Phenotypic effects and molecular mode-of-action of coumarin on *Arabidopsis thaliana.*

Stan Van Praet

Dissertation submitted for the degree of *Doctor of Philosophy*

Doctor in Sciences: Biochemistry & Biotechnology

2020

Language: English (United Kingdom)

Promotors: Prof. S. Depuydt and Prof. B. Vanholme

Ghent University
Faculty of Sciences
Department of Plant Biotechnology and Bioinformatics
UGent-VIB Centre for Plant Systems Biology
Ghent University Global Campus, Lab of Plant Growth Analysis

Research funded by the “Bijzonder Onderzoeksfonds” of Ghent Univerity for a PhD fellowship.

Examination commission

Chair

Prof. Geert De Jaeger

Universiteit Gent, Faculteit Wetenschappen
WE09 - Vakgroep Plantenbiotechnologie en Bio-informatica,
Technologiepark Zwijnaarde 71, 9052 Zwijnaarde
geert.dejaeger@ugent.be

Secretary

Prof. Steffen Vanneste

Universiteit Gent, Faculteit Wetenschappen
WE09 - Vakgroep Plantenbiotechnologie en Bio-informatica
Technologiepark Zwijnaarde 71, 9052 Zwijnaarde
steffen.vanneste@ugent.be

Supervisors

Prof. Stephen Depuydt

Universiteit Gent, Faculteit Wetenschappen
KR01 - Department of Environmental Technology, Food Technology and Molecular Biotechnology
WE09 - Vakgroep Plantenbiotechnologie en Bio-informatica
Sint-Pietersnieuwstraat 33, UFO, 9000, Gent
Technologiepark Zwijnaarde 71, 9052 Zwijnaarde
stephen.depuydt@ghent.ac.kr

Prof. Bartel Vanholme

Universiteit Gent, Faculteit Wetenschappen
WE09 - Vakgroep Plantenbiotechnologie en Bio-informatica
Technologiepark Zwijnaarde 71, 9052 Zwijnaarde
bartel.vanholme@ugent.be

Voting members

Prof. Wout Boerjan

Universiteit Gent, Faculteit Wetenschappen
WE09 - Vakgroep Plantenbiotechnologie en Bio-informatica
Technologiepark Zwijnaarde 71, 9052 Zwijnaarde
wout.boerjan@ugent.be

Prof. Godelieve Gheysen

Universiteit Gent, Faculteit Bio-ingenieurswetenschappen
BW25 - Vakgroep Biotechnologie
Coupure Links 653 geb. B, 9000 Gent
godelieve.gheysen@ugent.be

Prof. Dirk Inzé

Universiteit Gent, Faculteit Wetenschappen
WE09 - Vakgroep Plantenbiotechnologie en Bio-informatica
Technologiepark Zwijnaarde 71, 9052 Zwijnaarde
dirk.inze@ugent.be

Prof. Alexander Jones

Cambridge University, Sainsbury Laboratory
Bateman Street, Cambridge CB2 1LR, UK
alexander.jones@slcu.cam.ac.uk

Contents

Examination commission **3**

Abbreviations **9**

Chapter 1 – Phenylpropanoids, an underexplored group of biostimulants **13**

A brief history of coumarin 15

Addendum: other phenylpropanoids influencing plant development. 33

Chapter 2 – Hypocotyl elongation of *Arabidopsis thaliana:* a brief insight into the most important players during hypocotyl cell elongation **47**

Important players during (hypocotyl) cell elongation in *Arabidopsis thaliana*: from hormones to light. 49

Scientific scope and the aims of the project **73**

Chapter 3 – Coumarin induces elongation of the hypocotyl of *Arabidopsis thaliana* in the light.77

Coumarin induces hypocotyl elongation of light-grown *Arabidopsis thaliana* seedlings via increasing brassinosteroid signalling in an auxin-dependent manner. 79

Chapter 4 – Genome-wide transcriptional changes in the hypocotyl of *Arabidopsis thaliana* upon coumarin treatment **129**

RNA sequencing of hypocotyls of *Arabidopsis thaliana* treated with coumarin sheds light on the molecular basis of coumarin-induced phenotypes. 131

Coumarin induces dormancy in *Arabidopsis thaliana* 157

Chapter 5 – Coumarin reshapes the Root System Architecture of *Arabidopsis thaliana* **167**

Towards the molecular understanding of the coumarin-induced root response in *Arabidopsis thaliana*.... 169

Chapter 6 – Conclusion and perspectives **199**

General conclusion and perspectives. 201

Summary **211**

Nederlandstalige samenvatting **217**

Addendum **223**

References **381**

Curriculum vitae **435**

Personal 437

Scientific 442

Acknowledgements **448**

Abbreviations

AOPP	L-α-aminooxy-β-phenylpropionic Acid
BRs	Brassinosteroids
2,4-D	2,4-dichlorophenoxyacetic Acid
4-MU	4-methylumbelliferone
ABA	Abscisic Acid
ACC	1-amino-cyclopropane-1-carboxylate
AR	Adventitious roots
bHLH	Basic Helix-Loop-Helix
BL	Brassinolide
CA	Cinnamic Acid
CK(s)	Cytokinin(s)
CoA	Co-enzyme A
Col-0	*Arabidopsis thaliana Colombia*
DAG	Days After Germination
DMSO	Dimethylsulfoxide
EDTA	Ethylenediaminetetraacetic Acid
EXP(s)	Expansin(s)
FW	Forward
GA	Gibberellic Acid
GAs	Gibberellins
gDNA	Genomic DNA
GFP	Green Fluorescent Protein
IAA	Indole-3-acetic Acid
LR	Lateral Root
LRD	Lateral Root Density
MDCA	3,4-(methylenedioxy)cinnamic Acid
MES	2-(N-morpholino) ethanesulfonic Acid
MS	Murashige and Skoog
NAA	1-naphthaleneacetic Acid
NPA	N-1-naphthylphthalamic Acid
PA	Piperonylic Acid
PAC	Paclobutrazol
PAT	Polar Auxin Transport
PCR	Polymerase Chain Reaction
PCZ	Propiconazole
PHY	Phytochromes
PI	Propidium Iodide
PIN	Pin Formed
PP	Phenylpropanoid
PPP	Phenylpropanoid Pathway
rac-CA	Racemic Cinnamic Acid (a combination of the *trans*- and *cis*-isomer)
RSA	Root System Architecture
RV	Reverse
SA	Salicylic Acid
SAS	Shade Avoidance Syndrome
t/c-CA	*trans/cis*-Cinnamic Acid
t-CA	*trans*-Cinnamic Acid
TGG	*β*-thioglucoside glucohydrolase

UM	Umbelliferone
WT	Wild-type
YCS	Yucassin
Yucassin	5-(4-chlorophenyl)-4H-1,2,4-triazole-3-thiol

Chapter 1 – Phenylpropanoids, an underexplored group of biostimulants

A brief history of coumarin

Stan Van Praet[1,2,3], Stephen Depuydt[1,2,3], Bartel Vanholme[1,2]

1. Ghent University, Department of Plant Biotechnology and Bioinformatics, 9052 Ghent, Belgium
2. VIB Center for Plant Systems Biology, 9052 Ghent, Belgium
3. Ghent University Global Campus, Lab of Plant Growth Analysis, Incheon, South Korea

Author contribution:

S.V.P. and B.V. did write the manuscript and S.D. revised it.

Coumarin: a historical perspective

Equatorial America is home to *Dipterix odorata*, a large flowering tree belonging to the *Fabaceae*. It produces atypical round legumes, each composed of two fleshy carpels enfolding a single black and wrinkled seed, which is known as the Tonka bean (Fig. 1A). The beans spread a complex aroma resembling a mixture of almond and vanilla containing traces of cinnamon. The sweet odour mainly originates from a compound that accumulates in the legumes to levels at which it crystallizes at the surface of the bean and the inner side of the carpels (Ehlers *et al.*, 1995).

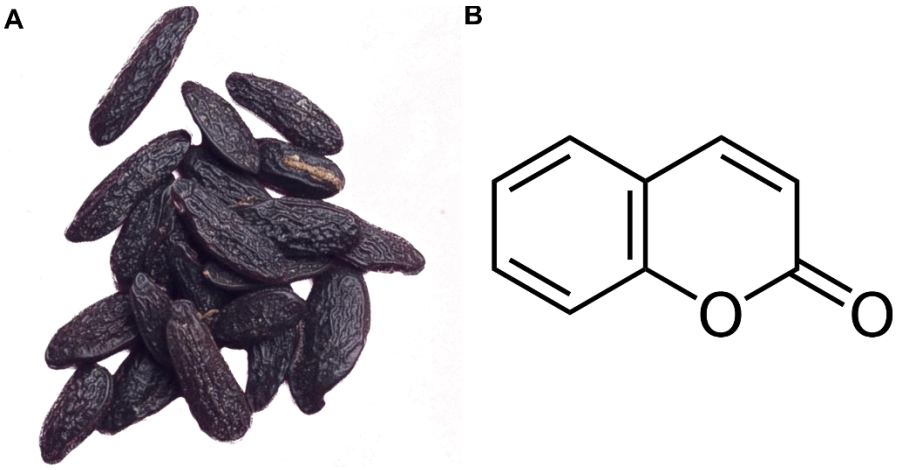

Figure1: (A) Tonka beans (https://www.thespicery.com, 2020) and (B) chemical structure of coumarin (Wikipedia, 2008).

In 1820, the German chemist August Vogel and the French pharmacist Nicholas Jean Baptiste Gaston Guibourt independently isolated the compound responsible for the typical flavour of Tonka beans (Guibourt, 1820; Vogel, 1820). Vogel's publication preceded the one of Guibourt, but he erroneously identified his purified compound as benzoic acid. Guibourt questioned Vogel's identification based on the chemical properties of the compound and later named the presumed novel compound "coumarine", referring to the vernacular name of *D. odorata*, being *Coumarouna odorata*. In a follow-up study, which largely confirmed the findings of Guibourt, coumarine was shortened to coumarin (Fig. 1B), the name under which the molecule is still known today (Boullay and Boutron-Charlard, 1825). Besides using Tonka beans as the source for coumarin, A. Vogel purified the compound from flowers of yellow sweet clover (Fig. 2 A) (*Melilotus officinalis*), a plant with a characteristic odour resembling the aroma of Tonka beans. Although not worked out in his initial paper, he also suggested that the same molecule could also be responsible for the sweet-smelling aroma of *Anthoxanthum odoratum* and *Holcus odoratus* (Fig. 2B, C) (later renamed to *Hierochloe odorata*) (Vogel, 1820). His assumption was later proven to be correct in several follow-up studies (Kosmann, 1844; Bleibtreu, 1846). Together, these early studies demonstrated that coumarin is not an odd metabolite restricted to an exotic plant, but is a more common secondary metabolite found in plants belonging to different families (i.e. *Fabaceae*, *Poaceae*, and *Rubiaceae*).

Around the same time, attempts were initiated to determine the structural composition of coumarin and the correct structure formula (i.e. $C_9H_6O_2$) was obtained in 1846 (Gerhardt, 1846). Final verification of the

formula was given in 1868 when the molecule was synthesised from organic building blocks (i.e. sodium salt of salicylaldehyde and acetic anhydride) by the English chemist William H. Perkin using a reaction still bearing his name (Fig. 2 D, E) (Perkin, 1868). Getting the formula correct was an important step towards the final identification of the molecular structure. Coumarin turned out to be a simple molecule composed of a planar bicyclic aromatic skeleton decorated with a keto group at the second position. The aromatic skeleton is a benzopyran (previously called chromene), which consists of a benzene and a pyran ring sharing two carbon atoms (Fig. 1B). The structure of coumarin is reflected in its official but hardly used IUPAC name: 2H-1-benzopyran-2-one.

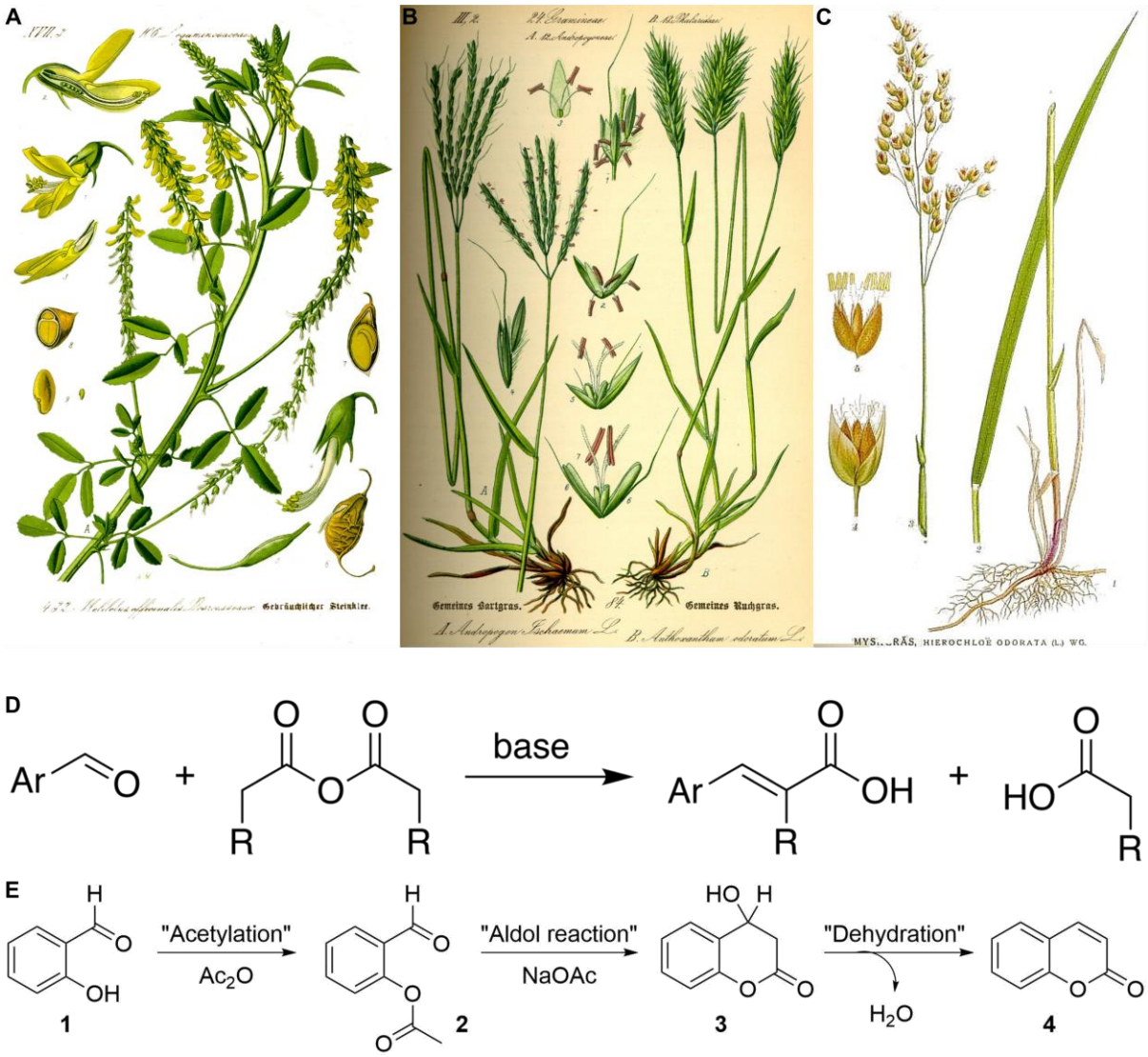

Figure 2: (A) *Melilotus officinalis* (Thomé, 1885b), *(B) Anthoxanthum odoratum* (Thomé, 1885a), *(C) Hierochloe odorata* (Lindman, 1901), (D) the Perkin reaction (Perkin, 1868) and (E) the synthesis of coumarin via the Perkin reaction: reaction of the sodium salt of salicylaldehyde (1) with acetic anhydride (Ac_2O). The same route was later also achieved by the reaction of salicylaldehyde with Ac_2O delivering O-acetyl salicylaldehyde (2) in a first step. Next, a base-catalyzed intramolecular aldol-type condensation of O-acetyl salicylaldehyde (3), followed by dehydration leads to coumarin (4) (Perkin, 1868; Heugebaert, 2015).

The perkin reaction allowed for the preparation of coumarin in a non-expensive way (Fig. 2 E). Coumarin is responsible for the familiar aroma of newly mowed grass or fresh hay. Therefore, coumarin was a popular source for flavour additives used in perfumes, desserts (sweets, pastries and ice cream), and tobacco and some alcoholic beverages (Cohen, 1979; Lake, 1999). Coumarin has been an integral part of the Fougère genre of perfumes since it was first used in Houbigant's “Fougère Royale” in 1882 (Fig. 3A). It was, however, not the French perfumer Jean-François Houbigant (Fig. 3B) who created the perfume with aromatic, spicy, oakmoss notes by adding synthetic coumarin, as claimed wrongly many times in literature (he died in 1806), but it was the joint owner of the Houbigant business, perfumer Paul Parquet, who developed the perfume in 1882 (Froissard et al., 2011; Houbigant Business, 2019). Today coumarin can still be found in multiple cosmetics, and also the “Fougère Royale” can still be purchased.

Benzopyrans are known to be very lipophilic in nature, explaining the ease by which they cross biological membranes and bind to other molecules through hydrophobic interactions. Such interactions could be at the basis of coumarin’s claimed toxicity in animal tests, causing liver problems and triggering tumour development when supplied at high concentrations (Cohen, 1979; Lake, 1999). Although the median lethal dose (LD50) value of coumarin is 10x higher than the one of vitamin D in rat oral acute toxicity studies (293 mg/kg and 33 mg/kg, respectively) (Cohen, 1979), the toxicity tests branded the compound and tanned its popularity as a food supplement. Based on its disputable but potential carcinogenic activity, the FDA also removed coumarin from the list of safe drugs in 1954, making it illegal to use it as a food additive in the USA. Interestingly, the tobacco industry has always opposed such a ban and delayed the adoption of legislation using the argument that revealing tobacco additives was a violation of trade secrets (Givel, 2003)[1].

The potential toxicity of coumarin has also been linked to a bleeding disorder of cattle that threatened the livelihood of farmers in the Northern US and Canada in the early 1920s (Smith, 1938). Preliminary investigations of this mysterious disease whereby cattle bled to death showed that affected cattle had eaten mouldy silage containing sweet clover. Subsequent fractionation of silage extracts resulted in the identification of dicoumarol as the haemorrhagic agent (Fig. 3C). This toxin is a metabolite of the fungi, formed from coumarin that accumulates to relatively high levels in clovers as was shown a century before by A. Vogel (Stahmann, Huebner and Link, 1941). Besides the identification of the anticoagulant dicoumarol as the causal agent of the bleeding disorder, the study led to the development of highly efficient anticoagulants used as either rodenticide

[1] The reluctant position of governments in these discussions most likely finds its origin in their conviction that smokers will die of cancer anyway, and if so they better do it with a pleasant scent (*pers. comm. Vanholme B.*).

(e.g. Warfarin (Fig. 3D)) or as drugs allowing the treatment of life-threatening blood clots and atrial fibrillation (Kresge, Simoni and Hill, 2005).

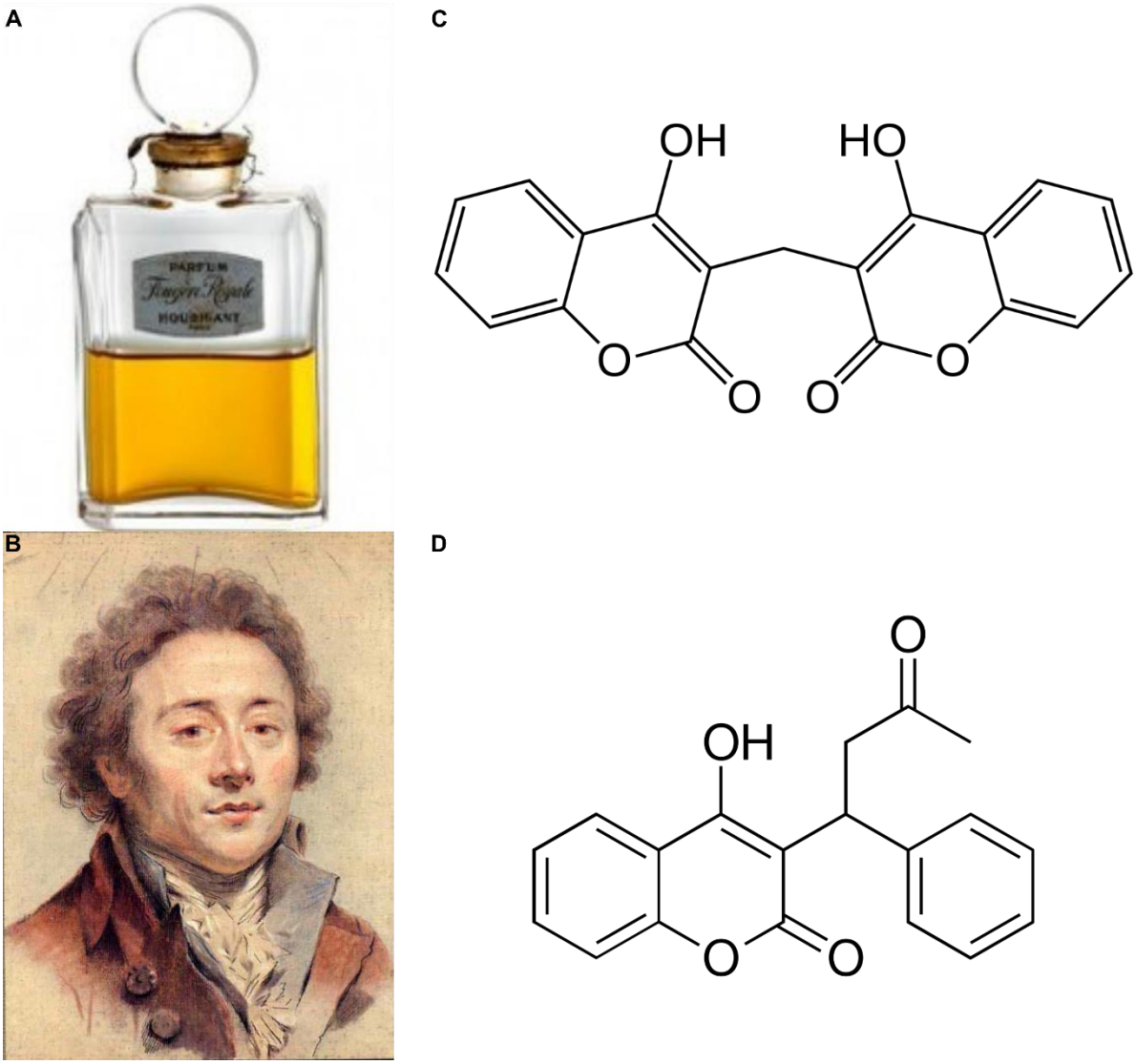

Figure 3: (A) Fougère Royale (Houbigant Business, 2019), (B) Jean-François Houbigant (© 2020 Parfums Houbigant Paris, 2020) (C) dicoumarol (Vasconcellos, 2006), and (D) warfarin (Vasconcellos, 2006).

Although being the first to have isolated coumarin, A. Vogel was not particularly interested in aromatic compounds of tropical plants with potential use as fragrance, nor in the toxicity of moulted silage (the bleeding disorder of cattle was not even an issue during his life). His main research interest was physiological in nature and focused on the question whether a compound found in the urine of herbivores and considered to be benzoic acid had a plant origin or whether the compound was a degradation product formed during digestion (Vogel, 1820). Identifying the compound in plants would definitely support his first hypothesis. Based on their odour, which he erroneously associated with the presence of benzoic acid, several meadow plants were suggested as potential sources of benzoic acid. The Tonka beans were merely included in his study as their odour was similar, yet much stronger and more intense compared the flavour of the meadow plants he brought up. The stronger

flavour suggested for a much higher level of the compound of interest, which would simplify the downstream purification process. Despite getting the compound wrong and having no initial interest in the aromatic compound of Tonka beans whatsoever, A. Vogel is recognised as the founding father of coumarin research. His purified compound turned out to serve as the structural skeleton for over 700 different plant metabolites, which are all categorized as coumarins, named after the parent compound they share (Collier, 1971; Harborne, 1999). Nomenclature-wise this turned out an unfortunate choice as it often leads to confusion when authors discuss characteristics of 'coumarin', referring to a member of the class of coumarins rather than coumarin itself. To avoid such confusion, we will use the plural form to refer to the class of coumarins, whereas we will restrict the use of the singular form to refer to the compound purified by A. Vogel in 1820 (i.e. 2H-1-benzopyran-2-one; (Vogel, 1820)).

The enigmatic pathway towards coumarin, a story to make Sweet clover 'sweeter'.

The biosynthesis of coumarins relies on the phenylpropanoid (PP) pathway, a plant-specific pathway with a central position in secondary metabolism (Vogt, 2010; Vanholme *et al.*, 2012). The different enzymatic steps of this pathway are arranged in a metabolic grid consisting of four levels corresponding to the four distinct classes of intermediates: acids, thioesters, aldehydes and alcohols, referring to the functional group on the phenylpropanoid side chain (Fig. 4). The majority of carbon entering the PP pathway via the aromatic amino acid phenylalanine ends up in one of the monolignols (i.e. coumaryl, coniferyl, or sinapyl alcohol) (Fig. 4, grey box). These end products of the PP pathway are the building blocks for the lignin polymer, which is deposited in the secondary thickened cell wall of plants. Thanks to its structural integrity and hydrophobicity, the polymer provides mechanical properties to the plant and allows long-distance water transport. For this reason, lignin and by extension the PP pathway has been considered a crucial evolutionary invention of plants to leave water environments and successfully colonize land (Boerjan, Ralph and Baucher, 2003; Muro-Villanueva, Mao and Chapple, 2019).

Besides the monolignols, the PP pathway also provides building blocks for a variety of other secondary metabolites, e.g. coumarins. The phenolic acids positioned on the first level of the metabolic grid of the PP pathway have always been considered the prime candidates for the branch points towards coumarins (Zobel and Brown, 1995; Bourgaud *et al.*, 2006). This preference is based on the core structure of the phenolic acids intermediates, consisting of nine carbon and two oxygen atoms in a configuration that easily leads to a coumarin skeleton. During the conversion, the side chain of the PP undergoes lactonisation, resulting in the formation of a benzopyran. Although lactonisation itself can occur spontaneously, it requires a hydroxyl group on the ortho-position of the aromatic ring and a *cis* configuration of the side chain (Bourgaud *et al.*, 2006). The hydroxylation reaction is strictly depending on an enzyme whereas the *trans-cis* isomerisation could be mediated by light.

When taking the PP pathway intermediate *trans*-cinnamic acid as the branch point, coumarin will be formed after ortho-hydroxylation, isomerisation and lactonization (Bourgaud *et al.*, 2006; Shimizu, 2014). At least in theory, as no enzyme involved in this pathway has been identified yet. An important obstacle in unravelling the pathway towards coumarin is the challenge to detect both start and end products of this pathway *in planta* (i.e. *trans*-cinnamic acid and coumarin, respectively). Both compounds are relatively insensitive

towards ionisation, making them almost undetectable in complex plant samples analysed by mass-spectrometry (Ghosh, Sil and Thakur, 1987; Zhou *et al.*, 2008). Although the presumed pathway intermediate *o*-coumaric acid should be easier to detect, this compound is unstable and quickly converts spontaneously to coumarin.

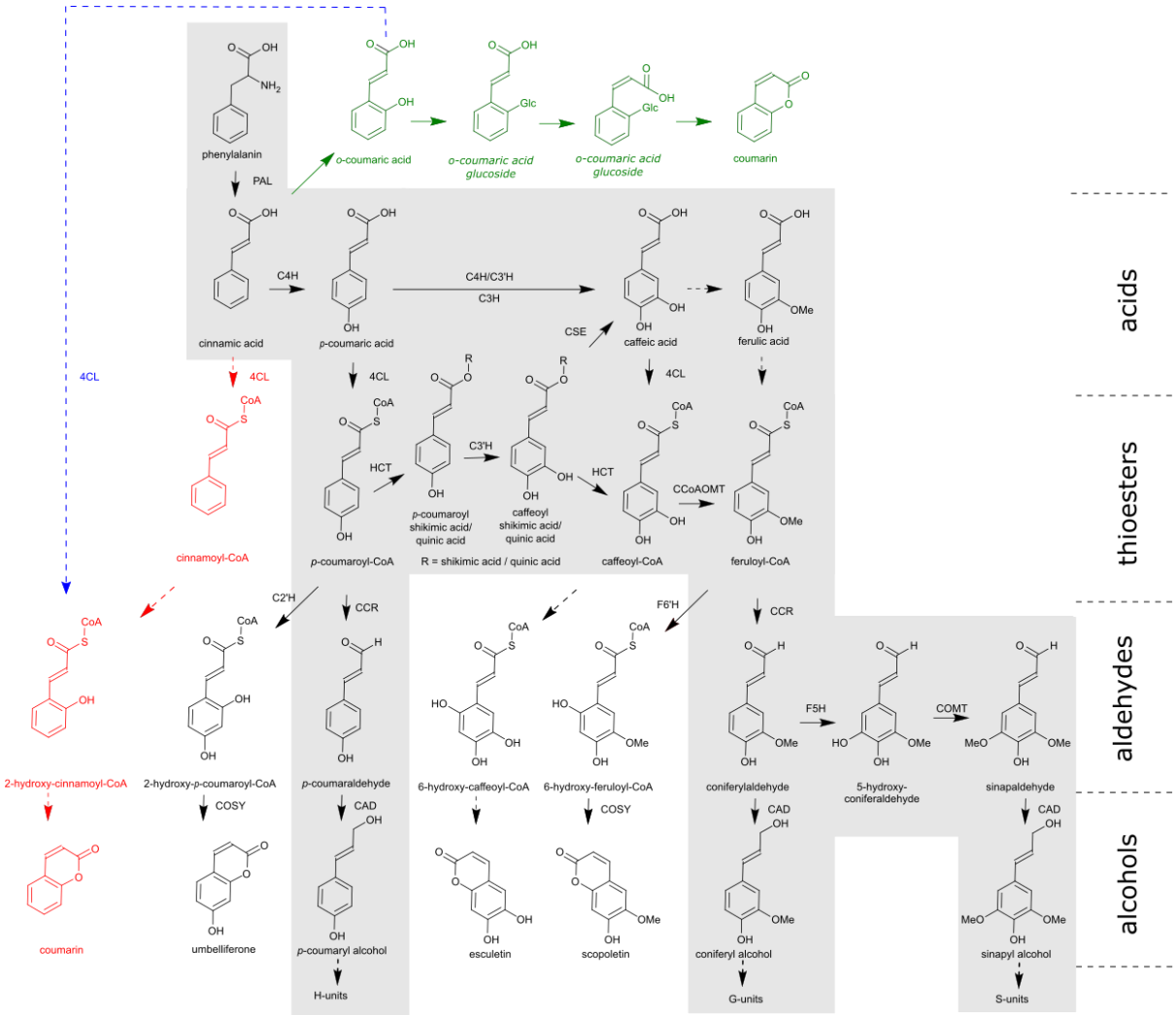

Figure 4: The biosynthetic pathways towards coumarins branching from the phenylpropanoid pathway

Grey background: The phenylpropanoid pathway involved in the biosynthesis of three monolignols which give rise to H-, G- and S-units when incorporated into the lignin polymer. Black: Biosynthetic pathway of the coumarins scopoletin, esculetin and umbelliferone to (Shimizu, 2014; Barros *et al.*, 2019; Vanholme *et al.*, 2019). Red: hypothetical biosynthetic pathway of coumarin via a putative 2ODD and an unknown COSY (Shimizu, 2014; Vanholme *et al.*, 2019). Green: hypothetical biosynthetic pathway of coumarin via a putative glucoside-intermediate (Brown, 1962; Collier, 1971). Blue: hypothetical biosynthetic pathway of coumarin via a putative 4CL. Arrows indicate the different enzymatic steps that are stated by literature. Dotted arrows indicate plausible enzymatic steps were solid proof is still lacking.

PAL: PHENYLALANINE-AMMONIA-LYASE; CAD: CINNAMYL-ALCOHOL-DEHYDROGENASE; 4CL: 4-COUMARATE-COA-LIGASE; C2H: CINNAMATE-2-HYDROXYLASE; C3H: CINNAMATE-3-HYDROXYLASE;

C3'H: 4-COUMAROYL-SHIKIMATE/QUINATE 3'-HYDROXYLASE; C4H: CINNAMATE-4-HYDROXYLASE; CCOAOMT: CAFFEOYL-COA-O-METHYLTRANSFERASE; CCR: CINNAMOYL-COA REDUCTASE; COMT: CAFFEIC-ACID-O-METHYLTRANSFERASE; CSE: CAFFEOYL SHIKIMATE ESTERASE; F5H: FERULATE-5-HYDROXYLASE; F6'H1:FERULOYL COA ORTHO-HYDROXYLASE 1; HCT: HYDROXYCINNAMOYL-COA SHIKIMATE / QUINATE HYDROXYCINNAMOYLTRANSFERASE ; 2ODD: 2-OXOGLUTARATE-DEPENDENT DIOXYGENASE; COSY: COUMARIN SYNTHASE

Oddly enough, the biosyntheses of coumarin derivatives, and in particular hydroxylated coumarins, are better characterised. The pathways towards these compounds branch from the PP pathway after the hydroxylation of the benzene ring. In the case of umbelliferone, this is after the formation of *p*-coumaric acid, whereas for scopoletin this is after the formation of ferulic acid or feruloyl-CoA (Bourgaud *et al.*, 2006). Feeding experiments of tobacco tissue cultures with labelled PP pathway intermediates led to the conclusion that ferulic acid itself is a branch point towards scopoletin (Fritig, Hirth and Ourisson, 1970). However, this idea was challenged by studies focusing on stress responses triggered by fungal elicitors in plant cell cultures, suggesting a role for CoA-esters as branch points towards coumarins (Matern, 1991). Genetic evidence provided final proof that *ortho*-hydroxylation does indeed occur at the level of feruloyl-CoA for the biosynthesis of scopoletin, resulting in the formation of 6-hydroxyferuloyl-CoA, a reaction catalysed by the 2-oxoglutarate-dependent dioxygenase *(*2-ODD) FERULOYL CoA 6′-HYDROXYLASE (F6′H) (Kai *et al.*, 2008). Later, a similar pathway was unravelled for umbelliferone. Here, *p*-COUMAROYL-CoA 2'-HYDROXYLASE (C2'H) catalyzes the conversion of *p*-coumaroyl-CoA to 2-hydroxy-*p*-coumaroyl-CoA (Vialart *et al.*, 2012). Similar 2-ODDs have been discovered in sweet potato (*Ipomoea batatas*), responsible for the biosynthesis of umbelliferone and scopoletin (Matsumoto *et al.*, 2012). Together these results imply that biosynthetic pathways towards coumarins withdraw carbon skeletons at the level of the thioesters, rather than the phenolic acid of the PP pathway (Fig. 4).

Once the hydroxyl-group is attached to the aromatic ring at the ortho-position, an isomerisation reaction takes place followed by a ring closure via lactonization. Both conversions can proceed without enzyme catalyst, but UV-light has been considered crucial for the isomerisation step preceding lactonization. On the other hand, it is well documented that plants can synthesise coumarins in roots, shielded from light. This ambiguity at the level of the isomerisation-step was recently solved by the identification of COUMARIN SYNTHASE (COSY), an enzyme catalysing *trans–cis* isomerisation and subsequent lactonization of the respective *o*-hydroxycinnamoyl-CoA thioesters (Fig. 4) (Vanholme *et al.*, 2019). Once the benzopyran skeleton is formed, the molecule can be further decorated with a range of functional groups (e.g. sugars, hydroxyls, sulfates, malonate, etc…), leading to the broad structural diversity found among coumarins. Based on its structure, the molecules are further classified as simple coumarins, furanocoumarins, pyranocoumarins and phenylcoumarins (Murray, Méndez and Brown, 1982; Murray, 1989; Bourgaud *et al.*, 2006).

As indicated earlier, in contrast to the profound insights we have in the biosynthesis of decorated coumarins, the biosynthesis of coumarin itself remains elusive. This is remarkable, in particular, because the genetic background of coumarin biosynthesis has been studied intensively in sweet clover in the light of the bleeding disorder of cattle, which was known to be caused indirectly by the high coumarin concentrations of clover (see above). Novel coumarin-deprived clover varieties were generated by plant breeders (Stevenson and

White, 1940; Goplen, Greenshields and Baenziger, 1957) and subsequent studies of these variants gave preliminary insight in the involvement of two genes ("*Cu"* and "*B"*) in coumarin metabolism. *Cu* was linked to the process of making '*bound-coumarin'*, while *B* was linked to the release of coumarin from bound-coumarin (Goplen, Greenshields and Baenziger, 1957). The bound-coumarin was later identified as a glucosylated form of *cis-o*-hydroxycinnamic acid (Rudorf and Schwarze, 1958), and in line with this, the B-gene was identified as a *β*-glucosidase (Schaeffer, Haskins and Gorz, 1960). These findings suggest a different pathway for coumarin as the one described above. The suggested pathway starts with *ortho*-hydroxylation of *trans*-cinnamic acid, followed by a glycosylation reaction on the ortho-position (Brown, Towers and Wright, 1960). Feeding studies with radioactive *o*-coumaryl glucoside led to the formation of coumarin, supporting the idea that *o*-coumaryl glucoside is an intermediate of the pathway (Brown, Towers and Wright, 1960). Moreover, the *o*-glucoside formation was shown to be a prerequisite for initiating the *trans-cis* isomerisation. The obtained data suggested that the *cis*- precedes the formation of the coumarin lactone ring (Kosuge and Conn, 1961; Brown, 1962). It should be emphasized that despite the listed experiments, limited molecular evidence is available for this alternative pathway towards coumarin and, to date, none of the enzymes has been identified at the genome sequence level.

A bioactive compound steering plant development

After Vogel's detection of coumarin in beans of *D. odorata* in 1820 (Vogel, 1820), the number of plants wherein coumarin was identified steadily increased and in 1911 coumarin had been found in over fifty different plant species (Wehmer, 1911). Its ubiquitous presence among plants suggested for a biological or physiological function, and one of the first hypotheses brought up was a role in allelopathy. According to this hypothesis, plants would release coumarin in the environment to suppress the growth of surrounding plants, giving the plant a competitive advantage (Gnonlonfin, Sanni and Brimer, 2012; Matos *et al.*, 2015). Whereas coumarin's role in allelopathy still hasn't been cleared up, its bioactivity is well documented. Numerous experiments have been performed to study the effect of coumarin on plant growth and development (Table 1). Unfortunately, contradictory results among the different studies make it difficult to draw unambiguous conclusions on which molecular processes are affected. The obtained contradictions are most likely the consequence of the use of a broad range of different plant species grown under different environmental conditions, all treated in different ways with coumarin at different concentrations. Moreover, the interpretation of the results is further complicated by the earlier mentioned confounding use of the name 'coumarin' in literature.

The first report on the activity of coumarin on algae was made by Klebs in 1896 (Klebs, 1896) and its activity on higher plants was described a decade later (Schreiner and Reed, 1907) by showing inhibitory effects on wheat germination and root growth. Numerous follow-up studies performed on a broad variety of plant species demonstrated that growth and germination are the main physiological processes affected by coumarin (Table 1). Interestingly, some studies showed that the inhibitory effect of coumarin on plant growth is reversible, leading to the conclusion that coumarin is phytostatic rather than phytocidal (Audus, 1950). In addition, also growth-promoting effects were observed when coumarin was used at low concentration (Bentley, 1958; Misra and Patnaik, 1959; Neumann, 1959, 1960a), resulting in a bell-shaped dose-response curve characteristic for growth regulators and phytohormones.

Coumarin shares its effect on elongation with auxin, the first identified and best-characterized phytohormone (for sure the best-characterized hormone at the moment most coumarin experiments were performed). This explains why the interaction between coumarin and auxin has been intensively investigated. However, no clear conclusion of the interaction of coumarin with auxin can be drawn from these studies. Based on the classical pea test bioassay[2], opposing effects of coumarin and the synthetic auxin analogue 1-naphthaleneacetic acid (NAA) led to the conclusion that they act antagonistically (Veldstra and Havinga, 1943). On the other hand, studies focusing on root growth inhibition reported an additive effect with the synthetic auxin 2,4-dichlorophenoxyacetic acid (2,4-D) (Pollock, Goodwin and Greene, 1954), or came to the conclusion that roots react differently to auxin than to coumarin (Burström, 1954). Also in shoot elongation assays, the effect of exogenous auxin treatment was observed to be additive (Neumann, 1960a). Interestingly, in this set-up, the order of treatments turned out to be crucial, as the additive elongation effect was only observed when the indole-3-acetic acid (IAA) treatment was followed by the coumarin treatment (Neumann, 1960a). This led to the conclusion that the effect of coumarin had to be separated from the auxin effect, indicating both compounds operate differently.

The other physiological process affected by coumarin is germination (Table 1) and two different explanations have been given for the coumarin effect: (1) toxicity, meaning the seed lost its viability or (2) dormancy, meaning that the seed lacks the capacity to germinate, despite favourable conditions (Baskin and Baskin, 2004). Abscisic Acid (ABA) is the main driver of seed dormancy (Sondheimer, Tzou and Galson, 1968) and in rice, it was shown that coumarin enhanced dormancy by inhibiting ABA catabolism (leading to higher ABA contents) via decreasing the expression of *(Oryza sativa) ABA 8'-HYDROXYLASE 2* and *3* (*OsABA8'ox2/3)*, which codes for ABA degrading oxidases (Chen *et al.*, 2019). Similar as for the effect of coumarin on elongation, some papers report on the stimulatory effect of coumarin on germination, especially when used at low concentrations (Knypl, 1964d; Saleh and Kebeish, 2018). At these lower concentrations, coumarin triggers the production of alpha-amylase in the aleurone layers of wheat, which are subsequently used to convert starchy endosperm to sugars. In addition, coumarin increased reactive oxygen species (ROS) production in wheat seeds (ROS is known to induce germination) as well as in Arabidopsis leaves (Araniti *et al.*, 2017; Saleh and Kebeish, 2018). In contrast to these studies, however, coumarin was found to stimulate the activity of superoxide dismutase and catalase in rice embryos, which avoids the accumulation of reactive oxygen species (ROS), and adds to its inhibitory effect on germination by inhibiting ABA catabolism (Chen *et al.*, 2019).

The preliminary insights in the physiological processes affected by coumarin (i.e. germination and elongation) were obtained in the first half of the previous century thanks to the joint effort of a whole community of chemists and plant physiologists. In contrast to this collaborative effort, the next period in coumarin research (1960-1970) was completely dominated by the Polish biochemist Jan Stanislaw Knypl. He focused on different model systems (e.g. *Rhodotorula rosea* cultures, fungi, hypocotyls of *Helianthus*) and provided evidence that

[2] The split pea test as invented by Went was a common tool in the first half of the 20th century to investigate effects on auxin. In short, growing stems of pea seedlings are split and immersed in a solution containing auxin and the others in solution of the compound that is investigated (e.g. coumarin). The two halves will curve inward, due to differential growth and this curvature is proportional to the auxin concentration. The epidermis side of the halved stems grows faster than the wounded inside, claimed by the unability of auxin to enter the stem through the wounded surface. If auxin is applied to the halved stems, the inside will grow just as much as the unwounded epidermis side (Went, 1934, 1939; Van Overbeek and Went, 1937).

coumarin operates as volatile (Knypl, 1961) and stimulates respiration (Knypl, 1964b). In addition, he largely confirmed previously shown positive effects of coumarin on plant growth (Knypl, 1964d, 1964a) and linked the growth effects to auxin. This conclusion was based on the observation that the growth inhibitory effect obtained by chlorocholine chloride (CCC; an inhibitor of gibberellin biosynthesis) could be reverted by both IAA as well as coumarin, but not in an additive manner (Knypl, 1964c, 1966a). Additional experiments made him conclude that coumarin-induced growth is auxin-like in type but that the primary mode of coumarin action is different from the one of IAA (Knypl, 1964a). Moreover, no additive effects could be observed between coumarin and auxin, GA or kinetin treatment in sunflower hypocotyl elongation assays (Knypl, 1966b). Besides the focus on elongation, Knyp also investigated the effect of coumarin and phytohormones on germination. Cytokinin could reverse the inhibitory effect of coumarin on germination of lettuce and kale seeds, while GA and auxin had no effect (Knypl, 1967b, 1967c). Initially, he tried to link this effect to light perception, as light plays a major role in lettuce germination, but as he observed the same effects with kale seeds (that are not sensitive to light for germination) he claimed that kinetin endogenously must counter the physiological changes induced by coumarin (Knypl, 1967b, 1967c). Interestingly, he also described how coumarin acts similarly as kinetin during leaf senescence by arresting chlorophyll loss in senescing kale leaf tissue while maintaining the synthesis of proteins (Knypl, 1967a). Contrary to the stimulation of protein synthesis for inducing respiration in sunflower hypocotyls (Knypl, 1968), it was found that coumarin inhibited protein formation in Kale leaves, leading to stimulation of senescence *sensu stricto* (Knypl, 1969), and so in the end coumarin was proposed to act antagonistically to kinetin. In conclusion, Knypl described numerous phenotypic effects of coumarin treatment but partly failed to link the effects to clear changes in the hormonal homeostasis of the plants. It can be noted that he mostly observed antagonistic effects with kinetin, hinting to auxin-like effects of coumarin. In addition, he distinguished the coumarin effect from the one of auxin, and concluded that the coumarin effect is auxin-like but not auxin-caused, confirming the statement Neumann forwarded a decade earlier (Neumann, 1959).

After the set of studies performed by Knypl, the research on the bioactivity of coumarin in plants largely faded in the following decades (i.e. 1970 – 1990). One important topic that got attention during that period was the coumarin induced swelling of roots (Svensson, 1971) and mesophyll cells (Harada, Rossini and Cheruel, 1971). Follow-up studies linked the phenotype to defects on the level of the microtubule and cellulose network (Hogetsu, Shiboaka and Shimokoriyama, 1974; Itoh, 1976a, 1976b; Satoh, Takahara and Matsuda, 1976; Burgess and Linstead, 1977). Interestingly, these observations were in line with older studies describing the effect of coumarin on the inhibition of mitosis in root meristems (Cornman, 1947; D'Amato and D'Amato-Avanzi, 1954; Avers and Goodwin, 1956). The topic was picked up again in the nineties, largely confirming those previous results without giving additional insight in the underlying molecular mechanism (Kupidlowska, Dobrzynska, *et al.*, 1994; Kupidlowska, Kowalec, *et al.*, 1994; Podbielkowska *et al.*, 1994, 1995, 1996; Keightley *et al.*, 1996).

The numerous reports on the effects of coumarin on plant growth, organ and tissue formation demonstrate that coumarin acts as a plant growth regulator, affecting plant growth by interfering with other hormones and therefore it can be considered as a hormone itself (Table 2). However, compared to the many papers illustrating the phenotypic effects of coumarin treatment, only a few studies tried to resolve the mode of coumarin action. Initially, the link with auxin was a main point of focus, but this did not result in a molecular

model explaining the working mechanism of coumarin. As described before, some links with ABA homeostasis have been described while investigating the effect of coumarin on germination. In the shoot, the link with GA homeostasis has been confirmed: coumarin induces elongation of wheat leaves and pea stem, an effect that was abolished when co-treated with paclobutrazol, an inhibitor of GA biosynthesis (Saleh and Abu El-Soud, 2015). One study investigated the potential role of ethylene, illustrating that coumarin induces ethylene biosynthesis, while ethylene mediates the inhibitory effect of coumarin on apical hook opening (Morgan and Powell, 1970). No link with brassinosteroids (BRs) has been illustrated so far, which can be explained by the fact that the majority of coumarin research was conducted in the 50s and 60s and BRs were only discovered in 1979 (Grove *et al.*, 1979). Whereas these studies all focused on the interaction between coumarin and one specific phytohormone, other studies tried to place coumarin in a hormonal network. When applied to root growth, the holistic approach did not reveal an overlap between the coumarin triggered effects and the effects of other hormones, whereupon it was concluded that the effect of coumarin on root growth must be direct (Svensson, 1972a). This conclusion is in agreement with the earlier statement of Neumann and Knypl, saying that the effects of coumarin are auxin-like but not auxin-caused (Neumann, 1960a; Knypl, 1966a). The auxin-like behaviour was later explained by observations illustrating the influence of coumarin on auxin transports. Feeding experiments with radioactive labelled exogenous auxin analogues illustrated that coumarin affects auxin transport in stem cuttings of *Phaseolus vulgaris* and *Impatiens balsamina L*. (Basu, 1972; Basler and Mcbride, 1977; Dhawan and Nanda, 1982). Moreover, coumarin also restored the diminished gravitropic response of Arabidopsis roots treated with the auxin transport inhibitor NPA (Lupini *et al.*, 2013). A follow-up study claimed that coumarin interferes with auxin polar transport by interaction with the *AUXIN RESISTANT 1 (AUX1)* influx carrier (Lupini *et al.*, 2014). However, additional evidence will be needed to further support this claim.

The lack of mutants in coumarin biosynthesis, signalling or transport is a major bottleneck in the study towards the physiological role of coumarin. In addition, the absence of tools to accurately measure coumarin in physiologically relevant concentrations further complicates coumarin research. Solving some of these factors could lead to the long-expected breakthrough towards the unravelling of the mode of coumarin action in plants.

Table 1: Phenotypes described for coumarin

Effect	**Used plant species**	**References**	**Concentration range**
Inducing germination	Wheat	(Knypl, 1964d; Rice, 1987; Saleh and Kebeish, 2018)	Up to 1000 µM
Inhibiting germination (inducing dormancy)	*Triticum turgidum* ssp. *Durum*, *Bidens pilosa,* Carrot, Cress, Lettuce, Radish*, Triticum durum,* Wheat*, Vicia faba. Italian ryegrass, Lens culinaris, Oryza sativa,* Peanut	(Nutile, 1945; Audus and Quastel, 1947; Mayer and Evenari, 1952; Misra and Patnaik, 1959; Bernhard, 1959; Blaim, 1960; Berrie *et al.*, 1968; Ketring and Morgan, 1972; Aliotta, Fuggi and Strumia, 1992; Aliotta *et al.*, 1993; Zobel and Brown, 1995; Abenavoli *et al.*, 2006; Pergo *et al.*, 2008; Saleh and Abu El-Soud, 2015; Saleh, Madany and González, 2015; Wu *et al.*, 2015; Yao *et al.*, 2017; Yuksel and Aksoy, 2017; Chen *et al.*, 2019)	0 to 1000 µM
Reducing germination speed	*Vicia faba*	(Saleh, Madany and González, 2015)	2000 – 4000 µM
Inducing alpha-amylase activity	*Vicia faba,* Wheat	(Saleh and Abu El-Soud, 2015; Saleh, Madany and González, 2015; Saleh and Kebeish, 2018)	500 – 4000 µM
Inhibiting alpha-amylase activity	*Barley, Vicia faba*	(Khan, 1969; Saleh, Madany and González, 2015)	1 – 340 µM
Stimulating ROS activity	*Arabidopsis thaliana,* Wheat	(Araniti *et al.*, 2017; Saleh and Kebeish, 2018)	*Not indicated*
Inhibiting ROS activity	*Oryza sativa, Arabidopsis thaliana*	(Lupini *et al.*, 2013; Chen *et al.*, 2019)	*Not indicated*
Inhibiting water uptake by the embryo	Wheat*, Triticum durum*	(Blaim, 1960; Abenavoli *et al.*, 2006)	1000 µM
Stimulating main root growth	*Avena sativa,* Cucumber, *Arabidopsis thaliana,* Maize, Rice	(Misra and Patnaik, 1959; Alexieva *et al.*, 1995; Abenavoli *et al.*, 2008; Lupini *et al.*, 2010)	10^{-3} M
Stimulating lateral root formation	Cress, Radish, Carrot, *Arabidopsis thaliana*	(Audus, 1948; Abenavoli *et al.*, 2008; Lupini *et al.*, 2014)	50 ppm

Inducing tuber formation	*Solanum tuberosum L., Helianthus tuberosus*	(Bagni and Fracassini, 1971; Stallknecht, 1972)	
Stimulating root hair formation	*Phleum pratense, Arabidopsis thaliana*	(Pollock, Goodwin and Greene, 1954; Svensson, 1971; Lupini *et al.*, 2014)	10^{-4} - 10^{-5} M
Stimulating root hair elongation	*Phleum pratense, Arabidopsis thaliana*	(Pollock, Goodwin and Greene, 1954; Svensson, 1971; Lupini *et al.*, 2014)	10^{-4} - 10^{-5} M
Inhibiting main root growth	Maize, *Avena sativa*, *Lepidium sativum, Pisum sativum*, Sweetclover, Alfalfa, *Phleum pratense*, Radish, Wheat, Cucumber, *Triticum durum, Bidens pilosa, pumpkin*, *Cichorium intybus, Arabidopsis thaliana,* Lettuce, *Vicia faba, Rice*	(Schreiner, Reed and Skinner, 1907; Audus and Quastel, 1947; Goodwin and Taves, 1950; Audus, 1950; San Antonio, 1952; Burström, 1954; Pollock, Goodwin and Greene, 1954; Avers and Goodwin, 1956; Misra and Patnaik, 1959; Bernhard, 1959; Goren and Tomer, 1971; Svensson, 1971, 1972a; Bagni and Fracassini, 1971; Aliotta *et al.*, 1993; Kupidlowska, Kowalec, *et al.*, 1994; Alexieva *et al.*, 1995; Abenavoli *et al.*, 2001, 2004, 2008; Hossain *et al.*, 2008; Pergo *et al.*, 2008; Takemura *et al.*, 2013; Lupini *et al.*, 2014; Saleh and Abu El-Soud, 2015; Saleh, Madany and González, 2015)	25 – 400 µM 2.5 * 10^{-5} M 1 – 500 µM
Inhibiting lateral root formation	Wheat, Maize, *Cichorium intybus, Arabidopsis thaliana*	(Audus, 1950; Bagni and Fracassini, 1971; Svensson, 1971; Abenavoli *et al.*, 2004, 2008)	2 * 10^{-4} M
Inducing adventitious root formation	*Phaseolus vulgaris Phaseolus vulgaris,* soybean*, Cedrus deodara, Glycine max L., Impatiens balsamina, Vigna radiata*	(Audus, 1950; Basu, 1972; Svensson, 1972a; Jansson and Svensson, 1980; Dhawan and Nanda, 1982; Grosser and Chandler, 1986; Nandi, Tamta and Palni, 2002; Tartoura, da Rocha and Youssef, 2004)	1 – 500 µM

Inhibiting root meristem division	*Allium cepa*, *Lilium longiflorum,* Wheat, Maize, *Allium sativum*, *Lens culinaris*	(Cornman, 1947; D'Amato and D'Amato-Avanzi, 1954; Avers and Goodwin, 1956; Svensson, 1971; Kupidlowska, Dobrzynska, *et al.*, 1994; Kupidlowska, Kowalec, *et al.*, 1994; Podbielkowska *et al.*, 1994, 1995, 1996; Keightley *et al.*, 1996; Yuksel and Aksoy, 2017)	200 – 1000 ppm $2.5 * 10^{-5}$ M
Inhibiting cell division/cell culture growth	*Carrot*	(Abenavoli *et al.*, 2003)	*Not indicated*
Stimulating hypertrophic swelling of roots	*Allium cepa, Phleum pratense, Avena sativa, Sweet clover,* Maize, cucumber, Pea, *Triticum durum*	(Cornman, 1947; San Antonio, 1952; Pollock, Goodwin and Greene, 1954; Avers and Goodwin, 1956; Svensson, 1971, 1972a; Kupidlowska, Kowalec, *et al.*, 1994; Abenavoli *et al.*, 2001, 2004)	10 – 300 μM
Affecting cell wall structure	Wheat, Sunflower, Maize, Potato, cucumber, Pine, Vine, Rice	(Misra and Patnaik, 1959; Svensson, 1971, 1972b; Harada, Ohyama and Cheruel, 1972; Hara, Umetsu and Miyamoto, 1973; Hogetsu, Shiboaka and Shimokoriyama, 1974; Itoh, 1976a, 1976b; Satoh, Takahara and Matsuda, 1976; Burgess and Linstead, 1977; Loewus, 1977; Uhrstrom and Svensson, 1979; Kupidlowska, Kowalec, *et al.*, 1994)	1 – 500 μM
Enhancing elongation of the stem (including hypocotyl and epicotyl segments)	Sunflower (*Helianthus*), *Phaseolus vulgaris*, Pea, Bean, *Vicia faba,* Wheat, Oat	(Moewus, 1949; Neumann, 1959, 1960b, 1960c; Knypl, 1964a; Morgan and Powell, 1970; Jansson and Svensson, 1980; Saleh and Abu El-Soud, 2015; Saleh, Madany and González, 2015)	500 – 4000 μM
Inducing coleoptile elongation	*Avena sativa*, Wheat, Rice	(Thimann and Bonner, 1949; Neumann, 1959, 1960b; Knypl, 1964d; Alexieva *et al.*, 1995)(Misra and Patnaik, 1959)	10 – 100 μM $0.01 – 0.1 * 10^{-4}$
Inducing leaf (cells) elongation	*Calystegia sepium,* Wheat	(Harada, Rossini and Cheruel, 1971; Saleh and Abu El-Soud, 2015; Saleh and Kebeish, 2018)	Up to 350 μM $4*10^{-4}$ M

Inhibiting stem elongation (including hypocotyl and epicotyl segments)	Pea, Pumpkin	(Thimann and Bonner, 1949; Alexieva *et al.*, 1995; Hossain *et al.*, 2008)	
Inhibiting coleoptiles elongation	*Avena sativa,* Wheat, Italian ryegrass	(Thimann and Bonner, 1949; Alexieva *et al.*, 1995; Saleh and Abu El-Soud, 2015; Wu *et al.*, 2015)	4 - 8000 μM
Inhibiting leaf growth	*Arabidopsis thaliana*	(Araniti *et al.*, 2017)	*Not indicated*
Inducing hypocotyl swelling	Pea	(Audus, 1950)	*Not indicated*
Influencing respiration	Sunflower, Onion, *Brassica oleracea L.,* Wheat, Lettuce, *Chlorella, Triticum durum,* spinach, *Bidens pilosa*	(Levari, 1953; Ron and Mayer, 1959; Knypl, 1961, 1967a, 1969; Svensson, 1972b; Moreland and Novitzky, 1987; Kupidlowska, Dobrzynska, *et al.*, 1994; Abenavoli *et al.*, 2001; Pergo *et al.*, 2008)	Vapours
Inhibition of degradation of chlorophyll in senescence leaves	*Brassica oleracea L.*	(Knypl, 1967a, 1969)	*Not indicated*
Alleviates salinity stress	Wheat	(Saleh and Madany, 2015)	50 ppm
Plant-plant interactions and allelopathy	*Pastinaca sativa, Gliricidia sepium*	(Whittaker and Feeny, 1971; Zobel and Brown, 1995; Razavi, 2011; Takemura *et al.*, 2013; Wu *et al.*, 2015)	*Not indicated*
Insecticidal activity	Sunflower, Sweetclover, Termites	(Gorz, Haskins and Manglitz, 1972; Mansour, Dimetry and Rofaeel, 1982; Reda and El-Banhawy, 1986)	*Not indicated*
Phytoalexin characteristics	*Helianthus annuus, Aspergillus niger, Penicillium glaucum, Rhizopus nigricans, Fusarium oxysporum f.sp. niveum,* Charcoal rot disease	(Knypl, 1960, 1963; Wu *et al.*, 2008; Al-Wakeel *et al.*, 2013; Lee *et al.*, 2014; Gutiérrez-Barranquero *et al.*, 2015; Zhang *et al.*, 2017; Reen *et al.*, 2018)	300 - 3000 μM 100 – 1000 ppm
Coumarin operates as volatile	Sunflower	(Knypl, 1961)	*Not indicated*
Enhances mineral uptake	*Triticum durum*	(Abenavoli *et al.*, 2001)	*Not indicated*

Table 2: Molecular effects and mode-of-action of coumarin

Effect	**Used plant species**	**References**	**Concentration range**
Increases formation of primary and secondary metabolites	*Vicia faba*	(Saleh, Madany and González, 2015)	500 to 4000 µM
Interferes with auxin homeostasis	Sunflower, Oat, Pea, Bean, *Helianthus annuus,*	(Thimann and Bonner, 1949; Neumann, 1960b; Knypl, 1964c; Svensson, 1972a)	*Not indicated*
Stimulating gibberellic acid biosynthesis	Faba bean (Vicia faba)	(Saleh and Abu El-Soud, 2015; Saleh, Madany and González, 2015)	1000 µM
Stimulating auxin biosynthesis or increasing free IAA levels	*Vicia faba, Vicia radiata*	(Tartoura, da Rocha and Youssef, 2004; Saleh and Abu El-Soud, 2015; Saleh, Madany and González, 2015)	1000 µM
Stimulation of auxin oxidation	Cucumber, *Impatiens balsamina*	(Goren and Tomer, 1971; Dhawan and Nanda, 1982)	*Not indicated*
Stimulation of ABA content	*Vicia faba, Oryza sativa*	(Saleh, Madany and González, 2015; Chen *et al.*, 2019)	*Not indicated*
Interfering with GA homeostasis	Wheat	(Svensson, 1972a)(Saleh and Abu El-Soud, 2015)	*Not indicated*
Interference with auxin transport	*Phaseolus vulgaris, Impatiens balsamina, Arabidopsis thaliana*	(Basu, 1972; Basler and Mcbride, 1977; Dhawan and Nanda, 1982; Lupini *et al.*, 2013, 2014)	*Not indicated*
Inducing H^+-ATPase activity leading to acidification of the apoplast	*Maize*	(Lupini *et al.*, 2010, 2018)	*Not indicated*
Stimulating ethylene biosynthesis	*Bean*	(Morgan and Powell, 1970)	*Not indicated*

Addendum: other phenylpropanoids influencing plant development.

Introduction

The phenylpropanoid pathway (PPP) is a large and well-known pathway that is at the basis of the production of several plant-specific metabolites. The phenylpropanoids fulfil numerous physiological functions that are essential for plant growth and development (Biala and Jasiński, 2018). There is even evidence that the conversion of phenylalanine (Phe) to cinnamic acid (CA) is conserved already for over 450 million years ago (Fellenberg and Vogt, 2015). Nowadays, it is known that 10 enzymatic steps convert phenylalanine to two of the three major building blocks for lignin and suberin production (Vanholme *et al.*, 2012). Lignin counts for approximately 30% of the organic carbon in the biosphere, is crucial for the structural integrity of the cell wall and strength of the stem (Jones, Ennos and Turner, 2001; Chabannes *et al.*, 2003), and therefore critical during the evolution of land plants to adapt from an aquatic to terrestrial environment. Moreover, lignin makes the cell wall waterproof allowing the development of the vascular system and as such enabled transport of water and solutes (Sarkanen and Ludwig, 1971).

Next to the formation of lignin, the pathway is also the basis for an enormous array of secondary metabolites (Vogt, 2010), e.g. the chalcone synthesis pathway that leads to flavonol and flavonoid biosynthesis (Vogt, 2010; Vanholme *et al.*, 2012). These more than 10 000 different compounds have various biological roles, for example in UV protection or radical scavenging (antioxidant) (Agati *et al.*, 2012; Yang *et al.*, 2018). Phenylpropanoids are also involved in flower and fruit pigmentation (Dixon, Liu and Jun, 2013), symbiotic associations (J. Zhang *et al.*, 2009; Nadal and Paszkowski, 2013; Liu and Murray, 2016), mineral shortage (Clemens and Weber, 2016), and defence reactions (Naoumkina *et al.*, 2010; Shalaby and Horwitz, 2015); Liu and Murray, 2016). Next to numerous roles in plant development, phenylpropanoids (especially flavonoids) have shown to have numerous positive effects on human health too (Dixon and Pasinetti, 2010).

It is well known that mutations in the PPP lead to dwarfism (Van Acker *et al.*, 2013), which is historically claimed to be caused by a lack of lignin and therefore named lignin modification-induced dwarfism (LMID) (Muro-Villanueva, Mao and Chapple, 2019). Moreover, it has been illustrated that the restoration of lignin biosynthesis in the vessels alone is enough to restore plant growth and even induce biomass production (De Meester *et al.*, 2017). It remains, however, questionable if the dwarf phenotypes are only the consequence of altered/perturbed lignin biosynthesis or if (part) of the effects can also be linked to the hypo- or hyper-accumulation of intermediates or derivatives of the phenylpropanoid pathway. Moreover, when genes producing enzymes in the monolignol-pathway are knocked-out (e.g. ferulate 5-hydroxylase (F5H), caffeic acid O-methyltransferase (COMT), and cinnamyl alcohol dehydrogenase (CAD)) - hampering the formation the lignin building blocks - the effect on growth is way less severe, to even no effect at all (Wang *et al.*, 2018). Furthermore, it has been illustrated that the phenylpropanoids 3,4-(methylenedioxy)cinnamic acid (MDCA) and cinnamic acid interfere with auxin transport and auxin signalling (Steenackers *et al.*, 2016, 2017; Kurepa *et al.*, 2018). Also, the PPP derivatives of cinnamic acid: umbelliferone, scopoletin and coumarin are known to influence plant growth in a wide variety of phenotypes (Podbielkowska *et al.*, 1995; Lacy and O'Kennedy, 2004; Kai *et al.*,

2006), and it has been known for a long time that also flavonoids interfere with auxin transport (Brown *et al.*, 2001; Peer and Murphy, 2007).

While most of the research is focussing on the roles and potential yield gains when modulating lignin biosynthesis (Muro-Villanueva, Mao and Chapple, 2019) and the many roles of flavonols and anthocyanins are mostly in the context of abiotic and biotic stress resistance, the intermediates and derivates (molecular) functions have been out of scope. Moreover, phenylpropanoids do not operate in a steady-state but are actively transported through the plant cell and tissues and their localisation is tightly controlled (Biala and Jasiński, 2018). Interesting is the compartmentalisation of several phenylpropanoids in the cell wall, independent of lignin biosynthesis, indicating potential interference with cell wall processes (Kulich and Žárský, 2014; Biala and Jasiński, 2018).

Coumarins are the biggest group of derivatives of the phenylpropanoid pathway, with over 700 members (Collier, 1971; Murray, 1989; Harborne, 1999). Coumarins have a broad role in plant development and are known to be involved in plant defence (as they accumulate rapidly at infection sites and operate often as phytoalexins) (Garcia *et al.*, 1995; Uritani, 1999; Kai *et al.*, 2006; Sun *et al.*, 2014; Beyer *et al.*, 2019), to have numerous roles in the rhizosphere (including iron chelation and influencing germination) (Zobel and Brown, 1995; Schmidt *et al.*, 2014; Tsai and Schmidt, 2017; Rajniak *et al.*, 2018; Stringlis *et al.*, 2018) and many coumarins are described as allelopathic compounds (Gnonlonfin, Sanni and Brimer, 2012; Matos *et al.*, 2015). The most well-known simple coumarins are pure coumarin, scopoletin, esculetin and umbelliferone. Coumarin has been discussed in detail before, here, the scope will be to give a brief overview of the state-of-the-art of how scopoletin and umbelliferone affect plant growth.

Scopoletin

Historical background and origin

Winkler isolated scopoletin (6-methoxy-7-hydroxycoumarin) out of more than 50 plant species encompassing both monocotyledons as well as dicotyledonous plants (Winkler, 1967). Others found it to be present in (to only name a few) *Chalcas exotica*, tobacco, *Avena sativa, Macaranga gigantifolia*, oat, plum tree, sunflower, sweet potato and *Arabidopsis thaliana* (Blas, 1868; Andreae and Andreae, 1949; Goodwin and Kavanagh, 1949; Hillis and Swain, 1959; Imbert and Wilson, 1970; Tal and Robeson, 1986; Darmawan *et al.*, 2012; Fourcroy *et al.*, 2014). Today, it is generally accepted that scopoletin is present in almost all plant species (Murray, Méndez and Brown, 1982; Gnonlonfin, Sanni and Brimer, 2012; Vanholme *et al.*, 2019). Scopoletin has the same structure as coumarin but contains an additional hydroxyl and methoxy group on the benzene ring (Fig. 5A). Scopoletin is a phytoalexin and is one of the major and most important coumarins that is formed as reaction of the plant towards microbial attacks, mechanical injuries and other types of biotic or abiotic stress (Tanaka *et al.*, 1983; Giesemann, Biehl and Lieberei, 1986; Tal and Robeson, 1986; Uritani, 1999; Gnonlonfin, Sanni and Brimer, 2012). Note that scopoletin is commonly found in plant species in its glycoside form (named scopolin), with on average an 85-fold higher abundance in Arabidopsis (Kai *et al.*, 2006). Moreover, scopoletin is on average 180-fold more abundant in roots than in shoots (Kai *et al.*, 2006). However, it is hypothesized that scopoletin is more active than its sugar-conjugate scopolin (Taguchi *et al.*, 2000).

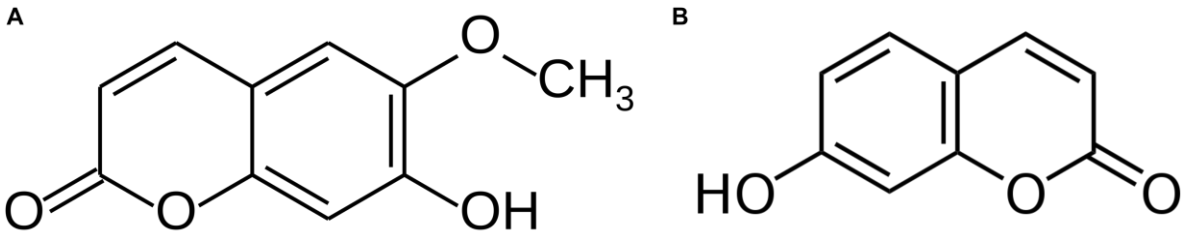

Figure 5: (A) Scopoletin (Kopiersperre, 2015), (B) Umbelliferone (Yikrazuul, 2010).

Roles in growth and development

Most effects (Table 3 and 4) can be divided into 3 majors roles: scopoletin operates as a (1) phytoalexin, as a (2) chelator for iron and (3) illustrates phytotoxic effects and allelopathic behaviour.

Phytoalexins are low molecular weight substances that are produced de novo in plants and accumulate rapidly at the infection site and function as antimicrobial, antifungal and/or antioxidative substance against (mostly) necrotrophs (Paxton, 1981). Scopoletin is well known for its negative effects on microbial and fungal growth, both in planta as *in vivo* (Tan and Low, 1975; Garcia *et al.*, 1995; Valle *et al.*, 1997; Perez-Rodriguez *et al.*, 2001; Ba *et al.*, 2017). Moreover, scopoletin has insecticidal properties (Olson and Roseland, 1991; Adfa *et al.*, 2010), and numerous papers are available illustrating its production after bacterial, viral, fungal or

mechanical infection at the site of infection in numerous plant species as for example cassava, tobacco, sunflower, rubber tree and Arabidopsis thaliana (Valle *et al.*, 1997; Kim *et al.*, 2000; Churngchow and Rattarasarn, 2001; Silva *et al.*, 2002; Peterson *et al.*, 2003; Carpinella, Ferrayoli and Palacios, 2005; Simon *et al.*, 2010; Sun *et al.*, 2014; Beyer *et al.*, 2019). A more than 20-fold increase in scopoletin concentration has been measured in tobacco (Costet, Fritig and Kauffmann, 2002). Furthermore, it has been illustrated that the disease-resistant hybrid of N. glutinosa x N. debneyi contains constitutively very high levels of scopoletin and scopolin (Goy *et al.*, 1993). Moreover, the scopoletin biosynthesis gene *F6'H1* had a 15 fold increase in expression upon infection with the fungus Phakopsora pachyrhizi, completely abolishing its germination (Beyer *et al.*, 2019). This result is so promising, that the method of increasing resistance against soybean rust in transgenic plants by increasing scopoletin biosynthesis was patented (US20180010144A1).

Interestingly, recently, it was also illustrated that scopoletin not only has antimicrobial characteristics but can also enhance the microbial activity, and thereby influences the root microbiome in a selective manner (Stringlis *et al.*, 2018). The role of scopoletin in the rhizosphere was originally discovered as aid in the mobilization and uptake of iron, whereby it was found that scopoletin is present in the rhizosphere in very high concentrations in iron limiting conditions (Lan *et al.*, 2011; Rodriguez-Celma *et al.*, 2013; Fourcroy *et al.*, 2014; Schmid *et al.*, 2014). Moreover, the scopoletin biosynthesis mutants, *f6'h1'* and *cosy* are hypersensitive towards iron limiting conditions (Rodriguez-Celma *et al.*, 2013; Schmid *et al.*, 2014; Vanholme *et al.*, 2019). Interestingly, Arabidopsis mutants impaired in the excretion scopoletin also lack the ability to mount rhizobacteria-mediated induced systemic resistance (ISR), suggesting for the first time a clear link between a stress response (iron starvation) and plant immunity (Lundberg and Teixeira, 2018).

Besides influencing the rhizosphere, it is also known that scopoletin has allelopathic behaviour (Araniti *et al.*, 2015). Scopoletin was first described to inhibit root growth of *Avena sativa* (Goodwin and Taves, 1950), but it was also found to inhibit germination, shoot growth, respiration, stomatal opening and in general plant growth (Goodwin and Taves, 1950; Pollock, Goodwin and Greene, 1954; Avers and Goodwin, 1956; Kohmuenzer, 1965; Einhellig *et al.*, 1970; Einhellig and Kuan, 1971; Shukla *et al.*, 1999; Dayan and Duke, 2006; Araniti *et al.*, 2015; Graña *et al.*, 2017). Nevertheless, also positive effects on root growth and germination have been described, illustrating that the role of scopoletin is concentration- and species-dependent (Andreae and Andreae, 1949; Einhellig and Kuan, 1971; Graña *et al.*, 2017). Scopoletin was found to stimulate root growth of potato plants when applied in low concentrations (1 ppm) (Andreae, 1952). Interestingly, scopoletin was strictly localised to elongating and mature portions of the root but was nearly absent in the meristem (Goodwin and Pollock, 1954). The effect on roots was linked to enhanced auxin metabolism via competitive inhibition of indol acetic acid oxidation by scopoletin (Andreae, 1952). It is a role of scopoletin that has been confirmed numerous times in the 2 decades following the original finding (Waywood, Oaks and Maclachlan, 1956; Sequeira, 1964; Schaeffer, Buta and Sharpe, 1967; Imbert and Wilson, 1970; Sirois and Miller, 1972). Thereby it has been illustrated that scopoletin, concentration-dependent, either inhibits or stimulates auxin oxidation (Imbert and Wilson, 1970), linking a mechanistic explanation to the phenotypes observed. Nevertheless, until today the exact mode-of-action has not been revealed on how scopoletin inhibits IAA-oxidation. The major IAA biosynthesis pathway in Arabidopsis - the indole-3-pyruvic acid (IPyA) route - is only discovered in the last decade (Mashiguchi *et al.*, 2011; Stepanova *et al.*, 2011; Won *et al.*, 2011; Dai *et al.*, 2013), and only in 2016

is the DIOXYGENASE FOR AUXIN OXIDATION (DAO) enzyme found, oxidizing IAA into 2-oxindole-3-acetic acid (oxIAA) (Stepanova and Alonso, 2016; Zhang *et al.*, 2016). Historically the oxidation of IAA has been linked to peroxidase activity (e.g. horseradish peroxidase), what today is no longer supported, and the inhibition of IAA oxidation by scopoletin was illustrated via inhibition of those peroxidases (Andreae, 1952; Schaeffer, Buta and Sharpe, 1967; Normanly, 1997; Peer, Cheng and Murphy, 2013). It will be interesting to test the effect of scopoletin on the expression of the DAO and the levels of IAA and oxIAA.

Graña et al., (2017) claimed that scopoletin as themselves mimics auxinic herbicides (e.g. 2,4-dichlorophenoxyacetic acid, 2,4-D). The synthetic auxin herbicides mimic the effect of IAA by interacting with the auxin receptor TIR1 and inducing a chain of effects similar to those of auxin (reviewed in Grossmann, 2009). In short, the following actions occur, first hormonal interactions are activated (e.g. ethylene biosynthesis and ABA accumulation) leading to all different growth phenotypes (e.g. tissue swelling, leaf epinasty, etc.) which later is followed by alterations in the actin cytoskeleton followed by induction of severe oxidative stress, stomatal closure, reduced transpiration, unsaturation of plasma membrane lipids and leakage of the cytosol what in the end will lead to cell death (Grossmann, 2009; Rodríguez-Serrano *et al.*, 2014; Christoffoleti *et al.*, 2015). Interesting is that also scopoletin can bind in the TIR1 pocket (Graña *et al.*, 2017), although only illustrated via modelling. Indeed, high concentrations of scopoletin mimic the auxin herbicide mechanism (i.e. compromising root development, inducing wrong microtubule assembling, mitochondrial membrane depolarization and ultimately cell death) (Graña *et al.*, 2017). Nevertheless, in low concentrations, 2,4-D behaves like auxin and is therefore commonly used in experiments as auxin analogue, while low concentrations of scopoletin (up to 5μM) had no effects on the analysed phenotypes (Graña *et al.*, 2017). Moreover, 2,4-D is a synthetic compound, not naturally occurring in plants and therefore a herbicide, while scopoletin is a natural compound, formed endogenously, with its less active form scopolin being stored in the vacuole, a compartmentalisation that will avoid herbicide actions.

Interestingly, scopoletin not only affects auxin metabolism, but also the opposite has been observed. 2,4-D treatment was found to induce scopoletin production in tobacco and shoots of Arabidopsis thaliana, indicating a feedback/crosstalk system between both (Skoog and Montaldi, 1961; Dieterman *et al.*, 1964; Kai *et al.*, 2006). Also, kinetin was observed to have a positive effect on scopoletin formation, with an additive effect in combination with IAA (Sargent and Skoog, 1960), therefore it was claimed that scopoletin played an important role in callus formation. In cell cultures, the first steps were taken in unravelling the feedback system between scopoletin formation and hormonal crosstalk. It was found that 2,4-D treatment of tobacco cells stimulated scopoletin uptake, where after the scopoletin was converted into scopolin in the cytoplasm, and then transferred into the vacuoles (Hino, Okazaki and Miura, 1982; Taguchi *et al.*, 2000). Not only 2,4-D but also other auxins and salicylic acid (SA) were found to stimulate the uptake of scopoletin, while the antiauxin p-chlorophenoxyisobutyric acid (PCIB), cytokinin and methyl jasmonate (MJ) suppressed the 2,4-D stimulated uptake (Taguchi *et al.*, 2001). Furthermore, it was found that MJ alone did induce scopoletin biosynthesis in tobacco cell cultures, whereby they illustrated that scopolin was mainly found within the cell, whereas scopoletin accumulated in the culture filtrate (Sharan *et al.*, 1998). Interesting is that they could uncouple the effect of MJ, a known stress hormone, and the role of scopoletin in plant defence: in response to stress a spike in scopoletin

concentration in the substrate was found originated from conjugation of scopolin to scopoletin and hence not by de novo synthesis as is the case by MJ treatment (Sharan *et al.*, 1998).

Moreover, it was found that JA signalling was activated in *Nicotiana tabacum* leaves after infection by Alternaria alternata (a necrotrophic fungus causing brown spot disease) and that this lead to scopoletin biosynthesis (Sun *et al.*, 2014). Interestingly, it was found that higher levels of scopoletin accumulated in young leaves while lower levels of scopoletin were observed in mature leaves in correlation with their respectively higher and lower resistance (Zhang *et al.*, 1998; Cheng and Sun, 2001; Sun *et al.*, 2014). They, furthermore, illustrated that this increase in scopoletin was MYC2 dependent, a master regulator of many JA-dependent defences against insect herbivores and pathogens, indicating scopoletin formation is a well-regulated response of the plant (Lorenzo *et al.*, 2004; Dombrecht *et al.*, 2007; Woldemariam *et al.*, 2013; Sun *et al.*, 2014). Moreover, also ethylene can induce scopoletin formation (Reuveni and Cohen, 1978) and, recently, it was shown that ethylene signalling is essential for the biosynthesis of the phytoalexin scopoletin for the resistance of Nicotiana attenuata against Alternaria alternata (Sun *et al.*, 2017).

These are the first steps in the unravelling of how phytohormonal pathways are connected to scopoletin and defence reactions. It is known that host plants activate the salicylic acid pathway to defend against biotrophic and hemibiotrophic pathogens, whereas jasmonic acid (JA) and ethylene pathways are induced as a response against necrotrophic pathogens (Glazebrook, 2005; Mengiste, 2012). It is found that both JA, as well as ethylene, lead to scopoletin production and scopoletin is causally found to operate as phytoalexin to reduce and even fully inhibit the negative effects of necrotrophs, and to be dependent on both ethylene and JA signalling for its production (Reuveni and Cohen, 1978; Sharan *et al.*, 1998; Sun *et al.*, 2014, 2017; Beyer *et al.*, 2019).

Table 3: Phenotypes described by scopoletin

Effect	Used plant species	References
Stimulation of root growth	*Potato spp., Pea, Arabidopsis*	(Andreae and Andreae, 1949; Andreae, 1952; Graña *et al.*, 2017)
Inhibition of root growth	*Phicum pratense L., Avena sativa L, Arabidopsis, Phleum pratense, wheat*	(Goodwin and Taves, 1950; Pollock, Goodwin and Greene, 1954; Avers and Goodwin, 1956; Shukla *et al.*, 1999; Graña *et al.*, 2017)
Stimulation of root hair growth and/of formation	*Arabidopsis*	(Graña *et al.*, 2017)
Stimulation of germination	*Arabidopsis*	(Graña *et al.*, 2017)
Inhibition of germination	*Panicum miliaceum*	(Peterson *et al.*, 2003)
Activating germination of seeds of plant parasite	*Striga astatic,*	(Worsham, A. D.Klingman and Moreland, 1962)
Inhibition of shoot growth	*Tobacco, Sunflower, Pigweed, Arabidopsis*	(Einhellig *et al.*, 1970; Dayan and Duke, 2006)
Phytotoxic effects and allelopathic behaviour	*Avena spp., Helianthuts annuns L, Arabidopsis, Wheat*	(Goodwin and Taves, 1950; Avers and Goodwin, 1956; Kohmuenzer, 1965; Shukla *et al.*, 1999; Araniti *et al.*, 2015; Graña *et al.*, 2017)
Decreased respiration	*Sunflower, tobacco, arabidopsis*	(Einhellig *et al.*, 1970; Dayan and Duke, 2006)
Stimulation of stomatal closure	*Tobacco, Sunflower*	(Einhellig and Kuan, 1971)
Stimulation of stomatal opening	*Tobacco, Sunflower*	(Einhellig and Kuan, 1971)
Alleviating biotic stress as a phytoalexin	*Cassava, Sunflower, Rubber Tree (Hevea brasiliensis),*	(Minamikawa, Akazawa and Uritani, 1963; Tan and Low, 1975; Tanaka *et al.*, 1983; Tal and Robeson, 1986; Giesemann,

	Tobacco, Arabidopsis, Sweet potato	Biehl and Lieberei, 1986; Snook, Chortyk and Csinos, 1991; Goy *et al.*, 1993; Garcia *et al.*, 1995; Valle *et al.*, 1997; Uritani, 1999; Kim *et al.*, 2000; Churngchow and Rattarasarn, 2001; Silva *et al.*, 2002; Peterson *et al.*, 2003; Carpinella, Ferrayoli and Palacios, 2005; Kai *et al.*, 2006; Simon *et al.*, 2010; Sun *et al.*, 2014; Beyer *et al.*, 2019)
Antifungal activity	*Ulmus pumila* and *Ulmus campestris, Melia azedarach L, Sweet potato, Cassava, Taro, Argyreia speciosa*	(Garcia *et al.*, 1995; Valle *et al.*, 1997; Shukla *et al.*, 1999; Uritani, 1999; Peterson *et al.*, 2003; Carpinella, Ferrayoli and Palacios, 2005; Soad A.L. Bayoumi *et al.*, 2008; Ba *et al.*, 2017)
Insecticide characteristics	*Protium javanicum Burm.*	(Olson and Roseland, 1991; Peterson *et al.*, 2003; Adfa *et al.*, 2010)
Chelator of iron	*Arabidopsis*	(Lan *et al.*, 2011; Rodriguez-Celma *et al.*, 2013; Fourcroy *et al.*, 2014, 2016; Schmid *et al.*, 2014)
Antiviral properties	*Tobacco*	(Kim *et al.*, 2000)
Antioxidant properties	*Sinomonium acutum*	(Shaw *et al.*, 2003)
Alleviating abiotic stress	*Dasycladus vermicularis*	(Perez-Rodriguez *et al.*, 2001)
Beneficial biotic interactions	*Arabidopsis*	(Stringlis *et al.*, 2018)
Beneficial effects on human health as an inflammation reducer, antivirulence and compound with anti-tumour characteristics etc.	*Humans*	(Ojewole and Adesina, 1983; Wulff *et al.*, 1998; Xia *et al.*, 2007; Ding *et al.*, 2008; Pan *et al.*, 2009; Gnonlonfin, Sanni and Brimer, 2012; Jinpei Zhou *et al.*, 2012; W. Liu *et al.*, 2012; Mogana, Teng-Jin and Wiart, 2013; Lee *et al.*, 2014; Li *et al.*, 2015; Basu *et al.*, 2016)

Table 4: Molecular effects described by scopoletin

Effect	Used plant species	References
Inhibition of the oxidation of indoleacetic acid	Potato spp., tobacco, Sweet potato	(Andreae, 1952; Waywood, Oaks and Maclachlan, 1956; Sequeira, 1964; Schaeffer, Buta and Sharpe, 1967; Imbert and Wilson, 1970; Sirois and Miller, 1972)
Interfering with IAA metabolism	Tobacco, Arabidopsis	(Skoog and Montaldi, 1961; Graña *et al.*, 2017)
IAA induced scopoletin biosynthesis	Tobacco	(Skoog and Montaldi, 1961; Dieterman *et al.*, 1964)
Jasmonate induces scopoletin biosynthesis	Tobacco	(Sharan *et al.*, 1998)
Ethylene induces scopoletin biosynthesis	Tobacco	(Reuveni and Cohen, 1978)

Umbelliferone

Historical background and origin

Umbelliferone's name is derived from the *Umbelliferae* (*Apiaceae*) family of plants, whose names refer to their umbrella-shaped inflorescences, each called an umbel (Burtt, 1997). The Umbelliferae family contains numerous economically important herbs and vegetables such as sanicle, alexanders, angelica, asafoetida, celery, carrot, cumin, fennel, coriander and parsley (Mazimba, 2017). Umbelliferone (7-hydroxycoumarin) is a coumarin, benzopyrone from nature, that is found in all higher plants (Vialart *et al.*, 2012). It is a pivotal intermediate in the synthesis of more complex derivatives, such as poly-hydroxylated-, methoxylated- and prenylated-coumarins, furanocoumarins and pyranocoumarins (Bourgaud *et al.*, 2006). Previous studies demonstrate that umbelliferone is widely used in Chinese herbal medicine (X. Bai *et al.*, 2012). Umbelliferone contains antioxidant properties and is, as such, often used as a sunscreen agent or optical brightener in textiles (Hoult and Payá, 1996; Leal *et al.*, 2000; Mazimba, 2017). Mutants in umbelliferone biosynthesis illustrate that its main role is in UV-protection based on the dramatic phenotype of those mutants exposed to high UV growth conditions and the strong upregulation of the gene p-coumaroyl-CoA 2'-hydroxylase upon UV treatment (Vialart *et al.*, 2012). Remarkably, 5 times more umbelliferone is observed to be present in shoots than in leaves (Zobel and Brown, 1989). Umbelliferone is an important coumarin distributed in many but not all plants, e.g. radish does not contain umbelliferone (Silva *et al.*, 2014; Deng and Lu, 2017; Mazimba, 2017; Hijazin *et al.*, 2019). Umbelliferone is often found in the root zone soils of plants (Guo *et al.*, 2015), linking its role to plant-plant interactions, allelopathy and its job as phytoalexin. In table 5 we give a full overview of the different phenotypes described of seedlings treated with umbelliferone and in table 6 we give an overview of what is known about the molecular interactions upon umbelliferone treatment.

Roles in growth and development

Often when looking for literature about umbelliferone you are guided to papers illustrating the effects of 4-methylumbelliferone (4-MU), which already was found to stimulate IAA oxidase in 1953 (Andreae and Andreae, 1953). It has been claimed, based on the similar root response of Avena seedlings treated with 4-MU or UM that also UM inhibits IAA oxidase or at least affects auxin homeostasis (Goodwin and Taves, 1950; Pollock, Goodwin and Greene, 1954), a claim that got some additional support some 20 years later (Vázquez, 1973; Jankay and Muller, 1976). Recently, also the effects on influencing auxin homeostasis of 4-MU got some additional support in which they suggested that auxin redistribution (by observing increased expression of two auxin efflux facilitator genes *PIN2* and *PIN3*) rather than its biosynthesis was responsible for root branching formation after 4-methylumbelliferone exposure (Li and Gao, 2011; Li *et al.*, 2011).

In general, however, umbelliferone (UM) was observed to have minor or no effects on plant growth, the effect on maize, pea and sweet pumpkin roots is not significant, no effect on hypocotyl elongation of sweet pumpkin was observed and also the germination of radish and lettuce is not influenced by UM treatment (Pollock, Goodwin and Greene, 1954; Bernhard, 1959; Berrie *et al.*, 1968; Kupidlowska, Kowalec, *et al.*, 1994; Podbielkowska *et al.*, 1994; Alexieva *et al.*, 1995; Hossain *et al.*, 2008). We assume based on those

observations illustrating minor or no effects on plant growth of UM that many data about umbelliferone are never published. Besides its role as UV protections, UM is often reported as phytoalexin based on its high effectivity in reducing biofilms (Lee *et al.*, 2014), therefor UM is often used to coat medical equipment (Cai *et al.*, 2016; Slobodníková *et al.*, 2016), what even led to a patent application (US8916227B2). UM also is reported numerous times as being involved in plant-plant interactions and allelopathy (Table 5). The latter revealed certain roles of UM in plant growth.

Only one paper illustrated enhancing effects of UM on root growth (Goodwin and Taves, 1950), while others only reported inhibition of main root length (Table 5). Its effects seem to be strongest in grasses (Guo *et al.*, 2015). Interestingly, just as for coumarin treatment with umbelliferone was found to decrease the elongation rate and initiates a swelling response in cucumber roots, an effect that was linked to increased peroxidase activity (Jankay and Muller, 1976). However, later the swelling of cucumber roots could not be observed anymore (Kupidlowska, Kowalec, *et al.*, 1994).

Table 5: Phenotypes described by umbelliferone

Effect	Used plant species	References
Activating germination of seeds of plant parasite	*Striga astatic*	(Worsham, A. D.Klingman and Moreland, 1962)
Stimulating ROS activity	Lettuce	(Pan *et al.*, 2015)
Inhibiting ROS activity		(Kato and Shimizu, 1985)
Stimulating main root growth	*Avena sativa*	(Goodwin and Taves, 1950)
Inhibiting root hair formation	*Pharbitis nil*	(Yaoya *et al.*, 2004)
Inhibiting main root growth	*Lactuca sativa,* cucumber*, Stellera* chamaejasme *L, A. retroflexus, lettuce, Festuca rubra, Medicago sativa,* Pea, Sorghum	(Jankay and Muller, 1976; Kupidlowska, Kowalec, *et al.*, 1994; Einhellig, 1996; Cutler *et al.*, 2003; Yaoya *et al.*, 2004; Morikawa *et al.*, 2011; Guo *et al.*, 2015; Pan *et al.*, 2015, 2017)
Inducing adventitious root formation	*Phaseolus vulgaris L.*	(Vázquez, 1973, 1974)
Inhibiting root meristem division	*Allium sativum*	(Keightley *et al.*, 1996)
Stimulating hypertrophic swelling of roots	Cucumber	(Jankay and Muller, 1976)
Inhibiting stem elongation (including hypocotyl and epicotyl segments)	*Lactuca sativa, Stellera chamaejasme L, A. retroflexus,* lettuce*, Medicago sativa, Zea mays, Glycine max, Abutilon theophrasti, Amaranthus retroflexus, Panicum miliaceum,* Sorghum	(Shettel and Balke, 1983; Einhellig, 1996; Guo *et al.*, 2015; Pan *et al.*, 2015, 2017)

Inhibiting coleoptiles elongation	*Avena sativa*	(Shettel and Balke, 1983)
Influencing respiration	Lettuce, Spinach	(Moreland and Novitzky, 1987; Pan *et al.*, 2015)
Alleviates abiotic stress	*Chamomilla recutita (L.)*	(Repčák, Imrich and Franeková, 2001)
Alleviates biotic stress	*Chamomilla recutita (L.)*	(Repčák, Imrich and Franeková, 2001)
Plant-plant interactions and allelopathy	*Stellera chamaejasme, Festuca rubra, Medicago sativa, Avena sativa, Ipomoea batatas (L.), Artemia salina,* Lettuce	(Whittaker and Feeny, 1971; Shettel and Balke, 1983; Djordjevic *et al.*, 1987; Einhellig, 1996; Ojala *et al.*, 1999; Smith *et al.*, 2001; Morikawa *et al.*, 2011; Razavi, 2011; Guo *et al.*, 2015)
Insecticidal activity		(Cottee, Bernays and Mordue, 1988; X. Bai *et al.*, 2012)
Trematoda killing activity		(Sunita, Kumar and Singh, 2014)
Phytoalexin characteristics	*Petroselinum crispum, Ruta graveolens,* Sweet potato, Grapefruit, Parsley	(Minamikawa, Akazawa and Uritani, 1962; Jurd, King and Mihara, 1971; Hamerski, Schmitt and Matern, 1990; Afek *et al.*, 1999; Ojala *et al.*, 2000; Al-Barwani and Eltayeb, 2004; Kováčik *et al.*, 2009; Farshori *et al.*, 2011; X. Bai *et al.*, 2012; Lee *et al.*, 2014; Yang *et al.*, 2017; Pan *et al.*, 2017)

Table 6: Molecular effects described by umbelliferone

Effect	**Used plant species**	**References**
Interferes with auxin homeostasis	*Phaseolus vulgaris L.*	(Vázquez, 1973)
Stimulation of auxin oxidation	Cucumber	(Jankay and Muller, 1976)
Interference with methyl jasmonate	*Pharbitis nil*	(Yaoya *et al.*, 2004)
Interference with SA homeostasis	*Matricaria chamomilla,* Sorghum	(Einhellig, 1996; Pastírová, Repčák and Eliašová, 2004)

Chapter 2 – Hypocotyl elongation of *Arabidopsis thaliana:* a brief insight into the most important players during hypocotyl cell elongation

Important players during (hypocotyl) cell elongation in *Arabidopsis thaliana*: from hormones to light.

Stephen Depuydt[1,2,3], Stan Van Praet[1,2,3], Hilde Nelissen[2,3], Bartel Vanholme[2,3] and Danny Vereecke[4].

1. Ghent University Global Campus, Songdomunhwa-Ro 119, Yeonsu-Gu, Incheon, 406-840 South Korea.
2. Department of Plant Biotechnology and Bioinformatics, Ghent University, Technologiepark 927, 9052 Ghent, Belgium.
3. Department of Plant Systems Biology, VIB, Technologiepark 927, 9052 Ghent, Belgium.
4. Department of Applied Biosciences, Ghent University, Valentin Vaerwyckweg 1, 9000 Ghent, Belgium.

Author contribution:

The main part of this chapter is based on the publication of Depuydt *et al.* (2016). S.D and S.V.P wrote the chapter, H.N. helped with the artwork, S.D., H.N., D.V and B.V. critically reviewed the manuscript. Here, it was updated, some clarifications regarding hormone signalling, the hypocotyl as a model system and light reception were added by S.V.P.

Introduction

The development and growth of plant organs requires orchestration between two seemingly separate phases: cell proliferation and cell expansion. These two phases are followed by cell maturation, which is mainly achieved by the stiffening of the plant cell wall (Sachs, 1882). The first phase of cell proliferation drives primordium growth, whereas the second phase of organ growth relies mainly on post-mitotic cell expansion of the differentiating cells via either endoreduplication and/or vacuolization (den Boer and Murray, 2000). Note that in plants the term 'cell expansion' refers merely to cell size increase, as the process is not necessarily accompanied by an increase in cytoplasmic content. It is also still unclear whether cell expansion or cell division initiates organ formation in plants (Sampathkumar *et al.*, 2014; Eng and Sampathkumar, 2018; Pałubicki, Kokosza and Burian, 2019).

The classical model of Heyn (1940) states that cell expansion occurs once a critical internal pressure, i.e. turgor pressure, is reached. A plant hormone, auxin, would subsequently mediate the extension of the plant cell wall. Although this turgor-driven cell expansion theory has been challenged, e.g. by Wei and Lintilhac, (2003, 2007) who claim that the cell wall would lose stability, rather than being rearranged by a signalling cascade, these two hypotheses do not differ in terms of the fundamental mechanism responsible for cell elongation: the cell wall needs to be altered in order for a plant cell to expand (Kutschera and Niklas, 2013). Indeed, plant cells are unique in the sense that they have fairly rigid cell walls that constitute their outermost layer and provide a protective physical barrier against biotic and abiotic stresses. The (cumulative) strength of the cell walls of individual cells provides plants with a structural alternative for a skeleton. As such, plants can deal with gravity forces that can be considerable, for example in giant trees, or with osmotic pressure within the cells. Additionally, this enables them to penetrate compact soil or withstand stormy weather (Burton, Gidley and Fincher, 2010). Nevertheless, the function of the plant cell walls ranges far beyond a structural role. The plant cell wall is also involved in signal transduction, for instance to switch on the defence machinery following pathogen attack (reviewed in Bellincampi, Cervone and Lionetti, 2014), in cell-to-cell adhesion (e.g. Knox, 1992), and in primary defence against pathogenic microorganisms (Metraux and Lionetti, 2014). Next to that, it is postulated that plant cell walls represent a significant source of metabolizable energy, required during the germination of many crops seeds, such as rice, wheat, maize, and barley (Knox, 2008).

The basic building blocks for plant cell walls are polysaccharides, but the different functions of the plant cell walls are somewhat reflected in their structure and composition: in young and growing cells, the so-called primary cell wall consists mainly of cellulose microfibrils embedded in a matrix of pectin and hemicellulose (predominantly xyloglucans in dicots and non-graminaceous monocots) (Somerville, 2004) and forms a tough, but extensible, extracellular matrix. In contrast, the secondary cell wall of terminally differentiated cells that stopped growing often becomes impregnated with lignin to increase wall strength (Boerjan, Ralph and Baucher, 2003), which also helps to resist compressive stresses. Thus, cell walls are highly dynamic with great structural and compositional plasticity. At the same time, the plant cell wall plays a crucial role in directing plant growth and development, as it determines the shape and architecture of the plant body: post-mitotic cell expansion is controlled by the cell wall because it can either restrict or tolerate growth of the cell (and thus the tissue and/or organ) in one or more directions. As the local flexibility of the cell wall matrix controls cell expansion, one might

actually argue that plant morphogenesis is the result of differential organ growth at the level of the cell walls. During plant growth and development, the cell proliferation and cell expansion phases and, thus, the biosynthesis and differentiation of cell walls, need to be tightly regulated in a spatiotemporal way and highly coordinated between different cells of the same organ or tissue in order to preserve organ integrity. To achieve such complex coordination and, hence, to actually steer plant growth and development, different growth effectors have been recruited throughout plant evolution (reviewed in e.g. Depuydt and Hardtke, 2011; Ubeda-Tomás, Beemster and Bennett, 2012; Wang *et al.*, 2015). Plant hormones are major intrinsic growth regulators that can adjust plant growth depending on environmental and/or developmental cues. As such, it would seem logical that plant hormone action and cell wall expansion are directly linked. However, the major hormones that are involved in cell expansion (see below) show surprisingly little overlap in transcriptional targets with one important exception: the EXPANSINS (EXPs) and their homologs that mediate loosening of the plant cell wall (Cosgrove, 2000; Nemhauser, Hong and Chory, 2006). Besides hormone signalling, several other signalling pathways are also controlling elongation in planta, including light signalling and the circadian clock. Mounting evidence suggests that these pathways could be integrated by PHYTOCHROME INTERACTING FACTORS (PIFs), members of the basic-loop-helix family of transcriptional regulators that take a central position in photomorphogenic plant development. This chapter will focus on how hormones and downstream signalling affect plant cell elongation with a major focus on the hypocotyl. Moreover, the hormonal independent and concerted activities and the role of light signalling for hypocotyl elongation will be descried. The link with cell wall remodelling will be briefly touched upon, but the reader is referred to the comprehensive review by Lampugnani *et al.*, (2018) for more in-depth information on this matter.

The Process of Cell Elongation

Post-mitotic cell enlargement, which usually follows cell proliferation, is considered to be the most important contributor to the final size of plant cells. As mentioned, turgor pressure is crucial for cell expansion, as well as cell wall extensibility (Cosgrove, 2005; Wolf, Hématy and Höfte, 2012). Although the 'acid growth theory' (also referred to as 'auxin-induced acidification') was proposed over 40 years ago, until today it is still believed to be key for cell expansion (Heyn, 1931, 1940; Hager, 2003). In short, plasma membrane proton pumps, specifically activated by the plant hormone auxin, would lower the pH in the apoplast, and as a result of the action of EXPs, amongst others, the cell wall would loosen, allowing turgor-driven cell enlargement (Cosgrove, 2000; Hager, 2003). The specific working mechanisms of EXPs remain obscure as it was shown that they do not alter covalent linkages between cell wall polysaccharides but rather they loosen non-covalent bonds in acidic conditions, temporarily releasing the cross-link between hemicellulose and cellulose fibrils (Cosgrove, 2000). The auxin class of phytohormones (see below) is considered to be the major and crucial orchestrator of plant development that originated early in evolution as well (Cooke *et al.*, 2002; Sergeeva, Liaimer and Bergman, 2002) but currently, it is well-known that nearly all other classes of plant hormones including brassinosteroids, gibberellins, cytokinins, abscisic acid, salicylic acid, jasmonic acid and ethylene can alter EXP gene expression (Cho and Kende, 1997; Fleming, 1997; Downes and Crowell, 1998; Cho and Cosgrove, 2002; Sánchez-Rodríguez *et al.*, 2010; Sun *et al.*, 2010; Zhao *et al.*, 2012).

Several model systems have significantly contributed to the understanding of cell elongation, hormones, and wall extensibility. For instance, pollen tubes show highly polarized cell expansion (reviewed in Hepler, Rounds and Winship, 2013) and root hairs uniquely grow via cell expansion after rather complex stages of cell fate acquisition (reviewed in Mendrinna and Persson, 2015). However, here the two most important model systems will be described in which the link between phytohormones and cell elongation is relatively well-characterized: the hypocotyl and primary root growth in *Arabidopsis thaliana.* More information on the use of the hypocotyl as a model system is given in the next paragraph. Also the Arabidopsis primary root is also considered to be a good model system for the action of phytohormones on cell elongation as it shows distinct zones of cell proliferation, cell elongation, and differentiation (Dolan *et al.*, 1993; Bennett and Scheres, 2010).

The hypocotyl as a model system.

Hypocotyl means literally "below the cotyledons" and is, as such, the part of stem underneath the two cotyledons and above the root. The anatomy of the Arabidopsis hypocotyl is rather simple: it consists of concentric cell layers, as observed in a cross/transverse section (Boron and Vissenberg, 2014). The outer epidermal cell layer of hypocotyls grown in the light surrounds two layers of cortical cells, the outer and inner cortical cells also referred to as the protruding and burrowed cell layer (Fig. 1). On a transverse section, the organisation of the hypocotyl exist out of (from the outside to the inside) epidermis, cortex endodermis, pericycle, and stele (Derbyshire *et al.*, 2007). Longitudinally, there are approximately 20 to 25 epidermal cells in an Arabidopsis hypocotyl cell row (Fig. 1) (Gendreau *et al.*, 1997; Gudesblat *et al.*, 2012) and as its growth is mainly regulated via cell elongation (Gendreau *et al.*, 1997), the hypocotyl is perfectly suited as tool to investigate cell elongation (Boron and Vissenberg, 2014). Hypocotyl growth consists of three closely related processes: (1) cell

division in the apical meristematic regions during embryogenesis; (2) turgor-driven cell elongation along the stem during the growth-phase; and (3) cell maturation in the basal region of the organ in the maturation-phase (Kutschera and Niklas, 2013). Hypocotyl growth is strongly influenced by both external and internal cues known to regulate cell elongation. For example, the hypocotyl is known to possess negative shoot gravitropism meaning that the hypocotyl grows in the opposite direction of the gravity response (Vandenbussche, Verbelen and Van Der Straeten, 2005). The negative shoot gravitropism is the main driver of the growth direction in the dark, while in light conditions the hypocotyl illustrates strong phototropism and grows in the direction of the light source. The importance of light signals in regulating plant growth already drew the attention of Charles Darwin (Charles Darwin and Darwin, 1881). Besides light and gravity, also temperature and hormones are drivers of the hypocotyl elongation process. These hormones include but are not limited to: auxins, cytokinins, ethylene, gibberellins, and brassinosteroids.

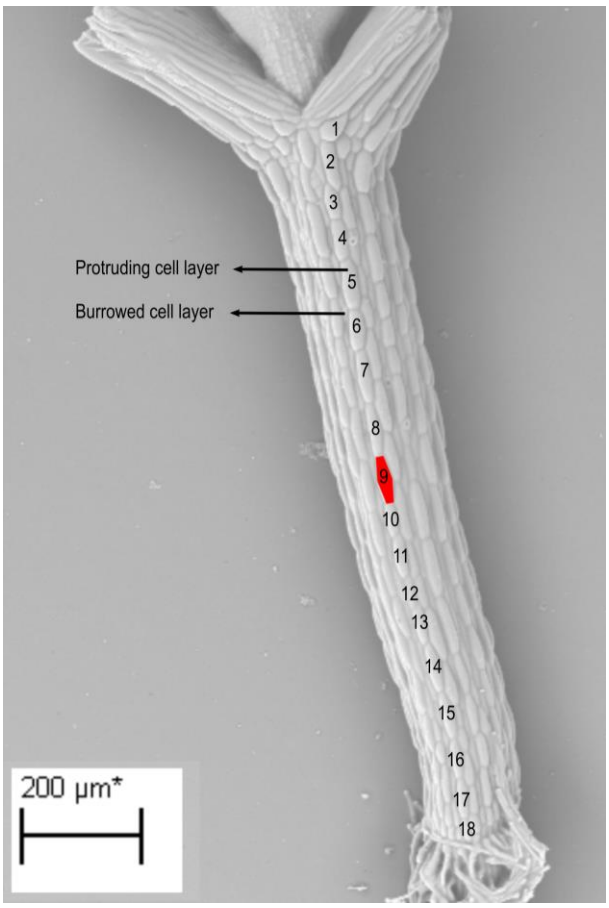

Figure 1: Scanning Electron Microscope picture of a 7-day old *Arabidopsis thaliana* hypocotyl.

Numbers indicate the different cells in 1 protruding cell layer. The red indicates 1 epidermal hypocotyl cell. The protruding and burrowed cell layer are shown via an arrow and name indication.

Different Hormones Have Been Implicated in Cell Elongation Processes

In the past years, the function, biosynthesis and signalling pathways of several classes of phytohormones became relatively well understood. Whereas auxins, cytokinins, gibberellins, and brassinosteroids take a central position in the context of plant growth and development, salicylic, jasmonic and abscisic acids act more as auxiliary signals in plant growth (although not exclusively (Tan *et al.*, 2020)) and are also involved in plant-biotic and plant-abiotic stresses (Derksen, Rampitsch and Daayf, 2013; N. Li *et al.*, 2019). Therefore, the latter three hormones will not be discussed in this chapter. It is difficult to pinpoint the action of a single hormone to specific effects on either cell proliferation or cell enlargement for three main reasons. Firstly, hormones have highly overlapping roles in plant development. Secondly, hormones interact with each other (a few examples are given below). Thirdly, whether hormones restrict or promote growth depends on the specific cell type, the concentration and the intensity of the signal. Although this adds to the complexity of studying hormone action *in planta,* it has been generally accepted for a long time that gibberellins, brassinosteroids and auxins promote cell elongation, while ethylene restricts cell enlargement. Cytokinins on the other hand, but auxins as well, are considered to regulate cell proliferation. More recently, the strigolactones, have been indirectly implicated in cell elongation as well, mainly via cross-talk with other hormonal pathways.

The Cell Elongation-Promoting Hormones: Brassinosteroids, Gibberellins, and Auxins

Brassinosteroids

Brassinosteroids (BRs) are a class of essential steroidal hormones with a wide spectrum of physiological effects on plants, including skotomorphogenesis, photomorphogenesis, cell elongation, flowering and even defence responses (Clouse and Sasse, 1998; Clouse, 2011; Singh and Savaldi-Goldstein, 2015; Zhang *et al.*, 2015). Brassinosteroids are relatively recently discovered in plants[3], unlike the other five "classical" plant hormones which were all discovered more than 60 years ago. It was, however, only in the mid-90s that brassinosteroids were generally accepted as authentic plant hormones. A number of BR-deficient and BR-insensitive mutants has been identified in Arabidopsis of which most of the mutants show a form of dwarfism. Mutants that are defective in the synthesis of BRs, such as *de-etiolated 2* (*det2*), *constitutive photomorphogenic dwarf* (*cpd*) and *cabbage* (*cbb1*), are constitutively photomorphogenic meaning that the hypocotyl is not etiolated and no apical hook is formed (Chory, Nagpal and Peto, 1991; Kauschmann *et al.*, 1996; Szekeres *et al.*, 1996). The exact biosynthesis pathway of brassinosteroids is still a matter of debate. In the classical pathway, four reactions lead to the formation of campesterol, which was general accepted as the starting point of BR biosynthesis. Campesterol is then converted via 10 steps involving, among others, the early mentioned genes *DET2, CPB* and *CBB1*, to brassinolide via a series of reductions, hydroxylations, epimerizations and oxidations (reviewed in Steven D. Clouse, 2011). However, more and more evidence is illustrating alternative routes towards brassinolide biosynthesis (Du *et al.*, 2017; Fujiyama *et al.*, 2019; Rozhon *et al.*, 2019). Classically, campesterol is converted by DET2 to campestanol (the precursor of DWARF4 (DWF4)), which was identified

[3] In 1979, 4 mg brassinolide was extracted out of 227 kg of rapeseed pollen and was as such the first discovery of brassinosteroids (Grove *et al.,* 1979).

as the rate-limiting step in BR biosynthesis. However, also campesterol itself can be the substrate for the DWF4 enzyme (Rozhon *et al.*, 2019), opening alternative entries in the BR biosynthesis pathway.

In contrast to the biosynthesis pathway, BR signalling is one of the best-characterized plant signalling pathways (reviewed in Singh and Savaldi-Goldstein, 2015). BRs are perceived by the surface receptor complex containing the leucine-rich repeat receptor-like kinase BRASSINOSTEROID INSENSITIVE 1 (BRI1) (Li and Chory, 1997) and co-receptors of the SOMATIC EMBRYOGENESIS RECEPTOR-LIKE KINASE (SERK) family (e.g. BRI1-ASSOCIATED RECEPTOR KINASE1 (BAK1), SOMATIC EMBRYOGENESIS RECEPTOR KINASE 1 (SERK1), and BAK1-LIKE KINASE 1 (BKK1)) (Fig. 2A) (Ma *et al.*, 2016; Hohmann *et al.*, 2018). Binding of the brassinosteroid ligand mediates hetero-dimerization of BRI1 and a SERK family member (e.g. BAK1) (Li *et al.*, 2002; Nam and Li, 2002), which in turn triggers extensive auto- and trans-phosphorylation of the intracellular BAK1 and BRI1 kinase domains (Fig. 2A) (Hohmann, Lau and Hothorn, 2017). BRI1 phosphorylates the inhibitory BRI1 kinase-bound protein BRI1 KINASE INHIBITOR1 (BKI1) on tyrosine residues to induce its dissociation and to allow the association of BRI1 with a second receptor kinase BAK1 (Jaillais *et al.*, 2011). BRI1 interacts with a downstream BR SIGNALING KINASE1 (BSK1) that binds and activates the protein phosphatase1 (PP1)-related protein BRI1 SUPPRESSOR1 (BSU1) (Mora-García *et al.*, 2004; Tang *et al.*, 2008; Kim *et al.*, 2009), which triggers BR-INSENSITIVE 2 (BIN2) dephosphorylation. Inactivation of BIN2, via its dephosphorylation, allows the accumulation of unphosphorylated transcription factors BRASSINAZOLE RESISTANT 1 (BZR1) and BRI1-EMS-SUPPRESSOR 1 (BES1) in the nucleus, which, in turn, regulates BR target genes (Fig. 2A) (Yin *et al.*, 2002; He *et al.*, 2005; Li and Deng, 2005). Interestingly, the latter seems to be a downstream target of strigolactone signalling too (Yuan Wang *et al.*, 2013). BZR1 forms a part of the trimeric module BZR1-ARF6-PIF that co-regulates cell elongation in the shoot via activating many genes with known functions in cell elongation (e.g. *EXPANSIN A8 (EXP8), BES1-INTERACTING MYC-LIKE1 (BIM1), BR-ENHANCED EXPRESSION 1/3 (BEE1/3), PACLOBUTRAZOL RESISTANCE (PREs), HISTONE ACETYLTRANSFERASE 2 (HAT2), ILI1 BINDING BHLH 1 (IBH1), LONG HYPOCOTYL IN FAR-RED (HFR1), PHY RAPIDLY REGULATED 1/2 (PAR1/2), EXORDIUM (EXO), SAUR19*) (Nemhauser, Mockler and Chory, 2004; Gallego-Bartolome *et al.*, 2012; M.-Y. Bai, Shang, *et al.*, 2012; Oh, Zhu and Wang, 2012; Oh *et al.*, 2014). One of the pathways that has been unravelled so far is the triple Helix-Loop-Helix/Basic Helix-Loop-Helix cascade downstream of BZR1 signalling that is known to induce cell elongation (Ikeda *et al.*, 2012; M.-Y. Bai, Fan, *et al.*, 2012; Oh *et al.*, 2014). In short, BZR1 activates the PRE-family basic helix-loop-helix (bHLH) factors that on their turn interact antagonistically with IBH1, the latter inhibits HOMOLOG OF BEE2 INTERACTING WITH IBH1 (HBI1), while HBI directly activates, by binding their promoters, *EXP1* and *EXP8,* and as such stimulates elongation (Fig. 2B) (L.-Y. Zhang *et al.*, 2009; Ikeda *et al.*, 2012; M.-Y. Bai, Fan, *et al.*, 2012; Oh *et al.*, 2014). Among the BR-induced transcription factors are cell-wall related genes strongly overrepresented, consistent with a growth-regulatory function of BR signalling (Sun *et al.*, 2010; Chaiwanon and Wang, 2015). In addition, the levels of enzymes involved in cellulose synthesis and in linking cellulose microfibrils were reduced in mutants impaired in brassinosteroid responses and/or signalling (reviewed in Sánchez-Rodríguez *et al.* (2010) and Singh and Savaldi-Goldstein (2015)). Moreover, in soybean hypocotyls, it has been demonstrated that adding brassinosteroids induces the activity of xyloglucan cleaving enzymes (Oh *et al.*, 1998), although the functional significance of this finding requires further research. Nevertheless, the general importance of

brassinosteroids in elongation processes is further illustrated by the clearly shorter hypocotyls observed in brassinosteroid biosynthesis and signalling mutants, such as *bri1*, *cpd, det2* and *dwf1* (Takahashi *et al.*, 1995; Clouse, 1996; Szekeres *et al.*, 1996; Li and Chory, 1997). Moreover, all those mutants illustrate a photomorphogenic growth in dark-grown conditions, with a small, non-etiolated hypocotyl and the absence of an apical hook is observed.

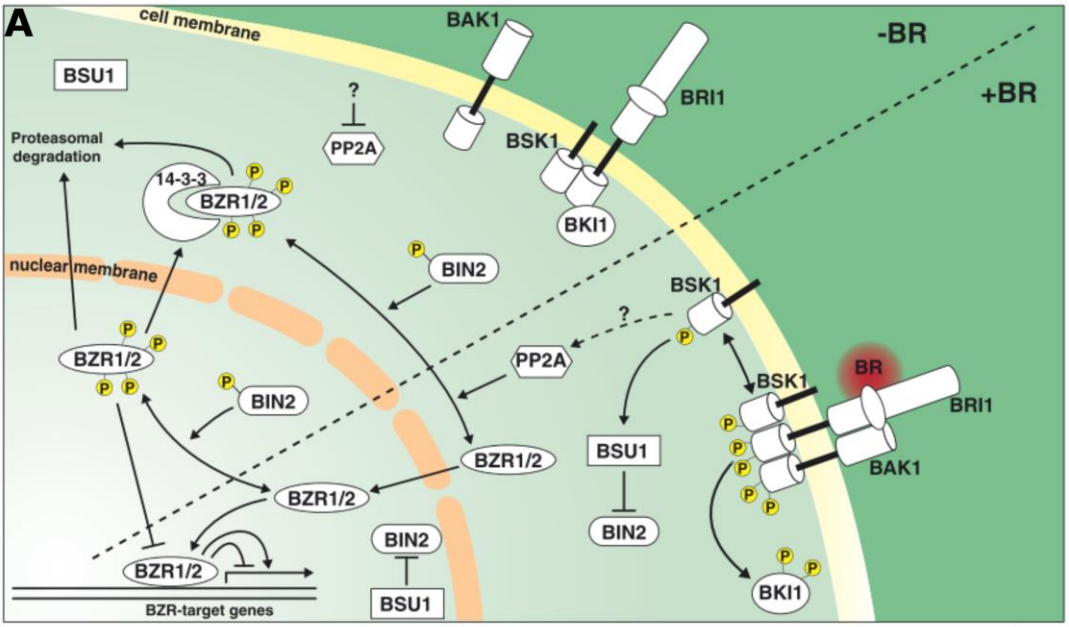

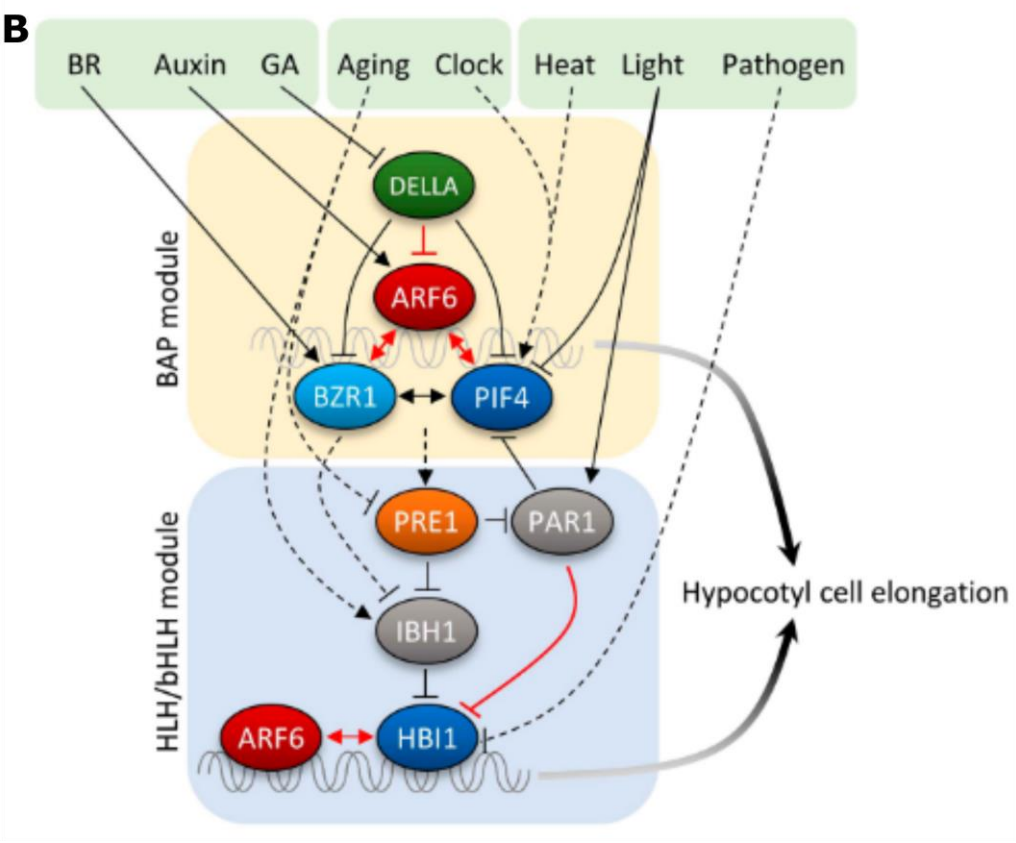

Figure 2: Brassinosteroid signalling

(A) BRs are perceived at the cell surface by direct binding to the extracellular domain BRI1. BRI1 heterodimers are formed and stabilized after BR binding, leading to activations of the intracellular BRI1 kinase. The inhibitory BRI1 kinase-bound protein BRI1 KINASE INHIBITOR1 (BKI1) is phosphorylated by BRI1 on its tyrosine residues to induce its dissociation and to allow the association of BRI1 with a second receptor kinase BRI1-ASSOCIATED RECEPTOR KINASE1 (BAK1). Autophosphorylation and sequential transphosphorylation between BRI1 and BAK1 fully activate the BRI1 kinase that triggers a downstream BR SIGNALING KINASE1 (BSK1). BSK1 binds to the protein phosphatase1 (PP1)-related protein BRI1 SUPPRESSOR1 (BSU1). BSU1 inactivates BIN2 by its dephosphorylation, in that way the BZR1 and BES1/BZR2 transcription factors are activated by dephosphorylation via a PP2A phosphatase. BIN2, in the absence of BR, phosphorylates BZR1 and BES1/BZR2 transcription factors leading to either their degradation or nuclear export and cytoplasmic retention. Dephosphorylated BZR1 and BZR2/BES1 translocate to the nucleus to regulate the expression of BR-responsive genes. (derived from Gudesblat and Russinova (2011))

(B) The diagram illustrates the triple Helix-Loop-Helix/Basic Helix-Loop-Helix cascade downstream of the tiple module BZR1-PIF4-ARF6, involved in BR signalling to induce cell elongation. Solid lines indicate protein-protein interaction or post-translational modification, and dashed lines indicate transcriptional regulation. Red lines indicate new discoveries made by Oh et al. (2014). The Brassinosteroid-Auxin-PIF (BAP) module combines BR, auxin, gibberellin and light responses and cooperatively regulate shared target genes and hypocotyl cell elongation. Downstream of the BAP module, the triple HLH/bHLH module, consisting of PRE1, IBH1/ PAR1 and HBI1/PIF, modulates BAP activities through HLH–bHLH interactions. The BAP transcription factors positively regulate *PRE1* in the HLH/bHLH module forming positive feedback loops. PRE1 inhibits IBH1, while the latter inhibits *HBI1* transcription. HBI1 is a positive regulator of cell elongation, and as such the BAP module can stimulate cell elongation. (derived from Oh *et al.* (2014))

Auxins

Because auxins are important regulators of the plant cell cycle (reviewed by del Pozo and Manzano, (2014)), many developmental processes in plants - from germination until senescence - depend on the general auxin status of the plant cells. Generally, auxin is known to stimulate cell elongation, and more specifically to induce hypocotyl elongation (Heyn, 1931, 1940; Hager, 2003; Cosgrove, 2005; Wolf, Hématy and Höfte, 2012). Auxin has a prominent role in the acid-growth hypothesis (see below) and there is ample evidence that auxin influences the expression and activity of crucial cell wall modifiers, such as expansins, pectin methylesterases, and polygalacturonases (Laskowski *et al.*, 2006; Kumpf *et al.*, 2013). Elegant experiments show that local application of auxin leads to demethylation of pectins at the shoot apical meristem, which causes tissue softening (Braybrook and Peaucelle, 2013). Notably, several links between auxin and secondary wall formation have also been reported, for instance in lignification processes and xyloglucan remodelling (Cecchetti *et al.*, 2013; Hentrich *et al.*, 2013; Velasquez *et al.*, 2019). Moreover, fully structured organ formation depends on the functioning of auxin transport regulation, supporting the presence of a mechano-chemical regulatory loop between auxin and organ outgrowth (Braybrook and Peaucelle, 2013; Kutschera and Niklas, 2013).

Auxin homeostasis is regulated by the coordination of biosynthesis, transport, conjugation, sequestration/storage and catabolism to optimize concentration-dependent growth responses and adaptive responses to temperature, water stress, herbivory, and pathogens (reviewed in Blakeslee, Spatola Rossi and Kriechbaumer, 2019).

Auxin biosynthesis

The major indole-3-acetic (IAA) biosynthesis pathway in Arabidopsis is named the indole-3-pyruvic acid (IPyA) route, which exists out of the conversion of tryptophan to indole-3-pyruvic acid via the gene *TRYPTOPHAN AMINOTRANSFERASE OF ARABIDOPSIS 1 (TAA1)*, followed by conversion via the YUCCA (YUC) proteins, to IAA (Mashiguchi *et al.*, 2011; Won *et al.*, 2011; Zhao, 2012; Dai *et al.*, 2013). Auxin catabolism is as much important as its biosynthesis, however, only in 2016 was the gene *DIOXYGENASE FOR AUXIN OXIDATION 1 (DAO1)* found as the primary IAA oxidase in seedlings, until then, the enzyme that catalyses oxidation of IAA to its primary catabolite 2-oxindole-3-acetic acid (oxIAA) remained uncharacterized (Stepanova and Alonso, 2016; Zhang *et al.*, 2016). 5-(4-chlorophenyl)-4H-1,2,4-triazole-3-thiol has been found to specifically blocks the activity of the YUCCA enzymes (and is therefore called yucassin) limiting IAA formation (Nishimura *et al.*, 2014). It has to be noted, however, that yucassin reduces the free IAA levels with only 20% in Arabidopsis seedlings as compared with the control, and that yucassin mainly limits the excess formation of auxin (Nishimura *et al.*, 2014). This makes it a handy tool to analyse the role of excess levels and *de novo* biosynthesis of auxin. Moreover, also a tryptophan-independent pathway contributes to the pool of IAA *in planta* (Woodward and Bartel, 2005; Chandler, 2009; Normanly, Slovin and Cohen, 2010). IAA molecules are mainly synthesized in the leaves and the shoot apical meristem (SAM) although root-borne auxin is important for development too. Indeed, higher-order *yucca* mutants (*yuc1/yuc4/yuc10/yuc11*), involved in tryptophan-dependent auxin biosynthesis, do not even develop a root meristem at all (Cheng, Dai and Zhao, 2006). Yucassin treatment has no effect on hypocotyl elongation and also lower order *yucca* mutants (*yuc4/yuc10)* develop a normal hypocotyl (Zhao, 2010; Mashiguchi *et al.*, 2011; Nishimura *et al.*, 2014). Interestingly, to the best of our knowledge, in standard light growth conditions (21 degrees Celsius, 16/8 hours light/dark), exogenous application of auxin (e.g. NAA, 2,4-D or IAA) cannot stimulate hypocotyl elongation (Hanson and Trewavas, 1982; Zhao, 2010; Barbez *et al.*, 2012), mutants (e.g *sur1/arlf1/hals3*) or plants (e.g. *p35S::YUC1*) that overproduce auxin have long hypocotyls (Boerjan *et al.*, 1995; Romano *et al.*, 1995; Delarue *et al.*, 1998; Zhao, Sioux K. Christensen, *et al.*, 2001; Zhao, 2010; Nishimura *et al.*, 2014; Adamowski and Friml, 2015; Velasquez *et al.*, 2016). Moreover, when added to isolated stem segments and coleoptiles, auxin is able to induce elongation, and when auxin signalling is reduced, in for example the *axr3* mutants or the transgenic *35S-iaaL* plants, in which free auxin levels are reduced by transferring auxin to its inactive conjugate, auxin can also stimulate elongation (Collett, Harberd and Leyser, 2000). Mark Estelle and his group, on the other hand, found longer hypocotyls in seedlings treated for 48 hours with 50 µM of IAA, though the seedlings were transferred to treatment when they were 5 days old (Chapman *et al.*, 2012), by that time the Polar Auxin Transport (PAT) system is fully established, which can explain this opposing result with other experiments where they use younger seedlings and when PAT is still developing (Blilou *et al.*, 2005; Petrášek and Friml, 2009).

Auxin signalling

Auxin signalling occurs in a 4-step process (reviewed in Leyser (2018) (Fig. 3). First, auxin will be perceived by the TRANSPORT INHIBITOR RESISTANT 1/AUXIN SIGNALING F-BOX (TIR1/AFB) family of F-box proteins. Together with the AUXIN BINDING PROTEIN1 (ABP1), they form the specific receptors of IAA (Jones, 1998; Dharmasiri, Dharmasiri and Estelle, 2005). The function of ABP1 as auxin receptor, however, is currently under high debate (Shi and Yang, 2011; Leyser, 2018; Gallei, Luschnig and Friml, 2020). Secondly, upon the perception of auxin by the TIR1/AFB F-box complex, AUX/IAA proteins, that in the absence of auxin heterodimerize with AUXIN RESPONSE FACTORS (ARFs) elements, will be degraded via the 26S proteasome (reviewed in Salehin, Bagchi and Estelle (2015)). Lastly, degradation of Aux/IAA proteins will lead to the liberation of AUXIN RESPONSE FACTORS (ARF) that then can bind AUXIN-RESPONSIVE ELEMENTS (AREs) in the promoter of primary auxin-responsive genes (Boer *et al.*, 2014). AREs have for instance been found in the promotors of cyclins, such as *CYCB; 1* and *CYCA; 2* (Hu, Xie and Chua, 2003; Roudier *et al.*, 2003). Various gain-of-function mutants in *AUX/IAA* genes in Arabidopsis have short hypocotyls as a consequence of cell elongation defects (Liscum and Reed, 2002; Mockaitis and Estelle, 2008), whereas ABP1 was shown to be involved in the auxin-induced enlargement of Arabidopsis hypocotyls as well (Steffens *et al.*, 2001).

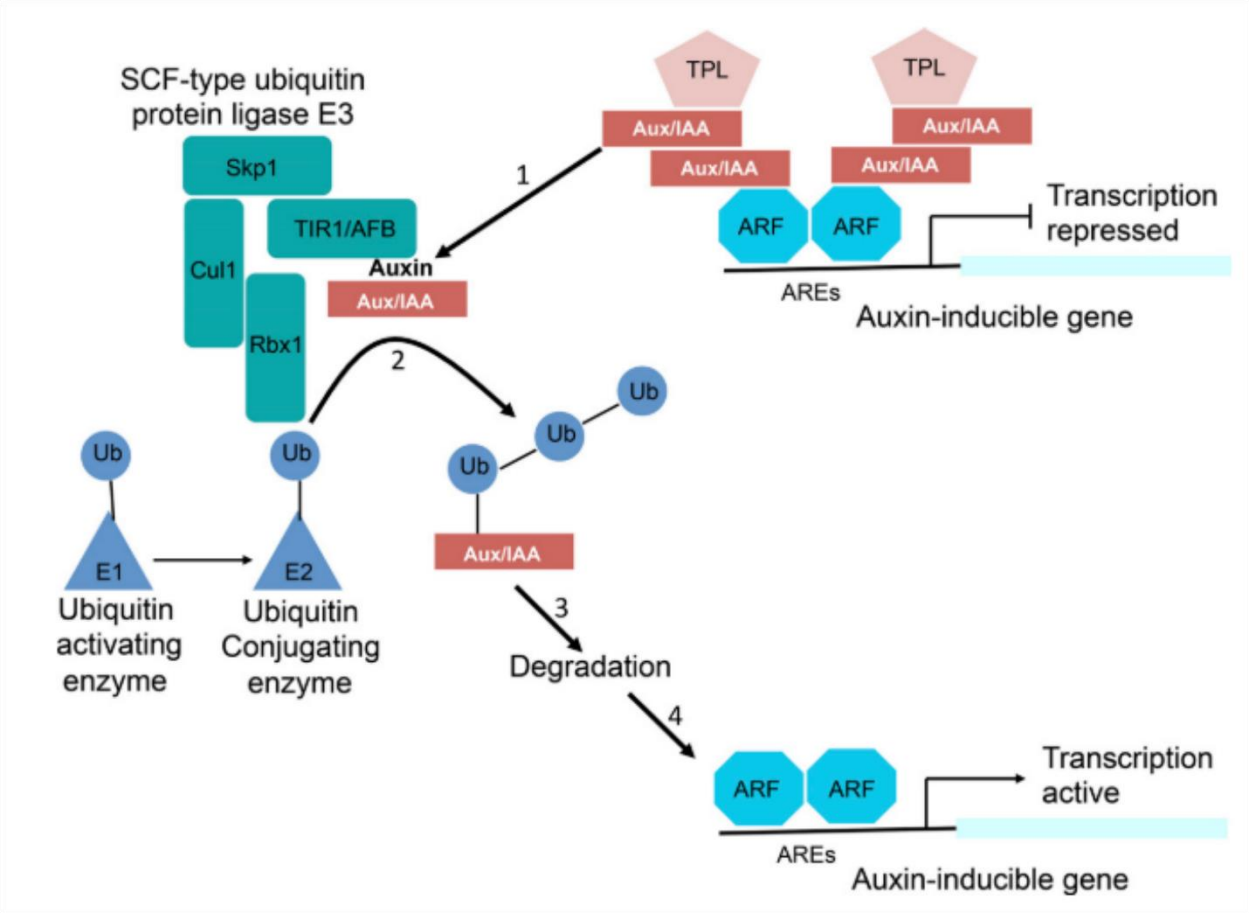

Figure 3: Auxin signalling

AREs are elements in the promoters of auxin-inducible genes. The AREs are bound by dimers of the ARFs that stimulate the transcription of auxin-inducible genes. However, gene expression is prevented by Aux/IAA proteins that interact with the ARFs and as such are transcriptional repressors. The steps in the auxin response pathway are indicated by the numbered arrows. 1, Auxin acts as a molecular glue bringing together Aux/IAAs and F-box proteins of the TIR1/AFB family. 2, These F-box proteins are part of an SCF-type E3 ubiquitin-protein ligase complex that transfers activated ubiquitin (Ub) from an E1/E2 enzyme system. 3, Polyubiquitination of the Aux/IAAs results in their degradation. 4, This releases repression at ARE-containing promoters what leads to active transcription of auxin response genes. (derived from Leyser (2018))

Auxin transport

Interestingly, although auxin plays a pivotal role to stimulate hypocotyl elongation in dark-grown seedlings (Fendrych, Leung and Friml, 2016), auxin transport, however, only seems to be crucially required for hypocotyl elongation in the light and is not needed in dark-grown Arabidopsis seedlings (Jensen, Hangarter and Estelle, 1998). Auxin is distributed in the plant by two transport systems: (1) a fast, non-directional stream in the phloem to deliver auxin from the sites of its synthesis (mostly in young leaves) to recipient organs and (2) a slow and directional cell-to-cell polar auxin transport (Adamowski and Friml, 2015). PAT distributes auxin in a precise manner that is critically important for the formation of local auxin maxima, mainly in developing tissues (Adamowski and Friml, 2015). Auxin can enter a cell via diffusion or by carrier-mediated uptake and leaves a cell through the action of efflux carriers (Kramer and Bennett, 2006; Barbosa, Hammes and Schwechheimer, 2018). Auxin import in cells is mediated by AUXIN-RESISTANT 1 (AUX1) and three LIKE AUXIN-RESISTANT (LAX 1, 2 and 3) carrier proteins and mutants therein show several auxin-related developmental defects (Parry *et al.*, 2001; Swarup, 2001; Péret *et al.*, 2012). The AUX/LAX family contains a well-conserved gene structure with the common role as auxin influx carrier. However, they mediate auxin-related developmental programmes in different organs and tissues. AUX1 regulates root gravitropism, root hair development and leaf phyllotaxy whereas LAX2 regulates vascular development in cotyledons (Péret *et al.*, 2012). Both AUX1 and LAX3 have been implicated in lateral root (LR) development as well as apical hook formation, with LAX3 being the major auxin influx carrier (Vandenbussche *et al.*, 2010). In the hypocotyl is AUX1 needed for basipetal auxin transport from the cotyledons to the hypocotyl, while LAX3, being localised in the basal part of the hypocotyl, is involved in the redistribution of auxin in the hypocotyl (Vandenbussche *et al.*, 2010; Zádníková *et al.*, 2010). Research towards the role of AUX/LAX auxin influx carriers during hypocotyl elongation is, however, seriously underrepresented.

Auxin efflux is mediated via the efflux carriers including the PIN family and a number of ABCB-type transporters (Geisler and Murphy, 2006; Lewis *et al.*, 2009). The PIN family is probably the most important and well-known family for the translocation of auxin, with eight discovered *PIN* genes in Arabidopsis: *PIN1* to *PIN8* (Křeček *et al.*, 2009; Christie and Murphy, 2013). *PIN1* to *PIN4* and *PIN7* are involved in directing auxin efflux at the plasma membrane, while *PIN5*, *PIN6* and *PIN8* are involved in intracellular auxin movement (Mravec *et al.*, 2009; Vanneste and Friml, 2009; Zádníková *et al.*, 2010; Ding *et al.*, 2011). Certain PIN proteins are

membrane-bound, expressed specifically in the basal or apical membrane of the cells, and in specific cell types of the root, and they are continuously recycled by endocytosis (Adamowski and Friml, 2015). For example in the hypocotyl, *PIN1* expression is restricted to the central cylinder, whereas *PIN3* and *PIN4* are expressed in the epidermis and cortex along the hypocotyl (Zádníková *et al.*, 2010). The PIN1 transporter is localized on the basal side of cells in the vascular tissue of the stem, emphasizing its importance in polar auxin transport from the shoot tip to the root tip, which is further confirmed by reduced PAT in *pin1* mutants (Galweiler *et al.*, 1998; Li *et al.*, 2005). While PIN1 is the main driver of PAT in the shoot, this role is directed to PIN2 in the root (Chen *et al.*, 1998; Luschnig *et al.*, 1998; Müller *et al.*, 1998). Altogether, this creates an effective and highly controlled auxin (re)distribution system that allows shoot-originated auxin to be (re)cycled in the root. The resulting typical graded auxin distribution pattern along the root's main trajectory provides positional information and steers cell fate. Single and higher-order mutants in the PIN proteins display severe growth defects, and modulation of PIN activity affects elongation rates and final cell sizes (Luschnig *et al.*, 1998; Friml and Palme, 2002; Friml *et al.*, 2002, 2003b; Benková *et al.*, 2003; Reinhardt *et al.*, 2003; Blilou *et al.*, 2005; Vieten *et al.*, 2005; Scarpella, 2006). Upon a directional stimulus of the shoot for example by light, auxin is redistributed by the PIN and ABCB proteins to the cells of the shaded side which leads to auxin accumulation, acidification and in the end cell elongation (Noh, Murphy and Spalding, 2001; Friml *et al.*, 2002; Rakusová *et al.*, 2011). The PIN1 transporter is strongly dependent on de-methyl-esterification of the pectin homogalacturonan. This de-methyl-esterification of pectin is sufficient to induce local tissue growth in the meristem.

Carrier-mediated transport of auxin can be regulated at three levels: by the regulation of (1) the abundance of a carrier (by determining its transcription, translation and degradation); (2) subcellular trafficking and targeting of auxin carriers to a specific position on the plasma membrane; and (3) transport activity (e.g. through the post-translational modification of carriers, the levels and activity of endogenous inhibitors, the regulation of the plasma membrane pH gradient, the composition of the plasma membrane and the interactions among individual transporters or transport systems). In general, auxin transport is mostly regulated on the proteome level (reviewed in Barbosa, Hammes and Schwechheimer (2018)).

Auxin and the 'acid-growth-theory'

As mentioned earlier, typically the elongation of the hypocotyl is referred to as the 'acid growth theory', as proposed over 45 years ago (Heyn 1931, 1940, Hager 2003). The process of elongation itself starts with the loosening of the cell wall, it induces a reduction in osmotic potential inside the cell due to the stress relaxation of the cell-wall. This causes water to rush into the cell, expanding the vacuole and stretching the entire cell due to the turgor pressure (Cosgrove, 2005; Wolf, Hématy and Höfte, 2012). From a biochemical point of view, the whole process starts with the auxin stimulated activation of proton hydrogen pumps embedded in the cell membrane. This results in a decrease in pH inside the cell-wall. This acidic environment activates, among others, EXPANSINS (EXPs) and XYLOGLUCAN ENDOTRANSGLUCOSYLASES/HYDROLASES which loosen the rigidity of the cell-wall and allows the cell to elongate (Cosgrove, 2014).

Until recently, it was unclear how auxin exactly regulated growth in the hypocotyl, as it was determined that auxin-induced growth operates in a timeframe of 15-20' after its stimulation (Kutschera, 1994; Fendrych,

Leung and Friml, 2016), which is considered to be too slow to be a direct effect (e.g. as in the case of stimulation through H^+-ATPase pumps via fusicoccin treatment that induces elongation in a few minutes (Fendrych, Leung and Friml, 2016)), but too fast to induce substantial protein formation. The SMALL AUXIN UP-RNA (SAUR) 19-24, as well as the SAUR63 subfamily, seem to be the missing link between auxin signalling and P-type H^+-ATPases activation (Franklin *et al.*, 2011; Chae *et al.*, 2012; Spartz *et al.*, 2012; Farquharson, 2014). *SAUR* genes, with 79 members in *Arabidopsis thaliana,* comprise the largest family of auxin-induced genes (Hagen and Guilfoyle, 2002). Auxin-induced expression of *SAUR* genes leads to activation of H^+-ATPases (AHAs) by promoting phosphorylation – via inhibition of type 2C protein phosphatases (PP2Cs) – of the penultimate threonine residue within the C-terminal autoinhibitory domain (Takahashi, Hayashi and Kinoshita, 2012; Spartz *et al.*, 2014). *Arabidopsis* contains 11 genes encoding PM H^+-ATPases: H(+)-ATPase 1 until 11 (*AHA1-11*) (Baxter *et al.*, 2005). *AHA1* and *AHA2* encode the two most highly expressed isoforms (Baxter *et al.*, 2005; Haruta *et al.*, 2010) but none of them seems to be transcriptionally induced by auxin. Therefore, the activation of the pumps would be affected rather than the production of them. *aha1* or *aha2* illustrate only modest phenotypes such as impaired root growth on alkaline pH, but the double mutant is embryo-lethal (Haruta *et al.*, 2010; Haruta and Sussman, 2012). Therefore, to clarify the functional relationship between auxin and H^+-ATPases directly *in planta*, often the dominant mutation for the *AHA1* locus, *open stomata 2 (ost2-2D)* is used: in that mutant the H^+-ATPases pump is constitutively active (Merlot *et al.*, 2007).

The SAUR proteins were not only the link between auxin and cell elongation but also between *PHYTOCHROME INTERACTING FACTOR 4 (PIF4)* and hypocotyl elongation. *SAUR19* overexpression alone is sufficient to restore hypocotyl elongation of *pif4* mutants at 28 °C (Franklin *et al.*, 2011). It is hypothesized that PIF4 stimulates auxin biosynthesis, promoting growth via SAUR19. Consistent with this idea, stem elongation during shade avoidance involves both PIF4- and *TAA1*-mediated auxin biosynthesis (Tao *et al.*, 2008).

Gibberellins

There are over 130 gibberellin metabolites in plants, but only a few are bioactive and their levels are tightly regulated (Yamaguchi, 2008; Shani *et al.*, 2013). Not only biosynthesis but also catabolism and metabolic deactivation will determine the pool of active gibberellins in the plant. Gibberellin can also inhibit its own biosynthesis via negative feedback mechanisms (Schomburg et al. 2003, reviewed in Hedden and Thomas 2012). Gibberellic acids are phytohormones that regulate a number of physiological responses in plants such as germination, greening and flowering time (Achard *et al.*, 2003, 2009; Alabadí *et al.*, 2008; Gallego-Bartolomé *et al.*, 2011), but primarily gibberellins promote cell growth: for instance, exogenous treatment promotes hypocotyl elongation (Derbyshire, McCann and Roberts, 2007). Moreover, gibberellin biosynthesis genes are associated with growing tissues in several plant systems and gibberellin inactivation leads to clear growth defects throughout the plant kingdom (Claeys, De Bodt and Inzé, 2013). GAs are even strictly required for hypocotyl elongation in dark-grown seedlings (Gendreau *et al.*, 1999).

In Arabidopsis, upregulation of gibberellin biosynthesis seems to affect both cell proliferation and cell expansion, dependent on the tissue/organ. In the proximal root meristem, gibberellins induce cell proliferation

(Achard *et al.*, 2007) and in leaves, for instance, both cell proliferation and cell expansion are stimulated by gibberellins (Gonzalez *et al.*, 2010). It has also been demonstrated that gibberellin-mediated cell expansion is required for adjacent cells to divide in the epidermis (Ubeda-Tomás *et al.*, 2009). In the hypocotyl, gibberellins clearly link to cell expansion. The latter happens via several mechanisms, including cell wall relaxation via induced expression of EXPs and XYLOGLUCAN ENDOTRANSGLUCOSYLASES/HYDROLASES (XETs) (Liu *et al.*, 2007), but also by controlling auxin biosynthesis and transport.

GA signalling is a de-repression model (Fig. 4): in the presence of GAs, the GA-INSENSITIVE-DWARF 1 (GID1) receptor (bound to a DELLA[4] protein) binds to GAs, which leads to the formation of an Skp–Cullin–F-box (SCF) complex with SLEEPY1 (SLY1) as the primary F-box protein (Daviere and Achard, 2013) and hence rapid degradation of the DELLA proteins via the 26S proteasome pathway (Fig. 4) (Peng *et al.*, 1997; Silverstone, Ciampaglio and Sun, 1998; Silverstone, 2001; Olszewski, Sun and Gubler, 2002). Arabidopsis has three gibberellin receptors that act redundantly because only double receptor mutants show dwarfisms (Suzuki *et al.*, 2009). In the absence of GAs, GA responses are repressed by proteins of the DELLA family. In Arabidopsis, there are five members of DELLA proteins: GA-INSENSITIVE (GAI), REPRESSOR-OF-GA1-3 (RGA), RGA-like 1 (RGL1), RGL2, and RGL3 (Claeys, De Bodt and Inzé, 2013).

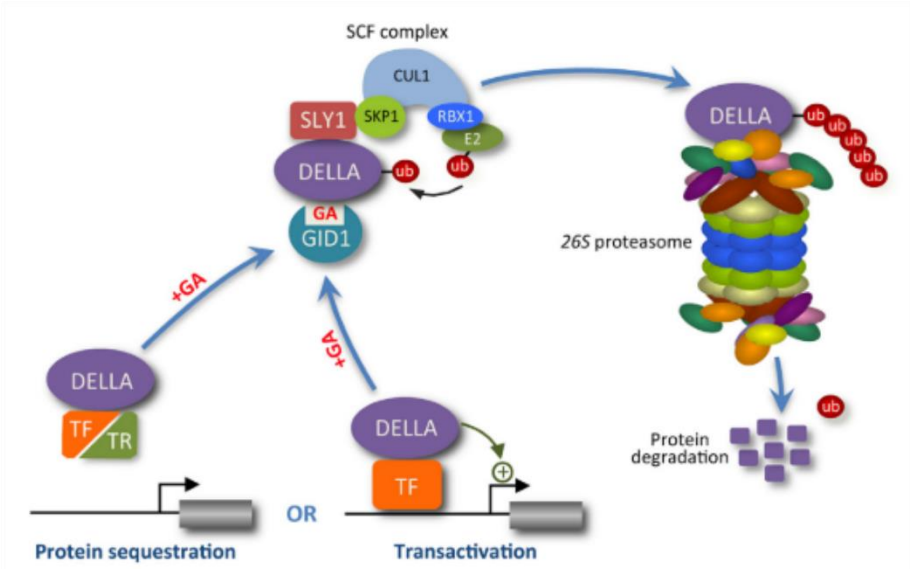

Figure 4: Gibberellin signalling

DELLAs repress GA responses by interacting with and inhibiting the activity of transcription factors (TF) or regulatory proteins (TR), or by activating the transcription of target genes associated with TF when GA concentrations are low. In the presence of GA or increasing concentrations of GA, GA binds to the GID1 receptor, stimulating the interaction of DELLA with the SCFSLY1 complex. Once recruited to SCF-SLY1

[4] DELLA proteins are characterized by the presence of a DELLA motif, excisting out ot the amino acids aspartate, glutamate, leucine, leucine and alanine, or in the single letter amino acid code: D-E-L-L-A.

complex, DELLAs are polyubiquitylated and then subsequently degraded through the 26S proteasome pathway, leading to the activation of GA responses. (derived from Davière and Achar (2016))

Gibberellin biosynthetic mutants (*ga1-3* and *ga3ox1/ga3ox2*) have shorter hypocotyls than wild-type plants (Ubeda-Tomás *et al.*, 2009) and *sly1-10* F-box receptor mutants are dwarfed as a result of inhibited gibberellin-induced cell growth (Dill, Jung and Sun, 2001; Strader *et al.*, 2004). Also gain-of-function mutants in the GID domain of the DELLA proteins – which make these proteins resistant to degradation by the 26S proteasome – illustrate a dwarfed phenotype and have, as such, shorter hypocotyls (Silverstone, Ciampaglio and Sun, 1998; Peng *et al.*, 1999; Dill, Jung and Sun, 2001). In the absence of GA's, the DELLA repressors accumulate in the nucleus and associate with diverse transcription factors or regulators (Zentella *et al.*, 2007; Davière, de Lucas and Prat, 2008), like the PIF-family ALCATRAZ (ALC) or the GRAS family member SCARECROW-LIKE 3 (SCL3) (De Lucas *et al.*, 2008; Feng *et al.*, 2008; Heo *et al.*, 2011; Zhang *et al.*, 2011). On the other hand, quadruple DELLA loss-of-function mutants show an exaggerated hypocotyl elongation (Alabadí *et al.*, 2004). The DELLA proteins are generally regarded as growth repressors since they are repressors of transcription factors that mediate gibberellin responses (Peng et al. 1997, Silverstone et al. 2001).

Moreover, DELLAs also form important points of cross-talk with other signalling cascades, including phytohormones, but also light signalling and circadian clock regulation. For instance, DELLAs interact with PIF3 and PIF4 that directly control cell expansion regulators (Achard *et al.*, 2007). This interaction can be inhibited by a negative regulator of jasmonic acid signalling which likely explains the negative effect of jasmonates on growth (Yang *et al.*, 2012). Also, gibberellins (via DELLAs) and phytochromes seem to share a common transcription module with brassinosteroids, in which DELLA degradation releases BZR1 inhibition (M.-Y. Bai, Shang, *et al.*, 2012). Furthermore, BZR1 also interacts with PIF4 and as such activates transcription of cell expansion genes (M.-Y. Bai, Shang, *et al.*, 2012). Auxin and ethylene also affect GA-mediated DELLA degradation (Achard *et al.*, 2003; Fu and Harberd, 2003). Next to that, DELLAs upregulate the CYCLIN DEPENDENT KINASE (CDK) inhibitors KIP-RELATED PROTEIN 2 (KRP2) and SIAMESE, thus affecting cell cycle progression (Achard *et al.*, 2009). Finally, DELLAs directly affect auxin transport via transcriptional and posttranslational control of PIN carriers. Auxin biosynthesis, on the other hand, can activate gibberellin biosynthesis too (Moubayidin *et al.*, 2010; Willige *et al.*, 2011).

Ethylene, the Growth-Inhibiting Hormone

Ethylene regulates many processes *in planta*, but its growth inhibitory role became clearly evident with the so-called triple-response: upon treatment of etiolated seedlings with ethylene, exaggerated apical hooks, stem swelling, and inhibition of hypocotyl elongation were observed (Guzmán and Ecker, 1990). In the dark, ethylene inhibits Arabidopsis hypocotyl elongation, whereas, contradictory, ethylene and its precursor 1-aminocyclopropane-1-carboxylate (ACC) increase hypocotyl elongation in light-grown Arabidopsis seedlings (Smalle *et al.*, 1997; Liang *et al.*, 2012). In root meristems, ethylene inhibits cell elongation (Tanimoto, Roberts and Dolan, 1995; Pitts, Cernac and Estelle, 1998; Růžička *et al.*, 2007). Indeed, mutants with increased levels of ethylene (e.g. *ctr1-1* and *eto1-2*) display shorter roots (Ortega-Martinez *et al.*, 2007; Thomann *et al.*, 2009). The ethylene signalling cascade is more complex than initially put forward and involves many regulatory circuits

(reviewed in Yang *et al.* (2015)). In short, five putative endoplasmic reticulum-bound receptors are involved: the His-Kinase two-component regulators ETHYLENE RESPONSE 1 (ETR1), ETR2, ETHYLENE RESPONSE SENSOR 1 (ERS1), ERS2, and ETHYLENE INSENSITIVE 4 (EIN4) (Fig. 5) (Hua *et al.*, 1995; Bleecker *et al.*, 1998; Hua and Meyerowitz, 1998; Sakai *et al.*, 1998). Upon binding with ethylene, CONSTITUTIVE TRIPLE RESPONSE 1 (CTR1), a serine/threonine-protein kinase that acts downstream of the ethylene receptors is inactivated (Kieber *et al.*, 1993; Zhong and Chang, 2018). In the absence of ethylene, CTR1 is active and represses downstream components, among which EIN2. Upon ethylene binding, EIN2 is derepressed which in turn allows transcriptional changes via EIN3, which will activate ETHYLENE RESPONSE FACTOR 1 (ERF1) and ETHYLENE INSENSITIVE3 LIKE (EIL) transcription factors. The *ein2* mutant is defective in all ethylene responses, demonstrating its critical importance in ethylene signalling (Fig. 5). Furthermore, in the absence of ethylene, specific F-box proteins trigger proteasome-mediated degradation of EIN2 and EIN3/EIL (Guo and Ecker, 2003; Gagne *et al.*, 2004; Konishi and Yanagisawa, 2008; Qiao *et al.*, 2009).

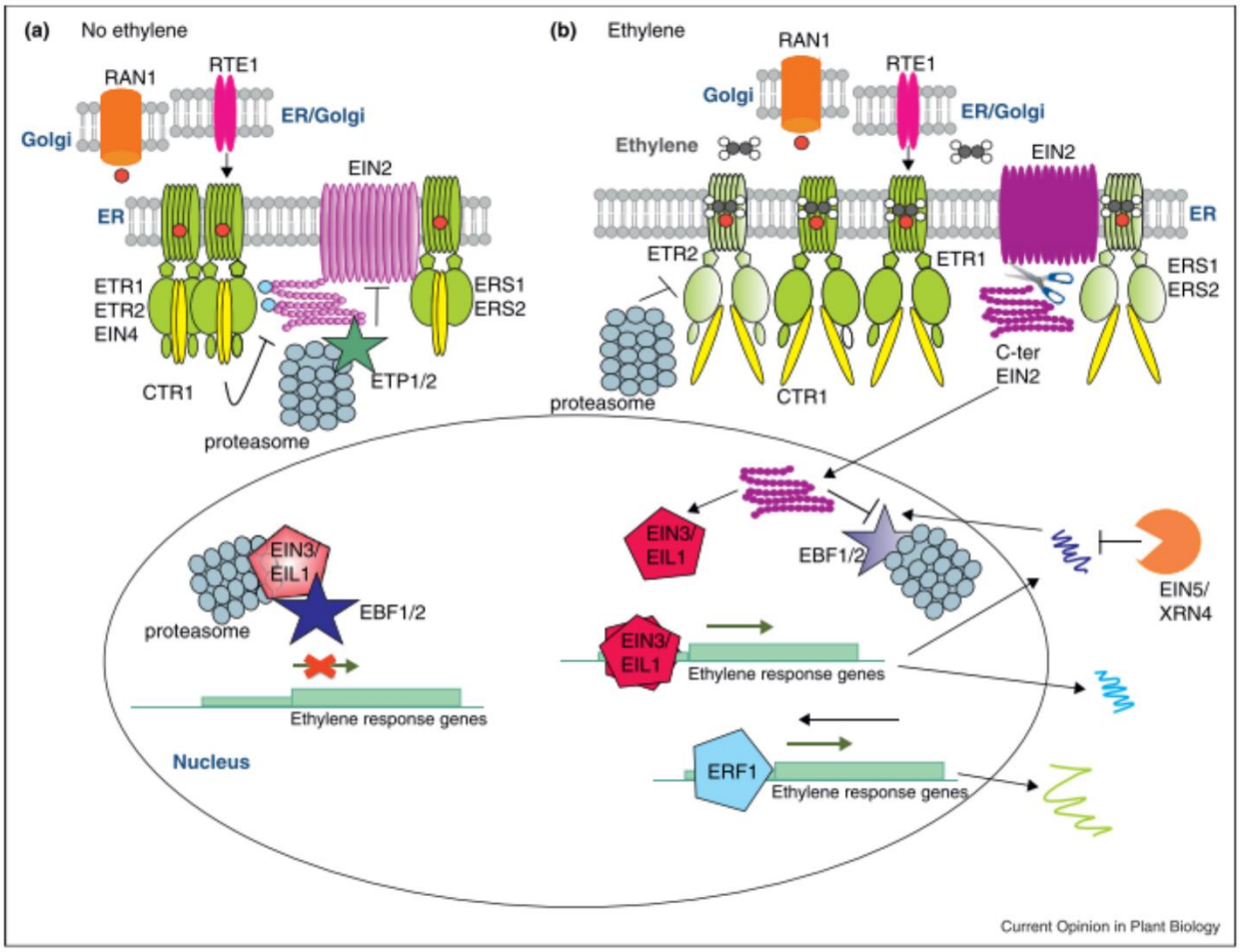

Figure 5: Ethylene signalling

The receptor proteins ETR1, ERS1, ETR2, ERS2 and EIN4 (represented in green) perceive ethylene. Copper (red circles) serves as a cofactor for ethylene binding and is delivered to the receptors by the copper transporter RAN1 (represented in orange). RTE1 (in pink) is associated with ETR1 and mediates the receptor signal output. The receptors are negative regulators of ethylene signalling. (a) In the absence of the hormone, the receptors

activate CTR1 (in yellow). CTR1, on its turn, inactivates EIN2 (in purple) by directly phosphorylating (blue circles) its C-terminal end. EIN2 can directly interact with the kinase domain of the receptors (represented as the larger ovals under the pentagons in the cytosolic domain of the receptors). The levels of EIN2 are negatively regulated by the F-box proteins ETP1 and ETP2 (green star) via the 26S proteasome (grey). In the nucleus, the transcription factors EIN3/EIL1 (in red) are being degraded by two other F-box proteins, EBF1/2 (blue star), through the proteasome. In the absence of EIN3/EIL1, transcription of the ethylene response genes is shut off. (b) In the presence of ethylene, the receptors bind the hormone and become inactivated, which in turn, switches off CTR1. This inactivation prevents the phosphorylation of the positive regulator EIN2. The C-terminal end of EIN2 is cleaved off by an unknown mechanism and moves to the nucleus where it stabilizes EIN3/EIL1 and induces degradation of EBF1/2. The transcription factors EIN3/EIL1 dimerize and activate the expression of ethylene target genes, Among the ethylene-responsive genes is the receptor gene ETR2 (green line), whose mRNA is upregulated by ethylene and is translated into the new batch of ethylene-free receptor molecules which then activate the negative regulator CTR1, thus providing the means of tuning down ethylene signalling in the absence of additional ethylene. Other regulatory nodes in the pathway are the exoribonuclease EIN5 (light orange), which controls the levels of EBF2 mRNA, and the F-box proteins ETP1 and ETP2 (green star) that are degraded in the presence of ethylene leading to the stabilization of EIN2. (derived from Merchante, Alonso and Stepanova, 2013))

Inhibition of cell expansion through ethylene takes place because of complex interactions with both auxin biosynthesis and auxin transport. Stepanova (2005) and Stepanova *et al.* (2007) demonstrated that auxin biosynthesis, as well as basipetal auxin transport, is stimulated by ethylene in root tips, setting the right conditions for inhibiting cell elongation via altering auxin disposibility (Luschnig *et al.*, 1998; Růžička *et al.*, 2007; Swarup *et al.*, 2007; Negi, Ivanchenko and Muday, 2008; Robles, Stepanova and Alonso, 2013). The increased auxin levels in their turn enhance ethylene synthesis, creating a positive feedback loop (Swarup *et al.*, 2007). Also, interactions and cross-talk between ethylene and gibberellins have been noted: for instance, DELLA double mutants are less responsive to ACC than the wild-type, and gibberellin can at least partly revert the ethylene mediated inhibition of root growth (Achard *et al.*, 2003). Likewise, it was shown that ethylene production in Arabidopsis seedlings can stimulate brassinosteroid production, highlighting an important cross-talk between ethylene and brassinosteroids (Woeste, Ye and Kieber, 1999).

Cytokinins and Strigolactones Indirectly Affect Elongation

Cytokinins

Classically, cytokinins have been described as controlling proliferation in the shoot and differentiation in the root by, among others, inducing *CYCD3;1* expression (Riou-Khamlichi, 1999; Ferreira and Kieber, 2005; Dello Ioio *et al.*, 2007, 2008). In short, there are three membrane-bound histidine kinase receptors: ARABIDOPSIS HISTIDINE KINASE 2 (AHK2), AHK3, and AHK4 (Hwang and Sheen, 2001; Inoue *et al.*, 2001), that after binding to cytokinin, induce a phosphorylation cascade involving ARABIDOPSIS HISTIDINE PHOSPHOTRANSFER PROTEINs (AHPs) that ultimately will phosphorylate ARABIDOPSIS RESPONSE REGULATORs (ARRs) in the nucleus. The so-called B-type ARRs are positive transcriptional regulators and

the A-type are repressors that likely act through cooperation with other transcription factors (To *et al.*, 2004; Argueso, Raines and Kieber, 2010). Specific members of these AHP and ARR protein families (e.g. ARR1, ARR12, and AHP6) represent important points of the interplay between cytokinins and auxins. It is that specific interplay that will ultimately determine root (meristem) size. In protoxylem development, for instance, high auxin levels upregulate cytokinin biosynthesis but at the same time, *AHP6* expression is upregulated, repressing cytokinin signalling (De Rybel *et al.*, 2014). For establishing the promotion of cell differentiation in the transition zone of the root meristem, cytokinin acts via dampening the PAT: ARR1 and ARR12 control an *AUX/IAA* gene, *SHORT HYPOCOTYL 2 (SHY2),* that inhibits PIN gene expression (Dello Ioio *et al.*, 2007, 2008) and in turn promotes differentiation and elongation of cells in the root meristem. At early stages of root meristem development, *ARR1* expression, in turn, is controlled by a specific DELLA factor, REPRESSOR OF GA1-3 (RGA), providing a clear link with gibberellin signalling (Moubayidin *et al.*, 2010). Also, brassinosteroid signalling, via BREVIX RADIX (BRX) is involved in this process: the BRX transcriptional coregulatory (Mouchel, 2004) is a target of the auxin response factor MONOPTEROS (MP) that can induce *PIN3* expression in complex feedback loops with cytokinin signalling via SHY2 (Scacchi *et al.*, 2010). Even more, cytokinins inhibit cell elongation also by interplaying with ethylene signalling via ETR1 and EIN2 (Růžička *et al.*, 2007; Kushwah, Jones and Laxmi, 2011).

Strigolactones

Strigolactones are the newest addition to the hormone classes *in planta*. Their hormonal actions were originally attributed to inhibitory effects on the outgrowth of axillary buds (Gomez-Roldan *et al.*, 2008; Umehara *et al.*, 2008), but nowadays multiple roles in plant growth and development have been described. At least two key components participate in the perception of strigolactones leading to ubiquitin-mediated protein degradation via an SCF mediated signalling pathway: MORE AXILLARY BRANCHES 2 (MAX2), an F-box protein, and DWARF 14 (D14), an α/β hydrolase, in Arabidopsis (Stirnberg, Furner and Ottoline Leyser, 2007; Hamiaux *et al.*, 2012). Among the downstream targets that have been described, there is BRANCHED 1/TEOSINTE BRANCHED1 LIKE1 (BRC1) (Braun *et al.*, 2012) and, interestingly, BES1, the positive regulator of the brassinosteroid signalling pathway (Yuan Wang *et al.*, 2013), pointing toward cross-talk with brassinosteroids. However, also direct effects of strigolactones on cell growth have been observed. In pea, for instance, it has been demonstrated that strigolactones affect stem elongation by stimulating cell division in the epidermal internode cells (de Saint Germain *et al.*, 2013). During germination and growth of rice, however, strigolactones were found to negatively regulate cell division in the mesocotyl in darkness (Hu *et al.*, 2010, 2014). Nonetheless, both reports clearly indicate that strigolactones did not interfere with cell elongation processes. Conversely, it was shown that strigolactones inhibit hypocotyl elongation in Arabidopsis (Tsuchiya *et al.*, 2010), which is dependent on several components of light signalling pathways, with the transcription factor LONG HYPOCOTYL 5 (HY5) as a possible integrator of the strigolactone and light signalling pathways (Tsuchiya *et al.*, 2010; Jia *et al.*, 2014). Lauressergues *et al.* (2015) showed a reduced shoot elongation in strigolactone-deficient *Medicago truncatula* mutants and demonstrated that this was not caused by reduced resource allocation as in strigolactone-related dwarf mutants from other species (Zou *et al.*, 2006; Kohlen *et al.*, 2012; Kretzschmar *et al.*, 2012). In root systems, strigolactones regulate lateral root development (Kapulnik, Delaux, *et al.*, 2011; Ruyter-Spira *et al.*, 2011) and they increase cell numbers in the primary root meristem and transition zones

probably through inhibitory effects on auxin efflux carriers (Ruyter-Spira *et al.*, 2011; Koren *et al.*, 2013). Strigolactones may indeed dampen auxin transport, as demonstrated by PIN1 depletion from the membrane in Arabidopsis stems (Shinohara, Taylor and Leyser, 2013; van Rongen *et al.*, 2019). In root meristems, however, although PIN1 was reported to be less abundant after long-term treatment with synthetic strigolactones (Ruyter-Spira *et al.*, 2011), there is no direct evidence of this so far (Shinohara, Taylor and Leyser, 2013). Nonetheless, PIN localization and polarization seem to be affected by strigolactone treatment or altered transport (Pandya-Kumar *et al.*, 2014; Sasse *et al.*, 2015). Furthermore, auxin can enhance strigolactone biosynthesis (Hayward *et al.*, 2009) and strigolactones, in turn, can inhibit auxin biosynthesis (Sang *et al.*, 2014). It was also recorded that strigolactones have a positive effect on root hair growth, which is, after cell fate acquisition, solely dependent on cell elongation. This effect, however, requires ethylene synthesis, and root hair elongation by strigolactones and ethylene seems to be relying on a common regulatory pathway, with ethylene being epistatic (Kapulnik, Resnick, *et al.*, 2011). Furthermore, auxin signalling contributed to the strigolactone mediated root hair response but was not absolutely required (Kapulnik, Resnick, *et al.*, 2011). The crosstalk between strigolactones and auxin seems to be key for every developmental aspect regulated by this new class of hormones, and future research will undoubtedly yield interesting points of convergence and divergence with other hormonal pathways (Bennett *et al.*, 2016; Matthys *et al.*, 2016). In terms of mechanisms of strigolactone-mediated cell expansion, more research is also required, but an interesting link has been uncovered between EXP genes and karrikinolide, a compound in smoke that structurally resembles strigolactones and even relies in part on the strigolactone signalling pathway (Jain, Ascough and Van Staden, 2008; Scaffidi *et al.*, 2014).

Cross-talk in Elongation: Influencing Biosynthesis, Transport, and Signal Transduction

An overview of the main players in the hormonal cross-talk for elongating cells in the hypocotyl and the proximal root meristem is presented (Fig. 6). Cross-talk *sensu stricto* occurs when two pathways are not independent. It can be positive (synergistic or additive) and it can be negative. One important thing to note is that all hormonal interactions are context-specific and tissue-dependent, which greatly adds to the complexity of understanding hormonal networks and their actions. Figure 6 shows clearly that there are numerous points of cross-talk, sometimes involving more than three hormones, again adding to the complexity of studying these interactions. It is also clear that the levels and/or signalling pathways of one hormone affect biosynthesis (or rather homeostasis) of other hormones, which in turn leads to altered signalling events that then again have repercussions on cell responses. Additionally, apart from influencing biosynthesis of other hormones, cross-talk can also affect transport, with the polar auxin transport machinery playing a very crucial role in this. Next to that, one hormone clearly influences signalling components of other hormones. Since the signalling machinery for the different classes of hormones shows great similarities, this is very plausible. For instance, auxin, strigolactones, ethylene, gibberellins and jasmonic acids all rely on the ubiquitin-dependent proteasome system for hormone perception, de-repression of hormone signalling pathways, degradation of hormone specific transcription factors, and/or regulation of hormone biosynthesis (Santner and Estelle, 2010). Furthermore, downstream targets of a specific hormone pathway can be important regulators and integrators of other hormonal processes too. In that respect, DELLAs, for instance, are involved in at least four hormonal pathways during hypocotyl growth, but also the most recently discovered class of phytohormones, the strigolactones, seem to share transcriptional regulators with other pathways. Altogether, this leads to the conclusion that the

action of a specific hormone on plant cell elongation cannot be isolated from other hormones, and that this, in fact, is one of the main mechanisms, partly explaining the pleiotropy of hormone-mediated processes *in planta* as well.

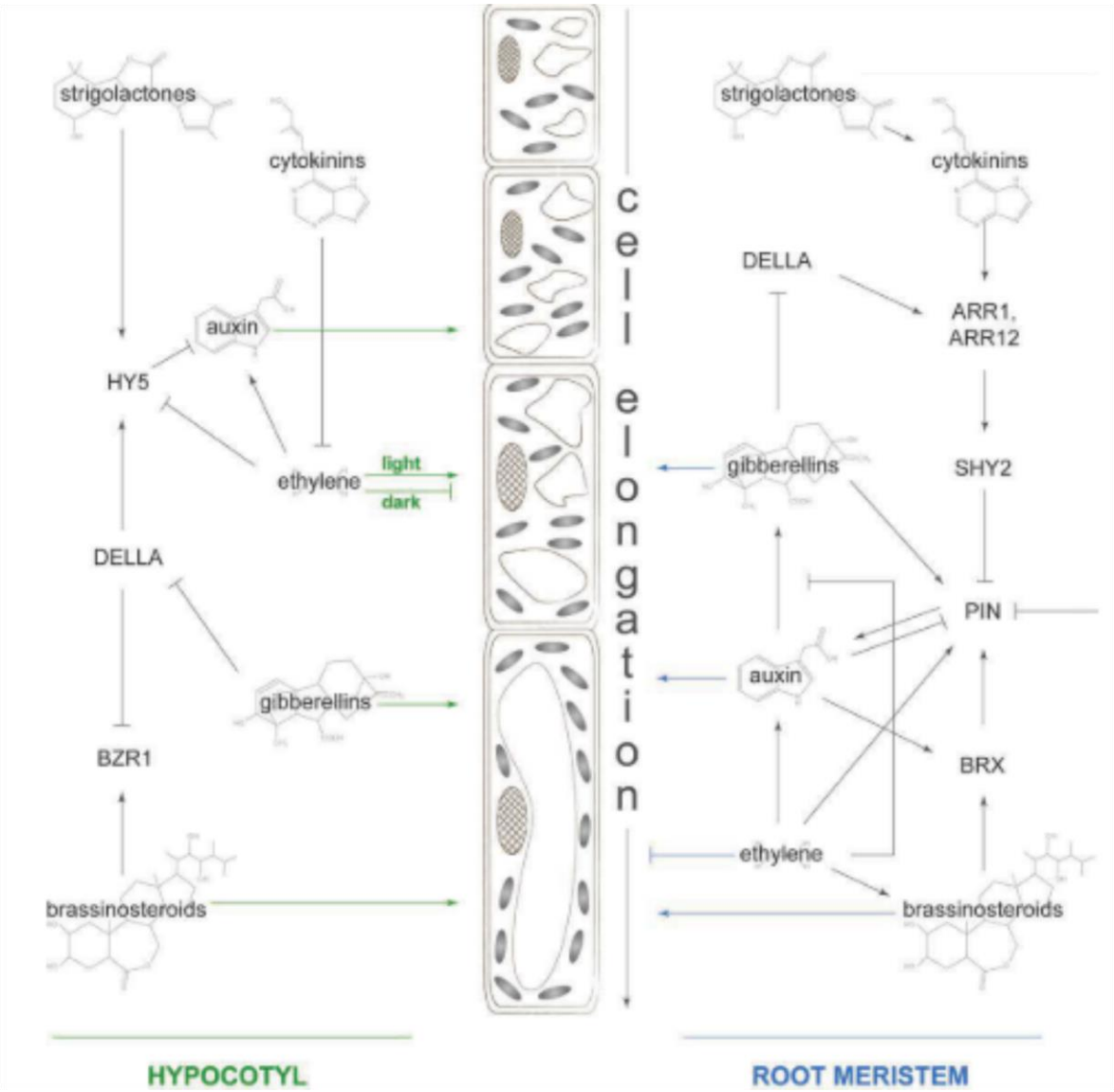

Figure 6: Model of hormonal interactions during hypocotyl elongation (left) and the root meristem (right)

This figure presents the main players and some of the cross-talk mechanisms that regulate hormone-mediated cell expansion in the hypocotyl (left) and the root meristem (right). Brassinosteroids, Gibberellins and auxin are the main drivers of hypocotyl elongation, while ethylene is an inhibitor of elongation in the dark, but a stimulator in the light. The role of strigolactones and cytokinin is not directly affecting cell elongation, but affecting other major players. In the root, just as in the hypocotyl, brassinosteroids, gibberellins and auxin are the main drivers of cell elongation, while ethylene is only known to inhibit elongation. Cytokinins have a well-known inhibiting function in elongation in the root by stimulating *SHY2* expression leading to reduced auxin transport and, as such, inhibition of elongation. Strigolactones are known to operate via cytokinins. (derived from Depuydt *et al.* (2016))

The influence of light on hypocotyl elongation.

Out of an evolutionary point of view, hypocotyl elongation helps the plant to push through the soil to reach the surface where the cotyledons and first leaves can catch sunlight and start photosynthesis. Plant development is completely different depending on the light conditions, evolved in such a way to create enormous plasticity to adapt to the changing environment The dark-grown growth mode is known as skotomorphogenesis in which it is generally accepted that light induces de-etiolation, also known as photomorphogenesis, leading to a reduction and stop in elongation of the hypocotyl (Quail *et al.*, 1995; Quail, 2002). The former is more studied but recently more attention is given to the process of elongation in the light (Smalle *et al.*, 1997; Collett, Harberd and Leyser, 2000; Zhong *et al.*, 2012; Zheng *et al.*, 2016).

The importance of light signals in regulating plant growth did already draw the attention of Charles Darwin (Charles Darwin and Darwin, 1881). Plants perceive light via at least 3 types of photoreceptors, the UV-B receptor, UV-A/blue- light receptors, and PHYTOCHROMES (PHYs) (Smith, 2000; Sakai *et al.*, 2001). PHYs are soluble chromoproteins of ~125 kDa can exist in two spectral forms, the inactive P_R form (upon absorption of far-red light) and the active P_{FR} form (upon absorption of red light) (Huq and Quail, 2002). PHYs represent a major class of photoreceptors first discovered in terrestrial plants as red (R) and far-red light (FR) sensors controlling key adaptive and developmental processes (Fortunato *et al.*, 2016). In *Arabidopsis thaliana*, and in fact, in all angiosperms, five phytochromes are present, named PHYA to PHYE (Sharrock and Quail, 1989; Mathews and Sharrock, 1997). Phylogenetic studies divide them into 4 families/types, the PHYA, PHYB/D, PHYC and PHYE types (i.e. PHYB and PHYD proteins form a related subgroup) (Mathews and Sharrock, 1997). These 5 PHYs are divided into 2 types. Type I phytochromes are highly abundant in etiolated seedlings and drastically decrease upon exposure to light (Reddy and Sharma, 1998; Sharrock and Clack, 2002; Xie, Kagawa and Takano, 2014). By contrast, type II phytochromes are relatively light-stable and present in de-etiolated seedlings and adult plants. The diversity in phytochromes gave flexibility to the plants to react to light signals as the different phytochromes have distinct roles during plant development. In *Arabidopsis thaliana*, only PHYA is classified as type I, its transcript is highly abundant in dark-grown (etiolated) seedlings but almost undetectable in light-grown seedlings. Therefore, PHYA plays an important role in seed germination, cotyledon expansion and photomorphogenesis under very low-intensity light (e.g. in dense canopy shade) (Sharrock and Quail, 1989; Mathews, Lavin and Sharrock, 1995; Smith, 2000; Inoue, Nishihama and Kohchi, 2017). The other four phytochromes belong to type II, of which, in Arabidopsis, PHYB is the most abundant. Transcripts of PHYB are present at lower levels in the dark and their expression is not strongly light-regulated. Therefore, PHYB plays a dominant role during photomorphogenesis, being involved in various processes such as seed germination, shade avoidance responses (including the effects of red light and of the R:FR ratio on hypocotyl elongation, flowering time and leaf morphology) (Sharrock and Quail, 1989; Mathews, Lavin and Sharrock, 1995; Smith, 2000; Inoue, Nishihama and Kohchi, 2017).

Phytochromes regulate plant growth by influencing gene expression via activation of specific transcription factors. The PIFs were the first transcription factor family (belonging to the BASIC HELIX-LOOP-HELIX (bHLH) transcription factor family) discovered to be directly regulated by phytochromes (Leivar & Monte 2014; Ni et al. 1998). Following conversion to the P_{FR} form, PHYs translocate to the nucleus (Sakamoto and

Nagatani, 1996; Nagatani, 2004; Kircher et al., 1999, 2002), there they physically interact with the PIFs via binding to a conserved N-terminal phytochrome-interacting domain. This domain is called the ACTIVE PHYB BINDING (APB) motif for all PIF members of Subfamily 15 and called the ACTIVE PHYA BINDING (APA) motif for the interaction of PHYA with PIF1 and PIF3 (Khanna *et al.*, 2004; Leivar and Quail, 2011). The physical interaction of PHYs with PIFs leads to phosphorylation, ubiquitination, and degradation via the 26S proteasome of the latter (reviewed in Franklin and Quail, 2010).

PIF3 appears to function in both PHYA and PHYB pathways and is involved in regulating not only the cell expansion responses underlying hypocotyl growth but also the expression of key regulatory genes, such as *CIRCADIAN CLOCK ASSOCIATED 1 (CCA1)* and *LATE ELONGATED HYPOCOTYL (LHY)*, which are involved in controlling chloroplast biogenesis and circadian rhythms (Ni et al., 1998; Martinez-Garcia et al., 2000). PIF4, by contrast, appears to be specific to the PHYB-pathway and does not seem to regulate *CCA1*, *LHY* or other genes of plastid development (Huq and Quail, 2002). PIF4 and PIF5 are positive stimulators of the Shade Avoidance Syndrome (SAS). The abundance of these proteins increases rapidly in the shade and *pif4*, *pif5* and *pif4pif5* mutants illustrate a reduced hypocotyl-elongation. Conversely, *PIF4*- and *PIF5*-overexpressors have the opposite phenotype, approaching constitutively long hypocotyls and petioles (Lorrain *et al.*, 2008). In conclusion: in the light, *PHYB* transcripts are upregulated, leading to a downregulation of *PIF4* transcripts, and as such inhibition of hypocotyl elongation, during the SAS, *PHYB* transcripts are low and *PIF4* transcripts are high stimulating hypocotyl elongation. Nevertheless, the story is not binominal and more complex, for example, PIF4 is also needed in the light to stimulate elongation when seedlings are grown in elevated temperature conditions (Franklin *et al.*, 2011). PIF4 is not only a key regulator of elongation in response to external signals, such as temperature, light, sucrose or the circadian clock (Greenham and McClung, 2015) but also to internal signals, including gibberellin, auxin and brassinosteroids (De Lucas *et al.*, 2008; Franklin *et al.*, 2011; M.-Y. Bai, Fan, *et al.*, 2012). In short, PIF4 is inhibited by DELLAs and BIN2, hence, both GAs (via DELLA breakdown), as well as BRs (via BES1), stimulate PIF4 leading to elongation (Choi and Oh, 2016). PIF4 itself stimulates auxin biosynthesis and IAAs (e.g. IAA19) leading to, respectively, elongation and phototropic responses. We indicated already that PHYB regulates PIF4 transcription (as illustrated earlier), but PHYB also inhibits BR signalling via interaction with BES1 (Wu *et al.*, 2019). In that way, via PIF4, light signalling integrates with phytohormone signalling to adjust plant development.

The BAP module (BZR1-ARF6-PIF4), integrating BRs, GAs, auxin and light signalling, regulates hypocotyl elongation via transcription of the BR-regulated *BZR1*, auxin-regulated *ARF6*, and GA/light-regulated *PIF4* genes. The BAP module interacts with each other and cooperatively regulate shared target genes (Oh *et al.*, 2014) and is the general cross-talk module in hypocotyl elongation. However, also this BAP module is too simple to illustrate and cover the many cross-talks during hypocotyl elongation. For examples, in the dark, ethylene inhibits hypocotyl elongation, but in the light ethylene stimulates hypocotyl elongation hinting on a current unknown interplay with light signalling. Overall, it can be concluded that cell elongation is a complex interaction of several external (e.g. light) and internal (phytohormones) signals that is species and time-dependent.

Scientific scope and the aims of the project

Coumarin is an intriguing molecule. Besides being small and aromatic, it possesses biological activity both in animals and plants. In animal systems the study of coumarin mainly focuses on the toxicity of the compound, paying special attention to its presumed role in carcinogenesis. Coumarin is also a known precursor for toxic metabolites that are formed during food storage or digestion. Obtaining insight in the direct or indirect toxicity of coumarin is important, especially since coumarin was once used as food additive, for enhancing flavour. In plants, the focus of coumarin research has mainly been on its capacity to steer growth and development, rather than studying its toxicity. Combined with the knowledge that coumarin is synthesized by plants, the big question is of course whether the bioactive compound also fulfills a physiological and/or biological function *in planta*. To date, this question remains to be answered, and here we attempted to get an insight into its role and function in plants.

The main reason for our poor understanding of the relevance of coumarin in plant physiology is our total lack of insight in the molecular mechanisms underlying coumarin activity. In addition, the biosynthetic pathway that leads to coumarin formation remains to be resolved, as quantifying coumarin at physiologically relevant concentrations in plants is near impossible. Together this results in a so-called coumarin black box, where the only thing we know is that exogenous coumarin treatment results in a plant response, which manifests itself as a particularly aberrant phenotype. The complete lack of insight in the underlying signalling cascade is surprising, especially since coumarin was already identified as a plant metabolite 200 years ago (which is even 100 year before the discovery of auxin!). Together with auxin, the activity of coumarin in plants has been intensely studied, especially in the middle of the previous century. At that time the studies were primarily descriptive in nature and focused on phenotypic defects caused by coumarin treatment. In contrast to the studies on auxin, which continued and even intensified over time, the study of coumarin was abandoned. The loss of interest in coumarin research at the end of last century also implies that this research field never benefited from *state-of-the-art* molecular tools that boosted the understanding of other plant growth regulators and phytohormones. As a consequence processes like coumarin biosynthesis, signalling and its *mode-of-action* were never studied in detail.

To get closer to the unravelling of coumarin's physiological relevance we here aim to re-open this research field and explore the coumarin black box by using state-of-the-art molecular techniques. Two different targets are set. First, we will study coumarin induced phenotypes using the early developmental stages of *Arabidopsis thaliana* as a model system. Based on a detailed phenotypic characterization we will select 2 particular phenotypes (a shoot and a root phenotype) to meet our second target: opening the coumarin black box by unraveling the signalling cascade linking the initial perception of coumarin with the final responses (mainly focusing on gene regulation). The obtained information will be used to build a molecular model explaining the mode of coumarin action. As such, we aim to clarify the sometimes opposing and contradictory findings in the literature about the effects of coumarin on plant growth, and describe the effects on shoot and root growth of Arabidopsis. Mutant analyses and pharmacological approaches will be used to unravel the relation with the known phytohormones and their role in the chosen physiological process. The presented model will subsequently be strengthened by an in-depth transcriptome analysis, whereby the early coumarin response will be monitored over time. Besides the insights in the dynamic behaviour of involved pathways, the transcriptome study will give new insights into the general context of growth and development influenced by

coumarin. In addition, the suggested model will be useful to draw general conclusions about the effect of coumarin on plant growth and can help in formulating hypotheses of how coumarin can affect other physiological processes in plants (e.g. germination).

In summary, the underlying research project aims to link the phenotypic effects induced by coumarin in *Arabopdisis thaliana* with molecular pathways and interactions with phytohormones in order to increase the understanding of its *modus operandi*.

Chapter 3 – Coumarin induces elongation of the hypocotyl of *Arabidopsis thaliana* in the light.

Coumarin induces hypocotyl elongation of light-grown *Arabidopsis thaliana* seedlings via increasing brassinosteroid signalling in an auxin-dependent manner.

Stan Van Praet[1,2,3], Annalisa Rizza[4], Bijun Tang[4], Alexander Jones[4], Dirk Inzé[1,2], Bartel Vanholme[1,2], Stephen Depuydt[1,2,3]

1. Ghent University, Department of Plant Biotechnology and Bioinformatics, (Technologiepark 71), 9052 Ghent, Belgium
2. VIB Center for Plant Systems Biology, (Technologiepark 71), 9052 Ghent, Belgium
3. Ghent University Global Campus, Lab of Plant Growth Analysis, Incheon, South Korea
4. Sainsbury Laboratory, Cambridge University, Cambridge, UK.

Author contributions:

S.V.P. and S.D. conceptualized and designed the research; S.V.P. performed the research/experiments. A.J., A.R. and B.T. contributed to the experiments using the *nlsGPS1* optic biosensor; S.V.P., B.V and S.D. interpreted the data. S.V.P. analysed the data, performed the statistics and made the figures; S.V.P. drafted the manuscript and A.J. D.I., B.V. and S.D. revised it.

Abstract

Coumarin is a derivative of the phenylpropanoid pathway, a well-known pathway that forms the basis for lignin biosynthesis (and other secondary metabolites). Coumarin is known to influence various plant developmental programs, ranging from germination, over root growth to stimulation of elongation in the shoot. Although the effect of coumarin on plant growth has already been described in 1943, until today its *mode-of-action* remains elusive. Here, we show that coumarin enhances hypocotyl growth of *Arabidopsis thaliana* by inducing cell elongation. A clear auxin response - illustrated by the analysis of pDR5::GFP reporter lines - is at the basis of coumarin-induced hypocotyl elongation, and mutant analysis revealed the need for auxin signalling. Moreover, we found that coumarin affects auxin transport, as the *pin1* mutant showed a diminished response towards coumarin in terms of hypocotyl elongation. We illustrated that coumarin-induced hypocotyl elongation occurs independently of ethylene and that probably also gibberellic acid signalling and/or biosynthesis play no major role during coumarin-induced hypocotyl elongation. Brassinosteroids (BRs), on the other hand, are crucial for coumarin-induced hypocotyl elongation, since we clearly illustrated a stong transcriptional BR response and BR mutants are impaired in their response. Coumarin also impacts on photomorphogenesis as transcription of relevant players is impacted. Moreover, no hypocotyl elongation was observed in the *phytochromeB-5* mutant upon coumarin treatment, suggesting that coumarin interferes with PHYB-mediated photomorphogenesis.

Introduction

The natural compound coumarin (2H-1-benzopyran-2-one) is chemically the simplest member of the coumarins, also known as *o*-hydroxycinnamic acid lactones. They are a ubiquitous group of plant secondary metabolites, comprising of at least 700 different structures (Collier, 1971; Harborne, 1999). Coumarin itself is a sweet-smelling plant substance and therefore previously used as an additive in perfumes, detergents, toothpaste, tobacco products and some alcoholic beverages (Cohen, 1979; Lake, 1999). Coumarin is present in almost every plant family (Wehmer, 1911; Harborne, 1999) and in all plant organs including roots, stems, leaves, flowers, fruits and seeds (Matos *et al.*, 2015).

Coumarins are derived from the general phenylpropanoid (PP) pathway (Zobel and Brown, 1995), a well-known pathway of which the biosynthesis of monolignols (providing the building blocks for lignin) is the best known (Vanholme *et al.*, 2010; Muro-Villanueva, Mao and Chapple, 2019). However, the PP pathway is also the basis for other plant-specific compounds (Vogt, 2010; Vanholme *et al.*, 2012). For example, the chalcone synthesis pathway leads to the biosynthesis of flavonoids (Vogt, 2010; Vanholme *et al.*, 2012), that have various biological roles ranging from UV protection, radical scavenging to the regulation of auxin transport (Brown *et al.*, 2001; Peer and Murphy, 2007; Agati *et al.*, 2012; Yang *et al.*, 2018). The PP pathway also provides a precursor of salicylic acid and hence plays a role in resistance to biotic stress (Widhalm and Dudareva, 2015).

Historically, coumarin biosynthesis was studied in sweet clover (*Melilotus alba*) as high concentrations of coumarin occurred therein, making the crop relatively unpalatable for cattle (Goplen, Greenshields and Baenziger, 1957; Haskins and Gorz, 1965, 1970; Kleinhofs, Haskins and Gorz, 1967; Gorz and Haskins, 1969). Sweet clover mutants (the *cucubb* mutants) were found that produced less coumarin and were, as such, more suited for feedstock (Schaeffer, Haskins and Gorz, 1960; Haskins and Gorz, 1965, 1970; Kleinhofs, Haskins and Gorz, 1966). Little is known about the enzymes involved in the formation and lactonization of coumarins (Collier, 1971; Bourgaud *et al.*, 2006; Kai *et al.*, 2008). Tracer feeding experiments indicate that coumarins are derived from cinnamic acid, which itself is derived from L-phenylalanine. Ortho-hydroxylation of cinnamate, under control of an unknown cytochrome P450 enzyme, leads to *o*-coumaric acid formation, which is followed by (spontaneous) lactonisation leading to coumarin production (Brown, Towers and Wright, 1960; Fritig, Hirth and Ourisson, 1970; Bourgaud *et al.*, 2006; Soad A. L. Bayoumi *et al.*, 2008; Shimizu, 2014).

It has been known for a long time that coumarin has an influence on plant growth (Kuhn *et al.*, 1943). Although species-dependent, coumarin affects nearly every plant developmental program in a concentration-dependent manner. For example, coumarin was reported to affect root growth, induce hypocotyl, coleoptile and stem elongation, influence germination and affect shoot yield (Audus and Quastel, 1947; Cornman, 1947; Thimann and Bonner, 1949; Neumann, 1959, 1960c, 1960a; Blaim, 1960; Knypl, 1964b; Alexieva *et al.*, 1995; Podbielkowska *et al.*, 1995; Abenavoli *et al.*, 2006; Hossain *et al.*, 2008; Saleh and Abu El-Soud, 2015; Saleh, Madany and González, 2015; Saleh and Kebeish, 2018). Coumarin interferes with physiological responses too, as it can induce respiration, influence photosynthesis and influence nitrogen uptake (Knypl, 1961; Macias *et al.*, 1999; Saleh, Madany and González, 2015). Moreover, coumarin accumulation is induced by biotic and abiotic stresses, suggesting a role in stress tolerance (Cabello-Hurtado *et al.*, 1998; Matern, Lüer and Kreusch, 1999;

Kai *et al.*, 2006; Al-Wakeel *et al.*, 2013). Furthermore, coumarin has pesticide properties and is generally described as an allelopathic chemical (i.e. an allelochemical) (Reda and El-Banhawy, 1986; Podbielkowska *et al.*, 1994; Pergo *et al.*, 2008; Razavi, 2011; Al-Wakeel *et al.*, 2013), which indicates that coumarin is a chemical, produced as secondary metabolite by plants (or other organisms) that influences the growth and development of surrounding biological systems (Whittaker and Feeny, 1971; Razavi, 2011).

Besides coumarin, several other PP derivatives (e.g. scopoletin and *cis*-cinnamic acid) can influence plant growth with far-reaching effects on plant growth and development (Einhellig *et al.*, 1970; Peterson *et al.*, 2003; Graña *et al.*, 2017; Steenackers *et al.*, 2017; Biala and Jasiński, 2018; Kurepa *et al.*, 2018), but in all cases, the underlying molecular networks are poorly understood (reviewed in Vanholme, El Houari and Boerjan, 2019). In the case of coumarin, it was shown that treated roots of *Arabidopsis thaliana* seedlings displayed a similar response as to auxin treatment: at the lower concentrations, root growth is stimulated, while at the higher concentrations it is inhibited (Abenavoli *et al.*, 2008). These phenotypes are due to the interference of coumarin with auxin polar transport and particularly with the AUX1 influx carrier (Lupini *et al.*, 2014). The stimulatory effect on root growth was also confirmed on maize roots, whereby it was found that coumarin stimulates root elongation by enhancing the plasma membrane H^+-ATPase activity leading to acidification of the apoplast (Lupini *et al.*, 2010). Also in the shoots, a link with auxin was found. Coumarin stimulates plumule elongation and biomass of *Vicia faba* seedlings, whereby elevated levels of indole-3-acetic acid (IAA) and gibberellic acid (GA3) were measured in leaves (Saleh, Madany and González, 2015). This finding is in line with the increased levels of IAA found in *Vigna radiata* stem cuttings treated with coumarin (Tartoura, da Rocha and Youssef, 2004). In pea stems, the stimulatory effect of coumarin on elongation was linked to gibberellic acid (GA), as the inhibitory effect of paclobutrazol was partially restored by coumarin treatment (Saleh and Abu El-Soud, 2015). The effect of coumarin on germination of wheat was also linked to GA, as coumarin was found to stimulate alpha-amylase activity (Saleh and Abu El-Soud, 2015; Saleh and Kebeish, 2018). Very recently, also links with abscisic acid (ABA) and coumarin were found (Saleh and Kebeish, 2018; Chen *et al.*, 2019). It was shown that coumarin delays rice seed germination by inhibiting ABA catabolism (leading to higher ABA contents) via decreasing the expression of *OsABA8'ox2/3* (Chen *et al.*, 2019). Moreover, coumarin also affects the Reactive Oxygen Species (ROS) content in seeds, but its effect seems species-, age- and concentration-dependent, leading to both stimulatory as well as inhibitory effects on ROS formation (Saleh and Kebeish, 2018; Chen *et al.*, 2019).

Growth of plant organs is an interplay between cell proliferation and cell expansion (Sachs, 1882). The acid-growth-theory as proposed by Heyn (1940) states that cell expansion occurs once a critical internal pressure, i.e. turgor pressure, is reached, and that cell enlargement is allowed because of loosening of the plant cell-well via acidification of the apoplast (Cosgrove, 2005; Wolf, Hématy and Höfte, 2012). The plant hormone auxin is historically claimed to be at the basis of this effect, and therefore the phenotype is often referred to as the 'auxin-induced acidification' (Depuydt *et al.*, 2016). Also brassinosteroids, ethylene and gibberellins are known to induce cell elongation (Box 1). Of those major hormones that are involved in cell expansion, there is substantial overlap in transcriptional targets Chapter 2), and almost all affect transcription of EXPANSINS (EXPs) and their homologs that mediate loosening of the plant cell wall (Cosgrove, 2000; Nemhauser, Hong and Chory, 2006).

BOX 1: The Major players during hypocotyl cell elongation.

Auxin: Auxin is essential for cell elongation responses to shade, elevated temperature, the circadian clock as well as light and gravity (Stewart and Nemhauser, 2010; Bianco and Kepinski, 2011). Auxin treatment of isolated stem segments or coleoptiles will induce cell elongation within a 10-minute timeframe (Evans and Cleland, 1985; Fendrych, Leung and Friml, 2016). The hypocotyl illustrates the typical bell-shaped response for auxin-induced phenotypes: mutants (e.g. *axr1*) with reduced responses to auxin (Lincoln, Britton and Estelle, 1990; Leyser *et al.*, 1993) and mutants (e.g. *axr3*) with an enhanced auxin response (Leyser *et al.*, 1996; Rouse, 1998), both have shorter hypocotyls than wild-type seedlings. The 'acid growth theory' is the mode of auxin action for cell expansion (Heyn, 1931, 1940; Hager, 2003). In short, plasma membrane proton pumps, specifically activated by the plant hormone auxin, lower the pH in the apoplast, and as a result of the action of EXPs, amongst others, the cell wall would loosen, allowing turgor-driven cell enlargement (Cosgrove, 2000; Hager, 2003).

SAURs and H^+-ATPases: The SMALL AUXIN UP-RNA (SAUR) gene family contains 79 known members in *Arabidopsis thaliana* and comprises, as such, the largest family of auxin-induced genes (Hagen and Guilfoyle, 2002). Auxin-induced expression of *SAUR* genes leads to activation of H^+-ATPases (AHAs), and as such, acidification of the apoplast (Franklin *et al.*, 2011; Chae *et al.*, 2012; Spartz *et al.*, 2012, 2014; Takahashi, Hayashi and Kinoshita, 2012; Farquharson, 2014). *AHA1* and *AHA2* encode for the two most highly expressed isoforms (Baxter *et al.*, 2005; Haruta *et al.*, 2010). Acidification of the apoplast activates EXPANSINS and XYLOGLUCAN ENDOTRANSGLUCOSYLASE/HYDROLASES that loosen the rigid cell-wall leading to turgor-assisted cell enlargement. SAUR19 overexpression lines have elongated hypocotyls illustrating their role in hypocotyl elongating (Spartz *et al.*, 2012). The SAUR proteins are also known, besides their clear role in elongation, to operate in various plant developmental programmes (reviewed in Stortenbeker and Bemer, 2019).

***EXPANSINS (EXPs) and XYLOGLUCAN ENDOTRANSGLUCOSYLASE/HYDROLASES (XTHs)*:** The plant cell wall is a complex structure comprised of polysaccharides (cellulose microfibrils and hemicellulose (e.g. xyloglucans), a pectin matrix and proteoglycans (e.g. extensins) (Cosgrove, 2005). Cell expansion needs loosening of that cell wall structure, a process that is mediated by EXPs and XTHs (Rose *et al.*, 2002; Cosgrove, 2005). EXPs are located in the cell wall and are activated by low apoplastic pH. The exact working mechanisms of EXPs are not fully unravelled yet (Fukuda, 2015), but basically, expansins disrupt non-covalent bonds between cell wall polysaccharides, i.e. they temporary release the cross-links between hemicellulose and cellulose (Cosgrove, 2000, 2005; Cosgrove *et al.*, 2002), allowing cell wall stretching by increased turgor pressure. XTHs, on the other hand, operate by modification of xyloglucan bindings. Xyloglucan binds non-covalently to cellulose, cross-linking adjacent cellulose microfibrils what leads to an extensive and rigid xyloglucan-cellulose network (Rose *et al.*, 2002). XTHs are involved in releasing those cross-linking structures resulting in loosening of the cell wall. Auxin is also known to directly loosen the cell wall by activating *XTH* expression in the hypocotyl (Velasquez *et al.*, 2019).

Brassinosteroids (BRs): BR biosynthesis mutants show severe dwarfism and illustrate a constitutive photomorphogenic growth (Choe *et al.*, 1998; Noguchi *et al.*, 1999). Treatment of seedlings with brassinolide, or overexpression lines of BR biosynthesis genes, on the other hand, leads to the formation of giants illustrating

the crucial role of BRs in cell enlargement (Szekeres *et al.*, 1996; Depuydt *et al.*, 2016). BRs typical induce elongation by affecting the number of cell wall biosynthesis and remodelling enzymes (Sun *et al.*, 2010), and by interacting with auxin (Oh *et al.*, 2014; Zheng *et al.*, 2017). BRASSINAZOLE RESISTANT1 (BZR1) interacts with PHYTOCHROME-INTERACTING FACTOR (PIF) factors, especially PIF4, and together they interact with AUXIN RESPONSE FACTOR 6 (ARF6), creating a trimeric complex whereby auxin, gibberellin and BR signalling are combined to regulates cell elongation (Gallego-Bartolome et al., 2012; M.-Y. Bai, Fan, et al., 2012; Oh et al., 2014). BRI1-EMS-SUPPRESSOR 1 (BES1) activates transcription of growth-promoting genes when bound to PIF4 during skotomorphogenesis (Wu *et al.*, 2019). In the light, however, PHYTOCHROMEB (PHYB) degrades PIF4 proteins and binds to BES1 deactivating transcription of growth-promoting genes, leading to photomorphogenic growth.

Gibberellins: Many developmental processes are regulated, or at least adjusted by gibberellins, as they can stimulate both cell division as well as cell elongation. Gibberellin loss-of-function biosynthesis mutants, as well as DELLA gain-of-function mutants, have shorter hypocotyls than wild-type seedlings (Koornneef and van der Veen, 1980; Sun, Goodman and Ausubel, 1992; Peng *et al.*, 1997). Exogenous gibberellin, on the other hand, promotes hypocotyl elongation, however, only in the light (Cowling and Harberd, 1999). In the hypocotyl, gibberellins induce cell expansion via several mechanisms, including cell wall relaxation via induced expression of EXPANSINs and XYLOGLUCAN ENDOTRANSGLUCOSYLASES/HYDROLASES (Liu *et al.*, 2007), but also by controlling auxin biosynthesis and transport (Willige *et al.*, 2011; Davière and Achard, 2016).

Ethylene: In general**,** ethylene is known to inhibit hypocotyl elongation, based on the typical triple response observed in etiolated hypocotyls treated with ethylene (Guzmán and Ecker, 1990; McKeon, Fernández-Maculet and Yang, 1995). However, in the light, it is observed that ethylene can stimulate hypocotyl elongation (Smalle *et al.*, 1997). Ethylene is a common target of hormonal interplay. Ethylene is known to stimulate brassinosteroid production (Woeste, Ye and Kieber, 1999), to interact with gibberellins (Achard *et al.*, 2003) and many interactions with auxin transport and signalling are observed (Růžička *et al.*, 2007; Stepanova *et al.*, 2007; Robles, Stepanova and Alonso, 2013).

Endoreduplication: Many *Arabidopsis thaliana* genes affect plant cell size by regulating the level of endoreduplication, and in that way, the latter is often correlated with mature cell size (Galbraith, Harkins and Knapp, 1991; Melaragno, Mehrotra and Coleman, 1993). Note, however, that not all plant species exhibit endoreduplication, which indicates that endoreduplication-driven cell size regulation is not universal among plants (Tsukaya, 2019). Nevertheless, in light-grown Arabidopsis hypocotyls, endoreduplication is linked to elongation and is hormonally regulated, for example, ethylene and GA are known to increase the 8C:4C ratio (Saibo *et al.*, 2003).

The historical use of different plant species and phenotypes to study the role of coumarin have hampered to reveal its mode-of-action. Moreover, significant fundamental research on the effects of coumarin on the model species *Arabidopsis thaliana* is lacking. Here, by zooming in on the effect of coumarin on hypocotyls of light-grown *Arabidopsis thaliana* seedlings, we unravel (part of) the molecular changes in auxin and brassinosteroid homeostases that we found to be crucial for coumarin-induced cell elongation. From apex

to base, there are only approximately 20 cells in the hypocotyl, and although the hypocotyl may increase more than 10-fold in length, there are no significant cortical or epidermal cell divisions (Gendreau *et al.*, 1997). By using the hypocotyl elongation model, we add a new piece of information to the underexplored field of the bioactivity of PP derivatives. Here we show that coumarin induces hypocotyl elongation in an auxin-dependent manner via increasing brassinosteroid signalling. Moreover, we show that PHYTOCHROME-B is crucial for coumarin-induced hypocotyl elongation, linking the observed phenotype to light signalling.

Material and Methods

Plant material and growth conditions

Wild-type Columbia (Col-0), Lansberg *erecta* (Ler) or Wassileskija (Ws) lines (depending on the background of the mutant) are used. All the *Arabidopsis thaliana* mutants used are described in Table S1. Seeds were surface-sterilized by treatment with 70 % ethanol for 5 minutes, followed by treatment with 100 % ethanol for 2 minutes, at room temperature while regularly inverting the Eppendorf tubes. The seeds were air-dried in the Laminar Air Flow (LAF) in a small sterile Petri dish Ø1 inch (SPL Life Science®, South Korea). Seeds were sown on 125x125 mm square Petri Dishes (SPL Life Science®, South Korea) containing 100 ml of ½ Murashige & Skoog growth medium (per litre demineralized water 2.15 g MS + vitamins, 0.5 g MES (2-(N-morpholino) ethanesulfonic acid), 0.1 g Myo-inositol, 10 g sucrose and 8 g agar (or 6.5 g gelrite) (Murashige and Skoog, 1962), the pH of the medium was adjusted to 5.7 using a 1 M KOH solution). Seeds were stratified at 4 °C for a minimum of 3 nights. Plates were positioned vertically at 21 °C, long-day conditions (16 h/8 h light/dark) and 120 PAR light.

Stock solutions

All chemicals that were used for treatments are described in Table S2 (the compounds' full name, abbreviation, the supplier, solvent and the stock concentration). The solvent of the compounds was always used as a mock control. All compounds were added to the growth medium after autoclaving and cooling down to 60 °C.

Phenotypic analysis of the hypocotyl length, cell number and leaf phenotype

Three or five days after germination (DAG), plates were scanned (Sindoh corp. Model DF-624; 400*400 dpi, JPEG) and the hypocotyl length was analyzed using ImageJ. The number of cells in the hypocotyl per seedling was counted using a stereomicroscope (Olympus corp. Model SZX2-ILLT), after clearance of the hypocotyls via Malamy and Benfey (Malamy and Benfey, 1997). Seedlings were first incubated in a 24 N HCl 20 % methanolic solution at 60 °C for 30 minutes, followed by incubation for 20 minutes in a 7 % (w/v) NaOH 60 % ethanol solution at room temperature. The samples were then dehydrated through 30-minute steps of 40 %, 20 %, and 10 % ethanol. As last plants were transferred to a solution containing 5 % ethanol and 25 % glycerol for 15 minutes, before being stored in 50 % glycerol.

Analysis of the leaf phenotype occurred following the protocol described in Nelissen *et al.*, 2013. In short, cotyledons were cleared in 100 % ethanol and mounted in 95 % lactic acid on a microscope slide. The total cotyledon area was measured for 15 representative cotyledons (per sample, per bio-repeat) under a dark-field binocular microscope. At least 100 abaxial epidermal cells positioned ¾ from the bottom of the cotyledon were drawn per cotyledon, via a microscope equipped with differential interference contrast optics (DM LB with 403 and 633 objectives; Leica) and a drawing tube. Photographs of cotyledons and scanned cell drawings were used to measure cotyledon and cell area, respectively, with ImageJ v1.50b (NIH; https://imagej.nih.gov/ij/), from which the cell numbers, stomatal index, and stomatal density were calculated according to the protocol explained in (Rymen *et al.*, 2010; Andriankaja *et al.*, 2012).

Cryo-SEM analysis

Hypocotyls of 5-day old *Arabidopsis thaliana* plants were prepared for imaging as outlined in Lyczakowski *et al.* (2019). Hypocotyls were dissected from roots and leaves and mounted on a sticky carbon pad on a stub. Hypocotyls were snap-frozen by submergence in liquid nitrogen, then transferred under vacuum and coated with 5 nm of platinum using a PT3010T cryo-apparatus fitted with a film thickness monitor (Quorum Technologies, Lewes, UK). The hypocotyls were maintained at -145 °C using a Quorum cryo-stage assembly and imaged using a Zeiss EVO HD15 Scanning Electron Microscope, with a Lanthanum Hexaboride HD filament as the electron source. Images were acquired using a secondary Backscattered Electron Detector at 25 kV.

Confocal microscopy

pDR5*rev*::GFP imaging and analysis

A Zeiss LSM 710 confocal laser scanning microscope was used for confocal imaging. 2 excitation filters at 488 nm for green fluorescent protein (GFP) and 561 nm for propidium iodide (PI) were set, with 3 band emission filters (1) 494 – 554 nm (for GFP), (2) 568 – 649 nm (for PI) and (3) 649 – 735 nm (for chloroplast reflection). Acquisition with multiple channels (4) was performed by sequential scanning. All settings remained the same to allow proper comparison of the different samples. Seedlings were stained with 0.1 % PI (Sigma-Aldrich) for 2–5 minutes. Images were analyzed using ImageJ v1.50b (NIH; https://imagej.nih.gov/ij/) and figures were prepared by using Inkscape (http://inkscape.org/en/).

*nls*GPS1 imaging

Imaging was performed as described in Rizza *et al.*, 2019. Seedlings were placed in a solution containing ¼ × MS medium (¼ × MS salts, 0.025% MES pH 5.7) with PI (1 mg/ml) for 5 –10 minutes, and prepared for imaging on glass slides. When the nlsGPS1 optic biosensor fused to the pUBQ10::PM-tdTomato line was used, no PI staining happened, as the tdTomato construct outlined cell membranes. Confocal images were acquired on a Leica SP8-FLIMan using a × 20 dry 0.70 HC PLAN APO objective, using a format of 512 x 512 pixels and a resolution of 12 bits. A 448 nm laser was used to excite the cyan fluorescent protein (CFP) and a 514 nm laser for yellow fluorescent protein (YFP). To excite PI (or the fluorescent protein tdTomato) a 552 nm laser line was used. The 448 nm laser line was set to 10% for GFP excitation. All settings remained the

same to allow proper comparison of the different samples. Fluorescence emission was detected by HyD SMD detectors, set to detect 460 to 500 nm for CFP, 525 to 560 nm for YFP, 590 to 635 nm for PI and 500 to 535 nm for GFP. The laser power was set between 0.5 % and 3 % with detector gain set to 110 to image CFP or YFP. A line average of four was used and the z-stacks were acquired with a step-size of 1–2 µm.

*nls*GPS1 processing and analysis.

Analysis occurred as described in Rizza *et al.*, 2019, by using the Fiji application. First, the Z-stack was combined in a 2D image via Stack > Z project (sum slices), followed by background subtraction (50 pixels) and splitting of the channels. The window corresponding to the YFP channel was used as the control. The images were adjusted for brightness and contrast after filtering them (Gaussian Blur of 1) to reduce the noise. The calculation of the ratio channel (DxAm/DxDm) was done by dividing the FRET-channel with the CFP channel (via image calculator), the obtained ratio was then multiplied with the YFP binary mask to show only pixels present in the YFP control channel. After a final adjustment of the brightness and contrast, a calibration bar is added and the picture exported as a .tiff file. To obtain values of the emission ratios the 'mean grey values' are calculated of at least 30 nuclei for every hypocotyl analyzed, in a pre-defined zone of the hypocotyl (indicated in the figure).

RNA extraction and quantitative real-time PCR (qRT-PCR)

Seedlings were harvested in 6-well plates containing RNAlater® (Thermo Fischer Scientific, United States) and stored at 4 °C. Hypocotyls of 3 and 5 DAG old seedlings were micro-dissected on ice, in RNA later, by the usage of a stereomicroscope and a syringe needle. 500-800 hypocotyls were collected per sample, snap-frozen in liquid nitrogen after dissection and stored at -80 °C. RNA was isolated by use of the RNeasy® Plant Mini Kit (Qiagen, Hilden, Germany) immediately followed by DNase treatment (Promega, RQ1 RNase-Free DNase kit). The RNA was treated for 30 minutes at 37 °C with a mixture containing RNA (30 µl), 10x RQ1 DNase-buffer (3.5 µl), RQ1 RNase-Free DNase enzyme (2U/µl) (1 µl), and water (H_2O-Diethylpyrocarbonate treated (DEPC) 1.5 µl). The reaction was stopped by adding 1 µl of RQ1 DNase stop solution and incubating the samples for 10 minutes at 65 °C. Sample quality was determined via spectrophotometry (Nanodrop® ND-1000)) and gel-electrophorese. If needed, the RNA was precipitated with 1 volume of 5 M NH_4Ac (dissolved in H_2O-DEPC) for 15 minutes on ice. The mixture was centrifuged for 15 minutes at 14000 rpm at 4 °C after which the pellet was washed with 70 % ethanol (RNase free). After vacuum-drying, the pellet was re-suspended in H_2O-DEPC (20 µl). Finally, 1 µg RNA was used to synthesize cDNA via the Cosmogene Synthesis Kit or the iScript™ cDNA Synthesis Kit following the manufacturer's instructions.

All qRT-PCR experiments were performed in three biological repeats and three technical repeats using 384-multiwell plates and detection by SYBR® Green. Reaction mixes were composed with a final volume of 5 µl and a 10 % cDNA fraction using the SYBR® Green Master Mix (PerkinElmer, Brussels, Belgium). The mix contains PCR-Buffer with SybRGreen, $MgCl_2$, dNTP's, DNA polymerase and the designed primers. The Roche Lightcycler® 480 system (Roche Diagnostics, Brussels, Belgium) was used to execute all qPCR reactions with following settings: one pre-incubation step at 95°C for 8', followed by 40 cycles of amplification at 95°C for 15";

60°C for 10"; 72°C for 10". After the final cycle, a melting curve was recorded: 95°C for 5" followed by heating from 95°C to 97°C for 1' and cooling down to 40°C for 10'. C_t-values and efficiency values were determined by the Lightcycler® 480 software and analyzed by the 2-ΔΔCt method (Livak and Schmittgen, 2001). The achieved expression data were normalized to the expression levels of the housekeeping genes *CBP20* and *PEX4* (Czechowski *et al.*, 2005; Pellino *et al.*, 2011). The primers that were used were originally designed with the primer design tool on Quantprime of the Max-Planck Institute, Germany (Arvidsson *et al.*, 2008). All primers were diluted with nuclease-free water (MiliQ) to a final concentration of 10 µM. The used primers are summarized in Table S3.

Statistical analysis

The statistical package 'R version 3.5.1' (https://www.r-project.org/) was used for all statistical analyses. The least-square means of the biological repeats were subjected to statistical analysis, in which the sample size (n) is the total number of seedlings analyzed per line/conditions. For the pairwise comparison of two experimental groups, statistical analysis has been performed using a Student t-test. To address the statistical difference between two or more experimental groups, a multiple-(mixed-)ANOVA (linear (Mixed-Effects) model) was used for the statistical analysis (Wilkinson and Rogers, 1973; Bates *et al.*, 2015). For discrete data (e.g. counting data) a Generalized Linear Mixed-Effects Models with 'Poisson' as the family function was used (McCullagh and Nelder, 1989; Dobson and Barnett, 2008). Posthoc analysis was performed via a Tukey correction. The statistical assumptions of (1) normal distribution (via histogram) and (2) homogeneity of variances (by analysis of the residuals (QQ-plot)), were tested, and where needed were log-transformed if data did not comply. For analysis of the emission ratios of the *nls*GPS1-CE line, the least-square means of all data were calculated and statistically compared between the samples via a multiple-(mixed-)ANOVA (linear (Mixed-Effects) model). For the analysis of the relative gene expression obtained via qRT-PCR, a Kruskal-Wallis rank-sum test was performed, followed by a Bonferroni correction (Hollander and Wolfe, 1973).

Results

Coumarin stimulates cell elongation in the shoot of Arabidopsis thaliana

We investigated the effect of coumarin on shoot growth of *Arabidopsis thaliana* by analyzing cotyledon and hypocotyl phenotypes. Detailed cellular analyses showed that seedlings grown until 5 days after germination (DAG) on medium containing 40 µM of coumarin had significantly smaller cotyledons because of a reduction in cell number (Fig. 1 A and B). Interestingly, the pavement cells of coumarin-treated seedlings were 23% bigger than the ones of mock-treated controls (Fig. 1B), indicating an effect on cell expansion. Stimulation of elongation could be a direct effect of coumarin, or it could be explained as a compensation phenotype: a well-known feature in plant growth whereby a reduction in cell numbers is often compensated for by an increase in cell size (Hisanaga, Kawade and Tsukaya, 2015). To further evaluate the effect of coumarin on elongation, a time-course analysis of light-grown *Arabidopsis* hypocotyls was performed. Seedlings were continuously treated with mock, 25, 40 or 100 µM coumarin and hypocotyl length was measured over time (Fig. 1C). Three days after germination hypocotyl length reached a plateau in mock conditions. Upon coumarin treatment, the hypocotyl extended for a longer period and only halted at 5 DAG (Fig. 1, C). Remarkably, in the dark, no significant difference in hypocotyl length was observed between treated and non-treated seedlings (Fig. 1D). The epidermis of light-grown hypocotyls is characterized by alternating protruding and non-protruding cell files (protruding cells face cortical cells whereas burrowed cells face anticlinal cortical cell walls) (Gendreau *et al.*, 1997; Gudesblat *et al.*, 2012). After coumarin treatment, as compared to before, no difference was found in the number of protruding cells in a single cell file (Fig. 1E, S1), indicating that no cell division took place (Fig. S1A). Altogether it is clear that coumarin induces cell elongation in the shoot, that coumarin-induced hypocotyl elongation is light-dependent and solely the consequence of cell elongation and not cell division.

Because exogenous coumarin treatment can interfere either directly, or indirectly with the biosynthesis of other derivatives of the phenylpropanoid (PP) pathway – for example by a feedback mechanism on the general PP derivative precursor cinnamic acid (Bourgaud *et al.*, 2006; Shimizu, 2014; Dare *et al.*, 2017) – we examined the effect of PP intermediates and derivatives on hypocotyl elongation. Interestingly, hypocotyl elongation cannot be mimicked by treatment with *trans*-cinnamic acid (*t*-CA), *rac*-CA (i.e. a racemic mixture of *trans*- and *cis*-cinnamic acid), *p*-coumaric acid, coniferyl alcohol, coniferyl aldehyde or feruloyl-CoA (Fig. S1, B). Moreover, exogenous treatment with different concentrations of scopoletin or umbelliferone could also not induce hypocotyl elongation (Fig. S1, B). These data illustrate that the enhanced hypocotyl elongation upon coumarin treatment is ascribed to coumarin and cannot be mimicked by interference with the PP pathway.

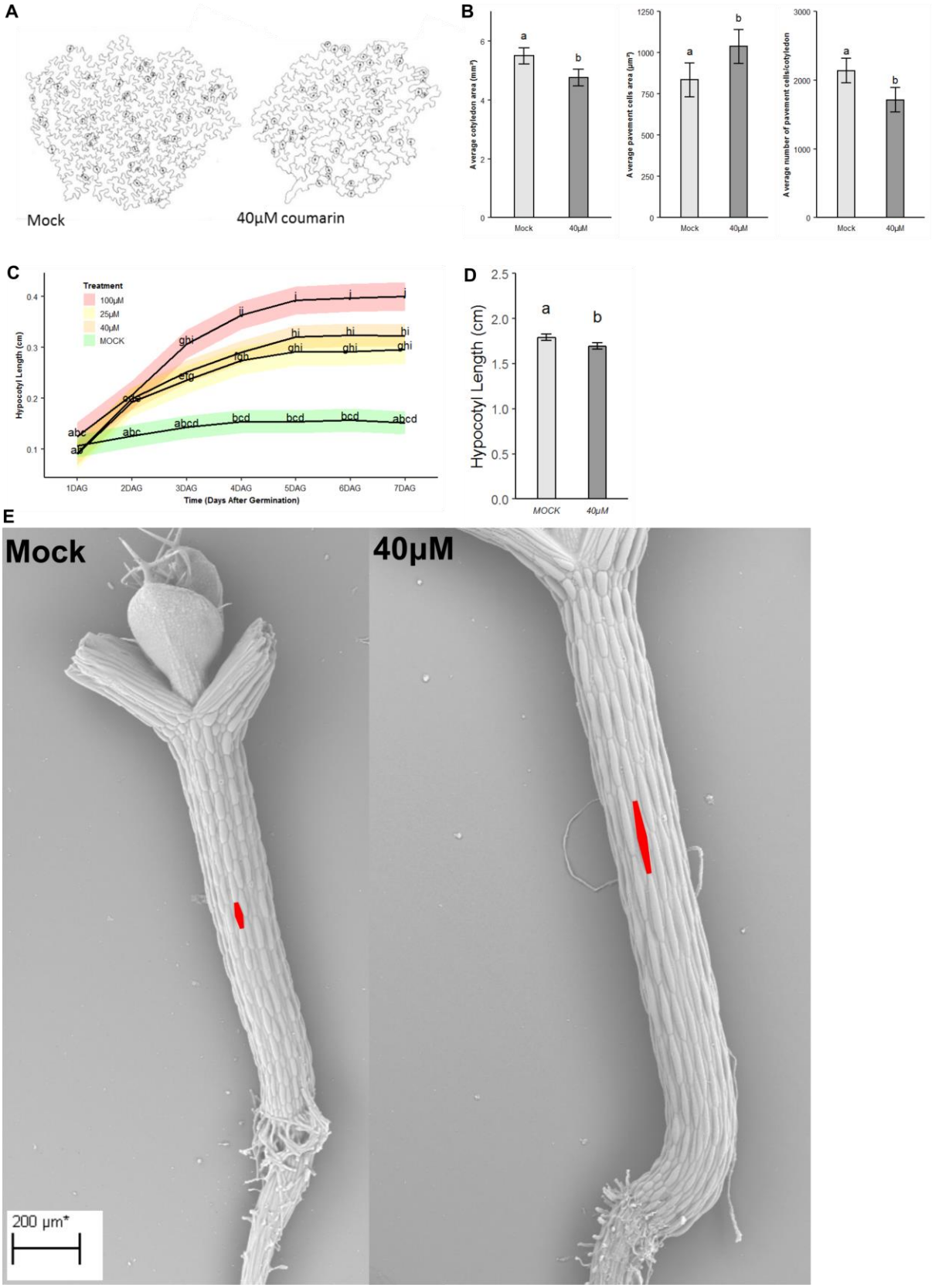
A
Mock
40µM coumarin
B
Average cotyledon area (mm²)
Average pavement cells area (µm²)
Average number of pavement cells/cotyledon
Mock
40µM
C
Treatment
100µM
25µM
40µM
MOCK
Hypocotyl Length (cm)
Time (Days After Germination)
1DAG
2DAG
3DAG
4DAG
5DAG
6DAG
7DAG
D
Hypocotyl Length (cm)
MOCK
40µM
E
Mock
40µM
200 µm*

Figure 1: Coumarin induces elongation in the shoot of *Arabidopsis thaliana.*

(A) Pavement cell analysis of cotyledons 5 days after germination (DAG) of seedlings continuously grown on mock (left) or 40 µM of coumarin (right). (B) Cotyledons area (µm²) (left), average pavement cell area (middle) and the average number of pavement cells per cotyledon (right) of 7DAG old seedlings continuously treated with 40 µM of coumarin compared to Mock (n ≥ 12). (C) Time-course analysis of hypocotyl length of seedlings continuously treated with different concentrations of coumarin compared to mock. (n≥75). (D) Hypocotyl length of 5 DAG old seedlings grown in the dark and transferred 2 days after to treatment: DMSO (Mock) or 40µM of coumarin (n≥32). (E) Scanning Electron Microscope images (via cryo freezing) of hypocotyls of 5 DAG old light-grown seedlings continuously treated with DMSO (i.e. Mock) or coumarin, (respectively left and right). The red box indicates 1 epidermal hypocotyl cell.

Data presented are means ± the confidence interval of at least three biological repeats. Letters indicate statistically different means ($p<0.05$).

Investigating the role of endoreduplication in coumarin-induced hypocotyl elongation

Endoreduplication plays a role in cell enlargements in Arabidopsis (Tsukaya, 2019) and especially during hypocotyl elongation (Saibo *et al.*, 2003). Moreover, we showed that cell elongation is solely responsible for the increase in hypocotyl length upon coumarin treatment. Therefore, we tested whether endoreduplication is involved in the process.

SIAMESE is a plant-specific cell cycle regulator that controls the endoreduplication onset in A*rabidopsis thaliana* (Churchman *et al.*, 2006). Therefore, we used the *SIAMESE RELATED 1 (SMR1)* gene as a marker for endoreduplication (Churchman *et al.*, 2006). Three DAG, in the middle of the elongation phase, we observed clear increased staining of the pSMR1::GUS reporter line in the hypocotyl epidermis upon continuous treatment with 40 µM of coumarin while this increase was absent in the mock control (Fig. 2A). Interestingly, while we still observe an increase in staining in 5 DAG old seedlings between coumarin and mock-treated seedlings, we observed a clear decrease in blue colouring upon coumarin treatment between 3 and 5 DAG old seedlings. This indicates that endoreduplication could be stimulated by coumarin in the middle of the elongation phase (i.e. 3 DAG), but not to the same extent at 5 DAG when elongation is terminated.

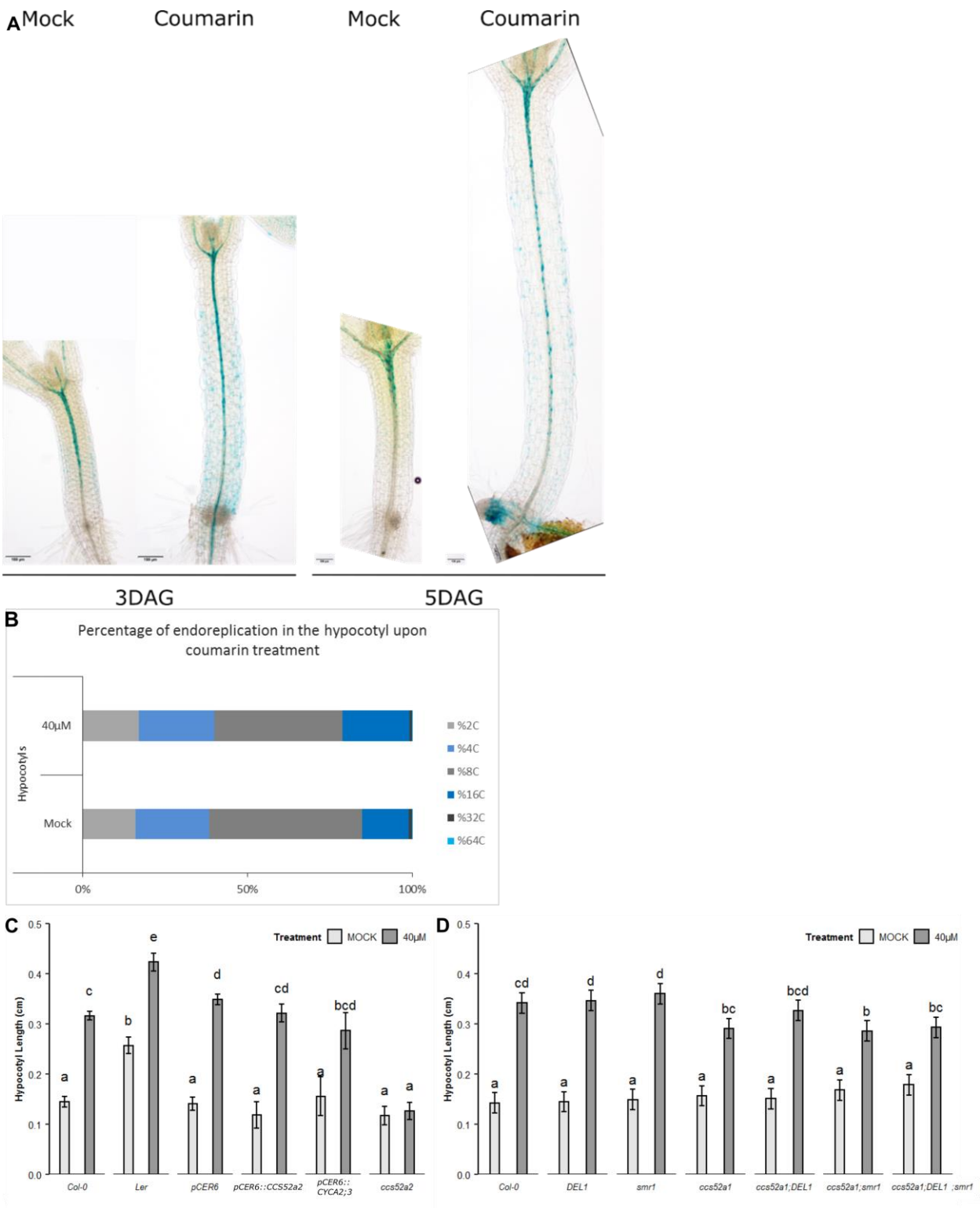

Figure 2: Investigating the role of endoreduplication during coumarin-induced hypocotyl elongation

(A) pSMR1::GUS staining of 3 and 5 DAG old seedlings continuously treated with either DMSO (mock) or 40 µM of coumarin. (B) The relative abundance of endoreduplication in the hypocotyl, expressed in terms of DNA content (C = haploid DNA content) (n = 200). (C, D) Hypocotyl length of 5 DAG old mutants in endoreduplication grown upon 40µM of coumarin treatment compared to mock.

Data presented are means ± the confidence interval of at least three biological repeats. Letters indicate statistically different means ($p<0.05$).

We next assessed endoreduplication levels via flow cytometric analyses. Our preliminary data illustrate a different abundance of endoreduplication levels in mock-treated seedlings than previously described (Saibo *et al.*, 2003). We observe a high abundance (46.6 %) of 8C nuclei and then an even distribution of 2C and 16C (±15 %), whereas there is a 22 % abundance of 4C in our mock sample (Fig. 2B). Interestingly, upon coumarin treatment, we observed a shift from 8C to 16C as the abundance of 8C nuclei drops to 38 % whereas the abundance of 16C nuclei will amount to 20 % (Fig. 2B). The level of 2C and 4C nuclei remained more or less the same and we have 1 % of 32C in both samples. Our data illustrate a shift in endoreduplication levels upon coumarin treatment, in line with the observed increased expression of *SMR1*.

To further analyse the role of *SMR1* and other genes involved in endoreduplication during coumarin-induced hypocotyl elongation, we tested several endoreduplication mutants. When endoreduplication is blocked in the whole seedlings, through mutation of *CELL CYCLE SWITCH PROTEIN 52 A2 (ccs52a2)*, the effect of coumarin is completely lost (Fig. 2C). It has to be noted that this mutation is rather severe, leading to a bad growth of the plants in general (Timmerman, Wassarman and Pourquié, 2010). Therefore, also mutants were tested that displayed a reduced level of endoreduplication but still illustrate normal growth. As a positive control, we examined the hypocotyl phenotype of seedlings with enhanced endoreduplication levels in the epidermis by overexpressing *CCS52a2* via the epidermal promoter *CER6* (i.e. the *pCER6::CCS52a2* seedlings)(Hooker, Millar and Kunst, 2002). We did not observe a different response upon coumarin treatment than the controls Col-0 and pCER6 (Fig. 2C). This indicates that enhanced endoreduplication in the epidermis is not sufficient to mimic the coumarin phenotype. When endoreduplication is negatively regulated in the epidermis (i.e. inhibited), via epidermal overexpression of the *CYCLIN A2;3 (CYCA2;3)* gene (*pCER6::CYCA2;3*), this had no effect on the length of the hypocotyl compared to the pCER6 mock-control (Fig. 2C). Moreover, those mutants responded in the same manner towards coumarin as the controls (Fig. 2C). The *smr1* mutant, the dominant gain-of-function mutant *DP-E2F-LIKE 1* (*DEL1*) and the *ccs52a1* mutant all three have a diminished endoreduplication level, but display a normal hypocotyl growth (Fig. 2D). Moreover, all three mutants are fully responsive towards coumarin treatment, i.e. no difference in hypocotyl length was observed upon coumarin treatment compared to Col-0. Also, the tested double and triple mutant(s) of *DEL1*, *smr1* and *ccs52a1* responded in the same manner as the *ccs52a1* single mutant (Fig. 2D), indicating there is no additive effect of the additional mutations blocking endoreduplication. Overall, we conclude that endoreduplication plays no major role in coumarin-induced hypocotyl elongation.

Coumarin induces an auxin response in the hypocotyl.

Auxin transport and accumulation play an important role in light-grown hypocotyl elongation (Jensen, Hangarter and Estelle, 1998; Chapman and Estelle, 2009). Therefore, we hypothesized that coumarin influences auxin homeostasis to induce hypocotyl elongation. Indeed, confocal analysis of the pDR5*rev*::GFP auxin reporter line revealed an auxin response in the hypocotyl upon coumarin treatment. A clear induced auxin maximum was observed at the apical and basal side (albeit more pronounced basally) of the hypocotyl of 3

DAG old seedlings treated continuously with 40 µM of coumarin (Fig. 3A), and also in the stomata, an increased auxin response upon coumarin could be observed (Fig. 3A). The clear auxin response was also shown transcriptionally by a 5-fold increase of *SMALL AUXIN UPREGULATED RNA 19 (SAUR19)* expression (assessed via qRT-PCR) (Fig. 3B). Moreover, auxin receptor and signalling mutants (the triple F-box receptor mutant *tir1-1afb2-1afb3-1* (Dharmasiri *et al.*, 2005; Dharmasiri, Dharmasiri and Estelle, 2005) and the gain-of-function *solitary root (slr-1)* mutant, which lacks an auxin response (Fukaki *et al.*, 2002)) do not respond towards coumarin treatment in terms of hypocotyl elongation (Fig. 3 C, D). These data illustrate that coumarin induces an auxin response in the hypocotyl and that stimulation of hypocotyl elongation occurs via an auxin-dependent signalling mechanism.

Generally, exogenous application of auxin (via 1-naphthaleneacetic acid (NAA), 2,4-dichlorophenoxyacetic acid (2,4-D), or the natural auxin indole-3-acetic acid (IAA)) does not lead to hypocotyl elongation in the light (Hanson and Trewavas, 1982; Zhao, 2010; Barbez *et al.*, 2012; Hu, Vandenbussche and Van Der Straeten, 2017), while plants that overproduce auxin have long hypocotyls (Boerjan *et al.*, 1995; Romano *et al.*, 1995; Delarue *et al.*, 1998; Zhao, Sioux K. Christensen, *et al.*, 2001; Adamowski and Friml, 2015; Velasquez *et al.*, 2016). Interestingly, co-treatment of coumarin with 1 µM of IAA or 0.1 µM of 2,4-D had small enhanced effects on hypocotyl elongation (Fig. S2). This indicates that coumarin treatment has distinct effects as compared to auxin treatment. Moreover, blocking auxin biosynthesis via 5-(4-chlorophenyl)-4H-1,2,4-triazole-3-thiol (yucassin) treatment (YCS) (Nishimura *et al.*, 2014), led to a slight positive effect on hypocotyl elongation that was additive in coumarin co-treated seedlings (Fig. 3 E, top), indicating that yuccasion treated seedlings responded to coumarin comparable to the WT (Fig. 3 E, bottom).

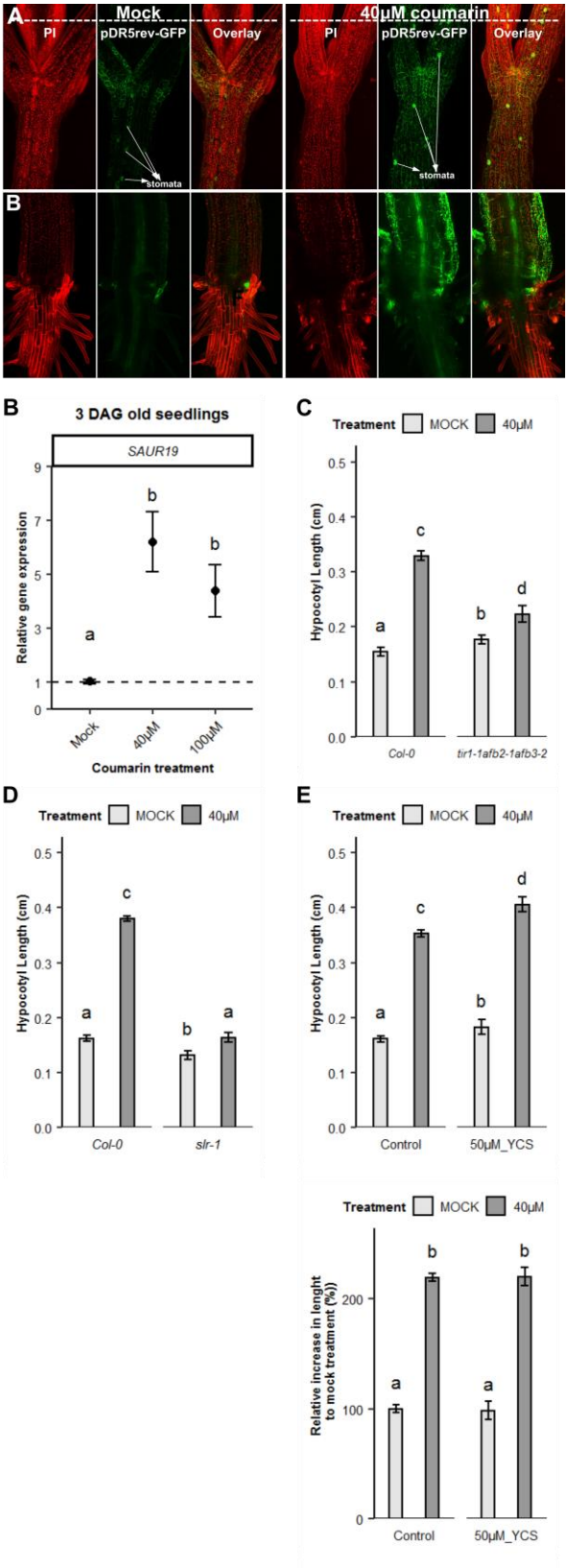

Figure 3: Coumarin induces an auxin response in the hypocotyl

(A) Confocal analysis of the pDR5rev::GFP reporter line in the hypocotyl of 3 DAG old seedlings, continuously treated with DMSO (Mock) or with 40 µM of coumarin (200x magnification). (B) Relative gene expression of the auxin response gene SAUR19 in hypocotyls harvested 3 days after germination of continuously treated seedlings with 40 or 100 µM of coumarin compared to the mock control (DMSO treatment). C) Hypocotyl length (cm) of 5 DAG old *tir1-1afb2-1afb3-2* mutants (n≥39) and (D) slr-1 mutants (n≥107) continuously treated with DMSO (Mock) or 40 µM of coumarin compared to the Col-0 control. (E) (top) Hypocotyl length (cm) of 5 DAG old seedlings continuously treated with DMSO (Mock) or 40 µM of coumarin in combination with 50 µM Yucassin (YCS); (bottom) relative increase in hypocotyl length, scaled to the mock treatment (n≥79).

Data presented are means ± the confidence interval of at least three biological repeats. Letters indicate statistically different means ($p<0.05$).

Coumarin-induced hypocotyl elongation and the 'acid growth theory'

Upon coumarin treatment, we observed a strong increase in *SAUR19* expression, indicating a clear auxin response, but potentially also a mechanism to induce hypocotyl growth through the acid-growth-theory (Farquharson, 2014). Therefore we investigated the role of H^+-ATPases during coumarin-induced hypocotyl elongation.

Our experiments with N,N′-dicyclohexylcarbodiimide (DCCD), a chemical blocker of H^+-ATPase pumps (Nelson and Harvey, 1999), illustrated that even when the H^+-ATPase pumps are pharmacologically inhibited, coumarin still induces elongation (Fig. 4A, B). Continuous treatment with 1 or 10 µM of DCCD could not block the effect of coumarin (Fig. 4A, B). To exclude the possibility that DCCD is broken down during the experiment[5], we transferred seedlings 2 days after germination from mock or 100 µM coumarin treatment to mock or 100 µM of coumarin, with or without 10 µM DCCD (Fig. 4A) for 24, 48 and 72 hours. Also here, DCCD could not block the effect of coumarin. To illustrate that the function of DCCD is not tissue or organ-specific a test was performed illustrating its inhibition of hypocotyl elongation in dark-grown seedlings (Fig. 4C). As it is known that SAUR19 activates mostly the *AHA2* pumps, we also analysed the *aha2-4* mutant (Haruta and Sussman, 2012). The *aha2-4* mutant was 12.3% smaller than Col-0 mock, but still, an 89% increase in length could be observed upon coumarin treatment, while in Col-0 seedlings a 129.5% increase was observed (Fig. 4D). This illustrates that the mutant is less responsive to coumarin than the wild-type (Fig. 4D, bottom), suggesting involvement of H^+-ATPases.

The difficulty in analysing the *SAUR* gene family in plant development is their high instability (Spartz *et al.*, 2012). However, it was found that the addition of an N-terminal green fluorescent protein (GFP) to the *SAUR19* transcript (a GFP-SAUR19 fusion protein) under the constitutive cauliflower mosaic virus 35S promoter, increases its stability enormously. We next analysed this *SAUR19* overexpression line (p35S::SAUR19-GFP) to see if *SAUR19* activation alone is enough to mimic our phenotype (Spartz *et al.*, 2012). However, constant activation of *SAUR19* only led to an increase of 11.5% in hypocotyl length compared to the control, while coumarin treatment alone leads to an increase of 133% (Fig. 4D). Moreover, no additive effects of both treatments could be observed (Fig. 4D, bottom). This finding is fully in line with the result of the *open stomata* (*ost2-2D*) mutant, a positive control (as the *ost2-2D* dominant gain-of-function mutant contains a constitutively active allele of the PM H^+-ATPase (Merlot *et al.*, 2007)), where a 13.3% increase was found compared to the control, and no additive effect when co-treated (Fig. 4D). In fact both, the *SAUR19* overexpression line end the *ost2-2D* mutant, even show a slightly reduced response towards coumarin (Fig. 4D, bottom).

Altogether, these data indicate that neither an enhanced *SAUR19* expression nor a constitutive H^+-ATPase activity can stimulate hypocotyl elongation as observed upon coumarin treatment. Nonetheless, when *AHA2* is knocked-out, the coumarin response is reduced.

[5] In literature, to the best of our knowledge, we didn't find any experiments using DCCD for such a long time period.

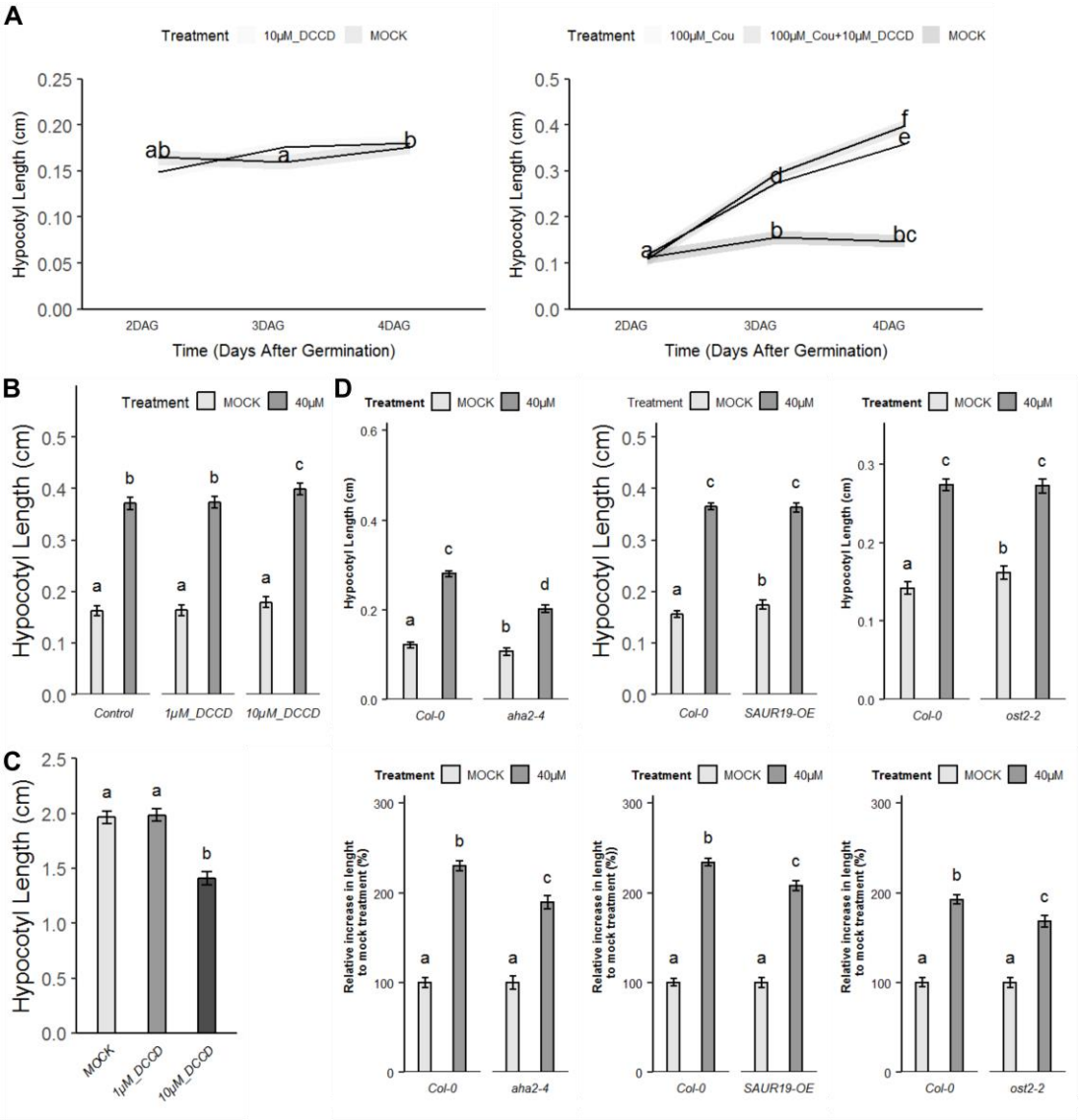

Figure 4: Investigating the role of the ‘acid growth theory’ during coumarin-induced hypocotyl elongation

(A) Hypocotyl length (cm) of seedlings grown on mock medium transferred 2 days after germination to mock medium (DMSO) or to medium supplemented with 10µM of DCCD (top, n≥62), or of seedlings grown on 100 µM of coumarin and transferred 2 days after germination to mock medium (DMSO), to medium supplemented with 10µM of DCCD or to medium supplemented with 10µM of DCCD and 100µM of coumarin (bottom, n≥41). The length is measured 24 h and 48 h later, respectively 3 and 4DAG. (B) Hypocotyl length of 5DAG seedlings continuously treated with DMSO, 1 or 10µM DCCD and co-treated with or without 40µM of coumarin (n≥57). (C) Hypocotyl length 5DAG of seedlings grown in the dark continuously treated with DMSO, 1 or 10µM DCCD (n≥75). (D) (top) Hypocotyl length and (bottom) relative increase in hypocotyl length of the *aha2-4* mutant (left), the p35S::SAUR19-GFP overexpression line (middle) and the *ost2-2* mutant (right) compared to the Col-0 control 5 DAG. All treated with or without 40µM of coumarin. (n≥ 77, 102 and 87 respectively).

Data presented are means ± the confidence interval of at least three biological repeats. Letters indicate statistically different means ($p<0.05$).

Coumarin affects auxin transport in the Arabidopsis hypocotyl.

The observed, albeit small, additional effect of combining coumarin and auxin on hypocotyl elongation, the clear auxin response and the fact that auxin transport plays a major role in light-grown hypocotyl elongation (Jensen, Hangarter and Estelle, 1998; Chapman and Estelle, 2009) made us investigate the effects of coumarin on auxin transport. Therefore, we analysed the response towards coumarin in auxin efflux mutants *pin-formed 1* (*pin1)* (we used the pML1::PIN1:GFP/*pin1* x pDR5::3xVENUS-N7 mutant (Kierzkowski *et al.*, 2013)[6]), *ethylene insensitive root 1 (eir1-1* (*pin2))*, *pin-formed 3 (pin3-4)* and *ATP-binding cassette b19 (abcb19)*, and the auxin influx mutants *auxin resistant 1* (*aux1-7),* and its analogues *like auxin resistant 1 - 1, 2* and *3 (lax1, lax2* and *lax3),* as well as the double mutant *aux1-21lax3*. Next, we also used the auxin efflux transport blocker N-1-naphthylphthalamic acid (NPA) to block polar auxin transport (PAT). Significantly longer hypocotyls could be observed upon coumarin treatment in the *lax1*, *lax2* and *lax3* mutant, with the greatest additional stimulation (13% longer hypocotyls compared to the wild-type) for the *lax3* mutant (Fig. 5A). When *AUX1* was knocked-out no difference in response to coumarin could be observed and, interestingly, also the double mutant *aux1-21lax3* did not show any significant difference in response. The expression of *LAX3* is not influenced upon 40 µM of coumarin treatment in 3 and 5 DAG old seedlings, while the expression of *AUX1* decreased with 15% in both 3 as well as 5 DAG old seedlings (Fig. 5B). In *pin3-4* and *abcb19* mutants, we observed a slightly enhanced effect of coumarin on hypocotyl elongation (Fig. 5C), which is in line with pharmacological experiments where the transport is blocked via NPA (Fig. 5D). NPA treatment leads to smaller hypocotyls, but the relative increase in hypocotyl length upon coumarin treatment was larger when co-treated with 1 µM of NPA (219 % vs. 307 %) (Fig. 5D, bottom). When *PIN1* or *PIN2* were knocked out, the induced elongation of coumarin was decreased by 50 % (Fig. 5C) and also the relative response to coumarin was decreased (Fig. 5C, bottom), illustrating the importance of auxin transport during coumarin-induced hypocotyl elongation. Interestingly, the expression of *ABCB19*, *PIN1* and *PIN3* was significantly increased upon 40 µM of coumarin treatment in 3 DAG old seedlings and remained significantly increased for *PIN3* in 5 DAG old seedlings (Fig. 5E). These data indicate that coumarin affects auxin transport in the Arabidopsis hypocotyl and that a functional PIN1 and PIN2 are needed for coumarin-induced hypocotyl elongation.

[6] This is a homozygous *pin1* mutant containing an expression construct whereby *PIN1* is expressed only in the L1 layer of the shoot meristem. Expression of *PIN1* in the L1 is sufficient for correct organ position, allowing the formation of a normal inflorescence and as such seed formation (Kierzkowski *et al.*, 2013). The *pin1* mutant does not form seeds and as such needs to be analysed in a heterozygous state, which is hampering analysis.

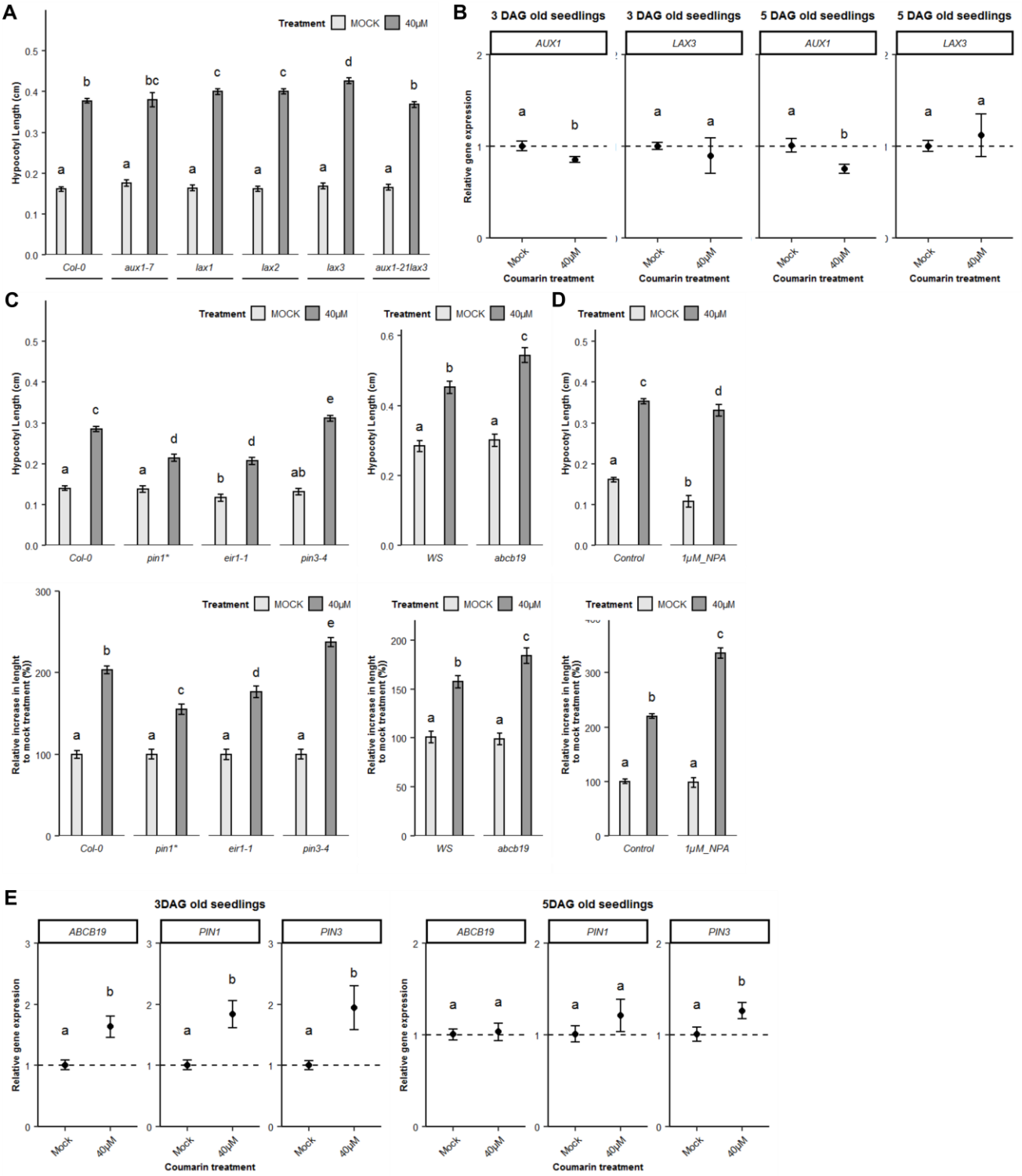

Figure 5: Coumarin influences auxin transport to stimulate hypocotyl elongation.

(A) Hypocotyl length (cm) of 5 DAG old mutants in auxin influx (*aux1-7, lax1, lax2, lax3 and aux1-21lax3*) continuously treated with DMSO (Mock) or 40 µM of coumarin compared to the Col-0 control (n≥112, except for aux1-7, n = 23). (B, E) Relative gene expression of (B) *AUX1* and *LAX3*; and (E) *ABCB19*, *PIN1* and *PIN3* in hypocotyls harvested 3 DAG (left), or 5 DAG (right) of continuously treated seedlings with DMSO (Mock) or 40 µM of coumarin. (C) (top) Hypocotyl length (cm) and (bottom) relative increase in hypocotyl length of 5 DAG old

mutants in auxin efflux (*pin1**, *eir1-1, pin3* and *abcb19*) continuously treated with DMSO (Mock) or 40 µM of coumarin compared to their corresponding control (n≥55); *pin1** is the pML1::PIN1:GFP/*pin1* x pDR5::3xVENUS-N7 mutant line. (D) (top) Hypocotyl length (cm) and (bottom) relative increase in hypocotyl length of 5 DAG old Col-0 seedlings continuously treated with DMSO (Mock) or 40 µM of coumarin in combination with 1 µM NPA (n≥58).

Data presented are relative means to the control ± lower/upper confidence interval of at least three biological repeats (A, C and D), and in (B and E) the data presented are relative means to the control ± SE of three biological repeats. Letters indicate statistically significant different means ($p < 0.05$).

Coumarin-induced hypocotyl elongation occurs independently of ethylene homeostasis

Ethylene is known to play a vital role in plant growth processes involving elongation, often by interplaying with auxin homeostasis (e.g. during apical hook opening ethylene influences AUX1 and LAX3 distribution in the hypocotyl) (Vandenbussche *et al.*, 2010; Zádníková *et al.*, 2010; Dubois, Van den Broeck and Inzé, 2018). Our data, however, illustrate that hypocotyl elongation induced by coumarin is independent of ethylene signalling. Hypocotyl length doubled compared to the control when seedlings were treated with 10 µM of 1-amino-cyclopropane-1-carboxylate (ACC), the precursor of ethylene, and its effect was blocked by silver nitrate ($AgNO_3$) (Fig. 6A). $AgNO_3$, however, could not block the effect of coumarin (Fig. 6A). Interestingly, there was also no difference in hypocotyl length of seedlings treated with both ACC (10, 50 or 100 µM) and 40 µM coumarin compared to their corresponding control treated with ACC alone. Moreover, those seedlings, even when treated with the highest concentration of ACC (100 µM) and 40 µM coumarin had hypocotyls that were smaller (37.3 mm) than those of seedlings treated with coumarin alone (43.4 mm). Interestingly, the gain-of-function mutant *CONSTITUTIVE TRIPLE RESPONSE 1* (*ctr1*-1) still reacted to coumarin although its hypocotyls reached slightly smaller lengths compared to those of the coumarin treated control, i.e. 37.9 mm versus 48.7 mm respectively, while in mock condition, hypocotyls of the *ctr1-1* mutant were significantly longer than those of Col-0 seedlings (Fig. 6B). Altogether these data indicate that high levels of ethylene prevent the action of coumarin on hypocotyl elongation. The clear increase in hypocotyl length of the loss-of-function ethylene signalling mutant *ETHYLENE RESPONSE 1* (*etr1-3)* (Fig. 6B) confirms that coumarin-induced hypocotyl elongation occurs independently of ethylene signalling. Moreover, no ethylene response was observed as there was no difference in *ETHYLENE INSENSITIVE 2* and *3* (*EIN2* and *EIN3*) expression 3 DAG, and even a significant decrease in *EIN2* and *EIN3* expression could be observed 5 DAG (Fig. S3 A, B). Remarkable, however, is the 2-fold increase in expression of the ethylene biosynthesis gene *1-AMINO-CYCLOPROPANE-1-CARBOXYLATE SYNTHASE 2 (ACS2)* 3 DAG (Fig. S3 A). However, 5 days after germination, no difference could be observed anymore (Fig. S3 B). Altogether these data lead to the conclusion that coumarin-induced hypocotyl elongation occurs independently of ethylene signalling, but that high levels of ethylene diminish the effect of coumarin.

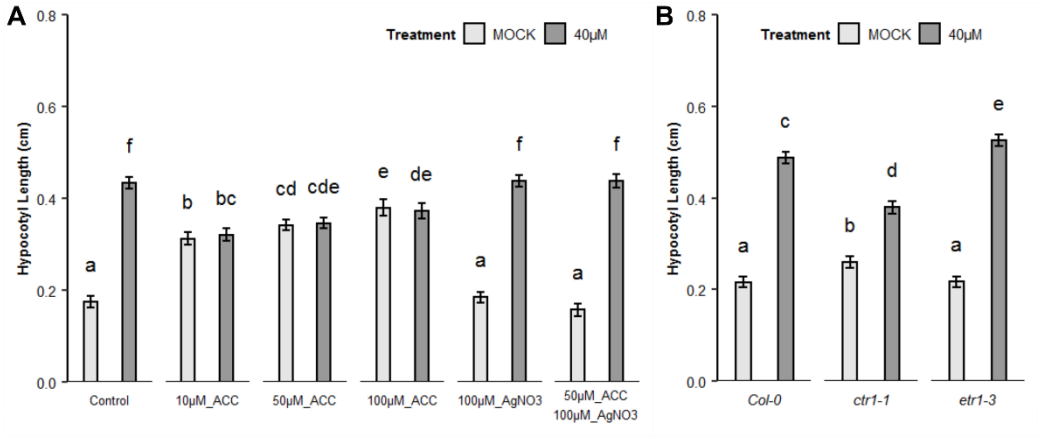

Figure 6: Coumarin induces hypocotyl elongation independent of ethylene homeostasis

(A) Hypocotyl length of 5 DAG old seedlings continuously treated with DMSO (the control), with a certain concentration of the ethylene precursor ACC (10, 50 or 100 µM), or with the ethylene signalling blocker AgNO3. All treatments are co-treated with DMSO or with 40 µM of coumarin. (n≥65). (B) Hypocotyl length of the mutants in ethylene signalling *etr1-3* and *ctr1-1* upon continuous treatment with 40 µM coumarin or DMSO. (n≥84).

Letters indicate statistically significant different means ($p < 0.05$). Data presented are means ± the confidence interval of up to three biological repeats.

Gibberellic Acid plays no or only a minor role for coumarin-induced hypocotyl elongation.

Gibberellins (GA) are known to play an important role during plant growth by stimulating organ growth, while biosynthesis or gain-of-function mutations in the DELLA proteins display dwarf phenotypes (Ross, Murfet and Reid, 1997; Peng *et al.*, 1999). Moreover, it is known that GA specifically induces hypocotyl growth via cell elongation (Smalle *et al.*, 1997; Cowling and Harberd, 1999), therefore we analysed the involvement of GA in coumarin-induced cell elongation. Pharmacological experiments revealed that hypocotyl elongation is induced by exogenous GA_3 treatment, i.e. 10 µM of GA_3 treatment stimulates hypocotyl elongation compared to the mock control (Fig. 5A). When co-treated with coumarin an additive effect is observed (Fig. 7A, left), leading to a similar response towards coumarin than the control (Fig. 7A, right). Note that treatment with paclobutrazol (PAC), a GA biosynthesis inhibitor (Rademacher, 1991), inhibited germination when co-treated with coumarin (Fig. 5A). Therefore we performed a transfer experiment whereby untreated 2 DAG old seedlings were transferred to mock condition or to PAC treatment alone or co-treated with coumarin (Fig. 7B). PAC treatment blocked coumarin-induced hypocotyl elongation (Fig. 7B). These findings imply that coumarin effects on hypocotyl elongation relies on *de novo* GA biosynthesis, which was further supported by the more than 7-fold increase in *GIBBERELLIN 20-OXIDASE 1* (*GA20OX1)* expression in the hypocotyls of 3 DAG old seedlings, a major GA biosynthesis gene (Rieu *et al.*, 2007) (Fig. 7C). This higher expression level was maintained in 5 DAG old seedlings (Fig. 7C). However, *GA20OX2* expression was not significantly enhanced in both 3 as well as 5 DAG old seedlings (Fig. 7D). Moreover, the expression of the GA catabolism gene *GIBBERELLIN 2-OXIDASE 1* (*GA2OX1*), a 2β-hydroxylase that converts bioactive GAs to their inactive forms (Thomas, Phillips and

Hedden, 1999), also significantly increased on both time points (Fig. 7D). Furthermore, when GA biosynthesis was (partly) blocked by the inactivation of the *GA20OX1* gene (the mutants *ga20ox1* and *ga5-1* in Col-0 and Ler background respectively), this had no influence on coumarin-induced hypocotyl elongation (Fig. 7E), and all mutants responded in the same extent to coumarin as the WT control (Fig. 7E, bottom). Even in the absence of a functional *GA20OX* gene, by analysis of the *ga20ox1,2,3* mutant, coumarin-induced hypocotyl elongation is not affected (Fig. 7F), and *ga20ox1,2,3* mutants even showed an enhanced response to coumarin (i.e. a 230% increase in length compared to mock, while Col-0 seedlings only illustrated a 172% increase in length) (Fig. 7F, bottom).

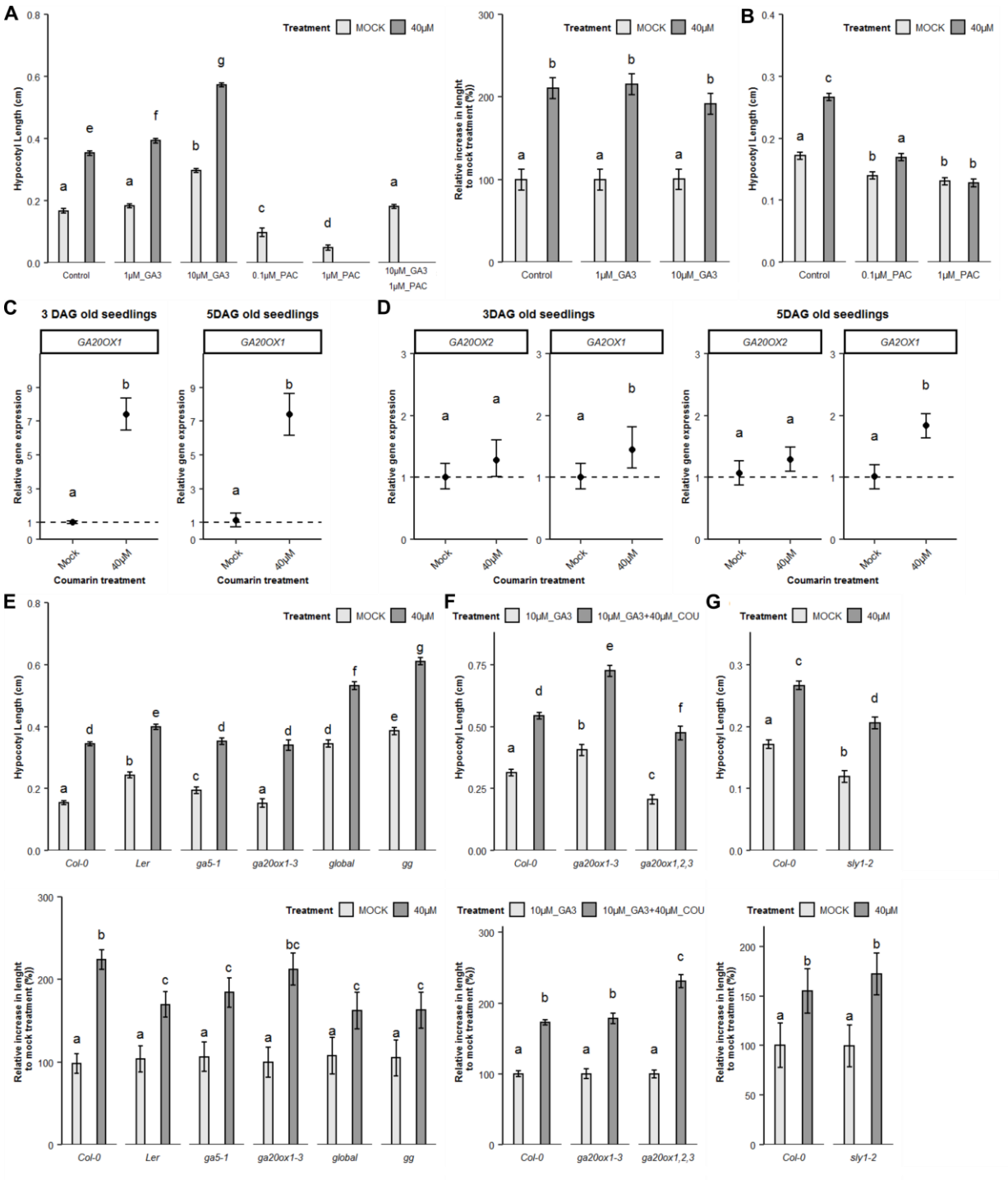

Figure 7: Coumarin induces hypocotyl elongation independently of gibberellic acid homeostasis

(A) (left) Hypocotyl length of 5 DAG old seedlings exogenous continuously treated with different concentrations of GA_3 and/or paclobutrazol (PAC) in combination with 40 µM of coumarin (n≥171). (right) The relative increase in hypocotyl length of 5 DAG old seedlings exogenous continuously treated with different concentrations of GA_3 in combination with 40 µM of coumarin (n≥197). (B) Hypocotyl length of 5 DAG old seedlings transferred 2 days after germination from mock treatment towards treatment with PAC with or without 40µM coumarin (n≥115). (C, D) Relative gene expression in hypocotyls harvested 3 (left) or 5 (right) DAG of continuously treated seedlings with 40 µM of coumarin compared to the mock control. (E) (top) Hypocotyl length (cm) and (bottom) relative increase in hypocotyl length of several mutants involved in GA biosynthesis or signalling. The *global* mutant is a knock-out mutant of all 5 DELLA proteins, i.e. *gai-t6;rga-t2;rgl1-1;rgl2-1;rgl3-4.* The *gg* mutant is the *global* mutant crossed with *ga1-3*, i.e. *global;ga1-1.* The *global, gg* and *ga5-1* are in the Ler background (n≥111). (F) (top) Hypocotyl length (cm) and (bottom) relative increase in hypocotyl length of 5DAG old mutants in GA biosynthesis *ga20ox1* and *ga20ox1,2,3* upon continuous treatment with 10 µM GA3 with or without 40µM coumarin (n≥42). (G) (top) Hypocotyl length (cm) and (bottom) relative increase in hypocotyl length of 5DAG old *sly1*-2 mutants transferred 2 days after germination from mock treatment towards treatment with PAC with or without 40µM coumarin (n≥62).

Data presented are means ± the confidence interval of up to three biological repeats (in A, B, E, F and G). Data presented are relative means to the control ± SE of three biological repeats in C and D. Letters indicate statistically different means ($p<0.05$).

Via an optogenetic biosensor, the GIBBERELLIN PERCEPTION SENSOR 1 (GPS1), that senses nanomolar levels of bioactive GAs (Rizza *et al.*, 2017), we analysed the GA-levels in the hypocotyl of 3 and 5 DAG old seedlings that were continuously treated with coumarin or mock (Fig. 8A). As a positive control, we treated seedlings for 5 days continuously with GA_4 (Fig. 8A). No difference in GA levels could be observed between mock and coumarin treated seedlings, while a clear increase in GA concentration was observed in the GA_4 treated seedlings (Fig. 8A). Quantitative analysis of the *nlsGPS1* emission ratios allows detecting minor changes in GA levels that are not detectable by qualitative analysis of the confocal images. Also quantitatively no differences could be observed between mock and coumarin treated seedling (Fig. 8B). To further study the putative role of GA during coumarin-induced hypocotyl elongation, we analysed mutants in GA signalling. The F-box receptor mutant *sleepy* (*sly1)* (Ariizumi, Lawrence and Steber, 2011), responded in the same manner to coumarin as the control (Fig. 7G). Moreover, when GA signalling was abolished via analysis of the DELLA quintuple mutant (named *global* in Ler background (Fuentes *et al.*, 2012)) the effect of coumarin was not diminished (Fig. 7E). Even the *gg* mutant (i.e. the *global* mutant crossed with the *ga1-3* mutant (*global;ga1-3):* besides a knock-out of all 5 DELLA proteins, this mutant also contains no endogenous GA levels (Fuentes *et al.*, 2012)), responded towards coumarin to the same extent as the wild type (Fig. 7E, bottom). Altogether, these data strongly suggest that coumarin elongation does not require an active *GA20ox* gene nor active GA signalling for exerting its effects and that, as such, GA is not the main driver of coumarin-induced hypocotyl elongation.

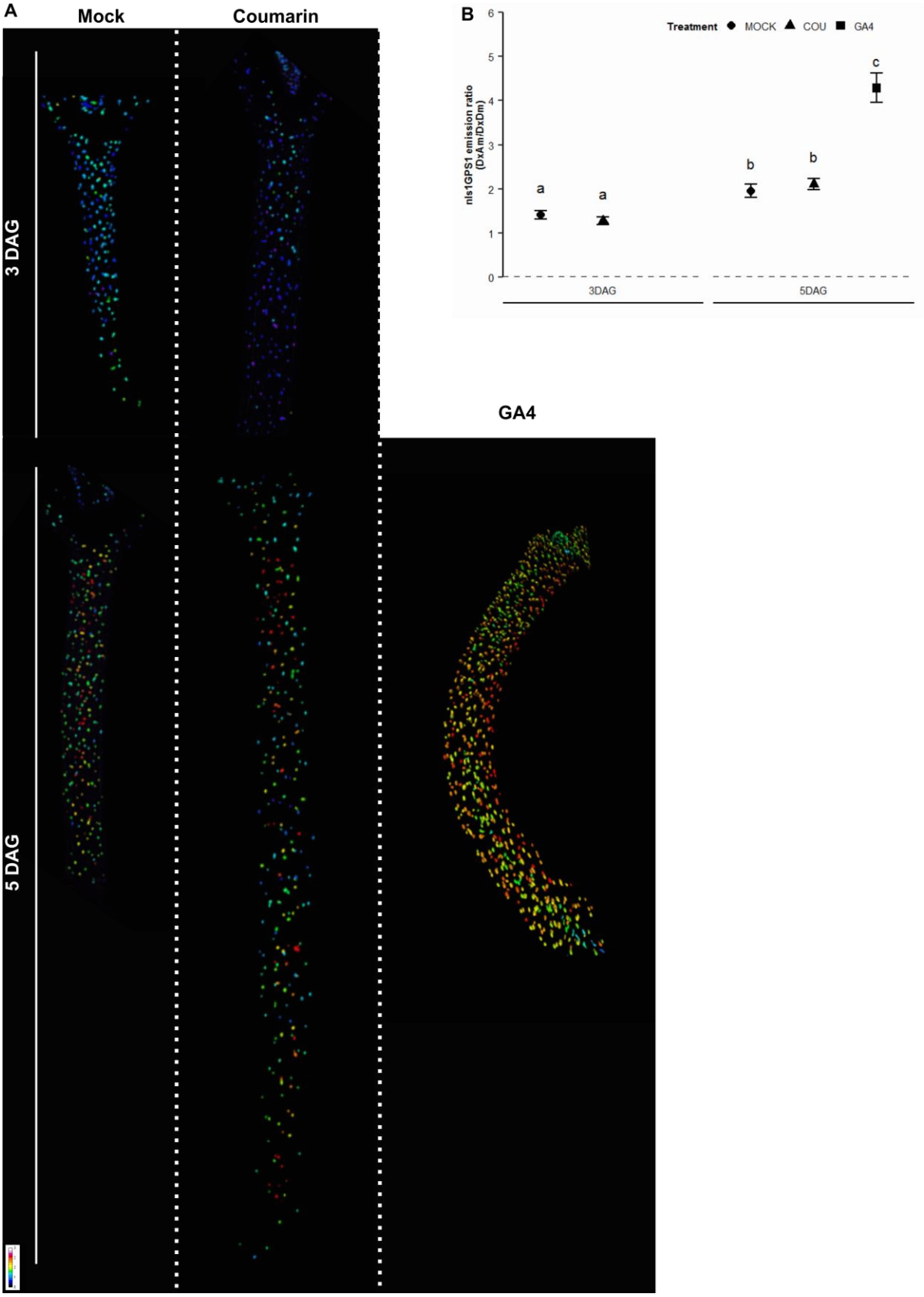

Figure 8: Emission ratios of *nlsGPS1* seedlings, focussing on the hypocotyls.

(A) Overview of emission ratio in the hypocotyl of 3 and 5 DAG old seedlings continuous treated with DMSO (mock) or 40µM coumarin, with GA_4 as positive control 5 DAG. (B) Line graph of the means ± the confidence interval of three biological repeats of the *nlsGPS1* emission ratios shown in (A) for all nuclei observed in the hypocotyl (n > 300 nuclei from three independent seedlings for each genotype).

Coumarin induces hypocotyl elongation via enhanced BR signalling and perception

Next to inhibiting GA biosynthesis, paclobutrazol also inhibits brassinosteroid (BR) biosynthesis (Asami and Yoshida, 1999; Rozhon *et al.*, 2019). Moreover, brassinosteroids are generally linked to cell elongation and BR-deficient, as well as BR-insensitive mutants, show a form of dwarfism (Clouse, 1996; Azpiroz *et al.*, 1998; Choe *et al.*, 1998; Noguchi *et al.*, 1999). Therefore, the role of BR during coumarin-induced hypocotyl elongation was investigated. Pharmacological experiments showed that coumarin-induced hypocotyl elongation is blocked by co-treatment with the BR-biosynthesis inhibitor propiconazole (PCZ, (Hartwig *et al.*, 2012)) (Fig. 9A). Interestingly, when BR signalling was enhanced via treatment with bikinin, a small molecule that directly binds and inhibits *BRASSINOSTEROID-INSENSITIVE 2 (BIN2)* and, as such, activates BR signalling (De Rybel *et al.*, 2009), hypocotyl length was more than doubled as compared to the control, and the relative increase by coumarin exceeded the control by 10% (Fig. 9A). In addition, the dominant mutant *bri1-EMS-suppressor 1* (*bes1-D*), which exhibits a constitutive BR response (Yin *et al.*, 2002), illustrated a strongly enhanced reaction towards coumarin. Upon coumarin treatment, the *bes1-D* mutant hypocotyls were 53 mm long compared with 33 mm of the Col-0 coumarin-treated control, while no difference in length could be observed between the mock-treated seedlings (i.e. *bes1*-D mock vs. Col-0 mock) (Fig. 9B).

The need for BRs during coumarin-induced hypocotyl elongation is further confirmed via mutant analysis. The BR biosynthesis mutants *dwarf 1* and *4* (*dwf1 and dwf4)* and *deetiolated 2* (*det2-1)* are insensitive towards coumarin in terms of hypocotyl elongation (Fig. 9B), illustrating the need for BRs. Moreover, the BR perception mutants *brassinosteroid insensitive 1 (bri1-116* and *bri1-5)* are insensitive towards coumarin in terms of hypocotyl elongation and the *bri1-associated receptor kinase 1* (*bak1-4*) mutant showed a strongly diminished response towards coumarin (Fig. 9B). Transcriptionally, increased expression of BR biosynthesis genes was observed: while the expression of *DET2* was not influenced, the expression of *DWF1* and *DWF4* was increased 3 DAG upon coumarin treatment and the expression of *DWF4* remained higher 5 DAG (Fig. 9C, D). Also, increased expression of the BR receptor *BRI1* was observed 3 DAG upon coumarin treatment, which remained slightly higher in 5 DAG old hypocotyls, while the expression of the co-receptor *BAK1* was not affected by coumarin at any time point (Fig. 9C, D).

To distinguish whether coumarin-induced hypocotyl elongation depends on an operational BR biosynthesis machinery, a complementation experiment was performed in which the *det2-1* mutant was exogenously treated with brassinolide (BL). It is known that BL treatment can rescue the leaf size of *det2-1* mutants by increasing both cell size and numbers (Nakaya *et al.*, 2002). We observed that upon 10 nM BL treatment, also hypocotyl length was partly restored (Fig. 9E). Moreover, hypocotyl length was significantly increased in *det2*-1 seedlings treated with 40 µM coumarin and 10 nM BL, compared with 10 nM BL treatment (Fig. 9E). However, *det2*-1 hypocotyls treated with10 nM BL responded less to coumarin than the WT control

(Fig. 9E, right). No difference in expression of *BIN2* and its antagonist *BRI1-EMS-SUPPRESSOR 1 (BES1)* was observed in 3 DAG old seedlings upon 40 µM of coumarin treatment, while a significant decrease in expression was observed of *BES1* in 5 DAG old seedlings (Fig. 9F). However, we did observe an increased expression of *BRASSINAZOLE RESISTANT 1* (*BZR1)* 3 DAG illustrating that coumarin increases BR signalling at the transcriptional level via *BZR1* (Fig. 9C). Altogether, these data indicate that BRs are needed for coumarin-induced hypocotyl elongation, but that at least part of the phenotype does not need increased BR biosynthesis, while coumarin clearly enhances BR signalling.

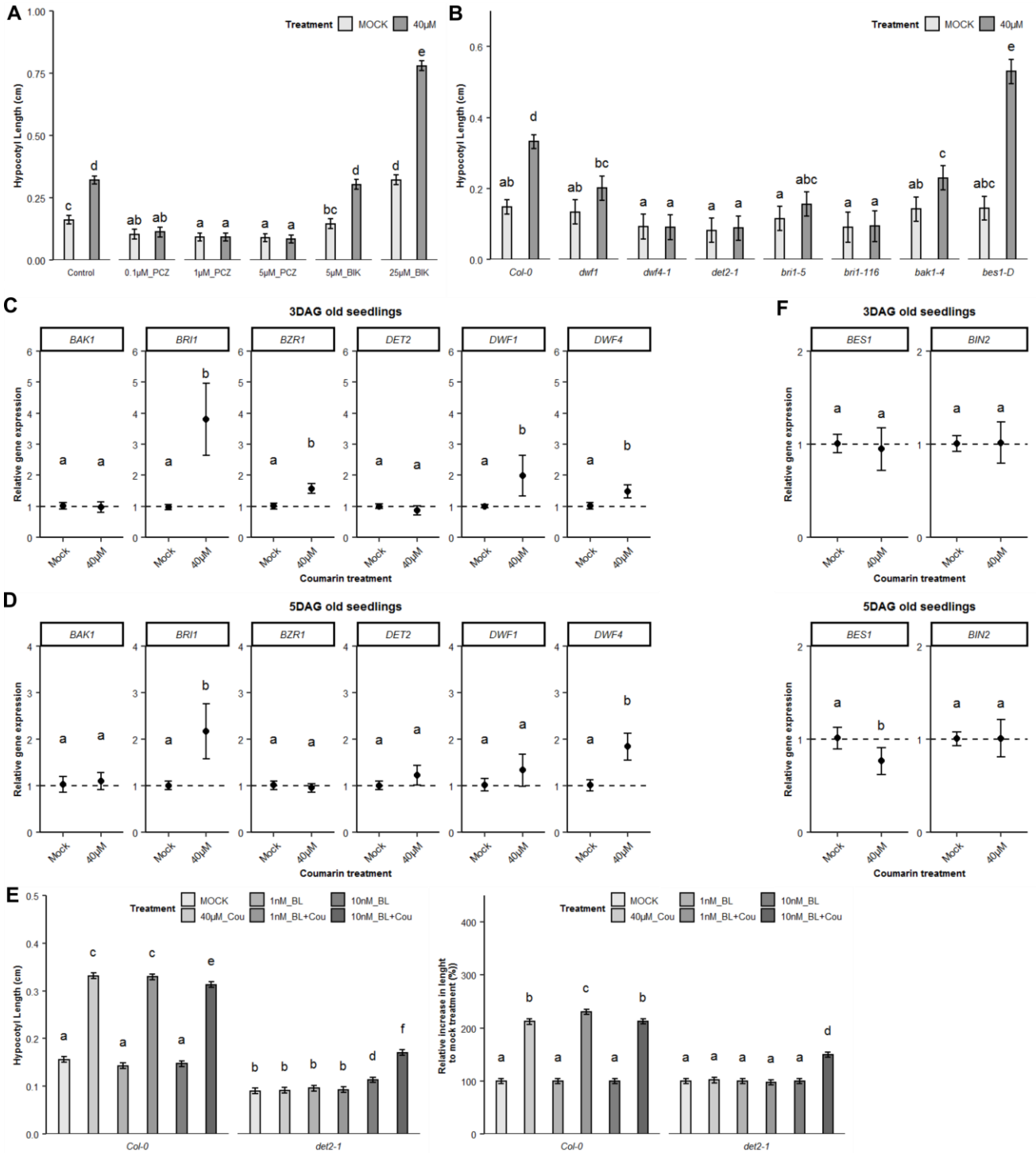

Figure 9: Coumarin induces hypocotyl elongation via increased brassinosteroid signalling

(A) Hypocotyl length of 5 DAG old seedlings continuous treated with mock or 40µM of coumarin in combination with treatment of propiconazole (PCZ) or bikinin (BIK) (n≥120). (B) Hypocotyl length of 5 DAG old seedlings mutated in genes involved in brassinosteroid synthesis or signalling. Col-0 and Ler are the corresponding control ecotypes. (C, D) Relative gene expression in hypocotyls harvested 3 (C) or 5 (D) days after germination of continuously treated seedlings with 40 µM of coumarin compared to the mock control. (E) (left) Hypocotyl length and (right) relative increase in hypocotyl length of 5DAG old Col-0 or *det2-1* seedlings that are treated with different concentrations of brassinolide (BL), in combination with DMSO or 40µM of coumarin. (F) Relative gene expression in hypocotyls harvested 3 (top) or 5 (bottom) DAG of continuously treated seedlings with 40 µM of coumarin compared to the mock control.

Data presented are means ± the confidence interval of up to three biological repeats (in A, B and E). Data presented are relative means to the control ± SE of three biological repeats in C, D and R. Letters indicate statistically different means ($p<0.05$).

Coumarin induces hypocotyl elongation by transcriptional activation of a BR response

BZR1 interacts with PHYTOCHROME-INTERACTING FACTOR (PIF) factors, especially PIF4, and together they interact with AUXIN RESPONSE FACTOR 6 (ARF6), creating a trimeric complex that regulates gene expression to induce elongation (Gallego-Bartolome *et al.*, 2012; M.-Y. Bai, Fan, *et al.*, 2012; Oh *et al.*, 2014). According to qRT-PCR analyses, the expression of *PIF4* was not changed upon coumarin treatment in 3 and 5 DAG old seedlings, while the expression of *ARF6* was significantly reduced at both time points (Fig. 10A). The *pif4-2* mutant is still responsive towards coumarin treatment in terms of hypocotyl elongation (Fig. 10B, left), although to a smaller extent than the WT (Fig. 10B, right).

Next, we studied how coumarin-mediated cell elongation involves genes acting downstream of the BR response. To this end, an expression analysis was performed of three well-known BR response genes, involved in elongation processes: *BR ENHANCED EXPRESSION 1 (BEE1), PACLOBUTRAZOL RESISTANT 1 (PRE1) and GATA TRANSCRIPTION FACTOR 2 (GATA2). BEE1* is an early response gene required for BR response and a direct downstream target of BES1 (Friedrichsen *et al.*, 2002; Yin *et al.*, 2005)*, PRE1* functions downstream of BZR1 to mediate BR regulation of cell elongation (L.-Y. Zhang *et al.*, 2009) and *GATA2* is a positive regulator of photomorphogenesis and thus an antagonist of cell elongation (i.e. an inhibitor of cell elongation) (Terzaghi and Cashmore, 1995; Luo *et al.*, 2010). We observed a 3-fold increase in expression of *PRE1*, 3 DAG upon 40 µM of coumarin treatment that further increased to 5-fold 5 DAG (Fig. 10C). The expression of *BEE1* increased 3-fold in 3 DAG old seedlings continuously grown upon 40 µM of coumarin and persisted in 5 DAG old hypocotyls (Fig. 10C). The expression of *GATA2* decreased with 80% upon 40 µM of coumarin treatment, but 5 DAG, no difference could be observed between mock and coumarin treated seedlings (Fig. 10C).

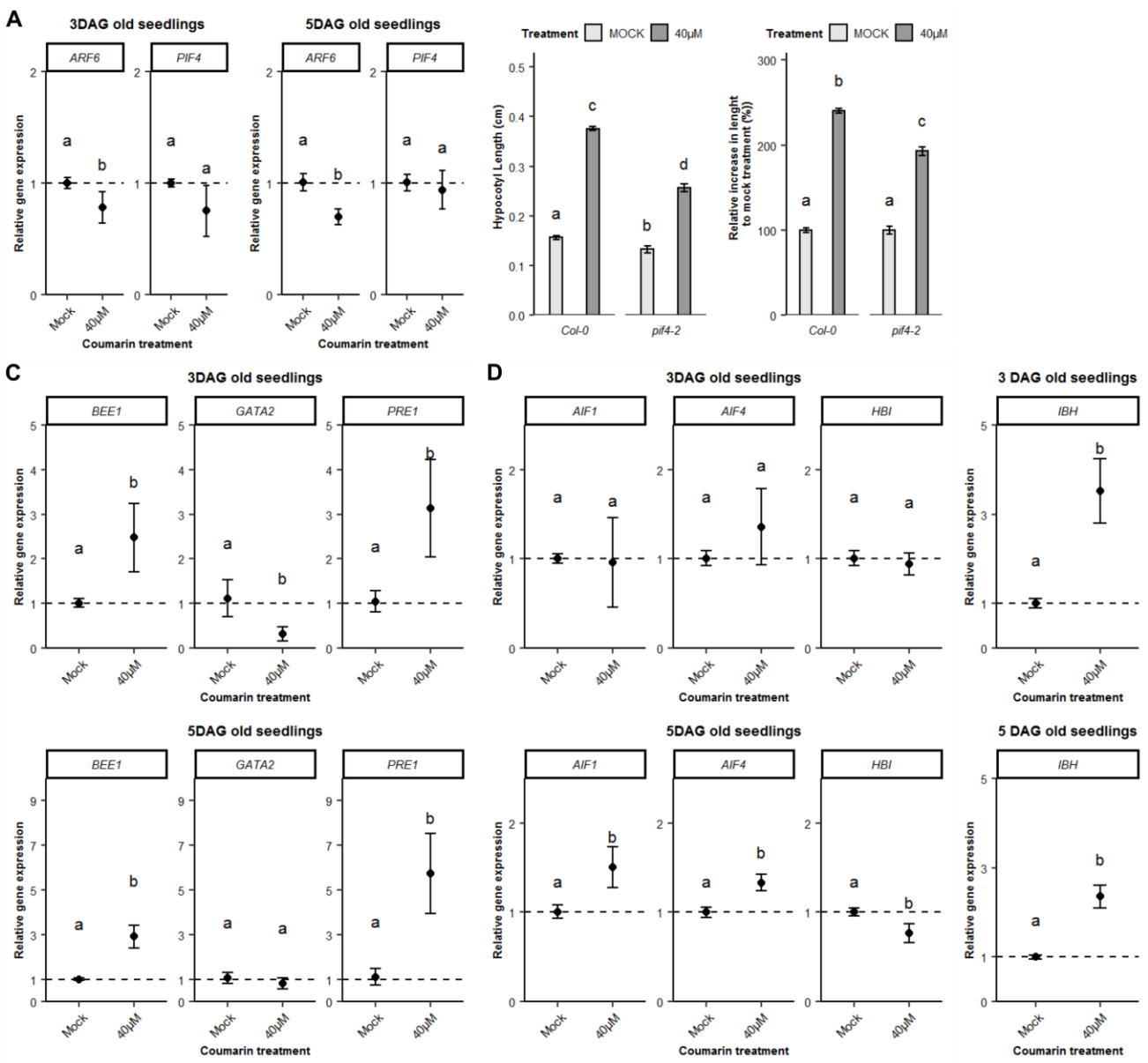

Figure 10: Coumarin induces a transcriptional BR response

(A, C and D) Relative gene expression in hypocotyls harvested 3 (left, up) or 5 (right, down) DAG of continuously treated seedlings with 40 µM of coumarin compared to the mock control. (B) (left) Hypocotyl length and (right) relative increase in hypocotyl length of the 5 DAG old *pif4-2* mutants continuously treated with 40 µM of coumarin compared to Col-0 (n≥134).

Data presented are means ± the confidence interval of at least three biological repeats (B), or (in A, C and D) the relative means to the control ± SE of three biological repeats. Letters indicate statistically different means ($p<0.05$)

BRs are known to induce cell elongation via a triple Helix-Loop-Helix/Basic Helix-Loop-Helix cascade (Fig. S4) (Ikeda *et al.*, 2012; M.-Y. Bai, Fan, *et al.*, 2012; Oh *et al.*, 2014). PRE-family basic helix-loop-helix (bHLH) factors promote cell elongation by interacting antagonistically with *ILI1 BINDING bHLH 1 (IBH1)* (L.-Y.

Zhang *et al.*, 2009; Ikeda *et al.*, 2012; M.-Y. Bai, Fan, *et al.*, 2012) and *ACTIVATION-TAGGED BRI1 SUPPRESSOR 1 (ATBS1) INTERACTING FACTORs (*AIFs) (Wang *et al.*, 2009; Ikeda, Mitsuda and Ohme-Takagi, 2013). There are four *AIF* genes in *Arabidopsis thaliana* of which *AIF1* is the direct target of BEE1 and is known to interact with *PRE3,* while AIF2-4 directly inhibits PRE1*,* whereby AIF4 has the highest affinity for PRE1 and is also the only member of the family upregulated in light-grown conditions (Wang *et al.*, 2009; Ikeda, Mitsuda and Ohme-Takagi, 2013). IBH1 inhibits HOMOLOG OF BEE2 INTERACTING WITH IBH1 (HBI1), a positive regulator of cell elongation. HBI1 directly activates, by binding their promoters, *EXP1* and *EXP8,* leading to stimulation of elongation (Fig. S4)(Oh *et al.*, 2014). The expression of *AIF1* and *AIF4* did not significantly change in 3 DAG old seedling upon coumarin treatment, while it was significantly increased in 5 DAG old hypocotyls upon 40 µM coumarin treatment (Fig. 10D). *IBH* and *HBI* are antagonists and this was also observable on the transcript level. However, while one would expect the opposite, the expression of *IBH1* increased a 3-fold upon 40 µM of coumarin treatment in 3 DAG old seedlings, and the expression of *HBI* did not change (Fig. 10D). In 5 DAG old hypocotyls, the expression levels of *IBH* remained 2.5-fold higher than the control, while the relative expression of *HBI* decreased to 75% of the control (Fig. 10D). These data indicate that coumarin induces a clear BR response, but that the increase of *PRE1* expression does not lead to activation of the triple antagonistic basic Helix-Loop-Helix cascade (PREs-IBH-AIFs) (Ikeda *et al.*, 2012; M.-Y. Bai, Fan, *et al.*, 2012; Ikeda, Mitsuda and Ohme-Takagi, 2013).

Coumarin stimulates elongation through PHYB mediated inhibition of photomorphogenesis

Upon coumarin treatment, there is a 3-fold increase in expression of *BEE1*, 3 DAG, and this elevated expression level persists in 5 DAG old hypocotyls (Fig. 10C). The enhanced expression of *BEE1*, could, besides showing a clear BR response, also hint to a role of the Shade Avoidance Syndrome (SAS), as BEE1 is a positive modulator of it (Cifuentes-Esquivel *et al.*, 2013). Therefore, we analysed the expression profile of *PHYTOCHROME RAPIDLY REGULATED1 (PAR1*), a negative regulator of the SAS acting by direct transcriptional repression of auxin- and BR-responsive genes (Bou-Torrent *et al.*, 2008). Transcriptional analysis revealed, however, that *PAR1* expression is not affected upon 40 µM of coumarin treatment 3 DAG and is even upregulated 5 DAG, at the end of the elongation phase (Fig. 11A). LONG HYPOCOTYL 5 (*HY5*) is known to work downstream of BRs to induce photomorphogenesis, and hence inhibits hypocotyl elongation (Gangappa and Botto, 2016). However, HY5 is also required for hypocotyl and petiole elongation during SAS through PHYTOCHROME A (PHYA) signalling (Ciolfi *et al.*, 2013; Nozue *et al.*, 2015). PHYA is classified as type I phytochrome and highly abundant in etiolated seedlings but drastically decreased upon exposure to light (Sharrock and Quail, 1989; Mathews, Lavin and Sharrock, 1995; Smith, 2000; Inoue, Nishihama and Kohchi, 2017). While *HY5* expression was significantly increased in 3 DAG old hypocotyls upon 40 µM coumarin treatment, no difference was observed anymore 5 DAG (Fig. 11A). The *hy5-1* mutant showed elongated hypocotyls in the light (Fig. 11B, top) but responded in the same manner to coumarin as the control (Fig. 11B, bottom), and also the *phya-201* mutant responded to coumarin treatment (Fig. 11B, top), although in a lesser extent than the WT (Fig. 11B, bottom). Altogether these data suggest that coumarin operates independently of the SAS – under control of *PHYA* and *HY5* – to induce hypocotyl elongation.

Coumarin induces hypocotyl elongation in the light, indicating a potential interaction with photomorphogenesis, supported by the strong transcriptional downregulation of the positive photomorphogenesis regulator *GATA2* (Fig. 10C). Besides *GATA2,* BZR1 is also known to inhibit photomorphogenesis by transcriptional repression of *PHYB* (Lau and Deng, 2010; Luo *et al.*, 2010; Wu *et al.*, 2019). PHYB belongs to the type II phytochromes, indicating they are relatively light-stable and present in de-etiolated seedlings and adult plants, where PHYB is known to be the main inducer of photomorphogenesis (Sharrock and Quail, 1989; Mathews, Lavin and Sharrock, 1995; Reddy and Sharma, 1998; Smith, 2000; Sharrock and Clack, 2002; Inoue, Nishihama and Kohchi, 2017). The *phyb-5* mutant and also the double mutant *phya-201;phyB-5* are completely insensitive towards coumarin in terms of hypocotyl elongation (Fig. 11B). These data indicate that coumarin stimulates hypocotyl elongation via activation of BR signalling and thereby affecting photomorphogenesis in a PHYB-dependent manner.

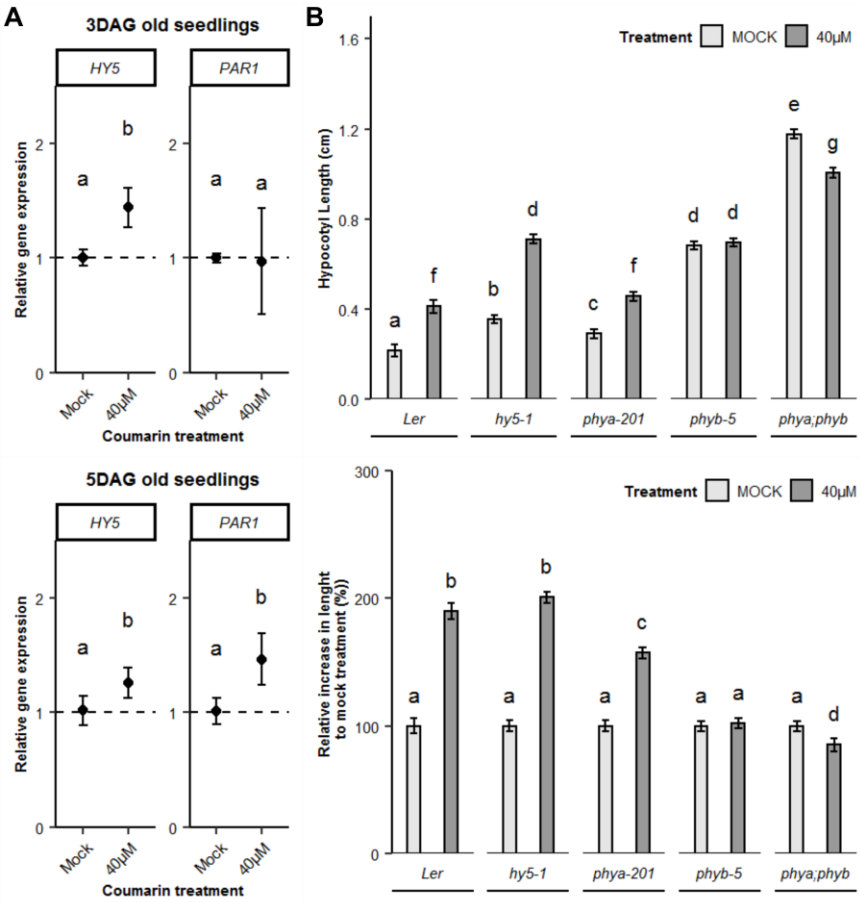

Figure 11: Coumarin stimulates elongation in a PHYB-dependent manner.

(A) Relative gene expression in hypocotyls harvested 3 (top) or 5 (bottom) DAG of continuously treated seedlings with 40 µM of coumarin compared to the mock control. (B) (top) Hypocotyl length and (bottom) relative increase in hypocotyl length of the 5DAG old mutants: *hy5-1*, *phya-201*, *phyb-5* and *phya-201*;*phyb-5*, with Ler as their control (n≥57). Data presented in (A) are relative means to the control ± SE of three biological repeats, and the data presented in (B) are means ± the confidence interval of three biological repeats. Letters indicate statistically different means (p<0.05).

Discussion

Here we show that coumarin relies on the interplay of auxin and brassinosteroid (BR) homeostasis in order to induce plant cell elongation in light-grown Arabidopsis hypocotyls. That coumarin interacts with auxin has been historically well documented (Audus and Quastel, 1947; Audus, 1948, 1950; Neumann, 1959; Dhawan and Nanda, 1982; Lupini *et al.*, 2014) yet the exact *mode-of-action* has hitherto not been clearly described.

The interaction of auxin and coumarin happens, likely, at the level of auxin transport. Polar auxin transport is crucial for hypocotyl elongation in the light and not for dark-grown Arabidopsis seedlings, i.e. NPA blocked the elongation of light-grown hypocotyls, while it didn't in the dark (Jensen, Hangarter and Estelle, 1998). That the polar auxin transport is influenced by coumarin was already reported specifically with regards to changes in root architecture upon coumarin treatment (i.e. reduction of the main root length while stimulating lateral root formation) (Lupini *et al.*, 2014). For these effects, the importance of AUX1 and LAX3 as auxin influx proteins was shown (Lupini *et al.*, 2014), but, remarkably, for coumarin-induced hypocotyl elongation, those proteins (and hence auxin influx in general) are not important, as mutants are still responsive to coumarin. Even more remarkable is that when *LAX3* is knocked out, an additional elongation by coumarin is apparent. All of this is no longer possible when additionally *AUX1* is knocked out too in double mutants. LAX3 localizes to the basal part of the hypocotyl and is involved in the redistribution of auxin to the neighbouring cells (Vandenbussche *et al.*, 2010; Zádníková *et al.*, 2010). AUX1, on the other hand, is needed for basipetal auxin transport from the cotyledons to the hypocotyl (Swarup and Bhosale, 2019). Together, this could indicate that the *LAX3* inactivation leads to a localized slightly higher increased auxin level, while this not the case in the double mutant *aux1-21lax3* because of the diminished PAT from the shoot in the double mutant (Zádníková *et al.*, 2010), rationalizing their different responses towards coumarin regarding hypocotyl elongation.

With regards to auxin efflux by PIN proteins, we showed that PIN1 and PIN2 are instrumental for coumarin to induce elongation. PIN1 is localized on the basal side of cells in the vascular tissue of the stem, and important for auxin transport from the shoot tip to the root tip, which is further confirmed by the reduced PAT in *pin1* mutants (Galweiler *et al.*, 1998; Li *et al.*, 2005). PIN1 localization overlaps with the regions in which we observed a clear auxin response upon coumarin treatment: at the base of the hypocotyl and close to the SAM (Omelyanchuk *et al.*, 2016). *PIN1* expression is upregulated upon coumarin treatment, in line with its known upregulation upon auxin treatment (Omelyanchuk *et al.*, 2016), and *pin1* or *pin2* mutants (PIN2 the main driver of PAT in the root (Luschnig *et al.*, 1998; Müller *et al.*, 1998)) display a 50% reduction in hypocotyl elongation upon coumarin treatment. PIN2 is mainly localised in the root tip (Friml *et al.*, 2003a), making this observation remarkably. We assume that reduced response to coumarin observed of *pin2* mutants is the consequence of a general reduced PAT, and hence an indirect effect rather than a direct effect. Remarkably, in *pin3* mutants, coumarin can induce elongation more than in the wild type. As it is known that PIN3, during phototropism and apical hook opening, restricts elongation at one side of the hypocotyl by directing auxin to the PAT (Zádníková *et al.*, 2010; Ding *et al.*, 2011), this could lead to a locally higher concentration of auxin, which in turn might stimulate elongation even further upon coumarin treatment. Note that the same enhanced elongation upon coumarin treatment is noted for the *abcb19* mutant. The ABC transporter, ABCB19 is predominantly localized at the plasma membrane to mediate polar auxin transport (Noh *et al.*, 2003; Blakeslee

et al., 2007) and displays an enhanced accumulation of auxin in the upper hypocotyl (Nagashima, Uehara and Sakai, 2008; Christie *et al.*, 2011; Christie and Murphy, 2013), which is exactly where we observe an enhanced auxin response (through pDR5rev::GFP reporter line analyses). To get a better idea on how coumarin affects auxin transport we suggest to spatiotemporally analyse translational reporter lines of the affected auxin transporters: LAX3, ABCB19, PIN1 and PIN3.

Through DR5rev::GFP analyses, we showed that there is an enhanced auxin response upon coumarin treatment, also underlined by the noted higher *SAUR19* expression. Moreover, auxin perception (through *TIR1, AFB2 and AFB3*) and downstream signalling (e.g., through *SLR-1*) were found to be crucial for coumarin induced cell elongation, but, interestingly, *de novo* auxin biosynthesis is not. Remarkably, high concentrations of exogenously added auxins blocked the elongation potential of coumarin, which is in line with the typical bell-shaped responses observed for auxin action on plant growth in which it is hypothesized that sub-optimal auxin levels are created once concentrations exceed a certain level (Collett, Harberd and Leyser, 2000; Chapman *et al.*, 2012). The canonical TIR1/AFB-Aux/IAA-ARF pathway can account for auxin-mediated polarization phenomena, for example in the shoot apical meristem where it was shown that auxin acts through MONOPTEROS (an ARF) to regulate plant cell polarity. As such nuclear auxin signalling affects auxin-regulated cell polarization. In other words: through the TIR/AFB-AUX/IAA-ARF system PINs can be reoriented (Bhatia *et al.*, 2016; Leyser, 2018). This could mean that the non-response of auxin signalling mutants toward coumarin (cf. above) could alternatively be attributed to altered auxin transport.

Spartz *et al.*, (2014) showed that auxin induces *SAUR* gene expression stimulating plasma membrane H^+-ATPase activity by adjusting its phosphorylation. Coumarin induces expression of *SAUR19* with more than a 5-fold in a 3 DAG old hypocotyl. It has been shown that *GFP-SAUR19* seedlings and a stronger overexpression line of *SAUR19*, the *35S::StrepII-SAUR19* line (Spartz *et al.*, 2012), reached hypocotyl lengths of 2.5 and 3 mm respectively, compared to 1.5mm mock Col-0 (Spartz *et al.*, 2012, 2014). Also in our set-up hypocotyls of p35S::SAUR19-GFP seedlings (Spartz *et al.*, 2012) and *ost2-2D* mutants are significantly longer than the control. The total lengths are, however, different than the ones published by (Spartz *et al.*, 2012) which can be explained by the different growth conditions: our experiments are performed in long-day conditions and seedling are analysed 5 days after germination, while in their set-up seedlings were grown under continuous light conditions and were analysed 8 days after germination. The *StrepII-SAUR19* transgene in the *aha2-4* background, displayed hypocotyls lengths that were not significantly different from the control (Spartz *et al.*, 2014), showing that the hypocotyl elongation effect of *SAUR19* fully depends on a functional *AHA2* gene. Coumarin-induced hypocotyl elongation, however, does not need a functional *AHA2* gene as the *aha2-4* mutant is only slightly less responsive to coumarin treatment. This limits the role of SAUR19 during coumarin-induced hypocotyl elongation. Nevertheless, we cannot exclude the role of auxin in the process, as it has been observed that hypocotyls of *aha2-4* mutants still respond to auxin-dependent phenotypes (Haruta *et al.*, 2010; de Wit, Lorrain and Fankhauser, 2014). Moreover, *AHA1* and *AHA2* are found to operate highly redundantly (Haruta and Sussman, 2012), indicating that indeed the role of SAUR19 in the process can be limited, but we cannot exclude the function of acidification, moreover, it can still be a main driver in the process. To further investigate the role of PM H^+-ATPase pumps during coumarin-induced hypocotyl elongation, we suggest analysing the pH changes in the apoplast as for example illustrated with HPTS staining (Barbez *et al.*, 2017).

Note that it was found that *SAUR19* also can operate independently from auxin and that *SAUR19* expression is also regulated via PIFs directly and via brassinosteroids. This indicates an auxin independent regulation of acidification of the cell wall leading to cell elongation (M.-Y. Bai, Shang, *et al.*, 2012; Oh, Zhu and Wang, 2012; Fendrych, Leung and Friml, 2016). Moreover, the expression of many *SAUR* genes is induced by other growth-promoting pathways, including brassinosteroids, gibberellin, and the PIF transcription factor (M.-Y. Bai, Shang, *et al.*, 2012; Oh, Zhu and Wang, 2012).

To the best of our knowledge, no reports thus far link coumarin action with brassinosteroid metabolism and/or signalling. BRs play a major role during hypocotyl elongation (Clouse, 1996; M.-Y. Bai, Fan, *et al.*, 2012). Since the BR biosynthesis mutants *dwf1*, *dwf4* and *det2-1* are completely insensitive towards coumarin in terms of hypocotyl elongation it is clear that adequate BR levels are also required for coumarin to push cells to elongate more. This is further confirmed via pharmacological experiments with propiconazole (PCZ) and with paclobutrazol (PAC) that both inhibit BR biosynthesis (Asami and Yoshida, 1999; Hartwig *et al.*, 2012). Note that the latter is more known for its effect on GA biosynthesis by interfering with the cytochrome P450-mediated conversion of ent-kaurene to ent-kaurenoic acid (Rademacher, 1991). The coumarin response of *det2-1* mutants supplemented with brassinolide shows that also without *de novo* formation of brassinosteroids, hypocotyl elongation can be induced by coumarin. However, the increase in *DWF1* and *DWF4* expression in 3 DAG old seedlings, could hint on increased BR biosynthesis upon coumarin treatment. More research will be needed to quantify the causality. *DWF4* is a key regulator in BR biosynthesis and BR homeostasis (Yoshimitsu *et al.*, 2011), and also a point of hormonal interplay as for example increased auxin levels are reported to lead to upregulation of *DWF4* expression (Chung *et al.*, 2011; Yoshimitsu *et al.*, 2011).

BR perception relies on the BRI1 receptor and multiple co-receptors of the SOMATIC EMBRYOGENESIS RECEPTOR-LIKE KINASE (SERK) family that can hetero-dimerize with BRI (Ma *et al.*, 2016; Hohmann *et al.*, 2018). *BRI1* expression increases in elongating tissues (Hategan *et al.*, 2014), and fully in line with this, its expression is upregulated at 3 DAG upon coumarin treatment, but no longer at 5 DAG when the hypocotyl ceased to elongate. Interestingly, hypocotyls of *bri1* mutants are non-responsive toward coumarin and the BRI1-ASSOCIATED RECEPTOR KINASE 1 (one of the co-receptors) mutant *bak1-4* has a strongly diminished response. The latter can be potentially explained by redundancy between SERK family members. Conversely, when BR signalling is activated – through bikinin treatment that inactivates BIN2 (De Rybel *et al.*, 2009) or in the dominant mutant BRI1-EMS-SUPPRESSOR 1 (*bes1-D*), which exhibits a constitutive BR response (Yin *et al.*, 2002) – a strongly enhanced effect of coumarin on hypocotyl elongation can be noted. Our transcript data suggest that BR target genes, which include numerous cell-wall-related proteins that ultimately induce elongation (Yin *et al.*, 2002; Sun *et al.*, 2010), are probably activated through the transcription factor BZR1 because BRI1-EMS-SUPPRESSOR1 (*BES1*) (another BR transcription factor) nor *BIN2* display any differential expression at 3 DAG. BZR1 forms a part of the trimeric module BZR1-ARF6-PIF that co-regulates cell elongation in the shoot via activating many genes with known functions in cell elongation (e.g. *EXPANSIN A8 (EXP8), BES1-INTERACTING MYC-LIKE1 (BIM1), BR-ENHANCED EXPRESSION 1/3 (BEE1/3), PACLOBUTRAZOL RESISTANCE (PREs), HISTONE ACETYLTRANSFERASE 2 (HAT2), ILI1 BINDING BHLH 1 (IBH1), LONG HYPOCOTYL IN FAR-RED (HFR1), PHY RAPIDLY REGULATED 1/2 (PAR1/2), EXORDIUM (EXO), SAUR19*) (Nemhauser, Mockler and Chory, 2004; Gallego-Bartolome *et al.*, 2012; M.-Y.

Bai, Shang, *et al.*, 2012; Oh, Zhu and Wang, 2012; Oh *et al.*, 2014). Next to the above-mentioned importance of BZR1, mutant analysis has shown that also PIF4 may play a role for coumarin action on elongation, as *pif4* mutants are less-responsive. In addition, the expression of *ARF6* is negatively regulated by auxin (Wang, Bai and Wang, 2014), making the involvement of the BZR1-ARF6-PIF module during coumarin induced elongation likely. However, more experiments and mutant analysis will be needed to prove this hypothesis.

PRE1 expression is induced by BRs, repressed by light, abundant in young and growing tissues (M.-Y. Bai, Fan, *et al.*, 2012; Oh, Zhu and Wang, 2012; Oh *et al.*, 2014), and is a target of the BZR1-ARF6-PIF module (Oh *et al.*, 2014). We observed a clear induced expression of *PRE1* in light-grown hypocotyls upon coumarin treatment. In its turn, PRE inhibits expression of *IBH1* (L.-Y. Zhang *et al.*, 2009), ATBS1 INTERACTING FACTORs (AIFs) (Wang *et al.*, 2009; Ikeda, Mitsuda and Ohme-Takagi, 2013), and PAR1/2 (Hao *et al.*, 2012). This inhibition leads to the activation of several other basic helix–loop–helix (bHLH) factors, such as HOMOLOG OF BEE2 INTERACTING WITH IBH1 (HBI1) and ACTIVATORS FOR CELL ELONGATION (ACEs) (Ikeda *et al.*, 2012; M.-Y. Bai, Fan, *et al.*, 2012; Fridman and Savaldi-Goldstein, 2013; Ikeda, Mitsuda and Ohme-Takagi, 2013; Singh and Savaldi-Goldstein, 2015). Upon coumarin treatment, *AIF1*, *AIF4* and *PAR1* did not significantly change in 3 DAG old seedlings while the expression of *IBH1* increased and the expression of *HBI* decreased significantly – markedly different than the reported expression profiles upon *PRE1* increase. This can indicate that coumarin operates independently of *PRE1* and that as such the transcriptional increase is not causal and other factors influence *PRE1* expression. However, it has been shown that *PRE1* overexpression alone is sufficient to induce hypocotyl elongation in Arabidopsis, leading to comparable lengths as upon coumarin treatment (3-4 mm) (S. Lee *et al.*, 2006) (and also stimulates cotton fibre elongation (Zhao *et al.*, 2018)). Moreover, until today it has not been shown that *PRE1*-induced elongation depends on the IBH-HBI signalling cascade to induce elongation but only that its increased expression activates that cascade (M.-Y. Bai, Fan, *et al.*, 2012; Oh *et al.*, 2014). Therefore, to induce hypocotyl elongation, it is possible that *PRE1* also operates via another, currently, unknown signalling cascade.

Other targets of the BZR1-ARF6-PIF module include *PIN* and *SAUR* genes (Oh *et al.*, 2014) linking auxin and BR homeostasis. Further complicating this interplay is the fact that increased auxin levels saturate the BR-stimulated growth leading to an inhibited phenotype (Nemhauser, Mockler and Chory, 2004) which might offer an alternative explanation for the diminished response toward coumarin under high auxin conditions. BR ENHANCED EXPRESSION 1 (BEE1), a direct downstream target of BES1 and a positive regulator of the Shade Avoidance Syndrome (SAS) (Friedrichsen *et al.*, 2002; Yin *et al.*, 2005; Cifuentes-Esquivel *et al.*, 2013) is also a target of the BZR1-ARF6-PIF module and also upregulated by coumarin. Finally, *GATA TRANSCRIPTION FACTOR 2 (GATA2)* expression, a positive regulator of photomorphogenesis and hence an antagonist of cell elongation (Terzaghi and Cashmore, 1995; Luo *et al.*, 2010), is inhibited by the BZR1-ARF6-PIF module, also upon coumarin treatment. All these data strongly suggest that the BZR1-ARF6-PIF module is stimulated by coumarin, facilitating elongation.

The involvement of PIFs, BEE1, and GATA2 also clearly link BR signalling with light signalling. The repression of *GATA2* has for instance been reported specifically for dark-grown plants but not for light grown-seedlings (Luo *et al.*, 2010). Our set-up concerns light-grown hypocotyls, yet we observe clear down-regulation.

Interestingly, it is reported that there are no differences in BR levels, nor in the phosphorylation status of BZR1 between light-grown and dark-grown Arabidopsis seedlings (Symons *et al.*, 2008; Luo *et al.*, 2010). Therefore, it claimed that BRs probably affect light signalling rather than vice-versa (Wang *et al.*, 2011). Moreover, very recently it was found that active PHYTOCHROME B antagonistically binds BES1 (Wu *et al.*, 2019). However, it has also been shown that BRs can operate rather independent of light-signalling: BRs can still induce elongation in the *phyB* mutant, while coumarin cannot, indicating that coumarin operates via *phyB*, for example by limiting its incorporation in the cells (Wu *et al.*, 2019), rather than directly affecting BR signalling. In the dark, when PHYB transcripts are low and PHYB is inactive (Sharrock and Quail, 1989; Mathews, Lavin and Sharrock, 1995; Smith, 2000; Inoue, Nishihama and Kohchi, 2017), BRs can induce elongation. In the light, when PHYB is active, the elongation potential of BRs is limited, though not completely abolished (Wu *et al.*, 2019). Indeed, when *PHYB* is knocked-out, hypocotyls are 8mm long in mock conditions, exactly the same hypocotyl length as seedlings co-treated with 40 µM coumarin and 25 µM bikinin. As such, it seems that coumarin releases the repression of PHYB on BR signalling and activates in that way hypocotyl elongation.

The main two other phytohormones that are commonly involved in elongation processes in *planta*, i.e. GA and ethylene (Depuydt and Hardtke, 2011; Depuydt *et al.*, 2016), do not seem to be functionally relevant. However, to completely abolish the role of GA in the process, some additional experiments are needed. Indeed, *GA20OX1* gene expression, the rate-limiting enzyme for GA biosynthesis (Rieu *et al.*, 2007), is highly upregulated upon coumarin treatment. However single- and higher-order *ga20ox* mutants are fully responsive, just like the GA receptor mutant *sly-1*. This suggest that the increased expression is probably counteracted by an increased GA catabolism (as also observed via increase *GA2OX1* expression) and is merely a result of the enhanced auxin and BR signalling (Olszewski, Sun and Gubler, 2002). Since these mutants do not germinate without GA, it needs to be noted that the experiments were carried out in the presence of GA. Nevertheless, they prove that *de novo* GA synthesis is not needed for coumarin-induced hypocotyl elongation. Next to that, no differences in GA levels in the hypocotyl epidermis could be demonstrated via the *nlsGPS1* optogenetic biosensor (Rizza *et al.*, 2017), however, the biosensor does not allow to analyse the GA levels in the endodermis and vasculature. The *global* mutant, on the other hand, illustrates that when GA signalling is maximized, coumarin can still induce hypocotyl elongation to the same extent as in the control. Altogether these data illustrate that neither GA biosynthesis nor increased GA signalling is crucial for coumarin-induced hypocotyl elongation. However, given the role of GA in phytochrome signalling and its clear involvement in the BAP module, further experiments are needed to quantify its role in the process, as so far we could not unambiguously prove that GA is not involved (as in all experiments performed GA was either present in the medium or GA signalling was activated via loss-of-function DELLA mutants).

As last, we can also conclude that endoreduplication – involved in cell elongation in Arabidossis and linked to cell wall modification (Bhosale, Maere and De Veylder, 2019) – plays no major role in coumarin-induced hypocotyl elongation. We observed a clear increase in *SMR1* expression via histochemical analysis of its GUS reporter line, a shift in 16C:8C ratio upon coumarin treatment and the *ccs52a2* mutant is not responsive anymore towards coumarin. The *ccs52a2* mutant, however, illustrates severe phenotypes and has an overall strong diminished growth (Y. Liu *et al.*, 2012). Moreover, when endoreduplication is affected less than in the *ccs52a2* mutant (e.g. in the mutants *DEL1, smr1* or *ccs52a1*), we could not observe a significant effect of the mutation

upon coumarin-induced hypocotyl elongation. Interestingly, also when endoreduplication is stimulated in the epidermis (the pCER6::CCS52A2 line), no additional effect could be observed. Note that that recently the role of endoreduplication on cell-size control is re-examinaed and under debate (Tsukaya, 2019).

In conclusion, we postulate a model on the mode-of-action of coumarin-induced hypocotyl elongation in *Arabidopsis thaliana* (Fig. 12).

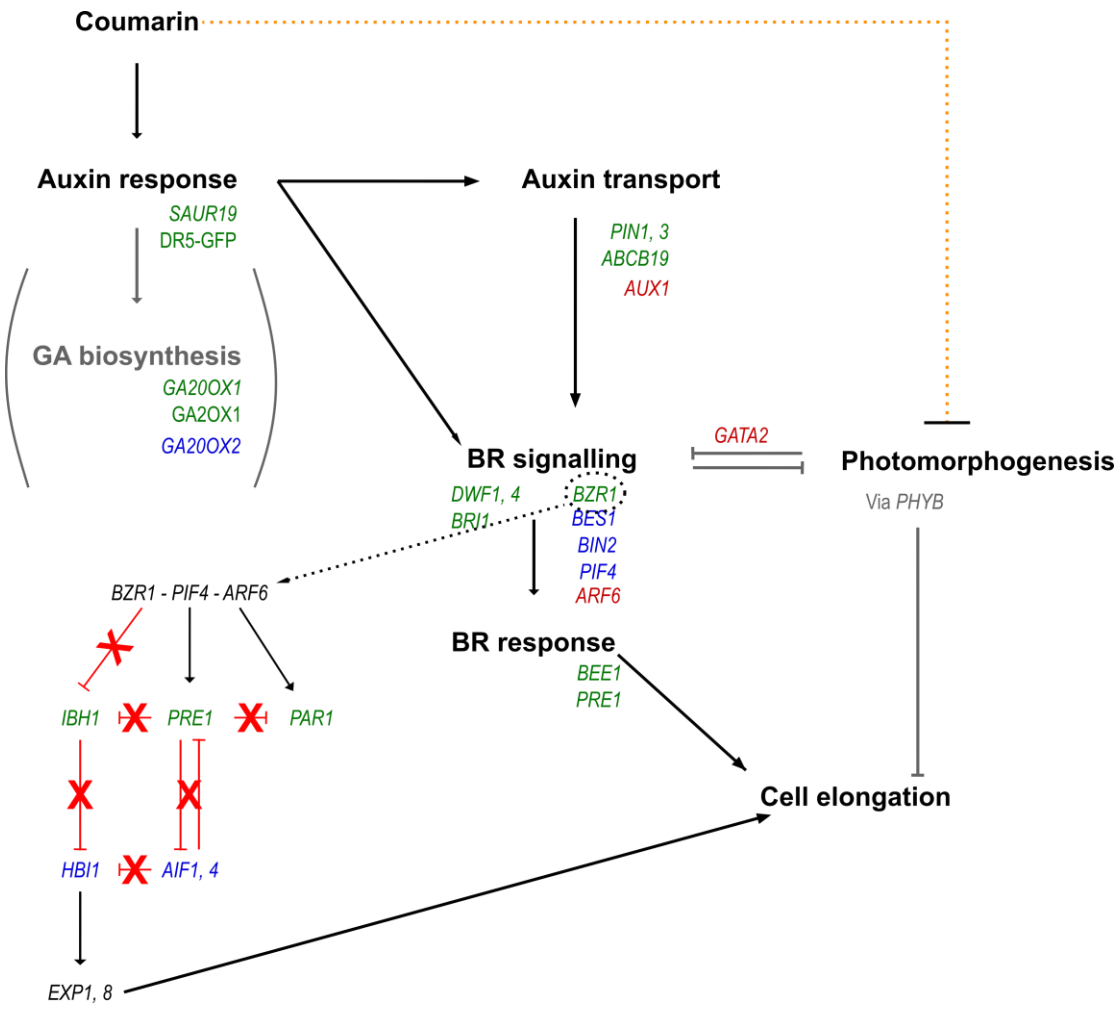

Figure 12: Model of the *mode-of-action* of coumarin-induced hypocotyl elongation in Arabidopsis thaliana.

Coumarin treatment induces an auxin response in the hypocotyl, observed via increased *SAUR19* expression and enhanced DR5rev::GFP transcription. Auxin signalling is crucial for coumarin-induced hypocotyl elongation and coumarin clearly affects auxin transport, whereby it has been shown that a diminished PAT inhibits the phenotype. Next, coumarin induces a clear BR response, observed by increased expression of *BEE1* and *PRE1*. *BZR1* expression is enhanced and the *pif4-2* mutants are less responsive towards coumarin hinting to a central role for the BZR1-ARF6-PIF module to stimulate elongation. We observed a mimicked skotomorphogenic growth based on the downregulation of *GATA2* expression and the crucial involvement of

PHYB. Note that GA biosynthesis is transcriptionally upregulated upon coumarin treatment, but not required for coumarin-induced hypocotyl elongation. Moreover, the antagonistic IBH-AIF-HBI module illustrates contrasting expression profiles than would be expected based on the expression profiles published for *PRE1* increased expression. It seems that cascade is not activated during coumarin-induced hypocotyl elongation and it has to be investigated more in detail how the observed BR response via *BEE1*, *PRE1* and *GATA2* relate to each other to stimulate hypocotyl elongation upon coumarin treatment in a PHYB-dependent manner.

Black arrows indicate the hypothesized model based on our data and literature. In green, red and blue we indicated the genes that are, respectively, transcriptionally up-, down- or not-regulated upon coumarin treatment. Grey arrows indicate unclarified interactions. The orange dotted line indicates a potential direct interaction of coumarin on photomorphogenesis, for which further experiments are needed. The black dotted line is used to extract the BZR1 module out of the BR response and to incorporate the model of Fig. S4.

Acknowledgements

The Microscopy Core Facility and the cryo-SEM Facility at the Sainsbury Laboratory, Cambridge, is supported by the Gatsby Charitable Foundation. This work was supported by the “Bijzonder Onderzoeksfonds” of Ghent University by indebtment of S.V.P. as a PhD fellowship and by the Ghent University ‘Bijzonder Onderzoeksfonds Methusalem Project’ no. BOF08/01M00408 of D.I.

Supplementary material

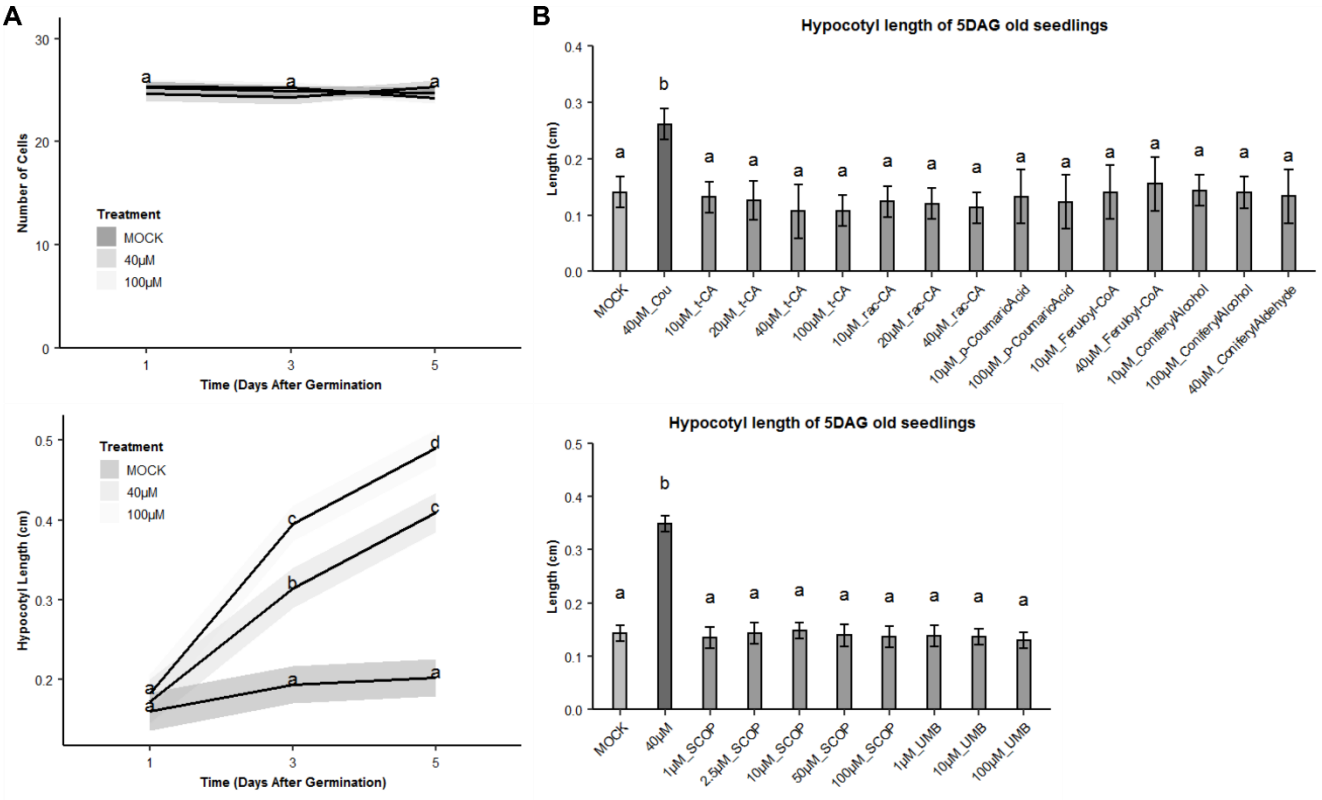

Figure S1: Coumarin-induced hypocotyl elongation is solely an effect of cell elongation and cannot be mimicked by the tested phenylpropanoid derivatives and intermediates.

(A) The number of hypocotyl protruding cells (top) and their corresponding hypocotyl length (bottom) of seedlings treated with 0, 40 or 100 µM of coumarin measured over time (1, 3 and 5 days after germination) (n≥57). (B) Hypocotyl length of 5 DAG old seedlings continuously treated with different concentrations of intermediates of the phenylpropanoid pathway (top) and with different concentration of the PP derivatives scopoletin (SCOP) or umbelliferone (UMB) (bottom). *t*-CA = *trans*-cinnamic acid, *rac*-CA = racemic mixture of *trans/cis*-cinnamic acid.

Letters indicate statistically significant different means ($p<0.05$). Data presented are means ± the confidence interval of at least three biological repeats.

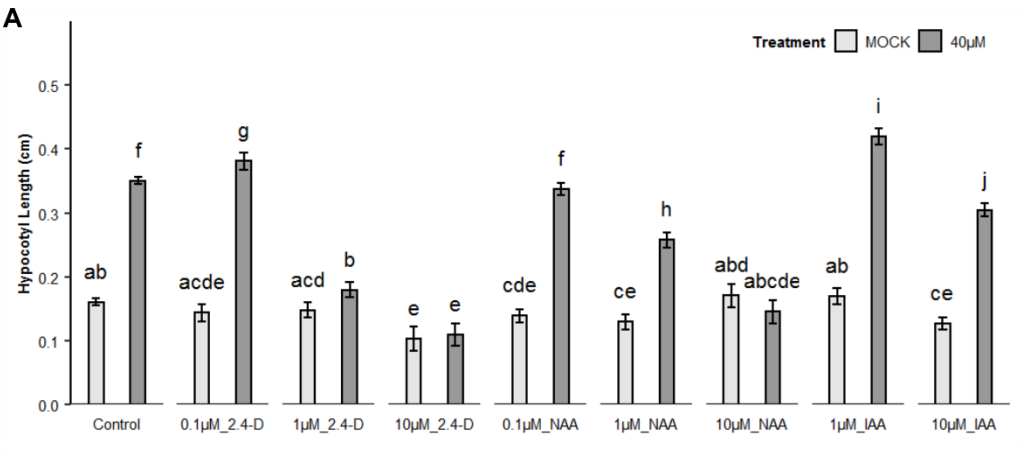

Figure S2: Co-treatment with coumarin and low concentrations of auxin lead to additive effects on hypocotyl elongation.

(A) Hypocotyl length (cm) of 5 DAG old seedlings continuously treated with DMSO (mock) or 40 µM of coumarin in combination with several auxin analogues in various concentrations (n≥30).

Data presented are means ± the confidence interval of at least three biological repeats. Letters indicate statistically different means (p<0.05).

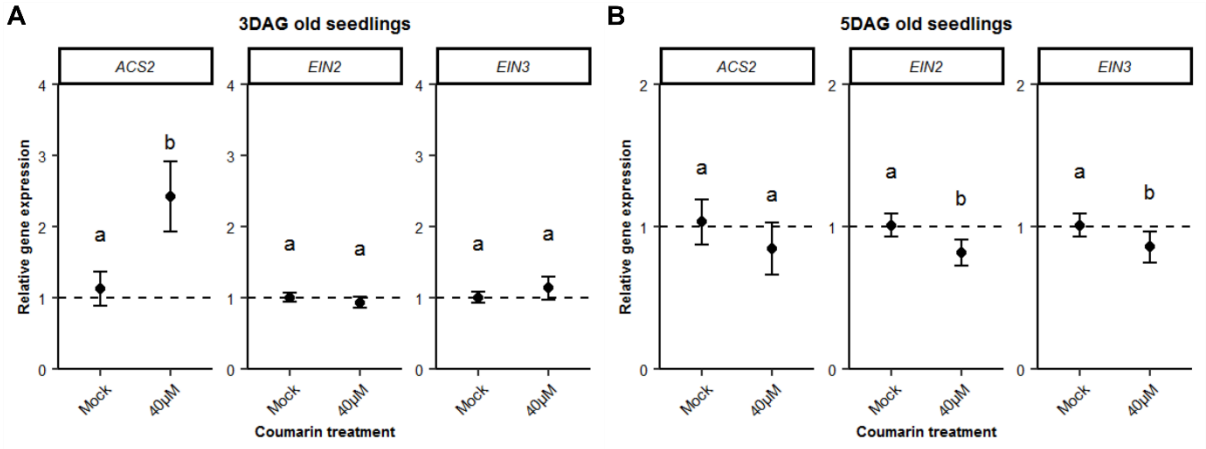

Figure S3: Coumarin induces hypocotyl elongation independent of ethylene homeostasis

(A, B) Relative gene expression in hypocotyls harvested 3 days after germination (DAG) (A), or 5 DAG (B), of continuously treated seedlings with 40 µM of coumarin compared to the mock control (DMSO treatment).

Letters indicate statistically significant different means (p <0.05). Data presented are means ± the confidence interval of up to three biological repeats.

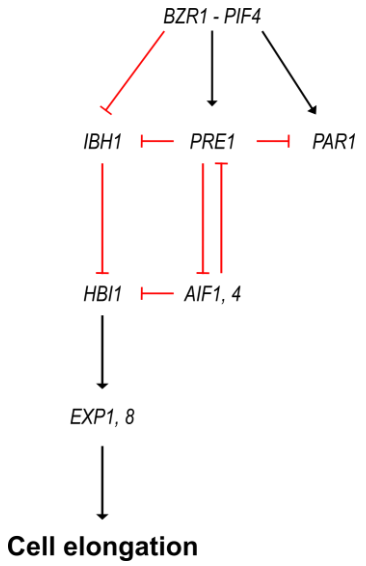

Figure S4: Illustration of the triple Helix-Loop-Helix/Basic Helix-Loop-Helix cascade known to be at the basis of BR induced cell elongation (Ikeda *et al.*, 2012; M.-Y. Bai, Fan, *et al.*, 2012; Oh *et al.*, 2014).

Red lines and black arrows illustrate, respectively, transcriptional inhibition and stimulation of the genes it is pointing to.

BZR1: BRASSINAZOLE RESISTANT 1; *PRE1: PACLOBUTRAZOL RESISTANT 1 (PRE1); PIF4: PHYTOCHROME INTERACTING FACTOR 4; PAR1: PHYTOCHROME RAPIDELY REGULATED; IBH1: ILI1 BINDING bHLH 1; AIF: ACTIVATION-TAGGED BRI1 SUPPRESSOR 1 (ATBS1) INTERACTING FACTORs; HBI:* HOMOLOG OF BEE2 INTERACTING WITH IBH1; *EXP1*, *8: EXPANSIN1, 8.*

Table S1: Information about the mutants and reporter lines used in this paper

Plant line	Background (ecotype)	Full name or description	Locus	Allele/Mutagen	Reference
Wild type	Colombia-0 (Col-0)		N/A	N/A	N/A
Wild type	Landsberg *erecta* (Ler)		N/A	N/A	N/A
Wild type	Wassilewskija		N/A	N/A	N/A
abcb19 (mdr1-1)	Wassilewskija	ATP-BINDING CASSETTE B19	AT3G28860.1	T-DNA insertion	(Noh, Murphy and Spalding, 2001)
aha2-4	*Colombia-0 (Col-0)*	*H(+)-ATPASE 2*	*AT4G30190*	*T-DNA insertion*	(Haruta and Sussman, 2012)
aux1-7	Colombia-0 (Col-0)	AUXIN RESISTANT 1	AT2G38120	Ethyl Methane Sulfonate (EMS)	(Stepanova *et al.*, 2007)
aux1-21	Colombia-0 (Col-0)	AUXIN RESISTANT 1	AT2G38120	Ethyl Methane Sulfonate (EMS)	(Marchant and Bennett, 1998)
aux1-21lax3	Colombia-0 (Col-0)	Cross of the mutants aux1-21 and lax3	AT2G38120	X-rays	(Swarup *et al.*, 2008)
bak1-4	Colombia-0 (Col-0)	BRI1-ASSOCIATED RECEPTOR KINASE	AT4G33430	T-DNA insertion	(Li *et al.*, 2002; Kemmerling *et al.*, 2007)
bri1-5, dwf2, cbb2	Wassilewskija-2	BRASSINOSTEROID INSENSITIVE 1	AT2G45400.1	Ethyl Methane Sulfonate (EMS)	(Clouse, Langford and McMorris, 1996; Noguchi *et al.*, 1999)
bri1-116, dwf2, cbb2	Colombia-0 (Col-0)	BRASSINOSTEROID INSENSITIVE 1	AT2G45400.1	Ethyl Methane Sulfonate (EMS)	(Li and Chory, 1997; Vert *et al.*, 2005)
bes1-D	Enkheim	BRI1-EMS-SUPPRESSOR 1	AT1G19350.3	Ethyl Methane Sulfonate (EMS)	(Yin *et al.*, 2002)
ctr1-1	Colombia-0 (Col-0)	CONSTITUTIVE TRIPLE RESPONSE 1	AT5G03730.2	Diepoxybutane	(Kieber *et al.*, 1993)
det2-1, dwf6	Colombia-0 (Col-0)	DE-ETIOLATED-2	AT2G38050	Ethyl Methane Sulfonate (EMS)	(Chory, Nagpal and Peto, 1991)
dwf1, dim1,	Colombia-0 (Col-0)	DWARF1, DIMINUTO 1,	AT3G19820.1	T-DNA insertion	(Feldmann *et al.*, 1989; Takahashi *et al.*, 1995)

cbb1		CABBAGE 1			
dwf4-1	Wassilewskija-2	DWARF4, CYTOCHROME P450 90B1, SHADE AVOIDANCE 1	AT3G50660.1	T-DNA insertion	(Azpiroz *et al.*, 1998; Choe *et al.*, 1998)
eir1-1 (pin2)	Colombia-0 (Col-0)	Ethylene Insensitive Root 1 (PIN-FORMED 2)	AT5G57090	Diepoxybutane	(Roman *et al.*, 1995)
etr1-3	Colombia-0 (Col-0)	ETHYLENE RESPONSE 1	AT1G66340	Ethyl Methane Sulfonate (EMS)	(Guzmán and Ecker, 1990)
ga5-1 (CS62)	Landsberg erecta (Ler)	GIBBERELLIN 20-OXIDASE 1	AT4G25420.1	Ethyl Methane Sulfonate (EMS)	(Koornneef and van der Veen, 1980)
ga20ox1-3	Colombia-0 (Col-0)	GIBBERELLIN 20-OXIDASE 1	AT4G25420.1	T-DNA insertion	(Alonso *et al.*, 2003)
ga20ox1-3;ga20ox2-1;ga20ox3-3	Colombia-0 (Col-0)	GIBBERELLIN 20-OXIDASE 1,2,3	AT4G25420	T-DNA insertion. Crossing of the double mutant ga20ox1-3;ga20ox2-1 (Rieu *et al.*, 2007) with the ga20ox3-3 mutant made by (Plackett *et al.*, 2012). Crossing done by (Plackett *et al.*, 2012).	(Rieu *et al.*, 2007; Plackett *et al.*, 2012)
gai-1(CS63), also known as rga2	Landsberg *erecta* (Ler)	GIBBERELLIC ACID INSENSITIVE - RESTORATION ON GROWTH ON AMMONIA	AT1G14920	Gain-of-function - X-rays	(Koorneef *et al.*, 1985)
Arabidopsis global-DELLA mutant = *global =* *gai-t6 rga-t2 rgl1-1 rgl2-1 rgl3-4*	Landsberg *erecta* (Ler)	GIBBERELLIC ACID INSENSITIVE REPRESSOR OF GA1-3 RGA-LIKE PROTEIN 1 RGA-LIKE PROTEIN 2 RGA-LIKE PROTEIN 3	AT1G14920.1 AT2G01570.1 AT1G66350.1 AT3G03450.1 AT5G17490.1	The quintuple mutant of all five DELLA genes (RGA, GAI, RGL1, RGL2 and RGL3) generated by genetic crosses.	(Fuentes *et al.*, 2012)

gg = *global;ga1-3*	Landsberg *erecta* (Ler)	*Global* (see up)	See up AT4G02780.1	Genetic cross of the *ga1-3* mutant with the global mutant	(Sun, Goodman and Ausubel, 1992; Fuentes *et al.*, 2012)
hy5-1	Landsberg *erecta* (Ler)	ELONGATED HYPOCOTYL 5	AT5G11260	Ethyl Methane Sulfonate (EMS)	(Koornneef, Rolff and Spruit, 1980)
lax1	Colombia-0 (Col-0)	LIKE AUXIN RESISTANT 1 1	AT5G01240.1	T-DNA insertion	(Tissier *et al.*, 1999; Alonso *et al.*, 2003; Swarup *et al.*, 2008)
lax2	Colombia-0 (Col-0)	LIKE AUXIN RESISTANT 1 2	AT2G21050.1	T-DNA insertion	(Tissier *et al.*, 1999; Alonso *et al.*, 2003; Swarup *et al.*, 2008)
lax3	Colombia-0 (Col-0)	LIKE AUXIN RESISTANT 1 3	AT1G77690.1	T-DNA insertion	(Tissier *et al.*, 1999; Alonso *et al.*, 2003; Swarup *et al.*, 2008)
lhy	Colombia-0 (Col-0)	LATE ELONGATED HYPOCOTYL 1	AT1G01060.1	T-DNA insertion	Arabidopsis Biological Resource Center - https://www.arabidopsis.org/entity/organization_detail/6
phya-201 (CS6219)	Landsberg *erecta* (Ler)	PHYTOCHROME A	AT1G09570.1	Ethyl Methane Sulfonate (EMS)	(Nagatani, Reed and Chory, 1993)
phyb-5 (CS6213)	Landsberg *erecta* (Ler)	PHYTOCHROME B	AT2G18790.1	Ethyl Methane Sulfonate (EMS)	(Koornneef, Rolff and Spruit, 1980)
phya-201;phyb-5 (CS6224)	Landsberg *erecta* (Ler)			Cross of the above mentioned mutants	(Nagatani, Reed and Chory, 1993)
pif4-2 (also known as *srl2)*	Colombia-0 (Col-0)	PHYTOCHROME INTERACTING FACTOR 4 (*short under red-light 2)*	AT2G43010.1	T-DNA insertion	(Huq and Quail, 2002)
pin1 (=pML1::PIN1:GFP/ pin1 + *pDR5::VENUS*	Colombia-0 (Col-0)	PIN-FORMED 1 + expression constructs	AT1G73590.1	Crossing	(Kierzkowski *et al.*, 2013)

pin3-4	Colombia-0 (Col-0)	PIN-FORMED 3	AT1G70940	T-DNA insertion	(Alonso *et al.*, 2003)
pin7-1	Landsberg *erecta* (Ler)	PIN-FORMED 7	AT1G23080.1	transposon insertion	(Friml *et al.*, 2003b)
ost2-2	*Colombia-0 (Col-0)*	*OPEN STOMATA 2*	*AT2G18960*	Dominant *gain-of-function* mutation of the gene *AHA1*	(Merlot *et al.*, 2007),
sly1-2	Landsberg *erecta* (Ler)	SLEEPY1	AT4G24210.1		(McGinnis *et al.*, 2003)
tir1-1afb2-1afb3-2	Chimeric Colombia-0 (Col-0) x Wassilewskija	TRANSPORT INHIBITOR RESPONSE 1 - AUXIN SIGNALLING F-BOX 2/3	AT3G62980 - AT3G26810 - AT1G12820	T-DNA insertion (afb2 and afb3), + EMS (tir1-1)	(Dharmasiri *et al.*, 2005; Dharmasiri, Dharmasiri and Estelle, 2005)
tir1-1afb2-3afb3-4	Colombia-0 (Col-0)	TRANSPORT INHIBITOR RESPONSE 1 - AUXIN SIGNALLING F-BOX 2/3	AT3G62980 - AT3G26810 - AT1G12820	T-DNA insertion (afb2 and afb3), + EMS (tir1-1)	(Parry *et al.*, 2009)
Reporter and overexpression lines	**Background (ecotype)**	**Full name or description**		**Additional mutation(s)/Information**	**Reference**
nlsGPS1(-NR/CE)	Colombia-0 (Col-0)	Nuclear localised GIBBERELLIN PERCEPTION SENSOR 1		FRET biosensor https://www.jove.com/video/58739/visualizing-cellular-gibberellin-levels-using-nlsgps1-forster	(Rizza *et al.*, 2017; Rizza and Jones, 2019)
pDR5rev::GFP	Colombia-0 (Col-0)	DR5 is a synthetic auxin-responsive promoter. Rev = reverse. Green Fluorescent Protein		To monitor auxin responses and their dynamics.	(Friml *et al.*, 2003b)
p35S::SAUR19-GFP	Colombia-0 (Col-0)	SMALL AUXIN UP RNA 19	AT5G18010		(Spartz *et al.*, 2012)

Table S2: Background of the chemical compounds used in treatments

Compound	**Abbreviation**	**Supplier**	**Solvent**	**Stock concentration (mM)**
1-amino-cyclopropane-1-carboxylate	ACC	Sigma-Aldrich	50% (v/v) DMSO/d H2O	50
Bikinin	BIK	Sigma-Aldrich	DMSO	25
Brassinolide	BL	MedChemExpress	DMSO	$10*10^{-3}$
cis/trans-Cinnamic acid*	rac-CA	Sigma-Aldrich	DMSO	40
trans-Cinnamic acid	t-CA	Sigma-Aldrich	DMSO	40
Coniferyl alcohol		Sigma-Aldrich	DMSO	100
Coniferyl aldehyde		Sigma-Aldrich	DMSO	40
Coumarin	COU	Tokyo Chemical Industry co., LTD	DMSO	40 and 100
p-Coumaric acid		Santa Cruz Biotechnology, Inc.	DMSO	100
2,4-dichlorophenoxyacetic acid	2.4-D	Sigma-Aldrich	DMSO	10
N,N′-Dicyclohexylcarbodiimide	DCCD	Sigma-Aldrich	DMSO	10
DMSO		Sigma-Aldrich	N/A	N/A
Feruloyl-CoA		PlantMetaChem	H2O	40
Gibberellic Acid	GA3	Duchefa Biochemie	DMSO	100
Indole-3-acetic acid	IAA	Duchefa	DMSO	10
N-1-napthylphthalamic acid	NPA	Supelco (Sigma-Aldrich)	DMSO	10
1-Naphthaleneacetic acid	NAA	Sigma-Aldrich	DMSO	10
Propiconazole (1-[2-(2,4-dichlorophenyl)-4-propyl-1,3-dioxolan-2-yl]methyl]-1,2,4-triazole)	PCZ	Sigma-Aldrich	DMSO	5
Paclobutrazol (α-tert-Butyl-β-(4-chlorobenzyl)-1H-1,2,4-triazole-1-ethanol)	PAC	Duchefa Biochemie	DMSO	100
Scopoletin	SCOP	Santa Cruz Biotechnology, Inc.	DMSO	50

Umbelliferone	UMB	Santa Cruz Biotechnology, Inc.	DMSO	100
Silvernitrate	AgNO3	Junsei	DMSO	100
Sinapyl alcohol		Santa Cruz Biotechnology, Inc.	DMSO	100
Yuccasin (5–(4–chlorophenyl)-4H-1,2,4–triazole-3–thiol)	YCS	Santa Cruz Biotechnology, Inc.	DMSO	50

**cis*/*trans*-cinnamic acid was made using a 40 mM stock solution of *trans*-cinnamic acid (Sigma-Aldrich) in DMSO that was exposed to UV-light (306 nm) for 48 h.

Table S3: Primer sequences used in qRT-PCR analysis

Gene	**Locus**	**Sequence (forward on top, reverse on the bottom**
CBP20	AT5G44200.1	TGGTGGTGGAAACTATGGTCAAGG
		TGTCGTTTCCGATGGTAGTCTCC
PEX4	AT5G25760.1	TCTCTCTCTCTCTCTCTCGCTCTC
		TGATGCCTGCATCTCTAATTTCCC
SAUR19	AT5G18010.1	GAAGAGATATTTGGTGCCGCTCTC
		TACTGAGCAGAGCTTGAAATGACG
PIN1	AT1G73590.1	GGCATGGCTATGTTCAGTCTTGGG
		ACGGCAGGTCCAACGACAAATC
PIN3	AT1G70940.1	TGACCAAGGTGCTAAAGAGATCCG
		TGCTGGATGAGCTACAGCTTTG
PIN4	AT2G01420.2	CATCATGGCTGTTGCTGGGATTG
		AGCCTGAACGATGGCTATACGG
ABCB19	AT3G28860.1	TAAAGGCTACGACACACAGGTTG
		TTGCAATTCTCTGCTTCTGTCCAC
AUX1	AT2G38120.1	AGGTCACGCGGTTACTGTTGAG
		CGTCTCCGAAAGCCCAGTAAAC
LAX3	AT1G77690.1	CGGAGCCACCAACATTCTCTACAC
		AGCGTGCATTATCTCCACTGTGAC
PIL5	AT2G20180.1	ATATCAGCAGTTCCGCGGTCTC
		TGGGTACGATGTTGCTTGATTCTG
GA20OX1	AT4G25420.1	CATCAACGTTCTCGAGCTTGATGTTC
		GCGGCTCGTGTATTCATGAGCG

GA20OX2	AT5G51810.1	CAAGAGTTCGAGCAGTTTGGGAAG
		TCGGAAATAGTCTCGGTTTACGC
GA2OX1	AT1G78440.1	AACGTTGGTGACTCTCTCCAGGTG
		AACCCTATGCCTCACGCTCTTG
PIF4	AT2G43010.1	TCAGATGCAGCCGATGGAGATG
		CGACGGTTGTTGACTTTGCTGTC
PRE1	AT5G39860.1	ACGTCGTTCTGATAAGGCATCAGC
		ACAAACGCTCGCTCAGATTGTC
ACS2	AT1G01480.1	ATGGGTCTTGCAGAGAATCAGC
		ACCTTCAAGGGTGCAAATAGAAGC
EIN2	AT5G03280.1	TCATGGCGATTTCGAAGGTCTG
		AGGAAGCCCTAACAGAGCAACC
EIN3	AT3G20770.1	AACTGGCATGTCCACATCGAGAC
		ATGAAACCTGGATGGTGCTGCTC
BES1	AT1G19350.1	TTGTTCTGAAGCTGGTTGGGTTG
		AGGTAGAGGCTTGTGTCCCTTG
BZR1	AT1G75080.2	TTGTGTTGAAGCTGGTTGGGTTG
		GTAAAGGCTTGCATCCCTTGCG
DET2	AT2G38050.1	ATATCCAGGCGAGGTGGGTTTC
		CGATAACAAACCGCCACCAGAAC
DWF1	AT3G19820.1	TCTTTACAAGGTTGGCGATGCAC
		GCAAAGCCAAATTGGATACACCTC
BIN2	AT4G18710.1	TGCACCCGAGCTCATATTTGGTG
		TCTCCGGGAAATAATGGCTGACC
BAK1	AT4G33430.2	TGTCCTGACGCTACAAGTTCTGG
		ACAGGAATATCTCCGGTGAGAGG
BRI1	AT4G39400.1	GTAAACGGCCAACGGATTCACC
		CGTGCTGTTTCACCCATCCAAC
BEE1	AT1G18400.1	AGATGCAGTTGATTCCATGCAGAG
		CAGGACTCCCATCTCTTGTTTGTC
DWF4	AT3G50660.1	AATCCTTGGAGATGGCAACAGC
		CTGAACCAGCACATAGCCTTGG
ARF6	AT1G30330.2	TTGGCGATCTGTCAAGGTTGGG
		AAACCCTTGGCTGTCTCTCTCC
GATA2	AT2G45050.1	CACGACATTTGCGTTCCCAGTG
		TCGTCCACGAATTGCGAAAGCC
HY5	AT5G11260.1	AGAACAAGCGGCTGAAGAGGTTG
		TCCTCTCTCTTGCTTGCTGAGCTG
IBH	AT2G43060.1	AGAGGCTGAGGAATCTTGTTCCG

		CCGTCTCTTCCATCAGCTTTGACG
HBI	AT2G18300.3	TTGAAGACCGGTGAAGAAACCAG
		GCTCTTCCCTTGTCTTAACCTCTG
PAR1	AT2G42870.1	TTTCGAGCGCAGAACCAAACGG
		TCTCGGTCTTCACGTACGCTTG
AIF1	AT3G05800.1	TCTGAAGAAGCTCCGGTAAGGC
		TATACCTTCTGCGCCGTTGTGG
AIF4	AT1G09250.1	TCGGATTAAGTTACCGGCGGTTG
		AACCAGGAACCAAACGGCCAAG

Chapter 4 – Genome-wide transcriptional changes in the hypocotyl of *Arabidopsis thaliana* upon coumarin treatment

RNA sequencing of hypocotyls of *Arabidopsis thaliana* treated with coumarin sheds light on the molecular basis of coumarin-induced phenotypes.

Stan Van Praet[1,2,3], Bartel Vanholme[1,2], Stephen Depuydt[1,2,3]

1. Ghent University, Department of Plant Biotechnology and Bioinformatics, (Technologiepark 71), 9052 Ghent, Belgium
2. VIB Center for Plant Systems Biology, (Technologiepark 71), 9052 Ghent, Belgium
3. Ghent University Global Campus, Lab of Plant Growth Analysis, Incheon, South Korea

Author contributions:

S.V.P. and S.D. conceptualized and designed the research; S.V.P. performed the research/experiments. S.V.P., B.V and S.D. interpreted the data. S.V.P. analysed the data, performed the statistics and made the figures; S.V.P. drafted the manuscript and B.V. and S.D. revised it.

Abstract

Coumarin, a derivative of the phenylpropanoid pathway, has profound effects on plant growth and development. Phenotypic effects on germination, root system architecture and shoot growth (elongation) have been described and noted in different plant species, among which *Arabidopsis thaliana*. Insights into the molecular *modus operandi* of coumarin are, however, notably lacking. This is partly due to the fact that coumarin research has historically mainly focused on unravelling its biosynthetic pathways, which to date remain elusive, and partly because of some contradictory phenotypes described in the scientific literature. Here, we attempted to gain insight into molecular networks underlying one of the specific phenotypes induced by coumarin: induction of hypocotyl elongation. Therefore, we made use of RNA sequencing to get insight into direct genome-wide expression changes in the Arabidopsis hypocotyl upon 30, 60 and 180 minutes of coumarin treatment. Coumarin-induced cell elongation has been linked with changes in phytohormone homeostasis (notably auxin and brassinosteroids seem to be involved) and light signalling as well. The RNAseq data obtained here confirm a clear auxin response: upregulation of numerous auxin response genes (SMALL AUXIN UP RNA (SAUR) genes, *Aux/IAA* response genes, *HISTONE ACETYLTRANSFERASE 1 (HAT)* genes and *AUXIN UPREGULATED F_BOX PROTEIN (AUF1)*) already after 30 minutes of coumarin treatment illustrates this. Upregulation of several PIN transporters was also clear from the RNAseq data. The brassinosteroid involvement during coumarin-induced elongation was further confirmed and linked with the upregulation of numerous genes (e.g. *PREs, BMI, BEE1*) that in the end stimulate *XYLOGLUCAN:XYLOGLUCOSYL TRANSFERASE (XET)* genes involved in cell wall remodelling. Through *PRE5*, the involvement of the BZR1-PIF4-ARF module is known to interact with light signalling via PHYB. The specific set-up of our experiments allowed us to refine the proposed model for coumarin-induced cell-elongation in the hypocotyl.

Introduction

In Chapter 3, we clearly showed that coumarin induces elongation in the shoot. By using the hypocotyl as a model, we have, through qRT-PCR, reporter line analyses, mutant analyses and pharmacological approaches, gained some insight into the molecular pathway(s) governing cell elongation. For instance, we showed that coumarin induces the expression of *SAUR19*, *PIN1*, *PIN3*, *GA20OX1*, *BRI1*, *BZR1*, *PRE1*, *BEE1* and *IBH* in the hypocotyl of 3 DAG old seedlings, while the expression of *HBI*, *GATA2* and *AUX1* significantly decreases. These analyses happened three days after germination of seedlings that have been continuously treated with coumarin (meaning that seeds have germinated and developed under constant exposure to coumarin) and can thus be regarded as fairly late responses. In fact, those data illustrate the transcriptional changes in steady-state conditions. As such, despite the relevance of the differential gene expressions (observed via qRT-PCR, and validated via mutant analysis), in the middle of the hypocotyl elongation phase, it cannot be stated that these are early transcriptional responses upon coumarin treatment.

In addition, to the best of our knowledge, there is no full transcriptome analysis available of Arabidopsis hypocotyls grown in the light, and our study also fills that gap. Despite this gap, some knowledge is already available. For instance, Zhao *et al.* (2013) showed that the *AT-HOOK MOTIF CONTAINING NUCLEAR LOCALIZED (AHL)* genes have a role in hypocotyl elongation in the light. More specifically, they showed that different members of the 29 AHL proteins in Arabidopsis, redundantly, albeit to different extents, suppress hypocotyl elongation in the light. Moreover, these proteins also interact with other nuclear proteins (e.g. transcription factors). Note that two Arabidopsis *AHL* genes (*SOB3/AHL29* and *ESC/AHL27*) repress hypocotyl growth specifically in the light and not in the dark (Street *et al.*, 2007). On the other hand, several other players are known that regulate hypocotyl elongation in the light as well as in the dark. For instance, Reed *et al.* (2018) showed that auxin-responsive hypocotyl elongation is dependent on three AUXIN RESPONSE FACTORS (ARFs) and suggested an involvement of Aux/IAA proteins to modulate ARF activity in the hypocotyl in a potential negative feedback loop. Note that, interestingly, these authors also provide evidence for the partially independent action of GA and brassinosteroids (Reed *et al.*, 2018). In addition, it is known that many pathways other than hormonal ones influence hypocotyl elongation. Among these are light perception, circadian rhythm or transcription in general. For instance, TANDEM ZINC-FINGER PLUS 3 (TZP), shown to upregulate growth-promoting and auxin-related genes in a blue light specific manner, interacts with ZINC-FINGER HOMEODOMAIN 10 (ZFHD10) to promote hypocotyl elongation (Perrella *et al.*, 2018). They do so via inducing the expression of *ATHB2, LONG HYPOCOTYL IN FAR-RED (HFR1), XYLOGLUCAN ENDOTRANSGLUCOSYLASE/HYDROLASE 17 (ATXTH17)* and *PHYTOCHROME INTERACTING FACTOR 7 (PIF7)* directly correlating with the hypocotyl phenotype described earlier (Perrella *et al.*, 2018).

The above illustrates that potentially much more players are involved in hypocotyl elongation and in order to get a complete view on early transcriptional changes during hypocotyl elongation induced by coumarin in the light, we performed an in-depth transcriptional analysis (RNA sequencing (RNAseq)) of seedlings treated with coumarin for only 30, 60 or 180 minutes. The use and developments of the technique were recently reviewed by Stark, Grzelak and Hadfield (2019), and we refer to this review for more details. This set-up allowed us to shed light on the temporal activation of the different hormonal pathways induced by coumarin. The results

not only confirm our earlier postulated hypotheses (Chapter 3), it allows us to gain insight in the dynamic behaviour of involved pathways and to update the mode of coumarin action to induce hypocotyl elongation.

Materials and methods

Sterilization, stratification, growth conditions, growth medium and treatment preparation

Seeds were surface-sterilized by treatment with 70 % ethanol for 5 minutes, followed by a treatment with 100 % ethanol for 2 minutes. Incubation took place at room temperature while regularly inverting the Eppendorf tubes. The seeds were dried in the Laminar Air Flow (LAF) in a small sterile Petri dish Ø1 inch (SPL Life Science®, South Korea). Seeds were sown on 125x125 mm square Petri Dishes (SPL Life Science®, South Korea) containing 100 ml of ½ Murashige & Skoog growth medium (per litre demineralized water 2.15 g MS + vitamins, 0.5 g MES (2-(N-morpholino) ethanesulfonic acid), 0.1 g Myo-inositol, 10 g sucrose and 8 g agar (or 6.5g gelrite), pH of the medium was adjusted to 5.7 using a 1 M KOH solution). Seeds were stratified for a minimum of 3 nights. Plants were grown vertically at 21 °C, long-day conditions (16 h/8 h light/dark) and 120 PAR light. A 40 mM stock of coumarin (Tokyo Chemical Industry co., LTD) was made by dissolving the compound in DMSO. DMSO was used as a mock control and was, just as for coumarin, added to the growth medium after autoclaving and cooling down to 60 °C.

Experimental set-up

Two DAG old seedlings, grown on an untreated medium, were transferred to either mock medium of medium supplemented with 40 µM of coumarin for 30, 90 or 180 minutes. Experiments were performed in 3 biological repeats. Seeds were sown with a density of 15 seeds/row and in 3 rows/plate, whereby the seedlings were grown on a nylon mesh (Ø20µm, Nytal® Prosep (Zaventem, Belgium)), allowing us to transfer the plants efficiently.

RNA Isolation and cDNA Library Preparation for RNA-Seq

Seedlings were harvested in 6-well plates containing RNAlater® (Thermo Fischer Scientific, United States) and stored at 4 °C for a maximum of 3 weeks. Per sample, 900 hypocotyls were micro-dissected on ice, in RNAlater®, by the usage of a stereomicroscope and a syringe needle and then snap-frozen in liquid nitrogen and stored at -80 °C. RNA was isolated by use of the RNeasy® Plant Mini Kit (Qiagen, Hilden, Germany) immediately followed by DNase treatment (Promega, RQ1 RNase-Free DNase kit). The RNA was treated for 30 minutes at 37 °C with a mixture containing RNA (30 µl), 10x RQ1 DNase-buffer (3.5 µl), RQ1 RNase-Free DNase enzyme (2U/µl) (1 µl), and water (H2O-Diethylpyrocarbonate treated (DEPC) 1.5 µl). The reaction was stopped by adding 1 µl of RQ1 DNase stop solution and incubating the samples for 10 minutes at 65 °C. Sample quality was determined via spectrophotometry (Nanodrop® ND-1000) and gel-electrophorese.

The sequencing was performed at the Nucleomics Core Facility (VIB, Leuven, Belgium, www.nucleomics.be). Library preparation was performed with the TruSeq RNA Sample Preparation Kit (Illumina, San Diego, CA, USA). The RNA quality and purity (A260/A280 and A260/A230 ratios > 1.8) was re-

checked with the Bioanalyzer 2100 (Agilent Technologies, Palo Alto, CA, USA), and all samples had a quality documented by RIN values > 7. Clusters were generated through amplification using the TruSeq3 Single-end Cluster Kit (Illumina, San Diego, CA, USA). Samples were sequenced on a HiSeq 2000 in single-end mode, 15M reads per sample with reads of 75 bp in length. Subsequent data analysis steps were performed in Galaxy. The quality of the sequences was verified with FASTQC (http:// bioinformatics.babraham.ac.uk/projects/fastqc/), and filtering of the adaptor and other overrepresented sequences was performed with the FASTX-Toolkit (http://hannonlab.cshl.edu/ fastx_toolkit/). The remaining reads were mapped to the Arabidopsis reference genome, using SALMON, according to TAIR10 (TAIR10_chr_all.fas; ftp.arabidopsis.org). Reads that did not map to a unique position were removed using SAMtools (v0.1.18). Differential expression analysis was performed with multifactorial ANOVA using the EdgeR and ggplot2 libraries in R3.0.1 (https://www.r-project.org) (Robinson, McCarthy and Smyth, 2010; McCarthy, Chen and Smyth, 2012). Rough counts were normalized to the library size. Very lowly expressed genes were removed by filtering for genes with counts >5 cpm (counts per million) in at least three samples. A generalized linear model was applied with time and treatment as factors using the glmQLFit function. Next, significant interactions were extracted using the glmQLFTest function. Differentially expressed genes in coumarin treatment versus mock conditions at each time point were calculated using predefined contrasts for each group, and we investigate the difference in response over time between the treatments. The cut-off was set on FDR = 0.05.

In R we drafted an additional paragraph to the script that automatically adds the gene symbols and explanation to the TAIR locus codes. This information is drafted from the TAIR library via the R-packages "AnnotationDbi" (Hervé Pagès, Marc Carlson, Seth Falcon and Nianhua Li (2019). AnnotationDbi: Manipulation of SQLite-based annotations in Bioconductor. R package version 1.48.0.) and "org.At.tair.db" (Marc Carlson (2019). org.At.tair.db: Genome-wide annotation for Arabidopsis. R package version 3.10.0).

Results and Discussion

To investigate the direct transcriptional responses in the hypocotyl, 2 DAG old seedlings (sown on a nylon mesh) were transferred from ½ MS medium to ½ MS medium containing DMSO (mock) or 40 µM of coumarin. Previous experiments illustrated that coumarin can still induce hypocotyl elongation when transferred at those time points, with clear increases in length after 24 hours of treatment (Chapter 3, Fig. 5B, E). We harvested the seedlings in RNAlater (see material and methods) after 30, 60 and 180 minutes of treatment, allowing us to investigate the direct changes in the transcriptome and their temporal evolution. The variance in the 3 biological repeats is acceptable: we observe a clear separation of the samples, illustrated via a Multi-Dimensional Scaling plot (Fig. S1), based on bio-repeat and time point of treatment.

Overall we found 97, 1278 and 904 differentially expressed genes between mock and coumarin treated seedlings for, respectively, 30, 60 and 180 minutes. Those differentially expressed genes can be found, respectivel,y in table 1, 2 and 3 in the addendum of this dissertation. After 30, 60 and 180 minutes of treatment, respectively, 83, 625 and 514 genes are upregulated, while, respectively, 14, 653 and 390 genes are downregulated. There are 19 genes that are upregulated after 30 minutes of coumarin treatment that are also upregulated after 1 hour of coumarin treatment (Table 4, see addendum) and there are 182 genes that are upregulated after 60 minutes of coumarin treatment and that remain higher expressed after 3 hours of treatment (Table 4). 63 genes are upregulated at all time-points, while only 4 genes are downregulated at all three time-points of harvesting (Table 5, see addendum). Data are presented as fold-changes (not log-fold changes), in order to facilitate interpretation. In tables 1, 2 and 3 we used a colour code to visually illustrate the change in expression as follows: (1) dark green indicates a higher than 5-fold increase in expression, (2) green illustrates a 2- to 5-fold increase in expression, (3) light green illustrates a 1- tot 2-fold increase in expression, (4) orange illustrates a decrease in expression of 0-50%, and (5) red illustrates a decrease in expression of more than 50%. In total this analysis creates 7 groups of genes based on their overlap in up- or down-regulation over the 3 timepoints, or their unique upregulation at one of the time points (Table 4 and 5).

For representing and clustering the numerous genes that are differentially expressed upon coumarin treated, we used the gene ontology (GO) enrichment tool PLAZA4 (p-value < 0.001) (Van Bel *et al.*, 2018). After clustering the differentially expressed genes based on their gene ontology, we visualized the biological processes and molecular function of those via REVIGO (Supek *et al.*, 2011) as shown in figures 1 to 10.

Transcriptional changes during coumarin-induced hypocotyl elongation

In Chapter 3, we postulated a model, based on transcriptional data and supported by pharmacological and mutant analyses, illustrating the molecular players involved in coumarin-induced hypocotyl elongation. Here, we investigated if those players are already from early on transcriptionally regulated by coumarin or if they are late responses. In addition, we pinpointed additional molecular players induced by coumarin.

Ethylene and Gibberellins are not central-players for coumarin-induced hypocotyl elongation

We observed an increase in expression of 1-*AMINO-CYCLOPROPANE-1-CARBOXYLATE SYNTHASE 2 (ACS2)* in 3 DAG old seedlings continuously treated with coumarin but claimed this to be a secondary effect as we clearly illustrated that ethylene is not involved in the process of coumarin-induced hypocotyl elongation (Chapter 3). Our RNAseq data support this hypothesis, as no differential expression is observed of *ACS2* after 30, 60 or 180 minutes of coumarin treatment (Table 1, 2 and 3). Moreover, we found no differential expression of the ethylene response genes *ETHYLENE-INSENSITIVE 2* (*EIN2)* and *EIN3* in any of the time points tested (Table 1, 2 and 3), in line with the findings in Chapter 3. We also observed a 2.5-fold increase in *GIBBERELLIN 20-OXIDASE 1 (GA20OX1)* and *GA3OX1* expression after 30' of coumarin treatment, which changed to a constant ±5- and a 2-fold increase respectively, after 60 and 180 minutes of treatment. This confirms the clear transcriptional upregulation of GA biosynthesis as observed earlier (Chapter 3). However, in Chapter 3, we illustrated that increased GA levels are probably not required for coumarin-induced hypocotyl elongation. We observed no increase in GA levels in the epidermis (analysed via the nlsGPS1 reporter line) and suggested that the potential increased GA biosynthesis is countered by an increase in GA catabolism. Indeed, in Chapter 3, we observed a 2-fold increase in *GA2OX1* expression, an enzyme involved in GA catabolism of C19 gibberellins (C. Li *et al.*, 2019), and also here, after 3 hours of coumarin treatment, we observed a 2.68 times higher expression of *GA2OX1* (Table 3). Moreover, the expression of *GA2OX8*, coding for an enzyme involved in GA catabolism of C20 gibberellins (C. Li *et al.*, 2019), is increased a 2.27-, 10.14- and 3.87-fold, respectively 30, 60 and 180 minutes after coumarin treatment (Table 1, 2 and 3). Together, these transcript data confirm that ethylene is not essential for coumarin-induced hypocotyl elongation. Moreover, this suggests indeed that the increased GA biosynthesis observed upon coumarin treatment is probably countered by increased catabolism limiting the role of GA during coumarin-induced hypocotyl elongation.

SAURs are both part of the fast and the continious transcriptional response upon coumarin treatment

In Table 1, the significant differential gene expression between hypocotyls treated with coumarin for 30 minutes compared to mock-treated ones is presented. Of the 19 genes that are a 5-fold or more upregulated, 17 are *SMALL AUXIN UP RNAs (SAURs)*, including *SAUR19*. In the gene pool that is expressed 2- to 5-fold higher after coumarin treatment, we observed the upregulation of an additional 6 *SAUR* genes (Table 1). Moreover, 1 hour after coumarin treatment, 14 *SAUR* genes are transcriptionally by more than a 5-fold while 16 *SAUR* genes illustrate a relative expression that is 2 to 5 times higher upon coumarin treatment (Table 2). Three hours after coumarin treatment, 9 *SAURs* are expressed 5-fold higher, while 9 *SAURs* are expressed between 2- and 5-fold higher (Table 3). Based on this overrepresentation of SAURs in our upregulated dataset, with a

significant upregulation of 23 *SAUR* genes already after 30 minutes of coumarin treatment (Fig. 1), there is a clear indication that auxin-induced acid growth plays a role during coumarin-induced hypocotyl elongation. Spartz *et al.* (2014) showed that SAUR proteins through inhibition of type 2C protein phosphatases (PP2Cs) prevent dephosphorylation of membrane H^+-ATPases, increasing their activity and as such induce acidification of the cell wall. Stimulation of the H^+-ATPases via SAUR was forwarded as the missing link in auxin-regulated growth in the hypocotyl: the response of hypocotyls to auxin was too slow to be direct and too fast to involve protein synthesis (Fendrych, Leung and Friml, 2016). The SAUR family contains 79 members in *Arabidopsis thaliana* and is as such the largest family of auxin-induced genes (Hagen and Guilfoyle, 2002). Nevertheless, SAURs not only play a central role in auxin-induced acid growth but also act independently of auxin to fine-tune plant growth in response to internal and external signals (reviewed Stortenbeker and Bemer, 2019). For example in tomato it has been shown that overexpression of stabilized *SAUR19* (fused to a GFP protein for stabilization of the protein) alone is sufficient to stimulate hypocotyl growth and this independently from auxin (Spartz *et al.*, 2017). However, we have shown that overexpression of *SAUR19* could not phenocopy the effect of coumarin on the hypocotyl (Chapter 3). Moreover, the dominant gain-of-function *ost2-2* (*AHA1*) mutant with a constitutive H^+-ATPase pump did not show the same hypocotyl elongation as induced by coumarin. This illustrates that acidification by activation of those pumps (potentially via SAURs) is not enough to induce hypocotyl elongation on itself. Nonetheless, when *H^+-ATPASE 2* (*AHA2)* is knocked-out, the coumarin response is reduced, suggesting at least a partial role of SAUR-induced acidification during coumarin-induced hypocotyl elongation Overall we can conclude that the strong up-regulation of the *SAUR*s illustrates that potentially acidification takes place in the hypocotyl upon coumarin treatment, but that also other factors and shifts in hormonal homeostasis are needed to induce hypocotyl elongation, as acidification alone seems not to be sufficient (Chapter 3). We suggest to analyse acidification of the cell wall in the hypocotyl upon coumarin directly via, for example, HPTS staining (Barbez *et al.*, 2017) or other tools, as HPTS staining in the hypocotyl is not straightforward (Chapter 3).

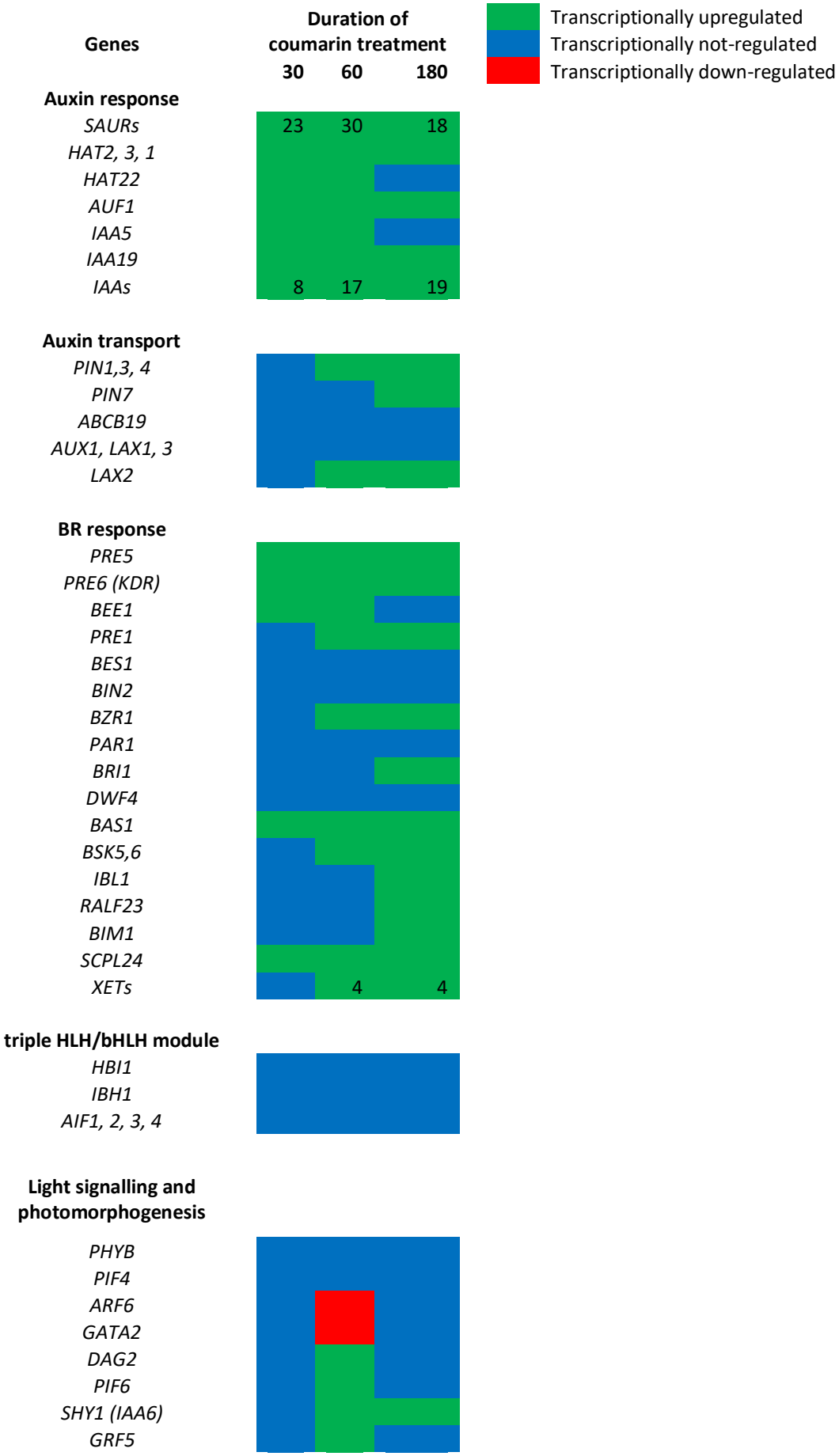
Genes
Duration of coumarin treatment
30
60
180
Transcriptionally upregulated
Transcriptionally not-regulated
Transcriptionally down-regulated
Auxin response
SAURs
HAT2, 3, 1
HAT22
AUF1
IAA5
IAA19
IAAs
23
30
18
8
17
19
Auxin transport
PIN1,3, 4
PIN7
ABCB19
AUX1, LAX1, 3
LAX2
BR response
PRE5
PRE6 (KDR)
BEE1
PRE1
BES1
BIN2
BZR1
PAR1
BRI1
DWF4
BAS1
BSK5,6
IBL1
RALF23
BIM1
SCPL24
XETs
4
4
triple HLH/bHLH module
HBI1
IBH1
AIF1, 2, 3, 4
Light signalling and photomorphogenesis
PHYB
PIF4
ARF6
GATA2
DAG2
PIF6
SHY1 (IAA6)
GRF5

Figure 1: Transcriptional up- and down-regulation of genes upon coumarin treatment.

Red and green indicate, respectively, significant down- and up-regulation, and blue indicate not differentially expressed. 30, 60 and 180 indicates the minutes of coumarin treatment. Black numbers illustrate the amount of genes that are differentially expressed, in case we mention a group of genes (e.g. *SAURs*)

Coumarin induces a clear auxin response in the hypocotyl followed by an upregulation of auxin efflux transporter genes.

In the group of genes that illustrate a 2- to 5-fold differential expression 30 minutes after coumarin treatment (Table 1), there are some candidates that may play an important role during coumarin-induced hypocotyl elongation. For example, the 2-fold increase in *HISTONE ACETYLTRANSFERASE 2 (HAT2)* expression, a homeobox-leucine zipper gene that uniquely is induced by auxin (hence not by other phytohormones) and found to be upregulated already after 15 minutes of IAA treatment (Sawa *et al.*, 2002) is an interesting candidate. *HAT2* is likely a direct target of the observed auxin response upon coumarin treatment. Indeed, also after 1 and 3 hours of coumarin treatment *HAT2* expression is increased compared to mock, respectively with a 4.8- and 3-fold (Table 2, 3). *HAT2* overexpression lines illustrate long hypocotyls (solely the effect of cell elongation) and small leaves (Sawa *et al.*, 2002), in line with the phenotypes observed upon coumarin treatment in the shoot (Chapter 3). The role of *HAT2* during coumarin-induced hypocotyl elongation should be investigated further. Moreover, although minor, we observed a significant increase in expression of other members of the HAT-family: *HAT1, HAT3* and *HAT22* expression is increased after 30 and 60 minutes of coumarin treatment (Fig. 1, Table 1, 2) and after 180 minutes of coumarin treatment the expression of *HAT1* and *HAT3* remained elevated upon coumarin treatment compared to the mock-control (Table 3).

Another interesting candidate is *AUXIN UP-REGULATED F-BOX PROTEIN 1 (AUF1)*, as its expression is increased a 2.9-, 2.98- and 2.23-fold, respectively, after 30, 60 and 180 minutes of coumarin treatment (Table 1, 2 and 3). *AUF1* expression is rapidly and transiently upregulated by auxin (Hurban *et al.*, 2003), making it an important auxin response gene. Moreover, *auf-1* mutants illustrate diminished auxin transport with decreased mRNA levels of *PIN* genes in the root (Zheng *et al.*, 2011). AUF1 is discovered as one of the small mobile RNAs being transported through the plant, indicating it can operate at distinct locations than where it is expressed (Thieme *et al.*, 2015). However, in the shoot, to the best of our knowledge, no data are available on its role in influencing auxin transport and we have no knowledge of available overexpression lines. Further research will be needed to investigate its importance for coumarin-induced hypocotyl elongation.

We showed, in Chapter 3, a diminished response of *pin2* mutants towards coumarin in terms of hypocotyl elongation. Based on the fact that PIN2 is of major importance in auxin-regulated root development (Luschnig *et al.*, 1998; Müller *et al.*, 1998), but only has minor roles in shoot development (Adamowski and Friml, 2015), we postulated that coumarin-induced hypocotyl elongation needs a functional, and potentially even stimulated Polar Auxin Transport (PAT) system. We observed no differential expression of *PIN2* in all 3 time-points (Table 1, 2 and 3), suggesting that, indeed, its role will potentially be secondary by maintaining the PAT system rather than being primarily involved. The importance of auxin transport during coumarin-induced

hypocotyl elongation is also shown by the direct transcriptional upregulation of *PIN-FORMED 1*(*PIN1)*, *PIN3* and *PIN4* by, respectively 1.67, 1.79, and 1.53 times, after 1 hour of coumarin treatment (Fig. 1) Table 2). Moreover, after 3 hours of treatment a 1.49-, 1.75-, 1.59- and 1.67-fold increase in *PIN1*, *PIN3*, *PIN4* and *PIN7* expression is found (Table 3). This in line with the observed increase in expression of *PIN1* and *PIN3* in hypocotyls of 3 DAG old seedlings continuously treated with coumarin (Chapter 3). The increase in *PIN1* and *PIN3* expression is as such a fast response induced by coumarin after 1 hour (Fig. 1) that is maintained during coumarin-induced hypocotyl elongation (Chapter 3), confirming the importance of auxin efflux. The increased expression observed of *ABCB19* in 3 DAG old seedlings continuously treated with coumarin (Chapter 3), is likely a late response as we observed no differential expression of the gene upon short-treatment with coumarin (Table 1, 2 and 3). Note that *SAUR* overexpression lines (e.g. 19, 39, 63) have been shown to increase PAT, auxin levels and expression of auxin response genes (Kant and Rothstein, 2009; Chae *et al.*, 2012; Spartz *et al.*, 2012), connecting the fast upregulation of *SAUR* expression to elevated *PIN* mRNA levels in the hypocotyl of coumarin treated seedlings. No differential gene expression could be observed for *AUXIN RESISTANT 1 (AUX1)*, *LIKE AUX1 1 (LAX1)* and *LAX3* in all 3 time-points of harvesting (Fig. 1, Table 1, 2 and 3), indicating that the observed decrease in *AUX1* expression in the hypocotyl of 3 DAG old seedlings continuously treated with coumarin is a late response (Chapter 3). LAX2 expression is significantly increased 1.56 and 1.23 times after, respectively 1 and 3 hours of coumarin treatment (Table 2 and 3). LAX2 has been shown to facilitate vascular development (Péret *et al.*, 2012), indicating its increased expression can be to support the elongating hypocotyl. However, it is questionable if such low expression values are biologically relevant. In addition, mutant analyses of *aux1, lax1, lax2* and *lax3* illustrate that the involvement of auxin influx during coumarin-induced hypocotyl elongation is minor (Chapter 3). Note that in general, the role of AUX and LAX proteins in the shoot is rather minor (reviewed in Swarup and Bhosale, 2019).

Overall, it is clear that coumarin affects auxin transport on different levels (e.g. via increased *PIN* expression) and this has to be analysed more in detail (e.g. via marker lines) to illustrate the changes in auxin fluxes induced by coumarin in the hypocotyl. Note that auxin transport is transcriptionally upregulated after 1 hour, following the fast upregulaton of SAURs and other auxin response genes already after 30 minutes of coumarin-treatment (Fig. 1).

Of the two remaining genes that illustrate a differential expression of more than a 5-fold after 30 minutes of coumarin treatment, one is unknown and referred to as long noncoding RNA, while the other is *INDOLE-3-ACETIC ACID INDUCIBLE 5 (IAA5)*, an auxin-inducible auxin repressor element (Table 1). IAA5 plays a major role in drought tolerance and has a link with stomata formation (Shani *et al.*, 2017; Salehin *et al.*, 2019). Besides *IAA5*, after 30 minutes of coumarin treatment, we also observed a 2-fold increase in expression of *IAA19* (Table 1). *IAA5* and *IAA19* are upregulated by brassinolide (BL) and indole-3-acetic acid (IAA), whereby it is illustrated that exogenous IAA induced these genes quickly and transiently, whereas exogenous BL induced them gradually and continuously (Nakamura *et al.*, 2003). The expression of *IAA5* and *IAA19* was even higher differentially expressed after 1 hour of treatment, 12.90 and 5.23 times respectively (Table 2), while after 3 hours of treatment no differential expression of *IAA5* could be observed any longer and the expression of *IAA19* dropped to a 4.84-fold increase (Table 3). It will be interesting to check the expression of *IAA5* and *IAA19* upon continuous treatment with coumarin, as to distinguish if this is a BR (a gradual and continuous increase in

expression of those genes) or an auxin (a fast and transiently increase in expression of those genes) response. Aux/IAA elements have been suggested as the link between auxin and BR signalling (Nakamura *et al.*, 2006). After 30, 60 and 180 minutes of coumarin treatment, respectively, 8, 17, 19 *Aux/IAA* genes are upregulated. More research is needed to analyse their role in plant development and to investigate (e.g. via mutant analysis) their significances during coumarin-induced hypocotyl elongation.

Coumarin induces a BR response within 30 minutes after treatment leading to upregulation of cell-wall remodelling enzymes to induce elongation.

After 30 minutes of coumarin treatment, also a clear BR response could be observed: we observed a significant increase in expression of *PACLOBUTRAZOL RESISTANT 5 (PRE5), PRE6* and *BR-ENHANCED EXPRESSION 1 (BEE1)* (Table 1), in line with the observed increase in *PRE1* and *BEE1* expression 3 DAG of seedlings continuously treated with coumarin as described in Chapter 3. In addition to *PRE1*, *PRE5* and *PRE6* are also reported to induce cell elongation by BRs (Ikeda *et al.*, 2012; M.-Y. Bai, Fan, *et al.*, 2012). Interestingly, *PRE6*, also known as *KIDARI* (*KDR*), plays a role in light signalling: the dominant gain-of-function mutant *kdr-D* illustrates hyposensitivity towards light and has elongated hypocotyls (Hyun and Lee, 2006). Note that no differential expression could be observed of *PRE1* after 30 minutes of coumarin treatment, but the expression of *PRE1*, *PRE6*, *PRE5* and *BEE1* are all increased after 60 minutes of coumarin treatment, with a 4.19-, 5.13-, 6.45- and 3.12-fold, respectively (Table 2). After 180 minutes of treatment with coumarin the expression of *PRE1*, *PRE6* and *PRE5* remained respectively, 3.81, 3.32 and 6.32 times higher, but no significant differential expression of *BEE1* was observed anymore (Table 3). Moreover, no differential expression was observed of *BRI1-EMS-SUPPRESSOR 1 (BES1)*, *BRASSINOSTEROID-INSENSITIVE 2 (BIN2)* and *PHYTOCHROME RAPIDLY REGULATED1 (PAR1)* (Table 1, 2 and 3), and we observed a 1.64 times increase of *BRASSINOSTEROID INSENSITIVE 1 (BRI1)* expression only after 3 hours of coumarin treatment (Table 3), all confirming our transcriptional observations in Chapter 3. No differential expression of *DWARF4 (DWF4)*, as observed in Chapter 3, was found (Table 1, 2 and 3), supporting the hypothesis that its increase in expression is part of the late auxin response (Chung *et al.*, 2011; Yoshimitsu *et al.*, 2011). In general, we can conclude that the auxin response likely precedes the BR signalling activation during coumarin-induced hypocotyl elongation (Fig. 1) and the RNAseq data have helped us to refine our model (Chapter 3) by including temporal changes.

Interesting is the 2.2-fold increase in expression after 30 minutes of coumarin treatment of *PHYB ACTIVATION TAGGED SUPPRESSOR 1 (BAS1)* (Table 1), of which the expression remained significantly higher (a 2.53 and 1.77 times increase respectively) 60 and 180 minutes after coumarin treatment (Fig. 1, Table 2 and 3). BAS1 is a negative regulator of BR biosynthesis and its expression is stimulated by PHYTOCHROME B (PHYB) (Neff *et al.*, 1999) and by BRASSINAZOLE-RESISTANT 1 (BZR1) (Youn *et al.*, 2016). The increased expression of *BAS1* indicates, as such, a negative feedback mechanism of increased BR signalling via increased expression of *BZR1* as observed in Chapter 3 (i.e. a 1.3-fold increase in expression) and confirmed here by a 1.29 and 1.28 times increase in expression, respectively, 1 and 3 hours after coumarin treatment (Table 2 and 3). No differential expression of *PHYTOCHROME INTERACTING FACTOR 4 (PIF4)* could be observed at any of the tested time points (Table 1, 2 and 3), in line with the observations in Chapter 3. The BRZ1-PIF4-(ARF6) module is known to activate a broad range of downstream targets, although those 3 genes

can also stimulate elongation independently of each other (Oh *et al.*, 2014). *AUXIN RESPONSE FACTOR 6 (ARF6)* expression is 28% downregulated after 60 minutes of coumarin treatment (Table 2), however, 30 or 180 minutes after coumarin treatment, no differential expression could be observed (Table 1 and 3). The expression profile of *ARF6* is as such not constant (Fig. 1), too small to be biologically relevant and in contrast with the decreased expression of the gene in 3 and 5 DAG old seedlings continuously treated with coumarin (Chapter 3). The role of the BRZ1-PIF4-(ARF6) module during coumarin-induced hypocotyl elongation is not clear out from these transcriptional data and should be investigated further by different methods.

The BRZ1-PIF4 module is known to stimulate BR-induced elongation via a Triple Helix-Loop-Helix/Basic Helix-Loop-Helix Cascade (M.-Y. Bai, Fan, *et al.*, 2012) with the PRE-family basic helix-loop-helix (bHLH) factors promoting cell elongation by interacting antagonistically with *ILI1 BINDING bHLH 1 (IBH1)* (L.-Y. Zhang *et al.*, 2009; Ikeda *et al.*, 2012; M.-Y. Bai, Fan, *et al.*, 2012) and *ACTIVATION-TAGGED BRI1 SUPPRESSOR 1 (ATBS1) INTERACTING FACTORs (*AIFs) (Wang *et al.*, 2009; Ikeda, Mitsuda and Ohme-Takagi, 2013). These in their turn activate (by reduced repression) *HOMOLOG OF BEE2 INTERACTING WITH IBH 1* leading to elongation (see the model in Fig. S4 in Chapter 3). However, we observed no differential expression of *HBI1*, *AIF1* and *AIF4,* and upregulation of *IBH1* expression in 3 DAG old seedlings continuously treated with coumarin (Chapter 3). Upon short treatment with coumarin, we found no differential expression of *IBH1*, *HBI1*, *AIF1-4* confirming that they are no part of the fast transcriptional response upon coumarin treatment (Fig. 1, Table 1, 2 and 3). Based on the contrasting expression profiles observed in the late responses upon coumarin treatment (Chapter 3), and the absence of early transcriptional responses, we can conclude that the role of this triple Helix-Loop-Helix/Basic Helix-Loop-Helix cascade during coumarin-induced hypocotyl is minor to non-existing.

We showed that coumarin interacts with photomorphogenesis to induce hypocotyl elongation, by for example downregulation of *GATA TRANSCRIPTION FACTOR 2 (GATA2)*, an activator of photomorphogenesis and by the fact that *phyb-5* mutants are non-responsive towards coumarin in terms of hypocotyl elongation (Chapter 3). Here, no differential expression of *PHYB* could be observed (Table 1, 2 and 3), while after 1 hour of coumarin treatment *GATA2* expression was downregulated by 41% (Table 2), although after 3 hours of coumarin treatment no differential expression could be observed any longer (Table 3). The transcriptional data of *GATA2* are as such not constant (Fig. 1), and the data are not in line with the clear downregulation of *GATA2* expression (>80 %) observed in 3 DAG old hypocotyls (Chapter 3). Therefore, the role of *GATA2* during coumarin-induced hypocotyl elongation, and in general the interplay with photomorphogenesis should be investigated further. Moreover, gene ontology (GO) analysis of the transcriptome data confirmed the interplay with light signalling and photomorphogensis. GO enrichment of the upregulated genes after 30 minutes of coumarin treatment illustrated no link with light-signalling yet (Fig. 3A), but after 60 minutes of coumarin treatment, GO analysis revealed an upregulation of responses to red and far-red light and genes involved in photomorphogenesis (Fig. 4). Detailed analysis of those GO enrichment groups illustrated following genes that are induced by coumarin: the cytochrome P450 *CYP707A1* (involved in ABA catabolism), *PRE1,6, ZINC-FINGER PROTEIN 1 (ZFP1), DOF AFFECTING GERMINATION 2 (DAG2), PIF6, SHY1 (IAA6)* and *GROWTH-REGULATING FACTOR 5 (GRF5).* Interestingly, GO enrichment of the genes that are significantly downregulated after 30 and 60 minutes of coumarin comprise genes involved in photoperiodism, circadian

rhythm and response to light signalling (Fig. 3B and Fig. 5). Also after 3 hours, we observe upregulation of genes involved in response to light (Fig. 6), however, enrichment of genes involved in light-signalling could not be observed of the downregulated group after 180 minutes of coumarin treatment (Fig. 7). Altogether it is clear, based on the reduced response of *pif4-2* mutants and the completely abolished response of the *phyb-5* mutant towards coumarin-induced hypocotyl elongation (Chapter 3), that light-signalling and photomorphogenesis are part of the molecular changes involved upon coumarin treatment. However, more research will be needed to clarify the exact interactions.

The constitutively upregulated transcriptional response upon coumarin-treatment in the hypocotyl

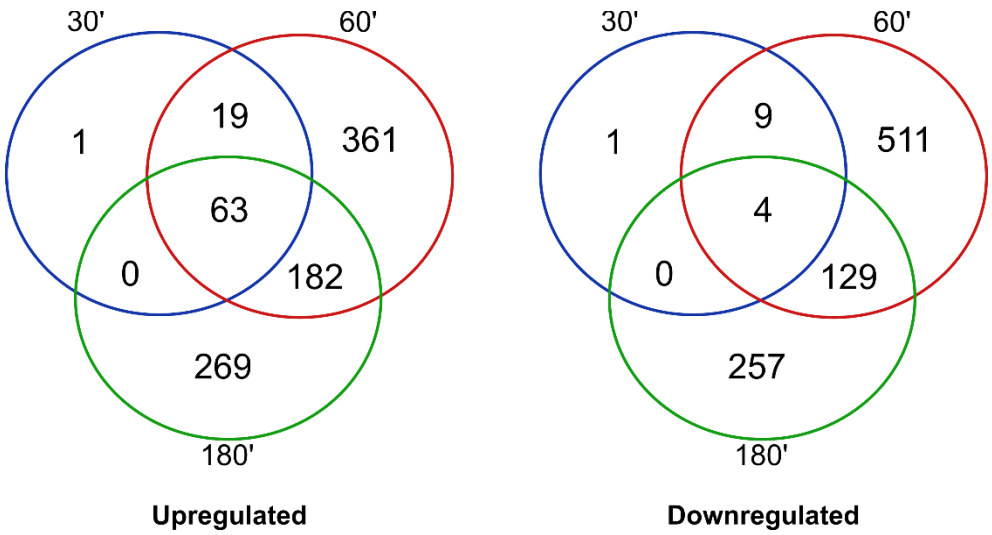

Figure 2: Differential gene expression over the three timepoints of harvesting of the up- and downregulated genes (left and right respectively).

In figure 2, via a VENN diagram, we illustrate the overlap in expression profiles between genes that are significantly and differentially expressed over the three time points of analysis. The genes are listed in table 4 and 5. Remarkably, except for the gene At1g24130 of which the function is currently unknown, all other genes (82 in total) that are upregulated after 30 minutes of coumarin treatment, are also upregulated after 1 hour of coumarin treatment and 63 genes remain expressed higher even after 3 hours of coumarin treatment (Fig. 6). After 60 minutes of coumarin treatment, 182 genes are upregulated that remain transcriptionally induced after 3 hours of treatment (Fig. 6). In total this analysis creates 7 groups of genes based on their overlap in up- or down-regulation over the 3 timepoints, or their unique upregulation at one of the time points (Table 4 and 5). Via gene ontology analysis we can comprehensively reveal the biological and molecular processes that are up- or down-regulated over the three time points of treatment and those will be discussed later. First, we will shortly discuss the 63 genes that are constitutively upregulated upon coumarin treatment. Most of those 63 genes are already discussed in this chapter as they are part of the observed auxin and BR response (e.g. *SAURs, IAAs, HATs, PINs, BAS1, PREs, BZR1* (Fig. 1) and genes involved in GA metabolism and catabolism). Numerous members of those 63 constitutively expressed genes have a role in reshaping the root system architecture and it would be interesting to check their expression in root-specific tissues upon coumarin treatment. Earlier in this

chapter, we already described the transcriptional upregulation of *AUF* at all timepoints of harvesting. Its transcription is rapidly and transiently upregulated by auxin (Hurban *et al.*, 2003), and *auf1* loss-of-function mutants have reduced rates of acropetal and basipetal auxin transport in roots (Zheng *et al.*, 2011). They are also hypersensitive to the auxin transport inhibitors 1-naphthylphthalamic acid (NPA) and 2,3,5- triiodobenzoic acid (TIBA) with respect to root elongation (Zheng *et al.*, 2011). Moreover, *AUF1* inhibits *RESPONSE REGULATOR 1 (ARR1)* expression, limiting *SHORT HYPOCOTYL 2 (SHY2)* expression in the roots (Zheng *et al.*, 2011). However, *SHY2* is another member of those 63 genes that are constitutively upregulated upon coumarin treatment, with an increase in expression by a 2.90-, 4.12- and 2.67-fold, respectively after 30, 60 and 180 minutes of coumarin treatment (Table 1-3). *SHY2* is involved in adjusting root growth by inhibiting meristem formation (Dello Ioio *et al.*, 2008). Moreover, in the hypocotyl *SHY2* is known to play a role in adventitious root formation (Verstraeten, Schotte and Geelen, 2014), a phenotype that is known to be induced by coumarin (see Chapter 6). Besides its well-known role in root development, *SHY2* also plays an important role in hypocotyl elongation (Vandenbussche, Verbelen and Van Der Straeten, 2005). The gain-of-function alleles of *shy2* have short hypocotyls because these mutants are constitutively photomorphogenic (Tian and Reed, 1999). This is, however, in contrast to our finding whereby *SHY2* expression is increased while the photomorphogenic inhibition of hypocotyl elongation is diminished. Also, *MEMBRANE-ASSOCIATED KINASE REGULATOR 4* and *6 (MAKR4* and *6*) are found to be upregulated at all 3 time-points of harvesting, suggesting another link with root formation. *MAKR4* and *6* are known to play a major role in auxin-regulated root spacing. They are upregulated after founder cell specification induced by *GATA23* and as such form the pre-branch-site for lateral root induction (Xuan *et al.*, 2015). Moreover, 30 minutes after coumarin treatment, we observed a 2.60-fold increase in *ASYMMETRIC LEAVES2-LIKE 18 (ASL18*) expression, a key-player in LR initiation (Goh, Joi, *et al.*, 2012). Its expression is increased 3.68- and 3.85-fold, respectively, 60 and 180 minutes after coumarin treatment. 30 minutes after coumarin treatment, the expression of *PROTEIN KINASE 3 ARABIDOPSIS THALIANA 2 (WAG2)* is increased by a 2-fold (Table 1), and its expression remains higher 60 and 180 minutes after treatment, respectively, a 2.37- and 1.85-fold increase in expression (Table 2, 3). *WAG1* and *WAG2* are involved in root waving by influencing auxin transport: the *wag1* and *wag2* mutants illustrate enhanced root waving (Santner and Watson, 2006). The genes *WAG1* and *WAG2* are nowadays incorporated in the PINOID (PID) gene family existing out of *PID* and its homologs *PID2, WAG1* and *WAG3* (Grones *et al.*, 2018). Recently, it was illustrated that this gene family interferes with *PIN3* during root gravitropism as well as during hypocotyl orientation/bending upon an external stimulus (Grones *et al.*, 2018). Alltogether these transcriptional data suggest an influence of coumarin on root formation and this should be investigated further. However, many of the genes mentioned here, with clear functions in the root, are also known to play a role in adventitious root fomation in the hypocotyl (Lakehal and Bellini, 2019). Additonal experiments will be needed to clarify the function of those gene during-coumarin induced hypocotyl elongation, and potentially additional research tracks investigating AR formation upon coumarin treatment should be followed.

Most remaining genes that are constitutively expressed in coumarin-treated hypocotyls have specific roles in plant development. For example, we observed a constitutive increase in expression of *HAIRY MERISTEM2 (HAM2)*, a gene with a clear role in shoot apical meristem proliferation: the HAIRY MERISTEM proteins define a domain within which WUSCHEL (WUS) cannot work, but beyond which WUS is left free to

promote stem cell proliferation (Zhou *et al.*, 2018). Other genes expressed at all 3 time-points of harvesting are *LONGIFOLIA1* (*LNG1*), *ROTUNDIFOLIA LIKE 16 (DLV6) and ROTUNDIFOLIA LIKE 13 (RTFL13).* The latter two are members of a class of small polypeptides known to influence plant development (Wen, Lease and Walker, 2004), while *LNG1*, together with its homolog *LNG2* regulates leaf morphology by promoting cell expansion in the leaf-length direction (Y. K. Lee *et al.*, 2006). The role of those genes in hypocotyl elongation is not known and should be investigated further.

Gene ontology analysis of the biological and molecular responses upon coumarin treatment

Thirty minutes after coumarin treatment, most upregulated genes have biological roles in auxin signalling as well as GA metabolism and are generally involved in growth and developmental responses (i.e. root and shoot development) (Fig. 3A). While the genes that are downregulated after 30 minutes of coumarin treatment are linked to sulphur metabolism and photoperiodism (Fig. 3B). Striking is the strong decrease (± 80 %) in *Low SUlfur1 (LSU1)* expression and its homologues *LSU2* and *LSU3* already after 30 minutes of coumarin treatment (Table 1). Their expression remained significantly lower (60 to 80 %) after 60 minutes of coumarin treatment compared to mock treatment (Table 2). No differential expression could be observed any longer after 3 hours of treatment (Table 3). The *LSU* gene family in Arabidopsis plays a role in sulphur uptake by the plant (Sirko *et al.*, 2015). It is known that coumarins, for example, scopoletin, can operate as chelators, for example for iron uptake (Clemens and Weber, 2016). It is possible that coumarin facilitates sulphur uptake, a negative feedback mechanism of the increased sulphur uptake could then lead to a downregulation of sulphur-starvation genes. It remains to be assessed how to link this observation to coumarin treatment and why those genes are downregulated, for example by playing with sulphur concentrations in the medium. Note, however, that these data are obtained via hypocotyl tissue and the link with sulphur metabolism (presumed to happen via root tissue) is as such even less clear.

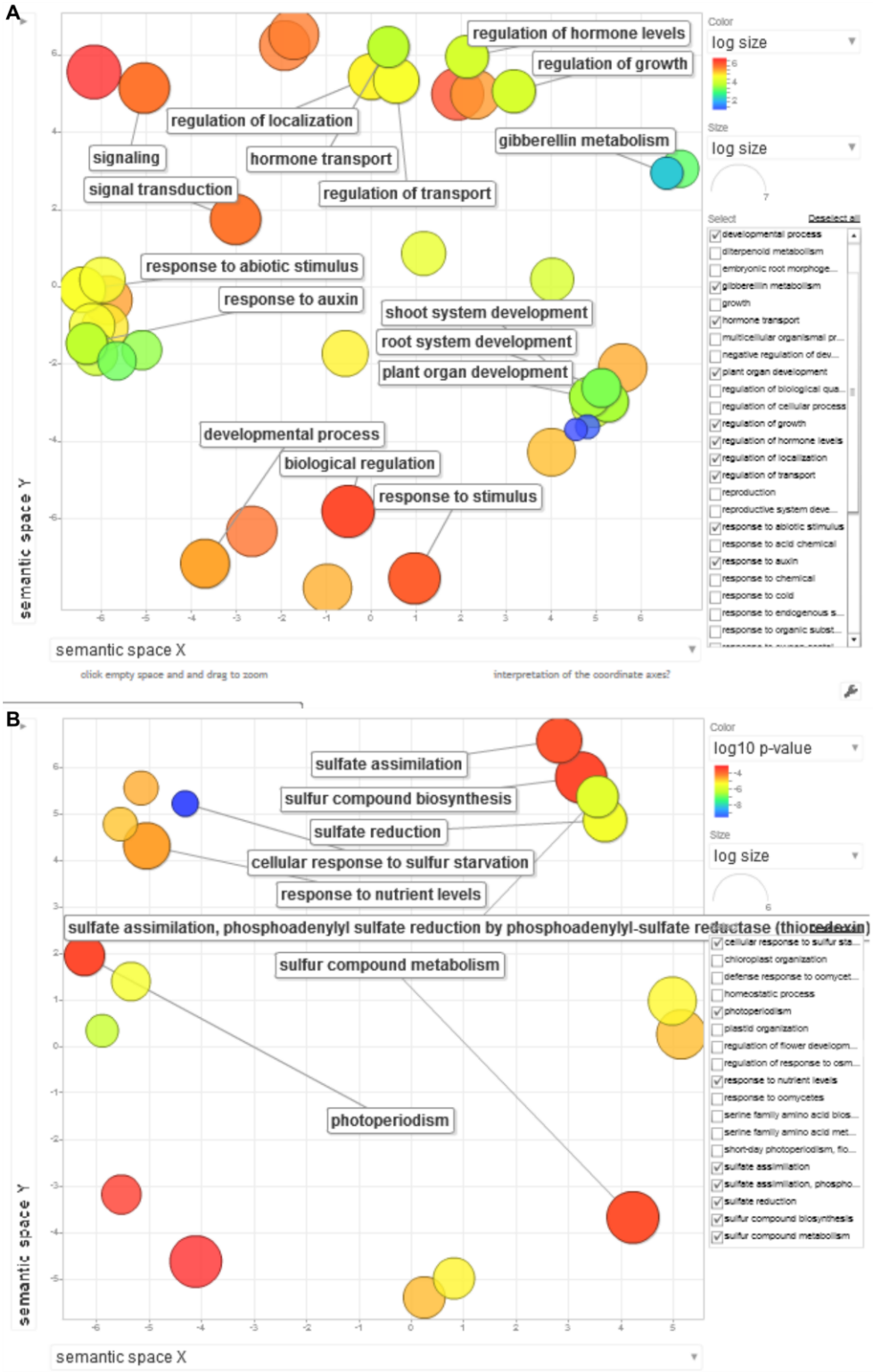

Figure 3: Gene ontology enrichment analysis (p< 0.001) via PLAZA4 of enriched groups in biological processes of the genes upregulated (A) or downregulated (B) after 30 minutes of coumarin treatment. Visual represented via Revigo (see M&M).

After 60 minutes of coumarin treatment, more than 600 genes are upregulated, hence the number of biological processes involved is large (Fig. 4A). We highlighted the processes that are upregulated the most, illustrating upregulation of developmental processes (e.g. seed, root and shoot growth, and meristem development), response to light (cf. above), gravitropism, responses to auxin and auxin activated signalling pathway, regulating auxin transport, BR and GA mediated signalling pathway, BR and GA responses and cytokinin catabolism (Fig. 4A). Regarding molecular processes, an increased hydrolase activity, calmodulin-binding and transferase activity and xyloglucan interactions (potentially involved in cell wall remodelling), RNA binding and DNA interacting factors (transcription factors) and enhanced IAA metabolism are to be noted (Fig. 4B). Interestingly, calmodulin-binding can relate to polar auxin transport, as this depends on calcium signalling (Vanneste and Friml, 2013). Note that also SAURs have a putative calmodulin-binding capacity and could as such potentially influence PAT (Ren and Gray, 2015). One hour after coumarin treatment gene ontology enrichments reveals downregulation of catabolism and of responses to stress, karrikins, ethylene, sulfur starvation, light and gibberellins (Fig. 5A). In terms of molecular processes, we observed a downregulation of genes involved in calmodulin-binding, sulphur metabolism, oxygen binding and numerous reductases as well as genes involved in methyl jasmonate esterase activity (Fig. 5B). The latter potentially explains the observed abiotic stress response.

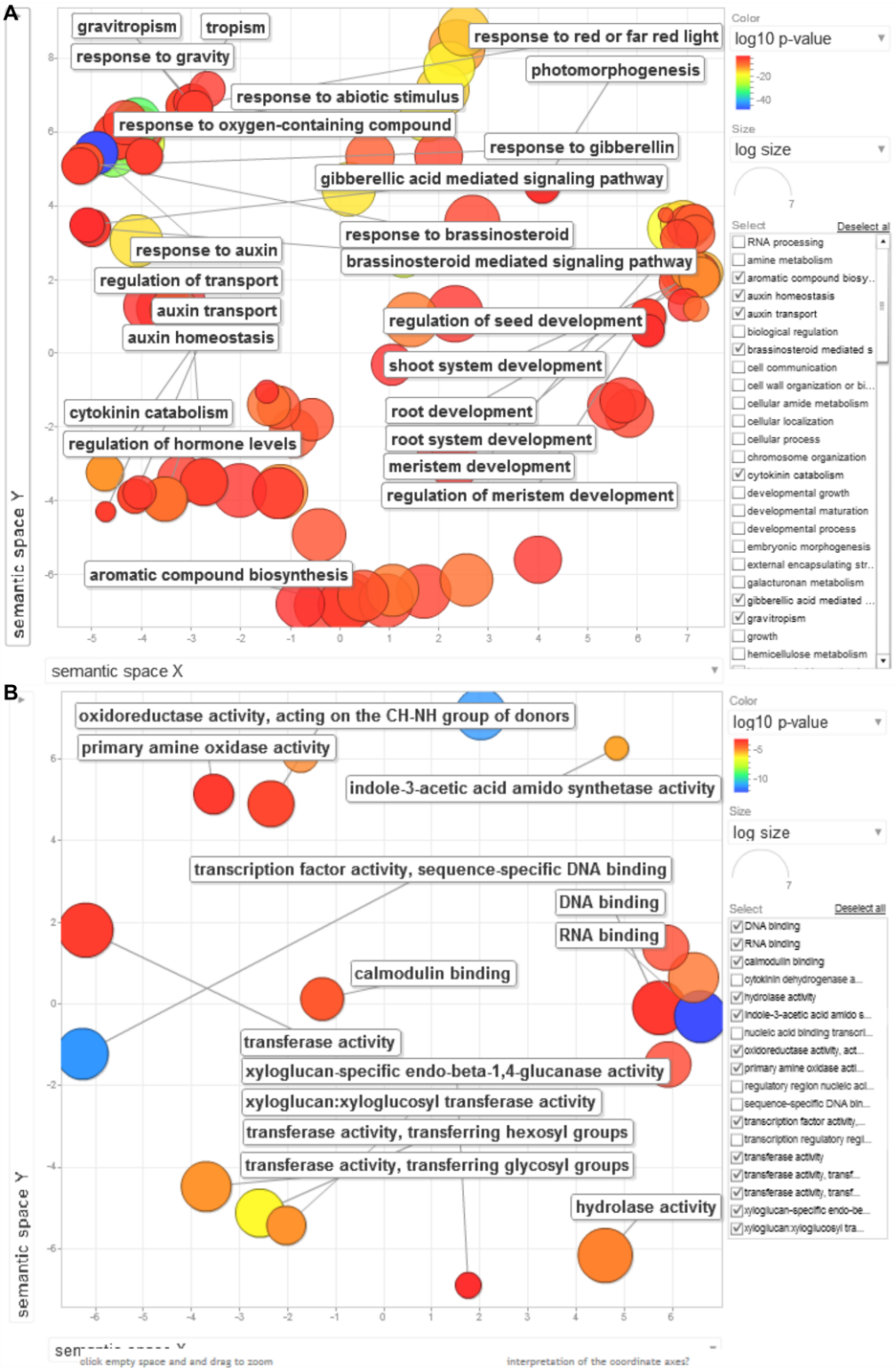

Figure 4: Gene ontology enrichment analysis ($p < 0.001$) via PLAZA4 of enriched groups in biological processes (A) and molecular function (B) of the genes upregulated after 60 minutes of coumarin treatment. Visual represented via Revigo (see M&M).

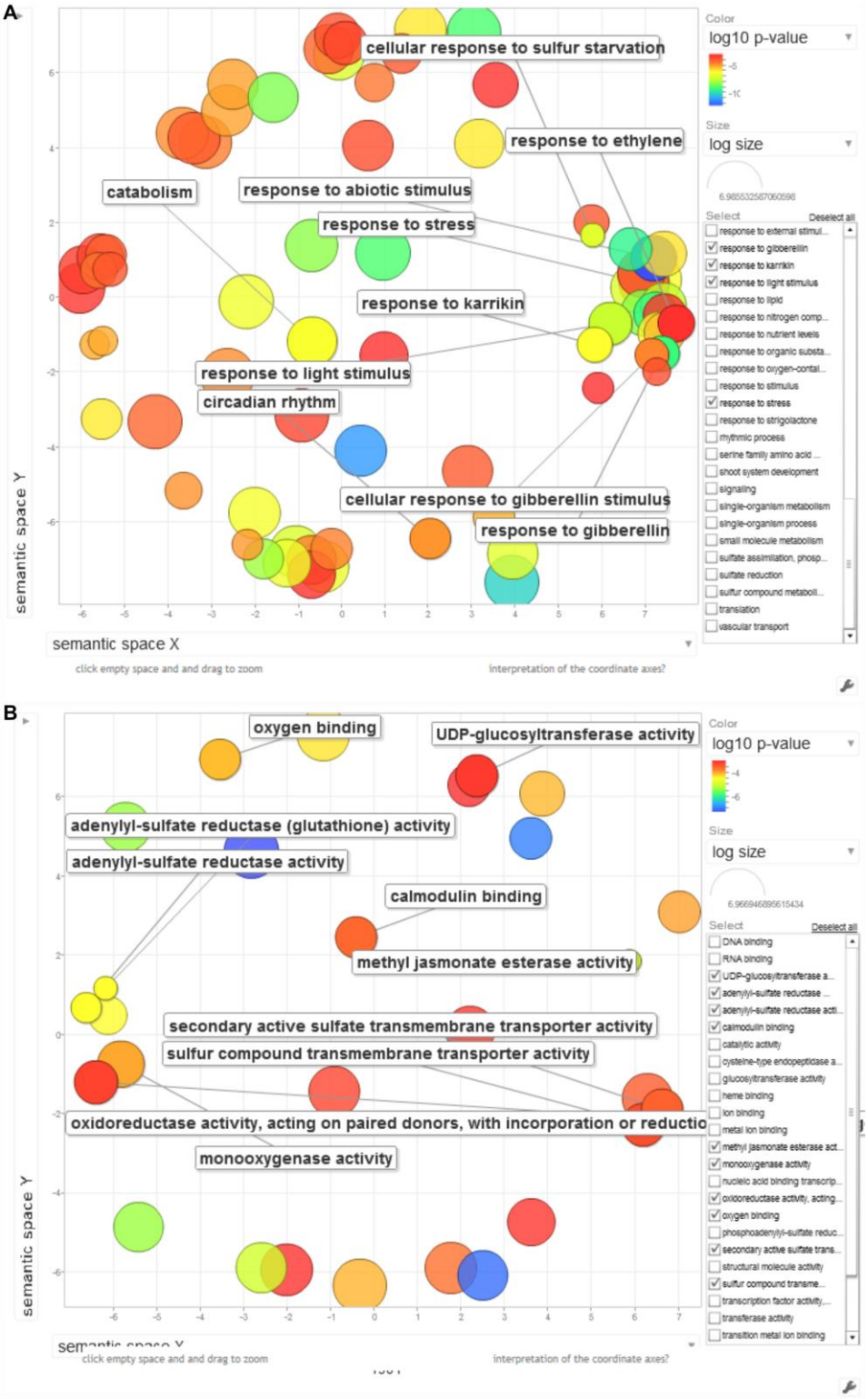

Figure 5: Gene ontology enrichment analysis (p< 0.001) via PLAZA4 of enriched groups in biological processes (A) or molecular function (B) of the genes downregulated after 60 minutes of coumarin treatment. Visual represented via Revigo (see M&M).

In terms of biological processes, we observe a similar picture 3 hours after coumarin treatment (Fig. 6A) as after 1 hour of coumarin treatment (Fig. 4A), although we observe a higher representation of BR and steroid responses (Fig. 6A). Those BR and steroid responses include a higher expression of *BZR1, RALF23, PRE1, PRE6, PRE5, BRASSINOSTEROID-SIGNALING KINASE 5 and 6 (BSK 5 and 6), IBL1, SCPL24, BRI1, and BES1-INTERACTING MYC-LIKE1 (BIM1)* (Table 3). We keep observing an overrepresentation of genes involved in RNA and DNA binding, IAA-amido synthetase activity and hydrolase activity, while also GTPase activity became apparent (Fig. 6B). Importantly, here we also notice the onset of cell wall remodelling (through activation of XETs) upon coumarin treatment, linking the signalling events with the mechanisms required to facilitate cell expansion. At last, after 180 minutes of coumarin treatment, we observed a significant downregulation of 390 genes that mainly have roles in responses to stress, cytokinin and ABA signalling, oxidation-reduction processes and seed development (Fig. 7A). Those downregulated processes relate to a reduction in oxygen binding and oxidoreductase activity (Fig. 7B), and just like after 1 hour of coumarin treatment, methyl jasmonate esterase activity remains reduced and, interestingly, we observe a reduced abscisic acid binding (Fig. 7B).

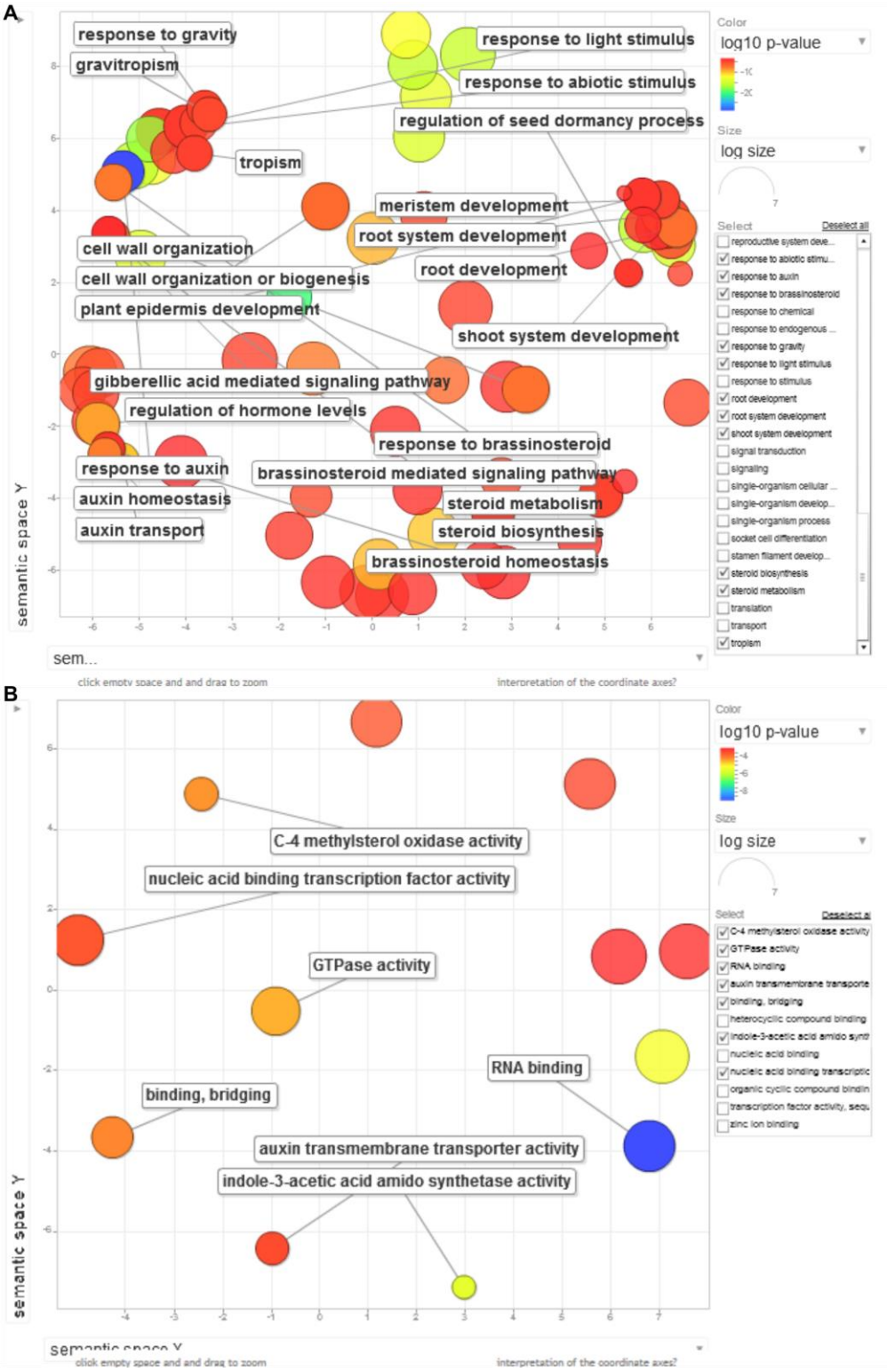

Figure 6: Gene ontology enrichment analysis (p< 0.001) via PLAZA4 of enriched groups in biological processes (A) and molecular function (B) of the genes upregulated after 180 minutes of coumarin treatment. Visual represented via Revigo (see M&M).

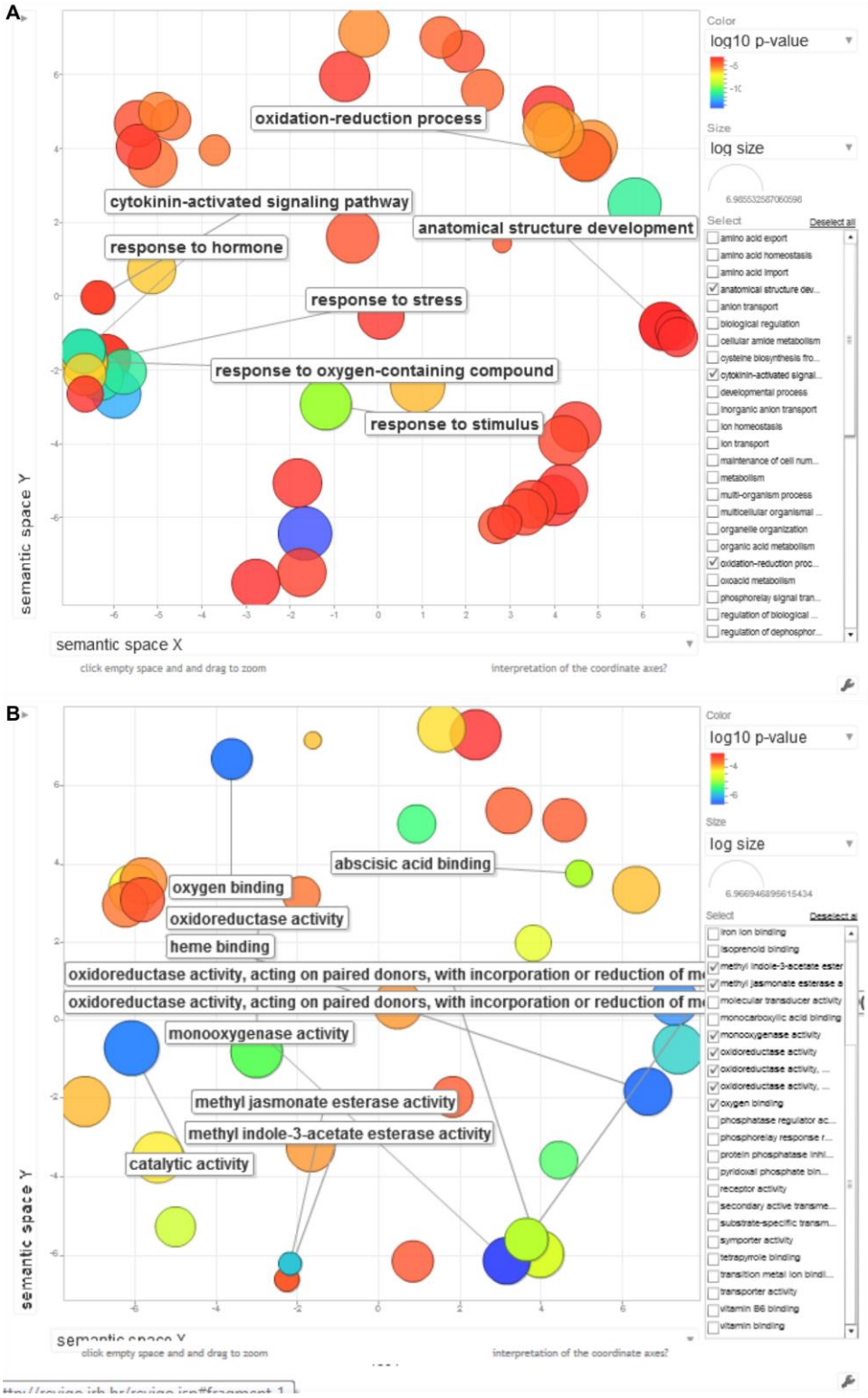

Figure 7: Gene ontology enrichment analysis (p< 0.001) via PLAZA4 of enriched groups in biological processes (A) and molecular function (B) of the genes downregulated after 180 minutes of coumarin treatment. Visual represented via Revigo (see M&M).

Overall this genome-wide transcriptome analysis of hypocotyls allowed us to (1) analyse the direct transcriptional changes upon coumarin, (2) observe the chronology of the interactions (Fig. 1) and (3) elaborate the postulated model in Chapter 3. Hence, in figure 8, we illustrate a refined and expanded model of the one illustrated in Chapter 3, showing the molecular players involved in coumarin-induced hypocotyl elongation. We revealed that first an auxin response upon coumarin treatment is established, inducing a high number of *SAUR* genes, followed by changes in auxin transport and the activation of several *Aux/IAA* genes. Next, these changes will lead to a clear induction and upregulation of BR signalling, followed by a strong BR response. Already after 3 hours of coumarin treatment, this will lead to cell wall remodelling via an increase in XYLOGLUCAN ENDOTRANSGLYCOSYLASES (Campbell and Braam, 1999; Clouse, 2015). While coumarin stimulates auxin and BR responses, the RNAseq data reveal that coumarin downregulate processes linked to cytokinin, jasmonate and ABA homeostasis.

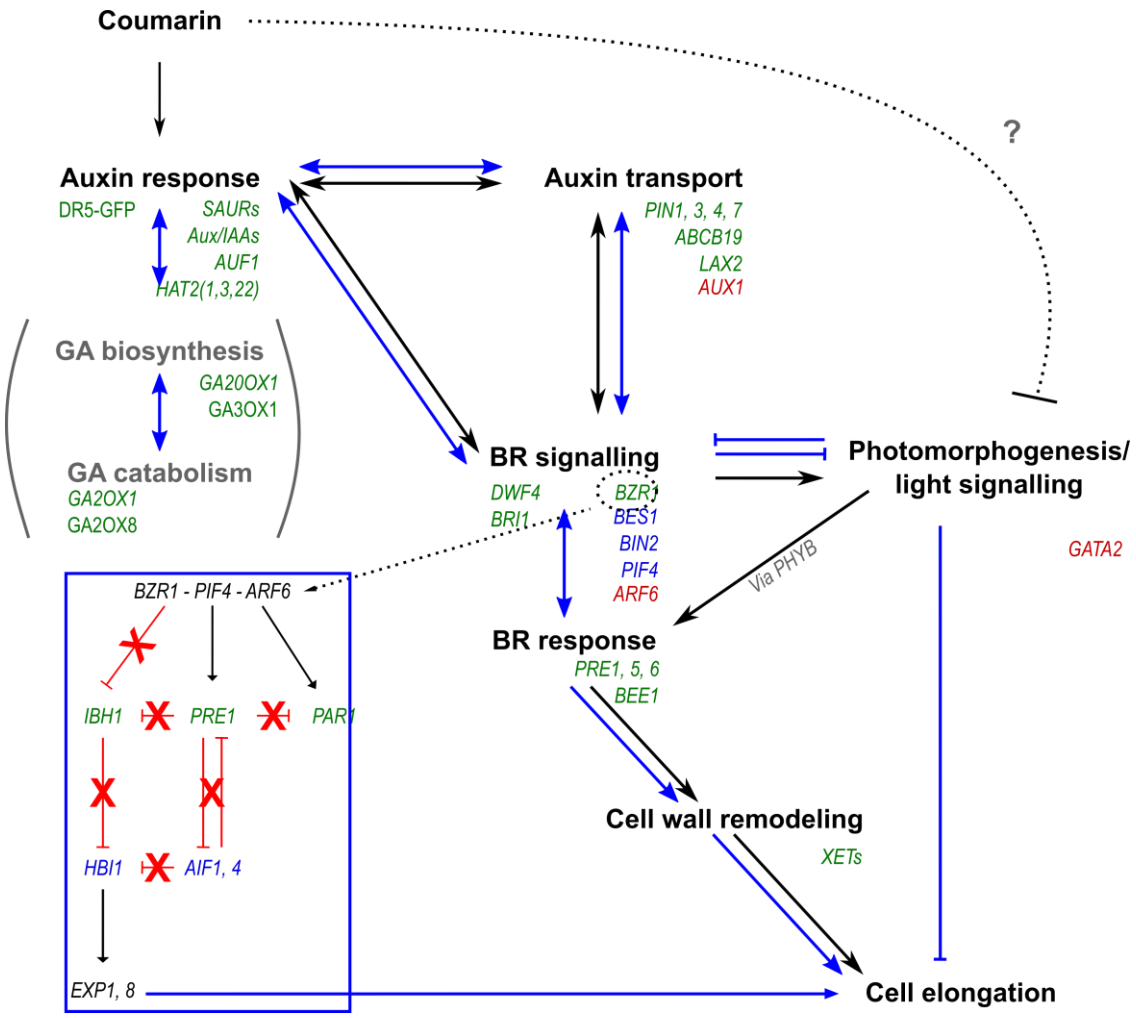

Figure 8: Model illustrating the transcriptional changes observed upon coumarin treatment. By taking into account the chronology of the gene upregulation this model shows the hypothetical mode-of-action of coumarin induced hypocotyl elongation.

Coumarin treatment induces an auxin response in the hypocotyl, observed via increased expression of numerous *SAUR* genes after 30 minutes of coumarin treatment, an increased expression that remained 3 hours

after coumarin treatment. Upon continuous treatment with coumarin, only the expression of *SAUR19* has been validated and showed an enhanced expression even 5 days after germination of seedlings continuously exposed to coumarin (Chapter 3). The auxin response is also observed via enhanced *pDR5rev::GFP* transcription (Chapter 3) and the fast upregulation of *IAAs*, *AUF1* and *HAT2*. Auxin signalling is crucial for coumarin-induced hypocotyl elongation and coumarin clearly affects auxin transport, with a fast upregulation of expression of *PIN1, 3* and *4* after 1 hour of coumarin treatment in the hypocotyl, whereby it has been shown that a diminished PAT inhibits the phenotype. Next, coumarin, already after 30 minutes of treatment, induces a BR response, observed by increased expression of *BEE1*, *PRE5 and PRE6*, however, most of the BR response genes are upregulated after 1 hour of coumarin treatment. The expression of *PRE1* and *BEE1* remains higher expressed even 3 and 5 days after germination. Based on this fast and constitutive upregulation it is unclear if this BR response is a direct effect of coumarin, or if coumarin operates via auxin (transport) or vice-versa. Therefore we represented the interactions with double arrows to illustrate that coumarin induces an auxin and brassinosteroid response while enhancing auxin transport, but the order of the interactions is unclear. Mutant analysis (in Chapter 3) revealed that those three players are at the basis of coumarin-induced hypocotyl elongation. Here we could also pinpoint the involvement of cell wall remodelling as we observed increased expression of XETs after 1 and 3 hours of coumarin treatment. In chapter 3, it has been shown that the *phyb-5* mutant is not responsive to coumarin in terms of hypocotyl elongation. It is known that BR can still induce elongation in *phyb* mutants indicating that BRs operate downstream of *PHYB*-signalling (Wu *et al.*, 2019). Therefore, we postulate that the induced BR signalling operates via PHYB to induce a BR response leading to cell elongation.

Black arrows indicate the postulated model based on the data gathered here and in Chapter 3. In green, red and blue we indicated the genes that are, respectively, transcriptionally up-, down- or not-regulated upon coumarin treatment. Arrows indicate stimulatory interactions, while T-lines indicate inhibitory interactions. Blue lines illustrate interactions as described in the scientific literature. The grey dotted line with a question mark indicates a potential direct interaction of coumarin on photomorphogenesis or vice-versa, but currently, any proof or clarification is lacking. The blue box presents the described triple Helix-Loop-Helix/Basic Helix-Loop-Helix Cascade that controls cell elongation downstream of BR signalling (M.-Y. Bai, Fan, *et al.*, 2012; Oh *et al.*, 2014) as done in Fig. S4 (Chapter 3). The red crosses indicate the opposing data gathered here and in Chapter 3, showing that this cascade is not at the basis of coumarin-induced hypocotyl elongation. The observed transcriptional interaction with GA biosynthesis and catabolism is placed in grey as its need for coumarin-induced hypocotyl elongation is not proven and therefore put aside in the model (illustrated with grey brackets).

Supplementary material

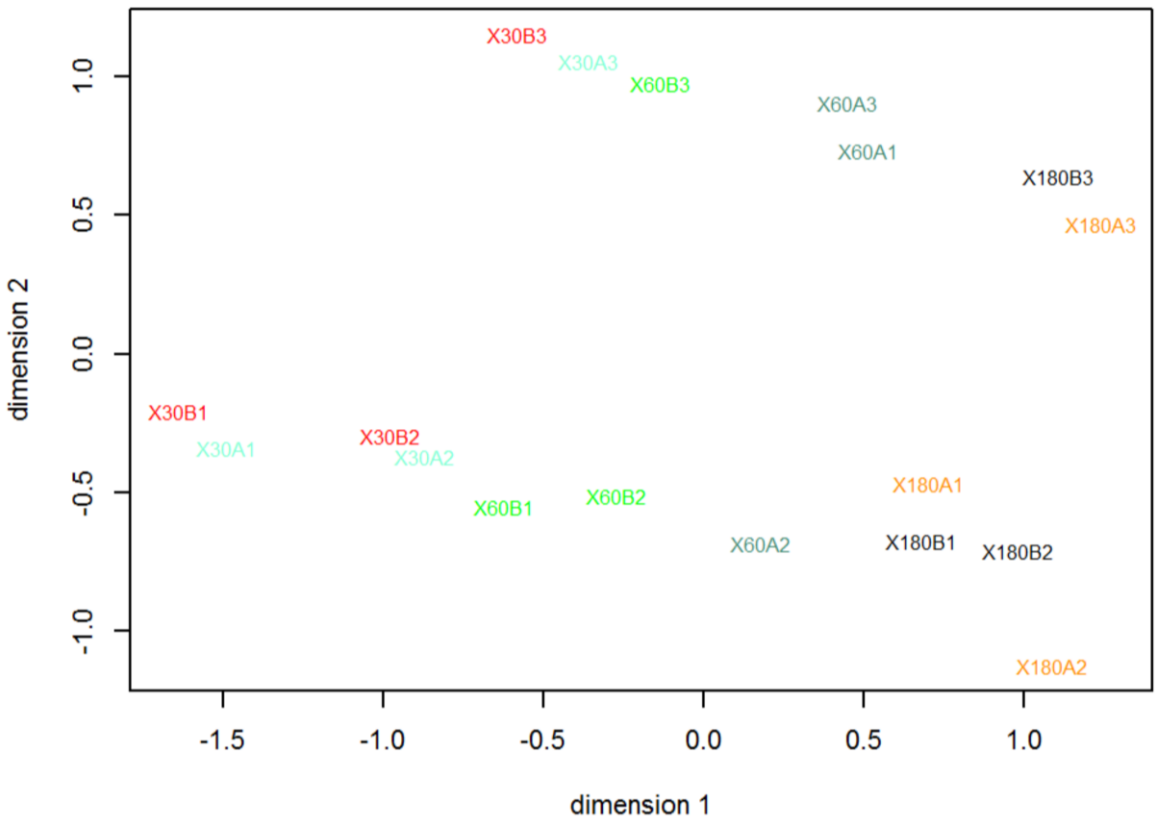

B

sampleID	Treatment	Transfer	group	Bio-repeat
30A1	Mock	30minutes	Mock_30	1
30A2	Mock	30minutes	Mock_30	2
30A3	Mock	30minutes	Mock_30	3
30B1	Coumarin	30minutes	Coumarin_30	1
30B2	Coumarin	30minutes	Coumarin_30	2
30B3	Coumarin	30minutes	Coumarin_30	3
60A1	Mock	60minutes	Mock_60	1
60A2	Mock	60minutes	Mock_60	2
60A3	Mock	60minutes	Mock_60	3
60B1	Coumarin	60minutes	Coumarin_60	1
60B2	Coumarin	60minutes	Coumarin_60	2
60B3	Coumarin	60minutes	Coumarin_60	3
180A1	Mock	180minutes	Mock_180	1
180A2	Mock	180minutes	Mock_180	2
180A3	Mock	180minutes	Mock_180	3
180B1	Coumarin	180minutes	Coumarin_180	1
180B2	Coumarin	180minutes	Coumarin_180	2
180B3	Coumarin	180minutes	Coumarin_180	3

Figure S1: Multi-Dimensional Scaling plot

MDS plot illustrating the grouping of the samples based on the duration of treatment and the bio-repeat (top). On the bottom information about the sampleID's used on the top. Transfer means the timeframe of treatment, e.g. 30 minutes means treated for 30 minutes.

Coumarin induces dormancy in *Arabidopsis thaliana*

Stan Van Praet[1,2,3], Bartel Vanholme[1,2], Stephen Depuydt[1,2,3]

4. Ghent University, Department of Plant Biotechnology and Bioinformatics, (Technologiepark 71), 9052 Ghent, Belgium
5. VIB Center for Plant Systems Biology, (Technologiepark 71), 9052 Ghent, Belgium
6. Ghent University Global Campus, Lab of Plant Growth Analysis, Incheon, South Korea

Author contributions:

S.V.P. and S.D. conceptualized and designed the research; S.V.P. performed the research/experiments. S.V.P., B.V and S.D. interpreted the data. S.V.P. analysed the data, performed the statistics and made the figures; S.V.P. drafted the manuscript and B.V. and S.D. revised it.

For limiting the number of pages, here, we will refer to the figures shown in the previous section 'RNA sequencing of hypocotyls of *Arabidopsis thaliana* treated with coumarin sheds light on the molecular basis of coumarin-induced phenotypes' and we will continue the numbering of figures.

Abstract

Via the gene ontology enrichment tool of PLAZA 4, we found a clear interaction of coumarin treatment with germination and dormancy processes. This is rather surprising as the transcript data where gathered from hypocotyl tissue only. Nevertheless, validation by some initial experiments showed that indeed coumarin affects germination by stimulation dormancy. We postulate that coumarin stimulates dormancy by inducing *RGL* and *GAI* expression, with an interplay with SMAX1, red-light receptors and abscisic acid (ABA) homeostasis. Further research will be needed to clarify its role during coumarin affect plant growth. The transcriptome data on the hypocotyl are currently not conclusive for the role of ABA in coumarin-induced dormancy which awaits further research.

Introduction

Germination is a complex trait balancing between germination (induced by gibberellins) and seed dormancy (induced by abscisic acid), involving the interaction of several plant hormones (Bewley, 1997; Koornneef, Bentsink and Hilhorst, 2002; Holdsworth, Bentsink and Soppe, 2008). By definition, germination of seeds starts with the uptake of water, followed by metabolic changes and later the rupture of the surrounding structures (the testa) (mostly by the radicle) (Bewley, 1997; Nonogaki, Bassel and Bewley, 2010). It is also named 'visible germination' and indicates the end of the germination process. Dormancy is a special trait of seeds, meaning that the seeds lack the capacity, at the time, to germinate, although it is in favourable conditions (Baskin and Baskin, 2004). Out of an evolutionary point of view, this is a very interesting trait: dormancy makes the seeds wait to germinate in favourable conditions until the prospects are good (Nonogaki, 2014; Née, Xiang and Soppe, 2017). Seeds can stay dormant for many years up to centuries (de Candolle, 1832; Turner, 1933), a useful feature in the restoration of heathlands (Putwain and Gillham, 1990). Dormancy, however, is species-dependent and also the environment (light, humidity, temperature and time) has a huge influence (Duvel, 1905; Koornneef, Bentsink and Hilhorst, 2002). Temperature and humidity play a role to keep seeds in their dormant state, without affecting their viability. A practical consequence, is the ability for us, as humans, to store seeds for 'doomsday' (Higgins, 2018). However, the international seed bank in Norway is, ironically, suffering from climate change, while the latter is already putting our natural seed banks under pressure (Ooi, 2012; Epstein, 2019). In Arabidopsis, seed dormancy can be released by a period of dry storage called after-ripening and by cold stratification, taking up or imbibing water in the cold (Ge and Steber, 2018), a treatment to stimulate synchronous germination in our experimental set-ups.

Abscisic Acid (ABA) is the main driver of seed dormancy as already described over 50 years ago (Sondheimer, Tzou and Galson, 1968). ABA levels are significantly upregulated during seed maturation (Karssen et al., 1983), preparing the seed for its dormancy (e.g. by inducing accumulation of storage proteins). ABA biosynthetic mutants such as *aba1* and *aba2* display reduced seed dormancy (Karssen et al., 1983; Koornneef and van der Veen, 1980; Marin et al., 1996), while seedlings treated with ABA illustrate enhanced dormancy. Dormancy is not a static process, as it has been shown that *de novo* ABA biosynthesis in imbibed seeds is required for the maintenance of seed dormancy (Ali-Rachedi *et al.*, 2004). More recently, additional hormones have been demonstrated to contribute to dormancy and germination. Among them, an important role has been identified for ethylene, by antagonising ABA effects (as reviewed in Linkies and Leubner-Metzger, 2012), and promoting germination in *Arabidopsis thaliana* (Linkies *et al.*, 2009). Nevertheless, the main driver of germination is gibberellic acid (GA). Its role to break dormancy has been described already in 1959 (Kallio and Piiroinen, 1959). ABA levels decrease strongly when dormancy ceases and then is followed by *de novo* GA biosynthesis needed for germination (Ogawa et al., 2003). The need for gibberellins is illustrated by the fact that GA biosynthetic mutants such as *ga1* are unable to germinate even under favourable conditions (Karssen et al., 1983; Koornneef and van der Veen, 1980; Marin et al., 1996), unless GA is exogenously applied or the seed coat is removed. The latter is the consequence of GA that facilitates germination via weakening of the mechanical restraint of the endosperm (Groot and Karssen, 1987). GA signalling is a de-repression model (Harberd, 2003), where DELLA proteins act as growth repressors and GA-mediated DELLA degradation is required to induce growth. Interestingly, GA-insensitive signalling mutants like the F-box protein signalling

mutant *sly1* (*sleepy1*) (Daviere and Achard, 2013), have an increased seed dormancy, whereas GA hypersensitive mutants like *spy* (*spindly*) display decreased seed dormancy. On the other hand, the loss-of-function mutation *rgl2* (RGL2 is a DELLA protein), allows plants to germinate even in the absence of *de novo* GA biosynthesis. Moreover, loss of the DELLA gene *RGL2* rescued the germination of the GA biosynthesis mutant *ga1-3* in the light, but the complete rescue of germination of *ga1-3* in the dark required additional mutations in the DELLA genes *RGA* and *GAI* (Cao *et al.*, 2005). As such, the current view is that domination of DELLA repression (and not the absence of GA) is the cause of dormancy (Seo *et al.*, 2009; Ge and Steber, 2018). An important feature of GA and ABA metabolism is their interaction. For example, ABA down-regulates GA biosynthesis and up-regulates GA deactivation (Seo *et al.*, 2006). In addition, besides ABA and GA involvement, seed germination is regulated by a large number of proteins, which are affected by both developmental and environmental factors touching upon all known hormones (reviewed in Née, Xiang and Soppe, 2017).

In general, coumarin inhibits germination in different plant species (both monocots as dicots) (Audus and Quastel, 1947; Blaim, 1960; Abenavoli *et al.*, 2006; Pergo *et al.*, 2008; Saleh and Abu El-Soud, 2015; Saleh, Madany and González, 2015). Inhibiting germination can occur in 2 ways, (1) toxicity, meaning the seed loses its viability or (2) through dormancy. In rice, it was illustrated that coumarin enhanced dormancy by inhibiting ABA catabolism (leading to higher ABA content) via decreasing the expression of the ABA catabolism genes *(Oryza sativa) ABA 8'-HYDROXYLASE 2* and *3 (OsABA8'ox2/3)* (Chen *et al.*, 2019). Moreover, it was illustrated that coumarin inhibited the accumulation of reactive oxygen species (ROS) in the rice embryo, by increasing the activity of superoxide dismutase and catalase (Chen *et al.*, 2019). However, a few papers also show that coumarin, at very low concentrations, stimulates germination in wheat (Knypl, 1964d; Saleh and Kebeish, 2018). It was shown that coumarin stimulated alpha-amylase activity in the aleurone layers of wheat (Saleh and Kebeish, 2018). In addition, an increase in ROS content was observed (Saleh and Kebeish, 2018). Also our transcript data hint on the role of coumarin in affecting germination. This is remarkably seen the RNAseq was performed on hypocotyl tissue only. For example, we observed an increase in *NINE-CIS-EPOXYCAROTENOID DIOXYGENASE 5 (NCED5)* expression, a key enzyme in the biosynthesis of abscisic acid at all timepoints of harvesting (Table 1, 2 and 3). *NCED5* plays a major role in seed dormancy, together with other NCED members (NCED 6 and 9), but does not influence GA content (Frey *et al.*, 2012). However, in vegetative tissue, hence also in the hypocotyl, *NCED5* (and in general ABA) plays a major role in drought tolerance (Frey *et al.*, 2012). Nevertheless, we also observed differential expression of genes that are only known to have a role in germination. For example, *MEDIATOR OF ABA-REGULATED DORMANCY 1* (*MARD1*) is involved in seed dormancy (He and Gan, 2004; Drechsel, Raab and Hoth, 2010) and is one of the 4 genes that is downregulated in all 3 timepoints of harvesting. Moreover, we observed downregulation of *SUPPRESSOR OF MAX2 1* (*SMAX1*) (Table 1, 2 and 3). *SMAX1* transcripts are most abundant in dry seeds, consistent with its function in seed germination control via karrikinins (Stanga *et al.*, 2013). This link could be an interesting path to pursue further (Waters *et al.*, 2014).

Here, via some small preliminary experiments, we aimed to get a first idea of how coumarin affects seed germination. In general, it is clear that coumarin induces seed dormancy and we could clearly indicate an

important role of light signalling. Seeds in the dark show an enhanced level of dormancy upon coumarin treatment compared to the light-germinated control.

Materials and methods

Sterilization, stratification, growth conditions, growth medium and treatment preparation

Seeds were surface-sterilized by treatment with 70 % ethanol for 5 minutes, followed by a treatment with 100 % ethanol for 2 minutes. Incubation took place at room temperature while regularly inverting the Eppendorf tubes. The seeds were dried in the Laminar Air Flow (LAF) in a small sterile Petri dish Ø1 inch (SPL Life Science®, South Korea). Seeds were sown on 90x90x20 mm round Petri Dishes (SPL Life Science®, South Korea) containing 100 ml of ½ Murashige & Skoog growth medium (per litre demineralized water 2.15 g MS + vitamins, 0.5 g MES (2-(N-morpholino) ethanesulfonic acid), 0.1 g Myo-inositol, 10 g sucrose and 8 g agar (or 6.5g gelrite), pH of the medium was adjusted to 5.7 using a 1 M KOH solution). Seeds were stratified for a minimum of 4 nights. Plants were grown vertically at 21 °C, long-day conditions (16 h/8 h light/dark) and 120 PAR light.

Stock solutions

All chemicals that were dissolved in DMSO, and, as such, DMSO was used as a mock control. All compounds were added to the growth medium after autoclaving and cooling down to 60 °C. A 40 mM stock of coumarin (Tokyo Chemical Industry co., LTD), a 10 mM stock of 1-Naphthaleneacetic acid (Sigma-Aldrich), a 50 mM stock of 1-amino-cyclopropane-1-carboxylate (ACC) Sigma-Aldrich and a 10 mM stock of Gibberellic Acid (Duchefa Biochemie) was made.

Experimental set-up

Experiments were performed in 3 biological repeats. Seeds were sown with a density of ±100 seeds per plate and 3 plates/bio-repeat. Germination assays performed in the dark are obtained by wrapping the petri dishes in aluminium foil after the seeds received a light pulse of 4 hours (i.e. by placing the plates unwrapped in the growth chambers for 4 hours).

Statistical analysis

The statistical package ‘R version 3.5.1’ (https://www.r-project.org/) was used for the statistical analyses. The least-square means of the biological repeats were subjected to statistical analysis, in which the sample size (n) is the total number of seedlings analyzed per line/conditions. For the pairwise comparison of two experimental groups, statistical analysis has been performed using a Student t-test. To address the statistical difference between two or more experimental groups a Generalized Linear Mixed-Effects Models with ‘Poisson’ as the family function was used (McCullagh and Nelder, 1989; Dobson and Barnett, 2008). Posthoc analysis was performed via a Tukey correction. The statistical assumptions of (1) normal distribution (via

histogram) and (2) homogeneity of variances (by analysis of the residuals (QQ-plot)), were tested, and where needed were log-transformed if data did not comply.

Results

To get an idea of how dormancy and germination of Arabidopsis are affected by coumarin treatment, we started by analyzing the effect of different concentrations of coumarin, ranging from 10 to 150 µM on the germination of *Arabidopsis thaliana* both in the light (long day conditions), as well as in the dark (after a 4-hour light pulse to induce germination). We found that coumarin inhibits germination but only at the higher concentrations: up to 50 µM of coumarin treatment the germination ratio was not significantly affected when germinated in the light (Fig. 8). Interestingly, for dark-grown germination, we observed already a significant reduction of 25% in germination rate upon 25 µM of coumarin treatment (Fig. 8). Moreover, upon 150 µM of coumarin treatment, 80% of the seeds still germinated in the light, while almost none of them germinated in the dark (Fig. 8).

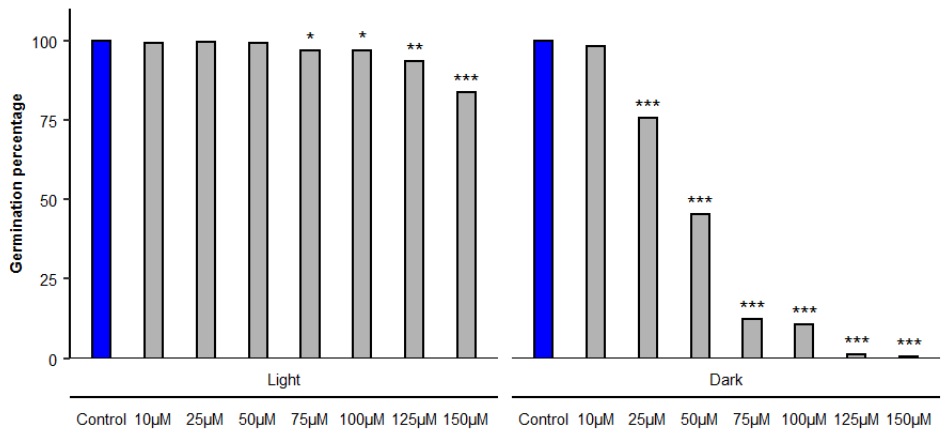

Figure 8: Coumarin inhibits germination in the dark more severely than in the light

(Left) seedlings germinated in the light (long day conditions). (Right) seedlings germinated in the dark after a 4-hour light pulse to induce germination. On the x-as, the different coumarin concentrations (in µM) are represented.

Data presented are means of at least three biological repeats. Asterisks denote significant differences between the mock control and treatment within the light-condition. (* = $p<0.05$, ** = $p<0.001$, *** = $p<0.001$).

To fully clarify these effects (i.e. the difference in germination inhibiting properties of coumarin depending on the light conditions) we performed an experiment to exclude the influence of (1) light on the technical aspects of our growing conditions (e.g. breakdown of coumarin in the light) and (2) the potential loss of the volatile coumarin (Fig. S2). In short, we observed the same inhibitory effect of coumarin on germination, even if the plates were primarily placed in the growth chamber in the light for 7 days, followed by sowing and placing them in the dark. This indicates that coumarin is not broken down by the light, nor significantly reduced

in concentration during exposure in the growth rooms. As such we can confidently state that the inhibitory effect of coumarin on germination is released by the light.

Although the germination ratio was barely affected by coumarin in the light, we observed a delay in germination. Indeed, in light-grown conditions, germination upon 40 µM of coumarin is 12 to 24 hours delayed, while upon 100 µM of coumarin we observed a 48-hour delay (Fig. 9). Note that we observed that a ±10 per cent of the seeds do not germinate upon 100 µM of coumarin (Fig. 8), we took this into account and rescaled the germination percentage to all germinated seeds counted 1 week after germination induction in the mock control (Fig. 9). We observed that no further germination occurred of seeds after 96 hours.

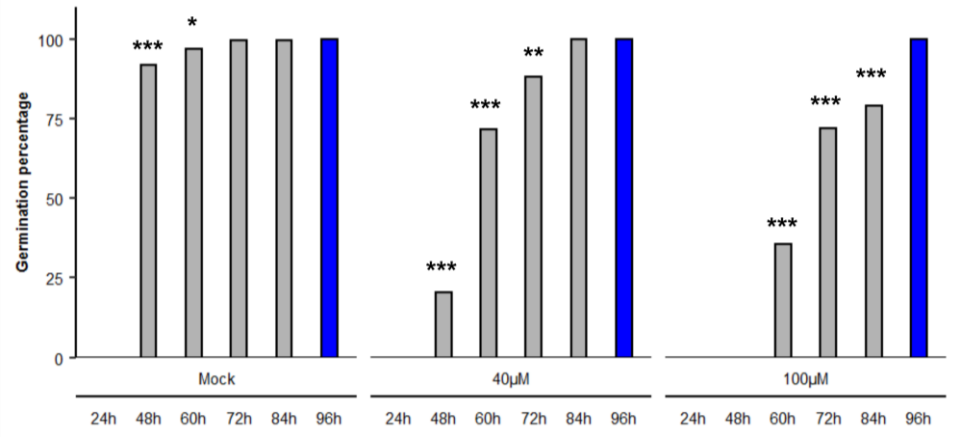

Figure 9: Coumarin reduces the germination rate of *Arabidopsis thaliana* in the light

Data presented are means of at least three biological repeats. Asterisks denote significant differences between the 96h control (blue bars) and the time-point of analysis within the treatment. (* = $p<0.05$, ** = $p<0.001$, *** = $p<0.001$).

Next, we analysed the effect of exogenous treatment with the hormone analogues 1-naphthaleneacetic acid (NAA) (auxin), 1-amino-cyclopropane-1-carboxylate (ACC) (the precursor of ethylene) and gibberellic acid 3 (GA3) (gibberellic acid). Although GA is known to induce germination (Koornneef and van der Veen, 1980), we observed no significant difference in germination ratio when combined with coumarin (Fig. 3). Note, however, that the concentration we applied is low. Interestingly, NAA treatment had an inhibitory effect when combined with coumarin, while a positive effect on germination was observed in mock conditions (Fig. 3). ACC had no significant effect on germination in mock conditions, while combined with coumarin it fully restored the phenotype and no difference in germination ratio could be observed between mock-treated seeds and seeds treated with coumarin and 50 µM of ACC.

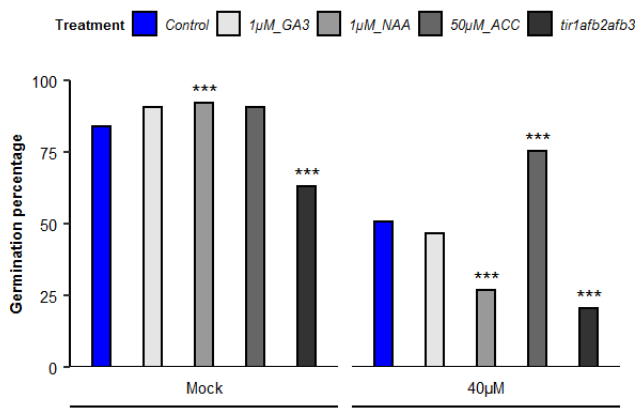

Figure 10: Ethylene alleviates coumarin-induced dormancy.

Seedlings are germinated in the dark after a 4-hour light pulse to induce germination. Data presented are means of at least three biological repeats. Asterisks denote significant differences between the control (blue bars) and treatment within the coumarin treatment (mock or μM of coumarin) (* = $p<0.05$, ** = $p<0.001$, *** = $p<0.001$).

Discussion

Arabidopsis seeds belong to the group of small-seeded plants that need light to germinate (e.g. lettuce) (Shinomura, 1997; Seo *et al.*, 2009). The influence of light on germination is since long known (reviewed in Evenari, 1965). More specifically, irradiation of dark-imbibed seeds with a red light pulse induces germination and a subsequent FR light pulse cancels the effect of R light (Borthwick *et al.*, 1952). Already in 1945, it was shown that coumarin had a profound effect on increasing dormancy in the dark compared to light germination, as was illustrated with lettuce (Nutile, 1945). Our data confirm these findings in Arabidopsis. In the dark, no significant difference in germination ratio could be observed upon 1 µM of GA3 treatment. However, we observed when GA biosynthesis is limited or blocked (Chapter 3), or better when DELLA repression is enhanced, increased dormancy upon coumarin treatment. For example, transfer experiments had to be performed when seedlings were treated with coumarin and paclobutrazol (PAC) as those did not germinate, while coumarin or PAC treatment alone does not affect germination (Chapter 3). Also the *sly1-2* mutant showed abolished germination upon coumarin treatment (Chapter 3). We observed that 50 µM of ACC treatment almost completely restored germination of coumarin treated seedlings in the dark. Ethylene is known to, besides reducing ABA-induced dormancy, stimulate expression of *GA3OX* and *GA20OX* and as such to stimulate germination (Corbineau *et al.*, 2014). Moreover, ethylene modifies the GA signalling pathway by altering the abundance and stability of DELLA proteins (Achard *et al.*, 2003, 2007). Also in the hypocotyl, the detailed transcriptional analysis showed the upregulation of 3 DELLA genes, *RGA2 (GAI), RGL1* and *RGL3* (and two splice-variants of RGL) upon coumarin treatment (Table 2, 3). Note that in the light, in the *ga1-3* mutant, loss of the DELLA gene *RGL2* is enough to rescue germination, but the complete rescue of germination of the *ga1-3* mutant in the dark required loss-of-function mutations in the DELLA genes *RGL2*, *RGA*, and *GAI* (Lee *et al.*, 2002; Cao *et al.*, 2005). Alterations of DELLA abundance or stabilization upon coumarin treatment is a possible explanation for the different response observed in germination upon coumarin in the dark versus the light. Although these preliminary data hint on the role of DELLA repression during coumarin-induced germination inhibition, further research is needed to clarify and quantify this possible interaction.

RGL2 is considered to be the main DELLA negatively regulating germination by stimulating ABA biosynthesis (Piskurewicz *et al.*, 2008). Moreover, auxin (treatment) is known to increase dormancy by enhancing ABA action (Liu *et al.*, 2013). This can explain the observed enhanced inhibition of germination of seedlings co-treated with NAA and coumarin. Recent findings illustrate the role of ABA for coumarin-induced dormancy (Saleh and Kebeish, 2018; Chen *et al.*, 2019). However, the triple F-box receptor mutant *tir1afb2afb3* is less sensitive to ABA and shows reduced dormancy (Liu *et al.*, 2013), while we observed enhanced dormancy of the *tir1afb2afb* mutant upon coumarin treatment. This indicates that the enhanced dormancy observed in the *tir1afb2afb3* Arabidopsis mutant upon coumarin treatment possibly has another origin than enhanced ABA action, for example, increased DELLA repression.

Overall, it is clear the coumarin induces dormancy in *Arabidopsis thaliana* in a concentration-dependent manner, with a clear link to light-signalling. These preliminary data hint on a link with DELLA repression, but numerous other experiments will have to be performed to support this hypothesis.

Supplementary material

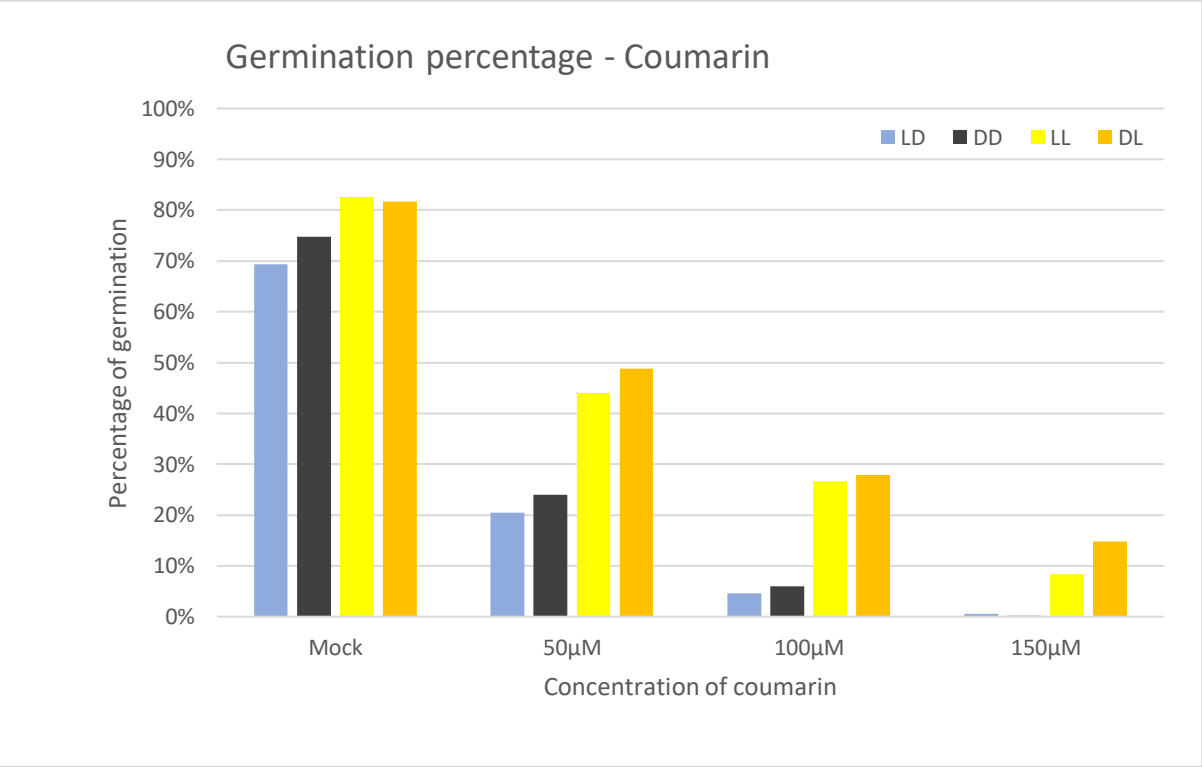

LD	Plates placed in the light for 7 days, moved to the dark after sowing for dark-grown germination
DD	Plates placed in the dark for 7 days, moved to the dark after sowing for dark-grown germination
LL	Plates placed in the light for 7 days, moved to the light after sowing for light-grown germination
DL	Plates placed in the dark for 7 days, moved to the light after sowing for light-grown germination

Germination %	Mock	50µM	100µM	150µM
LD	69.3%	20.5%	4.6%	0.6%
DD	74.8%	24.0%	5.9%	0.1%
LL	82.6%	44.0%	26.6%	8.4%
DL	81.7%	48.8%	27.9%	14.8%

Figure S2: Investigating the influence of (1) light on the technical aspects of our growth conditions, i.e. changes in the medium and potential breakdown of coumarin and (2) plates in the light are sealed with 3M tape allowing gas exchange, and as such potentially also loss of the volatile coumarin.

In this experiment, plates were placed in the growth chamber for 7 days, either exposed to the light or sealed with aluminium to foil to mimic the dark-grown conditions, containing no seeds and the growth medium was supplemented with 0, 25, 50 or 100 µM of coumarin. After 7 days, seeds were sown on those plates and placed in the dark or in the light. We observed a similar output: in the dark germination is inhibited by coumarin and no difference could be observed between the plates have been primarily exposed to the light for 7 days of to the dark.

Chapter 5 – Coumarin reshapes the Root System Architecture of *Arabidopsis thaliana*

Towards the molecular understanding of the coumarin-induced root response in *Arabidopsis thaliana*.

Stan Van Praet[1,2,3], Elke Barbez[4,5], Bartel Vanholme[1,2], Stephen Depuydt[1,2,3]

1. Ghent University, Department of Plant Biotechnology and Bioinformatics, 9052 Ghent, Belgium
2. VIB-UGent Centre for Plant Systems Biology, 9052 Ghent, Belgium
3. Ghent University Global Campus, Lab of Plant Growth Analysis, Incheon, South Korea
4. Gregor Mendel Institute, Austrian Academy of Sciences, Vienna Biocenter, 1030 Vienna, Austria
5. Department of Applied Genetics and Cell Biology, University of Natural Resources and Life Sciences, 1190 Vienna, Austria

Author contributions:

S.V.P. and S.D. conceptualized and designed the research; S.V.P. performed the research/experiments. E.B. performed the HPTS analysis and made figure 7 and S3. S.V.P., B.V and S.D. interpreted the data. S.V.P. analysed the data, performed the statistics and made the figures; S.V.P. drafted the manuscript and B.V. and S.D. revised it.

Abstract

Coumarin affects the development of almost every plant organ, but historically, in the light of investigating its roles as an allelopathic chemical, the root has been the centre of attention. From early onwards, the effects of coumarin were linked to auxin, based on the bell-shaped response of roots treated with auxin. Here, we confirm this bell-shaped response of roots towards coumarin in *Arabidopsis thaliana* (in both main root length as well as lateral root (LR) formation) and illustrate that coumarin increases lateral root density, adventitious root formation and root hair formation in a concentration-dependent manner. Moreover, we investigated the first steps of its *mode-of-action*. High concentrations of coumarin (≥ 25 µM) clearly inhibit root meristem cell division, shown by a reduction in meristem size and a decreased expression of *CYCB1*;*1*. Coumarin induces acidification of the apoplast in root meristems, a well-known feature of auxin treatment. We clearly illustrate that coumarin reduces auxin efflux in the root by adjusting abundance and localization of PIN1, PIN2 and PIN3 proteins in the root tip. Interestingly, while auxin efflux is reduced, coumarin enhances auxin influx by increasing AUX1 abundance. This is confirmed by a noted enhanced sensitivity to coumarin of the *aux1-7* mutant. Moreover, coumarin rescues the gravitropic response of *pin2* mutants, but not of *aux1-7* mutants, further adding to the hypothesis that coumarin affects root growth via AUX1. From our data, it is clear that brassinosteroids are not involved in the process and we postulate that SHY2 plays an important role during the coumarin-induced reduction of root meristem development. SHY2 is influenced by cytokinins and by auxin and the dominant gain-of-function mutant *shy2-2* has a diminished reduction in main root length upon coumarin treatment compared to the control. Lower concentrations of coumarin induce LR formation by enhancing *GATA23* expression, the main stimulator of LR initiation. Lastly, we observed a remarkable link with phytochrome signalling as the *phya-201* and *phyb-5* mutants are less responsive towards coumarin than the control. Altogether, our data reveal possible pathways through which coumarin can act, in order to establish it's well known and described root phenotypes.

Introduction

After the early discovery of the toxicity of coumarin to algae (Klebs, 1896), several reports illustrated its phytocidal action on plants (Cameron, 1910; Veldstra and Havinga, 1943). In an attempt to explain the allelochemical behaviour of coumarin, its effects on root growth were described (Audus and Quastel, 1947). Coumarin is chemically the most basic member of the coumarins, a large class of chemicals derived from the phenylpropanoid pathway with a large variety of effects on plant growth (Collier, 1971; Murray, Méndez and Brown, 1982; Harborne, 1999). Coumarin influences the root system architectures (RSA) of several plant species (both monocots as well as dicots): *Allium cepa, Lilium longiflorum, Phleum pratense, Maize, Avena sativa, Lepidium sativum, Pisum sativa, Radish, Arabidopsis thaliana, Sweetclover and Alfalfa* (Audus and Quastel, 1947; Cornman, 1947; Audus, 1948, 1950; Goodwin and Taves, 1950; San Antonio, 1952; Pollock, Goodwin and Greene, 1954; D'Amato and D'Amato-Avanzi, 1954; Avers and Goodwin, 1956; Neumann, 1960a, 1960b; Svensson, 1972a; Aliotta *et al.*, 1993; Podbielkowska *et al.*, 1995; Keightley *et al.*, 1996; Abenavoli *et al.*, 2004, 2006, 2008; Lupini *et al.*, 2010, 2014; Saleh and Madany, 2015; Ziegler *et al.*, 2015; Saleh and Kebeish, 2018; Voges *et al.*, 2019). In *Arabidopsis thaliana*, coumarin treatment leads to inhibition of primary root elongation, stimulation of lateral root formation, and induction of root swelling when high concentrations are applied (Abenavoli *et al.*, 2008; Lupini *et al.*, 2014). Swelling of roots by coumarin is a direct effect of increased cell volumes, a phenotype that for example also was observed in isolated mesophyll cells of *Calystegia sepium L* (Harada, Rossini and Cheruel, 1971). The effect on swelling was linked to inhibition of cellulose synthesis and microtubuli formation (Svensson, 1971; Hara, Umetsu and Miyamoto, 1973), and was seen as an auxin-effect based on phenotypic comparisons (i.e. exogenous auxin treatment also induced organ swelling) (Svensson, 1972a). It was found that the swelling was reduced by gibberellic acid (GA) treatment (Svensson, 1972a).

The inhibition of primary root elongation upon coumarin treatment was linked to reduced respiration in root tips, leading to inhibition of mitosis and as such smaller meristems (Cornman, 1947; D'Amato and D'Amato-Avanzi, 1954; Svensson, 1971; Kupidlowska, Dobrzynska, *et al.*, 1994; Podbielkowska *et al.*, 1994, 1995, 1996; Keightley *et al.*, 1996). Root growth is the result of both cell division and cell elongation – that occur in specific zones of the root (Péret *et al.*, 2009; Lavenus *et al.*, 2013; Sozzani and Iyer-Pascuzzi, 2014) – indicating that an effect on the meristem can indeed influence the whole development of the root (reviewed in Sozzani and Iyer-Pascuzzi, 2014). The root meristem size is determined by an interplay of hormones, but independent of those also reactive oxygen species (ROS) influence root meristem development (Sozzani and Iyer-Pascuzzi, 2014). In general, ROS are known to inhibit meristem development (Tsukagoshi, Busch and Benfey, 2010), while the hormones cytokinin (CK), auxin and GA interact to regulate root meristem development (Dello Ioio *et al.*, 2007, 2008; Moubayidin *et al.*, 2010). CKs play an important role during root differentiation, while auxin plays a major role in root division and gibberellic acid (GA) is involved in root elongation (Sozzani and Iyer-Pascuzzi, 2014). The meristem size is hormonally controlled via the AUX/IAA protein SHORT HYPOCOTYL 2 (SHY2), whose expression is activated by cytokinins via *ARABIDOPSIS RESPONSE REGULATOR* 1 (*ARR1*) and *ARR12*, leading to meristem inhibition and cell differentiation (Dello Ioio *et al.*, 2007, 2008; Moubayidin *et al.*, 2010). Transcription of *ARR1* is inhibited by GA, leading to low *SHY2* levels (Dello Ioio *et al.*, 2008; Ubeda-

Tomás *et al.*, 2009). The latter stimulates *PIN* gene expression leading to auxin flow and stimulation of cell division and thus meristem growth (Dello Ioio *et al.*, 2007, 2008; Moubayidin *et al.*, 2010).

The effects of coumarin on root growth have been linked to auxin. It has been illustrated that the inhibitory effect on the elongation zone of coumarin was diminished by kinetin (a CK) (Svensson, 1972a), illustrating that coumarin induces an auxin response (based on the antagonistic behaviour of auxin and CK (Deropp, 1956; Skoog and Miller, 1957; Pernisová *et al.*, 2009)). Moreover, coumarin induced tuber formation on excised shoots of *Solanum tuberosum L. in vitro*, an effect that also is linked to auxin (Stallknecht, 1972). Phenotypic overlap was also found between coumarin and the auxin analogue 2,4-dichlorophenoxyacetic acid (2,4-D) regarding adventitious root formation in hypocotyl cuttings of *Phaseolus vulgaris,* but when coumarin and 2,4-D were applied together, the respective effects cancelled out leading to a strong reduction in root formation (Basu, 1972). The stimulatory effect on adventitious rooting (AR) has been reported in *Phaseolus vulgaris, Glycine max, Cedrus deodara* and *Impatiens balsamina* (Basu, 1972; Svensson, 1972a; Jansson and Svensson, 1980; Dhawan and Nanda, 1982; Nandi, Tamta and Palni, 2002). The AR phenotype was the first system illustrating the effect of coumarin on auxin transport. When the basal end of the stem was treated with ^{14}C-labeled 2,4-D or naphthyl acetic acid (NAA), coumarin-induced auxin transport to the upper sections of the stem led to increased auxin concentrations, resulting in the induction of ARs (Basu, 1972). This was later confirmed by Basler and McBride (1977) illustrating that coumarin enhanced acropetal translocation of labelled 2,4,5-trichlorophenoxy acetic acid to the young shoots (Basler and Mcbride, 1977). Recently, the effect of coumarin on root growth of *Arabidopsis thaliana* has been linked to interference with auxin polar transport and particularly with the AUX1 carrier involved in basipetal auxin transport in the root (Lupini et al. 2014). It was shown that coumarin reduces the main root length while it stimulates the formation of lateral roots, an effect that was abolished in the *aux1-22* mutant (Lupini *et al.*, 2014).

Here we studied the effects of coumarin and its *mode-of-action* on root growth of *Arabidopsis thaliana,* focussing on meristem size, lateral- and main-root development and gravitropic responses.

Material and methods

Plant material, growth conditions and experimental set-up

Wild-type Columbia (Col-0) or Lansberg *erecta* (Ler) lines (depending on the background of the mutant) were used. All the *Arabidopsis thaliana* mutants and reporter lines used are described in Table S1. Seeds were surface-sterilized by treatment with 70 % ethanol for 5 minutes, followed by treatment with 100 % ethanol for 2 minutes, at room temperature while regularly inverting the Eppendorf tubes. The seeds were air-dried in the Laminar Air Flow (LAF) in a small sterile Petri dish Ø1 inch (SPL Life Science®, South Korea). Seeds were sown on 125x125 mm square Petri Dishes (SPL Life Science®, South Korea) containing 100 ml of ½ Murashige & Skoog growth medium (per litre demineralized water 2.15 g MS + vitamins, 0.5 g MES (2-(N-morpholino) ethanesulfonic acid), 0.1 g Myo-inositol, 10 g sucrose and 8 g agar (or 6.5 g gelrite) (Murashige and Skoog, 1962), the pH of the medium was adjusted to 5.7 using a 1 M KOH solution). Seeds were stratified at 4 °C for a minimum of 3 nights. Plates were positioned vertically at 21 °C, long-day conditions (16 h/8 h light/dark) and

120 PAR light. For RSA analysis, 12 seedlings were grown/plate and the root was analysed 9 days after germination (DAG). For analysing the effect of coumarin upon adventitious root formation we used a slightly adjusted experimental set-up as described in (Sorin *et al.*, 2005). Seedlings were grown in the dark for 5 days (after a light pulse of 4 hours) and were then transferred to medium containing coumarin or DMSO (i.e. mock) for another 6 days. The influence of coumarin on the gravitropic response of roots was analysed by rotating vertical plates 90 degrees 3 DAG, whereby the root tip was indicated with a marker dot. One day later (4 DAG), the angle was measured between the main root and the root tip location using the marker-dot as the corner.

Stock solutions

All chemicals that were used are described in table 1 (the compounds' full name, abbreviation, the supplier, solvent and the stock concentration). The solvent of the compounds was used as mock control in experiments. Compounds used as treatment and the solvent were added to the growth medium after autoclaving and cooling down to 60 °C.

Table 1: background of the chemical compounds used in treatments

Compound	**Abbreviation**	**Supplier**	**Solvent**	**Stock concentration (mM)**
Coumarin	COU	Tokyo Chemical Industry co., LTD	DMSO	40 and 100
DMSO		Sigma-Aldrich	N/A	N/A
8-hydroxypyrene-1,3,6-trisulfonic acid tri-sodium salt	HPTS	Sigma-Aldrich	¼ MS	100
Propidium iode	PI	Sigma-Aldrich	N/A	1mg/ml
5-Bromo-4-chloro-3-indolyl-β-D-glucuronide	X-gluc	Thermo Fisher Scientific	DMSO	0.261g/25ml

Phenotypic analysis of the root system architecture and adventitious roots formation

Nine days after germination (DAG), the number of lateral roots (of stage 8 or above (Malamy & Benfey 1997)) per seedling were counted using a stereomicroscope (Olympus corp. Model SZX2-ILLT). Afterwards, the plates were scanned (Sindoh corp. Model DF-624; 400*400 dpi, JPEG) and the main root length was analyzed using ImageJ. The number of adventitious roots formed on the etiolated hypocotyl per seedling after 11 days of growth was counted using a stereomicroscope (Olympus corp. Model SZX2-ILLT).

Histochemical analysis of GUS-reporter lines

Seedlings were harvested and placed in a 6-well plate containing ice-cold acetone (90 %) for 20 minutes and rinsed in NT buffer (100 mM Tris/50 mM NaCl). Staining was done as reported in (Vielle-Calzada et al., 1999). GUS staining of the plants was performed by transferring the plants to the GUS buffer supplied with 0.261 g X-gluc/25 ml (X-gluc was dissolved in 0,5 ml dimethyl sulfoxide (DMSO)) at 37 °C. The GUS buffer was

made by diluting the ferricyanide stock 50 times in NT buffer, whereby the ferricyanide stock was prepared by adding 0,32 g K3[Fe(CN)6] in 10 ml NT-buffer and stored at -20 °C. After the reaction, the medium was changed either by 70 % ethanol, or the plants were immediately cleared by the Malamy and Benfey protocol (Malamy and Benfey, 1997). Seedlings were first incubated in a 24 N HCL 20 % methanolic solution at 60 °C for 30 minutes, followed by incubation for 20 minutes in a 7 % (w/v) NaOH 60 % ethanol solution at room temperature. The samples were then dehydrated through 30-minute steps of 40 % ethanol, 20 % ethanol and 10 % ethanol. As last plants were transferred to a solution containing 5 % ethanol and 25 % glycerol for 15 minutes, thereafter the samples were stored in 50 % glycerol. 50% glycerol was used to mount the plants in microscope slides. Thereafter the seedlings were analysed by use of the differential interference contrast (DIC) microscopy technique (DMLB; Olympus BX51) (Arnison *et al.*, 2004). Pictures were taken with an Olympus digital camera connected to the microscope and controlled by an extra screen.

Confocal microscopy

Reporter line imaging and analysis

A Zeiss LSM 710 confocal laser scanning microscope was used for confocal imaging. 2 excitation filters at 488 nm for green/yellow fluorescent protein (G/YFP) and 561 nm for propidium iodide (PI) were set, with 2 band emission filters (1) 494 – 554 nm (for GFP) and (2) 568 – 649 nm (for PI). Acquisition with multiple channels was performed by sequential scanning. All settings remained the same to allow proper comparison of the different samples. Seedlings were stained with 0.1 % PI (Sigma-Aldrich) for 2–5 minutes. Images were analyzed using ImageJ v1.50b (NIH; https://imagej.nih.gov/ij/) and figures were prepared by using Inkscape (http://inkscape.org/en/).

Counting of the meristem cell number

Via confocal imaging, we analysed the length of the root meristem, i.e. the root meristematic zone. The length was expressed as the number of cortex cells in a file extending from the quiescent centre (QC; a small group of organizing cells (2 to 3) defining together with the stem cells the stem cell niche) as explained in (Dello Ioio *et al.*, 2007). Confocal images were acquired on the Zeiss LSM5 Exiter confocal laser scanning microscope with the excitation filter at 561 nm for propidium iodide (PI) and the emission filters at 568 – 735 nm. Seedlings were placed in a solution containing ¼ × MS medium (¼ × MS salts, 0.025% MES pH 5.7) with PI (1 mg/ml) for 5 –10 minutes, and prepared for imaging on glass slides. Images were stored and adjusted by ImageJ while counting the number of cells in a file.

HPTS Staining and Imaging

Seedlings were grown for 4 days upon the untreated medium and were then transferred to mock medium or medium supplemented with 100 µM coumarin. Twenty-four hours after transfer, the plates were scanned under a flatbed scanner to address root growth. In addition, seedlings were mounted on a slice of ½MS medium supplemented with 1 mM HPTS (and according to the sample with or without µM uM coumarin) on a microscope carrier slide. The seedlings were covered with a microscope cover slide or flipped into a plastic

Nunc imaging chamber and imaged using a LEICA SP5 upright confocal microscope. Fluorescent signals for the protonated HPTS form (Excitation 405 nm, emission peak 514 nm), as well as the deprotonated HPTS form [excitation, 458 nm (Zeiss) or 470 (LEICA); emission peak, 514 nm] were detected with a 63× (water immersion) objective. The image analysis was performed using the Fiji software (Fiji.sc), and data were statistically evaluated with Microsoft Excel 2011 as described in Barbez et al. (2017). For every imaged root, transversal cell walls of 5 cells were quantified.

Statistical analysis

The statistical package 'R version 3.10.1' (https://www.r-project.org/) was used for the statistical analyses. The least-square means of the biological repeats were subjected to statistical analysis, in which the sample size (n) is the total number of seedlings analyzed per line/conditions. For the pairwise comparison of two experimental groups, statistical analysis has been performed using a Student t-test. To address the statistical difference between two or more experimental groups of a continuous variable (e.g. root length), a multiple-(mixed-) ANOVA (linear (Mixed-Effects) model) was used for the statistical analysis (Wilkinson and Rogers, 1973; Bates *et al.*, 2015). For discrete data (e.g. number of lateral roots) a Generalized Linear Mixed-Effects Models with 'Poisson' as the family function was used (McCullagh and Nelder, 1989; Dobson and Barnett, 2008). Posthoc analysis was performed via a Tukey correction. The statistical assumptions of (1) normal distribution (via histogram) and (2) homogeneity of variances (by analysis of the residuals (QQ-plot)), were tested, and where needed were log-transformed if data did not comply.

Results

Coumarin induces a bell-shape response in the roots of *Arabidopsis thaliana*

We analysed the response of roots of *Arabidopsis thaliana* towards continuous coumarin treatment on a broad range of concentrations (Fig. 1A). Seven days after germination (DAG) roots of Arabidopsis showed a significant increase in main root length upon 1 and 2.5 µM of coumarin treatment (Fig. 1B), while concentrations of 25 µM of coumarin treatment or higher led to significant inhibition (Fig. 1B). Upon 1, 2.5, 5 and 10 µM of coumarin treatment, a significant increase in the number of lateral roots (LR) was observed (Fig. 1 C), while the number of LR was significantly decreased upon treatment with 50 or 75 µM of coumarin (Fig. 1 C). Interestingly, the decrease in LR formation was less than the decrease in main root length, leading to a gradual increase in lateral root density (LRD) (Fig. 1D). The effect on lower concentrations (<1 µM) was also analysed: 9 days after germination, no significant difference could be observed in main root length as well as in the number of LRs (Fig. S1A), and a small decrease in lateral root density could be observed (Fig. S1A). Based on the increase of the number of LRs, we analysed the effect of the stimulatory concentrations 1 and 10 µM of coumarin on the growth of roots over a longer timeframe. We found no significant increase in the number of LRs, but we observed a significant increase in lateral root length and as such also in total root length (Fig. 1S C). Consequently, the total root area increased (Fig. S1 D). We also found a strong increase in the number of junction/basal roots, i.e. adventitious roots that are formed on the transition zone between hypocotyl and the taproot (Fig. 1S E) (Steffens and Rasmussen, 2016; Zobel, 2016). We, therefore, analysed the effect of coumarin on adventitious root (AR)

formation on etiolated hypocotyls. A significant increase in the number of adventitious roots upon coumarin treatment in a concentration-dependent manner was found (Fig. S1 B). Lastly, we also observed a clear increase in number, density and length of root hairs upon coumarin treatment (Fig. S1 F).

Overall it can be concluded that coumarin treatment leads to a bell-shape response in both main root length as well as lateral root formation, and that coumarin stimulates lateral root density, adventitious root formation and root hair formation in a concentration-dependent manner. The Inhibitory Concentration 50 (IC_{50}) value of coumarin on the main root length was determined to be 50 µM. We, therefore, used 40 µM as the concentration to work with as it leads to clear inhibitory effects on main root length and LR formation, while it stimulates root hair formation and lateral root density. The root phenotype upon 40 µM of coumarin is robust and leads to an increase in LR formation when seedlings are transferred to treatment.

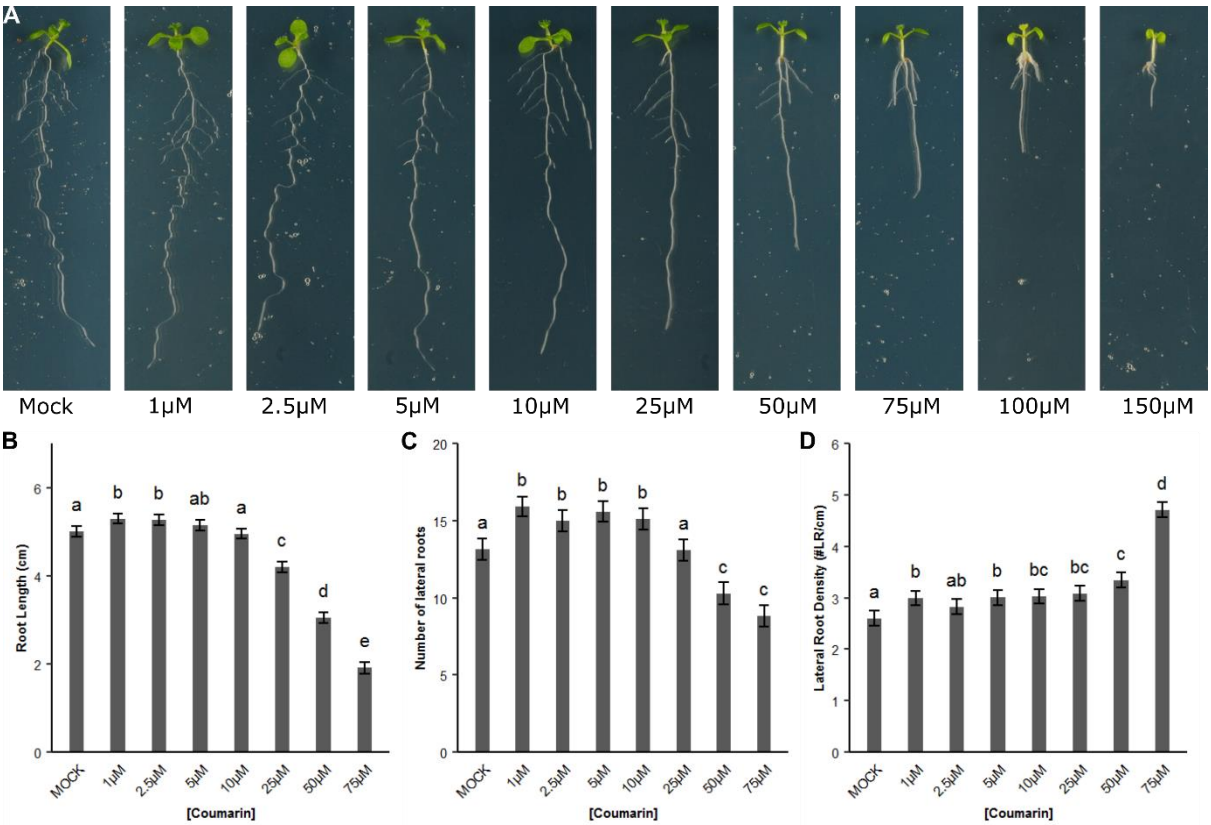

Figure 1: Coumarin treatment drastically reshapes the root system architecture

(A) Images of 7DAG old seedlings treated with different concentration of coumarin. (B) Main root length, (C) number of lateral roots and (D) lateral root density of seedlings grown for 7 DAG upon the mock medium, or 1, 2.5, 5, 10, 25, 50 or 75 µM of coumarin ($n \geq 70$).

Data presented are means ± the confidence interval of at least three biological repeats. Letters indicate statistically different means ($p<0.05$).

Coumarin inhibits cell division in the root meristem of *Arabidopsis thaliana*

Coumarin has been reported to inhibit root meristem division leading to inhibition of main root length in *Allium cepa*, *Lilium longiflorum,* Wheat, Maize, *Allium sativum* and *Lens culinaris* (Cornman, 1947; D'Amato and D'Amato-Avanzi, 1954; Podbielkowska *et al.*, 1994, 1995; Keightley *et al.*, 1996). Therefore we analysed the effect of coumarin on the root meristem of Arabidopsis seedlings. Via confocal imaging, we analysed the root meristematic zone. The length was determined, as explained in (Dello Ioio *et al.*, 2007)(see Materials and Methods), by the number of cortex cells in a file extending from the quiescent centre (QC; a small group of organizing cells (2 to 3) that together with the stem cells define the stem cell niche), until the cells doubled in size. Upon coumarin treatment, a minor and non-significant reduction in the number of cortex cells in the division zone of roots was observed in 3 DAG seedlings treated with 40 µM coumarin as compared to mock-treated seedlings (Fig. 2A, B), while a significant reduction of 20 % was observed in 5 DAG seedlings. In order to link those effects to interactions with cell division, the CYCB1;1 promotor activation was histochemically analysed upon coumarin treatment. We used the labile chimeric mitotic *cyclin::uidA* reporter, containing a mitotic destruction box (referred to here as the pCYCB1;1::GUS reporter line) (Colon-Carmona *et al.*, 1999). Coumarin clearly inhibits cell division in the root meristem as a decreased expression of *CYCB1*;1 was observed upon 40 µM coumarin as compared to mock in both 3 DAG as well as 5 DAG old seedlings (Fig. 2, C).

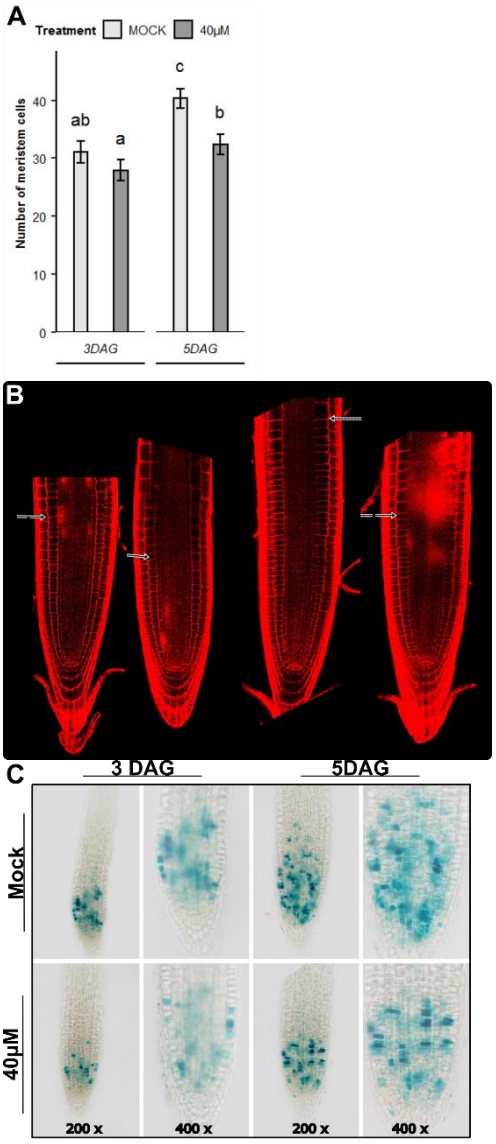

Figure 2: Coumarin inhibits meristem cell division in the early stages of development.

(A) The number of meristem cells in a cortex cell file counted according to (Dello Ioio *et al.*, 2007) in 3 DAG and 5 DAG old seedlings treated with mock of 40 µM of coumarin (n ≥ 16). (B) Confocal representation via PI stained root tips of the counted seedlings in (A). (C) Histochemical analysis of the *pCYCB1;1*::GUS reporter line upon 40 µM of coumarin treatment compared to mock in 3- and 5-DAG old seedlings. Visual representation of a 200 and 400 times magnification.

Data presented are means ± the confidence interval of at least three biological repeats. Letters indicate statistically different means ($p<0.05$).

We found a stimulatory effect on lateral root formation, while we observed a strong inhibition in main root length upon coumarin treatment. The negative effect on the root meristem influences both traits (Sozzani and Iyer-Pascuzzi, 2014). To overcome the inhibitory effect in the early stages of root development we performed a transfer experiment in which seedlings were transferred to treatment, 1, 2, 3, 4 of 5 days after germination and the roots were analysed 9 DAG (Fig. S2). When seedlings were transferred 1 DAG to mock, 10, 50 or 100 µM coumarin, no difference in phenotype was observed upon 10 µM of coumarin compared to mock, while a decrease in main root length and the number of LRs roots was found only upon 50 and 100 µM of coumarin. The decrease on main root length was more severe than the reduction in the number of lateral roots leading to a slight but significant increase in LRD upon 100 µM of coumarin treatment. The inhibition on main root length upon 50 µM of coumarin treatment is not observed anymore when transferred 3, 4 of 5 days after germination, while at all timepoints of transfer to 100 µM of coumarin, a significant reduction in main root length was clear (Fig. S2). The inhibitory effect on the number of lateral roots diminishes with the time of transfer, and an increase in the number of lateral roots is found upon all coumarin treatments compared to mock when

transferred 5DAG. Combined, the data show an increase in LRD upon 50 and 100 µM of coumarin when transferred 3DAG or later (Fig. S2). Altogether, these data indicate that the inhibitory effects of coumarin on root growth are established early on during root development.

Coumarin affects auxin transport in the root but does not lead to disruption of auxin maxima in the root.

Auxin-cytokinin interactions regulate meristem size (Su, Liu and Zhang, 2011). Moreover, it has been described that coumarin needs a functional AUX1 transporter to induce its effects on roots, confirming the role of auxin transport in the coumarin induced phenotype (Lupini et al. 2014). Therefore, we analysed the auxin response in roots upon coumarin treatment and analysed the effect on auxin transport using mutants and various reporter lines. Histochemical analysis of the pDR5::GUS reporter line illustrated that coumarin does not induce an altered auxin response in 7 DAG old roots grown continuously upon coumarin treatment as compared to the mock (Fig. 3A). As the pDR5::GUS reporter line is a robust marker line, it could be that a new steady-state is formed in the auxin response after 7 days of continuous coumarin treatment. Therefore, we analysed the direct response of the marker line to high concentrations of coumarin. Three DAG old seedlings were transferred to mock, 10 µM NAA or 100 µM of coumarin treatment for 4 or 24 hours (Fig. 3B). While a clear auxin response could be observed upon NAA treatment, no effect could be observed upon 100 µM of coumarin treatment compared to the mock (Fig. 3B). Remarkably, just as observed upon NAA treatment, also upon 100 µM of coumarin treatment, root swelling could be observed after 24 hours of treatment, although to a lesser extent than upon NAA treatment (Fig. 3B), indicating that the roots responded to coumarin treatment. An auxin response, at least of the DR5:GUS reporter was, however, not clear.

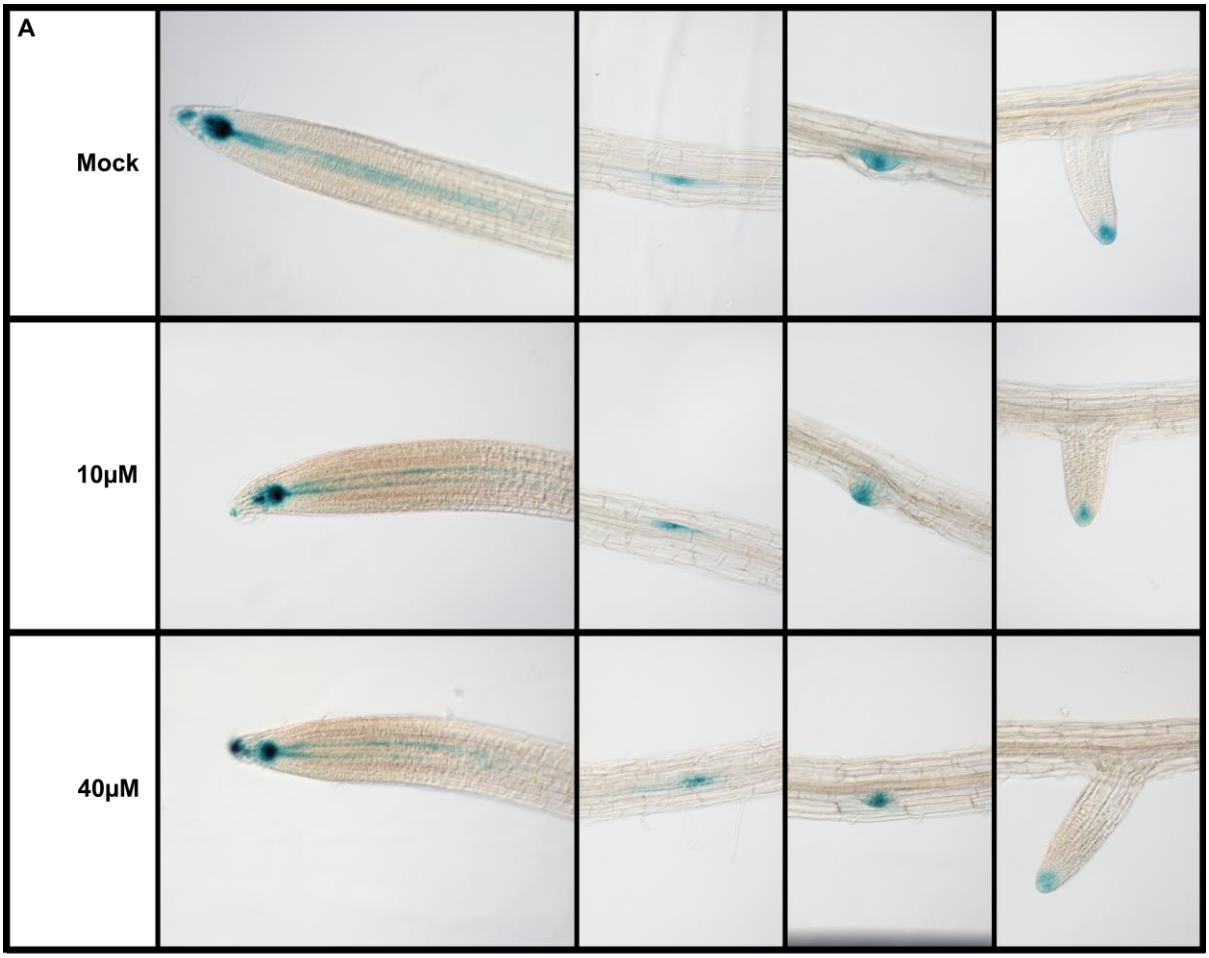
A
Mock
10µM
40µM

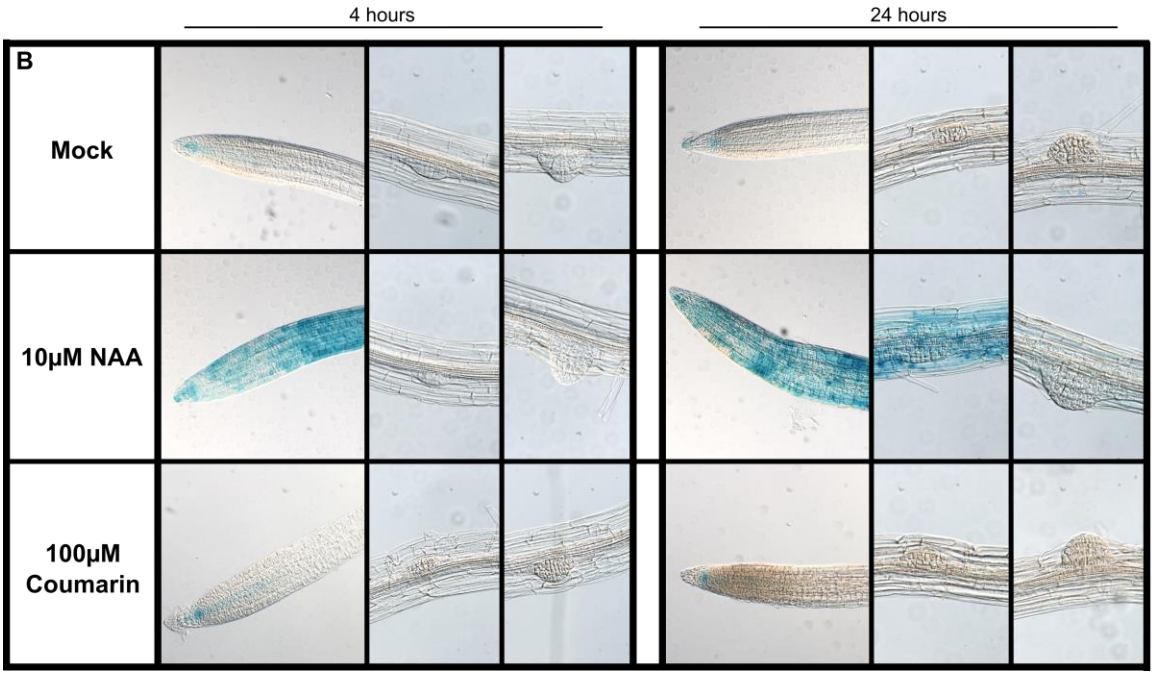
4 hours
24 hours
B
Mock
10µM NAA
100µM Coumarin

Figure 3: Coumarin does not affect DR5 expression in the root as analysed via histochemical analysis of the pDR5::GUS reporter line.

(A) Histochemical analysis of the pDR5::GUS reporter line in the roots of 7DAG old seedlings, continuously treated with DMSO (Mock), 10 or 40µM of coumarin (200x magnification). (B) Histochemical analysis of the pDR5::GUS reporter line in the roots of 3DAG old seedlings, treated for 4 (on the left) or 24 hours (on the right) with DMSO (Mock), 10 µM of NAA or 100 µM of coumarin (200x magnification).

In *Arabidopsis thaliana,* lateral root (LR) formation is regulated by the IAA28–ARFs (GATA23) module that regulates lateral root founder cell identity (De Rybel *et al.*, 2010) and the SOLITARY-ROOT (SLR)/IAA14–ARF7–ARF19 module that regulates nuclear migration and asymmetric cell divisions of the LR founder cells, required for LR initiation (Fukaki *et al.*, 2002). The *slr-1* mutant shows severe sensitivity towards coumarin treatment, as almost no main root is formed (Fig. 4A), and just like in the control, there is a complete absence of lateral root formation (Fig. 4A). To further unravel the effect on lateral root formation of coumarin, we histochemically analysed the reporter line p*GATA23*::GUS (De Rybel *et al.*, 2010). An increase in the number of root initiation spots and a slight increase in staining in the LR primordium was observed upon coumarin treatment compared to mock-treated seedlings (Fig. 4B). Interestingly, when the LR is formed, a decrease in *pGATA23*::GUS staining at the basis was observed (Fig. 4B), indicating a spatially confined downregulation of *GATA23* transcription.

We analysed the effects of the dominant gain-of-function mutant *shy2-2* in Ler background (Tian and Reed, 1999), as SHY2 is involved in LR development and *GATA23* expression is upregulated in the *shy2/iaa3* gain-of-function mutants (De Rybel *et al.*, 2010). A significant reduction in main root length and the number of lateral roots was observed when untreated *shy2-2* seedlings were compared to the Ler control (Fig. 4C, top). Upon coumarin treatment, however, no significant difference could be observed in the main root length and the number of lateral roots of the *shy2-2* mutants compared to the Ler control (Fig. 4C, top). The *shy2-2* mutant is significantly less responsive towards coumarin than the Ler control for reducing main root length (Fig. 4C, bottom). This reduced sensitivity of the main root length of *shy2-2* seedings to coumarin treatment also results in the absence of an increase in LRD upon coumarin treatment as observed in the Ler control (Fig. 4C).

Coumarin potentially activates SHY2 activation leads to a decrease in root meristem development and as such inhibition of main root growth (i.e. smaller roots upon coumarin treatment). On the other hand, coumarin increases *GATA23* transcription and as such stimulates LR formation.

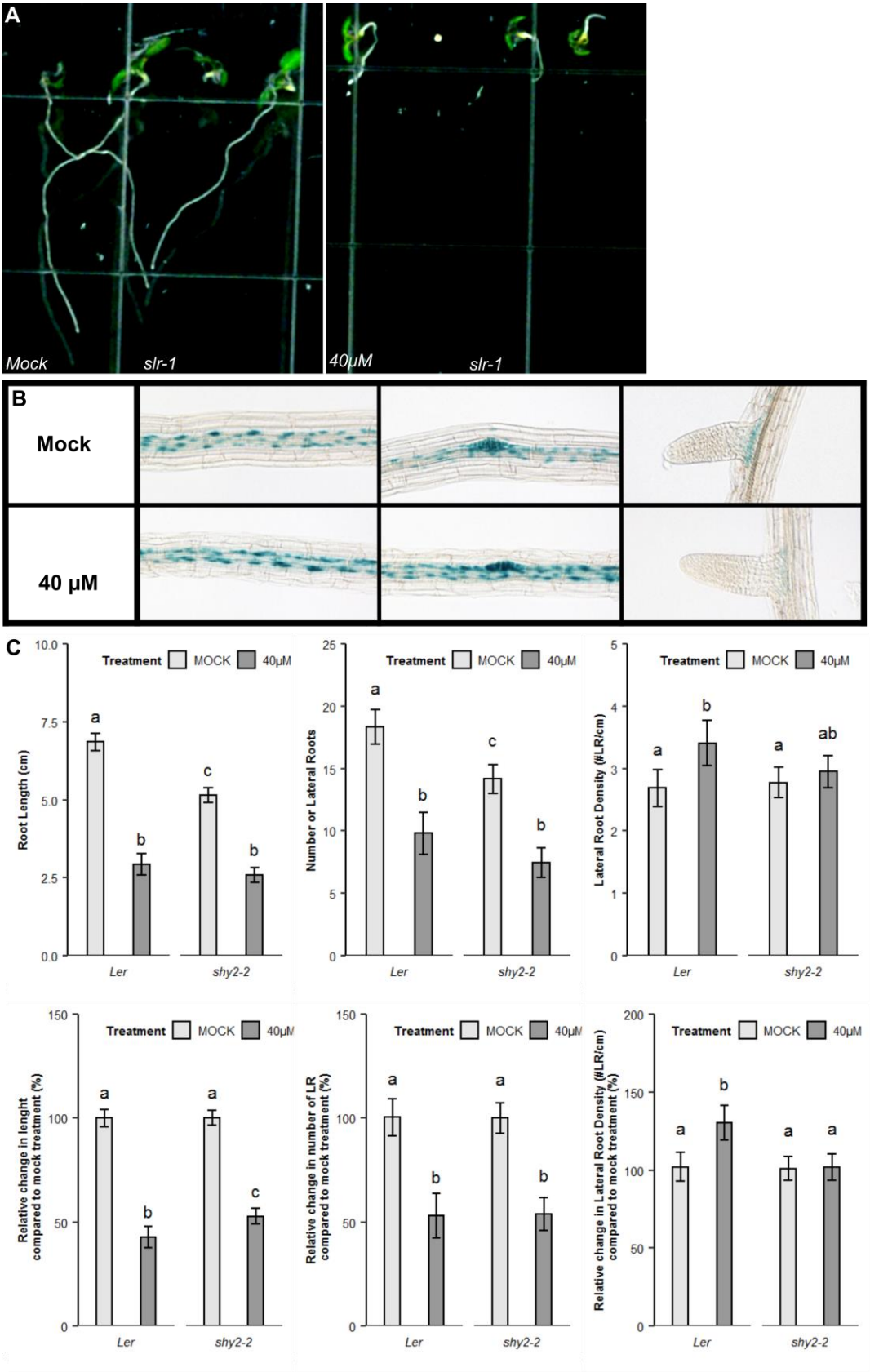

Figure 4: Coumarin slightly enhances transcription of *GATA23* in the root.

(A) *slr-1* mutants grown on mock medium (left) or 40 µM of coumarin treatment (right). (B) Histochemical analysis of the p*GATA23*::GUS reporter line in the roots of 7 DAG old seedlings, continuously treated with

DMSO (mock) or 40 µM of coumarin (200x magnification). (C) Root phenotype of *shy2-2* mutants grown for 9 DAG upon mock medium or 40 µM of coumarin treatment, (top) from left to right, main root length, number of lateral roots and lateral density (n≥11), (bottom) from left to right, relative change in main root length, number of lateral roots and lateral density compared to mock.

Data presented are means ± the confidence interval of at least three biological repeats. Letters indicate statistically different means ($p<0.05$).

Auxin transport is at the basis of lateral root initiation and reported to be pivotal for the induction of lateral root formation upon coumarin treatment (Lupini *et al.*, 2014). Moreover, the inhibition of the main root length upon coumarin treatment was absent in the *aux1* mutant (Lupini *et al.*, 2014). We, therefore, analysed the effect of coumarin on the main root length of the *AUXIN RESISTANT 1* (*aux1-7*) and the double mutant *AUXIN RESISTANT 1; LIKE AUXIN RESISTANT 1 3* (*aux1-21lax3*) upon coumarin treatment. Moreover, we tested the auxin efflux transport mutants *PIN-FORMED 1* (*pin1)* (we used the pML1::PIN1:GFP/*pin1* x pDR5::3xVENUS-N7 mutant (Kierzkowski *et al.*, 2013)) and *pin3*-4 for their root phenotype upon coumarin treatment. In mock conditions, we observed a significant reduction in main root length of the *pin1* and *pin3-4* mutant compared with the Col-0 control (Fig. 5A). Upon coumarin treatment, we observed a significant reduction in main root length of both mutants (to the same extent as the control, a reduction of 42 – 44% (Fig. 5A, bottom). The *pin3-4* mutant in mock conditions illustrated no difference in lateral root formation compared to the Col-0 control, while a significant reduction of LRs could be observed in the *pin1* mutant (Fig. 5A). Both *PIN* mutants responded to the same extent to coumarin treatment as the Col-0 control with a reduction of around 42% in the number of LRs (Fig. 5A, bottom). Col-0, *pin1* and *pin3-4* seedlings all illustrated an increase in LRD upon coumarin treatment, although only significantly in the *pin3-4* mutant, however this increase was not significantly different from the WT control (Fig. 5A). The *aux1-21;lax3* mutant has a significant reduction in main root length in mock conditions compared to Col-0, while the *aux1-7* and Col-0 do not differ in mock conditions (Fig. 5B). Interestingly, upon coumarin treatment a reduction of 39% in main root length is observed of the *aux1-21;lax3* double mutant, in line with the 37% reduction of the Col-0 control (Fig. 5B, bottom), while the *aux1-7* mutant has a 51% reduction. This indicates that the *aux1-7* mutant is more responsive to coumarin than the WT (Fig. 5B, bottom). Overal, the auxin transport mutants did not give conclusive ideas about the interference with auxin in the root and, moreover, stringent mutants in auxin homeostasis, e.g. the *slr-1* and *aux1lax3* mutants, showed such a drastic phenotype even in mock conditions (e.g. no LR are formed (Swarup *et al.*, 2008)) that it is hard to make conclusions for coumarin treatment.

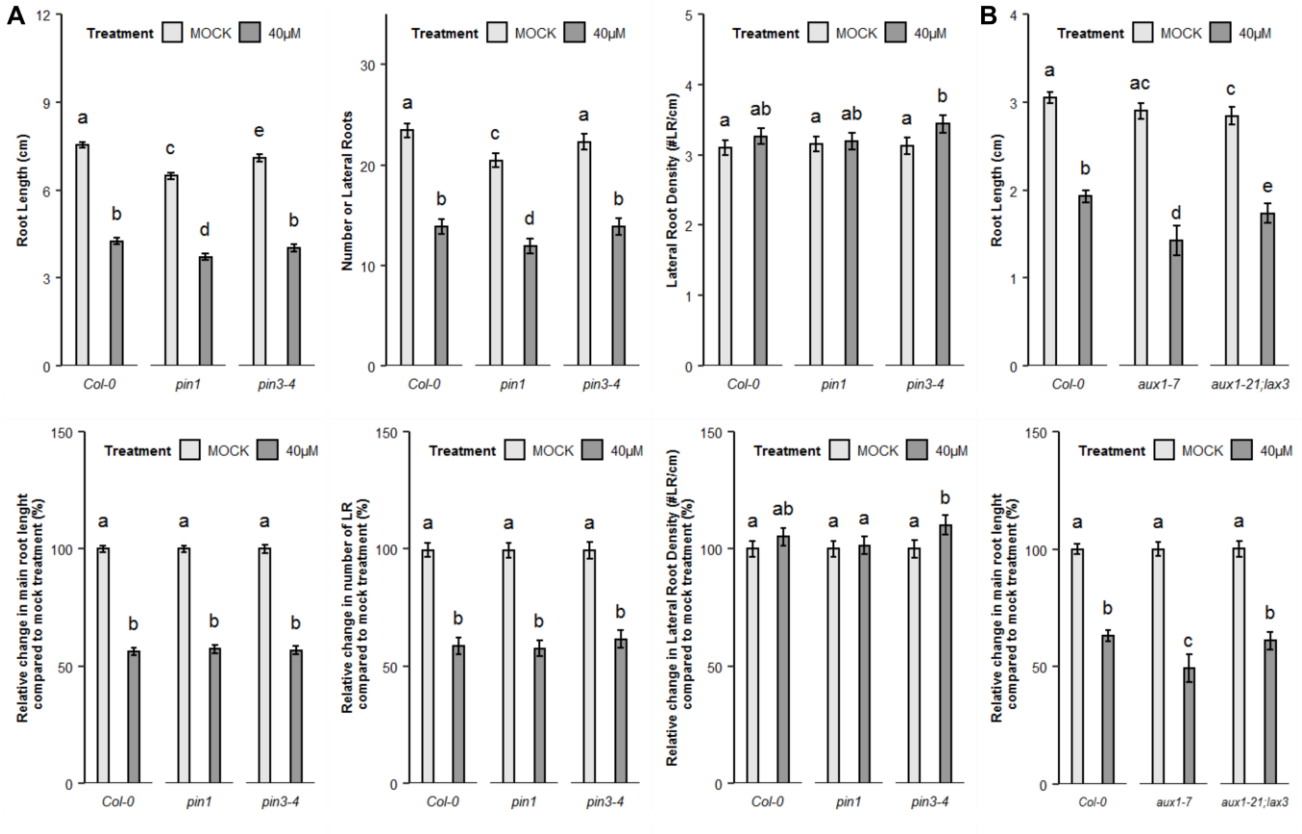

Figure 5: Analysis of the role of AUX1, PIN1 and PIN3 for coumarin adjusted root growth

(A) Analysis of *pin1* (we used the pML1::PIN1:GFP/*pin1* x pDR5::3xVENUS-N7 mutant (Kierzkowski *et al.,* 2013)) and *pin3-4* mutants grown for 9 DAG upon mock medium or 40 µM of coumarin treatment, from left to right (top), main root length, number of lateral roots and lateral density (n≥58), (bottom) relative change in main root length, number of lateral roots and lateral density upon 40 µM of coumarin treatment. (B) Analysis of the (top) main root length and (bottom) relative change in main root length of 5DAG old mutants *aux1-7* and *aux1-21lax3* compared to Col-0 upon mock medium or 40 µM of coumarin treatment.

Data presented are means ± the confidence interval of at least three biological repeats. Letters indicate statistically different means ($p<0.05$).

Next, we analysed the effect on the distribution of the auxin transporters AUX1, PIN1, PIN2, PIN3 and PIN7 via confocal analysis. No difference could be observed regarding distribution and abundance of PIN7 in the root upon coumarin treatment compared to mock (Fig. 6), while a slight reduction in the intensity of the pPIN3::PIN3-GFP signal was observed upon coumarin treatment compared to mock (Fig. 6). This indicates a reduced level of PIN3 transporters upon coumarin treatment. Moreover, we observed a less broad zone of PIN1 abundance in the root meristem, while a clear reduction in PIN2 abundance, as well as PIN2 distribution, could be observed upon coumarin treatment compared to the control (Fig. 6). AUX1 was observed in an extended epidermal cell file zone in the epidermis of coumarin treated roots as compared to the control (Fig. 6). We can conclude that coumarin affects auxin transport by reducing PIN1, PIN2 and PIN3 levels in the root meristem while enhancing AUX1 distribution.

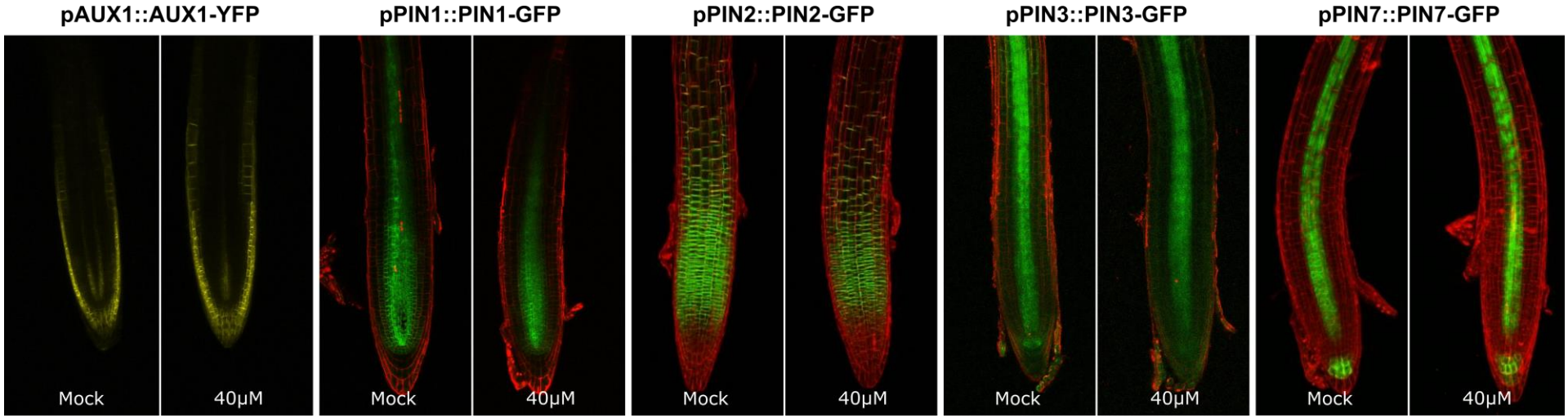

Figure 6: Coumarin affects auxin transport by slightly adjusting AUX1, PIN1 and PIN2 distribution

Analysis of translational fluorescent reporters lines of the transporters PIN1, PIN2, PIN3 and PIN7 fused to GFP and AUX1 fused to YFP. Images represented with PI staining of the root cells (except for the pAUX1::AUX1-YFP line, as the PI staining interfered too much with the yellow AUX1 expression in the epidermis of the main root) and we focused on the quiescent centre before taking of the picture.

Coumarin affects gravitropism of Arabidopsis roots

PIN2 plays an important role in the gravitropic response of Arabidopsis roots and was originally identified as mutated in the *AGRAVITROPIC 1* (*agr1*) mutant (Chen *et al.*, 1998). Since we observed a strong reduction in PIN2 abundance in the roots, we analysed the response of the roots of the *eir1-1* mutant (from now on referred to as the *pin2* mutant (Roman *et al.*, 1995)) towards coumarin treatment and analysed the effect of Col-0 roots in a gravitropism experiment. We observed that coumarin could almost completely restore the root curling phenotype of *pin2* mutants (Fig. 7A). WT roots, on the other hand, upon 10 and 40 µM of coumarin treatment had a slight but significant reduction in response to gravitropy (Fig. 7B). Next to PIN2, recent findings suggest that AUX1 acts upstream of PIN2 in regulating root gravitropism: AUX1 overexpression in *pin2* background restores the gravitropic response in *pin2* mutants (Liu *et al.*, 2018; Swarup and Bhosale, 2019). We observed that coumarin cannot restore the perturbed gravitropic response of *aux1-7* mutants (Fig. 7C), while it clearly can restore root gravitropism of *pin2* seedlings. Together these data indicate that coumarin possibly affects root gravitropism by interacting with AUX1.

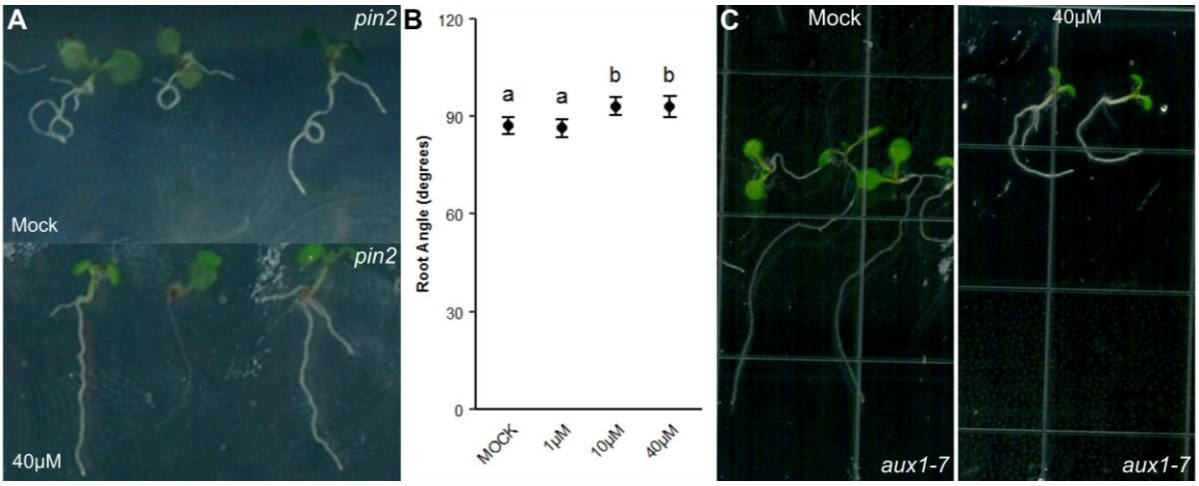

Figure 7: Coumarin influences root gravitropism of *Arabidopsis thaliana*

(A) The response of the roots of *pin2* (i.e. *eir1-1*) mutants upon coumarin treatment (down) compared to mock (top). (B) The gravitropic response of roots turned 90 degrees 3DAG expressed in the root angle measured 5DAG of seedlings treated with mock, 1, 10 or 40 µM of coumarin (n≥38). (C) The response of the roots of *aux1-7* mutants upon coumarin treatment (right) compared to mock (left).

Data presented are means ± the confidence interval of at least three biological repeats. Letters indicate statistically different means ($p<0.05$).

Coumarin acidifies the root

In Arabidopsis, it has been shown that acidification of the apoplast of root cells (e.g. via fusicoccin treatment) leads to cell expansion and as such an enhanced elongation rate (Barbez *et al.*, 2017). Auxin is known to induce acidification in root cells (Fu and Harberd, 2003; Sauer, Robert and Kleine-Vehn, 2013), however, Barbez et al. (2017) illustrated that auxin treatment first leads to immediate alkalinization (within 2

hours after treatment) of the apoplast and as such inhibition of root growth. In this way, for e.g. in gravistimulated roots, auxin accumulates at the inner side of the roots and induces alkalinization enabling root bending within minutes after the external signal (Barbez *et al.*, 2017). But indeed, longer treatment with auxin induces acidification of apoplast (Barbez *et al.*, 2017). The interplay of coumarin with auxin in the root meristem (e.g. the reduced PIN1/2 levels), could also lead to adjusted acidification in the root. Moreover, in maize roots, coumarin was found to induce H^+-ATPase activity, leading to an increase in elongation rate of the transition zone (a particular zone in the primary maize root localized 1.7–3.4 mm from the tip) (Lupini *et al.*, 2010). Via staining with 8-hydroxypyrene-1,3,6-trisulfonic acid trisodium salt (HPTS) (Barbez *et al.*, 2017), we aimed to investigate the acidification of the apoplast in the Arabidopsis root upon coumarin treatment. Two DAG old seedlings were transferred to mock or 100 µM of coumarin treatment for 24 hours after which the 458/405 ratio was calculated according to Barbez et al. (2017) (and serves as a proxy for the apoplastic pH, see material and methods). Note that a positive control with fusicoccin is missing to validate the experiment, moreover, treatment with (for example) auxin analogues would have been interesting to link our findings to an auxin response.

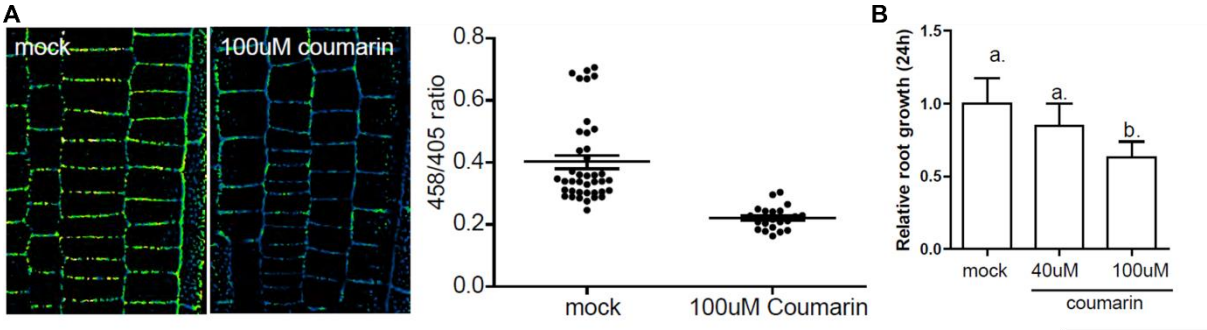

Figure 8: Coumarin reduces the apoplastic pH in the root meristem

(A) The effect of 100 µM of coumarin treatment for 24 hours on the apoplastic pH in *Arabidopsis thaliana* roots, visualized using HPTS staining (left), y-axis: mean 458/405 values of epidermal cells in root meristems of the pharmacologically treated seedlings relative to mock-treated seedlings (right). (B) Relative root growth after 24 hours of treatment upon 40 or 100 µM of coumarin treatment compared to mock.

Data presented are means ± SEM (n ≥ 6 roots per line/condition). Letters indicate statistically different means ($p<0.05$).

The pH of the medium was not affected by coumarin (Fig. S3), while the 458/405 ratio was significantly lower in the root meristem upon coumarin treatment (Fig. 8A). Besides this coumarin-induced reduction in apoplastic pH in this 24-hour timeframe compared to mock (Fig. 8A), coumarin treatment also led to a significant reduction in root growth (Fig. 8B).

The involvement of brassinosteroid homeostasis during coumarin inhibited root growth

Brassinosteroids (BRs) affect both cell proliferation and cell elongation in a concentration-dependent manner to control root meristem size (reviewed in Wei and Li, 2016). It has been shown in *Arabidopsis thaliana* that the loss-of-function *brassinosteroid insensitive 1* (*bri1-116)* as well as gain-of-function *BRI1-EMS suppressor 1* (*bes1-D)* (which exhibits a constitutive BR response (Yin *et al.*, 2002)), have a reduced meristem size (Gonzalez-Garcia *et al.*, 2011). This indicates that both, enhanced as well as reduced BR signalling, leads

to negative alterations of meristem development. We analysed the effect of coumarin on the BR signalling mutant *BRI1-ASSOCIATED RECEPTOR KINASE 1* (*bak1-4*) and the dominant mutant *bes1-D*. In mock conditions, we observed a shorter main root of the *bak1-4* mutant compared to Col-0, while *bes1-D* was not different from Col-0 (Fig. 9A). Interestingly, no reduction in the number of LR could be observed in the *bak1-4* mutant compared to Col-0 in mock conditions (Fig. 9B), leading to an increase in LRD of the mutant compared to Col-0 (Fig. 9C). The number of LRs of *bes1-D* mutants is significantly reduced compared to the WT (Fig. 9B). If we analyse the response to coumarin (Fig. 9, bottom), we observed an enhanced reduction in main root length upon coumarin treatment compared to mock conditions of *bak1-4* and *bes1-D mutants* – a reduction of 51.6% and 48.9%, respectively, compared to Col-0 seedlings that displayed a reduction of 43.6% – however this enhanced response was only significant for the *bak1-4* mutant (Fig. 9A, bottom). Also in the number of lateral roots, we found a significantly enhanced reduction upon coumarin treatment of the mutants compared to Col-0 (Fig. 9B, bottom): we observed a 40.39% reduction in number of lateral roots of Col-0 seedlings upon 40 µM of coumarin treatment compared to mock, while we observed a 49.84% and 50.73% reduction of *bak1-4* and *bes1-D* mutants (Fig. 9B, bottom). It is clear that both mutants show similar or even enhanced responses to coumarin treatment (Fig. 9, bottom). This indicates that reduced BR reception as well as enhanced BR signalling result in the same phenotype. We conclude that BRs act as a kind of modulaters but are not the main drivers of the effect of coumarin on roots.

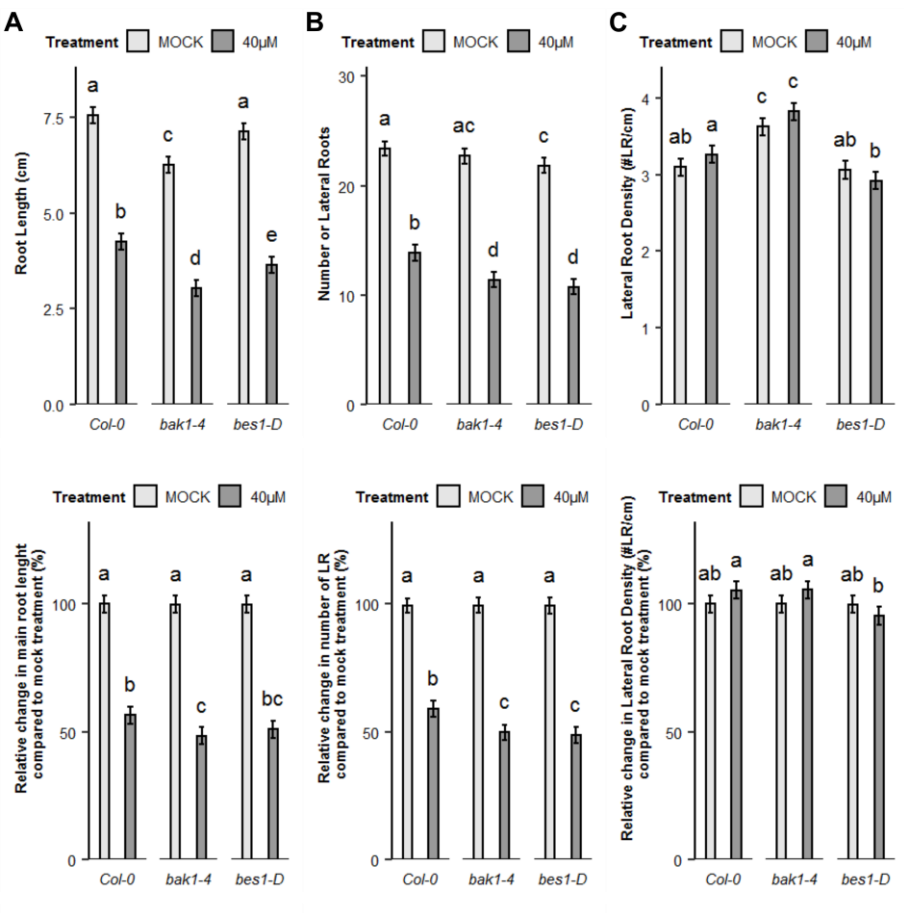

Figure 9: the interplay of BR homeostasis and coumarin to affect root growth

(top) The root phenotype of the *bak1-4* and *bes1-D* mutant grown for 7 DAG upon mock medium or 40 µM of coumarin treatment compared to the Col-0 control (A) main root length, (B) the number of lateral roots and (C) lateral density. (bottom) Illustration of the response to coumarin relative to the mock treatment for the phenotypes shown at the top (n≥91).

Data presented are means ± the confidence interval of at least three biological repeats. Letters indicate statistically different means ($p<0.05$).

Coumarin interferes with phytochromes to affect root growth

PHYTOCHROMES A and B (PHYA, PHYB) are involved in elongation of the primary root and root gravitropism (Correll and Kiss, 2005), and, moreover, are known to regulate lateral root emergence by, at least partly, controlling auxin distribution (Salisbury *et al.*, 2007). ELONGATED HYPOCOTYL 5 (HY5) is the central player in phytochrome signalling illustrated by the fact that *hy5* mutants are defective in phytochrome signalling. *hy5* mutants show altered lateral root production and reduced gravitropism with a clear link to an altered auxin pathway (Oyama, Shimura and Okada, 1997; Cluis, Mouchel and Hardtke, 2004). Given the pleiotropic root phenotype induced by coumarin, we analysed the response of the *phya-201, phyb-5, phya-201;phyb-5* and the *hy5-1* mutant towards coumarin treatment (Fig. 10).

The *hy5-1* mutant in mock conditions had longer main roots and more lateral roots than the Ler control (Fig. 10A, B). Upon coumarin treatment, however, no difference in main root length and number of LR was found of the *hy5-1* mutant compared to the WT, moreover, no significant difference in response towards coumarin for both phenotypes was observed (Fig. 10A, B, bottom). A clear reduced response towards coumarin was observed for the main root length of the *phya-201, phyb-5* and the double mutant *phya-201;phyb-5* compared to the Ler control (Fig. 10A): all three mutants have no significant different main root lengths in mock conditions compared to the WT, while all three mutants had significantly longer roots upon coumarin treatment compared to the WT (Fig. 10A). In mock conditions, only the *phya-201* mutant had slightly more LRs than the WT, while the *phyb-5* and the double mutant *phya-201;phyb-5* showed no significant difference in the number of lateral roots (Fig. 10B).The *phya-201, phyb-5* and the double mutant *phya-201;phyb-5* responded to 40 µM of coumarin treatment, comparable to WT in a reduction of the number of lateral roots (Fig. 10B, bottom), leading to a final number of LRs comparable to the WT (Fig. 10B). Overall, the *phya-201, phyb-5* and the double mutant *phya-201;phyb-5* showed a reduced decrease in main root length compared to the WT, while no difference in response could be observed in the number of lateral roots upon coumarin treatment compared with the Ler control. This suggest a role for PHY during inhibition of main root growth upon coumarin treatment, but no role in the LR formation process.

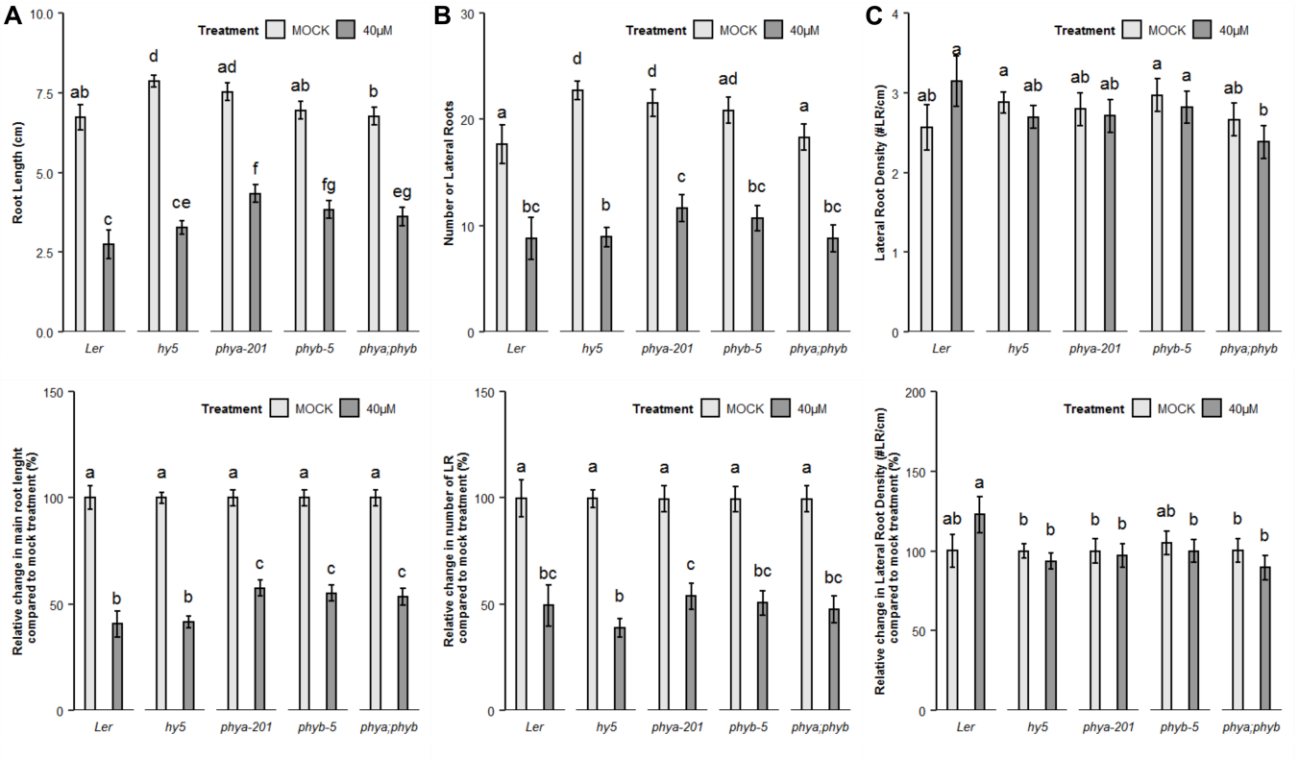

Figure 10: Coumarin interferes with phytochrome-mediated photomorphogenesis to affect root growth

The phenotype of the roots of the *hy5-1*, *phya-201, phyb-5* and *phya-201;phyb-5* mutants grown for 7 DAG upon mock medium or 40 µM of coumarin treatment: (A) main root length, (B) number of lateral roots and (C) lateral root density. (bottom) Illustration of the response to coumarin relative to the mock treatment for the phenotypes shown at the top. (n≥24).

Data presented are means ± the confidence interval of at least three biological repeats. Letters indicate statistically different means ($p<0.05$).

Discussion and conclusions.

Upon coumarin treatment, the main root length increases on lower concentrations and decreases on higher concentrations. This response is in line with observations made by Abenavoli et al. (2008), also confirming data by Lupini et al. (2014) who observed a 45% reduction in main root length of 4 day-old seedlings transferred to 100 µM of coumarin treatment for 1 week.

Our data show that both cell division and cell elongation in the root are affected by coumarin, leading to the noted short root phenotype at higher concentrations. In particular, the meristem size is severely reduced upon coumarin treatment, in line with historical data (D'Amato and D'Amato-Avanzi, 1954; Avers and Goodwin, 1956; Svensson, 1971; Kupidlowska, Kowalec, *et al.*, 1994; Podbielkowska *et al.*, 1994; Keightley *et al.*, 1996). Coumarin affects root growth at the early stages of root development, overlapping with the time-frame of root meristem development (from 1 to 5 DAG) (reviewed in Perilli, Di Mambro and Sabatini, 2012). An antagonistic cytokinin-auxin interplay regulates the primary root meristem development (Moubayidin *et al.*, 2010; Perilli, Moubayidin and Sabatini, 2010), with SHY2 being the central regulator. Increased levels of SHY2 (stimulated by cytokinin (CK)) lead to inhibition of PIN (re)distribution that in turn leads to cell differentiation/elongation (while inhibiting cell division) (Dello Ioio *et al.*, 2008; Moubayidin, Di Mambro and Sabatini, 2009; Perilli, Moubayidin and Sabatini, 2010). Degradation of SHY2 on the other hand (stimulated by auxin) will enhance cell division (Dello Ioio *et al.*, 2008; Moubayidin, Di Mambro and Sabatini, 2009; Perilli, Moubayidin and Sabatini, 2010).

Despite the fact that the root-specific *SHY2* expression still remains to be assessed upon coumarin treatment, we postulate that *SHY2* might be upregulated upon coumarin treatment, based on the diminished response of the *shy2-2* mutant to coumarin, a semi-dominant gain-of-function mutant that has both a reduced meristem size as well as a reduced distribution of PIN1/PIN3 (Dello Ioio *et al.*, 2008; Perilli, Moubayidin and Sabatini, 2010). This is further supported by the noted decrease in PIN1/PIN3 abundance upon coumarin treatment. The adjusted auxin distribution by coumarin has also been illustrated when examining the role of coumarin during gravitropic responses (Lupini *et al.*, 2013), and is further supported by the observed restoration of root gravitropism in the *pin2* mutant by coumarin treatment. Note, however, that merely looking at root size, *pin1* and *pin3* mutants are fully responsive toward coumarin indicating that suppression of *PIN1* or *PIN3* alone is not sufficient to establish the coumarin-induced reduction in root (meristem) size. We did not observe, via histochemical analysis of the pDR5::GUS reporter line, a differential auxin response in the roots upon long and short treatments with coumarin, but the spatial resolution and sensitivity of this auxin response marker is maybe too low and a more sensitive marker (e.g. pDII-VENUS (Brunoud *et al.*, 2012)) should be analysed to confirm this. Note that for example when *AUX1* is knocked-out also no auxin response could be observed via the synthetic pDR5::GUS reporter line (Liu *et al.*, 2018). In addition, the strong transcriptional upregulation of *SAURs* (a.o. auxin response genes) is one of the first events upon coumarin in the hypocotyl (Chapter 4) which makes the absence of an auxin response in the root unlikely. Moreover, we also observed acidification of the root meristem apoplast upon coumarin treatment, an effect typically exerted by auxin via stimulation of plasma membrane H^+-ATPase activity (Evans, Ishikawa and Estelle, 1994; Zhao, S K Christensen, *et al.*, 2001; Fu and Harberd, 2003; Sauer, Robert and Kleine-Vehn, 2013). Stimulation of plasma membrane H^+-ATPase activity by

coumarin has also been observed in maize roots (Lupini *et al.*, 2010). And while the role of the apoplast acidification in the root is currently debated – some papers illustrate that apoplast acidification, by low auxin concentrations, leads to enhanced root growth (Moloney, Elliott and Cleland, 1981; Evans, Ishikawa and Estelle, 1994; Fu and Harberd, 2003; Haruta *et al.*, 2010), while others show that acidification by high auxin concentrations inhibits root growth (Zhao, S K Christensen, *et al.*, 2001; Sauer, Robert and Kleine-Vehn, 2013) – it clearly illustrates the involvement of auxin during the coumarin-induced root response.

It is known that also BR homeostasis is influenced by coumarin (Chapter 3) and that BR mutants impaired in BR biosynthesis or signal transduction (e.g. *bak1-4*), as well as gain-of-function BR mutants with enhanced BR signalling (such as *bes1-D*), display a short-root phenotype by inhibition of meristem development (Gonzalez-Garcia *et al.*, 2011; Wei and Li, 2016). Moreover, similar to the main root phenotype, both reduced as well as enhanced levels of BRs inhibit LR formation (Bao *et al.*, 2004; Goh, Kasahara, *et al.*, 2012; Gupta, Singh and Laxmi, 2015; Wei and Li, 2016). Therefore, we hypothesized that BRs are involved in partly inhibiting meristem and LR formation upon coumarin treatment. The *bak1-4* mutant shows an enhanced reduction in root size upon coumarin treatment, while no significant different response was observed in the *bes1-D* mutant. Moreover, the *bak1-4* and *bes1-D* mutant respond more severely than the WT to coumarin in the reduction of the number of LR. Without further experiments, it is difficult to pinpoint the interplay between BRs and coumarin during root development. We suggest following up on this via hormone measurements in the root.

Reactive oxygen species (ROS) are also known to regulate the balance between cell division and cell differentiation, and this independently of auxin and CK (Tsukagoshi, Busch and Benfey, 2010; Sozzani and Iyer-Pascuzzi, 2014; Motte, Vanneste and Beeckman, 2019). Interestingly, coumarin is known to stimulate ROS production during germination (Saleh and Kebeish, 2018; Chen *et al.*, 2019) but also during shoot and root responses (e.g. gravitropic responses) (Lupini *et al.*, 2013; Araniti *et al.*, 2017), hence it is likely that ROS are involved too. In addition, the reduced inhibition of main root length upon coumarin treatment of the *phya-201* and the *phyb-5* mutant compared to the Ler control illustrates a role for phytochromes. This is in line with the role of phytochromes during coumarin-induced hypocotyl elongation (Chapter 3). However, not much light has been shed on the role of phytochromes during root development (Lymperopoulos, Msanne and Rabara, 2018; van Gelderen, Kang and Pierik, 2018), illustrating the need for additional research. Despite the fact that to the best of our knowledge no studies are available that demonstrate a functional link between AUX1 and root meristem size, and by extension auxin-influx as a whole, we also suspect for a role for auxin influx (especially via AUX1) in adjusting the root meristem. The first indication for this hypothesis is the fact that the extended distribution of AUX1 observed upon coumarin treatment, specifically overlaps with the zone where CKs induce degradation of auxin (via ARR1) (Di Mambro *et al.*, 2019). The enhanced decrease in main root length of the *aux1-7* mutant upon coumarin treatment potentially supports this. We thus postulate that enhanced AUX1 abundance in the root cap upon coumarin treatment (specifically inhibiting ARR1 (Moubayidin *et al.*, 2010)), partly saves the coumarin-induced activation of SHY2. This, however, has to be confirmed. The role of AUX1 for coumarin affected root growth, as also illustrated by Lupini et al. (2014), is further supported by its need to restore root-gravitropism. While coumarin can restore gravitropism in *pin2* roots, it cannot do so in the *aux1-7* mutant. It has been shown that AUX1 acts upstream of PIN2 in regulating root gravitropism (Liu *et al.*, 2018). Moreover, *AUX1* expression in the lateral root cap and epidermal cells were sufficient to rescue the root

gravitropic response in *aux1* mutants (Swarup *et al.*, 2005), overlapping with the enhanced abundance of AUX1 observed in coumarin-treated roots. The lack of research towards the role of auxin influx in main root growth (reviewed in Swarup and Bhosale, 2019), and the clear role of AUX1 during coumarin affected root growth makes it worthwhile to investigate this further. Although we could not visualize an auxin response in the root, there are several experiments that could be undertaken in order to clear out the role of phytohormones and/or ROS during the coumarin induced reduction in root length. Detailed analyses of the meristems (of the *shy2-2*, *aux1-7*, *phya/b* and ROS mutants (e.g. *UPBEAT1* (Tsukagoshi, Busch and Benfey, 2010)), expression analysis (*SHY2*, *PHYA/B* etc.) and spatio-temporal analyses of other players (e.g. CK and PHYs) need to be performed in order to support the above-made hypotheses.

The pathways governing LR formation have been well established (reviewed in Motte, Vanneste and Beeckman, 2019) and although coumarin is known to clearly stimulate the development of LRs in a concentration-dependent manner (Abenavoli *et al.*, 2008; Lupini *et al.*, 2014), its mode-of-action remains elusive. The strongest increase in LR formation by coumarin is found after the transfer of young seedlings (3 to 5 days old) to coumarin treatment (Abenavoli *et al.*, 2008; Lupini *et al.*, 2014; this study). Our hypothesis is that coumarin stimulates LR formation but inhibits meristem formation. When seedlings are treated with coumarin early in development, we assume that the inhibition on the meristem limits the LR formation potential of coumarin. To overcome this inhibition we suggest transferring seedlings to coumarin treatment after formation of the root meristem (3 to 5 days after germination (Sozzani and Iyer-Pascuzzi, 2014)). Here we showed that coumarin increases *GATA23* expression, a regulator of root founder cell identity (De Rybel *et al.*, 2010), and forward thereby its potential role as the main driver behind coumarin induced LR formation. In the *shy2/iaa3* gain-of-function mutants, *GATA23* expression is upregulated too (De Rybel *et al.*, 2010), confirming a role for SHY2 in LR development through regulation of *GATA23* expression. However, here we postulate that *SHY2* is not involved in coumarin-induced LR formation as the *shy2-2* mutant showed no differential response in LR formation towards coumarin treatment as the mock plants. Coumarin would, as such, act directly on *GATA23* expression, limiting the role of SHY2 to main root establishment (see above). Future experiments will have to clarify the role of GATA23 and SHY2 in adjusting the root system architecture of seedlings treated with coumarin.

Supplementary material

Table S1: *Information about the mutants and reporter lines used in this paragraph*

Plant line	Background (ecotype)	Full name or description	Locus	Allele/Mutagen	Reference
Wild type	Colombia-0 (Col-0)		N/A	N/A	N/A
Wild type	Landsberg erecta (Ler)		N/A	N/A	N/A
aux1-7	Colombia-0 (Col-0)	AUXIN RESISTANT 1	AT2G38120	Ethyl Methane Sulfonate (EMS)	(Maher and Martindale, 1980; Pickett, Wilson and Estelle, 1990)
aux1-21	Colombia-0 (Col-0)	AUXIN RESISTANT 1	AT2G38120	X-rays	(Marchant and Bennett, 1998)
aux1-21lax3	Colombia-0 (Col-0)	Cross of the mutants aux1-21 and lax3	AT2G38120	X-rays	(Swarup *et al.*, 2008)
bak1-4	Colombia-0 (Col-0)	BRI1-ASSOCIATED RECEPTOR KINASE	AT4G33430	T-DNA insertion	(Li *et al.*, 2002; Kemmerling *et al.*, 2007)
bes1-D	Enkheim	BRI1-EMS-SUPPRESSOR 1	AT1G19350.3	Ethyl Methane Sulfonate (EMS)	(Yin *et al.*, 2002)
ctr1-1	Colombia-0 (Col-0)	CONSTITUTIVE TRIPLE RESPONSE 1	AT5G03730.2	Diepoxybutane	(Kieber *et al.*, 1993)
eir1-1 (pin2)	Colombia-0 (Col-0)	Ethylene Insensitive Root 1 (PIN-FORMED 2)	AT5G57090	Diepoxybutane	(Roman *et al.*, 1995)
hy5-1	Landsberg erecta (Ler)	ELONGATED HYPOCOTYL 5	AT5G11260	Ethyl Methane Sulfonate (EMS)	(Koornneef, Rolff and Spruit, 1980)
phya-201 (CS6219)	Landsberg erecta (Ler)	PHYTOCHROME A	AT1G09570.1	Ethyl Methane Sulfonate (EMS)	(Nagatani, Reed and Chory, 1993)
phyb-5 (CS6213)	Landsberg erecta (Ler)	PHYTOCHROME B	AT2G18790.1	Ethyl Methane Sulfonate (EMS)	(Koornneef, Rolff and Spruit, 1980)
phya-201;phyb-5 (CS6224)	Landsberg erecta (Ler)			Cross of the above-mentioned mutants	(Nagatani, Reed and Chory, 1993)
pin1 (=pML1::PIN1:GFP/pin1 + pDR5::VENUS	Colombia-0 (Col-0)	PIN-FORMED 1 + expression constructs	AT1G73590.1	Crossing	(Kierzkowski *et al.*, 2013)
pin3-4	Colombia-0 (Col-0)	PIN-FORMED 3	AT1G70940	T-DNA insertion	(Alonso *et al.*, 2003)
shy2-2	Landsberg erecta (Ler)	SHORT HYPOCOTYL 2	AT1G04240.1	Ethyl Methane Sulfonate (EMS)	(Reed, Elumalai and Chory,

		(INDOLE-3-ACETIC ACID INDUCIBLE 3)			1998)
shy2-24 (IAA3)	Landsberg erecta (Ler)	SHORT HYPOCOTYL 2 (INDOLE-3-ACETIC ACID INDUCIBLE 3)	AT1G04240.1	transposon insertion	(Tian and Reed, 1999)
slr-1	Colombia-0 (Col-0)	*SOLITARY ROOT/IAA14*	*AT4G14550*	gain-of-function	(Fukaki *et al.*, 2002)
Reporter lines	**Background (ecotype)**	**Full name or description**	**Locus**	**Additional mutation(s)/Information**	**Reference**
pGATA23::GUS	Colombia-0 (Col-0)	GATA TRANSCRIPTION FACTOR 23	AT5G26930	Transcriptional reporter line. *GATA23* controls lateral root founder cell specification.	(De Rybel *et al.*, 2010)
pCYCB1;1::GUS	Colombia-0 (Col-0)	CYCLIN B1;1	AT4G37490	A labile chimeric mitotic cyclin::uidA reporter line, containing the CYCB1;1 destruction box. Cyclin-dependent protein kinase CYCB1;1 regulates cell cycle and this line is often used as cell division marker.	(Colon-Carmona *et al.*, 1999)
pDR5rev::GFP	Colombia-0 (Col-0)	DR5 is a synthetic auxin-responsive promoter. Rev = reverse. Green Fluorescent Protein		To monitor auxin responses and their dynamics.	(Sabatini et al., 1999)
pAUX1::AUX1-YFP	Colombia-0 (Col-0)	AUXIN RESISTANT 1	AT2G38120	Translational reporter line	(Swarup *et al.*, 2004)
pPIN1::PIN1-GFP	Colombia-0 (Col-0)	PIN-FORMED 1	AT1G73590	Translational reporter line	(Benková *et al.*, 2003)
pPIN2::PIN2-GFP	Colombia-0 (Col-0)	PIN-FORMED 2	AT5G57090	Translational reporter line	(Blilou *et al.*, 2005)
pPIN3::PIN3-GFP	Colombia-0 (Col-0)	PIN-FORMED 3	AT1G70940	Translational reporter line	(Zádníková *et al.*, 2010)
pPIN7::PIN7-GFP	Colombia-0 (Col-0)	PIN-FORMED 7	AT1G23080	Translational reporter line	(Blilou *et al.*, 2005)

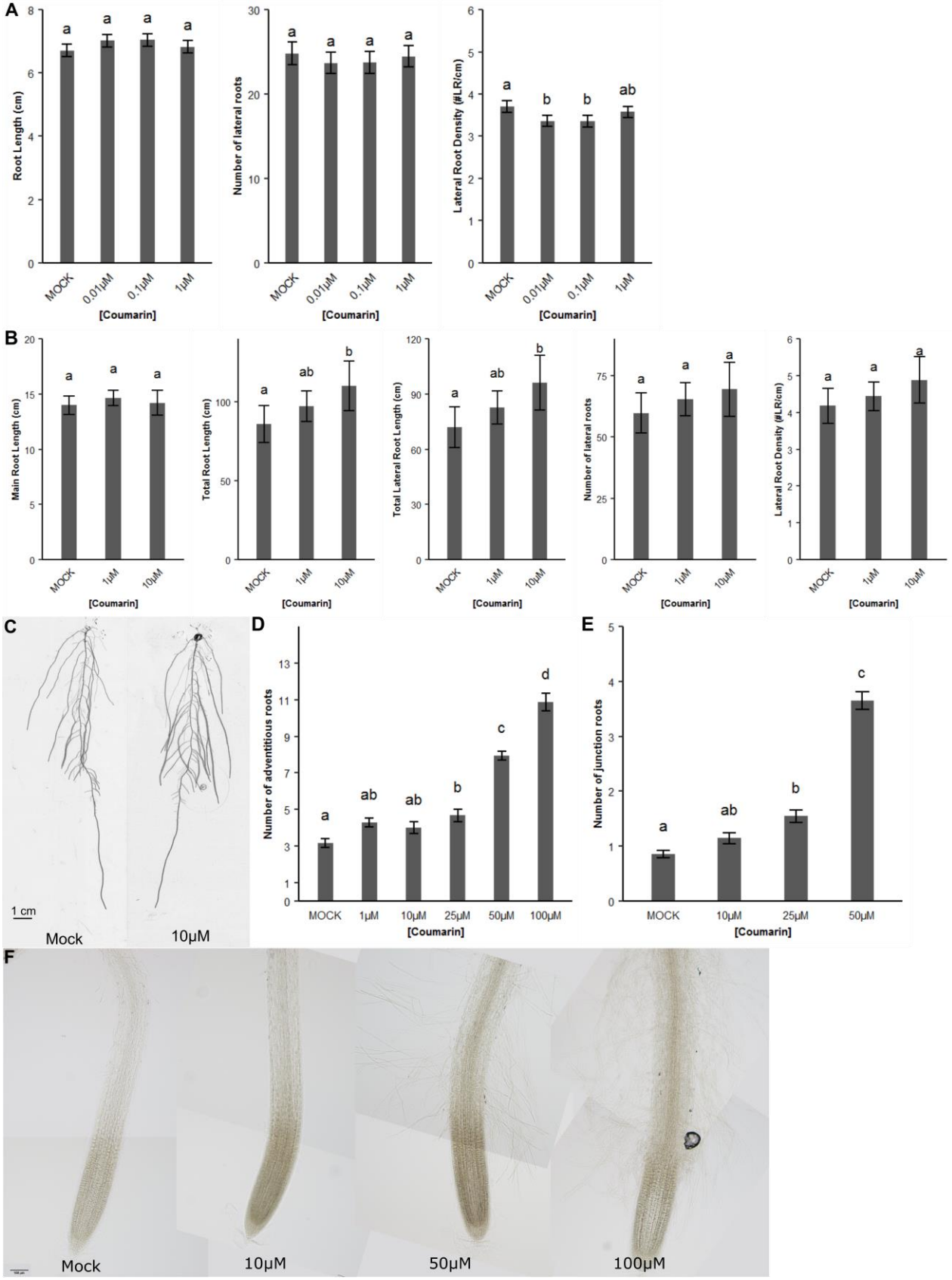
A
Root Length (cm)
Number of lateral roots
Lateral Root Density (#LR/cm)
MOCK
0.01µM
0.1µM
1µM
[Coumarin]
B
Main Root Length (cm)
Total Root Length (cm)
Total Lateral Root Length (cm)
Number of lateral roots
Lateral Root Density (#LR/cm)
MOCK
1µM
10µM
[Coumarin]
C
1 cm
Mock
10µM
D
Number of adventitious roots
MOCK
1µM
10µM
25µM
50µM
100µM
[Coumarin]
E
Number of junction roots
MOCK
10µM
25µM
50µM
[Coumarin]
F
Mock
10µM
50µM
100µM

Figure S1: Coumarin increases lateral root length, stimulates adventitious root formation and enhances root hair formation.

(A) From left to right: main root length, number of lateral roots and lateral root density of seedlings grown for 9DAG upon a mock medium, or 0.01, 0.1 or 1 µM of coumarin (n ≥ 29). (B) Analysis of the root phenotype of seedlings grown on mock, 1 or 10 µM of coumarin for 14 days (≥4). (C) Image of the seedlings analysed in (C). (D) Analysis of the number of adventitious formed on the etiolated hypocotyl of seedlings grown for 5 days in the dark and thereafter transferred to coumarin treatment and the light (n≥31). (E) Analysis of the number of adventitious formed on the etiolated hypocotyl of seedlings grown for 5 days in the dark and thereafter transferred to coumarin treatment and the light (n≥79). (F) Root hair formation upon 10, 50 or 100 µM of coumarin 9 days after germination.

Data presented are means ± the confidence interval of at least three biological repeats. Letters indicate statistically different means (p<0.05).

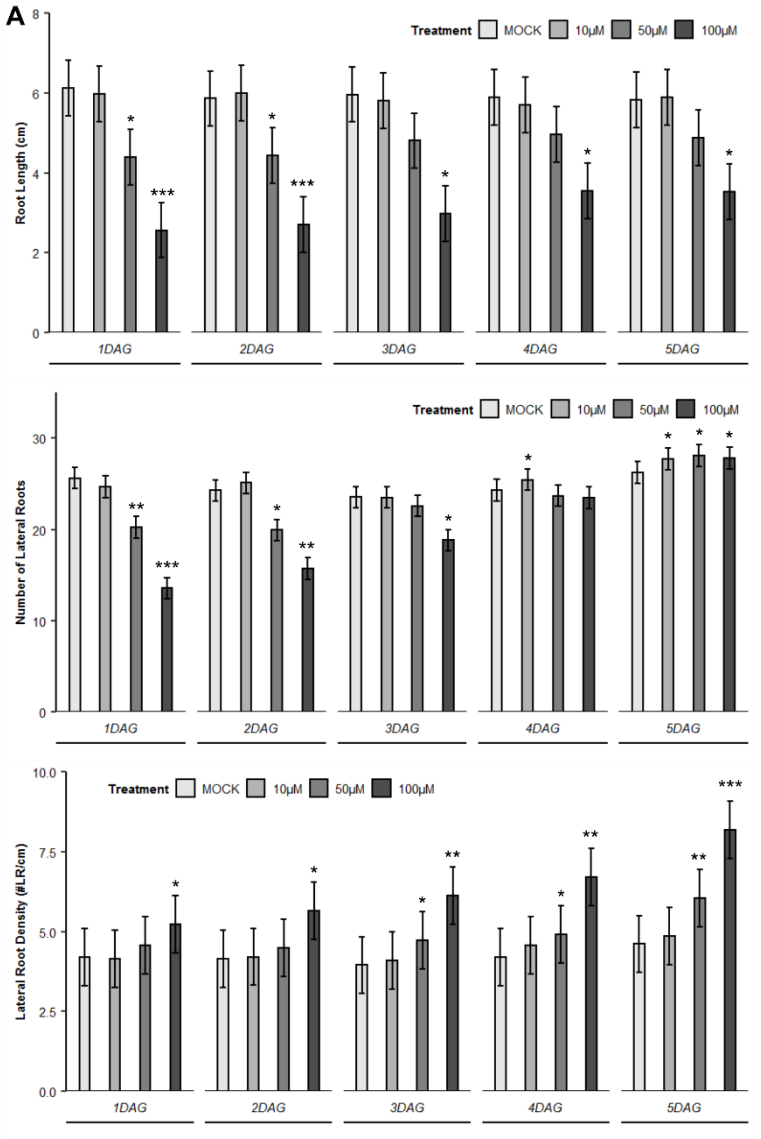

Figure S2: Coumarin inhibits meristem division in the early stages of development.

(A) From top to bottom, main root length, number of lateral roots and lateral root density of 1, 2, 3, 4 or 5 DAG old seedlings transferred from the untreated medium to mock medium, or medium supplemented with 10, 50 or 100 µM of coumarin and analysed 9DAG (n ≥ 63).

Data presented are means ± the confidence interval of at least three biological repeats. Letters indicate statistically different means ($p<0.05$).

Figure S3: Coumarin had no effect on the medium pH as measured by pH sticks.

Chapter 6 – Conclusion and perspectives

General conclusion and perspectives.

The natural compound coumarin (2H-1-benzopyran-2-one) was already described in 1820, as it could be found in high concentrations in Tonka beans (Vogel, 1820). This is a century before the description of auxin (Went and Thimann, 1937). Darwin and his son illustrated bending of coleoptiles to blue light, a phenotype linked to auxin afterwards, but at the time the responsible compound was uncharacterized (C. Darwin and Darwin, 1881). Given its early discovery, many researchers analysed the effects of both auxin (analogues) as well as coumarin on plant growth. However, although the biosynthesis, signalling and mode-of-action of auxin are well documented, most of it for coumarin remains elusive **(Introduction)**. Remarkably, while the biosynthesis of higher coumarins (e.g. scopoletin, umbelliferone) is known, the enzymatic steps of coumarin biosynthesis are not yet characterized (Shimizu, 2014).

Coumarin is known to influence the rhizosphere by influencing the rhizobiome, germination and root growth, but coumarin is also known to affect shoot growth, hypocotyl-, epicotyl- and coleoptile-elongation, respiration and photosynthesis (Table 1, **introduction**). However, the exact *modus operandi* is underexplored. Moreover, most research performed on investigating the effects of coumarin occurred some 50 to 60 years ago when the use of *Arabidopsis thaliana* as a model plant was not yet common. Here, we illustrated the effects of coumarin on hypocotyl elongation (**Chapter 3**) and on the root system architecture of *Arabidopsis thaliana* (**Chapter 5**). Genome-wide transcriptome analysis of Arabidopsis hypocotyls treated with coumarin for 30, 60 or 180 minutes (**Chapter 4**), gave a more in-depth picture of how coumarin affects plant growth and allowed us to confirm and elaborate previous findings.

Both in the root, as well in the hypocotyl we showed that coumarin influences auxin transport, although, remarkably, in an opposing manner. In the shoot coumarin induced auxin transport, by clear upregulation of the PIN-FORMED genes *PIN1*, *PIN3*, *PIN4* and *PIN7.* In the root we found, via translational reporter lines, that coumarin led to a reduction in the abundance of PIN1, PIN2 and PIN3 proteins, while we observed an increased abundance of the auxin influx transporter AUXIN RESISTANT 1 (AUX1). We, thereby, confirmed and elaborated early findings illustrating the influence of coumarin on auxin transport (Basu, 1972; Basler and Mcbride, 1977; Dhawan and Nanda, 1982; Lupini *et al.*, 2014). Analysis of translational reporter lines (via confocal microscopy) will be needed to clarify how coumarin exactly adjusts auxin transport in the hypocotyl. In the root, we were able to show the involvement of SHORT HYPOCOTYL 2/INDOLE-3-ACETIC ACID INDUCIBLE 3 (SHY2/IAA3) and forwarded, as such, an acceptable hypothesis of how coumarin inhibits meristem cell division (**Chapter 5**). *SHY2* is a central player in meristem development by inhibiting cell division via altering auxin transport (reducing distribution of PIN1 and PIN3) (Dello Ioio *et al.*, 2008; Perilli, Moubayidin and Sabatini, 2010). We postulated that *SHY2* might be upregulated upon coumarin treatment leading a reduced meristem size and altered auxin transport. Hereby, we confirm the numerous reports demonstrating the inhibitory effect on root meristem division of coumarin, without, however, providing evidence of the mode-of-action (Cornman, 1947; D'Amato and D'Amato-Avanzi, 1954; Avers and Goodwin, 1956; Svensson, 1971; Kupidlowska, Dobrzynska, *et al.*, 1994; Kupidlowska, Kowalec, *et al.*, 1994; Podbielkowska *et al.*, 1994, 1995, 1996; Keightley *et al.*, 1996; Yuksel and Aksoy, 2017). The upregulation of *SHY2* found in the hypocotyl (**Chapter 4**) should be confirmed in the root. To unravel its relevance for coumarin inhibited meristem cell division, downstream players should be analysed (e.g.

via analysis of the meristems of the mutant *shy2* and *arr1* upon coumarin treatment) (Dello Ioio *et al.*, 2008). The positive effects of coumarin on lateral root formation have been described numerous times before, and have also been observed in Arabidopsis (Abenavoli *et al.*, 2008; Lupini *et al.*, 2014). However, also here, no mode-of-action has been postulated. The interference with AUX1 has been postulated as a potential mechanism, but its role was mainly in mediating main root length inhibition upon coumarin treatment and not on the observed increase in lateral root formation. We have shown the upregulation of *GATA23* in the root via reporter analysis in the root (**Chapter 5**) and also observed its upregulation in the transcriptome data of the hypocotyl (**Chapter 4**). GATA23 is involved in lateral root initiation (De Rybel *et al.*, 2010) and as such suggests a potential mechanism of how coumarin can stimulate lateral root formation. Further research is however needed to unravel the role of GATA23 and its upstream players (IAA14, IAA12, IAA28 (De Rybel *et al.*, 2010)) during coumarin induced lateral root formation and to link this with the changed auxin transport in the root.

Coumarin stimulates cell elongation in the shoot: in cotyledons, pavement cells were enlarged by 23% upon coumarin treatment while hypocotyls increased a 3-fold in length (**Chapter 3**). The hypocotyl was used as a tool to investigate the effect of coumarin on cell elongation in *Arabidopsis thaliana*. Exogenous treatment with auxin analogues cannot induce hypocotyl elongation, indicating a different response of Arabidopsis towards coumarin than to auxin treatment. However, we clearly found that coumarin triggered an auxin response in the hypocotyl, this confirmed the claim by Neumann and Knypl that coumarin affects plant growth in an auxin-like manner, but not auxin-caused (Neumann, 1960a; Knypl, 1966a). Interesting fact, both also used the hypocotyl (from *Helianthus*) as a tool to analyse the coumarin-induced elongation. Numerous auxin reporter genes (*Aux/IAA* response genes, *HISTONE ACETYLTRANSFERASE 1 (HAT)* genes and *AUXIN UPREGULATED F_BOX PROTEIN (AUF1)*) are upregulated upon coumarin treatment (**Chapter 4**) and their causality, as well as their interdependence, needs to be investigated further. In the root as well as the hypocotyl we observed the potential role of H^+-ATPase mediated acidification. In the hypocotyl, 23 *SMALL AUXIN UP RNA (SAUR)* genes are upregulated after 30 minutes of coumarin treatment, an upregulation that remains during seedling development upon coumarin treatment. However, we were not able to exclude, neither fully prove their importance for coumarin-induced hypocotyl elongation (**Chapter 3, addendum 1**). In the root, via HPTS staining (Barbez *et al.*, 2017), we observed acidification of the root meristem upon short treatment with coumarin, in line with earlier findings in maize roots (Lupini *et al.*, 2010) (**Chapter 3**). Both findings illustrate (1) the involvement of auxin and (2) that coumarin influences acidification in at least 2 different organs. However, further research will be needed to analyse the role of acidification for coumarin-induced phenotypes, for example via pH reporter lines or HPTS staining (Moseyko and Feldman, 2001; Barbez *et al.*, 2017). Visualising acidification in the apoplast of hypocotyl cells will allow us to further identify the role of acidification during coumarin induced hypocotyl elongation. Furthermore, if acidification should take place, HPTS staining can be used as a tool to measure the acidification in the apoplast of hypocotyls cell of mutants that are non-responsive to coumarin (e.g. *pin1, bri1-116, slr-1*).

The effect of coumarin on ethylene, gibberellic acid (GA) and brassinosteroids (BRs) has either been limited or not all described (**Chapter 1, Table 2**). Here, we are the first to show a causal link with BR signalling to induce hypocotyl elongation by coumarin (**Chapter 3**). Note that our findings in the root are, however, not conclusive about the role of BR for the effect of coumarin. This would indicate that coumarin induces BR

signalling in a tissue-specific manner and this should be investigated further. The BR response is broad leading to upregulation of numerous genes (e.g. *PREs, BMI, BEE1*) that in the end stimulate *XYLOGLUCAN:XYLOGLUCOSYL TRANSFERASE (XET)* genes involved in cell wall remodelling (**Chapter 4**). It would be interesting to investigate the exact changes in cell wall composition further, definitely in the light of potential acidification induced by SAUR proteins. Moreover, it would be interesting to further analyse the interplay between auxin and BR as numerous *Aux/IAA* genes are known to be upregulated upon brassinolide treatment that are also found to be upregulated upon coumarin treatment (e.g. *IAA5* and *IAA19*), indicating a clear interaction between both observed responses (Nakamura *et al.*, 2003).

Lastly, both the transcriptome data in **Chapter 4**, as well as mutant analysis of the *phyb-5* mutant (**Chapter 3**), revealed a link with photomorphogenesis. The BZR1-PIF4 module is known to interact with light signalling via PHYB, but also by PRE6 (Zheng *et al.*, 2017; Wu *et al.*, 2019). Moreover, BRs, in general, illustrate a clear link with photomorphogenesis, by in fact by stimulating skotomorphogenesis. The *det2-1* mutants, for example, show a constitutive photomorphogenic phenotype, even when grown in the dark (Luccioni, 2002). More research will be needed to unravel the exact role of the observed light-signalling responses during coumarin-induced hypocotyl elongation. Recently it has been shown that BRs still can induce hypocotyl elongation of *phyb* mutants grown in the light, suggesting that PHYB operates upstream of BR signalling. We observed, despite the strong BR response in the WT, no increase in hypocotyl elongation of coumarin treated *phyb* mutants which suggest that also here, PHYB operates upstream of BR signalling. We suggest, for example, investigating the BR response (expression of *BEE1, PREs*, etc.) in the hypocotyl of coumarin treated *phyb* mutants.

Based on the results obtained in this research project, we propose (and have initiated) several sub-projects to further clarify how coumarin reshapes plant growth and development.

1. Link with the phenylpropanoid pathway – towards unravelling coumarin biosynthesis and biostimulant activity of PP pathway intermediates and derivatives.

In collaboration with the VIB Metabolomics Core Ghent (Specialized Metabolism), we were able to detect coumarin in methanol extracts of *Arabidopsis thaliana* via GC-MS profiling with a GC-qTOF, using a VF-5ms column and with helium as mobile phase (Material and Methods[7]). Preliminary data showed already that upon 40 µM of coumarin treatment, the endogenous concentration of coumarin in *Arabidopsis thaliana* is increased by a 10-fold compared to the mock-control. Interestingly, also in all the non-responsive mutants in terms of hypocotyl elongation (e.g. *pin1, bri1-116, det2, phyb-5*) we detected a 10-fold increase in coumarin concentration, with a final coumarin concentration that is statistically similar to the coumarin treated WT. This indicates that (1) coumarin is actively taken by Arabidopsis and (2) that the inhibited phenotype (i.e. absence of hypocotyl elongation) upon coumarin treatment is because of a change in physiology and not abolished uptake of coumarin.

In addition, these findings allow us to investigate potential biosynthetic pathways of coumarin. Historically, it has been claimed that coumarin is formed after a glycoside intermediate (Brown, 1962; Collier, 1971). Recently, this got some additional support from a proteomics approach that showed reduced levels of a specific B-GLUCOSIDASE MYROSINASE (E.C. Number: 3.2.1.21) upon coumarin treatment (Araniti *et al.*, 2017). The authors claimed a negative feedback regulation of coumarin on its own biosynthesis (Araniti *et al.,* 2017). Myrosinases (EC 3.2.1.147) are β-thioglycoside glycosidases with a specific role in protection against pathogens and insect pests by initiating the breakdown of secondary metabolites into toxic products (Andersson *et al.*, 2009). Interestingly, also coumarin is found to have insecticidal properties and is often described as phytoalexin (Knypl, 1960, 1963; Gorz, Haskins and Manglitz, 1972; Mansour, Dimetry and Rofaeel, 1982; Reda and El-Banhawy, 1986; Wu *et al.*, 2008; Al-Wakeel *et al.*, 2013; Lee *et al.*, 2014; Gutiérrez-Barranquero *et al.*, 2015; Zhang *et al.*, 2017; Reen *et al.*, 2018). In *Arabidopsis thaliana,* there are only six myrosinase genes (*TGG1–TGG6*), of which *TGG1* (*BETA GLUCOSIDASE 38)* and *TGG2* are the most highly expressed (Chadchawan *et al.*, 1993; Xue *et al.*, 1995). *TGG1* is specifically expressed in the guard cells and the phloem,

[7] GC-MS analysis

The obtained extracts were dissolved in 100 µL of methanol for GC-MS analysis and stock solutions for a standard curve (concentration range from 0.1 to 5.0 µg/ml) were prepared in 100% methanol. GC-MS analysis was carried out using a 7890B GC system equipped with a 7693A Automatic Liquid Sampler and a 7250 Accurate-Mass Quadrupole Time-of-Flight MS system (Agilent Technologies, Santa Clara, CA, USA). 1 µl of the sample was injected in splitless mode with the injector port set to 280°C. Separation was achieved with a VF-5ms column (30 m x 0.25 mm, 0.25 µm; Varian CP9013; Agilent Technologies) with helium carrier gas at a constant flow of 1.2 ml/min. The oven was held at 50°C for 1 min post-injection, ramped to 320°C at 10°C/min, held at 320°C for 1 min, and finally cooled to 50°C at 50°C/min at the end of the run. The total run time was 34.4 min. The MSD transfer line was set to 280°C and the electron ionization energy was 70 eV. Full EI-MS spectra were recorded between m/z 50-800 at a resolution of >25,000 and with a solvent delay of 5.0 min. The resulting GC-MS chromatograms were converted to TDA format and coumarin peak areas were determined using the MassHunter Quantitative Analysis (for Q-TOF) software package (Agilent Technologies). The fragment ion at m/z 118.0413 was selected as quantifier, with the ions at m/z 146.0362, m/z 89.0386, and m/z 63.0229 as qualifiers

while *TGG2* is only expressed in the phloem of Arabidopsis (Barth and Jander, 2006). It would be interesting to test the endogenous concentrations of coumarin in the *tgg1tgg2* mutant.

The role of *BETA GLUCOSIDASES* in the biosynthesis of coumarins is well-known. For example, recently it is has been shown that the BETA GLUCOSIDASE 42 (BGLU 42) plays a major role in scopoletin biosynthesis (Lundberg and Teixeira, 2018; Stringlis *et al.*, 2018). Note, however, that the function of *BGLU42* is to convert scopolin back to scopoletin (scopolin is formed after scopoletin biosynthesis) (Shimizu, 2014). Scopoletin is an active metabolite in plants, and recently, it has been shown, via modelling approaches, that scopoletin can bind in the TIR1 pocket and as such its bioactivity has been linked to herbicide actions (Graña *et al.*, 2017). Therefore, scopoletin is stored in the vacuole just like its less active glucoside variant scopolin (Goy *et al.*, 1993; Siwinska *et al.*, 2014). The glucoside variant of coumarin (*o*-coumaryl glucoside) is, however, claimed to be its precursor (Collier, 1971; Bourgaud *et al.*, 2006). Recently, it has been shown that COUMARIN SYNTHASE (COSY) is able to produce umbelliferone, esculetin and scopoletin from their respective *o*-hydroxycinnamoyl-CoA thioesters by two reaction steps — a *trans–cis* isomerisation followed by a lactonization (Vanholme *et al.*, 2019, Fig. 4 Chapter 1). Note that the S in the respective thioesters is claimed to be crucial for electron donation and allowing for ortho-hydroxylation (Kai *et al.*, 2008; Vanholme *et al.*, 2019). If the biosynthesis of coumarin would occur via myrosinase activity than a thio-glycoside intermediate is formed also donating an S to the reaction. *cosy* mutants are found to have strongly reduced levels of umbelliferone, esculetin and scopoletin (Vanholme *et al.*, 2019). Coumarin, however, could not be measured by the used techniques, hence the role of *COSY* in coumarin biosynthesis remains elusive. It would, therefore, be interesting to analyse, with the recently developed protocol, the role of COSY and *BETA GLUCOSIDASES* for the biosynthesis of coumarin via analysis of coumarin levels in their respective mutants compared to the control. Also feeding experiment with radioactively labelled precursors of coumarin (e.g. cinnamic acid) can give insight into the biosynthesis pathway. Note, however, that *o*-coumaric acid spontaneously converts to coumarin in the light, and can therefore not be used in feeding experiments in the light. But for example treatment with labelled cinnamoyl-CoA can give insights if this compound is an intermediate of coumarin biosynthesis, suggesting the involvement of the COSY enzyme or if coumarin biosynthesis occurs via another route.

Exogenous coumarin treatment can interfere either directly, or indirectly with the biosynthesis of other derivatives of the phenylpropanoid (PP) pathway – for example by a feedback mechanism on the general PP derivative precursor cinnamic acid (Bourgaud *et al.*, 2006; Shimizu, 2014; Araniti *et al.*, 2017; Dare *et al.*, 2017). Moreover, coumarin treatment is known to also upregulate the production of other PP derivatives (e.g. scopoletin) (Dhawan and Nanda, 1982). It is, as such, acceptable that coumarin treatment leads to accumulation of its precursors and/or other derivatives and in that way (indirectly) stimulates the PP pathway. We have shown that stimulation of hypocotyl elongation is relatively unique for coumarin as the derivatives scopoletin and umbelliferone and the intermediates trans-cinnamic acid (*t*-CA), *rac*-CA (i.e. a racemic mixture of *trans*- and *cis*-cinnamic acid), *p*-coumaric acid, coniferyl alcohol, coniferyl aldehyde or feruloyl-CoA could not induce hypocotyl elongation (Chapter 3). However, those data illustrate merely that exogenous treatment of other derivatives and intermediates of the PP pathway does not mimick the phenotype observed upon coumarin treatment, but it does not exclude a potential role for the PP pathway, neither reveal any potential interactions with the PP pathway.

Therefore, we suggest to further investigate the role of the PP pathway and any potential interactions with it during coumarin-induced hypocotyl elongation.

The phenylpropanoid pathway forms the basis of lignin formation by delivering the building blocks for it (i.e. the monolignols coniferyl alcohol, sinapyl alcohol and *p*-coumaryl alcohol) (Vanholme *et al.*, 2012). Lignin counts for approximately 30% of the organic carbon in the biosphere, is crucial for the structural integrity of the cell wall and strength of the stem (Jones, Ennos and Turner, 2001; Chabannes *et al.*, 2003), and therefore critical during the evolution of land plants to adapt from an aquatic to terrestrial environment. Moreover, lignin makes the cell wall waterproof allowing the development of the vascular system and as such enables transport of water and solutes (Sarkanen and Ludwig, 1971). The pathway is also the basis for an enormous array of secondary metabolites (Vogt, 2010), e.g. the chalcone synthesis pathway that leads to flavonol and flavonoid biosynthesis (Vogt, 2010; Vanholme *et al.*, 2012). These more than 10 000 different compounds have various biological roles, for example in UV protection or radical scavenging (antioxidant) (Agati *et al.*, 2012; Yang *et al.*, 2018), but are also involved in flower and fruit pigmentation (Dixon, Liu and Jun, 2013), symbiotic associations (J. Zhang *et al.*, 2009; Nadal and Paszkowski, 2013; Liu and Murray, 2016), mineral shortage (Clemens and Weber, 2016), and defence reactions (Naoumkina *et al.*, 2010; Shalaby and Horwitz, 2015).

It is well known that lignin is a restricting factor in the elongation of plant cells (Yin Wang *et al.*, 2013), whereby mutations in the PP pathway lead to dwarfism (Van Acker *et al.*, 2013), which is historically claimed to be caused by a lack of lignin and therefore named lignin modification-induced dwarfism (LMID) (Muro-Villanueva, Mao and Chapple, 2019). Therefore, it sounds contra-intuitive that the pathway should be involved in growth stimulation effects. However, it has been illustrated that the restoration of lignin biosynthesis in the vessels alone is enough to restore plant growth and even induce biomass production (De Meester *et al.*, 2017). It remains, however, questionable if the dwarf phenotypes are only the consequence of altered/perturbed lignin biosynthesis or if part of the effects can also be linked to the hypo- or hyper-accumulation of intermediates or derivatives of the phenylpropanoid pathway. Moreover, when genes producing enzymes in the monolignol-pathway are knocked-out (e.g. ferulate 5-hydroxylase (F5H), caffeic acid O-methyltransferase (COMT), and cinnamyl alcohol dehydrogenase (CAD)) - hampering the formation of lignin building blocks - the effect on growth is way less severe, to even no effect at all (Wang *et al.*, 2018). Furthermore, it has been illustrated that the phenylpropanoids 3,4-(methylenedioxy)cinnamic acid (MDCA) and cinnamic acid interfere with auxin transport and auxin signalling (Steenackers *et al.*, 2016, 2017; Kurepa *et al.*, 2018). Also, the PP derivatives of cinnamic acid: umbelliferone, scopoletin and coumarin are known to influence plant growth in a wide variety of phenotypes in a way resembling auxin accumulation (Chapter 1, Podbielkowska *et al.*, 1995; Lacy and O'Kennedy, 2004; Kai *et al.*, 2006; Lupini *et al.*, 2014; Graña *et al.*, 2017). Moreover, it has been known for a long time that even flavonoids interfere with auxin transport (Jacobs and Rubery, 1988; Brown *et al.*, 2001; Peer and Murphy, 2007; Yin *et al.*, 2014) and Arabidopsis mutants with changes in flavonol accumulation show defects in auxin transport (Kuhn *et al.*, 2011, 2017).

Most of the research is, however, focussing on the roles and potential yield gains (in fact trying to overcome the yield penalty) when modulating lignin biosynthesis (for bioenergy perposes) (Muro-Villanueva, Mao and Chapple, 2019). Moreover, the many roles of flavonols and anthocyanins are mostly investigated in

the context of abiotic and biotic stress resistance. Therefore, the intermediates and derivates (molecular) functions have been out of scope. Phenylpropanoids do not operate in a steady-state but are actively transported through the plant cell and tissues and their localisation is tightly controlled (Biala and Jasiński, 2018). Interesting is the compartmentalisation of several phenylpropanoids in the cell wall, independent of lignin biosynthesis, indicating potential interference with cell wall processes (Kulich and Žárský, 2014; Biala and Jasiński, 2018). Therefore, we suggest that more focus should be directed to the effects on plant growth and development of modulation in the PP pathway, rather than focusing on lignin only.

Here, we propose to investigate the link of coumarin with the PP pathway more in-depth and to gain, as such, a clear view on potential changes in the PP pathway induced by coumarin that can influence plant growth. In that way, we will be able to analyse if the observed effects of coumarin treatment are either caused by coumarin itself or (partly) by stimulating other compounds of the PP pathway. For example, the inhibitory effect on root growth can be a side-effect of enhanced cinnamic acid accumulation affecting auxin transport (Steenackers *et al.*, 2017). We suggest analysing the interference via a pharmacological approach whereby coumarin is co-treated with the PP pathway blockers L-α-aminooxy-3-phenyl propionic acid (AOPP), 3,4-(methylenedioxy)-cinnamic acid (MDCA) and Piperonylic acid (PA). AOPP blocks PHENYLALANINE AMMONIA LYASE, the first step in the pathway responsible for the formation of cinnamic acid out of phenylalanine (Amrhein and Gödeke, 1977). MDCA blocks the action of 4-COUMARATE-COA LIGASE (4CL), the enzyme converting *p*-coumaric acid to *p*-coumaroyl-CoA (Knobloch and Hahlbrock, 1977; Chakraborty, Karun and Mitra, 2009). It has to be noted, however, that MDCA treatment alone, also induces an auxin response in plants as it interferes with auxin transport (Steenackers *et al.*, 2016). PA inhibits CINNAMATE-4-HYDROXYLASE (C4H), the enzyme catalysing the conversion of *trans*-cinnamic acid to *p*-coumaric acid. Note that *p*-coumaric acid is the precursor or scopoletin, umbelliferone and esculetin (Shimizu, 2014).

In addition, we suggest analysing the response of mutants in the 10 biosynthetic steps of the central backbone of the PP[8] pathway to coumarin in terms of hypocotyl elongation. The analysis of those mutants will exclude if coumarin operates via the PP pathway or rather independently stimulates hypocotyl elongation. Moreover, a detailed phenolic outread of seedlings treated with coumarin can give us the first clues on the phenylpropanoid changes upon coumarin treatment. As such we will get an idea of the influence of coumarin on the phenylpropanoid pathway of which it is derived.

8 phenylalanine ammonia-lyase (PAL), Caffeoyl Skikimate Esterase (CSE), cinnamate 4-hydroxylase (C4H), p-coumarate 3-hydroxylase (C3H), ferulate 5-hydroxylase (F5H), caffeoyl-CoA O-methyltransferase (CCOAOMT), caffeic acid O-methyltransferase (COMT), cinnamoyl-CoA reductase (CCR), cinnamyl alcohol dehydrogenase (CAD), 4-coumarate-CoA ligase (4CL) and hydroxycinnamoyl-CoA shikimate/quinate hydroxycinnamoyl transferase (HCT) (Vanholme *et al.*, 2012, 2013).

2. A forward-genetics approach to unravel the *mode-of-action* of coumarin during seed germination

From the 80s onwards, *Arabidopsis thaliana* has gained interest as a model plant (Somerville and Koornneef, 2002), leading to its ubiquitousness in plant research today. Arabidopsis has a relatively small genome, only 25498 genes according to its first sequence in 2000 (The Arabidopsis Genome Initiative, 2000). Moreover, its short generation time (6-8 weeks), the production of a large number of seeds per plant and the fact that it is a self-fertilizer makes it an ideal plant for genetics (Koornneef and Meinke, 2010). Ethyl methane sulphonate (EMS) mutagenesis was proven to be an effective forward genetic screen in Arabidopsis (Koornneeff, Dellaert and van der Veen, 1982) and it is still a popular mutagen today (Koornneef and Meinke, 2010). EMS has high mutagenicity and low mortality and can be used in any basic laboratory (Maple and Møller, 2007). EMS mutagenesis will alkylate guanine bases and as such induce mispairing and in the end will lead to an amino acid change or deletion (Maple and Møller, 2007).

In chapter 4, we described an interesting phenotype for performing an EMS mutagenesis screen. Seeds in the dark, upon high concentrations of coumarin, do not germinate. This set-up allows for screening for seeds, after mutagenesis that do germinate upon coumarin treatment. The obtained mutants will be affected in the hormonal pathways involved (e.g. RGL2 or GAI (see chapter 4)), or will be mutants in coumarin signalling or reception, but it can as well be mutants involved in light signalling given the role of light in our phenotype. We believe that this set-up will deliver valuable information about how coumarin affects germination of *Arabidopsis thaliana*, and potentially, if interference with light is found, also reveal a broader mode-of-action.

Hypocotyl elongation is increased a 3-fold upon coumarin treatment. This means that hypocotyls are increased from on average a 1.2 mm in length in mock conditions to 3.5 mm upon coumarin treatment. In other words, this phenotype is easily visible with the bare eye and allows an accessible screening. In that way, we suggest screening for mutants that do not show an elongated hypocotyl upon coumarin treatment. It would also be interesting to screen for hypersensitive mutants to coumarin, illustrating an additional increase in hypocotyl length. Additional set-ups should be performed to exclude mutations in auxin and BR homeostasis as we already showed their role in the phenotype. One way to overcome this issue is for example to use the pDR5rev::GFP reporter line as seed stock for the EMS. In that way, mutated seedlings that do not respond to coumarin can be screened for their response to auxin.

3. A genome-wide association study (GWAS) to analyse the genetics underlying coumarin treatment in the hypocotyl and roots of *Arabidopsis thaliana*

Mendel was one of the first to postulate a relationship between genotype and phenotype, what is, in fact, the basis of a genome-wide association study (GWAS) analysis. The use of variation in physiological traits among natural accessions in Arabidopsis dates back until 1943 (Laibach, 1943). Later this track of research, with new molecular tools being discovered resulted in the current known GWAS analysis. It is a powerful tool to reconnect a trait of interest to its underlying genetics by comparing different responses of your phenotype of interest, linked to slightly different genotypes. A GWAS typically focusses on comparing the genome of closely linked individuals so that associations between single-nucleotide polymorphisms (SNPs) in the species of interest can be made (Korte and Ashley, 2013). By mapping back (e.g. by Quantitative Trait Locus (QTL) mapping) the underlying genetic differences of the individuals responding different for your phenotype of interest, you are able to detect the responsible loci (Korte and Ashley, 2013). The high level of homozygosity found in Arabidopsis accessions, in combination with the high density of molecular markers, make it a suitable organism for this approach (Nordborg and Weigel, 2008). In Arabidopsis, in general, different ecotypes and strains are used as they display a variety of SNPs (Korte and Ashley, 2013). In our specific case, we suggest analysing the effect of coumarin on hypocotyl elongation of around 200 different ecotypes. This population-scale has been shown to be sufficient to draw a clear conclusion about the phenotype of interest (Cao *et al.*, 2011). Preliminary data already showed that different ecotypes display a broad variety in responses to coumarin ranging from a severely diminished response to hypersensitivity towards coumarin in terms of hypocotyl elongation.

The power of this tool is its clear focus on the genome. Our transcriptome data reveal interesting information about the up- and down-regulation of gene expression, but it delivers no proof for the causality of the changes observed. An additional mutant analysis is needed to link the observed effects to the corresponding gene of interest. However, during our experiments, we observed that many mutants display severely reduced growth phenotypes (e.g. *dwf1, det2, slr-1*) leading to confounding factors in plant research. GWAS analysis focusses on small changes in the genome, allowing you to pinpoint the genes responsible for your phenotype without interfering with severe growth reductions. In that way, this GWAS approach has proven to be a powerful tool to investigate variations in the Root System Architecture of Arabidopsis (Rosas *et al.*, 2013; Lachowiec *et al.*, 2015; Kobayashi *et al.*, 2016; Satbhai *et al.*, 2017). As such, we postulate that a GWAS analysis is a valuable tool to investigate further the effect of coumarin on root growth.

However, one has to consider that the possibilities of GWAS analysis are also limited (Tam *et al.*, 2019). The approach is time-consuming, the multiple tests and experiments can be a burden. Moreover, a major limitation is the need to adopt a high level of significance to account for the multiple tests reducing the statistical power severely and therefore a conventional GWAS analysis is underpowered to detect all the heritability explained by SNPs (Tam *et al.*, 2019).

Summary

Coumarin, a bioactive compound steering plant development

Coumarin (2H-1-benzopyran-2-one) is a natural compound, derived from the phenylpropanoid pathway (PP) pathway, a large and well-known pathway leading to a high variety of compounds ranging from salicylic acid to monolignols. Ten different enzymatic steps of the backbone of the PP pathway converge the majority of carbon entering it via the aromatic amino acid phenylalanine to one of the monolignols (i.e. coumaryl, coniferyl, or sinapyl alcohol). These end products are the building blocks for the lignin polymer. Lignin is deposited in the secondary cell wall of plants, donating structural integrity and mechanical properties to it. It allows plants to (1) transport water and (2) to develop enlarged structures, i.e. to evolve from weeds to trees. Therefore, lignin and by extension the PP pathway has been considered a crucial evolutionary invention of plants to leave wetland environments and successfully colonize the land.

Coumarin is found in high concentrations in the Tonka bean and was already identified by A. Vogel in 1820. In 1860 its structure was unravelled and in 1868 Perkin showed the easy production of coumarin via the 'Perkin-reaction' allowing the production of coumarin in high quantities for a relatively cheap price. Chemically, coumarin is the simplest member of the *o*-hydroxycinnamic acid lactones, also known as the coumarins. They are a ubiquitous group of plant secondary metabolites, comprising of at least 700 different structures. Coumarin itself is a sweet-smelling plant substance responsible for the typical smell of freshly mown grass or young hay. Therefore, it was used as an additive in toothpaste, tobacco products, alcoholic beverages and as a flavour additive in food (mainly the French cuisine). Although proven to be 10 times less toxic than vitamin D, the potential convergence during digestion of coumarin to less healthy brothers (e.g. 7-hydroxycoumarin) put a ban on its use as a food additive. Today, it is still often used as an additive in cosmetics, and it gives the typical smell to the Fougière-type of perfumes.

Although the enzymatic steps of coumarin biosynthesis are not yet characterized, it is clear that coumarin is derived from cinnamic acid. Ortho-hydroxylation on the benzene ring structure, followed by cis-trans isomerisation and lactonization leads to the formation of coumarin. Its biosynthesis has been studied in detail between 1940 and 1960 as high concentrations of coumarin in sweet clover hay turned to the toxic dicoumarol when the hay was moulded. Dicoumarol is the cause of the bleeding syndrome in cattle as it avoided coagulation of the blood. Medicinal anticoagulants and rat poison are two inventions based on the knowledge gained with that finding. The research led to the discovery of *Melilotus officinalis* and *Melilotus alba* species that contained less coumarin, but even today, the biosynthesis of coumarin is not known. This is striking as the biosynthesis of higher coumarins (e.g. scopoletin and umbelliferone) is fully unravelled. The difficulties in detection coumarin via mass-spectrometry methods is probably the origin of this discrepancy.

Already in 1911, over fifty different plants were known to contain high concentrations of coumarin, illustrating its common presence in plants and the importance of the plant research performed. Coumarin was mainly seen as an allelochemical compound, since its rapid accumulation at infection sites and its proven role as phytoalexins. Coumarin is known to influence the rhizosphere by influencing the rhizobiome, germination and root growth, but coumarin is also known to affect shoot growth, hypocotyl-, epicotyl- and coleoptile-elongation, respiration, photosynthesis and even pollen tube elongation. The term 'coumarin' in literature is

often confusing as auteurs aim to indicate research to ‘their coumarin’, being a coumarin (e.g. scopoletin) and not the pure coumarin (2H-1-benzopyran-2-one). In this thesis, we used, as such, the term ‘coumarin’ for the pure compound, and we used the plural ‘coumarins’ to indicate the group.

Most research performed on investigating the effects of coumarin occurred some 50 to 60 years ago when the use of *Arabidopsis thaliana* as a model plant was not yet that common. Here, we illustrated the effects of coumarin on root growth and hypocotyl elongation of *Arabidopsis thaliana* and the data gained out of in-depth transcriptome analysis of Arabidopsis hypocotyls treated with coumarin for 30, 60 or 180 minutes.

Both in the root, as well in the hypocotyl, we showed that coumarin influenced auxin transport, although, interestingly, in an opposing manner. In the shoot coumarin induced auxin transport, by clear upregulation of PIN-FORMED genes, i.e. *PIN1*, *PIN3*, *PIN4* and *PIN7*. In the root we found, via translational reporter lines, that coumarin led to a reduction in the abundance of PIN1, PIN2 and PIN3 proteins, while we observed an increased abundance of AUXIN RESISTANT 1 (AUX1). Interestingly, we found that coumarin could restore the agravitropic response of *pin2* roots, probably a consequence of enhanced AUX1 presence as the latter is proven to overrule *pin2* mutations to restore gravitropism in the root. These data are in line with the findings of Lupini et al. (2014) illustrating the importance and need of AUX1 for coumarin to affect root growth. Moreover, the effect of coumarin is in line with historical findings, even dating back to 1952 claiming the interference of coumarin with auxin transport. Feeding experiments in 1972, 1978 and 1982 with radioactively labelled auxin and co-treatment with coumarin and auxin transport inhibitors, showed that coumarin indeed affects auxin transport. In line with earlier findings, we found that roots illustrate a bell-shaped response upon coumarin treatment: stimulating main root growth and lateral root formation on the lower concentrations while inhibiting both traits on the higher concentrations. Coumarin affects the early stages of root development with a clear inhibitory effect on meristem development. Coumarin treated seedlings show reduced meristem cell division, leading to a smaller root meristem and as such an affected development of the root system architecture. Via mutant analysis, we claimed the interference of SHORT HYPOCOTYL 2/INDOLE-3-ACETIC ACID INDUCIBLE 3 (SHY2/IAA3), which was confirmed in the transcriptome analysis, although performed on micro-dissected hypocotyls, by the clear increase in *SHY2* expression upon coumarin treatment. SHY2 is stimulated by cytokinins (via ARABIDOPSIS RESPONSE REGULATOR 1 (ARR1)), inhibiting, as such, auxin transport and auxin biosynthesis leading to reduced cell division in the meristem. Interestingly, coumarin induced acidification in the root tip, which supports the interplay with auxin. One would expect stimulation of cell elongation upon acidification based on the acid-growth-theory, we observed, however, the opposite. This adds to the current debate in the root research field where small auxin concentrations applied to the root lead to acidification of the apoplast and stimulated root growth, while higher concentrations of applied auxin lead to acidification and root growth inhibition. More research is needed to clarify the role of coumarin-induced acidification of the root and the phenotypes observed. We also observed that coumarin stimulates adventitious root formation and induces root hair formation and elongation and as such we can state that coumarin impacts the complete root system architecture

In the shoot, we observed a clear stimulatory effect of coumarin on cell elongation. In cotyledons, pavement cells were enlarged by 23% upon coumarin treatment while hypocotyls increased a 3-fold in length.

In cotyledons, we observed a decrease in cell number upon coumarin treatment. This indicates that the observed effect can be a consequence of compensation, or at least that coumarin affects both cell elongation as well as cell division. In the hypocotyl, however, we observed no difference in cell number of protruding cell files. Hence, the 3-fold increase in hypocotyl length is solely the consequence of cell elongation.

Coumarin induces a clear auxin response in the hypocotyl, observed via both microscopic analysis of the pDR5rev::GFP reporter lines as well as the transcriptional upregulation of numerous auxin reporter genes (*Aux/IAA* response genes, *HISTONE ACETYLTRANSFERASE 1 (HAT)* genes and *AUXIN UPREGULATED F_BOX PROTEIN (AUF1)*). In-depth analysis of the hypocotyl transcriptome upon coumarin treatment illustrated the upregulation of 23 *SMALL AUXIN UP RNA (SAUR)* genes after 30 minutes of coumarin treatment. The increased expression of numerous *SAUR* genes remained 3 hours after coumarin treatment, and the upregulation of *SAUR19* was also observed upon continuous treatment with coumarin for 3 or 5 days after germination. SAUR proteins are upregulated very fast upon auxin treatment and stimulate H^+-ATPase activity leading to acidification of the cell wall, within 15 minutes after auxin treatment (Fendrych et al. 2015). Remarkably, mutant analysis (both loss-of-function as well as gain-of-function) of H^+-ATPase genes and *SAUR19* overexpression lines illustrated that stimulation of acidification alone is not enough to stimulate cell elongation. As mentioned earlier, we observed a clear upregulation of auxin transport genes (*PIN1*, *PIN3*, *PIN4* and *PIN7*) and showed this response to be causal as the *pin1* mutant is less responsive towards coumarin in terms of hypocotyl elongation.

Ethylene plays a clear role in hypocotyl elongation, illustrated by the well-known triple response of etiolated seedlings treated with ethylene and its clear involvement in apical hook opening. In those phenotypes, ethylene is known to interfere with auxin transport. However, detailed pharmacological experiments and analysis of ethylene signalling mutants showed that ethylene plays no role during coumarin-induced hypocotyl elongation.

Both after continuous treatment with coumarin (for 3 DAG) as well as short treatment with coumarin (30 to 180 minutes) we observed a strong upregulation (> 5-fold) of the gibberellin acid biosynthesis gene *GIBBERELLIN-20-OXIDASE 1 (GA20OX1)*. Moreover, the transcriptome data revealed an additional upregulation of *GA3OX1*, indicating the involvement of GA biosynthesis during coumarin-induced hypocotyl elongation. However, mutant analysis of the *ga20ox1,2,3* mutant and loss-of-function DELLA mutants showed coumarin can still induce hypocotyl elongation illustrating that additional GA biosynthesis is not required for coumarin-induced hypocotyl elongation. In addition, our transcriptome data revealed a strong upregulation of *GA2OX8* and *GA2OX1*, involved in C19 and C20 catabolism of GA.

Our transcriptome data pinpointed the involvement of brassinosteroid (BR) signalling, as gene ontology enrichment revealed the upregulation of genes involved in BR signalling and steroid responses after 1 and 3 hours of coumarin treatment. We observed the clear upregulation of *BRASSINAZOLE-RESISTANT 1 (BZR1)*, an upregulation that persisted even after continuous treatment with coumarin in 3 DAG old seedlings. Moreover, mutant analysis of BR receptor, biosynthesis and signalling mutants showed complete inhibition of hypocotyl elongation upon coumarin treatment, illustrating their crucial role in coumarin-induced hypocotyl elongation.

Complementation studies whereby the BR biosynthesis mutant *DWARF 6* (*det2)* was co-treated with brassinolide and coumarin, revealed that BRs are needed but not *de novo* biosynthesis of it. In addition, analysis of *PHYTOCHROME INTERACTING FACTOR 4(pif4-2)* and *PHYTOCHROME-B (phyb-5)* mutants showed, respectively, a reduced and complete absence of response towards coumarin in terms of hypocotyl elongation. These data illustrate the involvement of light-signalling and photomorphogenesis during coumarin-induced hypocotyl elongation. In this thesis, however, we could not resolve how this light response is exactly involved. Gene ontology enrichment revealed the involvement of light-signalling and red and far-red responses, but further research is needed. We hypothesized that coumarin stimulates growth via the BZR1-PIF4 module that closely interacts with PHYB in many elongation phenotypes. The transcriptome data revealed the downstream BR response, illustrated by increased expression of (among others) *PACLOBUTRAZOL RESISTANCE 1 (PRE1), PRE5, PRE6* and *BR-ENHANCED EXPRESSION 1 (BEE1)*, followed by an upregulation of *XYLOGLUCAN:XYLOGLUCOSYL TRANSFERASE (XET)* genes involved in cell wall remodelling.

In conclusion, coumarin treatment leads to a clear auxin response, which besides the upregulation of numerous *Aux/IAA* elements and *HAT* genes, also stimulates a clear SAUR response. The latter, however, could not be linked to acidification of the apoplast yet. Next, auxin transport is stimulated and brassinosteroid signalling is enhanced. This is followed by upregulation of numerous BR response genes (e.g. *BEE1* and *PRE1,5,6*) leading to cell wall remodelling via XETs and, as such, hypocotyl elongation is induced.

Nederlandstalige samenvatting

Coumarine, een bioactieve component die plantontwikkeling aanstuurt.

Coumarine (2H-1-benzopyraan-2-on) is een natuurlijke component, afkomstig van de fenylpropanoid pathway, een goed gekende pathway die leidt tot een verscheidenheid aan stoffen variërend van salicylaat tot monolignolen. Tien verschillende enzymatische stappen van de fenylpropanoid pathway *ruggegraat* converteren de meerderheid aan binnengekomen koolstof via het aromatische aminozuur fenylalanine tot één van de monolignolen (d.i. coumaryl, coniferyl of sinapyl alcohol). Deze eindproducten zijn de bouwstenen voor lignine. Liginine wordt ingebouwd in de secondaire celwand van planten en zorgt zo voor structurele integriteit en mechanische eigenschappen van de celwand. Het laat planten toe om (1) water te transporteren en (2) grotere structuren te ontwikkelen (bv. bomen) Daarom wordt lignine en met uitbreiding de fenylpropanoid pathway, beschouwd als een cruciale evolutionaire stap bij planten om wetland omgevingen te kunnen verlaten en land succesvol te koloniseren.

Coumarine wordt in hoge concentraties gevonden in de Tonkaboon en werd reeds geïdentificeerd in 1820 door A. Vogel. De structuur werd ontleed in 1860 en in 1868 toonde Perkin aan dat coumarine op een eenvoudige manier kan geproduceerd worden via de 'Perkin-reactie', wat de relatief goedkope productie van coumarine toelaat in hoge concentraties. Chemisch is coumarine de eenvoudigste van de *o*-hydroxycinnamaat lactonen, beter gekend als coumarines. Deze zijn een alomtegenwoordige groep van secundaire plant metabolieten die minstens 700 verschillende structuren omvatten. Coumarine zelf is een zoet ruikende plant substantie verantwoordelijk voor de typische geur van vers gemaaid gras of jong hooi. Daarom ook dat het gebruikt werd als additief in tandpasta, tabaksproducten, alcoholische dranken en voedsel (als smaakadditief voornamelijk in de Franse keuken). Hoewel het bewezen is om 10 keer minder toxisch te zijn dan vitamine D, werd coumarine verboden als voedingsadditief omdat het tijdens de vertering mogelijks omgezet kan worden naar minder gezonde verbindingen zoals 7-hydroxycoumarine. Vandaag de dag wordt coumarine nog steeds vaak gebruikt als additief in cosmetische producten en geeft het de typische geur aan de Fougière parfums.

Hoewel het ontbreken van de karakteriscatie van de enzymatische stappen van coumarine biosynthese, is het toch duidelijk dat coumarine een derivaat is van cinnamaat. Ortho-hydroxylatie op de benzeenring structuur, gevolgd door *cis-trans* isomerisatie en lactonisatie leiden tot de vorming van coumarine. De biosynthese van coumarine werd in detail bestudeerd tussen 1940 en 1960 wegens de omzetting van coumarin in beschimeld hooi van de honingklaver tot het giftige dicoumarol, en men dus klaversoorten wou ontwikkelen met lagere coumarine concentraties. Dicoumarol is de oorzaak van het doodbloden van koeien gezien het bloedstolling verhinderd. Medicinale anticoagulanten en rattenvergif zijn twee uitvindingen gebaseerd op deze verkregen kennis. Onderzoek leidde naar de ontdekking van *Melilotus officinalis* en *Melilotus alba* soorten die minder coumarine bevatten. Maar tot de dag van vandaag is de biosynthese van coumarine niet gekend. Dit is opvallend gezien de biosynthese van hogere coumarines zoals bijvoorbeeld scopoletine en umbelliferone, volledig ontrafeld is. De moeilijkheid om coumarine te detecteren via massa-spectrometrische methodes ligt waarschijnlijk aan de basis van deze discrepantie.

Reeds in 1911 waren meer dan vijftig verschillende planten gekend die hoge concentraties van coumarine bevatten, wat de alom vertegenwoordiging in planten en de het belang van het gevoerde

plantonderzoek aantoont. Coumarine werd voornamelijk beschouwd als een allelochemische component, gezien de snelle accumulatie van coumarine op de plaats van infectie en zijn bewezen rol als fytoalexine. Het is gekend dat coumarine zijn invloed uitoefent op de rhizosfeer door zijn effect op het rhizobioom, kieming en wortelgroei, maar het is ook geweten van coumarine dat het een effect heeft op scheutgroei, hypocotyl-, epicotyl- en coleoptielelongatie, respiratie, fotosynthese en zelfs pollenbuiselongatie. In de literatuur wordt de term 'coumarine' vaak verward gezien auteurs spreken over 'hun coumarine', zijnde een coumarine zoals bijvoorbeeld scopoletine en niet het pure coumarine (2H-1-benzopyraan-2-on). In deze thesis wordt de term 'coumarine' gebruikt voor de zuivere component en owrdt de meervoudsvorm 'coumarines' gebruikt als groepsaanduiding.

Het meeste onderzoek gedaan naar de effecten van coumarine gebeurde 50 tot 60 jaar geleden wanneer het gebruik van *Arabidopsis thaliana* als modelsysteem nog niet zo gangbaar was. Hier illustreren we het effect van coumarine op wortelgroei en hypocotyl elongatie van *Arabidopsis thaliana* en de data verkregen uit een diepgaande transcriptoom analyse van Arabidopsis hypocotylen behandeld met coumarine gedurende 30, 60 of 180 minuten.

Zowel in de wortel als in de hypocotyl konden we aantonen dat coumarine auxine transport beinvloedt, echter, op een tegenovergestelde wijze. In de scheut induceert coumarine auxine transport, aangetoond door de duidelijke opregulatie van PIN-FORMED genen, d.i. *PIN1*, *PIN3*, *PIN4* en *PIN7.* Via translationele reporter lijnen vonden we in de wortel dat coumarine leidt tot reductie in de aanwezigheid van PIN1, PIN2 en PIN3 eiwitten, terwijl we een toename observeerden in de hoeveelheid van AUXIN RESISTANT 1 (AUX1). Interessant is ook de bevinding dat coumarine de agravitrope respons van *pin2* wortels kan herstellen, waarschijnlijk als een gevolg van de toename in AUX1, gezien het bewezen is dat deze laatste *pin2* mutaties overruled om gravitropie in de wortel te herstellen. Deze data zijn in lijn met de bevindingen van Lupini et al. (2014), wat het belang en de nood aantoont van AUX1 voor coumarine om wortelgroei te beinvloeden. Bovendien ligt het effect van coumarine in lijn met historische bevindingen, die zelfs teruggaan tot 1952 waar men de interferentie van coumarine met auxine transport aanhaalde. Experimenten in 1972, 1978 en 1982 illustreerden via het toedienen van radioactief gelabeld auxine en simultane behandeling met coumarine en auxine transport inhibitoren, dat coumarine auxin transport beinvloedt. In lijn met eerdere bevindingen vonden we dat wortels een Gauss-klok respons vertonen wanneer coumarine toegediend wordt: in lagere concentraties stimuleert coumarine de groei van de hoofdwortel en laterale wortel vorming, terwijl beiden geïnhibeerd worden in hogere concentraties. Coumarine heeft een effect op de vroege stadia van wortelontwikkeling door het duidelijke inhibitorische effect op meristeemontwikkeling. Zaailingen behandeld met coumarine tonen een verlaagde meristematische celdeling, leidend tot een smaller wortelmeristeem en coumarine beinvloedt zo ook de ontwikkeling van het wortelsysteem. Via mutantanalyse claimen we de tussenkomst van SHORT HYPOCOTYL 2/INDOLE-3-ACETIC ACID INDUCIBLE 3 (SHY2/IAA3), wat bevestigd werd in het transcriptoom, hoewel uitgevoerd op microgedissecteerde hypocotyen, door de duidelijke toename in *SHY2* expressie bij coumarinebehandeling. SHY2 wordt gestimuleerd door cytokinines (via ARABIDOPSIS RESPONSE REGULATOR 1 (ARR1)) en zal auxine transport en auxine biosynthese inhiberen, leidend tot verminderde celdeling in het meristeem. Interessant is de coumarine geïnduceerde verzuring in de worteltip, wat opnieuw de interplay met auxine aantoont. Op basis van de zuurgroeihypothese verwacht men stimulatie van celelongatie wanneer verzuring

optreedt. Wij observeerden echter het tegenovergestelde. Dit draagt bij tot het huidige debat in het wortel onderzoeksveld, waar lage auxine concentraties toevoegen aan de wortel leidt tot verzuring van de apoplast en wortelgroei stimuleert, terwijl hogere contraties van toegevoegd auxine leiden tot verzuring en wortelgroei-inhibitie. Meer onderzoek is nodig om deze rol van coumarine geïnduceerde verzuring van de wortel en de geobserveerde fenotypes te verduidelijken. Ook observeerden we dat coumarine bijwortelvorming stimuleert en de inductie en elongatie van wortelharen.

In de scheut observeerden we een duidelijk stimulerend effect van coumarine op celelongatie. In cotyledonen waren de pavement cellen 23% groter bij coumarine behandeling terwijl de hypocotylen 3 keer langer werden. In cotyledonen observeerden we bovendien een afname in hoeveelheid cellen bij comarine behandeling. Dit toont aan dat het geobserveerde effect een gevolg kan zijn van compensatie, of tenminste dat coumarine zowel celelongatie als celdeling beinvloedt. Echter, in de hypocotyl observeerden we geen verschil in hoeveelheid cellen van uitstekende celrijen. Hieruit besluiten we dan de 3-voudige toename in hypocotyl lengte enkel het gevolg is van celelongatie.

Coumarine induceert een duidelijke auxinerespons in de hypocotyl, dewelke we observeerden via zowel microscopische analyse van pDR5rev::GFP reporter lijnen als de transcriptionele opregulatie van talrijke auxine reportergenen (*Aux/IAA* respons genen, *HISTONE ACETYLTRANSFERASE 1 (HAT)* genen en *AUXIN UPREGULATED F_BOX PROTEIN (AUF1)*). Diepgaande analyse van het hypocotyl transcriptoom bij coumarine behandeling toont aan dat 23 *SMALL AUXIN UP RNA (SAUR)* genen opgereguleerd worden na 30 minuten behandeling. Deze verhoogde expressie van talrijke *SAUR* genen bleven we observeren 3 uur na behandeling met coumarine en de opregulatie van *SAUR19* werd zelfs waargenomen bij continue behandeling met coumarine voor 3 of 5 dagen na kieming. SAUR eiwitten worden snel opgereguleerd bij auxine behandeling en stimuleren H^+-ATPase activiteit wat celwandverzuring veroorzaakt binnen de 15 minuten na auxinebehandeling. Opmerkelijk is dat de mutant analyse (zowel loss-of-function als gain-of-function) van H^+-ATPase genen en *SAUR19* overexpressie lijnen illustreren dat stimulatie van verzuring alleen niet genoeg is om celelongatie te stimuleren. We observeerden, zoals eerder vermeld, een duidelijke opregulatie van auxine transport genen (*PIN1*, *PIN3*, *PIN4* en *PIN7*) en toonden we aan dat deze respons causaal is gezien de *pin1* mutant minder responsief is voor coumarine wat betreft hypocotyl elongatie.

Ethyleen speelt een duidelijke rol in hypocotyl elongatie, zoals geïllustreerd door de goed gekende triple respons van geëtioleerde zaailingen gehandeld met ethyleen en zijn duidelijke betrokkenheid in apicale haak opening. Het is geweten dat ethyleen (en deze fenotypes) interfereren met auxine transport. Hoewel gedetaileerde farmacologische experimenten en analyse van ethyleen signalisatie mutanten toonden dat ethyleen geen rol speelt bij coumarine geïnduceerde hypocotyl elonogatie.

Zowel na lange behandeling met coumarine (3 DAG) als korte behandeling met coumarine (30 tot 180 minuten), observeerden we een sterke opregulatie (> 5-voud) van het gibberelline zuur biosynthese gen *GIBBERELLIN-20-OXIDASE 1 (GA20OX1)*. Bovendien toonden de transcriptoom data een additionele opregulatie van *GA3OX1* aan, wat wijst op de betrokkenheid van GA biosynthese tijdens coumarine geïnduceerde hypocotyl elongatie. Echter, mutant analyse van de *ga20ox1,2,3* mutant en analyse van paclobutrazol (een inhibitor van

GA biosynthese) behandelde zaailingen, toonden aan dat coumarine nog steeds hypocotyl elongatie kan induceren, wat wijst op het feit dat additionele GA biosynthese niet nodig is voor coumarine geïnduceerde hypocotyl elongatie. Daarenboven toonden onze transcriptoom data de sterke opreguleratie aan van *GA2OX8* en *GA2OX1*, betrokken in C19 en C20 katabolisme van GA.

Onze transcriptoom data illustreren de betrokkenheid van brassinosteroïde (BR) signalisatie, gezien genontologische verrijkingsstudies de opregulatie van genen betrokken in de BR signalisatie en steroïde responsen aantonen na 1 en 3 uur behandeling met coumarine. We observeerden een duidelijke opregulatie van *BRASSINAZOLE-RESISTANT 1 (BZR1)*, een transcript dat opgereguleerd bleef zelfs na continue behandeling met coumarine in 3 DAG oude zaailingen. Bovendien toonden mutant analyse van BR receptor, biosynthese en signalisatie mutanten de complete inhibitie van hypocotyl elongatie aan bij coumarine behandeling. Dit is een goede illustratie van hun cruciale belang in coumarine geïnduceerde hypocotyl elongatie. Complementatiestudies waarbij de BR biosynthese mutant *DWARF 6* (*det2)* samen behandeld werd met brassinolide en coumarine, toonde aan dat BRs nodig zijn maar *de novo* biosynthese niet. Daarnaast gaf analyse van *PHYTOCHROME INTERACTING FACTOR 4 (pif4-2)* en *PHYTOCHROME-B (phyb-5)* mutanten ons het inzicht dat er respectivelijk een gereduceerde en complete afwezigheid van respons is op vlak van hypocotyl elongatie. Deze data illustreren de betrokkenheid van licht signalisatie en fotomorfogenese tijdens coumarine geïnduceerde hypocotyl elongatie. In deze thesis konden we echter niet volledig verklaren hoe deze lichtrespons exact betrokken is. Genontologische verrijkingsstudies wezen op de betrokkenheid van lichtsignalisatie en rode en ver-rode responsen, maar verder onderzoek is nodig. Onze hypothese is dat coumarine groei stimuleert via de BZR1-PIF4 module die nauw interageert met PHYB in verschillende elongatie fenotypes. De transcriptoom data onderbouwen de downstream BR respons, wat aangetoond wordt door onder andere de hogere expressie van *PACLOBUTRAZOL RESISTANCE 1 (PRE1), PRE5, PRE6* en *BR-ENHANCED EXPRESSION 1 (BEE1)*, gevolgd door een opregulatie van *XYLOGLUCAN:XYLOGLUCOSYL TRANSFERASE (XET)* genen betrokken bij celwand remodellering.

Als besluit kunnen we stellen dat coumarine behandeling leidt tot een duidelijke auxine respons, dewelke naast de opregulatie van talrijke *Aux/IAA* elementen en *HAT* genen, ook een duidelijke SAUR respons stimuleert. Deze laatste kon echter nog niet gelinkt worden met verzuring van de apoplast. Vervolgens is auxine transport gestimuleerd en brassinosteroïde signalisatie versterkt. Dit wordt gevolgd door de opregulatie van talrijke BR respons genen (vb. BEE1 en PRE1,5,6), wat leidt tot celwand remodellering via XETs en op deze manier hypocotyl elongatie induceert.

Addendum

Table 1: Significant differential expression of genes after 30 minutes of coumarin treatment

Gene locus	Fold change	FDR	Gene Symbol	Explanation
AT5G02865	18.75	0.00300	NA	Long noncoding RNA
AT3G03830	9.41	0.00395	SAUR28	SMALL AUXIN UP RNA gene
AT1G29490	7.74	0.01772	SAUR68	SMALL AUXIN UP RNA gene
AT1G29460	6.99	0.01338	SAUR65	SMALL AUXIN UP RNA gene
AT3G03850	6.95	0.01841	SAUR26	SMALL AUXIN UP RNA gene
AT4G36110	6.71	0.00069	SAUR9	SMALL AUXIN UP RNA gene
AT1G29440	6.47	0.00069	SAUR63	SMALL AUXIN UP RNA gene
AT5G18010	6.27	0.01349	SAUR19	SMALL AUXIN UP RNA gene
AT5G18030	6.16	0.03061	SAUR21	SMALL AUXIN UP RNA gene
AT1G29500	5.92	0.01264	SAUR66	SMALL AUXIN UP RNA gene
AT1G29430	5.65	0.02148	SAUR62	SMALL AUXIN UP RNA gene
AT1G29420	5.54	0.03589	SAUR61	SMALL AUXIN UP RNA gene
AT3G03840	5.51	0.00323	SAUR27	SMALL AUXIN UP RNA gene
AT5G18060	5.51	0.04823	SAUR23	SMALL AUXIN UP RNA gene
AT4G38850	5.40	0.00428	SAUR15	SMALL AUXIN UP RNA gene
AT1G29450	5.35	0.04823	SAUR64	SMALL AUXIN UP RNA gene
AT1G15580	5.32	0.00182	AUX2-27	AUXIN-INDUCIBLE 2-27, also known as INDOLE-3-ACETIC ACID INDUCIBLE 5 (IAA-5)
AT5G18080	5.11	0.03589	SAUR24	SMALL AUXIN UP RNA gene
AT1G29510	4.52	0.02181	SAUR67	SMALL AUXIN UP RNA gene
AT3G03820	4.47	0.03866	SAUR29	SMALL AUXIN UP RNA gene
AT5G66580	4.30	0.02796	NA	Protein coding, but unknown
AT3G28857	3.66	0.02786	PRE5	Encodes a atypical member of the bHLH (basic helix-loop-helix) family transcriptional factors.
AT4G34770	3.49	0.03310	SAUR1	SMALL AUXIN UP RNA gene
AT4G14819	3.43	0.00428	NA	Protein coding, but unknown
AT4G38825	3.42	0.01841	SAUR13	SMALL AUXIN UP RNA gene
AT5G47370	3.26	0.01584	HAT2	Homeobox-leucine zipper genes induced by auxin, but not by other phytohormones. Plays opposite roles in the shoot and root tissues in regulating auxin-mediated morphogenesis.

AT2G30040	3.25	0.03332	MAPKKK14	MITOGEN-ACTIVATED PROTEIN KINASE KINASE KINASE 14, member of MEKK subfamily.
AT4G38840	3.24	0.01349	SAUR14	SMALL AUXIN UP RNA gene
AT2G39370	3.13	0.00357	MAKR4	MEMBRANE-ASSOCIATED KINASE REGULATOR 4. Encodes a member of the MAKR gene family, that have putative kinase interacting motifs and membrane localization signals.
AT5G52900	3.08	0.00175	MAKR6	NA
AT4G34760	3.03	0.00333	SAUR50	SMALL AUXIN UP RNA gene
AT1G04240	2.94	0.00083	IAA3	SHY2/IAA3 regulates multiple auxin responses in roots. It is induced rapidly by IAA, and has been shown to be phosphorylated by oat phytochrome A in vitro.
AT1G78100	2.90	0.01201	AUF1	AUXIN UP-REGULATED F-BOX PROTEIN 1,
AT3G23635	2.83	0.00652	RTFL13	ROTUNDIFOLIA LIKE 13
AT3G25717	2.82	0.01338	DVL6	ROTUNDIFOLIA LIKE 16
AT1G30100	2.81	0.03910	NCED5	Encodes 9-cis-epoxycarotenoid dioxygenase, a key enzyme in the biosynthesis of abscisic acid. The expression of this gene increases during the first 6h of imbibition.
AT2G42430	2.80	0.01043	ASL18	ASYMMETRIC LEAVES2-LIKE 18, a LOB-domain protein gene This gene contains one auxin-responsive element (AuxRE) that regulates LR formation.
AT2G14960	2.77	0.00353	GH3.1	Encodes a protein similar to IAA-amido synthases. Lines carrying an insertion in this gene are hypersensitive to auxin.
AT1G15550	2.66	0.00069	GA3OX1	Involved in later steps of the gibberellic acid biosynthetic pathway. Activated by AGAMOUS in a cal-1, ap1-1 background. Deletion of 208 bp from -1016 to -809 (Δ-808) resulted in loss of GA-negative feedback (this sequence, which contains a 43-bp sequence GNFEI, was shown to be sufficient for GA-negative feedback).
AT4G25420	2.57	0.01436	GIBBERELLIN 20-OXIDASE 1	Encodes gibberellin 20-oxidase that is involved in the later steps of the gibberellin biosynthetic pathway. Regulated by a circadian clock. Weak expression response to far red light.
AT5G41400	2.56	0.02704	NA	NA
AT4G03140	2.55	0.02567	NA	NA
AT1G26945	2.53	0.04823	KDR	Encodes a basic helix-loop-helix (bHLH) protein involved in blue/far-red light signaling. Physically interacts with HFR1 and negatively regulates its activity.
AT2G23170	2.52	0.00437	GH3.3	Encodes an IAA-amido synthase that conjugates Asp and other amino acids to auxin in vitro.
AT2G28350	2.44	0.00069	ARF10	Involved in root cap cell differentiation.
AT5G65340	2.43	0.00203	NA	NA
AT4G21200	2.27	0.04188	GA2OX8	Encodes a protein with gibberellin 2-oxidase activity which acts specifically on C-20 gibberellins.

AT2G26710	2.21	0.02704	BAS1	Encodes a member of the cytochrome p450 family that serves as a control point between multiple photoreceptor systems and brassinosteroid signal transduction. Involved in brassinolide metabolism. Mediates response to a variety of light signals including hypocotyl elongation and cotyledon expansion.
AT1G29465	2.16	0.04276	NA	NA
AT1G65920	2.11	0.00149	NA	Regulator of chromosome condensation (RCC1) family with FYVE zinc finger domain-containing protein.
AT3G55720	2.08	0.00637	NA	BOUNDARY OF ROP DOMAIN7
AT3G14370	2.07	0.00746	WAG2	The WAG2 and its homolog, WAG1 each encodes protein-serine/threonine kinase that are nearly 70% identical to PsPK3 protein. All three together with CsPK3 belong to PsPK3-type kinases. At the N-terminus, all four possess a serine/threonine-rich domain. They are closely related to Arabidopsis kinases PINOID. wag1/wag2 double mutants exhibit a pronounced wavy root phenotype when grown vertically on agar plates (while wild-type plants develop wavy roots only on plates inclined to angles less than 90 degrees), indicating an overlapping role for WAG1 and WAG2 as suppressors of root waving. Simultaneous disruption of PID(AT2G34650) and its 3 closest homologs (PID2/AT2G26700, WAG1/AT1G53700, and WAG2/AT3G14370) abolishes the formation of cotyledons.
AT5G18070	2.06	0.00083	DRT101	DNA-DAMAGE-REPAIR/TOLERATION 101 is a novel protein involved in DNA repair from UV damage. Isolated by functional complementation of E. coli UV-sensitive mutants (UVR genes).
AT3G15540	2.01	0.03243	IAA19	Primary auxin-responsive gene. Involved in the regulation stamen filaments development.
AT4G37790	2.00	0.00149	HAT22	Encodes homeobox protein HAT22, member of the HD-Zip II family.
AT2G36220	2.00	0.00361	NA	NA
AT5G43700	1.99	0.00741	AUX2-11	IAA4, Auxin inducible protein similar to transcription factors.
AT1G53163	1.98	0.02366	NA	NA
AT1G24130	1.94	0.04064	NA	Transducin/WD40 repeat-like superfamily protein
AT3G60630	1.90	0.00003	HAM2	NA
AT1G18400	1.83	0.01341	BEE1	BR ENHANCED EXPRESSION 1 encodes the brassinosteroid signaling component BEE1, that positively modulates the shade avoidance syndrome in Arabidopsis seedlings.
AT3G28420	1.83	0.00652	NA	Putative membrane lipoprotein.
AT4G37390	1.82	0.00148	AUR3	Encodes an IAA-amido synthase that conjugates Asp and other amino acids to auxin in vitro. Lines carrying insertions in this gene are hypersensitive to auxin. May function as a negative component in auxin signaling by regulating auxin activity.
AT4G17460	1.79	0.03497	HAT1	Encodes homeobox protein HAT1.
AT1G63840	1.79	0.00175	NA	NA
AT4G09890	1.78	0.00353	NA	NA

AT5G15580	1.74	0.00428	LNG1	Encodes LONGIFOLIA1 (LNG1). Regulates leaf morphology by promoting cell expansion in the leaf-length direction. The LNG1 homologue LNG2 (At3g02170) has similar function.
AT1G51170	1.73	0.01043	AGC2-3	NA
AT5G64770	1.71	0.01694	CLEL	Encodes a root meristem growth factor (RGF). Belongs to a family of functionally redundant homologous peptides that are secreted, tyrosine-sulfated, and expressed mainly in the stem cell area and the innermost layer of central columella cells. RGFs are required for maintenance of the root stem cell niche and transit amplifying cell proliferation.
AT2G34650	1.68	0.00428	ABR	Encodes a protein serine/threonine kinase that may act as a positive regulator of cellular auxin efflux, as a a binary switch for PIN polarity, and as a negative regulator of auxin signaling. Recessive mutants exhibit similar phenotypes as pin-formed mutants in flowers and inflorescence but distinct phenotypes in cotyledons and leaves. Expressed in the vascular tissue proximal to root and shoot meristems, shoot apex, and embryos. Expression is induced by auxin. Overexpression of the gene results in phenotypes in the root and shoot similar to those found in auxin-insensitive mutants. The protein physically interacts with TCH3 (TOUCH3) and PID-BINDING PROTEIN 1 (PBP1), a previously uncharacterized protein containing putative EF-hand calcium-binding motifs. Acts together with ENP (ENHANCER OF PINOID) to instruct precursor cells to elaborate cotyledons in the transition stage embryo. Interacts with PDK1. PID autophosphorylation is required for the ability of PID to phosphorylate an exogenous substrate. PID activation loop is required for PDK1-dependent PID phosphorylation and requires the PIF domain. Negative regulator of root hair growth. PID kinase activity is critical for the inhibition of root hair growth and for maintaining the proper subcellular localization of PID.
AT3G60390	1.67	0.00861	HAT3	Encodes homeobox protein HAT3.
AT4G09970	1.66	0.00621	NA	NA
AT3G63440	1.66	0.00361	ATCKX6	This gene used to be called AtCKX7. It encodes a protein whose sequence is similar to cytokinin oxidase/dehydrogenase, which catalyzes the degradation of cytokinins.
AT1G26960	1.58	0.00568	AtHB23	Encodes a homeodomain leucine zipper class I (HD-Zip I) protein.
AT1G21050	1.57	0.01908	NA	NA
AT3G61460	1.55	0.01492	BRH1	Encodes a novel ring finger protein and forms an N-terminal hydrophobic domain and a C-terminal RING-H2 signature. Expression is down regulated by brassinolide.
AT4G28640	1.52	0.01772	IAA11	Auxin induced gene, IAA11 (IAA11).
AT2G41170	1.50	0.04064	NA	NA
AT5G43190	1.49	0.04978	NA	NA
AT1G54200	1.48	0.01197	NA	NA
AT1G67880	1.47	0.01178	NA	NA
AT3G17090	1.42	0.00637	NA	NA
AT1G67340	1.38	0.01584	NA	NA
AT1G36370	0.73	0.03628	SHM7	Encodes a putative serine hydroxymethyltransferase.

AT3G22970	0.71	0.01772	NA	NA
AT1G62180	0.71	0.00361	APR2	Encodes a adenosine 5'-phosphosulfate reductase, involved in sulfate assimilation. Is a major effect locus for natural variation of shoot sulfate content in Arabidopsis.
AT5G57710	0.70	0.02247	SMAX1	SMAX1 (SUPPRESSOR OF MAX2 1) is a member of an eight-gene family in Arabidopsis that has weak similarity to AtHSP101, a ClpB chaperonin required for thermotolerance. SMAX1 is an important component of KAR/SL signaling during seed germination and seedling growth, but is not necessary for all MAX2-dependent responses. The mRNA is cell-to-cell mobile.
AT3G63210	0.69	0.04823	MARD1	Encodes a novel zinc-finger protein with a proline-rich N-terminus, identical to senescence-associated protein SAG102
AT1G78170	0.67	0.00741	NA	NA
AT1G79160	0.65	0.01117	NA	NA
AT4G21990	0.64	0.02181	APR3	*APS REDUCTASE 3* encodes a protein disulfide isomerase-like (PDIL) protein, a member of a multigene family within the thioredoxin (TRX) superfamily. This protein also belongs to the adenosine 5'-phosphosulfate reductase-like (APRL) group.
AT2G29670	0.63	0.00361	NA	NA
AT1G74940	0.56	0.01201	NA	NA
AT1G04770	0.45	0.00087	NA	SULFUR DEFICIENCY INDUCED 2, SDI2 is a member of a small family of TPR proteins in Arabidopsis. Like SDI1 it is induced by low sulfer and appears to play a role in negative regulation of glucosinolate biosynthesis.
AT5G24660	0.43	0.00652	LSU2	NA
AT3G49580	0.27	0.00175	LSU1	NA
AT3G49570	0.21	0.00203	LSU3	NA

Table 2: Significant differential expression of genes after 60 minutes of coumarin treatment

Gene locus	Fold change	FDR	Gene Symbol	Explanation
AT4G13790	16.83	0.01321	SAUR25	NA
AT5G02865	14.93	0.00211	NA	NA
AT1G15580	12.90	0.00015	ATAUX2-27	auxin induced protein
AT3G58190	12.28	0.00581	ASL16	This gene contains two auxin-responsive element (AuxRE).
AT4G21200	10.14	0.00000	ATGA2OX8	Encodes a protein with gibberellin 2-oxidase activity which acts specifically on C-20 gibberellins.
AT1G52830	9.99	0.00009	IAA6	An extragenic dominant suppressor of the hy2 mutant phenotype. Also exhibits aspects of constitutive photomorphogenetic phenotype in the absence of hy2. Mutants have dominant leaf curling phenotype shortened hypocotyls and reduced apical hook. Induced by indole-3-acetic acid.
AT5G65800	9.31	0.00068	ACS5	1-aminocyclopropane-1-carboxylate synthase (ACS) is encoded by a multigene family consisting of at least five members whose expression is induced by hormones, developmental signals, and protein synthesis inhibition.
AT1G29490	8.68	0.00143	SAUR68	NA
AT2G23170	7.89	0.00000	GH3.3	encodes an IAA-amido synthase that conjugates Asp and other amino acids to auxin in vitro.
AT4G03140	7.19	0.00005	NA	NA
AT3G03830	6.92	0.00230	SAUR28	NA
AT3G28857	6.45	0.00110	PRE5	NA
AT4G36110	6.29	0.00010	SAUR9	NA
AT2G22810	6.28	0.00946	ACC4	key regulatory enzyme in the biosynthesis of the plant hormone ethylene. ACS4 is specifically induced by indoleacetic acid (IAA).
AT5G18010	6.17	0.00277	SAUR19	NA
AT4G38850	6.10	0.00067	ATSAUR15	mRNA is rapidly induced by auxin and is very short-lived. Has been used as a reporter gene in studying auxin mutants.
AT5G18050	6.02	0.01088	SAUR22	NA
AT1G09350	5.77	0.00954	AtGolS3	NA
AT2G39370	5.75	0.00003	MAKR4	NA
AT2G18010	5.71	0.01848	SAUR10	NA
AT5G05220	5.70	0.03238	NA	NA
AT5G18060	5.69	0.00964	SAUR23	NA

AT4G21745	5.69	0.00447	NA	NA
AT5G18030	5.66	0.00890	NA	NA
AT1G29460	5.54	0.00668	SAUR65	NA
AT3G03850	5.53	0.00890	SAUR26	NA
AT3G60650	5.53	0.00034	NA	NA
AT5G18080	5.37	0.00673	SAUR24	NA
AT5G26930	5.36	0.00378	GATA23	Encodes a member of the GATA factor family of zinc finger transcription factors.
AT3G24255	5.32	0.03486	NA	NA
AT4G32810	5.29	0.00090	ATCCD8	Encodes a protein with similarity to carotenoid cleaving deoxygenases, the enzymes that cleave beta-carotene. Involved in the production of a graft transmissable signal to suppress axillary branching. Protein is localized to chloroplast stroma and expressed primarily in root tip. Mutants in the gene exhibit increased shoot branching, and light-dependent defects in hook opening and hypocotyl/root elongation. Only upregulated by auxin in the root and hypocotyl, and this is not required for the inhibition of shoot branching.
AT1G29430	5.28	0.00573	SAUR62	NA
AT1G29420	5.26	0.00990	SAUR61	NA
AT3G15540	5.23	0.00002	IAA19	Primary auxin-responsive gene. Involved in the regulation stamen filaments development.
AT2G42440	5.16	0.03149	ASL15	NA
AT1G26945	5.13	0.00039	KDR	Encodes a basic helix-loop-helix (bHLH) protein involved in blue/far-red light signaling. Physically interacts with HFR1 and negatively regulates its activity.
AT1G14182	4.99	0.03556	NA	NA
AT5G18020	4.98	0.01857	SAUR20	NA
AT1G29450	4.97	0.01399	SAUR64	NA
AT1G10550	4.87	0.00089	XET	Encodes a membrane-localized protein that is predicted to function during cell wall modification.Overexpression of XTH33 results in abnormal cell morphology. It's expression is under epigenetic control by ATX1.
AT1G29440	4.85	0.00024	SAUR63	NA
AT1G29500	4.85	0.00555	SAUR66	NA
AT5G47370	4.83	0.00065	HAT2	homeobox-leucine zipper genes induced by auxin, but not by other phytohormones. Plays opposite roles in the shoot and root tissues in regulating auxin-mediated morphogenesis.
AT1G35140	4.75	0.00232	EXL1	At1g35140 (At1g35140/T32G9_32) mRNA, complete cds

AT4G25420	4.72	0.00010	AT2301	Encodes gibberellin 20-oxidase that is involved in the later steps of the gibberellin biosynthetic pathway. Regulated by a circadian clock. Weak expression response to far red light.
AT5G66580	4.71	0.00522	NA	NA
AT5G25190	4.67	0.00000	ESE3	encodes a member of the ERF (ethylene response factor) subfamily B-6 of ERF/AP2 transcription factor family. The protein contains one AP2 domain. There are 12 members in this subfamily including RAP2.11.
AT4G24275	4.53	0.00017	NA	Identified as a screen for stress-responsive genes.
AT5G14895	4.52	0.03907	NA	NA
AT3G03840	4.47	0.00118	SAUR27	NA
AT2G14960	4.36	0.00005	GH3.1	encodes a protein similar to IAA-amido synthases. Lines carrying an insertion in this gene are hypersensitive to auxin.
AT4G34419	4.36	0.02377	NA	NA
AT2G22460	4.35	0.02123	NA	NA
AT5G56970	4.27	0.01336	ATCKX3	It encodes a protein whose sequence is similar to cytokinin oxidase/dehydrogenase, which catalyzes the degradation of cytokinins.
AT4G14560	4.27	0.01025	AXR5	auxin (indole-3-acetic acid) induced gene (IAA1) encoding a short-lived nuclear-localized transcriptional regulator protein.
AT5G02760	4.22	0.00137	APD7	NA
AT3G03820	4.21	0.01035	SAUR29	NA
AT5G52900	4.18	0.00005	MAKR6	NA
AT5G39860	4.17	0.01772	BHLH136	Encodes PRE1 (PACLOBUTRAZOL RESISTANCE1). PRE1 and IBH1 form a pair of antagonistic HLH/bHLH transcription factors that function downstream of BZR1 to mediate brassinosteroid regulation of cell elongation. BNQ1 is directly and negatively regulated by AP3 and PI in petals.Required for appropriate regulation of flowering time.
AT3G45960	4.16	0.00370	ATEXLA3	member of EXPANSIN-LIKE. Naming convention from the Expansin Working Group (Kende et al, 2004. Plant Mol Bio)
AT1G04240	4.12	0.00002	IAA3	SHY2/IAA3 regulates multiple auxin responses in roots. It is induced rapidly by IAA, and has been shown to be phosphorylated by oat phytochrome A in vitro.
AT4G30280	4.08	0.00257	ATXTH18	Encodes a xyloglucan endotransglucosylase/hydrolase with only only the endotransglucosylase (XET; EC 2.4.1.207) activity towards xyloglucan and non-detectable endohydrolytic (XEH; EC 3.2.1.151) activity. Expressed in the mature or basal regions of both the main and lateral roots, but not in the tip of these roots where cell division occurs.

AT3G03660	4.05	0.00094	WOX11	Encodes a WUSCHEL-related homeobox gene family member with 65 amino acids in its homeodomain. Proteins in this family contain a sequence of eight residues (TLPLFPMH) downstream of the homeodomain called the WUS box.
AT5G24110	4.01	0.03232	ATWRKY30	member of WRKY Transcription Factor; Group III
AT2G10605	3.96	0.02401	NA	NA
AT4G14819	3.90	0.00078	NA	NA
AT4G34770	3.84	0.00329	SAUR1	NA
AT1G76610	3.84	0.00009	NA	NA
AT5G06760	3.83	0.02285	AtLEA4-5	Encodes LEA4-5, a member of the Late Embryogenesis Abundant (LEA) proteins which typically accumulate in response to low water availability conditions imposed during development or by the environment. Most of thediverse set of LEA proteins can be grouped according to properties such as high hydrophilicity and high content of glycine or other small amino acids in what has been termed hydrophilins. LEA4-5 protects enzyme activities from the adverse effects induced by freeze-thaw cycles in vitro.
AT5G57760	3.78	0.02718	NA	NA
AT5G50130	3.72	0.00006	NA	NA
AT1G29510	3.70	0.01028	SAUR67	NA
AT2G42430	3.68	0.00056	ASL18	LOB-domain protein gene LBD16. This gene contains one auxin-responsive element (AuxRE).
AT1G53163	3.63	0.00010	NA	NA
AT3G23030	3.56	0.01422	IAA2	auxin inducible gene expressed in the nucleus
AT3G07000	3.55	0.00006	NA	NA
AT3G23635	3.54	0.00040	RTFL13	NA
AT3G47090	3.51	0.02085	NA	NA
AT4G30290	3.51	0.00229	ATXTH19	Encodes a xyloglucan endotransglucosylase/hydrolase with only only the endotransglucosylase (XET; EC 2.4.1.207) activity towards xyloglucan and non-detectable endohydrolytic (XEH; EC 3.2.1.151) activity. Expressed throughout both the main and the lateral root, with intensive expression at the dividing and elongating regions. Is expressed in lateral root primordia but expression ceases after lateral root begins to grow.
AT3G55840	3.44	0.04936	NA	NA
AT2G01430	3.42	0.00060	ATHB-17	NA
AT3G04210	3.41	0.00055	NA	NA
AT4G04745	3.40	0.00015	NA	NA
AT5G37950	3.39	0.02574	NA	NA

AT4G12410	3.35	0.00415	SAUR35	NA
AT1G62440	3.29	0.00053	LRX2	encodes a paralog of LRX1 (LEUCINE-RICH REPEAT/EXTENSIN 1) which acts synergistically with LRX1 in root hair cell morphogenesis.
AT3G59900	3.26	0.00714	ARGOS	Encodes ARGOS (Auxin-Regulated Gene Involved in Organ Size). Inducible by auxin. Involved in lateral organ size control. Transgenic plants expressing sense or antisense ARGOS cDNA display enlarged or reduced aerial organs, respectively. The alteration in organ size is attributable mainly to changes in cell number and the duration of organ growth.
AT3G06370	3.22	0.00019	ATNHX4	member of Sodium proton exchanger family
AT4G16515	3.21	0.00094	CLEL	Encodes a root meristem growth factor (RGF). Belongs to a family of functionally redundant homologous peptides that are secreted, tyrosine-sulfated, and expressed mainly in the stem cell area and the innermost layer of central columella cells. RGFs are required for maintenance of the root stem cell niche and transit amplifying cell proliferation. Members of this family include: At5g60810 (RGF1), At1g13620 (RGF2), At2g04025 (RGF3), At3g30350 (RGF4), At5g51451 (RGF5), At4g16515 (RGF6), At3g02240 (RGF7), At2g03830 (RGF8) and At5g64770 (RGF9).
AT3G28420	3.20	0.00001	NA	NA
AT5G05365	3.16	0.00450	NA	NA
AT1G29465	3.14	0.00061	NA	NA
AT1G30100	3.14	0.00310	ATNCED5	Encodes 9-cis-epoxycarotenoid dioxygenase, a key enzyme in the biosynthesis of abscisic acid. The expression of this gene increases during the first 6h of imbibition.
AT3G45970	3.13	0.00066	ATEXLA1	member of EXPANSIN-LIKE. Naming convention from the Expansin Working Group (Kende et al, 2004. Plant Mol Bio)
AT1G18400	3.12	0.00003	BEE1	NA
AT5G50335	3.10	0.00346	NA	NA
AT1G67265	3.04	0.01829	DVL3	NA
AT4G38825	3.03	0.00578	SAUR13	NA
AT4G21730	3.00	0.01020	NA	NA
AT4G27260	2.99	0.00050	GH3.5	encodes an IAA-amido synthase that conjugates Asp and other amino acids to auxin in vitro. Lines carrying insertions in this gene are hypersensitive to auxin.
AT1G78100	2.98	0.00223	AUF1	NA
AT1G80730	2.98	0.00910	ATZFP1	Encodes a zinc finger protein and is expressed at high levels in the shoot apex, including the apical meristem, developing leaves and the developing vascular system. expression induced three days post germination. T-DNA insertion mutant has a dominant phenotype in leaf initiation.
AT4G01140	2.93	0.01198	NA	NA

AT5G44063	2.92	0.01011	NA	NA
AT5G41400	2.92	0.00297	NA	NA
AT4G25810	2.90	0.00065	XTH23	xyloglucan endotransglycosylase-related protein (XTR6)
AT1G65240	2.90	0.02975	NA	NA
AT3G63440	2.90	0.00000	ATCKX6	This gene used to be called AtCKX7. It encodes a protein whose sequence is similar to cytokinin oxidase/dehydrogenase, which catalyzes the degradation of cytokinins.
AT2G30040	2.89	0.01307	MAPKKK14	member of MEKK subfamily
AT1G49780	2.88	0.00001	PUB26	NA
AT4G23070	2.87	0.01335	ATRBL7	NA
AT1G65920	2.87	0.00002	NA	NA
AT2G21200	2.81	0.03449	SAUR7	NA
AT1G58340	2.81	0.00454	BCD1	NA
AT3G25717	2.80	0.00270	DVL6	NA
AT5G15160	2.78	0.00183	BHLH134	BNQ2 belongs to a family of atypical non-DNA binding basic helix-loop-helix (bHLH) proteins that heterodimerize with and negatively regulate bHLH transcription factors. Directly and negatively regulated by AP3 and PI in petals.Required for appropriate regulation of flowering time.
AT1G69570	2.77	0.03468	NA	NA
AT4G38400	2.76	0.00016	ATEXLA2	member of EXPANSIN-LIKE. Naming convention from the Expansin Working Group (Kende et al, 2004. Plant Mol Bio)
AT4G13190	2.76	0.00326	NA	NA
AT1G57560	2.74	0.01905	AtMYB50	Member of the R2R3 factor gene family.
AT3G42800	2.74	0.00956	NA	NA
AT1G13245	2.74	0.00866	DVL4	NA
AT2G42380	2.73	0.00089	ATBZIP34	Encodes a member of the BZIP family of transcription factors. Forms heterodimers with the related protein AtbZIP61. Binds to G-boxes in vitro and is localized to the nucleus in onion epidermal cells.
AT5G14360	2.71	0.04777	NA	NA
AT2G45410	2.70	0.02646	LBD19	NA
AT5G54230	2.68	0.03241	AtMYB49	Encodes a putative transcription factor (MYB49).
AT3G17690	2.67	0.03896	ATCNGC19	member of Cyclic nucleotide gated channel family
AT1G67900	2.66	0.00238	NA	NA
AT3G15670	2.66	0.02785	NA	NA

AT1G04877	2.65	0.02191	NA	NA
AT1G68825	2.64	0.04979	DVL5	NA
AT4G34760	2.63	0.00118	SAUR50	NA
ATMG01320	2.62	0.03039	NAD2	encodes subunit of mitochondrial NAD(P)H dehydrogenase that is trans-spliced from two precursors, NAD2A and NAD2B.
AT3G14362	2.61	0.01336	DVL19	NA
AT3G62100	2.61	0.00020	IAA30	Encodes a member of the Aux/IAA family of proteins implicated in auxin signaling. IAA30 lacks the conserved degron (domain II) found in many family members. IAA30 transcripts are induced by auxin treatment and accumulate preferentially in the quiescent center cells of the root meristem. Overexpression of IAA30 leads to defects in gravitropism, root development, root meristem maintenance, and cotyledon vascular development. Target of LEC2 and AGL15. Promotes somatyic embryogenesis.
AT5G20820	2.60	0.01488	SAUR76	NA
AT2G36220	2.59	0.00007	NA	NA
AT1G18835	2.58	0.00538	MIF3	NA
AT3G50280	2.58	0.00020	NA	NA
AT1G59740	2.58	0.00235	AtNPF4.3	NA
AT2G17080	2.58	0.01829	NA	NA
AT4G34800	2.57	0.00248	SAUR4	NA
AT1G15550	2.56	0.00009	ATGA3OX1	Involved in later steps of the gibberellic acid biosynthetic pathway. Activated by AGAMOUS in a cal-1, ap1-1 background. Deletion of 208 bp from -1016 to -809 (Δ-808) resulted in loss of GA-negative feedback (this sequence, which contains a 43-bp sequence GNFEI, was shown to be sufficient for GA-negative feedback).
AT2G28350	2.55	0.00006	ARF10	Involved in root cap cell differentiation.
AT4G37390	2.54	0.00000	AUR3	Encodes an IAA-amido synthase that conjugates Asp and other amino acids to auxin in vitro. Lines carrying insertions in this gene are hypersensitive to auxin. May function as a negative component in auxin signaling by regulating auxin activity.
AT3G19200	2.54	0.01518	NA	NA
AT3G25710	2.53	0.00006	ATAIG1	Encodes a basic helixloophelix transcription factor that is expressed in the hypophysis-adjacent embryo cells, and is required and partially sufficient for MP-dependent root initiation. Involved in response to phosphate starvation. Negative regulator of root hair development, anthocyanin formation and Pi content.

AT2G26710	2.53	0.00193	BAS1	Encodes a member of the cytochrome p450 family that serves as a control point between multiple photoreceptor systems and brassinosteroid signal transduction. Involved in brassinolide metabolism. Mediates response to a variety of light signals including hypocotyl elongation and cotyledon expansion.
AT4G00970	2.52	0.01041	CRK41	Encodes a cysteine-rich receptor-like protein kinase.
AT1G23340	2.51	0.00022	NA	NA
AT2G18969	2.51	0.00044	NA	NA
AT5G10430	2.50	0.01213	AGP4	Encodes arabinogalactan-protein (AGP4).
AT1G65310	2.49	0.00511	ATXTH17	Encodes a xyloglucan endotransglucosylase/hydrolase with only only the endotransglucosylase (XET; EC 2.4.1.207) activity towards xyloglucan and non-detectable endohydrolytic (XEH; EC 3.2.1.151) activity. Expressed in the mature or basal regions of both the main and lateral roots, but not in the tip of these roots where cell division occurs.
AT3G27500	2.49	0.00105	NA	NA
AT3G14440	2.48	0.02276	ATNCED3	Encodes 9-cis-epoxycarotenoid dioxygenase, a key enzyme in the biosynthesis of abscisic acid. Regulated in response to drought and salinity. Expressed in roots, flowers and seeds. Localized to the chloroplast stroma and thylakoid membrane.
AT5G66590	2.48	0.00056	NA	NA
AT3G15115	2.48	0.00578	NA	NA
AT4G21740	2.48	0.00006	NA	NA
AT5G54490	2.47	0.04040	PBP1	Encodes a PINOID (PID)-binding protein containing putative EF-hand calcium-binding motifs. The interaction is dependent on the presence of calcium. mRNA expression is up-regulated by auxin. Not a phosphorylation target of PID, likely acts upstream of PID to regulate the activity of this protein in response to changes in calcium levels.
AT1G76220	2.46	0.04509	NA	NA
AT1G07490	2.45	0.00074	DVL9	NA
AT1G54120	2.45	0.03039	NA	NA
AT3G28180	2.44	0.00118	ATCSLC04	encodes a gene similar to cellulose synthase
AT5G64770	2.44	0.00009	CLEL	Encodes a root meristem growth factor (RGF). Belongs to a family of functionally redundant homologous peptides that are secreted, tyrosine-sulfated, and expressed mainly in the stem cell area and the innermost layer of central columella cells. RGFs are required for maintenance of the root stem cell niche and transit amplifying cell proliferation. Members of this family include: At5g60810 (RGF1), At1g13620 (RGF2), At2g04025 (RGF3), At3g30350 (RGF4), At5g51451 (RGF5), At4g16515 (RGF6), At3g02240 (RGF7), At2g03830 (RGF8) and At5g64770 (RGF9).
AT5G65610	2.43	0.00201	NA	NA

AT1G61255	2.42	0.00615	NA	NA
AT2G14820	2.41	0.04196	MEL3	A member of the NPY gene family (NPY1/AT4G31820, NPY2/AT2G14820, NPY3/AT5G67440, NPY4/AT2G23050, NPY5/AT4G37590). Involved in auxin-mediated organogenesis.
AT5G50120	2.41	0.04455	NA	NA
AT1G68360	2.39	0.01999	NA	NA
AT3G25900	2.39	0.00050	ATHMT-1	NA
AT3G14370	2.37	0.00040	WAG2	The WAG2 and its homolog, WAG1 each encodes protein-serine/threonine kinase that are nearly 70% identical to PsPK3 protein. All three together with CsPK3 belong to PsPK3-type kinases. At the N-terminus, all four possess a serine/threonine-rich domain. They are closely related to Arabidopsis kinases PINOID. wag1/wag2 double mutants exhibit a pronounced wavy root phenotype when grown vertically on agar plates (while wild-type plants develop wavy roots only on plates inclined to angles less than 90 degrees), indicating an overlapping role for WAG1 and WAG2 as suppressors of root waving. Simultaneous disruption of PID(AT2G34650) and its 3 closest homologs (PID2/AT2G26700, WAG1/AT1G53700, and WAG2/AT3G14370) abolishes the formation of cotyledons.
AT3G06990	2.37	0.01174	NA	NA
AT5G64780	2.37	0.00024	NA	NA
AT3G59440	2.36	0.02295	NA	NA
AT5G65613	2.36	0.00274	NA	NA
AT1G01600	2.35	0.01931	CYP86A4	Encodes a member of the CYP86A subfamily of cytochrome p450 genes. Expressed significantly at highest level in mature stems and flowers.
AT5G65340	2.35	0.00050	NA	NA
AT4G09890	2.35	0.00003	NA	NA
AT5G24030	2.34	0.00000	SLAH3	Encodes a protein with ten predicted transmembrane helices. The SLAH3 protein has similarity to the SLAC1 protein involved in ion homeostasis in guard cells. Although it is not expressed in guard cells, it can complement an slac1-2 mutant suggesting that it performs a similar function. SLAH3:GFP localizes to the plasma membrane.
AT3G55720	2.32	0.00065	NA	NA
AT5G51810	2.32	0.04264	AT2353	Encodes gibberellin 20-oxidase. Involved in gibberellin biosynthesis. Up-regulated by far red light in elongating petioles. Not regulated by a circadian clock.
AT3G18200	2.31	0.00435	UMAMIT4	NA
AT5G20670	2.30	0.04714	NA	NA
AT1G53340	2.30	0.00275	NA	NA

AT1G22470	2.30	0.04241	NA	NA
AT4G10150	2.28	0.00297	NA	NA
AT3G50340	2.28	0.00416	NA	NA
AT5G43700	2.28	0.00041	ATAUX2-11	Auxin inducible protein similar to transcription factors.
AT1G64625	2.27	0.00090	NA	NA
AT1G52565	2.26	0.00890	NA	NA
AT4G13180	2.25	0.00010	NA	NA
AT1G14080	2.25	0.03757	ATFUT6	member of Xyloglucan fucosyltransferase family
AT2G20562	2.25	0.03299	NA	NA
AT1G68330	2.24	0.00088	NA	NA
AT4G38840	2.24	0.02276	SAUR14	NA
AT2G43340	2.23	0.00094	NA	NA
AT5G67450	2.23	0.02755	AZF1	Encodes zinc-finger protein. mRNA levels are elevated in response to low temperature, cold temperatures and high salt. The protein is localized to the nucleus and acts as a transcriptional repressor.
AT2G41170	2.23	0.00005	NA	NA
AT3G05320	2.22	0.03042	NA	NA
AT5G45580	2.22	0.03786	NA	NA
AT3G25250	2.21	0.04512	AGC2	Arabidopsis protein kinase
AT1G65840	2.21	0.00035	ATPAO4	encodes a peroxisomal polyamine oxidase, involved in the back-conversion polyamine degradation pathway. Among the five polyamine oxidases in the Arabidopsis genome, PAO4 is the major isoform in root peroxisomes.
AT5G13700	2.20	0.00327	APAO	Encodes a protein with polyamine oxidase activity. The mRNA of this gene is only expressed in very low amounts in the organs where it was detected (light-grown plants).
AT1G11120	2.18	0.00032	NA	NA
AT2G41480	2.17	0.03207	AtPRX25	NA
AT1G14185	2.17	0.00964	NA	NA
AT3G58120	2.15	0.00416	ATBZIP61	Encodes a member of the BZIP family of transcription factors. Forms heterodimers with the related protein AtbZIP34. Binds to G-boxes in vitro and is localized to the nucleus in onion epidermal cells.
AT5G15580	2.14	0.00007	LNG1	Encodes LONGIFOLIA1 (LNG1). Regulates leaf morphology by promoting cell expansion in the leaf-length direction. The LNG1 homologue LNG2 (At3g02170) has similar function.
AT4G20780	2.14	0.00137	CML42	Calcium sensor involved in trichome branching.

AT1G80240	2.14	0.00055	DGR1	NA
AT5G59220	2.14	0.03942	HAI1	NA
AT2G43290	2.14	0.00016	MSS3	Encodes calmodulin-like MSS3.
AT1G64640	2.13	0.00989	AtENODL8	NA
AT4G28640	2.12	0.00005	IAA11	Auxin induced gene, IAA11 (IAA11).
AT2G22470	2.12	0.02903	AGP2	Encodes arabinogalactan-protein (AGP2).
AT4G09970	2.11	0.00006	NA	NA
AT4G17460	2.10	0.00141	HAT1	Encodes homeobox protein HAT1.
AT5G54510	2.08	0.00529	DFL1	Encodes an IAA-amido synthase that conjugates Ala, Asp, Phe, and Trp to auxin. Lines overexpressing this gene accumulate IAA-ASP and are hypersensitive to several auxins. Identified as a dominant mutation that displays shorter hypocotyls in light grown plants when compared to wild type siblings. Protein is similar to auxin inducible gene from pea (GH3).
AT1G77640	2.08	0.04027	NA	encodes a member of the DREB subfamily A-5 of ERF/AP2 transcription factor family. The protein contains one AP2 domain. There are 15 members in this subfamily including RAP2.1, RAP2.9 and RAP2.10.
AT3G50890	2.07	0.03845	AtHB28	NA
AT5G14020	2.06	0.03918	NA	NA
AT4G13195	2.06	0.00772	CLE44	Belongs to a large gene family, called CLE for CLAVATA3/ESR-related, encoding small peptides with conserved carboxyl termini. The C-terminal 12 amino acid sequence of CLE44 is identical to that of a dodeca peptide (TDIF, tracheary element differentiation inhibitory factor) isolated from Arabidopsis and functions as a suppressor of plant stem cell differentiation. TDIF sequence is also identical to the C-terminal 12 amino acids of CLE41 (At3g24770).
AT4G28490	2.05	0.00109	HAE	member of Receptor kinase-like protein family
AT2G01200	2.04	0.03116	IAA32	Belongs to auxin inducible gene family.
AT4G22780	2.04	0.00057	ACR7	Member of a family of ACT domain containing proteins . ACT domains are involved in amino acid binding .
AT5G53250	2.04	0.03141	AGP22	NA
AT2G21220	2.03	0.01472	SAUR12	NA
AT3G54000	2.03	0.00903	NA	NA
AT3G19680	2.01	0.00890	NA	NA
AT1G70920	2.01	0.04722	ATHB18	NA
AT1G67880	2.01	0.00003	NA	NA

AT4G29310	2.01	0.03431	NA	NA
AT1G52827	2.00	0.00321	ATCDT1	Cysteine-rich protein that confers cadmium tolerance to yeast. Homologs are also found in rice, Brassica rapa and pine.
AT1G15520	2.00	0.02152	ABCG40	ABC transporter family involved in ABA transport and resistance to lead. Localizes to plasma membrane. Upregulated by lead. Expressed in leaves, flowers, stomata and roots.
AT3G20830	1.99	0.00171	AGC2-4	NA
AT3G25780	1.98	0.04365	AOC3	Encodes allene oxide cyclase, one of the enzymes involved in jasmonic acid biosynthesis. One of four genes in Arabidopsis that encode this enzyme. mRNA expression is upregulated in senescing leaves. Note: Nomenclature for Arabidopsis allene oxide cyclase 3 (AOC3, AT3G25780) gene is based on Stenzel et al. 2003 Plant Molecular Biology 51:895-911. AOC3 (AT3G25780) is also referred to as AOC2 in He et al. 2002 Plant Physiology, 128:876-884.
AT3G13310	1.98	0.02483	DJC66	NA
AT4G26470	1.98	0.04768	NA	NA
AT1G78120	1.97	0.02659	TPR12	NA
AT1G51170	1.97	0.00040	AGC2-3	NA
AT5G09970	1.95	0.00016	CYP78A7	member of CYP78A
AT5G59010	1.95	0.00174	BSK5	NA
AT3G54810	1.94	0.00137	BME3	Encodes a protein containing a GATA type zinc finger domain that is expressed in the embryo axis and involved in germination. Mutants have a reduced rate of germination even when stratified.
AT1G01200	1.93	0.00390	ATRAB-A3	NA
AT3G28340	1.93	0.01704	GATL10	Encodes a protein with putative galacturonosyltransferase activity.
AT3G62720	1.92	0.00115	ATXT1	Encodes a protein with xylosyltransferase activity, which is specific for UDP-xylose as donor substrate and for oligosaccharides with a degree of polymerization >4. Although the enzyme utilizes either cellopentaose or cellohexaose, its activity is four-fold higher with cellohexaose as an acceptor compared to cellopentaose. The enzyme is able to add several xylosyl residues to the acceptor forming mono-, di- and trixylosylated polysaccharides.
AT2G01150	1.91	0.00110	RHA2B	Encodes a RING-H2 finger protein that is expressed in vascular tissue, root tips, embryos and pistils.
AT1G32920	1.91	0.00442	NA	NA
AT1G17620	1.91	0.00030	NA	NA
AT2G23060	1.91	0.03449	NA	NA
AT1G54200	1.90	0.00006	NA	NA
AT3G49220	1.90	0.01115	NA	NA

AT3G19380	1.90	0.00021	PUB25	NA
AT3G02000	1.90	0.00015	ROXY1	Roxy1 encodes a glutaredoxin belonging to a subgroup specific to higher plants. It is required for proper petal initiation and organogenesis. It is likely to function in the temporal and spatial expression regulation of AGAMOUS in the first and second whorl. It's function is dependent on the Cysteine 49 residue and its nuclear localization. ROXY1 interacts in vitro and in vivo with members of the TGA family of transcription factors (e.g. TGA2, TGA3, TGA7 and PAN).
AT5G18930	1.89	0.00081	BUD2	NA
AT1G26960	1.89	0.00009	AtHB23	Encodes a homeodomain leucine zipper class I (HD-Zip I) protein.
AT1G14630	1.89	0.00116	NA	NA
AT1G11740	1.89	0.04350	NA	NA
AT2G41800	1.89	0.03449	NA	NA
AT3G22820	1.88	0.01383	CLL1	NA
AT4G19230	1.88	0.04926	CYP707A1	Encodes a protein with ABA 8'-hydroxylase activity, involved in ABA catabolism. Member of the CYP707A gene family. CYP707A1 appears to play an important role in determining the ABA levels in dry seeds. Gene involved in postgermination growth. Overexpression of CYP707A1 leads to a decrease in ABA levels and a reduction in after-ripening period to break dormancy.
AT2G41510	1.87	0.01416	ATCKX1	It encodes a protein whose sequence is similar to cytokinin oxidase/dehydrogenase, which catalyzes the degradation of cytokinins.
AT5G09805	1.87	0.04225	IDL3	Similar to Inflorescence deficient in abscission (IDA). Involved in floral organ abscission.
AT3G26960	1.87	0.04945	NA	NA
AT4G00080	1.87	0.02394	UNE11	NA
AT3G28200	1.87	0.00076	NA	NA
AT5G58630	1.86	0.02522	TRM31	NA
AT1G70990	1.86	0.00791	NA	NA
AT4G22560	1.86	0.00230	NA	NA
AT5G61570	1.85	0.03267	NA	NA
AT5G37540	1.85	0.00537	NA	NA
AT5G40540	1.85	0.04316	NA	NA
AT5G07110	1.84	0.00079	PRA1.B6	NA
AT5G50090	1.84	0.00145	NA	NA
AT2G17230	1.84	0.01602	EXL5	NA

AT4G35320	1.83	0.00105	NA	NA
AT1G29270	1.83	0.02454	NA	NA
AT1G74420	1.82	0.00167	ATFUT3	Predicted fucosyltransferase, based on similarity to FUT1, but not functionally redundantwith FUT1.
AT4G30180	1.82	0.02740	NA	NA
AT4G31000	1.82	0.00138	NA	NA
AT4G19460	1.81	0.01689	NA	NA
AT2G34930	1.81	0.01326	NA	NA
AT5G11740	1.81	0.00037	AGP15	Encodes arabinogalactan protein (AGP15).
AT3G06770	1.80	0.00636	NA	NA
AT4G09030	1.80	0.01169	AGP10	Encodes arabinogalactan protein (AGP10).
AT1G70940	1.79	0.00138	ATPIN3	A regulator of auxin efflux and involved in differential growth. PIN3 is expressed in gravity-sensing tissues, with PIN3 protein accumulating predominantly at the lateral cell surface. PIN3 localizes to the plasma membrane and to vesicles. In roots, PIN3 is expressed without pronounced polarity in tiers two and three of the columella cells, at the basal side of vascular cells, and to the lateral side of pericycle cells of the elongation zone. PIN3 overexpression inhibits root cell growth. Protein phosphorylation plays a role in PIN3 trafficking to the plasma membrane.
AT1G01120	1.79	0.00390	KCS1	Encodes a condensing enzyme KCS1 (3-ketoacyl-CoA synthase 1) which is involved in the critical fatty acid elongation process in wax biosynthesis.
AT5G63790	1.79	0.03664	ANAC102	Encodes a member of the NAC family of transcription factors. ANAC102 appears to have a role in mediating response to low oxygen stress (hypoxia) in germinating seedlings.
AT2G34080	1.79	0.04297	NA	NA
AT3G05490	1.78	0.00040	RALFL22	Member of a diversely expressed predicted peptide family showing sequence similarity to tobacco Rapid Alkalinization Factor (RALF), and is believed to play an essential role in the physiology of Arabidopsis. Consists of a single exon and is characterized by a conserved C-terminal motif and N-terminal signal peptide.
AT1G63840	1.78	0.00030	NA	NA
AT3G50900	1.78	0.00068	NA	NA
AT1G22882	1.78	0.00778	NA	NA
AT5G62865	1.77	0.00128	NA	NA
AT3G13520	1.77	0.00657	AGP12	Encodes a GPI-anchored arabinogalactan (AG) peptide with a short 'classical' backbone of 10 amino acids, seven of which are conserved among the 4 other Arabidopsis AG peptides. These peptides may be involved in cell signaling.

AT2G33310	1.77	0.00012	IAA13	Auxin induced gene, IAA13 (IAA13).
AT2G26440	1.77	0.00020	PME12	NA
AT4G37450	1.76	0.00022	AGP18	AGP18 is a lysine-rich arabinogalactan-protein (AGP) and part of a multi-gene family of glycoproteins with approx. 50 members. It falls into one subclass with AGP17 and AGP19, other lysine-rich AGPs. It is expressed in young leaves, shoots, roots and flowers.
AT5G54145	1.76	0.01126	NA	NA
AT4G08950	1.75	0.01025	EXO	NA
AT5G66940	1.75	0.00009	NA	NA
AT5G06930	1.75	0.03349	NA	NA
AT3G60260	1.75	0.00014	NA	NA
AT4G26490	1.74	0.00822	NA	NA
AT4G05020	1.74	0.03486	NDB2	NA
AT2G46570	1.74	0.00156	LAC6	putative laccase, a member of laccase family of genes (with 17 members in Arabidopsis).
AT5G12050	1.74	0.01292	NA	NA
AT1G29660	1.74	0.01477	NA	NA
AT2G26530	1.73	0.01455	AR781	unknown function
AT2G41820	1.72	0.00006	PXC3	NA
AT4G01575	1.72	0.02644	NA	NA
AT5G22690	1.72	0.04807	NA	NA
AT1G53470	1.72	0.01262	MSL4	NA
AT5G51790	1.71	0.03116	NA	NA
AT5G49300	1.71	0.00080	GATA16	Encodes a member of the GATA factor family of zinc finger transcription factors.
AT5G54530	1.71	0.01891	NA	NA
AT1G24170	1.71	0.00167	GATL8	Encodes a protein with putative galacturonosyltransferase activity.
AT4G30470	1.70	0.01152	NA	NA
AT3G06890	1.70	0.02781	NA	NA
AT4G39840	1.70	0.00065	NA	NA
AT3G17090	1.70	0.00005	NA	NA
AT1G21050	1.69	0.00146	NA	NA
AT1G02850	1.69	0.02879	BGLU11	NA

AT1G13670	1.69	0.00677	NA	NA
AT5G08790	1.69	0.00793	anac081	induced by wounding, belongs to a large family of putative transcriptional activators with NAC domain.
AT4G13340	1.69	0.00890	LRX3	NA
AT2G41070	1.69	0.02195	ATBZIP12	Transcription factor homologous to ABI5. Regulates AtEm1 expression by binding directly at the AtEm1 promoter. Located in the nucleus and expressed during seed maturation in the cotyledons and later in the whole embryo.
AT1G78970	1.69	0.00116	ATLUP1	Lupeol synthase. Converts oxidosqualene to multiple triterpene alcohols and a triterpene diols. This conversion proceeds through the formation of a 17β-dammarenyl cation.
AT5G47800	1.68	0.00659	NA	NA
AT4G28650	1.68	0.04226	NA	NA
AT5G43190	1.68	0.00171	NA	NA
AT5G47440	1.68	0.03624	NA	NA
AT1G74660	1.68	0.00314	MIF1	Constitutive overexpression of MIF1 caused dramatic developmental defects, seedlings were non-responsive to gibberellin (GA) for cell elongation, hypersensitive to the GA synthesis inhibitor paclobutrazol (PAC) and abscisic acid (ABA), and hyposensitive to auxin, brassinosteroid and cytokinin, but normally responsive to ethylene.
AT1G75450	1.67	0.01035	ATCKX5	This gene used to be called AtCKX6. It encodes a protein whose sequence is similar to cytokinin oxidase/dehydrogenase, which catalyzes the degradation of cytokinins.
AT5G57100	1.67	0.00390	NA	NA
AT1G30690	1.67	0.00305	NA	NA
AT5G55250	1.67	0.00162	AtIAMT1	Encodes an enzyme which specifically converts IAA to its methyl ester form MeIIAA. This gene belongs to the family of carboxyl methyltransferases whose members catalyze the transfer of the methyl group from S-adenosyl-L-methionine to carboxylic acid-containing substrates to form small molecule methyl esters. Expression of TCP genes is downregulated in mutant iamt1-D.
AT1G73590	1.67	0.00035	ATPIN1	Encodes an auxin efflux carrier involved in shoot and root development. It is involved in the maintenance of embryonic auxin gradients. Loss of function severely affects organ initiation, pin1 mutants are characterised by an inflorescence meristem that does not initiate any flowers, resulting in the formation of a naked inflorescence stem. PIN1 is involved in the determination of leaf shape by actively promoting development of leaf margin serrations. In roots, the protein mainly resides at the basal end of the vascular cells, but weak signals can be detected in the epidermis and the cortex. Expression levels and polarity of this auxin efflux carrier change during primordium development suggesting that cycles of auxin build-up and depletion accompany, and may direct, different stages of primordium development. PIN1 action on plant development does not strictly require function of PGP1 and PGP19 proteins.

AT5G44568	1.67	0.04454	NA	NA
AT1G75590	1.67	0.03351	SAUR52	NA
AT1G61667	1.66	0.04350	NA	NA
AT2G23100	1.66	0.01477	NA	NA
AT5G66600	1.66	0.00105	NA	NA
AT3G60550	1.66	0.04464	CYCP3;2	NA
AT5G20110	1.66	0.01635	NA	NA
AT1G02930	1.66	0.04011	ATGST1	Encodes glutathione transferase belonging to the phi class of GSTs. Naming convention according to Wagner et al. (2002).
AT4G34810	1.66	0.03845	SAUR5	NA
AT3G07010	1.65	0.02208	NA	NA
AT3G06868	1.65	0.02879	NA	NA
AT5G25440	1.65	0.02491	NA	NA
AT2G34650	1.64	0.00145	ABR	Encodes a protein serine/threonine kinase that may act as a positive regulator of cellular auxin efflux, as a a binary switch for PIN polarity, and as a negative regulator of auxin signaling. Recessive mutants exhibit similar phenotypes as pin-formed mutants in flowers and inflorescence but distinct phenotypes in cotyledons and leaves. Expressed in the vascular tissue proximal to root and shoot meristems, shoot apex, and embryos. Expression is induced by auxin. Overexpression of the gene results in phenotypes in the root and shoot similar to those found in auxin-insensitive mutants. The protein physically interacts with TCH3 (TOUCH3) and PID-BINDING PROTEIN 1 (PBP1), a previously uncharacterized protein containing putative EF-hand calcium-binding motifs. Acts together with ENP (ENHANCER OF PINOID) to instruct precursor cells to elaborate cotyledons in the transition stage embryo. Interacts with PDK1. PID autophosphorylation is required for the ability of PID to phosphorylate an exogenous substrate. PID activation loop is required for PDK1-dependent PID phosphorylation and requires the PIF domain. Negative regulator of root hair growth. PID kinase activity is critical for the inhibition of root hair growth and for maintaining the proper subcellular localization of PID.
AT2G42800	1.64	0.03124	AtRLP29	NA
AT1G25425	1.64	0.00380	CLE43	NA

AT1G80100	1.64	0.04454	AHP6	AHP6 lacks the conserved histidine residue (Asn83 in AHP6b), which is required for phosphotransfer, present in the other AHPs. AHP6 does not appear to have phosphotransfer activity. Acts as an inhibitor of cytokinin signaling by interacting with the phosphorelay machinery. Expressed in developing protoxylem and associated pericycle cell files. Negative regulator of cytokinin signaling. Expression is down-regulated by cytokinins. There are two alternatively spliced genes for this locus, AHP6a and AHP6b, differing in the length of the first exon. In ahp6-2 seedlings, only the AHP6a transcript is present. Members of the AHP gene family include: AT3G21510 (AHP1), AT3G29350 (AHP2), AT5G39340 (AHP3), AT3G16360 (AHP4), AT1G03430 (AHP5) and AT1G80100 (AHP6).
AT4G10040	1.63	0.00721	CYTC-2	Encodes cytochrome c. Promoter directs preferential expression in vascular tissues of cotyledons, leaves, roots, and hypocotyls, and in anthers.
AT3G59310	1.63	0.03171	NA	NA
AT3G50350	1.63	0.04145	NA	NA
AT5G50670	1.63	0.00255	SPL13	NA
AT3G10720	1.63	0.01422	NA	NA
AT1G72790	1.62	0.00034	NA	NA
AT3G54030	1.62	0.00056	BSK6	NA
AT4G25760	1.62	0.00957	ATGDU2	Encodes a member of the GDU (glutamine dumper) family proteins involved in amino acid export: At4g31730 (GDU1), At4g25760 (GDU2), At5g57685 (GDU3), At2g24762 (GDU4), At5g24920 (GDU5), At3g30725 (GDU6) and At5g38770 (GDU7).
AT1G72430	1.62	0.04378	SAUR78	NA
AT3G18010	1.62	0.04870	WOX1	Encodes a WUSCHEL-related homeobox gene family member with 65 amino acids in its homeodomain. Proteins in this family contain a sequence of eight residues (TLPLFPMH) downstream of the homeodomain called the WUS box. Its mRNA is expressed in the initiating vascular primordium of the cotyledons during heart and torpedo stages.
AT3G13650	1.61	0.00116	NA	NA
AT2G35880	1.61	0.00772	NA	NA
AT3G23170	1.61	0.02326	NA	NA
AT4G37590	1.61	0.00009	MEL1	A member of the NPY gene family (NPY1/AT4G31820, NPY2/AT2G14820, NPY3/AT5G67440, NPY4/AT2G23050, NPY5/AT4G37590). Involved in auxin-mediated organogenesis.
AT1G61170	1.61	0.01518	NA	NA
AT5G58620	1.61	0.02728	TZF9	NA
AT1G72230	1.61	0.00014	NA	NA

AT5G62220	1.61	0.00235	ATGT18	NA
AT1G01130	1.60	0.02438	NA	NA
AT4G05010	1.60	0.02530	AtFBS3	NA
AT5G54500	1.60	0.00018	FQR1	Encodes a flavin mononucleotide-binding flavodoxin-like quinone reductase that is a primary auxin-response gene.
AT5G51460	1.60	0.00056	ATTPPA	homologous to the C-terminal part of microbial trehalose-6-phosphate phosphatases
AT1G53830	1.60	0.04714	ATPME2	encodes a pectin methylesterase
AT4G03190	1.60	0.00093	AFB1	Encodes an F box protein belonging to the TIR1 subfamily. This protein forms SCF complexes with ASK1 and CUL1 and interacts with Aux/IAA proteins in an auxin-dependent manner. It also has sequence similarity to the yeast protein GRR1, which is involved in glucose repression.
AT5G66280	1.60	0.01174	GMD1	GDP-D-mannose 4,6-dehydratase
AT3G26760	1.59	0.00050	NA	NA
AT1G05420	1.59	0.01194	ATOFP12	NA
AT5G48150	1.59	0.00023	PAT1	Member of GRAS gene family. Semi-dominant mutant has a reduced response to far-red light and appears to act early in the phytochrome A signaling pathway.
AT1G34110	1.59	0.00778	NA	NA
AT1G21830	1.59	0.00472	NA	NA
AT2G33570	1.58	0.00293	GALS1	NA
AT3G17420	1.58	0.00283	GPK1	serine/threonine protein kinase-like protein
AT3G12610	1.58	0.01689	DRT100	Plays role in DNA-damage repair/toleration. Partially complements RecA- phenotypes.
AT1G63420	1.57	0.00470	NA	NA
AT4G22530	1.57	0.02317	NA	NA

AT5G03150	1.57	0.03465	JKD	JKD is a nuclear-localized putative transcription factor with three zinc finger domains. jkd mutants show a number of root patterning defects including ectopic periclinal divisions in the cortex, increased cell numbers in the cortical and epidermal layers, a disrupted QC marker expression pattern, and disorganized QC and columella cells. jkd mutants also have a reduced number of meristematic cells in their roots. JKD can interact with the SCR and SHR proteins implicated in root patterning, as well as another zinc finger transcription factor, MAGPIE. All of these interactions require the first zinc finger in JKD according to a Y2H assay. There are also transcriptional interactions among these proteins. The initiation of JKD transcription does not appear to depend on SCR and SHR, but later expression in the post-embryonic QC cells and ground tissue initials is reduced in scr and shr mutants. JKD also appears to be required for SCR transcription beginning in the embryo. There is also some evidence that JKD plays a role in promoting the movement of SHR into the nucleus, particularly in QC cells, but this may be indirect.
AT4G35160	1.57	0.01262	NA	NA
AT3G14540	1.57	0.02619	NA	NA
AT4G32350	1.57	0.01169	NA	NA
AT5G45280	1.57	0.00249	NA	NA
AT5G52060	1.56	0.00515	ATBAG1	A member of Arabidopsis BAG (Bcl-2-associated athanogene) proteins, plant homologs of mammalian regulators of apoptosis. Plant BAG proteins are multi-functional and remarkably similar to their animal counterparts, as they regulate apoptotic-like processes ranging from pathogen attack, to abiotic stress, to plant development.
AT4G15800	1.56	0.00296	RALFL33	Member of a diversely expressed predicted peptide family showing sequence similarity to tobacco Rapid Alkalinization Factor (RALF), and is believed to play an essential role in the physiology of Arabidopsis. Consists of a single exon and is characterized by a conserved C-terminal motif and N-terminal signal peptide.
AT5G45730	1.56	0.04365	NA	NA
AT1G67400	1.56	0.00643	NA	NA
AT3G60630	1.56	0.00010	ATHAM2	NA
AT2G21050	1.56	0.00035	LAX2	Encodes LAX2 (LIKE AUXIN RESISTANT), a member of the AUX1 LAX family of auxin influx carriers. Required for the establishment of embryonic root cell organization.
AT3G57450	1.55	0.00786	NA	NA
AT1G21840	1.55	0.01729	UREF	Encodes a urease accessory protein which is essential for the activation of plant urease.
AT1G11545	1.55	0.04787	XTH8	NA

AT1G14920	1.54	0.01934	GAI	Similar to a putative transcription factor and transcriptional coactivators. Repressor of GA responses and involved in gibberellic acid mediated signaling. Member of the DELLA proteins that restrain the cell proliferation and expansion that drives plant growth. The protein undergoes degradation in response to GA via the 26S proteasome. GAI may be involved in reducing ROS accumulation in response to stress by up-regulating the transcription of superoxide dismutases. Represses GA-induced vegetative growth and floral initiation. Rapidly degraded in response to GA.
AT3G60640	1.54	0.01463	ATG8G	NA
AT2G47930	1.54	0.00935	AGP26	NA
AT1G61260	1.54	0.00623	NA	NA
AT5G15350	1.53	0.03449	AtENODL17	NA
AT5G53590	1.53	0.01336	SAUR30	NA
AT2G01420	1.53	0.04701	ATPIN4	Encodes a putative auxin efflux carrier that is localized in developing and mature root meristems. It is involved in the maintenance of embryonic auxin gradients. A role for AtPIN4 in generating a sink for auxin below the quiescent center of the root meristem that is essential for auxin distribution and patterning is proposed. In the root, PIN4 is detected around the quiescent center and cells surrounding it, and localizes basally in provascular cells. PIN4 expression is upregulated in brassinosteroid-insensitive mutant (PMID 16141452).
AT1G62045	1.53	0.02619	NA	NA
AT1G33800	1.53	0.03437	AtGXMT1	NA
AT5G17490	1.52	0.04705	AtRGL3	DELLA subfamily member involved in GA signal transduction
AT3G47510	1.52	0.01278	NA	NA
AT4G39390	1.52	0.00088	ATNST-KT1	Encodes a golgi localized nucleotide sugar transporter.
AT5G05810	1.52	0.03116	ATL43	NA
AT4G30440	1.52	0.00538	GAE1	UDP-D-glucuronate 4-epimerase
AT1G12990	1.51	0.00669	NA	NA
AT1G32170	1.51	0.01472	XTH30	xyloglucan endotransglycosylase-related protein (XTR4)
AT1G27210	1.51	0.02011	NA	NA
AT5G56980	1.51	0.00501	NA	NA
AT5G25170	1.51	0.00167	NA	NA
AT2G14890	1.51	0.00772	AGP9	putative proline-rich protein (At2g14890) mRNA, complete

AT1G72470	1.51	0.00523	ATEXO70D1	A member of EXO70 gene family, putative exocyst subunits, conserved in land plants. Arabidopsis thaliana contains 23 putative EXO70 genes, which can be classified into eight clusters on the phylogenetic tree.
AT1G75500	1.51	0.00337	UMAMIT5	An Arabidopsis thaliana homolog of Medicago truncatula NODULIN21 (MtN21). The gene encodes a plant-specific, predicted integral membrane protein and is a member of the Plant-Drug/Metabolite Exporter (P-DME) family (Transporter Classification number: TC 2.A.7.3).
AT5G66920	1.51	0.00105	sks17	NA
AT4G37790	1.51	0.01287	HAT22	Encodes homeobox protein HAT22, member of the HD-Zip II family.
AT1G76160	1.50	0.00270	sks5	NA
AT1G80280	1.50	0.00013	NA	NA
AT2G47060	1.50	0.02584	PTI1-4	NA
AT1G67340	1.50	0.00056	NA	NA
AT1G04250	1.50	0.00105	AXR3	Transcription regulator acting as repressor of auxin-inducible gene expression. Auxin-inducible AUX/IAA gene. Short-lived nuclear protein with four conserved domains. Domain III has homology to beta alpha alpha dimerization and DNA binding domains. Involved in auxin signaling. Auxin induces the degradation of the protein in a dosage-dependent manner in a process mediated by AtRac1. Auxin induced the relocalization of the protein within the nucleus from a diffused nucleoplasmic pattern to a discrete particulated pattern named nuclear protein bodies or NPB in a process also mediated by Rac1. Colocalizes with SCF, CSN and 26S proteasome components.
AT2G24300	1.50	0.01336	NA	NA
AT2G47860	1.50	0.01893	SETH6	NA
AT3G19390	1.50	0.04139	NA	NA
AT3G17100	1.50	0.04071	AIF3	NA
AT1G31880	1.49	0.03168	BRX	Belongs to five-member BRX gene family. Arabidopsis BRX genes share high levels of similarity among each others, with several conserved domains. The most distinct is BRX domain - highly conserved in all BRX genes among distantly related species. This protein-protein interaction domain is required and sufficient for BRX activity. BRX encodes a key regulator of cell proliferation and elongation in the root, which has been implicated in the brassinosteroid (BR) pathway as well as regulation of auxin-responsive gene expression. Also involved in cytokinin-mediated inhibition of lateral root initiation. A loss-of-function allele, named brx-2 in Rodrigues et al. (2009) Plant Physiol. but changed to brx-3 to resolve nomenclature conflict (Li et al. Planta 2009:229(3):593-603), shows enhanced response to ABA-mediated inhibition of root growth.
AT5G10830	1.49	0.02531	NA	NA

AT5G27000	1.49	0.00669	ATK4	Encodes a kinesin-like protein that binds microtubules in an ATP-dependent manner.
AT3G62090	1.48	0.02584	PIF6	encodes a novel Myc-related bHLH transcription factor, which physically associated with APRR1/TOC1 and is a member of PIF3 transcription factor family.
AT5G62170	1.48	0.03698	TRM25	NA
AT1G65845	1.48	0.03598	NA	NA
AT2G39180	1.48	0.01685	ATCRR2	NA
AT1G77450	1.48	0.01857	anac032	NA
AT1G68810	1.48	0.00197	NA	NA
AT1G79760	1.47	0.03331	DTA4	Identified as target of the AGL15 binding motif CArG.
AT2G22830	1.47	0.02781	SQE2	NA
AT3G12920	1.47	0.01278	BRG3	NA
AT1G11125	1.47	0.02641	NA	NA
AT3G57010	1.47	0.01241	NA	NA
AT5G51670	1.47	0.03514	NA	NA
AT2G41660	1.46	0.04455	MIZ1	Essential for hydrotropism in roots. Mutant roots are defective in hydrotropism, and have slightly reduced phototropism and modified wavy growth response. Has normal gravitropism and root elongation.
AT1G14330	1.46	0.00937	NA	NA
AT4G31020	1.46	0.03327	NA	NA
AT2G25790	1.46	0.02181	SKM1	NA
AT2G45310	1.46	0.01033	GAE4	UDP-D-glucuronate 4-epimerase
AT3G14870	1.46	0.02068	NA	NA
AT5G45720	1.45	0.00914	NA	NA
AT2G19460	1.45	0.03834	NA	NA
AT5G23850	1.45	0.03241	NA	NA
AT3G51790	1.45	0.00791	AtCCME	putative transmembrane protein G1p (AtG1) mRNA, complete
AT5G39850	1.45	0.01228	NA	NA
AT1G32190	1.45	0.00380	NA	NA
AT3G17390	1.44	0.00370	MAT4	S-adenosylmethionine synthetase
AT1G68410	1.44	0.00194	NA	NA
AT4G09460	1.44	0.04046	AtMYB6	Encodes myb6 DNA-binding protein.

AT5G44060	1.44	0.01472	NA	NA
AT3G44610	1.44	0.04819	NA	NA
AT1G66350	1.44	0.01395	RGL	Negative regulator of GA responses, member of GRAS family of transcription factors. Also belongs to the DELLA proteins that restrain the cell proliferation and expansion that drives plant growth. RGL1 may be involved in reducing ROS accumulation in response to stress by up-regulating the transcription of superoxide dismutases. Rapidly degraded in response to GA. Involved in flower and fruit development.
AT5G55380	1.44	0.03606	NA	NA
AT1G26770	1.43	0.00514	AT-EXP10	Encodes an expansin. Naming convention from the Expansin Working Group (Kende et al, Plant Mol Bio). Involved in the formation of nematode-induced syncytia in roots of Arabidopsis thaliana.
AT3G17185	1.43	0.00841	NA	NA
AT1G24625	1.43	0.00581	ZFP7	Encodes a zinc finger protein containing only a single zinc finger.
AT5G44670	1.43	0.04028	GALS2	NA
AT1G14190	1.43	0.00925	NA	NA
AT3G61460	1.43	0.01205	BRH1	Encodes a novel ring finger protein and forms an N-terminal hydrophobic domain and a C-terminal RING-H2 signature. Expression is down regulated by brassinolide.
AT4G39800	1.42	0.03436	ATIPS1	** Referred to as MIPS2 in Mitsuhashi et al 2008. myo-inositol-1-phosphate synthase isoform 1.Expressed in leaf, root and silique. Immunolocalization experiments with an antibody recognizing MIPS1, MIPS2, and MIPS3 showed endosperm localization.
AT2G34770	1.42	0.04539	ATFAH1	encodes a fatty acid hydroxylase, required for the AtBI-1-mediated suppression of programmed cell death.
AT5G18070	1.42	0.02454	DRT101	encodes a novel protein involved in DNA repair from UV damage. Isolated by functional complementation of E. coli UV-sensitive mutants (UVR genes).
AT3G07470	1.42	0.00956	NA	NA
AT5G05380	1.42	0.02438	PRA1.B3	NA
AT4G18890	1.41	0.00666	BEH3	NA
AT4G24805	1.41	0.00263	NA	NA
AT2G41110	1.41	0.04010	ATCAL5	Encodes a touch-inducible calmodulin that has higher affinity to kinesin-like calmodulin binding motor protein than CAM4 or CAM6.
AT2G38610	1.41	0.00209	NA	NA
AT5G49630	1.41	0.00032	AAP6	Is a high affinity amino acid transporter capable of transporting aspartate and tryptophan. May be involved in the amino acid uptake from xylem.
AT1G55910	1.41	0.04860	ZIP11	member of Putative zinc transporter ZIP2 - like family

AT3G62420	1.41	0.00953	ATBZIP53	Encodes a group-S bZIP transcription factor. Forms heterodimers with group-C bZIP transcription factors. The heterodimers bind to the ACTCAT cis-element of proline dehydrogenase gene.
AT3G12700	1.41	0.01011	NANA	NA
AT4G31910	1.40	0.00244	BAT1	NA
AT1G69295	1.40	0.00349	PDCB4	Encodes a member of the X8-GPI family of proteins. It localizes to the plasmodesmata and is predicted to bind callose.
AT1G21980	1.40	0.00778	ATPIP5K1	Type I phosphatidylinositol-4-phosphate 5-kinase. Preferentially phosphorylates PtdIns4P. Induced by water stress and abscisic acid in Arabidopsis thaliana. Expressed in procambial cells of leaves, flowers and roots. A N-terminal Membrane Occupation and Recognition Nexus (MORN)affects enzyme activity and distribution.
AT3G13000	1.40	0.00241	NA	NA
AT2G31680	1.40	0.01115	AtRABA5d	NA
AT1G51660	1.40	0.00936	ATMEK4	Encodes a mitogen-activated map kinase kinase (there are nine in Arabidopsis) involved in innate immunity. This protein activates MPK3/MPK6 and early-defense genes redundantly with MKK5. In plants with both MKK5 and MKK6 levels reduced by RNAi plants, floral organs do not abscise suggestion a role for both proteins in mediating floral organ abscission.
AT2G34070	1.40	0.00254	TBL37	Encodes a member of the TBL (TRICHOME BIREFRINGENCE-LIKE) gene family containing a plant-specific DUF231 (domain of unknown function) domain. TBL gene family has 46 members, two of which (TBR/AT5G06700 and TBL3/AT5G01360) have been shown to be involved in the synthesis and deposition of secondary wall cellulose, presumably by influencing the esterification state of pectic polymers. A nomenclature for this gene family has been proposed (Volker Bischoff & Wolf Scheible, 2010, personal communication).
AT3G04860	1.40	0.03666	NA	NA
AT3G08630	1.39	0.01890	NA	NA
AT2G38360	1.39	0.01025	PRA1.B4	NA
AT3G06740	1.38	0.03374	GATA15	Encodes a member of the GATA factor family of zinc finger transcription factors.
AT3G13970	1.38	0.04316	APG12	NA
AT3G62630	1.38	0.01359	NA	NA
AT1G17170	1.38	0.04687	ATGSTU24	Encodes glutathione transferase belonging to the tau class of GSTs. Naming convention according to Wagner et al. (2002).
AT4G32880	1.38	0.01266	ATHB-8	member of homeodomain-leucine zipper family, acting as a differentiation-promoting transcription factor of the vascular meristems.
AT3G62660	1.38	0.00890	GATL7	Encodes a protein with putative galacturonosyltransferase activity.

AT1G57680	1.38	0.01383	Cand1	NA
AT4G34750	1.38	0.01336	SAUR49	NA
AT1G01540	1.37	0.03890	NA	NA
AT2G22680	1.37	0.03039	WAVH1	NA
AT1G76090	1.37	0.03499	SMT3	Encodes S-adenosyl-methionine-sterol-C-methyltransferase, an enzyme in the sterol biosynthetic pathway.
AT3G60390	1.37	0.04069	HAT3	Encodes homeobox protein HAT3.
AT4G27270	1.37	0.02377	NA	NA
AT2G01190	1.36	0.02255	PDE331	NA
AT4G19120	1.36	0.01167	ERD3	NA
AT2G20370	1.36	0.00478	AtMUR3	Encodes a xyloglucan galactosyltransferase located in the membrane of Golgi stacks that is involved in the biosynthesis of fucose. It is also involved in endomembrane organization. It is suggested that it is a dual-function protein that is responsible for actin organization and the synthesis of cell wall materials.
AT4G35070	1.36	0.03151	NA	NA
AT1G69690	1.36	0.03797	AtTCP15	NA
AT2G21195	1.36	0.03267	NA	NA
AT5G15150	1.36	0.04145	ATHB-3	homeobox-containing gene with an unusual feature: a leucine zipper motif adjacent to the carboxyl-terminal of the homeodomain structure. This gene is expressed primarily in the cortex of the root and the stem.
AT3G56810	1.36	0.04631	NA	NA
AT3G02070	1.36	0.02220	NA	NA
AT5G01765	1.36	0.00848	NA	NA
AT1G52290	1.36	0.02789	AtPERK15	NA
AT4G17695	1.36	0.04280	KAN3	NA
AT3G50410	1.36	0.04046	OBP1	Arabidopsis Dof protein containing a single 51-amino acid zinc finger DNA-binding domain, which may play an important roles in plant growth and development.
AT1G12580	1.35	0.00885	PEPKR1	NA
AT3G63430	1.35	0.04110	TRM5	NA
AT4G08930	1.35	0.01862	APRL6	Encodes a protein disulfide isomerase-like (PDIL) protein, a member of a multigene family within the thioredoxin (TRX) superfamily. This protein also belongs to the adenosine 5'-phosphosulfate reductase-like (APRL) group.
AT5G56170	1.35	0.00847	LLG1	NA

AT3G28455	1.35	0.03874	CLE25	Member of a large family of putative ligands homologous to the Clavata3 gene. Consists of a single exon. Can not replace CLV3 function in vivo.
AT4G22550	1.35	0.01886	LPPbeta	NA
AT3G11700	1.35	0.03074	FLA18	NA
AT1G13250	1.35	0.01399	GATL3	Encodes a protein with putative galacturonosyltransferase activity.
AT4G37890	1.35	0.04144	EDA40	NA
AT1G04040	1.35	0.04936	NA	NA
AT1G04550	1.35	0.00545	BDL	IAA12/BDL plays a role in auxin-mediated processes of apical-basal patterning in the embryo. bdl mutants lack a primary root meristem
AT2G22000	1.34	0.03624	PROPEP6	NA
AT2G46590	1.34	0.02906	DAG2	encodes a protein containing Dof zinc finger motifs. expression is limited to vascular system of the mother plant. recessive mutation is inherited as maternal-effect and expression is not detected in the embryo. mutants are defective in seed germination. mutants are more dependent on light and cold treatment and less sensitive to gibberellin during seed germination.
AT2G05940	1.34	0.01873	RIPK	NA
AT5G66200	1.34	0.00755	ARO2	Armadillo repeat protein. One of a family of four in Arabidopsis. Expressed in vegetative tissues, anthers and ovules.
AT5G19530	1.33	0.00321	ACL5	Encodes a spermine synthase. Required for internode elongation and vascular development, specifically in the mechanism that defines the boundaries between veins and nonvein regions. This mechanism may be mediated by polar auxin transport. Though ACL5 has been shown to function as a spermine synthase in E. coli, an ACL5 knockout has no effect on the endogenous levels of free and conjugated polyamines in Arabidopsis, suggesting that ACL5 may have a very specific or altogether different in vivo function.
AT3G12670	1.33	0.00477	emb2742	NA
AT3G63120	1.33	0.02138	CYCP1;1	NA
AT1G48040	1.33	0.02906	NA	NA
AT5G11970	1.33	0.00816	NA	NA
AT4G32790	1.33	0.04602	NA	NA
AT2G37940	1.33	0.01934	AtIPCS2	I
AT3G49350	1.32	0.03973	NA	NA
AT4G20170	1.32	0.04722	GALS3	NA
AT3G56800	1.32	0.01326	ACAM-3	encodes a calmodulin
AT3G61560	1.32	0.04777	NA	NA

AT4G31550	1.32	0.00490	ATWRKY11	member of WRKY Transcription Factor; Group II-d; negative regulator of basal resistance to Pseudomonas syringae.
AT3G10820	1.32	0.03499	NA	NA
AT4G32285	1.32	0.00586	NA	NA
AT5G64310	1.32	0.02574	AGP1	Encodes arabinogalactan-protein (AGP1).
AT5G45670	1.32	0.00805	NA	NA
AT4G12110	1.31	0.00936	ATSMO1-1	Encodes a member of the SMO1 family of sterol 4alpha-methyl oxidases. More specifically functions as a 4,4-dimethyl-9beta,19-cyclopropylsterol-4alpha- methyl oxidase.
AT1G78480	1.31	0.03359	NA	NA
AT1G47860	1.31	0.04776	NA	NA
AT3G17120	1.31	0.01179	NA	NA
AT2G44830	1.31	0.02770	NA	NA
AT2G34300	1.31	0.00390	NA	NA
AT4G31590	1.30	0.02377	ATCSLC05	encodes a gene similar to cellulose synthase
AT4G12130	1.30	0.03874	NA	NA
AT5G54860	1.30	0.04671	NA	NA
AT1G59710	1.30	0.00989	NA	NA
AT2G31730	1.30	0.02209	NA	NA
AT3G24530	1.30	0.02386	NA	NA
AT2G17990	1.30	0.00170	NA	NA
AT5G11000	1.30	0.01083	NA	NA
AT1G74380	1.29	0.01226	XXT5	NA
AT1G75080	1.29	0.00555	BZR1	Encodes a positive regulator of the brassinosteroid (BR) signalling pathway that mediates both downstream BR responses and negative feedback regulation of BR biosynthesis. There is evidence for phosphorylation-dependent nucleocytoplasmic shuttling of BZR1. GSK3-like kinases (including BIN2), 14-3-3 proteins, and the phosphatase BSU1 seem to participate in this process. Phosphorylation also appears to affect BZR1's transcriptional activities.
AT5G48450	1.29	0.03317	sks3	Encodes a protein with two DUF26 domains and a signal peptide for secretion. The protein is transported to the apoplast when it is expressed as a GFP fusion protein.

AT5G64740	1.29	0.03060	CESA6	Encodes a cellulose synthase isomer. CESA6 mutants have cellulose defect in the primary cell wall. Multiple lines of evidence suggest that CESA6, along with CESA1 and CESA3 are present in the same plasma membrane complex for cellulose biosynthesis. CESA2 and CESA5 are related to CESA6, having partially redundant roles. As inferred from the null role of secondary wall-type CesAs, included in a set of five primary wall-type CesAs that may support trichome cell wall thickening.
AT2G41880	1.29	0.04235	AGK1	Guanylate kinase. Involved in nucleotide metabolism.
AT3G07360	1.29	0.03232	ATPUB9	Encodes a protein containing a U-box and an ARM domain. This protein has E3 ubiquitin ligase activity based on in vitro assays.
AT2G37250	1.29	0.03359	ADK	encodes adenylate kinase that is located in the chloroplast involved in the coordination of metabolism and growth
AT2G39870	1.29	0.01819	NA	NA
AT5G01710	1.28	0.02630	NA	NA
AT5G05180	1.28	0.04605	NA	NA
AT2G33320	1.28	0.03186	NA	NA
AT5G27760	1.28	0.01028	NA	NA
AT2G41410	1.28	0.02879	NA	NA
AT2G39130	1.27	0.01189	NA	NA
AT4G00480	1.27	0.04487	ATMYC1	MYC-related protein with a basic helix-loop-helix motif at the C-terminus and a region similar to the maize B/R family at the N-terminus
AT4G08170	1.27	0.03187	NA	NA
AT1G66940	1.27	0.04291	NA	NA
AT2G41130	1.27	0.03035	NA	NA
AT5G66310	1.27	0.02830	NA	NA
AT5G03040	1.27	0.02412	iqd2	NA
AT5G60200	1.26	0.01967	TMO6	Encodes a Dof-type transcription factor.
AT4G21850	1.26	0.02387	ATMSRB9	NA
AT3G29360	1.26	0.01375	UGD2	NA
AT5G48500	1.26	0.02454	NA	NA
AT1G45688	1.25	0.03814	NA	NA
AT3G54920	1.25	0.01485	PMR6	Powdery mildew resistant mutant encodes a pectate lyase-like protein
AT1G72750	1.25	0.04145	ATTIM23-2	NA

AT4G30996	1.25	0.03282	NKS1	NA
AT3G60200	1.25	0.04768	NA	NA
AT5G05160	1.25	0.04046	RUL1	NA
AT5G09600	1.25	0.03890	SDH3-1	Encodes one of the membrane anchor subunits of the mitochondrial respiratory complex II. The protein is encoded by the nuclear genome but is imported into the mitochondrion. There are two genes that encode this protein, the other is SDH3-2.
AT5G61310	1.25	0.03124	NA	NA
AT5G65670	1.25	0.01435	IAA9	auxin (indole-3-acetic acid) induced gene
AT3G15820	1.24	0.02276	ROD1	Functions as phosphatidylcholine:diacylglycerol cholinephosphotransferase, a major reaction for the transfer of 18:1 into phosphatidylcholine for desaturation and also for the reverse transfer of 18:2 and 18:3 into the triacylglycerols synthesis pathway
AT5G26800	1.24	0.03410	NA	NA
AT1G52280	1.24	0.02975	AtRABG3d	NA
AT1G49740	1.24	0.04211	NA	NA
AT4G02290	1.24	0.04827	AtGH9B13	NA
AT1G76340	1.24	0.03449	GONST3	Encodes a nucleotide-sugar transporter.
AT2G20840	1.24	0.03186	AtSCAMP3	NA
AT1G63500	1.23	0.03874	BSK7	NA
AT4G39220	1.22	0.02688	ATRER1A	Key player of retrieval of ER membrane proteins
AT3G15040	1.22	0.03954	NA	NA
AT4G39920	1.22	0.04844	POR	Microtubule-folding cofactor, produces assembly-competent alpha-/beta-tubulin heterodimers.
AT5G13500	1.22	0.02912	NA	NA
AT2G31280	1.22	0.04041	CPUORF7	Upstream open reading frames (uORFs) are small open reading frames found in the 5' UTR of a mature mRNA, and can potentially mediate translational regulation of the largest, or major, ORF (mORF). CPuORF7 represents a conserved upstream opening reading frame relative to major ORF AT2G31280.1
AT5G55850	1.21	0.02483	NOI	NOI protein
AT5G01970	1.21	0.04350	NA	NA
AT3G13960	1.21	0.04602	AtGRF5	Growth regulating factor encoding transcription activator. One of the nine members of a GRF gene family, containing nuclear targeting domain. Involved in leaf development and expressed in root, shoot and flower.

AT1G08030	1.21	0.03698	AQC1	Encodes a tyrosylprotein sulfotransferase (TPST). This protein is a 500-aa type I transmembrane protein that shows no sequence similarity to animal TPSTs. Activity confirmed by protein expression in yeast. TPST is expressed throughout the plant body, and the highest levels of expression are in the root apical meristem. A loss-of-function mutant TPST displayed a marked dwarf phenotype accompanied by stunted roots, pale green leaves, reduction in higher order veins, early senescence, and a reduced number of flowers and siliques.
AT5G37475	1.20	0.03037	NA	NA
AT1G08010	1.20	0.01893	GATA11	Encodes a member of the GATA factor family of zinc finger transcription factors.
AT4G26480	1.18	0.03043	NA	NA
AT4G23710	1.18	0.02658	VAG2	NA
AT5G45420	1.17	0.04617	maMYB	NA
AT5G15400	0.87	0.04874	MUSE3	NA
AT1G34210	0.86	0.03808	ATSERK2	Plasma membrane LRR receptor-like serine threonine kinase expressed during embryogenesis in locules until stage 6 anthers, with higher expression in the tapetal cell layer. SERK1 and SERK2 receptor kinases function redundantly as an important control point for sporophytic development controlling male gametophyte production.
AT1G56700	0.86	0.03039	NA	NA
AT5G58440	0.86	0.04235	SNX2a	NA
AT5G16540	0.84	0.04699	ZFN3	Encodes a zinc finger protein.
AT5G21326	0.84	0.03124	CIPK26	NA
AT5G62890	0.84	0.03468	NA	NA
AT4G28610	0.84	0.03353	AtPHR1	Similar to phosphate starvation response gene from Chlamydomonas. Weakly responsive to phosphate starvation. Acts upstream of PHO2 in phosphate signaling.
AT1G68720	0.84	0.03186	ATTADA	Encodes the chloroplastic A-to-I tRNA editing enzyme.
AT5G37020	0.84	0.04211	ARF8	Encodes a member of the auxin response factor family. Mediates auxin response via expression of auxin regulated genes. Acts redundantly with ARF6 to control stamen elongation and flower maturation. Expression of ARF8 is controlled by miR167.
AT3G24040	0.84	0.02831	NA	NA
AT4G36860	0.84	0.02438	NA	NA
AT1G16320	0.84	0.03486	NA	NA
AT1G78670	0.84	0.03468	ATGGH3	NA
AT1G16680	0.84	0.04280	NA	NA

AT2G01570	0.84	0.03612	RGA	Member of the VHIID/DELLA regulatory family. Contains homopolymeric serine and threonine residues, a putative nuclear localization signal, leucine heptad repeats, and an LXXLL motif. Putative transcriptional regulator repressing the gibberellin response and integration of phytohormone signalling. DELLAs repress cell proliferation and expansion that drives plant growth. The protein undergoes degradation in response to GA via the 26S proteasome. RGA1 binds to PIF3 and inhibits its DNA binding activity and thus affects the expression of PIF3 regulated genes. RGA may be involved in reducing ROS accumulation in response to stress by up-regulating the transcription of superoxide dismutases. Represses GA-induced vegetative growth and floral initiation. Rapidly degraded in response to GA. Involved in fruit and flower development.
AT1G59580	0.83	0.04979	ATMPK2	encodes a mitogen-activated kinase involved in innate immunity
AT3G12950	0.83	0.04213	NA	NA
AT3G56590	0.83	0.02684	NA	NA
AT4G16130	0.83	0.04945	ARA1	Similar to galactokinase.
AT3G45300	0.83	0.03168	ATIVD	Encodes isovaleryl-coenzyme a dehydrogenase. Mutants have increases in 12 seed free amino acids, accumulation of seed homomethionine and 3-isovaleroyloxypropyl-glucosinolate, with a concomitant decrease in seed 3-benzoyloxypropyl-glucosinolate.
AT2G45810	0.83	0.04203	NA	NA
AT1G80790	0.82	0.04046	FDM5	NA
AT3G46540	0.82	0.01287	NA	NA
AT1G07990	0.82	0.04145	NA	NA
AT4G37440	0.82	0.03447	NA	NA
AT1G53580	0.82	0.00993	ETHE1	Mononuclear Fe(II)-containing member of the b-lactamase fold superfamily. ETHE1 is homodimeric in solution, exhibits low-level esterase activity, and specifically binds a single Fe(II) atom in the active site.
AT1G02720	0.82	0.04969	AtGATL5	Encodes a protein with putative galacturonosyltransferase activity.
AT1G73980	0.82	0.01998	NA	NA
AT1G60490	0.82	0.01882	ATVPS34	Encodes a phosphatidylinositol 3-kinase that is expressed in most plant tissues. Defects in VPS34 affect a number of cellular processes. Loss of function mutations are not transmitted through the male gametophyte due to defects in microgametogenesis therefore it is difficult to assess the effects of loss of VPS34 function in the whole plant. Involved in salt-stress responses.
AT1G10682	0.82	0.02811	NA	NA
AT1G67480	0.82	0.03114	NA	NA
AT2G22540	0.82	0.04291	AGL22	Encodes a nuclear protein that acts as a floral repressor and that functions within the thermosensory pathway. SVP represses FT expression via direct binding to the vCArG III motif in the FT promoter.

AT2G23610	0.82	0.01963	ATMES3	Encodes a protein shown to have carboxylesterase activity, methyl IAA esterase activity, and methyl jasmonate esterase activity in vitro. This protein does not act on methyl salicylate, MeGA4, or MEGA9 in vitro.
AT5G59830	0.82	0.03874	NA	NA
AT2G42490	0.82	0.02938	NA	NA
AT4G32820	0.82	0.04291	NA	NA
AT5G24520	0.82	0.03646	ATTTG1	Required for the accumulation of purple anthocyanins in leaves and stems. Involved in trichome and root hair development. Controls epidermal cell fate specification. Affects dihydroflavonol 4-reductase gene expression. It is thought that a ternary complex composed of TT2, TT8 and TTG1 is necessary for correct expression of BAN in seed endothelium. Based on clonal analysis and other methonds TTG1 has been shown to act non-cell autonomously and to move via plasmodesmata between cells.Localization and levels of TTG1 affect patterning of leaf trichomes.
AT2G33770	0.82	0.04329	ATUBC24	Encodes a ubiquitin-conjugating E2 enzyme. UBC24 mRNA accumulation is suppressed by miR399f, miR399b and miR399c. Involved in phosphate starvation response.
AT1G53910	0.82	0.01646	RAP2.12	encodes a member of the ERF (ethylene response factor) subfamily B-2 of ERF/AP2 transcription factor family (RAP2.12). The protein contains one AP2 domain. There are 5 members in this subfamily including RAP2.2 AND RAP2.12.
AT1G28320	0.82	0.03130	DEG15	Mutants in this gene are defective in the processing of pre-glyoxysomal malate dehydrogenase (pre-gMDH) to gMDH.
AT1G58110	0.82	0.02501	NA	NA
AT1G72500	0.81	0.04211	NA	NA
AT3G20930	0.81	0.03230	ORRM1	NA
AT2G36350	0.81	0.04936	NA	NA
AT2G27360	0.81	0.03486	NA	NA
AT3G44880	0.81	0.04454	ACD1	Encodes a pheide a oxygenase (PAO). Accelerated cell death (acd1) mutants show rapid, spreading necrotic responses to both virulent and avirulent Pseudomonas syringae pv. maculicola or pv. tomato pathogens and to ethylene.
AT1G31650	0.81	0.02285	ATROPGEF14	Encodes a member of KPP-like gene family, homolog of KPP (kinase partner protein) gene in tomato. Also a member of the RopGEF (guanine nucleotide exchange factor) family, containing the novel PRONE domain (plant-specific Rop nucleotide exchanger), which is exclusively active towards members of the Rop subfamily.
AT5G14370	0.81	0.04145	NA	NA
AT4G02480	0.81	0.04827	NA	NA

AT1G79970	0.81	0.03934	NA	NA
AT5G02250	0.81	0.03486	ATMTRNASEII	Encodes a exoribonuclease involved in rRNA processing in mitochondria and chloroplasts.Loss of function mutations are pale green and require supplementation with sucrose for germination and early development. Plants are pale green due to defects in chloroplast biogenesis.
AT5G55530	0.81	0.00874	NA	NA
AT5G25900	0.81	0.02619	ATKO1	Encodes a member of the CYP701A cytochrome p450 family that is involved in later steps of the gibberellin biosynthetic pathway.
AT5G07290	0.81	0.03374	AML4	AML4 A member of mei2-like gene family, predominantly plant-based family of genes encoding RNA binding proteins with characteristic presence of a highly conserved RNA binding motif first described in the mei2 gene of the fission yeast S. pombe. In silico analyses reveal nine mei2 -like genes in A. thaliana. They were grouped into four distinct clades, based on overall sequence similarity and subfamily-specific sequence elements. AML4 is a member of two sister clades of mei2-like gene family, AML1 through AML5, and belongs to the clade named ALM14. AML4 is expressed during embryo development (heart and torpedo stage) and in vegetative and floral apices.
AT3G29390	0.81	0.02748	RIK	Nuclear localized K-homology containing protein that interacts with AS1.
AT5G10960	0.81	0.03447	NA	NA
AT4G16380	0.81	0.03174	NA	NA
AT1G50840	0.81	0.04251	POLGAMMA2	DNA Polymerase gamma2. Dual targeting to mitochondria and plastids due to alternative translation initiation.
AT3G63340	0.81	0.03174	NA	NA
AT2G48110	0.81	0.04145	MED33B	Encodes a novel protein of unknown function with homologs in non-seed plants. Sequence analysis predicts membrane spanning domains and a putative protein-protein interaction domain. Semi-dominant mutations display defects in phenylpropanoid accumulation suggesting a role in phenylpropanoid metabolism.
AT2G37480	0.81	0.03318	NA	NA
AT1G60940	0.81	0.03168	SNRK2-10	encodes a member of SNF1-related protein kinases (SnRK2) whose activity is activated by ionic (salt) and non-ionic (mannitol) osmotic stress.
AT5G04290	0.81	0.03331	KTF1	Encodes SPT5-Like, a member of the nuclear SPT5 (Suppressor of Ty insertion 5) RNA polymerase (RNAP) elongation factor family that is characterized by the presence of a carboxy-terminal extension with more than 40 WG/GW motifs. Interacts with AGO4. Required for RNA-directed DNA methylation.
AT4G15840	0.80	0.03449	NA	NA

AT1G16710	0.80	0.03698	HAC12	Encodes an enzyme with histone acetyltransferase activity that can use both H3 and H4 histones as substrates. No single prior lysine acetylation is sufficient to block HAC12 acetylation of the H3 or H4 peptides, suggesting that HAC12 can acetylate any of several lysines present in the peptides.
AT4G28300	0.80	0.00791	NA	Encodes a protein with 13.6% proline amino acids that is predicted to localize to the cell wall.
AT1G54510	0.80	0.02684	ATNEK1	Encodes AtNEK1, a member of the NIMA-related serine/threonine kinases (Neks) that have been linked to cell-cycle regulation in fungi and mammals. Plant Neks might be involved in plant development processes.
AT5G24460	0.80	0.03307	NA	NA
AT3G06170	0.80	0.04145	NA	NA
AT3G63000	0.80	0.02500	NPL41	NA
AT3G48190	0.80	0.03353	ATATM	encodes a homolog of the human ATM gene, which is mutated in ataxia telangiectasia, a chromosome instability disorder. Characterization of mutants suggest a role in repairing DNA in response to ionizing radiation as well as during meiosis. The protein has kinase domains and shows kinase activity in orthologs. There is also evidence that ATM might be involved in the telomerase-independent process known as Alternative Lengthening of Telomeres.
AT1G45130	0.80	0.02000	AtBGAL5	NA
AT2G46060	0.80	0.03730	NA	NA
AT2G45620	0.80	0.01848	URT1	NA
AT1G07040	0.80	0.03187	NA	NA
AT2G37050	0.80	0.03808	NA	NA
AT3G62770	0.80	0.02780	AtATG18a	Required for autophagosome formation during nutrient deprivation and senescence.
AT3G44310	0.80	0.03124	ATNIT1	Mutants are resistant to indole-3-acetonitrile (IAN). NIT1 catalyzes the terminal activation step in indole-acetic acid biosynthesis. Predominantly expressed isoform of nitrilase isoenzyme family. Aggregation of NIT1 in cells directly abutting wound sites is one of the earliest events associated with wound and herbicide-induced cell death. The protein undergoes thiolation following treatment with the oxidant tert-butylhydroperoxide. It is also involved in the conversion of IAN to IAM (indole-3-acetamide) and other non-auxin-related metabolic processes.
AT5G12350	0.80	0.04444	NA	NA
AT1G34300	0.80	0.01949	NA	NA
AT5G25610	0.80	0.03888	ATRD22	responsive to dehydration 22 (RD22) mediated by ABA
AT3G20120	0.80	0.03039	CYP705A21	member of CYP705A
AT1G70890	0.79	0.03451	MLP43	NA

AT4G21960	0.79	0.03527	PRXR1	Encodes AT4g21960 (AT4g21960/T8O5_170).
AT1G70660	0.79	0.01262	MMZ2	MMZ2/UEV1B encodes a protein that may play a role in DNA damage responses and error-free post-replicative DNA repair by participating in lysine-63-based polyubiquitination reactions. UEV1A can form diubiquitin and triubiquitin chains in combination with UBC13A/UBC35 in vitro. It can also functionally complement an mms2 mutation in budding yeast, both by increasing mms2 mutant viability in the presence of the DNA damaging agent MMS, and by reducing the rate of spontaneous DNA mutation. However, a combination of MMZ2/UEV1B and UBC13A do not do a good job of rescuing an mms2 ubc13 double mutant in yeast. MMZ2/UEV1B transcripts are found in most plant organs, but not in the pollen or in seedlings 6 hours or 2 days post-germination. The transcript levels do not appear to be stress-inducible.
AT3G52240	0.79	0.04677	NA	NA
AT1G26150	0.79	0.03917	AtPERK10	NA
AT4G00355	0.79	0.01999	ATI2	NA
AT3G19290	0.79	0.03449	ABF4	bZIP transcription factor with specificity for abscisic acid-responsive elements (ABRE). Mediate ABA-dependent stress responses.
AT2G18960	0.79	0.04196	AHA1	Encodes a plasma membrane proton ATPase. Mutants have a reduced ability to close their stomata in response to drought and are affected in stomatal but not seed responsiveness to ABA.
AT3G01770	0.79	0.04722	ATBET10	NA
AT4G11570	0.79	0.02599	NA	NA
AT2G38970	0.79	0.03241	NA	NA
AT2G02080	0.79	0.04768	AtIDD4	NA
AT4G05320	0.79	0.03255	UBI10	One of five polyubiquitin genes in A. thaliana. These genes encode the highly conserved 76-amino acid protein ubiquitin that is covalently attached to substrate proteins targeting most for degradation. Polyubiquitin genes are characterized by the presence of tandem repeats of the 228 bp that encode a ubiquitin monomer. Induced by salicylic acid. Independent of NPR1 for their induction by salicylic acid.
AT3G26300	0.79	0.04483	CYP71B34	putative cytochrome P450
AT1G18270	0.79	0.01205	NA	NA
AT5G10770	0.79	0.03783	NA	NA
AT3G55610	0.79	0.04291	P5CS2	encodes delta 1-pyrroline-5-carboxylate synthetase B. Gene expression is induced by dehydration, high salt and ABA. Knock-out mutations in P5CS2 are embryo-lethal. P5CS2 appears to be present in different cells and/or different subcellular locations from P5CS1 in a tissue-dependent manner.
AT1G21640	0.79	0.04339	ATNADK2	Encodes a protein with NAD kinase activity. The protein was also shown to bind calmodulin.
AT3G19000	0.79	0.03432	NA	NA

AT1G07530	0.79	0.03436	ATGRAS2	Encodes a member of the GRAS family of transcription factors. The protein interacts with the TGA2 transcription factor and affects the transcription of stress-responsive genes. The protein is found in the nucleus and is also exported to the cytoplasm.
AT5G43850	0.79	0.03138	ARD4	NA
AT3G60850	0.79	0.03318	NA	NA
AT1G09010	0.79	0.03932	NA	NA
AT4G03415	0.79	0.03644	PP2C52	NA
AT3G55070	0.79	0.01432	NA	NA
AT1G25375	0.79	0.01691	NA	NA
AT3G09920	0.78	0.02658	PIP5K9	NA
AT5G64280	0.78	0.01577	DiT2.2	NA
AT3G20015	0.78	0.04510	NA	NA
AT2G31800	0.78	0.04350	NA	NA
AT4G23680	0.78	0.04016	NA	NA
AT1G78010	0.78	0.02179	NA	NA
AT5G48180	0.78	0.03834	AtNSP5	Encodes a nitrile-specifier protein NSP5. NSP5 is one out of five (At3g16400/NSP1, At2g33070/NSP2, At3g16390/NSP3, At3g16410/NSP4 and At5g48180/NSP5) A. thaliana epithiospecifier protein (ESP) homologues that promote simple nitrile, but not epithionitrile or thiocyanate formation.
AT2G35800	0.78	0.03612	SAMTL	NA
AT1G71480	0.78	0.04605	NA	NA
AT3G25840	0.78	0.01237	NA	NA
AT1G70160	0.78	0.02487	NA	NA
AT4G17940	0.78	0.00925	NA	NA
AT5G18460	0.78	0.01849	NA	NA
AT1G28310	0.78	0.03374	NA	NA
AT2G20950	0.78	0.04710	NA	NA
AT3G01180	0.78	0.03039	AtSS2	NA
AT4G13530	0.78	0.04143	NA	NA

AT2G35940	0.78	0.03938	BLH1	Encodes a member of the BEL-like homeodomain protein family. Ecotopic expression in the embryo sac leads to defects in nuclear migration and cellularization and embryo sacs with multiple egg cells. Loss of function alleles have no female gametophyte defects. The ecotopic expression phenotype requires KNAT3 because it can be suppressed by loss of KNAT3 function alleles. Localized to the nucleus but interaction with OFP1 relocates it to the cytoplasm.
AT4G36840	0.78	0.04860	NA	NA
AT4G37330	0.78	0.02646	CYP81D4	member of CYP81D
AT1G22360	0.78	0.02092	AtUGT85A2	NA
AT1G54710	0.77	0.00885	ATATG18H	NA
AT1G19650	0.77	0.03144	NA	NA
AT5G62910	0.77	0.02231	NA	NA
AT1G55350	0.77	0.02877	ATDEK1	Similar to maize DEK1, a gene encoding a membrane protein of the calpain gene superfamily required for aleurone cell development in the endosperm of maize grains. A key component of the embryonic L1 cell-layer specification pathway.
AT2G35680	0.77	0.00834	NA	NA
AT5G59430	0.77	0.03635	ATTRP1	Encodes a telomeric repeat binding protein with a DNA binding domain at its C terminus. The DNA binding domain has a preference for GGTTTAG sequences and at least five of these repeats are required for recognition by a nearly full-length TRP1 protein.
AT3G54720	0.77	0.03932	AMP1	Encodes glutamate carboxypeptidase. Various alleles show-increased cotyledon number and rate of leaf initiation, show transformation of leaves to cotyledons, altered flowering time and photomorphogenesis and an increased level of cytokinin biosynthesis. Involved in ethylene enhanced hypocotyl elongation in the light. Strong genetic interaction between TGH and AMP1.
AT1G26930	0.77	0.04926	NA	NA
AT2G15695	0.77	0.03193	NA	NA
AT1G78890	0.77	0.02438	NA	NA
AT1G71240	0.77	0.01270	NA	NA
AT1G53510	0.77	0.01765	ATMPK18	member of MAP Kinase
AT2G42600	0.77	0.02684	ATPPC2	Encodes one of four Arabidopsis phosphoenolpyruvate carboxylase proteins.
AT3G61150	0.77	0.03977	HD-GL2-1	Encodes a homeobox-leucine zipper family protein belonging to the HD-ZIP IV family.
AT2G34150	0.77	0.04539	ATRANGAP2	Encodes a member of the SCAR family.These proteins are part of a complex (WAVE) complex.The SCAR subunit activates the ARP2/3 complex which in turn act as a nucleator for actin filaments.

AT2G18915	0.77	0.01873	ADO2	encodes a member of F-box proteins that includes two other proteins in Arabidopsis (ZTL and FKF1). These proteins contain a unique structure containing a PAS domain at their N-terminus, an F-box motif, and 6 kelch repeats at their C-terminus. Overexpression results in arrhythmic phenotypes for a number of circadian clock outputs in both constant light and constant darkness, long hypocotyls under multiple fluences of both red and blue light, and a loss of photoperiodic control of flowering time. Although this the expression of this gene itself is not regulated by circadian clock, it physically interacts with Dof transcription factors that are transcriptionally regulated by circadian rhythm. LKP2 interacts with Di19, CO/COL family proteins.
AT5G42140	0.77	0.03193	NA	NA
AT5G14390	0.77	0.02368	NA	NA
AT5G14780	0.77	0.01397	FDH	Encodes a NAD-dependent formate dehydrogenase.
AT5G62350	0.77	0.03023	NA	NA
AT2G47240	0.77	0.03814	CER8	Encodes an acyl-CoA synthetase that acts on long-chain and very-long-chain fatty acids, involved in cuticular wax and cutin biosynthesis
AT5G59540	0.77	0.03778	NA	NA
AT2G29970	0.77	0.01826	SMXL7	NA
AT3G22380	0.77	0.04211	TIC	Encodes a nucleus-acting plant-specific clock regulator working close to the central oscillator and affecting the circadian gating of light responses. Circadian gating is the alteration of circadian phase according to the photoperiod of the entraining day/light cycle and the rhythmic antagonism of light responses in the early subjective night. TIC differentially regulates CCA1 and PRR9 from LHY, with LHY expression as a dominant genetic target of TIC action.
AT3G06510	0.77	0.04979	ATSFR2	Encodes a protein with beta-glucosidase activity, mutants show increased sensitivity to freezing
AT5G26230	0.77	0.04145	MAKR1	NA
AT5G24930	0.77	0.04280	ATCOL4	NA
AT5G26820	0.77	0.04526	ATIREG3	Mutations in MAR1 confer resistance, while MAR1 overexpression causes hypersensitivity to multiple aminoglycoside antibiotics. Localizes to the chloroplast envelope. MAR1 may act as a plastid transporter involved in cellular iron homeostasis.
AT2G33835	0.77	0.04454	FES1	Encodes a zinc finger domain containing protein that is expressed in the shoot/root apex and vasculature, and acts with FRI to repress flowering.FES1 mutants in a Col(FRI+) background will flower early under inductive conditions.
AT2G25070	0.77	0.02209	NA	NA
AT4G01450	0.77	0.03598	UMAMIT30	NA
AT1G72010	0.77	0.01780	NA	NA

AT2G35155	0.77	0.01118	NA	NA
AT5G51970	0.77	0.04979	NA	Encodes a putative sorbitol dehydrogenase that can be thiolated in vitro.
AT3G21690	0.77	0.01372	NA	NA
AT2G18750	0.77	0.00349	NA	NA
AT5G45800	0.77	0.00219	MEE62	NA
AT2G40460	0.76	0.04690	NA	NA
AT2G22660	0.76	0.04145	NA	NA
AT3G20640	0.76	0.04534	NA	NA
AT2G20210	0.76	0.03447	NA	NA
AT2G01950	0.76	0.00361	BRL2	Encodes a leucine rich repeat receptor kinase and associated with provascular/procambial cells. Similar to BRI, brassinosteroid receptor protein.
AT3G04760	0.76	0.02574	NA	NA
AT1G32530	0.76	0.04278	NA	NA
AT1G17200	0.76	0.02339	NA	NA
AT5G01810	0.76	0.03039	ATPK10	Encodes a CBL-interacting serine/threonine protein kinase, also has similarities to SOS2 kinase.
AT1G73950	0.76	0.02502	NA	NA
AT2G28840	0.76	0.00727	XBAT31	NA
AT1G77480	0.76	0.01399	NA	NA
AT4G13100	0.76	0.01163	NA	NA
AT2G28930	0.76	0.01205	APK1B	NA
AT4G18020	0.76	0.01262	APRR2	Encodes pseudo-response regulator 2 (APRR2) that interacts with a calcium sensor (CML9).
AT1G76890	0.76	0.03932	AT-GT2	encodes a plant trihelix DNA-binding protein
AT1G67840	0.76	0.02798	CSK	Encodes a chloroplast sensor kinase (CSK) that shares common ancestors with cyanobacterial histidine sensor kinases. CSK is synthesised in the cytosol and imported into the chloroplast as a protein precusor. CSK is autophosphorylated and required for control of transcription of chloroplast genes by the redox state of an electron carrier connecting photosystems I and II.
AT2G36895	0.76	0.04455	NA	NA
AT3G16940	0.76	0.02906	NA	NA
AT4G37300	0.76	0.04822	MEE59	NA

AT5G65970	0.76	0.01214	ATMLO10	A member of a large family of seven-transmembrane domain proteins specific to plants, homologs of the barley mildew resistance locus o (MLO) protein. The Arabidopsis genome contains 15 genes encoding MLO proteins, with localization in plasma membrane. Phylogenetic analysis revealed four clades of closely-related AtMLO genes. ATMLO10 belongs to the clade III, with AtMLO5, AtMLO7, AtMLO8, and AtMLO9. The gene is expressed in root and cotyledon vascular system, in root-shoot junction and lateral root primordia and in developing siliques, as shown by GUS activity patterns. The expression of several phylogenetically closely-related AtMLO genes showed similar or overlapping tissue specificity and analogous responsiveness to external stimuli, suggesting functional redundancy, co-function, or antagonistic function(s
AT1G69360	0.76	0.03560	NA	NA
AT5G16820	0.76	0.00361	ATHSF3	Encodes a putative transcription factor whose expression is not induced by heat but whose stable overexpression leads to expression of HSP. Required early in the stress response for transient expression of heat shock genes.
AT3G62980	0.76	0.00907	AtTIR1	Encodes an auxin receptor that mediates auxin-regulated transcription. It contains leucine-rich repeats and an F-box and interacts with ASK1, ASK2 and AtCUL1 to form SCF-TIR1, an SCF ubiquitin ligase complex. Related to yeast Grr1p and human SKP2 proteins, involved in ubiquitin-mediated processes. Required for normal response to auxin and repressed in response to flagellin. As part of the SCF complex and in the presence of auxin, TIR1 interacts with Aux/IAA transcriptional repressor proteins and mediates their degradation.
AT4G38520	0.75	0.02781	APD6	NA
AT3G51730	0.75	0.01472	NA	NA
AT3G45900	0.75	0.00506	NA	NA
AT3G09770	0.75	0.00569	AIRP3	NA
AT1G68670	0.75	0.01772	NA	NA
AT3G62700	0.75	0.02297	ABCC14	member of MRP subfamily
AT4G40060	0.75	0.01616	ATHB-16	Encodes a homeodomain leucine zipper class I (HD-Zip I) protein.
AT1G66330	0.75	0.01950	NA	NA
AT3G10250	0.75	0.02317	NA	NA
AT3G10550	0.75	0.03175	AtMTM1	Has 3'-phosphatase activity against both phosphatidylinositol-3,5-bisphosphate (PtdIns3,5P2) and Phosphatidylinositol-3-phosphate (PtdIns3P). The in vitro activity was higher with PtdIns3,5P2 than with PtdIns3P.

AT3G54140	0.75	0.04145	AtNPF8.1	Encodes a di- and tri-peptide transporter that recognizes a variety of different amino acid combinations. GFP-tagged PTR1 localizes to the plasma membrane and has 8 to 11 predicted transmembrane domains. PTR1 is expressed in a number of different vascular tissues throughout the plant based on promoter:GUS expression analysis. ptr1 mutants have a lower dry weight than wild type plants when both are grown with Pro-Ala or Ala-Ala dipeptides as their nitrogen source, suggesting that PTR1 plays a role in dipeptide uptake in the roots. Furthermore N content of ptr1 mutants is lower than that of wild type plants when grown with Pro-Ala or a mixture of dipeptides as nitrogen source
AT5G67385	0.75	0.03449	NA	NA
AT5G60890	0.75	0.01295	ATMYB34	Myb-like transcription factor that modulates expression of ASA1, a key point of control in the tryptophan pathway; mutant has deregulated expression of ASA1 in dominant allele. Loss of function allele suggests ATR1 also functions at a control point for regulating indole glucosinolate homeostasis.
AT4G37540	0.74	0.04490	LBD39	NA
AT3G58940	0.74	0.04145	NA	NA
AT3G21750	0.74	0.04350	UGT71B1	Encodes a glucosyltransferase that can attach glucose to a number of hydroxylated phenolic compounds as well as quercetins in vitro
AT1G78680	0.74	0.01262	ATGGH2	The Arabidopsis protein AtGGH2 is a gamma-glutamyl hydrolase acting specifically on monoglutamates. The enzyme is involved in the tetrahydrofolate metabolism and located to the vacuole.
AT3G46640	0.74	0.04354	LUX	Encodes a myb family transcription factor with a single Myb DNA-binding domain (type SHAQKYF) that is unique to plants and is essential for circadian rhythms, specifically for transcriptional regulation within the circadian clock. LUX is required for normal rhythmic expression of multiple clock outputs in both constant light and darkness. It is coregulated with TOC1 and seems to be repressed by CCA1 and LHY by direct binding of these proteins to the evening element in the LUX promoter.
AT3G28130	0.74	0.03449	UMAMIT44	NA
AT1G12240	0.74	0.04509	ATBETAFRUCT4	NA
AT4G39510	0.74	0.04558	CYP96A12	member of CYP96A
AT1G56460	0.74	0.00170	NA	NA
AT4G15500	0.74	0.03267	UGT84A4	Encodes a protein that might have sinapic acid:UDP-glucose glucosyltransferase activity.
AT3G14230	0.74	0.00380	RAP2.2	encodes a member of the ERF (ethylene response factor) subfamily B-2 of ERF/AP2 transcription factor family (RAP2.2). The protein contains one AP2 domain. There are 5 members in this subfamily including RAP2.2 AND RAP2.12.
AT2G39000	0.74	0.00370	NA	NA
AT3G50430	0.74	0.01026	NA	NA
AT1G33050	0.74	0.01372	NA	NA

AT5G04360	0.74	0.03612	ATLDA	Encodes an enzyme thought to be involved in the hydrolysis of the α-1,6 linkages during starch degradation in seed endosperm. However, a knockout mutant of Arabidopsis lacking limit dextrinase has normal rates of starch degradation in the leaf at night, indicating that more than one isoamylases might be involved in this process.
AT2G46370	0.74	0.00270	AtGH3.11	Encodes a jasmonate-amido synthetase that is a member of the GH3 family of proteins. JAR1 catalyzes the formation of a biologically active jasmonyl-isoleucine (JA-Ile) conjugate. JA-Ile promotes the interaction between JAZ1 and COI1 in the jasmonate signaling pathway. JAR1 localizes to the cytoplasm and is also a phytochrome A signaling component. JAR1 is an auxin-induced gene. Loss of function mutants are defective in a variety of responses to jasmonic acid. JAR1 has additional enzymatic activities in vitro, (e.g. the ability to synthesize adenosine 5'-tetraphosphate and other JA conjugates), but there are no data to show whether JAR1 catalyzes many of these reactions in vivo. JAR1 is involved in pathogen defense, sensitivity to ozone, and wound responses.
AT5G41110	0.74	0.03698	NA	NA
AT2G17640	0.74	0.04446	ATSERAT3;1	Encodes a cytosolic serine O-acetyltransferase involved in sulfur assimilation and cysteine biosynthesis. Expressed in the vascular system. Expression is induced after long-term sulfur starvation.
AT1G28100	0.74	0.03598	NA	NA
AT2G43900	0.74	0.01477	5PTase12	NA
AT3G01750	0.74	0.00224	NA	NA
AT4G05150	0.74	0.00761	NA	NA
AT5G15230	0.74	0.01108	GASA4	gibberellin-regulated (GASA4)
AT1G30320	0.74	0.04145	NA	NA
AT3G04350	0.73	0.01250	NA	NA
AT1G21590	0.73	0.02599	NA	NA
AT5G27730	0.73	0.03698	NA	NA
AT3G21760	0.73	0.02852	HYR1	Encodes HYR1, a UDP glycosyltransferase (UGT). HYR1 glucosylates hypostatin, an inhibitor of cell expansion in vivo to form a bioactive glucoside.
AT5G24165	0.73	0.01123	NA	NA
AT2G46890	0.73	0.01209	NA	NA
AT5G67420	0.73	0.02377	ASL39	NA
AT1G60800	0.73	0.01642	AtNIK3	NA
AT5G10150	0.73	0.04046	NA	NA
AT1G10600	0.73	0.02520	AMSH2	NA

AT2G19570	0.73	0.00354	AT-CDA1	Encodes a cytidine deaminase that deaminates cytidine and deoxycytidine and is competitively inhibited by cytosine-containing compounds.
AT3G56140	0.73	0.03130	NA	NA
AT2G46690	0.73	0.02380	SAUR32	NA
AT4G02920	0.73	0.00845	NA	NA
AT1G75820	0.73	0.02261	ATCLV1	Putative receptor kinase with an extracellular leucine-rich domain. Controls shoot and floral meristem size, and contributes to establish and maintain floral meristem identity. Negatively regulated by KAPP (kinase-associated protein phosphatase). CLV3 peptide binds directly CLV1 ectodomain.
AT5G04810	0.73	0.01296	NA	NA
AT5G56850	0.73	0.04316	NA	NA
AT1G08980	0.73	0.03685	AMI1	Encodes an enzyme with similarity to bacterial acylamidohydrolases and exhibits indole-3-acetamide amidohydrolase activity in vitro. This enzyme may be involved in the in vivo biosynthesis of indole-acetic acid from indole-3-acetamide, a native metabolite of A. thaliana. It appears to exist as a monomer.
AT4G27730	0.73	0.01882	ATOPT6	oligopeptide transporter
AT2G15050	0.73	0.04317	LTP	Predicted to encode a PR (pathogenesis-related) protein. Belongs to the lipid transfer protein (PR-14) family with the following members: At2g38540/LTP1, At2g38530/LTP2, At5g59320/LTP3, At5g59310/LTP4, At3g51600/LTP5, At3g08770/LTP6, At2g15050/LTP7, At2g18370/LTP8, At2g15325/LTP9, At5g01870/LTP10, At4g33355/LTP11, At3g51590/LTP12, At5g44265/LTP13, At5g62065/LTP14, At4g08530/LTP15.
AT4G20070	0.72	0.02503	AAH	The gene encoding Arabidopsis thaliana Allantoate Amidohydrolase (AtAAH)which catalyzes the allantoate deiminase reaction (EC 3.5.3.9)is expressed in all parts of the plant being consistent with a function in purine turnover in Arabidopsis.
AT4G27710	0.72	0.04380	CYP709B3	member of CYP709B
AT2G19580	0.72	0.01483	TET2	Member of TETRASPANIN family
AT2G25930	0.72	0.03130	ELF3	Encodes a novel nuclear protein that is expressed rhythmically and interacts with phytochrome B to control plant development and flowering through a signal transduction pathway. Required component of the core circadian clock regardless of light conditions.

AT3G25070	0.72	0.02879	RIN4	Encodes a member of the R protein complex and may represent a virulence target of type III pili effector proteins (virulence factors) from bacterial pathogens, which is 'guarded' by R protein complex (RPM1 and RPS2 proteins). RIN4 physically interacts with RPS2 and RPM1 in vivo. Bacterial avirulence (Avr) effectors AvrB, AvrRpm1, and AvrRpt2 induce a mobility shift in RIN4 and expression of AvrRpt2 induces rapid degradation of RIN4. RIN4 contains 2 sites for AvrRpt2 autocleavage, called RCS1 and RCS2. Overexpression of RIN4 inhibits multiple phenotypes associated with AvrRpt2 function and also inhibits PAMP-induced defense signaling. Attached to the plasma membrane at its carboxyl terminus. Cleaved by AvrRpt2 at two PxFGxW motifs, one releasing a large portion of RIN4 from the plasma membrane and both exposing amino-terminal residues that destabilized the carboxyl-terminal cleavage products by targeting them for N-end ubiquitylation and proteasomal degradation. Major virulence target of the TTSE HopF2Pto.
AT1G30330	0.72	0.00415	ARF6	Encodes a member of the auxin response factor family. Mediates auxin response via expression of auxin regulated genes. Acts redundantly with ARF8 to control stamen elongation and flower maturation. Expression of ARF6 is controlled by miR167.
AT2G24762	0.72	0.00243	AtGDU4	Encodes a member of the GDU (glutamine dumper) family proteins involved in amino acid export: At4g31730 (GDU1), At4g25760 (GDU2), At5g57685 (GDU3), At2g24762 (GDU4), At5g24920 (GDU5), At3g30725 (GDU6) and At5g38770 (GDU7).
AT1G07230	0.72	0.00509	NPC1	NA
AT5G57250	0.72	0.03449	NA	NA
AT5G61420	0.72	0.02309	AtMYB28	Encodes a nuclear localized member of the MYB transcription factor family. Involved in positive regulation of aliphatic glucosinolate biosynthesis.Expression is induced by touch, wounding and glucose.
AT5G57710	0.72	0.00822	SMAX1	NA
AT4G32980	0.72	0.00511	ATH1	Encodes transcription factor involved in photomorphogenesis. Regulates gibberellin biosynthesis. Activated by AGAMOUS in a cal-1, ap1-1 background. Expressed at low levels in developing stamens. Increased levels of ATH1 severely delay flowering in the C24 accession. Most remarkably, ectopically expressed ATH1 hardly had an effect on flowering time in the Col-0 and Ler accessions. ATH1 physically interacts with STM, BP and KNAT6 and enhances the shoot apical meristem defect of some of these genes suggesting a role in SAM maintenance. Nuclear localization is dependent upon interaction with STM.
AT1G55000	0.72	0.01372	NA	NA
AT2G15230	0.72	0.03449	ATLIP1	Lipase active on medium and short chain triacylglycerols, but not on phospho- or galactolipids. Active between pH4 and 7 with an optimum at pH6. Knock-out mutant has not obvious phenotype. Predicted to be extracellular.
AT4G02050	0.72	0.04071	STP7	NA

AT1G28580	0.72	0.00887	NA	NA
AT1G03000	0.72	0.00620	PEX6	Encodes an apparent ATPase similar to yeast and human protein required for peroxisomal biogenesis. May facilitate recycling of PEX5, the peroxisomal matrix protein receptor, and thereby promote peroxisomal matrix protein import.
AT1G11350	0.72	0.02975	CBRLK1	NA
AT1G09390	0.72	0.03116	NA	NA
AT3G15070	0.72	0.01973	NA	NA
AT2G33050	0.72	0.03792	AtRLP26	NA
AT5G18680	0.72	0.00544	AtTLP11	Member of TLP family
AT1G64270	0.72	0.04936	NA	NA
AT1G44770	0.72	0.01083	NA	NA
AT5G27150	0.72	0.00041	AT-NHX1	Encodes a vacuolar sodium/proton antiporter involved in salt tolerance, ion homeostasis, and leaf development.
AT4G37310	0.72	0.00680	CYP81H1	member of CYP81H
AT4G02710	0.72	0.00422	NET1C	NA
AT4G11320	0.72	0.01474	AtCP2	NA
AT2G36320	0.72	0.02815	NA	NA
AT4G28260	0.71	0.00380	NA	NA
AT2G24755	0.71	0.03039	NA	NA
AT1G33110	0.71	0.02611	NA	NA
AT5G64550	0.71	0.03153	NA	NA
AT1G67530	0.71	0.01613	NA	NA
AT4G25620	0.71	0.02609	NA	NA
AT1G01420	0.71	0.02584	UGT72B3	NA
AT3G16450	0.71	0.00935	JAL33	NA
AT4G01020	0.71	0.00666	NA	NA
AT5G10860	0.71	0.00539	CBSX3	NA
AT4G08290	0.71	0.01772	UMAMIT20	NA
AT1G07440	0.71	0.01691	NA	NA
AT3G16460	0.71	0.03034	JAL34	NA

AT2G26690	0.71	0.04350	AtNPF6.2	NA
AT1G19700	0.71	0.00767	BEL10	Encodes a member of the BEL family of homeodomain proteins. Its interaction with PLP (PAS/LOV PROTEIN) is diminished by blue light.
AT1G27320	0.71	0.01609	AHK3	Encodes a histidine kinases, a cytokinin receptor that controls cytokinin-mediated leaf longevity through a specific phosphorylation of the response regulator, ARR2.
AT1G22630	0.71	0.03666	NA	NA
AT2G03340	0.71	0.01118	WRKY3	Encodes WRKY DNA-binding protein 3 (WRKY3).
AT1G09530	0.71	0.02903	PAP3	Transcription factor interacting with photoreceptors phyA and phyB. Forms a ternary complex in vitro with G-box element of the promoters of LHY, CCA1. Acts as a negative regulator of phyB signalling. It degrades rapidly after irradiation of dark grown seedlings in a process controlled by phytochromes. Does not play a significant role in controlling light input and function of the circadian clockwork. Binds to G- and E-boxes, but not to other ACEs. Binds to anthocyanin biosynthetic genes in a light- and HY5-independent fashion. PIF3 function as a transcriptional activator can be functionally and mechanistically separated from its role in repression of PhyB mediated processes.
AT1G70000	0.71	0.04822	NA	NA
AT2G37450	0.70	0.02112	UMAMIT13	NA
AT1G24440	0.70	0.03932	NA	NA
AT5G11460	0.70	0.00890	NA	NA
AT2G03550	0.70	0.01905	NA	NA
AT5G38510	0.70	0.03267	NA	NA
AT3G18930	0.70	0.03193	NA	NA
AT5G65480	0.70	0.01846	CCI1	NA
AT4G13830	0.70	0.02150	DJC26	DnaJ-like protein (J20); nuclear gene
AT3G09390	0.70	0.04970	ATMT-1	metallothionein, binds to and detoxifies excess copper and other metals, limiting oxidative damage
AT5G54980	0.70	0.01517	NA	NA
AT5G58520	0.70	0.00316	NA	NA
AT5G63190	0.70	0.02415	NA	NA
AT4G16190	0.70	0.03606	NA	NA
AT3G14067	0.70	0.02684	NA	NA
AT5G25630	0.70	0.04317	NA	NA
AT5G37790	0.70	0.00482	NA	NA

AT4G02715	0.70	0.00145	NA	NA
AT1G25560	0.70	0.03449	AtTEM1	Encodes a member of the RAV transcription factor family that contains AP2 and B3 binding domains. Involved in the regulation of flowering under long days. Loss of function results in early flowering. Overexpression causes late flowering and repression of expression of FT. Novel transcriptional regulator involved in ethylene signaling. Promoter bound by EIN3. EDF1 in turn, binds to promoter elements in ethylene responsive genes.
AT1G12280	0.70	0.02688	SUMM2	NA
AT2G40110	0.70	0.00801	NA	NA
AT3G10360	0.69	0.01400	APUM4	Encodes a member of the Arabidopsis Pumilio (APUM) proteins containing PUF domain (eight repeats of approximately 36 amino acids each). PUF proteins regulate both mRNA stability and translation through sequence-specific binding to the 3' UTR of target mRNA transcripts.
AT1G42550	0.69	0.03168	PMI1	Encodes a plant-specific protein of unknown function that appears to be conserved among angiosperms.
AT4G30790	0.69	0.00817	NA	NA
AT2G23840	0.69	0.01262	NA	NA
AT3G61960	0.69	0.00450	NA	NA
AT1G55110	0.69	0.00767	AtIDD7	NA
AT5G63710	0.69	0.00607	NA	NA
AT5G46270	0.69	0.03594	NA	NA
AT5G08520	0.69	0.01875	NA	NA
AT3G30180	0.69	0.02785	BR6OX2	Encodes a cytochrome p450 enzyme that catalyzes the last reaction in the production of brassinolide. It is capable of converting 6-deoxocastasterone into castasterone, a C-6 oxidation, as well as the further conversion of castasterone into brassinolide by a Baeyer-Villinger oxidation reaction at C-6, resulting in the formation of an unusual seven-membered lactone ring. The enzyme possesses high affinity for both C28- and C27-Brassinosteroids. The expression of the gene using a CYP85A2 promoter:LUC fusion construct was shown to be under circadian and light control.
AT1G74840	0.69	0.00211	NA	NA
AT1G26560	0.69	0.00370	BGLU40	NA

AT1G22770	0.69	0.01033	FB	Together with CONSTANTS (CO) and FLOWERING LOCUS T (FT), GIGANTEA promotes flowering under long days in a circadian clock-controlled flowering pathway. GI acts earlier than CO and FT in the pathway by increasing CO and FT mRNA abundance. Located in the nucleus. Regulates several developmental processes, including photoperiod-mediated flowering, phytochrome B signaling, circadian clock, carbohydrate metabolism, and cold stress response. The gene's transcription is controlled by the circadian clock and it is post-transcriptionally regulated by light and dark. Forms a complex with FKF1 on the CO promoter to regulate CO expression.
AT3G52490	0.69	0.02377	SMXL3	NA
AT1G01430	0.69	0.01882	TBL25	Encodes a member of the TBL (TRICHOME BIREFRINGENCE-LIKE) gene family containing a plant-specific DUF231 (domain of unknown function) domain. TBL gene family has 46 members, two of which (TBR/AT5G06700 and TBL3/AT5G01360) have been shown to be involved in the synthesis and deposition of secondary wall cellulose, presumably by influencing the esterification state of pectic polymers. A nomenclature for this gene family has been proposed (Volker Bischoff & Wolf Scheible, 2010, personal communication).
AT2G41180	0.69	0.03435	SIB2	NA
AT5G13770	0.69	0.03080	NA	NA
AT2G39705	0.69	0.03953	DVL11	NA
AT1G04280	0.69	0.03598	NA	NA
AT2G33060	0.69	0.04225	AtRLP27	NA
AT2G14080	0.69	0.03094	NA	NA
AT5G35670	0.69	0.03353	iqd33	NA
AT4G05070	0.69	0.00167	NA	NA
AT3G21360	0.68	0.02639	NA	NA
AT5G13550	0.68	0.00847	SULTR4;1	Encodes a sulfate transporter.
AT5G57887	0.68	0.00483	NA	NA
AT5G18640	0.68	0.01265	NA	NA
AT4G15530	0.68	0.00683	PPDK	The product of this long transcript was shown to be targeted to the chloroplast, whereas the shorter transcript (no targeting sequence) accumulates in the cytosol. They were also found in slightly different tissues.
AT1G66140	0.68	0.02729	ZFP4	Encodes a zinc finger protein containing only a single zinc finger.
AT2G41560	0.68	0.03277	ACA4	encodes a calmodulin-regulated Ca(2+)-ATPase that improves salt tolerance in yeast. localized to the vacuole.

AT1G68130	0.68	0.00866	AtIDD14	NA
AT2G46030	0.68	0.02502	UBC6	Ubiquitin conjugating enzyme E2
AT3G16520	0.68	0.01205	UGT88A1	NA
AT4G28652	0.68	0.03267	NA	NA
AT1G64500	0.68	0.02150	NA	NA
AT1G79160	0.68	0.00451	NA	NA
AT3G13040	0.67	0.00390	NA	NA
AT3G56040	0.67	0.03027	UGP3	NA
AT1G35290	0.67	0.00345	ALT1	NA
AT3G09162	0.67	0.02603	NA	NA
AT1G03090	0.67	0.02740	MCCA	MCCA is the biotinylated subunit of the dimer MCCase, which is involved in leucine degradation. Both subunits are nuclear coded and the active enzyme is located in the mitochondrion.
AT3G45290	0.67	0.02789	ATMLO3	A member of a large family of seven-transmembrane domain proteins specific to plants, homologs of the barley mildew resistance locus o (MLO) protein. The Arabidopsis genome contains 15 genes encoding MLO proteins, with localization in plasma membrane. Phylogenetic analysis revealed four clades of closely-related AtMLO genes. ATMLO3 belongs to the clade IV, with AtMLO2, AtMLO6 and AtMLO12. The gene is expressed during early seedling growth, in primary root and lateral root primordia, in fruit abscission zone, in vascular system of cotyledons and in trichomes of young leaves,; it was not expressed in mature rosette leaves, as shown by GUS activity patterns. The expression of several phylogenetically closely-related AtMLO genes showed similar or overlapping tissue specificity and analogous responsiveness to external stimuli, suggesting functional redundancy, co-function, or antagonistic function(s).
AT5G58787	0.67	0.01267	NA	NA
AT5G64430	0.67	0.00104	NA	NA
AT1G66840	0.67	0.03267	PMI2	Encodes a coiled-coil protein WEB2 (weak chloroplast movement under blue light 2, also named PMI2/plastid movement impaired 2). Involved in chloroplast avoidance movement under intermediate and high light intensities. WEB2, together with another coiled-coil protein WEB1 (AT2G26570), maintains the chloroplast photorelocation movement velocity.
AT4G31450	0.67	0.02325	NA	NA
AT2G37460	0.67	0.01399	UMAMIT12	NA
AT3G25020	0.67	0.03046	AtRLP42	NA
AT4G37250	0.66	0.00890	NA	NA

AT1G52870	0.66	0.03803	NA	NA
AT4G31620	0.66	0.03695	NA	NA
AT2G43910	0.66	0.00679	ATHOL1	NA
AT5G59960	0.66	0.00150	NA	NA
AT2G18890	0.66	0.01724	NA	NA
AT1G25550	0.66	0.04669	NA	NA
AT3G21090	0.66	0.02455	ABCG15	NA
AT3G52540	0.66	0.03039	ATOFP18	NA
AT1G18880	0.66	0.00620	AtNPF2.9	NA
AT3G47430	0.66	0.00791	PEX11B	member of the peroxin11 (PEX11) gene family, located on the peroxisome membrane, controls peroxisome proliferation.
AT4G23890	0.66	0.00442	CRR31	NA
AT3G54990	0.66	0.03117	SMZ	Encodes a AP2 domain transcription factor that can repress flowering. SMZ and its paralogous gene, SNARCHZAPFEN (SNZ), share a signature with partial complementarity to the miR172 microRNA, whose precursor is induced upon flowering.
AT3G02910	0.66	0.03527	NA	NA
AT5G06800	0.66	0.01144	NA	NA
AT3G57190	0.66	0.04195	PrfB3	NA
AT5G01720	0.66	0.00254	NA	NA
AT2G30100	0.66	0.01969	NA	NA
AT5G65210	0.66	0.00874	TGA1	Encodes TGA1, a redox-controlled regulator of systemic acquired resistance. TGA1 targets the activation sequence-1 (as-1) element of the promoter region of defense proteins. TGA1 are S-nitrosylated.
AT5G38895	0.65	0.03318	NA	NA
AT5G27280	0.65	0.01490	NA	NA
AT3G24110	0.65	0.02454	NA	NA
AT2G45850	0.65	0.00416	AHL9	NA
AT1G58030	0.65	0.02159	CAT2	Encodes a member of the cationic amino acid transporter (CAT) subfamily of amino acid polyamine choline transporters. Localized to the tonoplast.
AT3G22104	0.65	0.00321	NA	NA
AT1G03380	0.65	0.01829	ATATG18G	NA
AT5G40670	0.65	0.00673	NA	NA

AT2G17550	0.65	0.03803	TRM26	NA
AT1G77660	0.65	0.00236	NA	NA
AT3G10910	0.65	0.01432	DAFL1	NA
AT1G56010	0.65	0.01128	anac021	Encodes a transcription factor involved in shoot apical meristem formation and auxin-mediated lateral root formation. The gene is thought not to be involved in stress responses (NaCl, auxins, ethylene). NAC1 (NAC1)
AT4G18220	0.65	0.00641	NA	NA
AT1G31770	0.65	0.00145	ABCG14	NA
AT3G05120	0.65	0.00346	ATGID1A	Encodes a gibberellin (GA) receptor ortholog of the rice GA receptor gene (OsGID1). Has GA-binding activity, showing higher affinity to GA4. Interacts with DELLA proteins in vivo in the presence of GA4. The DELLA region alone can interact with GID1A in GA-dependent manner in a Y2H assay.
AT4G34920	0.65	0.00704	NA	NA
AT5G04330	0.65	0.01562	CYP84A4	NA
AT3G47800	0.65	0.03124	NA	NA
AT5G57630	0.64	0.04455	CIPK21	CBL-interacting protein kinase
AT1G11700	0.64	0.02209	NA	NA
AT1G55020	0.64	0.02609	ATLOX1	lipoxygenase, a defense gene conferring resistance Xanthomonas campestris
AT5G62900	0.64	0.00321	NA	NA
AT3G55130	0.64	0.00340	ABCG19	Encodes a vacuole localized protein of the ABC transporter White-Brown Complex (WBC) family. When overexpressed in planta, confers resistance to kanamycin.
AT5G65040	0.64	0.03186	NA	NA
AT3G08660	0.64	0.04953	NA	NA
AT5G24120	0.64	0.00390	ATSIG5	Encodes a specialized sigma factor that functions in regulation of plastid genes and is responsible for the light-dependent transcription at the psbD LRP. Activation of SIG5 is dependent upon blue light and mediated by cryptochromes.
AT4G33150	0.64	0.03186	LKR	NA
AT2G31560	0.64	0.00946	NA	NA
AT1G77280	0.64	0.01246	NA	NA

AT1G29400	0.64	0.00762	AML5	A member of mei2-like gene family, predominantly plant-based family of genes encoding RNA binding proteins with characteristic presence of a highly conserved RNA binding motif first described in the mei2 gene of the fission yeast S. pombe. In silico analyses reveal nine mei2 -like genes in A. thaliana. They were grouped into four distinct clades, based on overall sequence similarity and subfamily-specific sequence elements. AML5 is a member of two sister clades of mei2-like gene family, AML1 through AML5, and belongs to the clade named ALM235. Among mei2-like genes, AML5 is the transcript with highest frequency of alternative splicing. Expression was detected during embryo development (heart and torpedo stage) and in vegetative and floral apices.
AT2G04690	0.64	0.00778	NA	NA
AT3G48350	0.64	0.00890	CEP3	NA
AT2G03890	0.64	0.00885	ATPI4K	Phosphoinositide kinase which undergo autophosphorylation and phosphorylate serine/threonine residues of protein substrates. Contains phosphoinositide 3/4-kinase and ubiquitin-like domains.
AT1G61590	0.64	0.02551	NA	NA
AT2G32970	0.64	0.01404	NA	NA
AT3G44970	0.63	0.00468	NA	NA
AT1G05300	0.63	0.04235	ZIP5	member of Fe(II) transporter isolog family
AT1G13260	0.63	0.04145	EDF4	Encodes an AP2/B3 domain transcription factor which is upregulated in response to low temperature. It contains a B3 DNA binding domain. It has circadian regulation and may function as a negative growth regulator.
AT4G39770	0.63	0.04117	TPPH	NA
AT1G01770	0.63	0.02068	NA	NA
AT5G39760	0.63	0.01772	AtHB23	NA
AT1G19000	0.63	0.03953	NA	NA
AT4G29110	0.63	0.01284	NA	NA
AT3G19030	0.63	0.01011	NA	NA
AT2G21560	0.63	0.00305	NA	NA
AT1G49320	0.62	0.00854	ATUSPL1	Encodes USPL1, a BURP domain protein targeted to the protein storage vacuoles. Overexpression of USPL1 affects seed development, protein storage vacuoles and lipid vesicles morphology and function.
AT2G24580	0.62	0.00511	NA	NA
AT5G27320	0.62	0.00249	ATGID1C	Encodes a gibberellin (GA) receptor ortholog of the rice GA receptor gene (OsGID1). Has GA-binding activity, showing higher affinity to GA4. Interacts with DELLA proteins in vivo in the presence of GA4.
AT2G30230	0.62	0.04446	NA	NA

AT3G05165	0.62	0.00035	NA	NA
AT2G46220	0.62	0.03486	NA	NA
AT1G76990	0.62	0.00078	ACR3	NA
AT1G70300	0.62	0.01189	KUP6	potassium transporter
AT5G58500	0.62	0.01395	LSH5	NA
AT1G47128	0.62	0.00614	RD21	cysteine proteinase precursor-like protein/ dehydration stress-responsive gene (RD21)
AT4G24015	0.62	0.00326	NA	NA
AT1G73920	0.62	0.03401	NA	NA
AT3G60690	0.62	0.03174	SAUR59	NA
AT1G49230	0.62	0.00386	AtATL78	NA
AT4G39090	0.62	0.01671	RD19	Similar to cysteine proteinases, induced by desiccation but not abscisic acid. Required for RRS1-R mediated resistance against Ralstonia solanacearum. Interacts with the R. solanacearum type III effector PopP2. RD19 associates with PopP2 to form a nuclear complex that is required for activation of the RRS1-Rmediated resistance response.
AT5G24150	0.62	0.00582	SQE5	squalene monooxygenase gene homolog
AT2G23600	0.61	0.00065	ACL	Encodes a protein shown to have carboxylesterase activity, methyl salicylate esterase activity, methyl jasmonate esterase activity, and methyl IAA esterase activity in vitro. MES2 appears to be involved in MeSA hydrolysis in planta. This protein does not act on MeGA4, or MEGA9 in vitro.
AT2G36870	0.61	0.00904	AtXTH32	NA
AT5G64570	0.61	0.00015	ATBXL4	Encodes a beta-d-xylosidase that belongs to family 3 of glycoside hydrolases.
AT3G56200	0.61	0.00145	NA	Encodes a putative amino acid transporter.
AT5G61270	0.61	0.03722	PIF7	Basic helix-loop-helix (bHLH) phytochrome interacting factor. Interacts specifically with the far-red lightabsorbing Pfr form of phyB through a conserved domain called the active phyB binding motif. Upon light exposure, PIF7 rapidly migrates to intranuclear speckles, where it colocalizes with phyB. Role as negative regulator of phyB-mediated seedling deetiolation.
AT3G16180	0.61	0.00435	NRT1.12	NA
AT1G69080	0.61	0.02089	NA	NA
AT2G45080	0.61	0.01882	cycp3;1	NA
AT1G70420	0.61	0.00492	NA	NA
AT5G44410	0.61	0.03437	NA	NA

AT2G39250	0.61	0.00034	SNZ	Encodes a AP2 domain transcription factor that can repress flowering. SNZ and its paralogous gene, SCHLAFMUTZE (SMZ), share a signature with partial complementarity to the miR172 microRNA, whose precursor is induced upon flowering.
AT2G32390	0.61	0.03449	ATGLR3.5	Encodes a ionotropic glutamate receptor ortholog, a member of a putative ligand-gated ion channel subunit family
AT1G32540	0.61	0.04260	LOL1	Encodes a protein with 3 plant-specific zinc finger domains that acts as a positive regulator of cell death.
AT3G10740	0.61	0.03311	ARAF	Encodes a bifunctional alpha-l-arabinofuranosidase/beta-d-xylosidase that belongs to family 51 of glycoside hydrolases. It may be involved in cell wall modification.
AT1G76590	0.61	0.00990	NA	NA
AT2G35170	0.61	0.00573	NA	NA
AT3G11660	0.61	0.00539	NHL1	encodes a protein whose sequence is similar to tobacco hairpin-induced gene (HIN1) and Arabidopsis non-race specific disease resistance gene (NDR1). Expression of this gene is induced by cucumber mosaic virus. Localization of the gene product is similar to that of NHL3 (plasma membrane) but it is yet inconclusive.
AT3G45680	0.61	0.00069	NA	NA
AT1G78090	0.61	0.04976	ATTPPB	homologous to the C-terminal part of microbial trehalose-6-phosphate phosphatases
AT1G02300	0.61	0.01862	NA	NA
AT4G08300	0.61	0.00284	UMAMIT17	NA
AT5G47560	0.61	0.04316	ATSDAT	Encodes a tonoplast malate/fumarate transporter.
AT5G14880	0.60	0.00372	KUP8	NA
AT3G59300	0.60	0.00249	NA	NA
AT5G13090	0.60	0.00128	NA	NA
AT5G04950	0.60	0.01169	ATNAS1	Encodes a nicotianamide synthase.
AT3G26890	0.60	0.04145	NA	NA
AT1G32090	0.60	0.02068	NA	NA
AT5G57770	0.60	0.03842	NA	NA
AT1G74900	0.60	0.04453	OTP43	NA
AT4G11460	0.60	0.03598	CRK30	Encodes a cysteine-rich receptor-like protein kinase.
AT1G62510	0.60	0.04101	NA	NA

AT2G26980	0.60	0.00353	CIPK3	encodes a serine-threonine protein kinase whose expression increases in response to abscisic acid, cold, drought, high salt, and wounding conditions. The gene is expressed in developing seeds and seedlings. Lines carrying a T-DNA insertions have reduced germination efficiency and expression of cold, high-salt, and abscisic acid marker genes are altered, but not drought-response markers.
AT1G14890	0.60	0.00568	NA	NA
AT2G27830	0.59	0.01278	NA	NA
AT2G45050	0.59	0.00041	GATA2	Encodes a member of the GATA factor family of zinc finger transcription factors.
AT4G37925	0.59	0.03486	NDH-M	Encodes subunit NDH-M of NAD(P)H:plastoquinone dehydrogenase complex (Ndh complex) present in the thylakoid membrane of chloroplasts. This subunit is thought to be required for Ndh complex assembly.
AT5G44572	0.59	0.01103	NA	NA
AT4G27470	0.59	0.00032	ATRMA3	Encodes a RING finger E3 ubiquitin ligase.
AT1G07280	0.59	0.01262	NA	NA
AT5G54080	0.59	0.00723	AtHGO	homogentisate 1,2-dioxygenase
AT2G34960	0.59	0.04413	CAT5	Encodes a member of the cationic amino acid transporter (CAT) subfamily of amino acid polyamine choline transporters. Mediates efficient uptake of Lys, Arg and Glu in a yeast system. Localized to the plasma membrane.
AT4G03510	0.59	0.00533	ATRMA1	RMA1 encodes a novel 28 kDa protein with a RING finger motif and a C-terminal membrane-anchoring domain that is involved in the secretory pathway. Has E3 ubiquitin ligase activity.
AT5G16410	0.59	0.03359	NA	NA
AT5G15860	0.59	0.00109	ATPCME	Encodes a protein with prenylcysteine methylesterase activity.
AT3G46590	0.59	0.01763	ATTRP2	Encodes a protein that specifically binds plant telomeric DNA (TTTAGGG)n repeats. Involved in bending DNA. Expressed throughout the plant with highest levels in flowers.
AT2G46550	0.59	0.04819	NA	NA
AT3G43800	0.59	0.00088	ATGSTU27	Encodes glutathione transferase belonging to the tau class of GSTs. Naming convention according to Wagner et al. (2002).
AT4G04830	0.59	0.00074	ATMSRB5	NA
AT4G02075	0.58	0.02377	PIT1	NA
AT1G07200	0.58	0.00241	SMXL6	NA
AT1G56220	0.58	0.00890	NA	NA
AT2G36970	0.58	0.00886	NA	NA

AT4G04610	0.58	0.00841	APR	Encodes a protein disulfide isomerase-like (PDIL) protein, a member of a multigene family within the thioredoxin (TRX) superfamily. This protein also belongs to the adenosine 5'-phosphosulfate reductase-like (APRL) group.
AT3G05400	0.58	0.00191	NA	NA
AT3G56080	0.58	0.01237	NA	NA
AT1G15740	0.58	0.01070	NA	NA
AT2G22890	0.57	0.03578	NA	NA
AT2G18560	0.57	0.00105	NA	NA
AT1G77990	0.57	0.00093	AST56	cDNA encoding a sulfate transporter.
AT3G50440	0.57	0.00044	ATMES10	Encodes a protein shown to have methyl jasmonate esterase activity in vitro. This protein does not act on methyl IAA, MeSA, MeGA4, or MEGA9 in vitro.
AT4G12310	0.57	0.00702	CYP706A5	member of CYP706A
AT5G20030	0.57	0.03174	NA	NA
AT5G56860	0.57	0.03594	GATA21	Encodes a member of the GATA factor family of zinc finger transcription factors.
AT1G63800	0.56	0.01829	UBC5	NA
AT1G01180	0.56	0.02742	NA	NA
AT5G11060	0.56	0.00413	KNAT4	A member of Class II KN1-like homeodomain transcription factors (together with KNAT3 and KNAT5), with greatest homology to the maize knox1 homeobox protein. Expression regulated by light. Detected in all tissues examined, but most prominent in leaves and young siliques. Transient expression of GFP translational fusion protein suggests bipartite localization in nucleus and cytoplasm. KNAT4 promoter activity showed cell-type specific pattern along longitudinal root axis; GUS expression pattern started at the elongation zone, predominantly in the phloem and pericycle cells, extending to endodermis toward the base of the root.
AT5G15830	0.56	0.01508	AtbZIP3	NA
AT5G07670	0.56	0.00112	NA	NA
AT1G77920	0.56	0.00305	TGA7	NA
AT1G80180	0.56	0.01517	NA	NA
AT1G67110	0.56	0.01319	CYP735A2	member of CYP709A
AT2G24240	0.56	0.02150	NA	NA
AT5G59780	0.56	0.00078	ATMYB59	Encodes a putative transcription factor (MYB59).
AT3G07310	0.55	0.02619	NA	NA

AT2G17730	0.55	0.01727	NIP2	Intrinsic thylakoid membrane protein that fixes RPOTmp on the stromal side of the thylakoid membrane.
AT5G65010	0.55	0.02011	ASN2	Encodes asparagine synthetase (ASN2).
AT1G19660	0.55	0.04827	AtBBD2	NA
AT3G12520	0.55	0.00035	SULTR4;2	Encodes a sulfate transporter that in induced under sulfate limitation.
AT4G35640	0.55	0.00935	ATSERAT3;2	Encodes a cytosolic serine O-acetyltransferase involved in sulfur assimilation and cysteine biosynthesis. Expressed in the vascular system. Expression is induced in both roots and shoots under sulfur-starved conditions.
AT5G58580	0.55	0.00868	ATL63	NA
AT1G32700	0.55	0.00589	NA	NA
AT4G19860	0.55	0.00443	NA	NA
AT5G53160	0.55	0.00006	PYL8	Encodes RCAR3, a regulatory component of ABA receptor. Interacts with protein phosphatase 2Cs ABI1 and ABI2. Stimulates ABA signaling.
AT2G01890	0.55	0.03834	ATPAP8	Encodes a purple acid phosphatase (PAP) belonging to the low molecular weight plant PAP group.
AT3G51910	0.55	0.03355	AT-HSFA7A	member of Heat Stress Transcription Factor (Hsf) family
AT1G22500	0.54	0.00845	AtATL15	NA
AT4G38060	0.54	0.00380	CCI2	NA
AT2G38180	0.54	0.00118	NA	NA
AT1G48260	0.54	0.03883	CIPK17	Encodes a member of the SNF1-related kinase (SnRK) gene family (SnRK3.21), which has also been reported as a member of the CBL-interacting protein kinases (CIPK17).
AT3G57520	0.54	0.04291	AtSIP2	NA
AT1G61795	0.54	0.01730	NA	NA
AT5G03995	0.54	0.00203	NA	NA
AT2G20180	0.54	0.01893	PIF1	Encodes a novel Myc-related bHLH transcription factor that has transcriptional activation activity in the dark. It is a key negative regulator of phytochrome-mediated seed germination and acts by inhibiting chlorophyll biosynthesis, light-mediated suppression of hypocotyl elongation and far-red light-mediated suppression of seed germination, and promoting negative gravitropism in hypocotyls. Light reduces this activity in a phy-dependent manner. The protein preferentially interacts with the Pfr forms of Phytochrome A (PhyA) and Phytochrome B (PhyB), is physically associated with APRR1/TOC1 and is degraded in red (R) and far-red (FR) light through the ubiquitin (ub)-26S proteasome pathway to optimize photomorphogenic development in Arabidopsis. It also negatively regulates GA3 oxidase expression.
AT1G78000	0.54	0.01399	SEL1	Encodes a sulfate transporter that can restore sulfate uptake capacity of a yeast mutant lacking sulfate transporter genes.

AT3G52360	0.53	0.00078	NA	NA
AT5G50450	0.53	0.00321	NA	NA
AT5G10030	0.53	0.00029	OBF4	Encodes a member of basic leucine zipper transcription gene family. Nomenclature according to Xiang, et al. (1997).
AT5G57180	0.53	0.00133	CIA2	Transcription regulator responsible for specific upregulation of the translocon genes atToc33 and atToc75 in leaves. Involved in protein import into chloroplast.
AT1G69440	0.53	0.00270	AGO7	Encodes ARGONAUTE7, a member of the ARGONAUTE family, characterised by the presence of PAZ and PIWI domains. Involved in the regulation of developmental timing. Required for the accumulation of TAS3 ta-siRNAs but not for accumulation of miR171, miR173, miR390 or mi391. Localized in mature rosette leaves and floral buds.
AT5G03960	0.53	0.04278	IQD12	NA
AT4G37225	0.52	0.03124	NA	NA
AT5G42680	0.52	0.00637	NA	NA
AT3G09450	0.52	0.03594	NA	NA
AT5G05690	0.52	0.00016	CBB3	Encodes a member of the CP90A family, a cytochrome P450 monooxygenase which converts 6-deoxocathasterone to 6-deoxoteasterone in the late C6 oxidation pathway and cathasterone to teasterone in the early C6 oxidation pathway of brassinolide biosynthesis. Expressed in cotyledons and leaves. Mutants display de-etiolation and derepression of light-induced genes in the dark, dwarfism, male sterility and activation of stress-regulated genes in the light. The expression of the gene using a CPD promoter:LUC fusion construct was shown to be under circadian and light control. Additionally, the circadian regulation was shown to be independent of BR levels as it remains unchanged in bri1 mutant lines. CPD appears to be involved in the autonomous pathway that regulates the transition to flowering, primarily through a BRI1-mediated signaling pathway that affects FLC expression levels, as uncovered by double mutant analyses.
AT1G25440	0.52	0.00961	BBX15	NA
AT5G01520	0.52	0.01189	AIRP2	NA
AT1G12200	0.52	0.00018	FMO	NA
AT3G29670	0.52	0.03465	PMAT2	NA

AT3G50630	0.52	0.00014	ICK2	Kip-related protein (KRP) gene, encodes CDK (cyclin-dependent kinase) inhibitor (CKI), negative regulator of cell division. A member of seven KRP genes found in Arabidopsis thaliana. Differential expression patterns for distinct KRPs were revealed by in situ hybridization. Gene was isolated from a yeast two hybrid screen as an interacting protein of CDC2A. Recombinant protein has a strong kinase inhibitor activity in vitro. Transcript is expressed in all tissues examined but is differentially distributed from ICK1. Controls the onset of the endoreduplication cycle through inhibition of CDKA;1. The KRP2 protein abundance is regulated by proteolysis through CDKB1;1 phosphorylation.
AT2G15080	0.51	0.01319	AtRLP19	NA
AT4G33666	0.51	0.03241	NA	NA
AT4G04630	0.51	0.02609	NA	NA
AT2G22200	0.51	0.00390	NA	encodes a member of the DREB subfamily A-6 of ERF/AP2 transcription factor family. The protein contains one AP2 domain. There are 8 members in this subfamily including RAP2.4.
AT3G44990	0.51	0.03241	AtXTH31	xyloglucan endo-transglycosylase
AT1G08810	0.51	0.01123	AtMYB60	putative transcription factor of the R2R3-MYB gene family. Transcript increases under conditions that promote stomatal opening (white and blue light, abi1-1 mutation) and decreases under conditions that trigger stomatal closure (ABA, desiccation, darkness), with the exception of elevated CO2. Expressed exclusively in guard cells of all tissues. It is required for light-induced opening of stomata. Mutant shows reduced stomatal aperture which helps to limit water loss during drought.
AT2G29670	0.51	0.00003	NA	NA
AT1G60590	0.51	0.00788	NA	NA
AT1G80920	0.50	0.02515	AtJ8	A nuclear encoded soluble protein found in the chloroplast stroma.
AT1G37130	0.50	0.00530	ATNR2	Identified as a mutant resistant to chlorate. Encodes nitrate reductase structural gene. Involved in nitrate assimilation. Has nitrate reductase activity. Up-regulated by the fungus P. indica. Binds transcription factor At2g35940.
AT3G13750	0.50	0.04093	BGAL1	beta-galactosidase, glycosyl hydrolase family 35
AT3G03470	0.50	0.03076	CYP89A9	member of CYP89A
AT3G52060	0.50	0.00330	AtGnTL	NA
AT1G74940	0.50	0.00035	NA	NA
AT4G19160	0.49	0.04071	NA	NA
AT1G60140	0.49	0.02584	ATTPS10	Encodes an enzyme putatively involved in trehalose biosynthesis. The protein has a trehalose synthase (TPS)-like domain that may or may not be active as well as a trehalose phosphatase (TPP)-like domain.
AT5G01820	0.49	0.00331	ATCIPK14	Encodes a CBL-interacting serine/threonine protein kinase.

AT2G17710	0.49	0.00011	NA	NA
AT1G36370	0.49	0.00001	SHM7	Encodes a putative serine hydroxymethyltransferase.
AT2G03310	0.49	0.00973	NA	NA
AT4G33960	0.48	0.00211	NA	NA
AT1G75380	0.48	0.03692	ATBBD1	Encodes a nucleases AtBBD1 involved in ABA-mediated callose deposition.
AT2G32540	0.48	0.02551	ATCSLB04	encodes a gene similar to cellulose synthase
AT5G13730	0.48	0.02879	SIG4	Encodes sigma 4 factor, involved in regulating the activity of the plastid-encoded RNA polymerase PEP. Regulates the overall quantity of NDH complexes and thus influences NDH activity.
AT4G30110	0.48	0.00145	ATHMA2	encodes a protein similar to Zn-ATPase, a P1B-type ATPases transport zinc
AT3G59010	0.48	0.01668	PME35	NA
AT1G77870	0.48	0.00791	MUB5	NA
AT5G10210	0.48	0.01540	NA	NA
AT3G22970	0.48	0.00001	NA	NA
AT2G36792	0.48	0.02059	NA	NA
AT5G39080	0.48	0.01808	NA	NA
AT2G36800	0.48	0.04316	DOGT1	Encodes a DON-Glucosyltransferase. The UGT73C5 glucosylates both brassinolide and castasterone in the 23-O position. The enzyme is presumably involved in the homeostasis of those steroid hormones hence regulating BR activity. Transgenic plants overexpressing UGT73C5 show a typical BR-deficient phenotype.
AT3G47160	0.47	0.00511	NA	NA
AT4G35750	0.47	0.00357	NA	NA
AT4G23700	0.47	0.04383	ATCHX17	member of Putative Na+/H+ antiporter family
AT2G39400	0.47	0.00903	NA	NA
AT3G29035	0.47	0.00677	ANAC059	Encodes a protein with transcription factor activity. Note: this protein (AT3G29035) on occasion has also been referred to as AtNAC3, not to be confused with the AtNAC3 found at locus AT3G15500.
AT1G31820	0.46	0.03666	PUT1	NA
AT2G30070	0.46	0.01848	ATKT1	Encodes a high affinity potassium transporter.
AT3G46130	0.46	0.00028	ATMYB48	Encodes a putative transcription factor (MYB48) that functions to regulate flavonol biosynthesis primarily in cotyledons.
AT5G65683	0.46	0.00118	WAVH2	NA
AT3G50840	0.46	0.00014	NA	NA

AT4G32940	0.45	0.00050	GAMMA-VPE		Encodes a vacuolar processing enzyme belonging to a novel group of cysteine proteinases that is expressed in vegetative organs and is upregulated in association with various types of cell death and under stressed conditions. They are essential in processing seed storage proteins and for mediating the susceptible response of toxin-induced cell death.
AT2G27420	0.45	0.00090	NA		NA
AT4G37150	0.45	0.00179	ATMES9		Encodes a protein shown to have carboxylesterase activity, methyl salicylate esterase activity, methyl jasmonate esterase activity, and methyl IAA esterase activity in vitro. MES9 appears to be involved in MeSA hydrolysis in planta. Expression of MES9 can restore systemic acquired resistance in SAR-deficient tobacco plants. This protein does not act on MeGA4, or MEGA9 in vitro.
AT2G17890	0.45	0.04145	CPK16		member of Calcium Dependent Protein Kinase
AT3G52525	0.44	0.00293	ATOFP6		NA
AT4G24050	0.44	0.00025	NA		NA
AT5G24660	0.43	0.00067	LSU2		NA
AT5G24155	0.43	0.00823	NA		NA
AT4G28270	0.43	0.00386	ATRMA2		Encodes a RING finger E3 ubiquitin ligase. Binds and ubiquitinates ABP1 in vivo and in vitro.
AT3G04060	0.43	0.02797	anac046		NA
AT5G27350	0.43	0.00074	SFP1		Encodes a sugar-porter family protein that is induced during leaf senescence. The increase in its gene expression during leaf senescence is paralleled by an accumulation of monosaccharides.
AT4G12440	0.43	0.01422	APT4		NA
AT3G21670	0.43	0.00890	AtNPF6.4		NA
AT5G44574	0.42	0.00032	NA		NA
AT5G44920	0.42	0.03449	NA		NA
AT5G23050	0.42	0.00560	AAE17		NA
AT5G19970	0.42	0.00074	NA		NA
AT1G62180	0.42	0.00000		37347	encodes a adenosine 5'-phosphosulfate reductase, involved in sulfate assimilation. Is a major effect locus for natural variation of shoot sulfate content in Arabidopsis.
AT3G16560	0.42	0.00019	NA		NA

AT4G36380	0.41	0.00001	ROT3		Encodes a cytochrome P-450 gene that is involved in leaf blade expansion by controlling polar cell expansion in the leaf length direction. Member of the CYP90C CYP450 family. ROT3 was shown to be involved in brassinosteroid biosynthesis, most likely in the conversion step of typhasterol (TY) to castasterone (CS). As 6-deoxo-CS was unable to restore the phenotype of rot3-1, it has been postulated that ROT3 might be specifically involved in the conversion of TY to CS in the C6-oxidation pathway of brassinolide. Recently, CYP90C1 was shown to catalyse the C-23 hydroxylation of several brassinosteroids (the enzyme has a broad specificity for 22-hydroxylated substrates).
AT1G21360	0.41	0.01296	GLTP2		NA
AT3G51400	0.41	0.03374	NA		NA
AT4G12320	0.40	0.01328	CYP706A6		member of CYP706A
AT3G19850	0.40	0.01123	NA		NA
AT4G11360	0.39	0.00331	RHA1B		Encodes a putative RING-H2 finger protein RHA1b.
AT1G68570	0.39	0.00074	AtNPF3.1		NA
AT1G13080	0.39	0.01025	CYP71B2		cytochrome P450 monooxygenase
AT5G56870	0.38	0.02906	BGAL4		NA
AT4G32860	0.38	0.02658	NA		NA
AT4G04435	0.37	0.00167	NA		NA
AT3G23880	0.37	0.03039	NA		NA
AT5G45650	0.37	0.00048	NA		NA
AT4G21990	0.37	0.00001		37712	Encodes a protein disulfide isomerase-like (PDIL) protein, a member of a multigene family within the thioredoxin (TRX) superfamily. This protein also belongs to the adenosine 5'-phosphosulfate reductase-like (APRL) group.
AT2G32530	0.37	0.00492	ATCSLB03		encodes a gene similar to cellulose synthase
AT1G77760	0.37	0.00607	GNR1		Encodes the cytosolic minor isoform of nitrate reductase (NR). Involved in the first step of nitrate assimilation, it contributes about 15% of the nitrate reductase activity in shoots. Similar to molybdopterin oxidoreductases at the N-terminus, and to FAD/NAD-binding cytochrome reductases at the C-terminus. Cofactors: FAD, heme iron (cytochrome B-557), and molybdenum-pterin.
AT3G52480	0.36	0.00305	NA		NA
AT3G63210	0.36	0.00000	MARD1		encodes a novel zinc-finger protein with a proline-rich N-terminus, identical to senescence-associated protein SAG102
AT3G17510	0.35	0.00330	CIPK1		Encodes a CBL-interacting protein kinase. Specifically interacts with ECT1 and ECT2.
AT1G04770	0.35	0.00001	NA		NA

AT5G41590	0.33	0.00040	NA	NA
AT1G68520	0.32	0.00078	BBX14	NA
AT3G47340	0.32	0.02879	ASN1	encodes a glutamine-dependent asparagine synthetase, the predicted ASN1 peptide contains a purF-type glutamine-binding domain, and is expressed predominantly in shoot tissues, where light has a negative effect on its mRNA accumulation. Expression is induced within 3 hours of dark treatment, in senescing leaves and treatment with exogenous photosynthesis inhibitor. Induction of gene expression was suppressed in excised leaves supplied with sugar. The authors suggest that the gene's expression pattern is responding to the level of sugar in the cell.
AT5G26220	0.31	0.01038	AtGGCT2;1	NA
AT2G40200	0.30	0.00529	NA	NA
AT4G19170	0.29	0.03039	CCD4	chloroplast-targeted member of a family of enzymes similar to nine-cis-epoxycarotenoid dioxygenase
AT3G08860	0.28	0.00014	PYD4	Encodes a protein that is predicted to have beta-alanine aminotransferase activity.
AT4G20820	0.28	0.00234	NA	NA
AT3G07425	0.27	0.02255	NA	NA
AT3G15720	0.26	0.00010	NA	NA
AT3G28270	0.26	0.04979	NA	NA
AT4G31330	0.22	0.00005	NA	NA
AT3G49580	0.22	0.00007	LSU1	NA
AT3G49570	0.18	0.00012	LSU3	NA
AT3G48360	0.18	0.03492	ATBT2	encodes a protein (BT2) that is an essential component of the TAC1-mediated telomerase activation pathway. Acts redundantly with BT3 and BT1 during female gametophyte development and with BT3 during male gametophyte development. BT2 also mediates multiple responses to nutrients, stresses, and hormones.
AT5G48850	0.12	0.00014	ATSDI1	homologous to the wheat sulphate deficiency-induced gene sdi1. Expression in root and leaf is induced by sulfur starvation. Knockout mutants retained higher root and leaf sulfate concentrations, indicating a role in regulation of stored sulfate pools.
AT1G60540	0.03	0.03646	NA	NA

Table 3: Significant differential expression of genes after 180 minutes of coumarin treatment

Gene locus	Fold change	FDR	Gene Symbol	Explanation
AT5G02865	28.55	0.01100	NA	NA
AT4G13790	20.36	0.00125	SAUR25	NA
AT2G37030	15.69	0.02695	SAUR46	NA
AT1G67265	13.94	0.00012	DVL3	NA
AT4G21745	12.07	0.00179	NA	NA
AT4G10020	10.11	0.04269	AtHSD5	Encodes a putative hydroxysteroid dehydrogenase (HSD). Genes that encode HSD include: At5g50600 and At5g50700 (HSD1), At3g47350(HSD2), At3g47360(HSD3), At5g50590 and At5g50690(HSD4), At5g50770(HSD6) (Plant Cell Physiology 50:1463). Two copies of HSD1 and HSD4 exist due to a gene duplication event. In Plant Physiology 145:87, At5g50690 is HSD7, At4g10020 is HSD5.
AT5G18010	8.13	0.00357	SAUR19	NA
AT4G30290	8.11	0.00021	ATXTH19	Encodes a xyloglucan endotransglucosylase/hydrolase with only only the endotransglucosylase (XET; EC 2.4.1.207) activity towards xyloglucan and non-detectable endohydrolytic (XEH; EC 3.2.1.151) activity. Expressed throughout both the main and the lateral root, with intensive expression at the dividing and elongating regions. Is expressed in lateral root primordia but expression ceases after lateral root begins to grow.
AT5G18050	8.10	0.01168	SAUR22	NA
AT1G29490	8.02	0.00561	SAUR68	NA
AT4G08040	7.25	0.00007	ACS11	encodes an aminotransferase that belongs to ACC synthase gene family structurally
AT5G65800	7.19	0.00974	ACS5	1-aminocyclopropane-1-carboxylate synthase (ACS) is encoded by a multigene family consisting of at least five members whose expression is induced by hormones, developmental signals, and protein synthesis inhibition.
AT5G37950	7.19	0.00255	NA	NA
AT5G66080	6.53	0.00006	APD9	NA
ATMG00580	6.37	0.04133	NAD4	NADH dehydrogenase subunit 4
AT3G03830	6.35	0.00863	SAUR28	NA
AT3G28857	6.32	0.00125	PRE5	NA
AT2G23170	6.18	0.00004	GH3.3	encodes an IAA-amido synthase that conjugates Asp and other amino acids to auxin in vitro.
AT1G52830	5.84	0.00748	IAA6	An extragenic dominant suppressor of the hy2 mutant phenotype. Also exhibits aspects of constitutive photomorphogenetic phenotype in the absence of hy2. Mutants have dominant leaf curling phenotype shortened hypocotyls and reduced apical hook. Induced by indole-3-acetic acid.

AT5G18030	5.67	0.01769	NA	NA
AT5G18020	5.56	0.02240	SAUR20	NA
AT1G29460	5.37	0.01497	SAUR65	NA
AT4G14560	5.28	0.00644	AXR5	auxin (indole-3-acetic acid) induced gene (IAA1) encoding a short-lived nuclear-localized transcriptional regulator protein.
AT5G18060	5.10	0.02435	SAUR23	NA
AT4G25420	4.91	0.00021	AT2301	Encodes gibberellin 20-oxidase that is involved in the later steps of the gibberellin biosynthetic pathway. Regulated by a circadian clock. Weak expression response to far red light.
AT4G32280	4.86	0.02419	IAA29	Auxin inducible protein.
AT3G14362	4.85	0.00133	DVL19	NA
AT2G22460	4.85	0.00373	NA	NA
AT3G15540	4.84	0.00009	IAA19	Primary auxin-responsive gene. Involved in the regulation stamen filaments development.
AT4G27260	4.69	0.00009	GH3.5	encodes an IAA-amido synthase that conjugates Asp and other amino acids to auxin in vitro. Lines carrying insertions in this gene are hypersensitive to auxin.
AT5G02760	4.68	0.00129	APD7	NA
AT1G76610	4.67	0.00006	NA	NA
AT4G21730	4.62	0.00274	NA	NA
AT5G44260	4.62	0.01162	AtTZF5	NA
AT5G66580	4.54	0.00863	NA	NA
AT3G23030	4.34	0.00859	IAA2	auxin inducible gene expressed in the nucleus
AT3G53232	4.19	0.00012	DVL20	NA
AT3G29370	4.10	0.02000	P1R3	NA
AT3G14880	4.00	0.04452	NA	NA
AT4G38850	4.00	0.00665	ATSAUR15	mRNA is rapidly induced by auxin and is very short-lived. Has been used as a reporter gene in studying auxin mutants.
AT4G21200	3.87	0.00051	ATGA2OX8	Encodes a protein with gibberellin 2-oxidase activity which acts specifically on C-20 gibberellins.
AT2G42430	3.85	0.00117	ASL18	LOB-domain protein gene LBD16. This gene contains one auxin-responsive element (AuxRE).
AT3G03840	3.82	0.00514	SAUR27	NA
AT1G29500	3.81	0.02611	SAUR66	NA

AT5G39860	3.81	0.03853	BHLH136	Encodes PRE1 (PACLOBUTRAZOL RESISTANCE1). PRE1 and IBH1 form a pair of antagonistic HLH/bHLH transcription factors that function downstream of BZR1 to mediate brassinosteroid regulation of cell elongation. BNQ1 is directly and negatively regulated by AP3 and PI in petals.Required for appropriate regulation of flowering time.
AT1G70270	3.80	0.00198	NA	NA
AT5G18560	3.76	0.00736	PUCHI	Encodes PUCHI, a member of the ERF (ethylene response factor) subfamily B-1 of ERF/AP2 transcription factor family. The protein contains one AP2 domain. There are 15 members in this subfamily including ATERF-3, ATERF-4, ATERF-7, and leafy petiole. PUCHI is required for morphogenesis in the early lateral root primordium of Arabidopsis. Expressed in early floral meristem (stage 1 to 2). Required for early floral meristem growth and for bract suppression. Triple mutant with bop1 and bop2 displays a strong defect in the determination of floral meristem identity with reduced LFY expression and the lack of AP1 expression.
AT2G39370	3.71	0.00051	MAKR4	NA
AT5G18080	3.70	0.03865	SAUR24	NA
AT4G03140	3.64	0.00132	NA	NA
AT3G14440	3.60	0.00614	ATNCED3	Encodes 9-cis-epoxycarotenoid dioxygenase, a key enzyme in the biosynthesis of abscisic acid. Regulated in response to drought and salinity. Expressed in roots, flowers and seeds. Localized to the chloroplast stroma and thylakoid membrane.
AT4G14819	3.54	0.00253	NA	NA
AT1G30100	3.37	0.00918	ATNCED5	Encodes 9-cis-epoxycarotenoid dioxygenase, a key enzyme in the biosynthesis of abscisic acid. The expression of this gene increases during the first 6h of imbibition.
AT3G25620	3.35	0.04617	ABCG21	NA
AT5G66590	3.32	0.00014	NA	NA
AT1G62440	3.32	0.00178	LRX2	encodes a paralog of LRX1 (LEUCINE-RICH REPEAT/EXTENSIN 1) which acts synergistically with LRX1 in root hair cell morphogenesis.
AT1G26945	3.32	0.00445	KDR	Encodes a basic helix-loop-helix (bHLH) protein involved in blue/far-red light signaling. Physically interacts with HFR1 and negatively regulates its activity.
AT3G23635	3.32	0.00089	RTFL13	NA
AT5G57760	3.25	0.04093	NA	NA
AT1G69570	3.17	0.03045	NA	NA
AT4G25410	3.17	0.01575	NA	NA
AT5G01740	3.14	0.00132	NA	NA
AT5G47370	3.09	0.00657	HAT2	homeobox-leucine zipper genes induced by auxin, but not by other phytohormones. Plays opposite roles in the shoot and root tissues in regulating auxin-mediated morphogenesis.

AT1G29440	3.09	0.00735	SAUR63	NA
AT1G54120	2.96	0.01025	NA	NA
AT5G37940	2.92	0.00736	NA	NA
AT5G38970	2.89	0.00066	ATBR6OX	Encodes a polypeptide involved in the C-6 oxidation of brassinosteroids. Heterologous expression of the protein in yeast conferred the ability to catalyze multiple reactions in which the C-6 position of 6-deoxocastasterone, 6-deoxotyphasterol, 3-dehydro-6-deoxoteasterone and 6-deoxoteasterone are oxidized.
AT1G67900	2.80	0.00242	NA	NA
AT1G69140	2.77	0.04230	NA	NA
AT5G52900	2.77	0.00125	MAKR6	NA
AT1G65920	2.76	0.00006	NA	NA
AT4G23070	2.76	0.04358	ATRBL7	NA
AT3G59900	2.70	0.02611	ARGOS	Encodes ARGOS (Auxin-Regulated Gene Involved in Organ Size). Inducible by auxin. Involved in lateral organ size control. Transgenic plants expressing sense or antisense ARGOS cDNA display enlarged or reduced aerial organs, respectively. The alteration in organ size is attributable mainly to changes in cell number and the duration of organ growth.
AT1G78440	2.68	0.03602	ATGA2OX1	Encodes a gibberellin 2-oxidase that acts on C19 gibberellins.
AT1G04240	2.67	0.00040	IAA3	SHY2/IAA3 regulates multiple auxin responses in roots. It is induced rapidly by IAA, and has been shown to be phosphorylated by oat phytochrome A in vitro.
AT3G42800	2.64	0.01453	NA	NA
AT1G52750	2.63	0.03010	NA	NA
AT5G57790	2.59	0.00088	NA	NA
AT1G29465	2.55	0.00644	NA	NA
AT2G05810	2.50	0.00372	NA	NA
AT1G11740	2.49	0.01012	NA	NA
AT2G42380	2.49	0.00241	ATBZIP34	Encodes a member of the BZIP family of transcription factors. Forms heterodimers with the related protein AtbZIP61. Binds to G-boxes in vitro and is localized to the nucleus in onion epidermal cells.
AT5G51790	2.49	0.00125	NA	NA
AT2G01200	2.49	0.00386	IAA32	Belongs to auxin inducible gene family.
AT4G34760	2.47	0.00272	SAUR50	NA
AT3G29575	2.44	0.00122	AFP3	NA
AT1G23060	2.44	0.00462	MDP40	NA

AT5G57785	2.44	0.00052	NA	NA
AT5G63820	2.44	0.02069	NA	NA
AT1G02850	2.42	0.00129	BGLU11	NA
AT5G03553	2.42	0.00211	NA	NA
AT4G36110	2.40	0.03921	SAUR9	NA
AT4G24275	2.39	0.00855	NA	Identified as a screen for stress-responsive genes.
AT4G22545	2.36	0.00248	NA	NA
AT3G50890	2.36	0.02424	AtHB28	NA
AT3G24715	2.35	0.00478	NA	NA
AT2G18969	2.34	0.00132	NA	NA
AT4G12410	2.34	0.04220	SAUR35	NA
AT3G25717	2.32	0.01067	DVL6	NA
AT5G54510	2.32	0.00274	DFL1	Encodes an IAA-amido synthase that conjugates Ala, Asp, Phe, and Trp to auxin. Lines overexpressing this gene accumulate IAA-ASP and are hypersensitive to several auxins. Identified as a dominant mutation that displays shorter hypocotyls in light grown plants when compared to wild type siblings. Protein is similar to auxin inducible gene from pea (GH3).
AT5G12940	2.31	0.00012	NA	NA
AT2G19660	2.30	0.03632	NA	NA
AT4G13190	2.28	0.01562	NA	NA
AT1G14185	2.25	0.01017	NA	NA
AT5G65610	2.24	0.00565	NA	NA
AT5G10430	2.23	0.03107	AGP4	Encodes arabinogalactan-protein (AGP4).
AT1G78100	2.23	0.01698	AUF1	NA
AT2G42990	2.23	0.04414	NA	NA
AT1G64660	2.20	0.01000	ATMGL	Encodes a functional methionine gamma-lyase, a cytosolic enzyme catalyzes the degradation of methionine into methanethiol, alpha-ketobutyrate and ammonia. The catabolism of excess methionine is important to methionine homeostasis.
AT5G06860	2.19	0.00142	ATPGIP1	Encodes a polygalacturonase inhibiting protein involved in defense response. PGIPs inhibit the function of cell wall pectin degrading enzymes such as those produced by fungal pathogens. PGIP1 is induced by fungal infection.
AT2G18480	2.18	0.04697	NA	NA

AT5G15580	2.17	0.00012	LNG1	Encodes LONGIFOLIA1 (LNG1). Regulates leaf morphology by promoting cell expansion in the leaf-length direction. The LNG1 homologue LNG2 (At3g02170) has similar function.
AT4G01680	2.16	0.04838	AtMYB55	Encodes a putative transcription factor (MYB55).
AT1G52565	2.15	0.01935	NA	NA
AT3G28180	2.14	0.00478	ATCSLC04	encodes a gene similar to cellulose synthase
AT3G45970	2.13	0.01479	ATEXLA1	member of EXPANSIN-LIKE. Naming convention from the Expansin Working Group (Kende et al, 2004. Plant Mol Bio)
AT5G38200	2.13	0.01694	NA	NA
AT1G13245	2.11	0.04557	DVL4	NA
AT4G38400	2.11	0.00256	ATEXLA2	member of EXPANSIN-LIKE. Naming convention from the Expansin Working Group (Kende et al, 2004. Plant Mol Bio)
AT5G50130	2.10	0.00538	NA	NA
AT1G76620	2.10	0.00812	NA	NA
AT4G16515	2.09	0.02128	CLEL	Encodes a root meristem growth factor (RGF). Belongs to a family of functionally redundant homologous peptides that are secreted, tyrosine-sulfated, and expressed mainly in the stem cell area and the innermost layer of central columella cells. RGFs are required for maintenance of the root stem cell niche and transit amplifying cell proliferation. Members of this family include: At5g60810 (RGF1), At1g13620 (RGF2), At2g04025 (RGF3), At3g30350 (RGF4), At5g51451 (RGF5), At4g16515 (RGF6), At3g02240 (RGF7), At2g03830 (RGF8) and At5g64770 (RGF9).
AT4G14550	2.07	0.03849	IAA14	IAA14 is a member of the Aux/IAA protein family. Involved in lateral root development. Gain of function mutation decreases auxin-inducible gene expression. Protein is localized to the nucleus. Expressed in stele and root tip epidermis. Functions as a negative regulator of ARF7/19.
AT2G14960	2.06	0.02124	GH3.1	encodes a protein similar to IAA-amido synthases. Lines carrying an insertion in this gene are hypersensitive to auxin.
AT5G65340	2.04	0.00213	NA	NA
AT5G43700	2.03	0.00182	ATAUX2-11	Auxin inducible protein similar to transcription factors.
AT2G14900	2.02	0.00918	NA	NA
AT4G30180	2.02	0.01694	NA	NA
AT1G48330	2.02	0.00125	NA	NA
AT5G54530	2.01	0.00328	NA	NA
AT1G36940	2.01	0.00126	NA	NA
AT3G13520	2.00	0.00242	AGP12	Encodes a GPI-anchored arabinogalactan (AG) peptide with a short 'classical' backbone of 10 amino acids, seven of which are conserved among the 4 other Arabidopsis AG peptides. These peptides may be involved in cell signaling.

AT2G39450	2.00	0.00014	ATMTP11	Encodes a Golgi-localized manganese transporter that is involved in Mn tolerance. When expressed into yeast cells, this gene confer Mn²⁺ and Cu²⁺ tolerance.
AT5G65613	2.00	0.01583	NA	NA
AT5G59010	1.99	0.00193	BSK5	NA
AT3G54030	1.99	0.00008	BSK6	NA
AT1G76240	1.99	0.03061	NA	NA
AT3G28340	1.99	0.02435	GATL10	Encodes a protein with putative galacturonosyltransferase activity.
AT3G27500	1.99	0.02240	NA	NA
AT1G12080	1.98	0.02010	NA	NA
AT3G23050	1.98	0.00011	AXR2	Transcription regulator acting as repressor of auxin-inducible gene expression. Plays role in the control of gravitropic growth and development in light-grown seedlings. Auxin induces the degradation of the protein in a dosage-dependent manner in a process mediated by AtRac1. Auxin induced the relocalization of the protein within the nucleus from a diffused nucleoplasmic pattern to a discrete particulated pattern named nuclear protein bodies or NPB in a process also mediated by Rac1. Colocalizes with SCF, CSN and 26S proteasome components.
AT5G41400	1.95	0.04297	NA	NA
AT5G43190	1.95	0.00047	NA	NA
AT1G11120	1.95	0.00156	NA	NA
AT5G49630	1.95	0.00001	AAP6	Is a high affinity amino acid transporter capable of transporting aspartate and tryptophan. May be involved in the amino acid uptake from xylem.
AT5G06930	1.94	0.01804	NA	NA
AT4G22780	1.91	0.00193	ACR7	Member of a family of ACT domain containing proteins . ACT domains are involved in amino acid binding .
AT3G13980	1.91	0.04065	NA	NA
AT4G25260	1.91	0.02637	NA	NA
AT1G05680	1.90	0.01529	UGT74E2	Encodes a UDP-glucosyltransferase, UGT74E2, that acts on IBA (indole-3-butyric acid) and affects auxin homeostasis. The transcript and protein levels of this enzyme are strongly induced by H2O2 and may allow integration of ROS (reactive oxygen species) and auxin signaling. This enzyme can also transfer glycosyl groups to several compounds related to the explosive TNT when this synthetic compound is taken up from the environment.
AT1G51170	1.90	0.00105	AGC2-3	NA
AT1G78970	1.90	0.00041	ATLUP1	Lupeol synthase. Converts oxidosqualene to multiple triterpene alcohols and a triterpene diols. This conversion proceeds through the formation of a 17β-dammarenyl cation.

AT1G04250	1.90	0.00007	AXR3	Transcription regulator acting as repressor of auxin-inducible gene expression. Auxin-inducible AUX/IAA gene. Short-lived nuclear protein with four conserved domains. Domain III has homology to beta alpha alpha dimerization and DNA binding domains. Involved in auxin signaling. Auxin induces the degradation of the protein in a dosage-dependent manner in a process mediated by AtRac1. Auxin induced the relocalization of the protein within the nucleus from a diffused nucleoplasmic pattern to a discrete particulated pattern named nuclear protein bodies or NPB in a process also mediated by Rac1. Colocalizes with SCF, CSN and 26S proteasome components.
AT3G58120	1.90	0.01591	ATBZIP61	Encodes a member of the BZIP family of transcription factors. Forms heterodimers with the related protein AtbZIP34. Binds to G-boxes in vitro and is localized to the nucleus in onion epidermal cells.
AT5G65390	1.89	0.04422	AGP7	NA
AT3G12610	1.89	0.00271	DRT100	Plays role in DNA-damage repair/toleration. Partially complements RecA- phenotypes.
AT1G08500	1.89	0.00622	AtENODL18	NA
AT4G37390	1.89	0.00014	AUR3	Encodes an IAA-amido synthase that conjugates Asp and other amino acids to auxin in vitro. Lines carrying insertions in this gene are hypersensitive to auxin. May function as a negative component in auxin signaling by regulating auxin activity.
AT1G75500	1.88	0.00019	UMAMIT5	An Arabidopsis thaliana homolog of Medicago truncatula NODULIN21 (MtN21). The gene encodes a plant-specific, predicted integral membrane protein and is a member of the Plant-Drug/Metabolite Exporter (P-DME) family (Transporter Classification number: TC 2.A.7.3).
AT1G11000	1.88	0.00075	ATMLO4	A member of a large family of seven-transmembrane domain proteins specific to plants, homologs of the barley mildew resistance locus o (MLO) protein. The Arabidopsis genome contains 15 genes encoding MLO proteins, with localization in plasma membrane. Phylogenetic analysis revealed four clades of closely-related AtMLO genes. ATMLO4 belongs to the clade I, with AtMLO11 and AtMLO14. The gene is expressed during early seedling growth, in roots and lateral root primordia, in flower and fruit abscission zone, in vascular system of root, cotyledons and young leaves, it was not expressed in mature rosette leaves, as shown by GUS activity patterns. The expression of several phylogenetically closely-related AtMLO genes showed similar or overlapping tissue specificity and analogous responsiveness to external stimuli, suggesting functional redundancy, co-function, or antagonistic function(s).
AT3G13310	1.87	0.04551	DJC66	NA
AT3G18200	1.86	0.03849	UMAMIT4	NA

AT3G14370	1.85	0.00857	WAG2	The WAG2 and its homolog, WAG1 each encodes protein-serine/threonine kinase that are nearly 70% identical to PsPK3 protein. All three together with CsPK3 belong to PsPK3-type kinases. At the N-terminus, all four possess a serine/threonine-rich domain. They are closely related to Arabidopsis kinases PINOID. wag1/wag2 double mutants exhibit a pronounced wavy root phenotype when grown vertically on agar plates (while wild-type plants develop wavy roots only on plates inclined to angles less than 90 degrees), indicating an overlapping role for WAG1 and WAG2 as suppressors of root waving. Simultaneous disruption of PID(AT2G34650) and its 3 closest homologs (PID2/AT2G26700, WAG1/AT1G53700, and WAG2/AT3G14370) abolishes the formation of cotyledons.
AT1G29660	1.84	0.01096	NA	NA
AT5G45280	1.83	0.00056	NA	NA
AT4G17460	1.82	0.00748	HAT1	Encodes homeobox protein HAT1.
AT2G28350	1.82	0.00235	ARF10	Involved in root cap cell differentiation.
AT2G41170	1.82	0.00114	NA	NA
AT4G13195	1.82	0.03139	CLE44	Belongs to a large gene family, called CLE for CLAVATA3/ESR-related, encoding small peptides with conserved carboxyl termini. The C-terminal 12 amino acid sequence of CLE44 is identical to that of a dodeca peptide (TDIF, tracheary element differentiation inhibitory factor) isolated from Arabidopsis and functions as a suppressor of plant stem cell differentiation. TDIF sequence is also identical to the C-terminal 12 amino acids of CLE41 (At3g24770).
AT4G30410	1.82	0.00105	NA	NA
AT3G07010	1.81	0.01100	NA	NA
AT5G15265	1.80	0.04322	NA	NA
AT4G00050	1.78	0.00633	UNE10	NA
AT1G15550	1.78	0.00538	ATGA3OX1	Involved in later steps of the gibberellic acid biosynthetic pathway. Activated by AGAMOUS in a cal-1, ap1-1 background. Deletion of 208 bp from -1016 to -809 (Δ-808) resulted in loss of GA-negative feedback (this sequence, which contains a 43-bp sequence GNFEI, was shown to be sufficient for GA-negative feedback).
AT5G25440	1.78	0.02427	NA	NA
AT2G26710	1.77	0.04220	BAS1	Encodes a member of the cytochrome p450 family that serves as a control point between multiple photoreceptor systems and brassinosteroid signal transduction. Involved in brassinolide metabolism. Mediates response to a variety of light signals including hypocotyl elongation and cotyledon expansion.
AT3G30180	1.77	0.00244	BR6OX2	Encodes a cytochrome p450 enzyme that catalyzes the last reaction in the production of brassinolide. It is capable of converting 6-deoxocastasterone into castasterone, a C-6 oxidation, as well as the further conversion of castasterone into brassinolide by a Baeyer-Villinger oxidation reaction at C-6, resulting in the formation of an unusual seven-membered lactone ring. The enzyme possesses high affinity for both C28- and C27-Brassinosteroids. The expression of the gene using a CYP85A2 promoter:LUC fusion construct was shown to be under circadian and light control.
AT5G60860	1.77	0.00047	AtRABA1f	NA

AT1G13670	1.76	0.00501	NA	NA
AT2G36220	1.76	0.00406	NA	NA
AT3G50280	1.76	0.01570	NA	NA
AT4G13180	1.76	0.00235	NA	NA
AT4G09890	1.75	0.00125	NA	NA
AT1G59740	1.75	0.04503	AtNPF4.3	NA
AT4G14548	1.75	0.03778	NA	NA
AT1G70940	1.75	0.00256	ATPIN3	A regulator of auxin efflux and involved in differential growth. PIN3 is expressed in gravity-sensing tissues, with PIN3 protein accumulating predominantly at the lateral cell surface. PIN3 localizes to the plasma membrane and to vesicles. In roots, PIN3 is expressed without pronounced polarity in tiers two and three of the columella cells, at the basal side of vascular cells, and to the lateral side of pericycle cells of the elongation zone. PIN3 overexpression inhibits root cell growth. Protein phosphorylation plays a role in PIN3 trafficking to the plasma membrane.
AT5G22860	1.75	0.00193	NA	NA
AT5G03150	1.74	0.01535	JKD	JKD is a nuclear-localized putative transcription factor with three zinc finger domains. jkd mutants show a number of root patterning defects including ectopic periclinal divisions in the cortex, increased cell numbers in the cortical and epidermal layers, a disrupted QC marker expression pattern, and disorganized QC and columella cells. jkd mutants also have a reduced number of meristematic cells in their roots. JKD can interact with the SCR and SHR proteins implicated in root patterning, as well as another zinc finger transcription factor, MAGPIE. All of these interactions require the first zinc finger in JKD according to a Y2H assay. There are also transcriptional interactions among these proteins. The initiation of JKD transcription does not appear to depend on SCR and SHR, but later expression in the post-embryonic QC cells and ground tissue initials is reduced in scr and shr mutants. JKD also appears to be required for SCR transcription beginning in the embryo. There is also some evidence that JKD plays a role in promoting the movement of SHR into the nucleus, particularly in QC cells, but this may be indirect.
AT4G09970	1.74	0.00102	NA	NA
AT3G23170	1.74	0.01318	NA	NA
AT2G35880	1.73	0.00386	NA	NA
AT1G75590	1.73	0.03267	SAUR52	NA
AT5G51670	1.73	0.00664	NA	NA
AT4G39390	1.73	0.00016	ATNST-KT1	Encodes a golgi localized nucleotide sugar transporter.
AT5G48150	1.72	0.00012	PAT1	Member of GRAS gene family. Semi-dominant mutant has a reduced response to far-red light and appears to act early in the phytochrome A signaling pathway.
AT1G75880	1.72	0.03061	NA	NA

AT2G41820	1.72	0.00011	PXC3	NA
AT5G17490	1.72	0.01548	AtRGL3	DELLA subfamily member involved in GA signal transduction
AT4G31000	1.71	0.00663	NA	NA
AT4G32460	1.71	0.02128	NA	NA
AT2G47130	1.71	0.02448	AtSDR3	NA
AT5G64780	1.71	0.00989	NA	NA
AT3G22820	1.70	0.03411	CLL1	NA
AT3G49220	1.70	0.03848	NA	NA
AT3G13970	1.69	0.00275	APG12	NA
AT3G55720	1.69	0.02408	NA	NA
AT3G05880	1.69	0.03948	RCI2A	Induced by low temperatures, dehydration and salt stress and ABA. Encodes a small (54 amino acids), highly hydrophobic protein that bears two potential transmembrane domains.
AT5G48900	1.69	0.00501	NA	NA
AT1G13970	1.68	0.01017	NA	NA
AT5G64770	1.68	0.00565	CLEL	Encodes a root meristem growth factor (RGF). Belongs to a family of functionally redundant homologous peptides that are secreted, tyrosine-sulfated, and expressed mainly in the stem cell area and the innermost layer of central columella cells. RGFs are required for maintenance of the root stem cell niche and transit amplifying cell proliferation. Members of this family include: At5g60810 (RGF1), At1g13620 (RGF2), At2g04025 (RGF3), At3g30350 (RGF4), At5g51451 (RGF5), At4g16515 (RGF6), At3g02240 (RGF7), At2g03830 (RGF8) and At5g64770 (RGF9).
AT1G66350	1.68	0.00256	RGL	Negative regulator of GA responses, member of GRAS family of transcription factors. Also belongs to the DELLA proteins that restrain the cell proliferation and expansion that drives plant growth. RGL1 may be involved in reducing ROS accumulation in response to stress by up-regulating the transcription of superoxide dismutases. Rapidly degraded in response to GA. Involved in flower and fruit development.
AT2G14890	1.68	0.00213	AGP9	putative proline-rich protein (At2g14890) mRNA, complete
AT3G07000	1.67	0.04936	NA	NA
AT3G23640	1.67	0.00147	HGL1	NA
AT4G26140	1.66	0.01252	BGAL12	putative beta-galactosidase

AT1G14920	1.66	0.00946	GAI	Similar to a putative transcription factor and transcriptional coactivators. Repressor of GA responses and involved in gibberellic acid mediated signaling. Member of the DELLA proteins that restrain the cell proliferation and expansion that drives plant growth. The protein undergoes degradation in response to GA via the 26S proteasome. GAI may be involved in reducing ROS accumulation in response to stress by up-regulating the transcription of superoxide dismutases. Represses GA-induced vegetative growth and floral initiation. Rapidly degraded in response to GA.
AT2G26700	1.66	0.00132	PID2	Encodes PID2, a homolog of PID. Simultaneous disruption of PID(AT2G34650) and its 3 closest homologs (PID2/AT2G26700, WAG1/AT1G53700, and WAG2/AT3G14370) abolishes the formation of cotyledons.
AT1G32170	1.66	0.00478	XTH30	xyloglucan endotransglycosylase-related protein (XTR4)
AT5G10100	1.66	0.00313	TPPI	NA
AT2G04570	1.65	0.03116	NA	NA
AT5G55380	1.65	0.01184	NA	NA
AT1G12990	1.64	0.00293	NA	NA
AT2G42800	1.64	0.04157	AtRLP29	NA
AT1G63420	1.64	0.00373	NA	NA
AT4G39400	1.64	0.00213	ATBRI1	Encodes a plasma membrane localized leucine-rich repeat receptor kinase involved in brassinosteroid signal transduction. BRI1 ligand is brassinolide which binds at the extracellular domain. Binding results in phosphorylation of the kinase domain which activates the BRI1 protein leading to BR responses. Residue T-1049 and either S-1044 or T-1045 were essential for kinase function in vitro and normal BRI1 signaling in planta. Although BAK1 and BRI1 alone localize in the plasma membrane, when BAK1 and BRI1 are coexpressed, the heterodimer BAK1/BRI1 they form is localized in the endosome. BRI1 appears to be involved in the autonomous pathway that regulates the transition to flowering, primarily through its effects on FLC expression levels, as uncovered by double mutant analyses. This most likely occurs as a result of BRI1-dependent effects on histone acetylation, but not histone triMeH3K4 methylation, at the FLC locus.
AT5G66800	1.64	0.00117	NA	NA
AT3G17050	1.63	0.03061	NA	NA
AT5G57050	1.63	0.01546	ABI2	Encodes a protein phosphatase 2C and is involved in ABA signal transduction. Binds fibrillin preprotein in vitro and in vivo.
AT3G13965	1.63	0.01207	NA	NA
AT1G72230	1.63	0.00019	NA	NA
AT1G14390	1.63	0.04496	NA	NA
AT5G09970	1.63	0.00289	CYP78A7	member of CYP78A

AT1G25425	1.63	0.00562	CLE43	NA
AT1G23080	1.63	0.03147	ATPIN7	Encodes a novel component of auxin efflux that is located apically in the basal cell and is involved during embryogenesis in setting up the apical-basal axis in the embryo. It is also involved in pattern specification during root development. In roots, it is expressed at lateral and basal membranes of provascular cells in the meristem and elongation zone, whereas in the columella cells it coincides with the PIN3 domain. Plasma membrane-localized PIN proteins mediate a saturable efflux of auxin. PINs mediate auxin efflux from mammalian and yeast cells without needing additional plant-specific factors. The action of PINs in auxin efflux is distinct from PGPs, rate-limiting, specific to auxins and sensitive to auxin transport inhibitors. PINs are directly involved of in catalyzing cellular auxin efflux.
AT2G43290	1.63	0.00717	MSS3	Encodes calmodulin-like MSS3.
AT3G04730	1.62	0.01223	IAA16	early auxin-induced (IAA16)
AT1G05420	1.62	0.01587	ATOFP12	NA
AT1G23030	1.62	0.01769	NA	NA
AT4G35060	1.61	0.00975	HIPP25	NA
AT5G08790	1.61	0.01583	anac081	induced by wounding, belongs to a large family of putative transcriptional activators with NAC domain.
AT1G12845	1.60	0.02182	NA	NA
AT1G02816	1.60	0.01789	NA	NA
AT1G11545	1.59	0.04697	XTH8	NA
AT3G16360	1.59	0.01264	AHP4	Encodes AHP4, a histidine-containing phosphotransmitter involved in Histidine (His)-to-Aspartate (Asp) phosphorelay signal transduction. AHP4 is one of the six Arabidopsis thaliana histidine phosphotransfer proteins (AHPs). AHPs function as redundant positive regulators of cytokinin signaling. Members of the AHP gene family include: AT3G21510 (AHP1), AT3G29350 (AHP2), AT5G39340 (AHP3), AT3G16360 (AHP4), AT1G03430 (AHP5) and AT1G80100 (AHP6).
AT2G01420	1.59	0.03909	ATPIN4	Encodes a putative auxin efflux carrier that is localized in developing and mature root meristems. It is involved in the maintenance of embryonic auxin gradients. A role for AtPIN4 in generating a sink for auxin below the quiescent center of the root meristem that is essential for auxin distribution and patterning is proposed. In the root, PIN4 is detected around the quiescent center and cells surrounding it, and localizes basally in provascular cells. PIN4 expression is upregulated in brassinosteroid-insensitive mutant (PMID 16141452).
AT4G19120	1.58	0.00129	ERD3	NA
AT3G63470	1.58	0.01000	scpl40	NA
AT1G54200	1.57	0.00132	NA	NA
AT1G49780	1.57	0.00717	PUB26	NA

AT3G28420	1.57	0.01489	NA	NA
AT5G27000	1.57	0.00261	ATK4	Encodes a kinesin-like protein that binds microtubules in an ATP-dependent manner.
AT5G23870	1.56	0.02435	NA	NA
AT3G10720	1.56	0.03853	NA	NA
AT2G46640	1.56	0.02427	TAC1	NA
AT5G54500	1.56	0.00054	FQR1	Encodes a flavin mononucleotide-binding flavodoxin-like quinone reductase that is a primary auxin-response gene.
AT1G63300	1.55	0.03848	NA	NA
AT3G13650	1.55	0.00333	NA	NA
AT5G44670	1.55	0.02207	GALS2	NA
AT3G44610	1.55	0.02435	NA	NA
AT3G06770	1.55	0.04452	NA	NA
AT5G11740	1.54	0.00501	AGP15	Encodes arabinogalactan protein (AGP15).
AT4G30270	1.54	0.04384	MERI-5	encodes a protein similar to endo xyloglucan transferase in sequence. It is also very similar to BRU1 in soybean, which is involved in brassinosteroid response.
AT1G61170	1.54	0.04019	NA	NA
AT4G22560	1.53	0.03581	NA	NA
AT3G60260	1.53	0.00180	NA	NA
AT4G39800	1.52	0.01890	ATIPS1	** Referred to as MIPS2 in Mitsuhashi et al 2008. myo-inositol-1-phosphate synthase isoform 1.Expressed in leaf, root and silique. Immunolocalization experiments with an antibody recognizing MIPS1, MIPS2, and MIPS3 showed endosperm localization.
AT5G08130	1.52	0.00235	BIM1	Arabidopsis thaliana basic helix-loop-helix (bHLH) family protein involved in brassinosteroid signaling. It synergistically interacts with BES1 to bind to E box sequences (CANNTG).
AT1G75450	1.52	0.04609	ATCKX5	This gene used to be called AtCKX6. It encodes a protein whose sequence is similar to cytokinin oxidase/dehydrogenase, which catalyzes the degradation of cytokinins.
AT4G26690	1.52	0.01464	GDPDL3	Glycerophosphoryl diester phosphodiesterase-like protein involved in cell wall cellulose accumulation and pectin linking. Impacts root hair, trichome and epidermal cell development.
AT5G06870	1.52	0.00222	ATPGIP2	Encodes a polygalacturonase inhibiting protein involved in plant defense response. PGIPs inhibit the activity of pectin degrading enzymes such as those produced by fungal pathogens. PGIP2 is induced by fungal infection and methyl jasmonate.
AT5G03760	1.52	0.00435	ATCSLA09	encodes a beta-mannan synthase that is required for agrobacterium-mediated plant genetic transformation involves a complex interaction between the bacterium and the host plant. 3' UTR is involved in transcriptional regulation and the gene is expressed in the elongation zone of the root.

AT1G72180	1.51	0.01910	NA	NA
AT1G63840	1.51	0.00499	NA	NA
AT3G17090	1.51	0.00064	NA	NA
AT4G17550	1.51	0.00372	AtG3Pp4	NA
AT3G20130	1.51	0.03076	CYP705A22	member of CYP705A
AT4G35320	1.51	0.02299	NA	NA
AT3G16570	1.51	0.02403	ATRALF23	Encodes RALF23, a member of a diversely expressed predicted peptide family showing sequence similarity to tobacco Rapid Alkalinization Factor (RALF), and is believed to play an essential role in the physiology of Arabidopsis. Consists of a single exon and is characterized by a conserved C-terminal motif and N-terminal signal peptide. RALF23 is significantly downregulated by brassinolide treatment of seedlings. Overexpression of AtRALF23 impairs brassinolide-induced hypocotyls elongation, and mature overexpressing plants are shorter and bushier. RALF23 overexpression produces slower growing seedlings with roots that have reduced capacity to acidify the rhizosphere.
AT3G19380	1.51	0.00896	PUB25	NA
AT3G47295	1.51	0.03232	NA	NA
AT2G23180	1.50	0.02196	CYP96A1	member of CYP96A
AT1G63260	1.50	0.01546	TET10	Member of TETRASPANIN family
AT4G21740	1.50	0.03206	NA	NA
AT5G57780	1.49	0.02111	P1R1	NA
AT1G73590	1.49	0.00304	ATPIN1	Encodes an auxin efflux carrier involved in shoot and root development. It is involved in the maintenance of embryonic auxin gradients. Loss of function severely affects organ initiation, pin1 mutants are characterised by an inflorescence meristem that does not initiate any flowers, resulting in the formation of a naked inflorescence stem. PIN1 is involved in the determination of leaf shape by actively promoting development of leaf margin serrations. In roots, the protein mainly resides at the basal end of the vascular cells, but weak signals can be detected in the epidermis and the cortex. Expression levels and polarity of this auxin efflux carrier change during primordium development suggesting that cycles of auxin build-up and depletion accompany, and may direct, different stages of primordium development. PIN1 action on plant development does not strictly require function of PGP1 and PGP19 proteins.
AT5G56170	1.49	0.00170	LLG1	NA
AT2G47930	1.49	0.01869	AGP26	NA
AT4G37590	1.49	0.00067	MEL1	A member of the NPY gene family (NPY1/AT4G31820, NPY2/AT2G14820, NPY3/AT5G67440, NPY4/AT2G23050, NPY5/AT4G37590). Involved in auxin-mediated organogenesis.

AT1G05835	1.49	0.00863	NA	NA
AT5G24120	1.48	0.02098	ATSIG5	Encodes a specialized sigma factor that functions in regulation of plastid genes and is responsible for the light-dependent transcription at the psbD LRP. Activation of SIG5 is dependent upon blue light and mediated by cryptochromes.
AT1G75780	1.48	0.02364	TUB1	beta tubulin gene downregulated by phytochrome A (phyA)-mediated far-red light high-irradiance and the phytochrome B (phyB)-mediated red light high-irradiance responses
AT4G16980	1.48	0.04358	NA	NA
AT1G50630	1.47	0.01550	NA	NA
AT4G17170	1.47	0.00689	AT-RAB2	member of RAB gene family
AT3G28200	1.47	0.02695	NA	NA
AT3G25710	1.47	0.03418	ATAIG1	Encodes a basic helixloophelix transcription factor that is expressed in the hypophysis-adjacent embryo cells, and is required and partially sufficient for MP-dependent root initiation. Involved in response to phosphate starvation. Negative regulator of root hair development, anthocyanin formation and Pi content.
AT2G26690	1.47	0.03152	AtNPF6.2	NA
AT1G69690	1.47	0.01575	AtTCP15	NA
AT5G08330	1.46	0.03411	AtTCP11	NA
AT1G34110	1.46	0.03381	NA	NA
AT5G63650	1.46	0.04441	SNRK2-5	encodes a member of SNF1-related protein kinases (SnRK2) whose activity is activated by ionic (salt) and non-ionic (mannitol) osmotic stress.
AT5G66920	1.46	0.00274	sks17	NA
AT1G70750	1.46	0.04396	MyoB2	NA
AT5G66460	1.46	0.02403	AtMAN7	NA
AT1G67880	1.46	0.00435	NA	NA
AT1G07420	1.45	0.00157	ATSMO1	Arabidopsis thaliana sterol 4-alpha-methyl-oxidase mRNA
AT2G39010	1.45	0.00293	PIP2;6	NA
AT4G20870	1.45	0.00429	ATFAH2	encodes a fatty acid hydroxylase, required for the AtBI-1-mediated suppression of programmed cell death.
AT2G37380	1.44	0.04810	MAKR3	NA
AT5G57970	1.44	0.00375	NA	NA
AT5G61660	1.44	0.04297	NA	NA
AT3G63440	1.44	0.01193	ATCKX6	This gene used to be called AtCKX7. It encodes a protein whose sequence is similar to cytokinin oxidase/dehydrogenase, which catalyzes the degradation of cytokinins.

AT1G69295	1.43	0.00296	PDCB4	Encodes a member of the X8-GPI family of proteins. It localizes to the plasmodesmata and is predicted to bind callose.
AT1G30690	1.43	0.03400	NA	NA
AT1G31070	1.43	0.00429	GlcNAc1pUT1	Encodes a protein that functions as an N-acetylglucosamine-1-phosphate uridylyltransferase that catalyzes the formation of UDP-N-acetylglucosamine (UDP-GlcNAc). This is an essential precursor for glycolipid and glycoprotein synthesis and is also used for regulatory protein modification in signaling pathways. The enzyme can also catalyze the reverse reaction using both UDP-GlcNAc and the less common UDP-N-acetylgalactosamine as substrates.
AT2G39800	1.43	0.02643	ATP5CS	encodes a delta1-pyrroline-5-carboxylate synthase that catalyzes the rate-limiting enzyme in the biosynthesis of proline. Gene is expressed in reproductive organs and tissues under non-stress conditions but in the whole plant under water-limiting condition. Expression is also induced by abscisic acid and salt stress in a light-dependent manner. P5CS1 appears to be involved in salt stress responses related to proline accumulation, including protection from reactive oxidative species. P5CS1 appears to be present in different cells and/or different subcellular locations from P5CS2 in a tissue-dependent manner.
AT1G32190	1.43	0.00663	NA	NA
AT1G13250	1.43	0.00650	GATL3	Encodes a protein with putative galacturonosyltransferase activity.
AT4G12110	1.43	0.00213	ATSMO1-1	Encodes a member of the SMO1 family of sterol 4alpha-methyl oxidases. More specifically functions as a 4,4-dimethyl-9beta,19-cyclopropylsterol-4alpha- methyl oxidase.
AT4G28640	1.43	0.01564	IAA11	Auxin induced gene, IAA11 (IAA11).
AT5G12250	1.42	0.02235	TUB6	Encodes a beta-tubulin. Expression of TUB6 has been shown to decrease in response to cold treatment.
AT3G50900	1.42	0.02448	NA	NA
AT1G53290	1.42	0.02094	NA	NA
AT3G54400	1.42	0.04363	NA	NA
AT2G29420	1.42	0.01264	ATGSTU7	Encodes glutathione transferase belonging to the tau class of GSTs. Naming convention according to Wagner et al. (2002). Induced by Salicylic acid. Independent of NPR1 for their induction by salicylic acid.
AT1G29300	1.41	0.04705	UNE1	NA
AT1G17620	1.41	0.03257	NA	NA
AT3G57800	1.41	0.02424	NA	NA
AT3G05945	1.41	0.02128	NA	NA
AT3G05910	1.41	0.01627	NA	NA
AT4G24510	1.41	0.02394	CER2	Involved in C28 to C30 fatty acid elongation.
AT2G41740	1.41	0.02181	ATVLN2	Encodes a protein with high homology to animal villin.
AT3G23750	1.40	0.03147	BARK1	NA

AT1G53840	1.40	0.01194	ATPME1	encodes a pectin methylesterase
AT2G34070	1.40	0.00296	TBL37	Encodes a member of the TBL (TRICHOME BIREFRINGENCE-LIKE) gene family containing a plant-specific DUF231 (domain of unknown function) domain. TBL gene family has 46 members, two of which (TBR/AT5G06700 and TBL3/AT5G01360) have been shown to be involved in the synthesis and deposition of secondary wall cellulose, presumably by influencing the esterification state of pectic polymers. A nomenclature for this gene family has been proposed (Volker Bischoff & Wolf Scheible, 2010, personal communication).
AT3G26760	1.40	0.00562	NA	NA
AT1G70950	1.40	0.04093	NA	NA
AT2G31680	1.40	0.01550	AtRABA5d	NA
AT1G17700	1.40	0.04735	PRA1.F1	NA
AT1G72160	1.40	0.04065	NA	NA
AT4G36780	1.40	0.00854	BEH2	NA
AT5G46730	1.40	0.01716	NA	NA
AT5G15150	1.40	0.03848	ATHB-3	homeobox-containing gene with an unusual feature: a leucine zipper motif adjacent to the carboxyl-terminal of the homeodomain structure. This gene is expressed primarily in the cortex of the root and the stem.
AT4G33625	1.39	0.02953	NA	NA
AT5G11970	1.39	0.00375	NA	NA
AT2G34300	1.39	0.00129	NA	NA
AT1G64330	1.39	0.04109	NA	NA
AT3G27960	1.39	0.01477	KLCR2	NA
AT1G59710	1.39	0.00296	NA	NA
AT5G65670	1.39	0.00135	IAA9	auxin (indole-3-acetic acid) induced gene
AT4G25280	1.38	0.04033	NA	NA
AT3G07360	1.38	0.01084	ATPUB9	Encodes a protein containing a U-box and an ARM domain. This protein has E3 ubiquitin ligase activity based on in vitro assays.
AT1G22910	1.38	0.04080	NA	NA
AT1G14460	1.38	0.03632	NA	NA
AT4G30610	1.38	0.00946	BRS1	Encodes a secreted glycosylated serine carboxypeptidase with broad substrate preference that is involved in brassinosteroid signalling via BRI1. It is proteolytically processed in vivo by a separate as yet unidentified protease.
AT5G66600	1.37	0.02953	NA	NA
AT1G69780	1.37	0.01583	ATHB13	Encodes a homeodomain leucine zipper class I (HD-Zip I) protein.

AT4G36648	1.37	0.04297	NA	NA
AT3G60390	1.37	0.04672	HAT3	Encodes homeobox protein HAT3.
AT3G60630	1.37	0.00223	ATHAM2	NA
AT4G32285	1.36	0.00350	NA	NA
AT3G56800	1.36	0.00900	ACAM-3	encodes a calmodulin
AT4G39840	1.36	0.03341	NA	NA
AT5G61810	1.36	0.01099	APC1	NA
AT3G02000	1.36	0.03085	ROXY1	Roxy1 encodes a glutaredoxin belonging to a subgroup specific to higher plants. It is required for proper petal initiation and organogenesis. It is likely to function in the temporal and spatial expression regulation of AGAMOUS in the first and second whorl. It's function is dependent on the Cysteine 49 residue and its nuclear localization. ROXY1 interacts in vitro and in vivo with members of the TGA family of transcription factors (e.g. TGA2, TGA3, TGA7 and PAN).
AT2G35190	1.36	0.00392	ATNPSN11	plant-specific SNARE located in cell plate of dividing cells. cofractionates with the cytokinesis-specific syntaxin, KNOLLE, which is required for the formation of the cell plate.
AT1G32410	1.36	0.03619	NA	NA
AT5G47550	1.36	0.02087	NA	NA
AT5G57340	1.36	0.04520	NA	NA
AT1G62430	1.36	0.03427	ATCDS1	Encodes a CDP-diacylglycerol synthase, involved in phospholipid biosynthesis.
AT5G37790	1.35	0.01921	NA	NA
AT1G11905	1.35	0.00858	NA	NA
AT1G45688	1.35	0.01084	NA	NA
AT5G03520	1.35	0.04852	ATRAB-E1D	NA
AT2G21050	1.35	0.00863	LAX2	Encodes LAX2 (LIKE AUXIN RESISTANT), a member of the AUX1 LAX family of auxin influx carriers. Required for the establishment of embryonic root cell organization.
AT4G18670	1.34	0.03778	NA	NA
AT5G65440	1.34	0.01546	NA	NA
AT2G23150	1.34	0.01017	ATNRAMP3	Encodes a member of the Nramp2 metal transporter family; like its homolog Atnramp4, localized in vacuolar membrane. Seedlings of double mutant, atnramp3-1 atnramp4-1, were arrested at early germination.
AT3G07470	1.34	0.03539	NA	NA
AT2G33310	1.34	0.02184	IAA13	Auxin induced gene, IAA13 (IAA13).

AT1G21980	1.34	0.02403	ATPIP5K1	Type I phosphatidylinositol-4-phosphate 5-kinase. Preferentially phosphorylates PtdIns4P. Induced by water stress and abscisic acid in Arabidopsis thaliana. Expressed in procambial cells of leaves, flowers and roots. A N-terminal Membrane Occupation and Recognition Nexus (MORN)affects enzyme activity and distribution.
AT5G52430	1.34	0.00883	NA	NA
AT1G19835	1.34	0.03268	NA	NA
AT1G76670	1.34	0.00170	NA	NA
AT3G11700	1.33	0.04617	FLA18	NA
AT3G62630	1.33	0.03434	NA	NA
AT5G64250	1.33	0.03602	NA	NA
AT4G38900	1.33	0.02087	NA	NA
AT3G10525	1.33	0.04761	LGO	Encodes LGO (loss of giant cells from organs) required for giant cell formation. Giant cells in both leaves and sepals are absent in lgo mutants. LGO is a member of a plant specific cell cycle inhibitor family SIAMESE and was originally named as SMR1(SIAMESE RELATED 1).
AT2G41760	1.33	0.03206	NA	NA
AT5G45550	1.33	0.00274	MOB1-like	NA
AT1G48240	1.33	0.04630	ATNPSN12	member of NPSN Gene Family
AT1G78490	1.33	0.02846	CYP708A3	member of CYP708A
AT3G01470	1.33	0.02692	ATHB-1	Encodes a homeodomain leucine zipper class I (HD-Zip I) transcriptional activator involved in leaf development.
AT5G65810	1.33	0.00762	CGR3	NA
AT2G21060	1.32	0.03849	ATCSP4	glycine-rich protein (AtGRP2b)
AT4G27840	1.32	0.01339	NA	NA
AT3G54690	1.32	0.03352	SETH3	NA
AT5G44340	1.32	0.03938	TUB4	beta tubulin gene
AT3G51470	1.32	0.04133	NA	NA
AT1G55840	1.32	0.00129	NA	NA
AT2G38610	1.32	0.01308	NA	NA
AT4G18380	1.32	0.04114	NA	NA

AT1G19850	1.32	0.00650	ARF5	Encodes a transcription factor (IAA24) mediating embryo axis formation and vascular development. Similar to AUXIN RESPONSIVE FACTOR 1 (ARF1) shown to bind to auxin responsive elements (AREs), and to the maize transcriptional activator VIVIPAROUS 1(VP1). In situ hybridization shows expression in provascular tissue of embryos, the emerging shoot primordia, then is restricted to provascular tissue, and in the root central vascular cylinder.
AT1G57700	1.31	0.02427	NA	NA
AT3G18820	1.31	0.00685	ATRAB7B	NA
AT5G47180	1.31	0.04297	NA	NA
AT4G00300	1.31	0.03061	NA	NA
AT3G48610	1.31	0.00242	NPC6	NA
AT4G25770	1.31	0.03380	NA	NA
AT3G49720	1.31	0.00857	NA	NA
AT2G28950	1.31	0.00481	ATEXP6	Encodes an expansin. Naming convention from the Expansin Working Group (Kende et al, 2004. Plant Mol Bio). Involved in the formation of nematode-induced syncytia in roots of Arabidopsis thaliana.
AT5G56730	1.30	0.01938	NA	NA
AT4G20890	1.30	0.02639	TUB9	tubulin 9
AT1G67340	1.30	0.01449	NA	NA
AT1G68910	1.30	0.02748	WIT2	Encodes one of the WPP domain-interacting proteins (WIT1/AT5G11390, WIT2/AT1G68910) required for RanGAP nuclear envelope association in root tip cells. Ran GTPase plays essential roles in multiple cellular processes, including nucleocytoplasmic transport, spindle formation, and postmitotic nuclear envelope reassembly. The cytoplasmic Ran GTPase activating protein RanGAP is critical to establish a functional RanGTP/RanGDP gradient across the nuclear envelope and is associated with the outer surface of the nuclear envelope in metazoan and higher plant cells. Arabidopsis thaliana RanGAP association with the root tip nuclear envelope requires a family of likely plant-specific nucleoporins combining coiled-coil and transmembrane domains (CC-TMD) and WPP domain-interacting proteins (WIPs). WIT1 and WIT2 have been identified as a second family of CC-TMD proteins, structurally similar, yet clearly distinct from the WIP family, that is required for RanGAP nuclear envelop association in root tip cells.
AT3G17120	1.30	0.01811	NA	NA
AT5G09890	1.30	0.02488	NA	NA
AT3G08030	1.30	0.00870	NA	NA
AT4G28050	1.30	0.03010	TET7	Member of TETRASPANIN family
AT4G24790	1.30	0.04979	NA	NA
AT5G43310	1.30	0.02094	NA	NA

AT3G50830	1.29	0.02908	ATCOR413-PM2	cold acclimation protein WCOR413-like protein beta form. Transcript is not detectable.
AT5G42420	1.29	0.03116	NA	NA
AT1G49740	1.29	0.02360	NA	NA
AT5G19530	1.28	0.01025	ACL5	Encodes a spermine synthase. Required for internode elongation and vascular development, specifically in the mechanism that defines the boundaries between veins and nonvein regions. This mechanism may be mediated by polar auxin transport. Though ACL5 has been shown to function as a spermine synthase in E. coli, an ACL5 knockout has no effect on the endogenous levels of free and conjugated polyamines in Arabidopsis, suggesting that ACL5 may have a very specific or altogether different in vivo function.
AT4G23400	1.28	0.04057	PIP1;5	NA
AT3G29360	1.28	0.01223	UGD2	NA
AT1G75080	1.28	0.00858	BZR1	Encodes a positive regulator of the brassinosteroid (BR) signalling pathway that mediates both downstream BR responses and negative feedback regulation of BR biosynthesis. There is evidence for phosphorylation-dependent nucleocytoplasmic shuttling of BZR1. GSK3-like kinases (including BIN2), 14-3-3 proteins, and the phosphatase BSU1 seem to participate in this process. Phosphorylation also appears to affect BZR1's transcriptional activities.
AT4G31590	1.28	0.04240	ATCSLC05	encodes a gene similar to cellulose synthase
AT3G12670	1.28	0.01569	emb2742	NA
AT3G01750	1.28	0.01223	NA	NA
AT4G31910	1.28	0.02360	BAT1	NA
AT5G66420	1.28	0.00538	NA	NA
AT1G78040	1.27	0.02098	NA	NA
AT2G41420	1.27	0.03853	WIH2	NA
AT1G52280	1.27	0.02182	AtRABG3d	NA
AT1G04430	1.27	0.01084	NA	NA
AT3G13720	1.27	0.03848	PRA1.F3	NA
AT3G14790	1.27	0.00564	ATRHM3	NA
AT1G10410	1.27	0.02846	NA	NA
AT1G27350	1.26	0.04133	NA	NA
AT3G14000	1.26	0.03632	ATBRXL2	Belongs to five-member BRX gene family. Arabidopsis BRX genes share high levels of similarity among each others, with several conserved domains. The most distinct is BRX domain - highly conserved in all BRX genes among distantly related species. This protein-protein interaction domain is required and sufficient for BRX activity.

AT3G15820	1.26	0.02098	ROD1	Functions as phosphatidylcholine:diacylglycerol cholinephosphotransferase, a major reaction for the transfer of 18:1 into phosphatidylcholine for desaturation and also for the reverse transfer of 18:2 and 18:3 into the triacylglycerols synthesis pathway
AT1G73760	1.26	0.02184	NA	NA
AT4G35880	1.26	0.01434	NA	NA
AT1G20970	1.26	0.02455	NA	NA
AT5G55850	1.26	0.01084	NOI	NOI protein
AT2G29390	1.26	0.02388	ATSMO2	Encodes a sterol 4-alpha-methyl-oxidase, specifically a 4-alpha-methyl-delta-7-sterol-4alpha-methyl-oxidase.
AT5G13460	1.26	0.03814	IQD11	NA
AT1G68410	1.26	0.04977	NA	NA
AT5G65310	1.26	0.03848	ATHB-5	Encodes a class I HDZip (homeodomain-leucine zipper) protein that is a positive regulator of ABA-responsiveness, mediating the inhibitory effect of ABA on growth during seedling establishment.
AT1G74380	1.25	0.03297	XXT5	NA
AT4G33580	1.25	0.00386	ATBCA5	NA
AT1G08200	1.25	0.00926	AXS2	Encodes a putative UDP-D-apiose/UPD-D-xylose synthetase.
AT1G51160	1.25	0.00622	NA	NA
AT4G22010	1.25	0.04462	sks4	NA
AT5G62580	1.25	0.03844	NA	NA
AT5G11000	1.25	0.03433	NA	NA
AT1G54100	1.25	0.02870	ALDH7B4	Aldehyde dehydrogenase
AT2G26730	1.25	0.00721	NA	NA
AT5G57270	1.24	0.03591	NA	NA
AT2G27950	1.24	0.00988	NA	NA
AT5G26667	1.24	0.01038	PYR6	encodes a uridine 5'-monophosphate (UMP)/cytidine 5'-monophosphate (CMP) kinase.
AT1G28960	1.24	0.02982	ATNUDT15	NA
AT3G12360	1.24	0.04213	ITN1	Encodes a protein with an ankyrin motif and transmembrane domains that is involved in salt tolerance. Expressed throughout the plant and localized to the plasma membrane. Loss of function mutations show an increased tolerance to salt based on assaying seedling growth in the presence of salt. In the mutants, induction of genes required for production of reactive oxygen species is reduced suggesting that itn1 promotes ROS production.
AT5G48500	1.24	0.04190	NA	NA
AT1G79990	1.24	0.01238	NA	NA

AT5G57460	1.23	0.01239	NA	NA
AT3G12620	1.23	0.02964	NA	NA
AT2G20760	1.23	0.03865	NA	NA
AT4G23710	1.23	0.00857	VAG2	NA
AT1G55520	1.23	0.03115	ATTBP2	TATA-box binding protein. Required for basal transcription. Acts facilitating the recruitment of TFIID to the promoter, which together with the RNA polymerase form the preinitiation complex.
AT4G24220	1.23	0.01485	5[beta]-StR	encodes a novel protein containing mammalian death domain involved in programmed cell death. Gene is expressed in vascular system and mutants carrying dominant mutation in the gene have defective vascular patterning. Gene expression is induced specifically by wounding.
AT1G18840	1.23	0.02182	IQD30	NA
AT2G27860	1.23	0.04626	AXS1	Encodes UDP-d-apiose/UDP-d-xylose synthase that requires NAD+ for enzymatic activity and is strongly inhibited by UDP-d-galacturonate.
AT5G47200	1.23	0.04240	ATRAB1A	NA
AT2G36300	1.23	0.04384	NA	NA
AT5G61240	1.23	0.01000	NA	NA
AT5G28040	1.23	0.04883	NA	NA
AT2G04780	1.23	0.02902	FLA7	fasciclin-like arabinogalactan-protein 7 (Fla7)
AT1G08280	1.23	0.02911	NA	NA
AT2G40540	1.22	0.03530	ATKT2	putative potassium transporter AtKT2p (AtKT2) mRNA,
AT1G06870	1.22	0.03848	Plsp2A	NA
AT1G12850	1.22	0.03139	NA	NA
AT3G15480	1.21	0.03076	NA	NA
AT4G13350	1.21	0.04066	NIG	Encodes a GTPase that interacts with nuclear shuttle proteins (NSPs) from a number of different plant viruses. The gene is widely expressed and NIG transcript levels do not rise in response to viral infection. This cytoplasmic protein does not directly interact with a viral movement protein (MP), but, it does promote the movement of NSP from the nucleus to the cytoplasm. Overexpression of NIG in Arabidopsis plants renders them more sensitive to geminivirus infection.
AT1G14670	1.21	0.01969	NA	NA
AT1G60660	1.21	0.04810	ATCB5LP	member of Cytochromes b5
AT1G14830	1.21	0.01223	ADL1C	Encodes a dynamin-like protein that is involved in mitochondrial morphogenesis and pollen development. Protein is localized as speckles in the cytoplasm, partially co-localizes with mitochondrial markers, cell plate of dividing cells, and the tip of root hairs, root cap cells, and expanding part of trichoblasts.

AT4G08685	1.21	0.04551	SAH7	Encodes a protein, expressed in leaves, with similarity to pollen allergens.
AT3G48780	1.21	0.04986	ATSPT1	Encodes one of the two LCB2 subunits (LCB2a and LCB2b) of serine palmitoyltransferase, an enzyme involved in sphingolipid biosynthesis. LCB2a and LCB2b are functional redundant. Double mutants are gametophytic lethal.
AT1G75680	1.21	0.04977	AtGH9B7	NA
AT3G01780	1.20	0.01430	TPLATE	Encodes TPLATE, a cytokinesis protein targeted to the cell plate. Functions in vesicle-trafficking events required for site-specific cell wall modifications during pollen germination and for anchoring of the cell plate to the mother wall at the correct cortical position.
AT3G43740	1.20	0.03893	NA	NA
AT1G19440	1.20	0.04093	KCS4	Encodes KCS4, a member of the 3-ketoacyl-CoA synthase family involved in the biosynthesis of VLCFA (very long chain fatty acids).
AT5G08590	1.20	0.02062	ASK2	Encodes a member of SNF1-related protein kinases (SnRK2) whose activity is activated by ionic (salt) and non-ionic (mannitol) osmotic stress. Similar to the calcium/calmodulin-dependent protein kinase subfamily and the SNF1 kinase subfamily.
AT1G53050	1.20	0.02087	NA	NA
AT4G34490	1.20	0.02611	ATCAP1	CYCLASE ASSOCIATED PROTEIN
AT5G61480	1.19	0.04824	PXY	NA
AT1G11890	1.19	0.04291	ATSEC22	member of SEC22 Gene Family
AT3G15980	1.19	0.02190	NA	NA
AT2G37550	1.19	0.02448	AGD7	A member of ARF GAP domain (AGD), A thaliana has 15 members, grouped into four classes.
AT4G11820	1.18	0.04060	FKP1	Encodes a protein with hydroxymethylglutaryl-CoA synthase activity which was characterized by phenotypical complementation of the S. cerevisiae mutant.
AT1G48230	1.18	0.03085	NA	NA
AT1G53040	1.18	0.04098	NA	NA
AT5G03080	1.18	0.04350	LPPgamma	NA
AT2G17990	1.18	0.03848	NA	NA
AT2G33120	1.18	0.03010	ATVAMP722	Encodes a member of Synaptobrevin -like protein family.
AT2G02870	1.18	0.04297	NA	NA
AT1G11280	1.18	0.04415	NA	NA
AT1G53000	1.18	0.02182	AtCKS	Encodes a putative CMP-KDO (3-deoxy-D-manno-octulosonate) synthetase.

AT3G46830	1.17	0.03355	ATRAB-A2C	NA
AT5G18520	1.17	0.04735	Cand7	NA
AT5G37850	0.86	0.04358	ATSOS4	Encodes a pyridoxal kinase required for root hair development. Mutants are hypersensitive to Na+, K+ and Li+.
AT2G35490	0.85	0.04251	NA	NA
AT1G53580	0.84	0.02702	ETHE1	Mononuclear Fe(II)-containing member of the b-lactamase fold superfamily. ETHE1 is homodimeric in solution, exhibits low-level esterase activity, and specifically binds a single Fe(II) atom in the active site.
AT4G36860	0.84	0.03286	NA	NA
AT3G26710	0.84	0.03148	CCB1	NA
AT4G14410	0.84	0.04452	bHLH104	NA
AT3G53180	0.84	0.02907	NodGS	NA
AT5G20990	0.84	0.02910	B73	Involved in molybdenum cofactor (Moco) biosynthesis, inserting Mo into Molybdopterin. sir loss-of-function mutants are resistant to sirtinol, a modulator of auxin signaling.
AT2G34690	0.83	0.03085	ACD11	Gene product transports the glycolipid precursor sphingosine between membranes in vitro. Mutant constitutively expresses defense-related genes that accompany the hypersensitive response normally triggered by avirulent pathogens.
AT5G36160	0.83	0.02455	NA	NA
AT3G46540	0.83	0.02087	NA	NA
AT3G04520	0.83	0.03092	THA2	Encodes a threonine aldolase, involved in threonine degradation to glycine. Expressed in vascular tissue through out the plant.
AT5G21326	0.83	0.02260	CIPK26	NA
AT5G46250	0.83	0.03606	AtLARP6a	NA
AT1G70310	0.82	0.02241	SPDS2	Spermidine synthase.
AT5G27380	0.82	0.03237	AtGSH2	Encodes a protein with similarity to glutathione synthetases, which catalyzes one of the early steps in glutathione biosynthesis. Two transcripts have been detected; the longer transcript is less abundant and the protein is localized to the chloroplast. The smaller transcript, in which the transit peptide is truncated, is localized to the cytosol.
AT1G53910	0.82	0.02403	RAP2.12	encodes a member of the ERF (ethylene response factor) subfamily B-2 of ERF/AP2 transcription factor family (RAP2.12). The protein contains one AP2 domain. There are 5 members in this subfamily including RAP2.2 AND RAP2.12.
AT1G09430	0.82	0.02408	ACLA-3	Encodes subunit A of the heteromeric enzyme ATP citrate lyase (ACL). In animals, ACL is encoded by a single gene; ACL in Arabidopsis is composed of two polypeptides, ACLA (encoded by 3 genes) and ACLB (encoded by 2 genes). The holoenzyme has an A(4)B(4)stoichiometry. Expression of both ACLA and ACLB but not of either of the subunits alone results in ACL activity.

AT1G34210	0.82	0.01000	ATSERK2	Plasma membrane LRR receptor-like serine threonine kinase expressed during embryogenesis in locules until stage 6 anthers, with higher expression in the tapetal cell layer. SERK1 and SERK2 receptor kinases function redundantly as an important control point for sporophytic development controlling male gametophyte production.
AT2G43750	0.82	0.01464	ACS1	Arabidopsis thaliana O-acetylserine (thiol) lyase (OAS-TL) isoform oasB, the key enzyme for fixation of inorganic sulfide. It catalyzes the formation of cysteine from O-acetylserine and inorganic sulfide.
AT2G29180	0.82	0.03482	NA	NA
AT1G28320	0.82	0.03778	DEG15	Mutants in this gene are defective in the processing of pre-glyoxysomal malate dehydrogenase (pre-gMDH) to gMDH.
AT2G24762	0.81	0.04617	AtGDU4	Encodes a member of the GDU (glutamine dumper) family proteins involved in amino acid export: At4g31730 (GDU1), At4g25760 (GDU2), At5g57685 (GDU3), At2g24762 (GDU4), At5g24920 (GDU5), At3g30725 (GDU6) and At5g38770 (GDU7).
AT2G38800	0.81	0.03978	NA	NA
AT3G16190	0.81	0.04313	NA	NA
AT5G24460	0.81	0.04629	NA	NA
AT4G16250	0.81	0.03893	PHYD	Encodes a phytochrome photoreceptor with a function similar to that of phyB that absorbs the red/far-red part of the light spectrum and is involved in light responses. It cannot compensate for phyB loss in Arabidopsis but can substitute for tobacco phyB in vivo.
AT3G16470	0.81	0.01852	JAL35	JA-responsive gene
AT3G23790	0.81	0.04452	AAE16	NA
AT4G38160	0.81	0.00412	pde191	NA
AT4G28300	0.81	0.01060	NA	Encodes a protein with 13.6% proline amino acids that is predicted to localize to the cell wall.
AT1G34300	0.81	0.03061	NA	NA
AT1G68220	0.81	0.03848	NA	NA
AT2G37200	0.81	0.04810	NA	NA
AT5G67290	0.80	0.04013	NA	NA
AT3G21690	0.80	0.04626	NA	NA
AT2G23610	0.80	0.01294	ATMES3	Encodes a protein shown to have carboxylesterase activity, methyl IAA esterase activity, and methyl jasmonate esterase activity in vitro. This protein does not act on methyl salicylate, MeGA4, or MEGA9 in vitro.
AT2G28190	0.80	0.03092	CSD2	Encodes a chloroplastic copper/zinc superoxide dismutase CSD2 that can detoxify superoxide radicals. Its expression is affected by miR398-directed mRNA cleavage.
AT1G69760	0.80	0.04824	NA	NA
AT2G34470	0.80	0.01099	PSKF109	Encodes a urease accessory protein which is essential for the activation of plant urease.

AT4G00040	0.80	0.01870	NA	NA
AT2G01830	0.79	0.04452	AHK4	Histidine kinase: cytokinin-binding receptor that transduces cytokinin signals across the plasma membrane
AT1G50480	0.79	0.01282	THFS	10-formyltetrahydrofolate synthetase (THFS) mRNA, complete
AT5G14780	0.79	0.03085	FDH	Encodes a NAD-dependent formate dehydrogenase.
AT1G13740	0.79	0.02514	AFP2	Encodes a member of a small plant-specific gene family whose members interact with ABI5 and appear to be involved in mediating stress responses. AFP2 mutants affect a number of ABA mediated processes such as germination and response to osmotic and sugar stress. AFP2 nuclear localization is stress dependent.
AT1G77230	0.79	0.00918	NA	NA
AT3G05410	0.79	0.03010	NA	NA
AT5G55790	0.79	0.03844	NA	NA
AT2G01290	0.78	0.02182	RPI2	Cytosolic ribose-5-phosphate isomerase. Knockout mutation causes chloroplast dysfunction, late flowering and premature cell death.
AT5G57930	0.78	0.04314	APO2	ACCUMULATION OF PHOTOSYSTEM ONE 2
AT5G19250	0.78	0.03061	NA	NA
AT1G51070	0.78	0.01694	bHLH115	NA
AT2G28840	0.78	0.01650	XBAT31	NA
AT3G61440	0.78	0.04297	ARATH;BSAS3;1	Encodes a cysteine synthase isomer CysC1. The isomer is however less effective in cysteine biosynthesis. It is involved in beta-cyanoalanine biosynthesis, an intermediate of cyanide detoxification pathway.
AT5G20740	0.78	0.04269	NA	NA
AT3G48990	0.78	0.04617	AAE3	NA
AT4G05070	0.78	0.02910	NA	NA
AT5G10180	0.78	0.02465	AST68	Encodes a low-affinity sulfate transporter expressed in the root cap and central cylinder, where it is induced by sulfur starvation. Expression in the shoot vascular system is not induced by sulfur starvation.
AT3G45310	0.77	0.01583	NA	NA
AT5G02710	0.77	0.01450	NA	NA
AT2G36460	0.77	0.03085	FBA6	NA
AT3G16910	0.77	0.04952	AAE7	Encodes a peroxisomal protein with acetyl-CoA synthetase activity that is responsible for the activation of acetate for entry into the glyoxylate cycle.
AT5G04230	0.77	0.01906	ATPAL3	Member of Phenylalanine ammonialyase (PAL) gene family. Differs significantly from PAL1 and PAL2 and other sequenced plant PAL genes. Arabidopsis has four PALs: AT2G37040 (PAL1), AT3G53260 (PAL2), AT5G04230 (PAL3) and AT3G10340 (PAL4).
AT4G21190	0.77	0.04213	emb1417	NA

AT5G23920	0.77	0.04810	NA	NA
AT1G16650	0.77	0.02488	NA	NA
AT5G41700	0.77	0.02319	ATUBC8	One of the polypeptides that constitute the ubiquitin-conjugating enzyme E2
AT1G78010	0.77	0.01715	NA	NA
AT1G27980	0.77	0.00858	ATDPL1	NA
AT2G26650	0.77	0.03627	AKT1	Encodes AKT1, a member of the Shaker family inward rectifying potassium channel predominantly expressed in predominantly in root hairs and root endodermis. This family includes five groups based on phylogenetic analysis (FEBS Letters (2007) 581: 2357): I (inward rectifying channel): AKT1 (AT2G26650), AKT5 (AT4G32500) and SPIK (also known as AKT6, AT2G25600); II (inward rectifying channel): KAT1 (AT5G46240) and KAT2 (AT4G18290); III (weakly inward rectifying channel): AKT2 (AT4G22200); IV (regulatory subunit involved in inwardly rectifying conductance formation): KAT3 (also known as AtKC1, AT4G32650); V (outward rectifying channel): SKOR (AT3G02850) and GORK (AT5G37500).
AT1G56700	0.77	0.00126	NA	NA
AT1G70560	0.77	0.04321	CKRC1	TAA1 is involved in the shade-induced production of indole-3-pyruvate (IPA), a precursor to IAA, a biologically active auxin. It is also involved in regulating many aspects of plant growth and development from embryogenesis to flower formation and plays a role in ethylene-mediated signaling. This enzyme can catalyze the formation of IPA from L-tryptophan. Though L-Trp is expected to be the preferred substrate in vivo, TAA1 also acts as an aminotransferase using L-Phe, L-Tyr, L-Leu, L-Ala, L-Met, and L-Gln.
AT3G47250	0.76	0.00883	NA	NA
AT2G20950	0.76	0.04098	NA	NA
AT1G62810	0.76	0.01497	CuAO1	NA
AT4G14930	0.76	0.04140	NA	NA
AT2G24100	0.76	0.04129	ASG1	NA
AT1G58110	0.76	0.00445	NA	NA
AT4G23670	0.76	0.03296	NA	NA
AT1G70890	0.76	0.01569	MLP43	NA
AT2G41720	0.76	0.01921	EMB2654	NA
AT3G48000	0.76	0.00768	ALDH2	Encodes a putative (NAD+) aldehyde dehydrogenase.
AT2G45510	0.76	0.02094	CYP704A2	member of CYP704A
AT3G60300	0.76	0.01539	NA	NA
AT2G27360	0.75	0.00857	NA	NA

AT5G05110	0.75	0.04384	NA	NA
AT5G13090	0.75	0.04936	NA	NA
AT1G50420	0.75	0.04550	SCL-3	Encodes a scarecrow-like protein (SCL3) Putative transcription factors interacting with the gene product of VHA-B1 (vacuolar ATPase subunit B1; as shown through yeast two-hybrid assay).
AT1G53430	0.75	0.04065	NA	NA
AT5G53160	0.75	0.01497	PYL8	Encodes RCAR3, a regulatory component of ABA receptor. Interacts with protein phosphatase 2Cs ABI1 and ABI2. Stimulates ABA signaling.
AT5G59790	0.75	0.04297	NA	NA
AT3G50430	0.74	0.01575	NA	NA
AT2G43900	0.74	0.02128	5PTase12	NA
AT2G01590	0.74	0.02000	CRR3	Likely a subunit of the chloroplast NAD(P)H dehydrogenase complex, involved in PSI cyclic electron transport. Located in the membrane fraction of chloroplast. Mutant has impaired NAD(P)H dehydrogenase activity.
AT5G54940	0.74	0.04882	NA	NA
AT4G21850	0.74	0.00768	ATMSRB9	NA
AT3G27190	0.74	0.00858	UKL2	One of the homologous genes predicted to encode proteins with UPRT domains (Uracil phosphoribosyltransferase). Five of these genes (At5g40870, At3g27190, At1g55810, At4g26510 and At3g27440) show a high level of identity, and are annotated as also containing a N-terminal uracil kinase (UK) domain. These genes are referred to as UKL1 (UK-like 1), UKL2, UKL3, UKL4 and UKL5, respectively.
AT3G62700	0.74	0.02182	ABCC14	member of MRP subfamily
AT1G45201	0.74	0.03848	ATTLL1	Target of AtGRP7 regulation.
AT3G01210	0.74	0.00565	NA	NA
AT1G12200	0.74	0.03914	FMO	NA
AT1G64710	0.74	0.03296	NA	NA
AT5G18140	0.73	0.03606	DJC69	NA
AT3G22970	0.73	0.00863	NA	NA
AT1G78580	0.73	0.00918	ATTPS1	Encodes an enzyme putatively involved in trehalose biosynthesis. The protein has a trehalose synthase (TPS)-like domain but no trehalose phosphatase (TPP)-like domain. ATTPS1 is able to complement yeast tps1 mutants in vivo. The gene product modulates cell growth but not cell differentiation by determining cell wall deposition and cell division.
AT4G24660	0.73	0.04452	ATHB22	NA
AT2G28930	0.73	0.00657	APK1B	NA
AT3G17670	0.73	0.04592	NA	NA

AT5G40390	0.73	0.04935	RS5	Encodes a protein which might be involved in the formation of verbascose. A T-DNA insertion mutant was shown to have a decreased amount of verbascose (as well as mannitol) whereas the levels of raffinose and stachyose remained unchanged.
AT3G14020	0.73	0.03033	NF-YA6	NA
AT2G42600	0.73	0.01017	ATPPC2	Encodes one of four Arabidopsis phosphoenolpyruvate carboxylase proteins.
AT3G45210	0.73	0.01099	NA	NA
AT3G47430	0.73	0.04551	PEX11B	member of the peroxin11 (PEX11) gene family, located on the peroxisome membrane, controls peroxisome proliferation.
AT1G60989	0.73	0.04952	SCRL7	Encodes a member of a family of small, secreted, cysteine rich proteins with sequence similarity to SCR (S locus cysteine-rich protein).
AT2G34490	0.73	0.02695	CYP710A2	Encodes a protein with C22-sterol desaturase activity. The enzyme was shown to catalyze the conversion of both 24-epi-campesterol and β-sitosterol to brassicasterol and stigmasterol, respectively, in the presence of NADPH.
AT1G74880	0.73	0.03453	NDH-O	Encodes subunit NDH-O of NAD(P)H:plastoquinone dehydrogenase complex (Ndh complex) present in the thylakoid membrane of chloroplasts. This subunit is thought to be required for Ndh complex assembly.
AT4G27730	0.72	0.02242	ATOPT6	oligopeptide transporter
AT5G07830	0.72	0.00211	AtGUS2	Belongs to the plant glycoside hydrolase family 79. Encodes a protein with several posttranslational modification sites including O-β-GlcNAc attachment sites and serine-, threonine- and tyrosine-phosphorylation sites, suggesting that this protein is extensively modified posttranslationally. The protein is predicted (WoLF PSORT program) to be membrane-associated.
AT1G64680	0.72	0.03341	NA	NA
AT1G68238	0.72	0.04697	NA	NA
AT1G28580	0.72	0.01180	NA	NA
AT2G05520	0.72	0.04286	ATGRP-3	Encodes a glycine-rich protein that is expressed mainly in stems and leaves. mRNA levels are upregulated in response to ABA, salicylic acid and ethylene but downregulated in response to dessication.
AT1G72300	0.72	0.04240	PSY1R	Encodes a leucine-rich repeat receptor kinase (LRR-RK) involved in the perception of PSY1. PSY1 is an 18-aa tyrosine-sulfated glycopeptide encoded by AT5G58650 that promotes cellular proliferation and expansion.
AT5G03780	0.72	0.04810	TRFL10	Encodes a protein whose sequence is similar to human telomere proteins. This belongs to TRFL family 2, which do not show DNA binding in vitro.
AT1G67810	0.72	0.02435	SUFE2	Encodes a protein capable of stimulating the cysteine desulfurase activity of CpNifS (AT1G08490) in vitro. SufE2:GFP localizes to the chloroplasts where it is likely to play a role in iron-sulfur cluster assembly. Transcript levels for this gene are high in the pollen relative to other organs based on RT-PCR analysis.
AT1G79160	0.72	0.01797	NA	NA

AT2G47910	0.72	0.02087	CRR6	Encodes a chloroplast thylakoid membrane protein. Required for the assembly/accumulation of the NAD(P)H dehydrogenase complex of the photosynthetic electron transport chain.
AT2G26355	0.72	0.04230	NA	NA
AT1G71480	0.72	0.01485	NA	NA
AT3G63210	0.71	0.01517	MARD1	encodes a novel zinc-finger protein with a proline-rich N-terminus, identical to senescence-associated protein SAG102
AT3G12520	0.71	0.02182	SULTR4;2	Encodes a sulfate transporter that in induced under sulfate limitation.
AT2G38010	0.71	0.00396	NA	NA
AT2G29720	0.71	0.02435	CTF2B	Encodes CTF2B.
AT2G26975	0.71	0.02304	COPT6	NA
AT2G03890	0.71	0.04697	ATPI4K	Phosphoinositide kinase which undergo autophosphorylation and phosphorylate serine/threonine residues of protein substrates. Contains phosphoinositide 3/4-kinase and ubiquitin-like domains.
AT3G43800	0.71	0.02427	ATGSTU27	Encodes glutathione transferase belonging to the tau class of GSTs. Naming convention according to Wagner et al. (2002).
AT2G15050	0.71	0.04222	LTP	Predicted to encode a PR (pathogenesis-related) protein. Belongs to the lipid transfer protein (PR-14) family with the following members: At2g38540/LTP1, At2g38530/LTP2, At5g59320/LTP3, At5g59310/LTP4, At3g51600/LTP5, At3g08770/LTP6, At2g15050/LTP7, At2g18370/LTP8, At2g15325/LTP9, At5g01870/LTP10, At4g33355/LTP11, At3g51590/LTP12, At5g44265/LTP13, At5g62065/LTP14, At4g08530/LTP15.
AT1G02860	0.71	0.01345	BAH1	Encodes a likely ubiquitin E3 ligase with RING and SPX domains that is involved in mediating immune responses. Targeted by MIR827.
AT2G39310	0.71	0.00863	JAL22	NA
AT1G44760	0.71	0.00213	NA	NA
AT2G41700	0.71	0.01862	ABCA1	NA
AT3G11280	0.71	0.00622	NA	Putative transcription factors interacting with the gene product of VHA-B1 (vacuolar ATPase subunit B1; as shown through yeast two-hybrid assay).
AT2G17820	0.71	0.01562	AHK1	Encodes a member of the histidine kinase family.
AT3G49940	0.71	0.00847	LBD38	NA
AT5G21482	0.71	0.03042	ATCKX5	This gene used to be called AtCKX5. It encodes a protein whose sequence is similar to cytokinin oxidase/dehydrogenase, which catalyzes the degradation of cytokinins.
AT5G28020	0.71	0.02182	ATCYSD2	Encodes cysteine synthase CysD2.
AT1G79970	0.70	0.00230	NA	NA
AT3G26330	0.70	0.01583	CYP71B37	putative cytochrome P450

AT5G14090	0.70	0.01223	AtLAZY1	NA
AT1G31710	0.70	0.00304	NA	NA
AT4G01450	0.70	0.00748	UMAMIT30	NA
AT1G10682	0.69	0.00070	NA	NA
AT5G15860	0.69	0.01734	ATPCME	Encodes a protein with prenylcysteine methylesterase activity.
AT5G54960	0.69	0.04697	PDC2	pyruvate decarboxylase-2
AT4G23570	0.69	0.00649	SGT1A	Closely related to SGT1B, may function in SCF(TIR1) mediated protein degradation. AtSGT1a and AtSGT1b are functionally redundant in the resistance to pathogenes. AtSGT1b was more highly expressed than AtSGT1. The N-terminal TPR domain of AtSGT1a reduces the steady-state level of Arabidopsis SGT1 proteins whereas the same domain from AtSGT1b enhances SGT1 accumulation. The TPR domain is dispensable for SGT1 resistance. AtSGT1a is induced upon pathogen infection and can function in R gene-mediated resistance.
AT1G62200	0.69	0.00794	AtNPF8.5	NA
AT2G33050	0.69	0.02435	AtRLP26	NA
AT2G31110	0.69	0.01862	TBL40	Encodes a member of the TBL (TRICHOME BIREFRINGENCE-LIKE) gene family containing a plant-specific DUF231 (domain of unknown function) domain. TBL gene family has 46 members, two of which (TBR/AT5G06700 and TBL3/AT5G01360) have been shown to be involved in the synthesis and deposition of secondary wall cellulose, presumably by influencing the esterification state of pectic polymers. A nomenclature for this gene family has been proposed (Volker Bischoff & Wolf Scheible, 2010, personal communication).
AT4G21410	0.69	0.01172	CRK29	Encodes a cysteine-rich receptor-like protein kinase.
AT5G04330	0.69	0.04384	CYP84A4	NA
AT4G04830	0.69	0.01160	ATMSRB5	NA
AT4G16380	0.69	0.00125	NA	NA
AT1G77990	0.69	0.01965	AST56	cDNA encoding a sulfate transporter.
AT1G58602	0.68	0.01756	NA	NA
AT2G24260	0.68	0.03443	LRL1	Encodes a basic helix-loop-helix (bHLH) protein that regulates root hair development. One of the three Arabidopsis homologs of the Lotus japonicus ROOTHAIRLESS1 (LjRHL1) gene: At2g24260 (AtLRL1), At4g30980 (AtLRL2), and At5g58010 (AtLRL3).
AT1G28570	0.68	0.02277	NA	NA
AT2G30870	0.68	0.00741	ATGSTF10	early dehydration-induced gene ERD13 homologous to tobacco and maize glutathione S-transferases. Encodes glutathione transferase belonging to the phi class of GSTs. Naming convention according to Wagner et al. (2002)
AT5G64570	0.68	0.00158	ATBXL4	Encodes a beta-d-xylosidase that belongs to family 3 of glycoside hydrolases.

AT2G36320	0.68	0.01570	NA	NA
AT3G16560	0.68	0.04662	NA	NA
AT3G58710	0.68	0.00870	ATWRKY69	member of WRKY Transcription Factor; Group II-e
AT5G11670	0.67	0.01018	ATNADP-ME2	The malic enzyme (EC 1.1.1.40) encoded by AtNADP-ME2 is presumably a cytosolic enzyme involved in malate metabolism and possibly assisting the oxidative pentose phosphate pathway. AtNADP-ME2 counts for the major part of NADP-ME activity in mature tissues of Arabidopsis.
AT3G16450	0.67	0.00429	JAL33	NA
AT5G51970	0.67	0.00637	NA	Encodes a putative sorbitol dehydrogenase that can be thiolated in vitro.
AT5G67110	0.67	0.00650	ALC	encodes a myc/bHLH transcription factor-like protein. Gene product is involved in fruit dehiscence. Mutant siliques fail to dehisce.
AT1G35560	0.67	0.01724	AtTCP23	NA
AT3G15353	0.67	0.00017	ATMT3	metallothionein, binds to and detoxifies excess copper and other metals, limiting oxidative damage
AT3G14230	0.66	0.00066	RAP2.2	encodes a member of the ERF (ethylene response factor) subfamily B-2 of ERF/AP2 transcription factor family (RAP2.2). The protein contains one AP2 domain. There are 5 members in this subfamily including RAP2.2 AND RAP2.12.
AT2G46680	0.66	0.02643	ATHB-7	encodes a putative transcription factor that contains a homeodomain closely linked to a leucine zipper motif. Transcript is detected in all tissues examined. Is transcriptionally regulated in an ABA-dependent manner and may act in a signal transduction pathway which mediates a drought response.
AT5G53550	0.66	0.00473	ATYSL3	NA
AT2G33480	0.66	0.04240	ANAC041	NA
AT5G37600	0.66	0.00117	ATGLN1;1	encodes a cytosolic glutamine synthetase, the enzyme has high affinity with substrate ammonium
AT3G05165	0.66	0.00168	NA	NA
AT1G48320	0.66	0.02973	DHNAT1	NA
AT5G25810	0.66	0.04321	tny	encodes a member of the DREB subfamily A-4 of ERF/AP2 transcription factor family (TINY). The protein contains one AP2 domain. There are 17 members in this subfamily including TINY. Ectopic or overexpression of this gene in a Ds tagged line has reduced cell expansion. The expression of this gene is induced by ethylene and light and appears to stimulate cytokinin biosynthesis.
AT4G39510	0.66	0.01223	CYP96A12	member of CYP96A
AT1G59870	0.66	0.03914	ABCG36	ATP binding cassette transporter. Localized to the plasma membrane in uninfected cells. In infected leaves, the protein concentrated at infection sites. Contributes to nonhost resistance to inappropriate pathogens that enter by direct penetration in a salicylic aciddependent manner. Required for mlo resistance. Has Cd transporter activity (Cd2+ extrusion pump) and contributes to heavy metal resistance.

AT5G05860	0.66	0.01017	UGT76C2	NA
AT4G29110	0.66	0.03085	NA	NA
AT5G10280	0.66	0.02360	ATMYB64	Encodes a putative transcription factor (MYB92).
AT4G17870	0.66	0.00256	PYR1	Encodes a member of the PYR (pyrabactin resistance)/PYL(PYR1-like)/RCAR (regulatory components of ABA receptor) family proteins with 14 members. PYR/PYL/RCAR family proteins function as abscisic acid sensors. Mediate ABA-dependent regulation of protein phosphatase 2Cs ABI1 and ABI2.
AT1G28100	0.66	0.00650	NA	NA
AT1G74940	0.66	0.01583	NA	NA
AT4G18220	0.66	0.01099	NA	NA
AT4G23680	0.66	0.00193	NA	NA
AT1G07440	0.66	0.00538	NA	NA
AT5G61290	0.65	0.00650	NA	NA
AT5G26280	0.65	0.00208	NA	NA
AT4G19810	0.65	0.00444	ChiC	NA
AT5G46780	0.65	0.00474	NA	NA
AT1G64500	0.65	0.02637	NA	NA
AT3G13404	0.65	0.04066	NA	NA
AT1G11175	0.65	0.04143	NA	NA
AT2G39705	0.65	0.02098	DVL11	NA
AT2G29340	0.65	0.00275	NA	NA
AT4G39070	0.65	0.04084	BBX20	NA
AT4G24350	0.65	0.02143	NA	NA
AT3G61430	0.65	0.01629	ATPIP1	a member of the plasma membrane intrinsic protein subfamily PIP1. localizes to the plasma membrane and exhibits water transport activity in Xenopus oocyte. expressed ubiquitously and protein level decreases slightly during leaf development.
AT1G33110	0.64	0.00857	NA	NA
AT1G71880	0.64	0.03767	ATSUC1	Sucrose transporter gene induced in response to nematodes; member of Sucrose-proton symporter family.
AT1G09390	0.63	0.00661	NA	NA
AT3G23430	0.63	0.00261	ATPHO1	mutant is deficient in the transfer of phosphate from root epidermal and cortical cells to the xylem. encodes protein with the mainly hydrophilic N-terminal and the C-terminal containing 6 potential membrane-spanning domains.

AT4G21960	0.63	0.00059	PRXR1	Encodes AT4g21960 (AT4g21960/T8O5_170).
AT2G40100	0.63	0.01575	LHCB4.3	Lhcb4:3 protein (Lhcb4.3, light harvesting complex of photosystem II
AT4G28250	0.63	0.01327	ATEXPB3	putative beta-expansin/allergen protein. Naming convention from the Expansin Working Group (Kende et al, 2004. Plant Mol Bio). Involved in the formation of nematode-induced syncytia in roots of Arabidopsis thaliana.
AT4G21910	0.63	0.01029	NA	NA
AT1G75430	0.63	0.00716	BLH11	NA
AT5G22460	0.63	0.00946	NA	NA
AT2G45660	0.63	0.02672	AGL20	Controls flowering and is required for CO to promote flowering. It acts downstream of FT. Overexpression of (SOC1) AGL20 suppresses not only the late flowering of plants that have functional FRI and FLC alleles but also the delayed phase transitions during the vegetative stages of development. AGL20/SOC1 acts with AGL24 to promote flowering and inflorescence meristem identity.AGL20 upregulates expression of AGL24 in response to GA.
AT4G15530	0.63	0.00256	PPDK	The product of this long transcript was shown to be targeted to the chloroplast, whereas the shorter transcript (no targeting sequence) accumulates in the cytosol. They were also found in slightly different tissues.
AT3G25870	0.62	0.01464	NA	NA
AT1G13110	0.62	0.02833	CYP71B7	member of CYP71B
AT1G11700	0.62	0.02128	NA	NA
AT1G53700	0.62	0.04508	PK3AT	The WAG1 and its homolog, WAG2 each encodes a protein-serine/threonine kinase that are nearly 70% identical to PsPK3 protein. All three together with CsPK3 belong to PsPK3-type kinases. At the N-terminus, all four possess a serine/threonine-rich domain. They are closely related to Arabidopsis kinases PINOID. wag1/wag2 double mutants exhibit a pronounced wavy root phenotype when grown vertically on agar plates (while wild-type plants develop wavy roots only on plates inclined to angles less than 90 degrees), indicating an overlapping role for WAG1 and WAG2 as suppressors of root waving. Simultaneous disruption of PID(AT2G34650) and its 3 closest homologs (PID2/AT2G26700, WAG1/AT1G53700, and WAG2/AT3G14370) abolishes the formation of cotyledons.
AT5G57887	0.62	0.00117	NA	NA
AT1G05570	0.62	0.00242	ATGSL06	Encodes a callose synthase 1 catalytic subunit . Member of Glycosyltransferase Family- 48.
AT1G08180	0.62	0.00174	NA	NA
AT4G25940	0.61	0.00781	NA	NA
AT3G22460	0.61	0.04313	OASA2	Encodes a member of a family of genes with O-acetylserine(thiol)lyase activity.
AT1G31770	0.61	0.00105	ABCG14	NA
AT4G08290	0.61	0.00213	UMAMIT20	NA
AT5G58500	0.61	0.01650	LSH5	NA

AT3G50440	0.61	0.00193	ATMES10	Encodes a protein shown to have methyl jasmonate esterase activity in vitro. This protein does not act on methyl IAA, MeSA, MeGA4, or MEGA9 in vitro.
AT2G37460	0.61	0.00501	UMAMIT12	NA
AT5G15830	0.61	0.04810	AtbZIP3	NA
AT5G62900	0.61	0.00132	NA	NA
AT5G65510	0.61	0.04810	AIL7	NA
AT4G31620	0.61	0.01464	NA	NA
AT1G13100	0.61	0.00121	CYP71B29	putative cytochrome P450
AT1G80180	0.60	0.03710	NA	NA
AT3G61630	0.60	0.01583	CRF6	CRF6 encodes one of the six cytokinin response factors. CRF5 belongs to the AP2/ERF superfamily of the transcriptional factors. CRF proteins rapidly relocalize to the nucleus in response to cytokinin. Analysis of loos-of-function mutants revealed that the CRFs function redundantly to regulate the development of embryos, cotyledons and leaves.
AT1G69440	0.60	0.01778	AGO7	Encodes ARGONAUTE7, a member of the ARGONAUTE family, characterised by the presence of PAZ and PIWI domains. Involved in the regulation of developmental timing. Required for the accumulation of TAS3 ta-siRNAs but not for accumulation of miR171, miR173, miR390 or mi391. Localized in mature rosette leaves and floral buds.
AT1G27030	0.60	0.00007	NA	NA
AT4G22690	0.60	0.00107	CYP706A1	member of CYP706A
AT1G80050	0.60	0.00070	APT2	Encodes an adenosine phosphoribosyl transferase(E.C:2.4.2.7), a constitutively expressed enzyme involved in the one-step salvage of adenine to AMP. This isozyme has high affinity for cytokinins and is likely to be localized to the cytosol.
AT5G59780	0.60	0.00381	ATMYB59	Encodes a putative transcription factor (MYB59).
AT3G25020	0.60	0.00946	AtRLP42	NA
AT4G39780	0.60	0.02424	NA	encodes a member of the DREB subfamily A-6 of ERF/AP2 transcription factor family. The protein contains one AP2 domain. There are 8 members in this subfamily including RAP2.4.
AT5G66490	0.60	0.04913	NA	NA
AT2G27420	0.60	0.04445	NA	NA
AT4G24015	0.60	0.00211	NA	NA

AT4G32940	0.60	0.01181	GAMMA-VPE	Encodes a vacuolar processing enzyme belonging to a novel group of cysteine proteinases that is expressed in vegetative organs and is upregulated in association with various types of cell death and under stressed conditions. They are essential in processing seed storage proteins and for mediating the susceptible response of toxin-induced cell death.
AT2G38310	0.60	0.00304	PYL4	Encodes a member of the PYR (pyrabactin resistance)/PYL(PYR1-like)/RCAR (regulatory components of ABA receptor) family proteins with 14 members. PYR/PYL/RCAR family proteins function as abscisic acid sensors. Mediate ABA-dependent regulation of protein phosphatase 2Cs ABI1 and ABI2.
AT1G01180	0.60	0.04624	NA	NA
AT5G05440	0.59	0.03848	PYL5	Encodes a member of the PYR (pyrabactin resistance)/PYL(PYR1-like)/RCAR (regulatory components of ABA receptor) family proteins with 14 members. PYR/PYL/RCAR family proteins function as abscisic acid sensors. Mediate ABA-dependent regulation of protein phosphatase 2Cs ABI1 and ABI2.
AT1G13400	0.59	0.04556	JGL	Along with JAG, it is involved in stamen and carpel development. Expression is limited to the adaxial side of lateral organs. Activated by AGAMOUS in a cal-1, ap1-1 background.
AT2G24580	0.59	0.00284	NA	NA
AT3G54720	0.59	0.00054	AMP1	Encodes glutamate carboxypeptidase. Various alleles show-increased cotyledon number and rate of leaf initiation, show transformation of leaves to cotyledons, altered flowering time and photomorphogenesis and an increased level of cytokinin biosynthesis. Involved in ethylene enhanced hypocotyl elongation in the light. Strong genetic interaction between TGH and AMP1.
AT4G30250	0.59	0.01640	NA	NA
AT2G28670	0.59	0.03647	ESB1	NA
AT4G27300	0.59	0.00031	NA	NA
AT1G78850	0.58	0.00034	NA	curculin-like (mannose-binding) lectin family protein, low similarity to ser/thr protein kinase from Zea mays (GI:2598067); contains Pfam lectin (probable mannose binding) domain PF01453 but not the protein kinase domain of the Z. mays protein
AT3G50840	0.58	0.00373	NA	NA
AT2G36870	0.58	0.00622	AtXTH32	NA
AT5G14730	0.58	0.04114	NA	NA
AT5G39030	0.58	0.02611	NA	NA
AT3G62150	0.58	0.00014	ABCB21	NA
AT5G04950	0.58	0.00883	ATNAS1	Encodes a nicotianamide synthase.

AT1G08810	0.58	0.03147	AtMYB60	putative transcription factor of the R2R3-MYB gene family. Transcript increases under conditions that promote stomatal opening (white and blue light, abi1-1 mutation) and decreases under conditions that trigger stomatal closure (ABA, desiccation, darkness), with the exception of elevated CO2. Expressed exclusively in guard cells of all tissues. It is required for light-induced opening of stomata. Mutant shows reduced stomatal aperture which helps to limit water loss during drought.
AT1G77885	0.58	0.00099	NA	NA
AT1G22400	0.57	0.00274	ATUGT85A1	NA
AT2G27310	0.57	0.01008	NA	NA
AT2G13665	0.57	0.00193	NA	NA
AT4G37150	0.57	0.02846	ATMES9	Encodes a protein shown to have carboxylesterase activity, methyl salicylate esterase activity, methyl jasmonate esterase activity, and methyl IAA esterase activity in vitro. MES9 appears to be involved in MeSA hydrolysis in planta. Expression of MES9 can restore systemic acquired resistance in SAR-deficient tobacco plants. This protein does not act on MeGA4, or MEGA9 in vitro.
AT3G62040	0.57	0.02968	NA	NA
AT1G77380	0.57	0.02427	AAP3	Amino acid permease which transports basic amino acids.
AT5G43910	0.57	0.01056	NA	NA
AT3G60690	0.56	0.01154	SAUR59	NA
AT3G51910	0.56	0.04617	AT-HSFA7A	member of Heat Stress Transcription Factor (Hsf) family
AT4G02850	0.56	0.00598	NA	NA
AT4G36670	0.56	0.00256	AtPLT6	NA
AT1G78830	0.56	0.01073	NA	NA
AT1G52270	0.56	0.00211	NA	NA
AT3G52525	0.56	0.02274	ATOFP6	NA
AT3G11660	0.55	0.00259	NHL1	encodes a protein whose sequence is similar to tobacco hairpin-induced gene (HIN1) and Arabidopsis non-race specific disease resistance gene (NDR1). Expression of this gene is induced by cucumber mosaic virus. Localization of the gene product is similar to that of NHL3 (plasma membrane) but it is yet inconclusive.
AT1G22500	0.55	0.01398	AtATL15	NA
AT1G32450	0.55	0.03574	AtNPF7.3	Transmembrane nitrate transporter. Involved in xylem transport of nitrate from root to shoot. Induced in response to nitrate. Not involved in nitrate uptake. expressed in root pericycle cells.
AT5G11930	0.55	0.04629	NA	NA

AT5G41590	0.55	0.03479	NA	NA
AT1G44970	0.55	0.02031	NA	NA
AT5G19260	0.55	0.03139	FAF3	NA
AT4G11290	0.55	0.02672	NA	NA
AT5G65040	0.54	0.00565	NA	NA
AT2G31160	0.54	0.01870	LSH3	NA
AT5G38610	0.54	0.00883	NA	NA
AT2G31230	0.54	0.01456	ATERF15	encodes a member of the ERF (ethylene response factor) subfamily B-3 of ERF/AP2 transcription factor family. The protein contains one AP2 domain. There are 18 members in this subfamily including ATERF-1, ATERF-2, AND ATERF-5.
AT3G63110	0.54	0.01862	ATIPT3	Encodes cytokinin synthase involved in cytokinin biosynthesis. IPT3 subcellular localization is modulated by farnesylation- when farnesylated it is localized to the nucleus, otherwise to the chloroplast.
AT2G23600	0.54	0.00015	ACL	Encodes a protein shown to have carboxylesterase activity, methyl salicylate esterase activity, methyl jasmonate esterase activity, and methyl IAA esterase activity in vitro. MES2 appears to be involved in MeSA hydrolysis in planta. This protein does not act on MeGA4, or MEGA9 in vitro.
AT5G06800	0.54	0.00107	NA	NA
AT1G69520	0.53	0.03619	NA	NA
AT1G76990	0.53	0.00014	ACR3	NA
AT5G59090	0.53	0.00242	ATSBT4.12	NA
AT1G73330	0.53	0.00445	ATDR4	encodes a plant-specific protease inhibitor-like protein whose transcript level in root disappears in response to progressive drought stress. The decrease in transcript level is independent from abscisic acid level.
AT3G50740	0.52	0.00064	UGT72E1	UGT72E1 is an UDPG:coniferyl alcohol glucosyltransferase which specifically glucosylates sinapyl- and coniferyl aldehydes. The enzyme is thought to be involved in lignin metabolism.
AT2G34960	0.52	0.02630	CAT5	Encodes a member of the cationic amino acid transporter (CAT) subfamily of amino acid polyamine choline transporters. Mediates efficient uptake of Lys, Arg and Glu in a yeast system. Localized to the plasma membrane.
AT3G59270	0.52	0.00233	NA	NA
AT2G15080	0.52	0.01535	AtRLP19	NA
AT3G10910	0.51	0.00159	DAFL1	NA
AT5G35732	0.51	0.02455	NA	NA

AT3G16770	0.51	0.00213	ATEBP	Encodes a member of the ERF (ethylene response factor) subfamily B-2 of the plant specific ERF/AP2 transcription factor family (RAP2.3). The protein contains one AP2 domain. There are 5 members in this subfamily including RAP2.2 AND RAP2.12.It is localized to the nucleus and acts as a transcriptional activator through the GCC-box. It has been identified as a suppressor of Bax-induced cell death by functional screening in yeast and can also suppress Bax-induced cell death in tobacco plants. Overexpression of this gene in tobacco BY-2 cells confers resistance to H2O2 and heat stresses. Overexpression in Arabidopsis causes upregulation of PDF1.2 and GST6. It is part of the ethylene signaling pathway and is predicted to act downstream of EIN2 and CTR1, but not under EIN3.
AT4G30110	0.51	0.00357	ATHMA2	encodes a protein similar to Zn-ATPase, a P1B-type ATPases transport zinc
AT2G41180	0.51	0.00101	SIB2	NA
AT1G74890	0.51	0.02448	ARR15	Encodes a nuclear response regulator that acts as a negative regulator in cytokinin-mediated signal transduction. Transcript accumulates in leaves and roots in response to cytokinin treatment.
AT5G65530	0.51	0.01430	NA	NA
AT3G52480	0.50	0.04286	NA	NA
AT2G17710	0.50	0.00021	NA	NA
AT2G29740	0.50	0.00436	UGT71C2	NA
AT3G48100	0.50	0.04114	ARR5	Encodes a transcription repressor that mediates a negative feedback loop in cytokinin signalling. ARR5 expression is upregulated by Class I KNOX genes. Arr5 protein is stabilized by cytokinin in a two-component phosphorelay.
AT2G36100	0.50	0.03153	CASP1	NA
AT5G52830	0.50	0.02403	ATWRKY27	Encodes a WRKY transcription factor WRKY27. Mutation in Arabidopsis WRKY27 results in delayed symptom development in response to the bacterial wilt pathogen Ralstonia solanacearum.
AT1G21100	0.50	0.02094	IGMT1	NA
AT3G15356	0.50	0.00098	NA	NA
AT4G13580	0.49	0.03647	NA	NA
AT3G26210	0.49	0.01852	CYP71B23	putative cytochrome P450
AT3G44970	0.49	0.00022	NA	NA
AT1G71740	0.49	0.03844	NA	NA
AT2G38180	0.49	0.00065	NA	NA
AT5G61412	0.48	0.03976	NA	NA
AT1G19050	0.48	0.02748	ARR7	Encodes a member of the Arabidopsis response regulator (ARR) family, most closely related to ARR15. A two-component response regulator protein containing a phosphate accepting domain in the receiver domain but lacking a DNA binding domain in the output domain. Involved in response to cytokinin and meristem stem cell maintenance. Arr7 protein is stabilized by cytokinin.

AT5G58580	0.48	0.00249	ATL63	NA
AT1G67110	0.48	0.00408	CYP735A2	member of CYP709A
AT1G72200	0.48	0.01398	NA	NA
AT3G45680	0.48	0.00006	NA	NA
AT5G44580	0.48	0.00006	NA	NA
AT3G46130	0.47	0.00067	ATMYB48	Encodes a putative transcription factor (MYB48) that functions to regulate flavonol biosynthesis primarily in cotyledons.
AT5G48010	0.47	0.03115	AtTHAS1	Encodes an oxidosqualene cyclase involved in the biosynthesis of thalianol, a tricyclic triterpenoid of unknown function. Overexpression of THAS leads to dwarfing in the aerial tissues of Arabidopsis plants, but increases their root length. THAS is part of a small operon-like cluster of genes (with At5g48000 (THAH) and At5g47990 (THAD)) involved in thalianol metabolism.
AT1G10470	0.46	0.00016	ARR4	Encodes a two-component response regulator. Acts redundantly with ARR3 in the control of circadian period in a cytokinin-independent manner.
AT3G55230	0.46	0.02702	NA	NA
AT5G11320	0.46	0.00102	AtYUC4	Belongs to the YUC gene family. Encodes a predicted flavin monooxygenase YUC4 involved in auxin biosynthesis and plant development.
AT5G45650	0.45	0.00429	NA	NA
AT3G45700	0.45	0.00342	NA	NA
AT2G36970	0.45	0.00089	NA	NA
AT2G37130	0.45	0.00883	NA	NA
AT1G61590	0.44	0.00071	NA	NA
AT1G05300	0.44	0.00169	ZIP5	member of Fe(II) transporter isolog family
AT4G21870	0.44	0.00012	NA	NA
AT2G40113	0.44	0.02427	NA	NA
AT5G47990	0.43	0.00748	CYP705A5	encodes a member of the CYP705A family of cytochrome P450 enzymes. It appears to catalyze the addition of a double bond to thalian-diol at carbon 15. Reduced levels of THAD expression lead to a build up of thalian-diol in root extracts. thad1-1 mutants also have longer roots than wild type seedlings.
AT1G06160	0.43	0.01449	ORA59	encodes a member of the ERF (ethylene response factor) subfamily B-3 of ERF/AP2 transcription factor family. The protein contains one AP2 domain. There are 18 members in this subfamily including ATERF-1, ATERF-2, AND ATERF-5.
AT5G42180	0.43	0.00803	PER64	NA
AT1G27020	0.43	0.00015	NA	NA

AT3G23550	0.43	0.02348	NA	NA
AT4G31330	0.42	0.00198	NA	NA
AT3G01260	0.42	0.00397	NA	NA
AT3G48740	0.42	0.03691	AtSWEET11	NA
AT5G06570	0.41	0.00461	NA	NA
AT3G29670	0.41	0.00863	PMAT2	NA
AT4G16563	0.41	0.02616	NA	NA
AT4G11460	0.41	0.00148	CRK30	Encodes a cysteine-rich receptor-like protein kinase.
AT4G08300	0.41	0.00006	UMAMIT17	NA
AT3G08860	0.40	0.00193	PYD4	Encodes a protein that is predicted to have beta-alanine aminotransferase activity.
AT5G48000	0.40	0.00503	CYP708	Encodes a member of the CYP708A family of cytochrome P450 enzymes. THAH appears to add a hydroxyl group to the triterpene thalianol. thah1 mutants have an elevated accumulation of thalianol. thah1-1 mutants have longer roots than wild type plants. Thalian-diol and desaturated thalian-diol are lost from the root extracts of thah1-1 mutants. Overexpression of the sequence from At5g48000.1 rescues the thah1-1 mutant phenotype (Field 2008); it is unknown whether the shorter sequences associated with other gene models would provide functional complementation.
AT3G15720	0.40	0.00213	NA	NA
AT4G26950	0.40	0.02695	NA	NA
AT4G15700	0.40	0.02083	NA	NA
AT5G61520	0.40	0.00023	NA	NA
AT3G24463	0.39	0.01692	NA	NA
AT2G38170	0.39	0.00125	ATCAX1	Encodes a high affinity vacuolar calcium antiporter. The residue His 338 is critical to Ca2+ transport activity. Disruption of CAX1 reduces manganese and zinc of shoot tissue and results in a decrease in the activity of vacuolar V-type proton ATPase.
AT1G15125	0.39	0.02128	NA	NA
AT4G15330	0.38	0.01262	CYP705A1	a member of the cytochrome P450 family
AT2G32300	0.38	0.00031	UCC1	Encodes a uclacyanin, a protein precursor that is closely related to precursors of stellacyanins and a blue copper protein from pea pods.
AT3G04210	0.38	0.02016	NA	NA
AT4G12450	0.38	0.02128	NA	NA
AT5G36220	0.37	0.01181	CYP81D1	member of CYP81D

AT5G56870	0.37	0.02695	BGAL4	NA
AT2G40330	0.36	0.02128	PYL6	Encodes a member of the PYR (pyrabactin resistance)/PYL(PYR1-like)/RCAR (regulatory components of ABA receptor) family proteins with 14 members. PYR/PYL/RCAR family proteins function as abscisic acid sensors. Mediate ABA-dependent regulation of protein phosphatase 2Cs ABI1 and ABI2.
AT3G26320	0.35	0.02723	CYP71B36	putative cytochrome P450
AT4G06746	0.35	0.00556	DEAR5	encodes a member of the DREB subfamily A-5 of ERF/AP2 transcription factor family (RAP2.9). The protein contains one AP2 domain. There are 16 members in this subfamily including RAP2.1 and RAP2.10.
AT5G61610	0.35	0.02275	NA	NA
AT5G62920	0.34	0.00828	ARR6	Encodes a Type-A response regulator that is responsive to cytokinin treatment. Its C-ter domain is very short in comparison to other Arabidopsis ARRs (17 total). Arr6 protein is stabilized by cytokinin.
AT1G10770	0.34	0.01595	NA	Encodes a putative pectin methylesterase/invertase inhibitor. Anti-sense reduction of this gene's transcript results in pollen tube growth retardation and then partial male sterility and reduced seed set.
AT5G10210	0.33	0.00181	NA	NA
AT1G43020	0.33	0.00213	NA	NA
AT5G43290	0.32	0.01084	ATWRKY49	member of WRKY Transcription Factor; Group II-c
AT5G44572	0.31	0.00007	NA	NA
AT3G16530	0.29	0.00444	NA	Lectin like protein whose expression is induced upon treatment with chitin oligomers.
AT5G44574	0.28	0.00006	NA	NA
AT3G46880	0.28	0.01181	NA	NA
AT3G44990	0.20	0.00026	AtXTH31	xyloglucan endo-transglycosylase
AT3G05770	0.11	0.01531	NA	NA

Table 4: Overlap in significant upregulated expressed genes over the three timepoints of analysis

Names	total	elements	GeneSymbol
180' 30' 60'	63	AT4G17460	HAT1
		AT3G25717	DVL6
		AT4G34760	SAUR50
		AT2G26710	BAS1
		AT2G23170	GH3.3
		AT4G36110	SAUR9
		AT2G28350	ARF10
		AT1G29460	SAUR65
		AT5G66580	NA
		AT1G26945	KDR
		AT5G43190	NA
		AT1G67880	NA
		AT3G60390	HAT3
		AT5G41400	NA
		AT3G28857	PRE5
		AT4G09970	NA
		AT5G18010	SAUR19
		AT1G54200	NA
		AT3G60630	ATHAM2
		AT3G03830	SAUR28
		AT3G15540	IAA19
		AT1G29490	SAUR68
		AT4G14819	NA
		AT1G78100	AUF1
		AT5G18030	NA
		AT5G47370	HAT2
		AT5G43700	ATAUX2-11
		AT4G37390	AUR3
		AT3G28420	NA
		AT5G18080	SAUR24
		AT4G21200	ATGA2OX8
		AT1G29500	SAUR66
		AT4G28640	IAA11
		AT3G17090	NA
		AT3G03840	SAUR27
		AT2G14960	GH3.1
		AT1G30100	ATNCED5
		AT2G36220	NA
		AT1G63840	NA
		AT1G15550	ATGA3OX1
		AT3G55720	NA
		AT1G04240	IAA3

		AT5G65340	NA
		AT1G51170	AGC2-3
		AT4G09890	NA
		AT4G38850	ATSAUR15
		AT3G63440	ATCKX6
		AT1G67340	NA
		AT4G25420	AT2301
		AT4G03140	NA
		AT5G52900	MAKR6
		AT5G15580	LNG1
		AT1G65920	NA
		AT2G39370	MAKR4
		AT5G02865	NA
		AT1G29465	NA
		AT2G41170	NA
		AT2G42430	ASL18
		AT3G23635	RTFL13
		AT1G29440	SAUR63
		AT3G14370	WAG2
		AT5G64770	CLEL
		AT5G18060	SAUR23
30' 60'	19	AT1G29510	SAUR67
		AT1G29420	SAUR61
		AT2G30040	MAPKKK14
		AT1G18400	BEE1
		AT3G03820	SAUR29
		AT3G03850	SAUR26
		AT4G37790	HAT22
		AT4G34770	SAUR1
		AT2G34650	ABR
		AT1G15580	ATAUX2-27
		AT3G61460	BRH1
		AT1G29450	SAUR64
		AT1G21050	NA
		AT4G38825	SAUR13
		AT1G53163	NA
		AT4G38840	SAUR14
		AT1G29430	SAUR62
		AT1G26960	AtHB23
		AT5G18070	DRT101
180' 60'	182	AT2G42380	ATBZIP34
		AT5G03150	JKD
		AT4G39840	NA
		AT2G35880	NA
		AT5G54500	FQR1
		AT3G26760	NA

AT1G04250	AXR3
AT1G13670	NA
AT5G66600	NA
AT5G45280	NA
AT2G14890	AGP9
AT1G66350	RGL
AT1G68410	NA
AT3G50280	NA
AT1G73590	ATPIN1
AT4G13195	CLE44
AT4G23710	VAG2
AT4G32285	NA
AT2G34070	TBL37
AT1G76610	NA
AT3G13970	APG12
AT3G28180	ATCSLC04
AT3G50890	AtHB28
AT3G29360	UGD2
AT1G61170	NA
AT3G59900	ARGOS
AT1G49740	NA
AT2G47930	AGP26
AT3G13650	NA
AT1G52565	NA
AT5G64780	NA
AT4G16515	CLEL
AT3G17120	NA
AT2G31680	AtRABA5d
AT5G55380	NA
AT1G75450	ATCKX5
AT4G31000	NA
AT2G21050	LAX2
AT4G27260	GH3.5
AT4G31910	BAT1
AT2G01200	IAA32
AT2G42800	AtRLP29
AT4G22780	ACR7
AT3G12670	emb2742
AT5G08790	anac081
AT2G38610	NA
AT1G74380	XXT5
AT1G69295	PDCB4
AT5G48500	NA
AT3G28340	GATL10
AT1G70940	ATPIN3
AT4G22560	NA

AT4G21730	NA
AT2G43290	MSS3
AT4G12410	SAUR35
AT5G65610	NA
AT2G18969	NA
AT4G13180	NA
AT1G59710	NA
AT1G14185	NA
AT3G12610	DRT100
AT2G34300	NA
AT2G41820	PXC3
AT1G52830	IAA6
AT1G05420	ATOFP12
AT5G56170	LLG1
AT5G27000	ATK4
AT3G02000	ROXY1
AT5G66590	NA
AT1G02850	BGLU11
AT4G13790	SAUR25
AT1G29660	NA
AT3G06770	NA
AT1G59740	AtNPF4.3
AT3G42800	NA
AT3G22820	CLL1
AT3G49220	NA
AT1G67265	DVL3
AT5G11970	NA
AT4G39390	ATNST-KT1
AT1G32190	NA
AT3G25710	ATAIG1
AT1G21980	ATPIP5K1
AT5G55850	NOI
AT5G09970	CYP78A7
AT5G02760	APD7
AT3G13520	AGP12
AT5G65800	ACS5
AT3G45970	ATEXLA1
AT1G11545	XTH8
AT1G75500	UMAMIT5
AT1G30690	NA
AT3G07010	NA
AT4G30180	NA
AT3G44610	NA
AT4G39800	ATIPS1
AT5G65670	IAA9
AT1G72230	NA

AT5G11740	AGP15
AT2G33310	IAA13
AT3G60260	NA
AT4G24275	NA
AT4G30290	ATXTH19
AT5G54510	DFL1
AT1G13250	GATL3
AT5G19530	ACL5
AT5G15150	ATHB-3
AT1G34110	NA
AT4G12110	ATSMO1-1
AT5G51790	NA
AT5G50130	NA
AT3G19380	PUB25
AT1G25425	CLE43
AT1G32170	XTH30
AT5G10430	AGP4
AT4G21745	NA
AT1G11120	NA
AT1G78970	ATLUP1
AT5G48150	PAT1
AT5G18050	SAUR22
AT5G11000	NA
AT3G58120	ATBZIP61
AT4G14560	AXR5
AT5G59010	BSK5
AT3G18200	UMAMIT4
AT4G35320	NA
AT5G57760	NA
AT5G18020	SAUR20
AT3G62630	NA
AT5G25440	NA
AT5G06930	NA
AT3G10720	NA
AT1G62440	LRX2
AT3G56800	ACAM-3
AT1G54120	NA
AT3G54030	BSK6
AT1G75080	BZR1
AT5G54530	NA
AT5G37950	NA
AT3G14362	DVL19
AT3G11700	FLA18
AT1G13245	DVL4
AT4G19120	ERD3
AT1G17620	NA

		AT5G66920	sks17
		AT1G12990	NA
		AT3G07360	ATPUB9
		AT1G11740	NA
		AT1G14920	GAI
		AT5G65613	NA
		AT1G75590	SAUR52
		AT1G63420	NA
		AT4G31590	ATCSLC05
		AT5G44670	GALS2
		AT1G45688	NA
		AT1G69690	AtTCP15
		AT1G49780	PUB26
		AT3G23170	NA
		AT2G17990	NA
		AT3G07470	NA
		AT4G21740	NA
		AT1G67900	NA
		AT3G50900	NA
		AT2G22460	NA
		AT5G49630	AAP6
		AT1G52280	AtRABG3d
		AT2G01420	ATPIN4
		AT4G37590	MEL1
		AT3G13310	DJC66
		AT3G07000	NA
		AT5G51670	NA
		AT4G23070	ATRBL7
		AT1G69570	NA
		AT3G28200	NA
		AT3G23030	IAA2
		AT4G13190	NA
		AT3G14440	ATNCED3
		AT5G17490	AtRGL3
		AT4G38400	ATEXLA2
		AT3G27500	NA
		AT5G39860	BHLH136
		AT3G15820	ROD1
30'	1	AT1G24130	NA
60'	361	AT4G09460	AtMYB6
		AT1G51660	ATMEK4
		AT1G78120	TPR12
		AT2G25790	SKM1
		AT4G30470	NA
		AT2G47060	PTI1-4
		AT1G76220	NA

AT2G26440	PME12
AT5G56980	NA
AT4G26490	NA
AT2G18010	SAUR10
AT2G34770	ATFAH1
AT5G53250	AGP22
AT1G14330	NA
AT2G47860	SETH6
AT5G62865	NA
AT1G57680	Cand1
AT2G39130	NA
AT1G77640	NA
AT5G52060	ATBAG1
AT3G63120	CYCP1;1
AT5G37540	NA
AT5G05365	NA
AT4G05020	NDB2
AT5G05180	NA
AT1G14190	NA
AT5G64740	CESA6
AT5G54860	NA
AT1G33800	AtGXMT1
AT2G39180	ATCRR2
AT2G17230	EXL5
AT4G27270	NA
AT1G78480	NA
AT4G32810	ATCCD8
AT2G46570	LAC6
AT2G41660	MIZ1
AT2G41110	ATCAL5
AT1G68810	NA
AT5G44063	NA
AT5G54490	PBP1
AT2G41510	ATCKX1
AT3G19200	NA
AT3G06890	NA
AT5G22690	NA
AT1G09350	AtGolS3
AT4G17695	KAN3
AT1G79760	DTA4
AT4G28490	HAE
AT1G80100	AHP6
AT1G80280	NA
AT3G62420	ATBZIP53
AT3G15115	NA
AT1G76340	GONST3

AT2G44830	NA
AT3G13000	NA
AT3G17420	GPK1
AT1G72470	ATEXO70D1
AT2G22000	PROPEP6
AT3G05320	NA
AT1G53340	NA
AT1G07490	DVL9
AT1G53470	MSL4
AT5G61570	NA
AT1G68825	DVL5
AT5G66280	GMD1
AT2G21195	NA
AT3G50350	NA
AT4G25760	ATGDU2
AT1G04040	NA
AT5G56970	ATCKX3
AT1G64625	NA
AT2G34930	NA
AT5G50670	SPL13
AT2G41800	NA
AT4G34800	SAUR4
AT3G17390	MAT4
AT2G19460	NA
AT3G51790	AtCCME
AT3G02070	NA
AT2G45410	LBD19
AT5G37475	NA
AT5G53590	SAUR30
AT3G60650	NA
AT5G48450	sks3
AT2G41070	ATBZIP12
AT3G28455	CLE25
AT1G22882	NA
AT2G22470	AGP2
AT3G57450	NA
AT4G01140	NA
AT3G15040	NA
AT5G07110	PRA1.B6
AT1G65310	ATXTH17
AT2G33570	GALS1
AT4G19460	NA
AT5G58630	TRM31
AT4G24805	NA
AT4G00480	ATMYC1
AT4G19230	CYP707A1

AT5G05810	ATL43
AT4G35160	NA
AT1G10550	XET
AT1G68360	NA
ATMG01320	NAD2
AT4G02290	AtGH9B13
AT5G50090	NA
AT1G21840	UREF
AT5G01710	NA
AT5G57100	NA
AT5G50120	NA
AT5G26800	NA
AT5G03040	iqd2
AT1G52290	AtPERK15
AT1G76160	sks5
AT4G08170	NA
AT3G04860	NA
AT2G45310	GAE4
AT3G26960	NA
AT1G58340	BCD1
AT1G01120	KCS1
AT2G41410	NA
AT5G10830	NA
AT3G03660	WOX11
AT1G72750	ATTIM23-2
AT1G21830	NA
AT5G45730	NA
AT1G55910	ZIP11
AT4G29310	NA
AT2G22680	WAVH1
AT5G18930	BUD2
AT2G23100	NA
AT1G01600	CYP86A4
AT1G17170	ATGSTU24
AT4G31550	ATWRKY11
AT2G01190	PDE331
AT4G34810	SAUR5
AT4G39220	ATRER1A
AT5G24030	SLAH3
AT2G21200	SAUR7
AT3G18010	WOX1
AT3G13960	AtGRF5
AT5G66200	ARO2
AT1G35140	EXL1
AT1G24170	GATL8
AT2G42440	ASL15

AT2G41880	AGK1
AT4G34750	SAUR49
AT3G04210	NA
AT5G20110	NA
AT1G11125	NA
AT3G62720	ATXT1
AT2G41480	AtPRX25
AT3G60550	CYCP3;2
AT4G05010	AtFBS3
AT2G37250	ADK
AT5G61310	NA
AT3G10820	NA
AT1G62045	NA
AT3G14540	NA
AT1G74420	ATFUT3
AT2G10605	NA
AT5G45580	NA
AT2G26530	AR781
AT4G26480	NA
AT1G47860	NA
AT4G10150	NA
AT3G60640	ATG8G
AT1G23340	NA
AT5G62220	ATGT18
AT2G20840	AtSCAMP3
AT2G33320	NA
AT5G45420	maMYB
AT3G56810	NA
AT5G54145	NA
AT5G58620	TZF9
AT4G12130	NA
AT5G51810	AT2353
AT2G21220	SAUR12
AT3G59440	NA
AT3G24255	NA
AT1G72790	NA
AT4G04745	NA
AT3G17100	AIF3
AT4G35070	NA
AT4G31020	NA
AT4G32880	ATHB-8
AT2G14820	MEL3
AT2G39870	NA
AT4G22530	NA
AT5G25190	ESE3
AT1G70920	ATHB18

AT2G01430	ATHB-17
AT1G68330	NA
AT4G18890	BEH3
AT3G06990	NA
AT3G50340	NA
AT2G24300	NA
AT5G25170	NA
AT1G26770	AT-EXP10
AT5G27760	NA
AT5G05220	NA
AT5G23850	NA
AT5G66310	NA
AT5G14895	NA
AT3G15670	NA
AT3G19390	NA
AT1G08030	AQC1
AT5G13500	NA
AT2G31280	CPUORF7
AT1G76090	SMT3
AT5G14020	NA
AT1G12580	PEPKR1
AT3G17690	ATCNGC19
AT1G61260	NA
AT4G30440	GAE1
AT3G54810	BME3
AT5G47440	NA
AT2G17080	NA
AT2G01150	RHA2B
AT4G00080	UNE11
AT5G44060	NA
AT3G17185	NA
AT1G80240	DGR1
AT1G15520	ABCG40
AT2G31730	NA
AT4G25810	XTH23
AT4G20170	GALS3
AT3G25780	AOC3
AT5G44568	NA
AT5G64310	AGP1
AT4G08930	APRL6
AT1G01540	NA
AT5G50335	NA
AT3G63430	TRM5
AT1G57560	AtMYB50
AT1G48040	NA
AT1G52827	ATCDT1

AT1G24625	ZFP7
AT3G08630	NA
AT5G15350	AtENODL17
AT5G24110	ATWRKY30
AT1G22470	NA
AT3G47510	NA
AT1G02930	ATGST1
AT5G06760	AtLEA4-5
AT3G55840	NA
AT3G58190	ASL16
AT3G62100	IAA30
AT5G09600	SDH3-1
AT3G54920	PMR6
AT5G12050	NA
AT3G19680	NA
AT2G22830	SQE2
AT1G65845	NA
AT1G01200	ATRAB-A3
AT5G60200	TMO6
AT4G37890	EDA40
AT4G20780	CML42
AT5G40540	NA
AT1G65840	ATPAO4
AT4G00970	CRK41
AT4G09030	AGP10
AT1G61255	NA
AT2G46590	DAG2
AT5G14360	NA
AT3G05490	RALFL22
AT2G20562	NA
AT1G77450	anac032
AT3G25900	ATHMT-1
AT1G64640	AtENODL8
AT3G62660	GATL7
AT1G80730	ATZFP1
AT3G06740	GATA15
AT4G28650	NA
AT2G38360	PRA1.B4
AT5G09805	IDL3
AT1G61667	NA
AT1G08010	GATA11
AT3G61560	NA
AT5G45670	NA
AT4G01575	NA
AT1G27210	NA
AT4G08950	EXO

AT4G13340	LRX3
AT5G47800	NA
AT5G67450	AZF1
AT5G54230	AtMYB49
AT4G22550	LPPbeta
AT5G20820	SAUR76
AT3G25250	AGC2
AT1G04550	BDL
AT3G45960	ATEXLA3
AT1G14182	NA
AT3G60200	NA
AT1G18835	MIF3
AT2G05940	RIPK
AT3G24530	NA
AT5G15160	BHLH134
AT3G54000	NA
AT1G04877	NA
AT4G21850	ATMSRB9
AT1G14630	NA
AT4G03190	AFB1
AT5G59220	HAI1
AT2G34080	NA
AT1G53830	ATPME2
AT1G66940	NA
AT4G10040	CYTC-2
AT1G01130	NA
AT5G20670	NA
AT4G15800	RALFL33
AT5G05380	PRA1.B3
AT5G62170	TRM25
AT5G66940	NA
AT1G67400	NA
AT1G32920	NA
AT2G41130	NA
AT5G13700	APAO
AT5G26930	GATA23
AT2G37940	AtIPCS2
AT4G34419	NA
AT5G01970	NA
AT5G45720	NA
AT2G43340	NA
AT3G06868	NA
AT5G05160	RUL1
AT5G63790	ANAC102
AT3G62090	PIF6
AT3G47090	NA

		AT1G72430	SAUR78
		AT3G14870	NA
		AT2G22810	ACC4
		AT3G12920	BRG3
		AT5G01765	NA
		AT5G55250	AtIAMT1
		AT1G65240	NA
		AT1G14080	ATFUT6
		AT4G30280	ATXTH18
		AT1G29270	NA
		AT2G23060	NA
		AT3G57010	NA
		AT3G50410	OBP1
		AT2G20370	AtMUR3
		AT3G59310	NA
		AT1G70990	NA
		AT1G74660	MIF1
		AT3G12700	NANA
		AT4G37450	AGP18
		AT3G06370	ATNHX4
		AT4G32790	NA
		AT1G63500	BSK7
		AT5G49300	GATA16
		AT3G49350	NA
		AT3G20830	AGC2-4
		AT5G51460	ATTPPA
		AT4G30996	NKS1
		AT4G39920	POR
		AT5G39850	NA
		AT4G32350	NA
		AT1G31880	BRX
		AT4G26470	NA
180'	269	AT1G70950	NA
		AT2G29390	ATSMO2
		AT1G13970	NA
		AT1G78040	NA
		AT4G20890	TUB9
		AT1G68910	WIT2
		AT3G48610	NPC6
		AT2G37550	AGD7
		AT1G63300	NA
		AT2G21060	ATCSP4
		AT4G08685	SAH7
		AT4G32280	IAA29
		AT1G23030	NA
		AT5G61480	PXY

AT2G14900	NA
AT3G16360	AHP4
AT4G27840	NA
AT1G72160	NA
AT3G01750	NA
AT4G13350	NIG
AT3G63470	scpl40
AT4G24790	NA
AT4G25280	NA
AT5G57970	NA
AT1G07420	ATSMO1
AT1G11000	ATMLO4
AT3G46830	ATRAB-A2C
AT5G18560	PUCHI
AT4G17550	AtG3Pp4
AT5G52430	NA
AT3G04730	IAA16
AT5G65310	ATHB-5
AT1G53290	NA
AT2G40540	ATKT2
AT3G01470	ATHB-1
AT1G05680	UGT74E2
AT4G17170	AT-RAB2
AT1G73760	NA
AT2G41420	WIH2
AT5G08330	AtTCP11
AT2G27860	AXS1
AT3G10525	LGO
AT4G25410	NA
AT1G19850	ARF5
AT1G70270	NA
AT5G57270	NA
AT4G26690	GDPDL3
AT1G75780	TUB1
AT2G26730	NA
AT5G37940	NA
AT5G66420	NA
AT5G63820	NA
AT4G25770	NA
AT2G33120	ATVAMP722
AT1G23080	ATPIN7
AT4G10020	AtHSD5
AT3G14790	ATRHM3
AT1G05835	NA
AT1G14830	ADL1C
AT1G60660	ATCB5LP

AT1G27350	NA
AT3G01780	TPLATE
AT4G26140	BGAL12
AT3G23050	AXR2
AT1G48330	NA
AT1G63260	TET10
AT4G30610	BRS1
AT1G08500	AtENODL18
AT1G04430	NA
AT3G51470	NA
AT3G17050	NA
AT5G65440	NA
AT4G33580	ATBCA5
AT1G69780	ATHB13
AT2G20760	NA
AT1G19835	NA
AT5G66080	APD9
AT3G50830	ATCOR413-PM2
AT2G42990	NA
AT2G18480	NA
AT4G18670	NA
AT5G22860	NA
AT1G11905	NA
AT3G12360	ITN1
AT1G48240	ATNPSN12
AT4G33625	NA
AT1G22910	NA
AT2G05810	NA
AT2G46640	TAC1
AT1G08200	AXS2
AT1G76620	NA
AT1G55520	ATTBP2
AT2G02870	NA
AT5G62580	NA
AT2G04780	FLA7
AT3G05910	NA
AT3G13965	NA
AT1G64660	ATMGL
AT3G23750	BARK1
AT5G28040	NA
AT1G57700	NA
AT1G14390	NA
AT5G61810	APC1
AT4G00050	UNE10
AT1G64330	NA

AT1G19440	KCS4
AT3G20130	CYP705A22
AT5G46730	NA
AT5G61660	NA
AT4G08040	ACS11
AT2G26690	AtNPF6.2
AT5G13460	IQD11
AT1G20970	NA
AT2G36300	NA
AT5G57785	NA
ATMG00580	NAD4
AT5G26667	PYR6
AT5G66800	NA
AT5G57790	NA
AT4G22010	sks4
AT3G49720	NA
AT1G23060	MDP40
AT3G05880	RCI2A
AT5G65810	CGR3
AT4G18380	NA
AT5G48900	NA
AT1G02816	NA
AT1G31070	GlcNAc1pUT1
AT1G08280	NA
AT2G37030	SAUR46
AT5G66460	AtMAN7
AT4G22545	NA
AT1G55840	NA
AT1G12850	NA
AT5G57780	P1R1
AT3G47295	NA
AT4G11820	FKP1
AT3G25620	ABCG21
AT5G47550	NA
AT1G50630	NA
AT1G36940	NA
AT1G11280	NA
AT5G10100	TPPI
AT2G23150	ATNRAMP3
AT2G29420	ATGSTU7
AT2G04570	NA
AT2G23180	CYP96A1
AT1G76240	NA
AT3G14880	NA
AT3G43740	NA
AT5G57340	NA

AT5G15265	NA
AT5G37790	NA
AT1G18840	IQD30
AT4G38900	NA
AT5G03520	ATRAB-E1D
AT4G24510	CER2
AT1G28960	ATNUDT15
AT3G15980	NA
AT1G62430	ATCDS1
AT5G44340	TUB4
AT4G30410	NA
AT2G27950	NA
AT4G28050	TET7
AT2G37380	MAKR3
AT1G69140	NA
AT5G57460	NA
AT1G10410	NA
AT5G45550	MOB1-like
AT1G75880	NA
AT3G14000	ATBRXL2
AT4G14548	NA
AT4G32460	NA
AT2G28950	ATEXP6
AT4G35880	NA
AT5G08130	BIM1
AT1G54100	ALDH7B4
AT5G23870	NA
AT3G08030	NA
AT2G39800	ATP5CS
AT5G09890	NA
AT5G12250	TUB6
AT3G48780	ATSPT1
AT2G41760	NA
AT4G36780	BEH2
AT3G24715	NA
AT5G12940	NA
AT1G29300	UNE1
AT5G47200	ATRAB1A
AT2G39010	PIP2;6
AT1G53040	NA
AT5G61240	NA
AT5G57050	ABI2
AT3G30180	BR6OX2
AT4G00300	NA
AT1G53840	ATPME1
AT1G70750	MyoB2

AT4G16980	NA
AT3G23640	HGL1
AT1G53000	AtCKS
AT1G75680	AtGH9B7
AT3G12620	NA
AT5G64250	NA
AT5G03080	LPPgamma
AT3G54690	SETH3
AT5G24120	ATSIG5
AT4G30270	MERI-5
AT1G78490	CYP708A3
AT4G35060	HIPP25
AT1G14460	NA
AT5G18520	Cand7
AT5G01740	NA
AT5G03760	ATCSLA09
AT5G60860	AtRABA1f
AT5G06860	ATPGIP1
AT4G24220	5[beta]-StR
AT3G29370	P1R3
AT5G43310	NA
AT4G39400	ATBRI1
AT1G72180	NA
AT2G39450	ATMTP11
AT1G53050	NA
AT4G01680	AtMYB55
AT3G13720	PRA1.F3
AT4G14550	IAA14
AT5G42420	NA
AT1G76670	NA
AT1G14670	NA
AT1G78440	ATGA2OX1
AT3G53232	DVL20
AT4G23400	PIP1;5
AT3G54400	NA
AT1G51160	NA
AT1G12845	NA
AT5G06870	ATPGIP2
AT3G27960	KLCR2
AT2G41740	ATVLN2
AT5G65390	AGP7
AT1G12080	NA
AT1G79990	NA
AT1G17700	PRA1.F1
AT4G20870	ATFAH2
AT5G38970	ATBR6OX

AT3G16570	ATRALF23
AT3G57800	NA
AT2G47130	AtSDR3
AT1G11890	ATSEC22
AT5G56730	NA
AT1G48230	NA
AT3G05945	NA
AT1G32410	NA
AT5G63650	SNRK2-5
AT3G18820	ATRAB7B
AT2G26700	PID2
AT5G38200	NA
AT4G25260	NA
AT2G35190	ATNPSN11
AT3G15480	NA
AT4G34490	ATCAP1
AT3G13980	NA
AT2G19660	NA
AT5G08590	ASK2
AT5G03553	NA
AT3G29575	AFP3
AT4G36648	NA
AT1G52750	NA
AT5G44260	AtTZF5
AT1G06870	Plsp2A
AT5G47180	NA

Table 5: Overlap in significant downregulated expressed genes over the three timepoints of analysis

Names	total	elements	GeneSymbol
180' 30' 60'	4	AT1G74940	NA
		AT3G63210	MARD1
		AT3G22970	NA
		AT1G79160	NA
30' 60'	9	AT4G21990	APR3
		AT1G36370	SHM7
		AT3G49570	LSU3
		AT3G49580	LSU1
		AT1G62180	APR2
		AT2G29670	NA
		AT5G57710	SMAX1
		AT1G04770	NA
		AT5G24660	LSU2
180' 60'	129	AT4G30110	ATHMA2
		AT2G23610	ATMES3
		AT4G24015	NA
		AT3G50840	NA
		AT4G31620	NA
		AT5G04950	ATNAS1
		AT1G67110	CYP735A2
		AT5G58580	ATL63
		AT3G11660	NHL1
		AT3G45680	NA
		AT2G15080	AtRLP19
		AT5G53160	PYL8
		AT1G11700	NA
		AT5G51970	NA
		AT3G15720	NA
		AT3G08860	PYD4
		AT3G51910	AT-HSFA7A
		AT2G03890	ATPI4K
		AT3G50440	ATMES10
		AT2G38180	NA
		AT4G04830	ATMSRB5
		AT2G23600	ACL
		AT5G14780	FDH
		AT2G27360	NA
		AT2G36970	NA
		AT4G16380	NA
		AT5G65040	NA
		AT4G28300	NA
		AT5G62900	NA
		AT5G21326	CIPK26

AT4G39510	CYP96A12
AT1G28100	NA
AT5G15860	ATPCME
AT2G17710	NA
AT1G58110	NA
AT5G15830	AtbZIP3
AT1G71480	NA
AT4G11460	CRK30
AT1G33110	NA
AT4G21960	PRXR1
AT1G56700	NA
AT3G14230	RAP2.2
AT2G43900	5PTase12
AT1G78010	NA
AT1G28580	NA
AT3G52480	NA
AT3G54720	AMP1
AT3G25020	AtRLP42
AT1G28320	DEG15
AT4G37150	ATMES9
AT4G36860	NA
AT1G76990	ACR3
AT3G46130	ATMYB48
AT1G69440	AGO7
AT5G41590	NA
AT1G05300	ZIP5
AT3G12520	SULTR4;2
AT5G56870	BGAL4
AT4G18220	NA
AT1G70890	MLP43
AT1G80180	NA
AT1G64500	NA
AT3G44970	NA
AT2G41180	SIB2
AT3G60690	SAUR59
AT1G53580	ETHE1
AT5G10210	NA
AT2G37460	UMAMIT12
AT4G29110	NA
AT2G24580	NA
AT4G23680	NA
AT3G47430	PEX11B
AT4G32940	GAMMA-VPE
AT5G13090	NA
AT3G52525	ATOFP6
AT5G59780	ATMYB59

AT2G36870	AtXTH32
AT5G24460	NA
AT3G46540	NA
AT5G44574	NA
AT2G28930	APK1B
AT3G16450	JAL33
AT1G08810	AtMYB60
AT1G01180	NA
AT5G45650	NA
AT3G29670	PMAT2
AT2G27420	NA
AT3G10910	DAFL1
AT1G79970	NA
AT4G05070	NA
AT4G15530	PPDK
AT1G12200	FMO
AT5G58500	LSH5
AT3G62700	ABCC14
AT1G22500	AtATL15
AT2G33050	AtRLP26
AT3G21690	NA
AT1G07440	NA
AT4G27730	ATOPT6
AT4G01450	UMAMIT30
AT1G34210	ATSERK2
AT4G31330	NA
AT3G43800	ATGSTU27
AT4G08290	UMAMIT20
AT2G42600	ATPPC2
AT1G77990	AST56
AT1G09390	NA
AT5G44572	NA
AT2G28840	XBAT31
AT2G39705	DVL11
AT5G06800	NA
AT3G16560	NA
AT3G50430	NA
AT1G34300	NA
AT2G34960	CAT5
AT3G44990	AtXTH31
AT5G57887	NA
AT1G31770	ABCG14
AT2G15050	LTP
AT2G24762	AtGDU4
AT2G36320	NA
AT1G53910	RAP2.12

		AT2G20950	NA
		AT1G61590	NA
		AT1G10682	NA
		AT4G08300	UMAMIT17
		AT3G05165	NA
		AT5G04330	CYP84A4
		AT5G64570	ATBXL4
30'	1	AT1G78170	NA
60'	511	AT5G59960	NA
		AT3G14067	NA
		AT5G03995	NA
		AT1G09530	PAP3
		AT3G57520	AtSIP2
		AT1G07040	NA
		AT4G15840	NA
		AT5G57180	CIA2
		AT2G45050	GATA2
		AT4G02715	NA
		AT5G39760	AtHB23
		AT2G24755	NA
		AT4G02920	NA
		AT5G65010	ASN2
		AT3G47340	ASN1
		AT3G09450	NA
		AT3G56080	NA
		AT5G23050	AAE17
		AT3G58940	NA
		AT2G46220	NA
		AT3G06510	ATSFR2
		AT1G19650	NA
		AT1G70420	NA
		AT4G16130	ARA1
		AT3G24040	NA
		AT1G55110	AtIDD7
		AT4G28652	NA
		AT5G38895	NA
		AT3G52360	NA
		AT3G08660	NA
		AT2G22540	AGL22
		AT2G19580	TET2
		AT3G62980	AtTIR1
		AT1G66140	ZFP4
		AT1G21360	GLTP2
		AT3G09390	ATMT-1
		AT3G04060	anac046
		AT1G26560	BGLU40

AT1G49320	ATUSPL1
AT5G10150	NA
AT3G25070	RIN4
AT1G32700	NA
AT1G31820	PUT1
AT1G58030	CAT2
AT2G25070	NA
AT3G01750	NA
AT1G55350	ATDEK1
AT5G62890	NA
AT5G26820	ATIREG3
AT3G23880	NA
AT5G10770	NA
AT5G60890	ATMYB34
AT5G57770	NA
AT2G32390	ATGLR3.5
AT1G68130	AtIDD14
AT5G18680	AtTLP11
AT3G10250	NA
AT2G03340	WRKY3
AT1G01420	UGT72B3
AT1G33050	NA
AT1G78670	ATGGH3
AT3G20930	ORRM1
AT3G19000	NA
AT2G30230	NA
AT5G57250	NA
AT3G61150	HD-GL2-1
AT2G01950	BRL2
AT2G33770	ATUBC24
AT1G70660	MMZ2
AT5G14370	NA
AT5G25630	NA
AT5G39080	NA
AT5G44920	NA
AT2G35155	NA
AT1G75380	ATBBD1
AT3G48360	ATBT2
AT5G65683	WAVH2
AT3G63340	NA
AT4G04630	NA
AT4G11570	NA
AT1G24440	NA
AT1G67530	NA
AT3G21360	NA
AT1G68670	NA

AT5G65480	CCI1
AT4G37540	LBD39
AT1G02300	NA
AT1G63800	UBC5
AT4G33960	NA
AT1G48260	CIPK17
AT1G19700	BEL10
AT4G36840	NA
AT4G11360	RHA1B
AT1G80920	AtJ8
AT3G24110	NA
AT1G18880	AtNPF2.9
AT2G46370	AtGH3.11
AT3G21090	ABCG15
AT2G46030	UBC6
AT5G26220	AtGGCT2;1
AT5G59540	NA
AT3G48350	CEP3
AT3G10550	AtMTM1
AT4G15500	UGT84A4
AT3G54140	AtNPF8.1
AT3G56040	UGP3
AT2G15695	NA
AT3G59010	PME35
AT5G64280	DiT2.2
AT3G46590	ATTRP2
AT1G52870	NA
AT2G19570	AT-CDA1
AT3G48190	ATATM
AT4G12320	CYP706A6
AT1G42550	PMI1
AT1G64270	NA
AT1G62510	NA
AT2G43910	ATHOL1
AT1G07530	ATGRAS2
AT5G11060	KNAT4
AT3G26890	NA
AT2G38970	NA
AT2G17550	TRM26
AT4G31450	NA
AT2G40110	NA
AT5G27320	ATGID1C
AT3G46640	LUX
AT2G20180	PIF1
AT1G03000	PEX6
AT3G52540	ATOFP18

AT3G51730	NA
AT2G15230	ATLIP1
AT2G45810	NA
AT1G68520	BBX14
AT2G40460	NA
AT2G37480	NA
AT4G34920	NA
AT3G12950	NA
AT2G21560	NA
AT4G32860	NA
AT3G01180	AtSS2
AT1G32090	NA
AT1G68720	ATTADA
AT1G80790	FDM5
AT2G20210	NA
AT2G35940	BLH1
AT3G52490	SMXL3
AT3G10360	APUM4
AT3G19290	ABF4
AT1G15740	NA
AT3G20015	NA
AT5G62350	NA
AT1G21640	ATNADK2
AT4G16190	NA
AT4G05320	UBI10
AT5G18640	NA
AT3G21750	UGT71B1
AT3G01770	ATBET10
AT4G37310	CYP81H1
AT1G26930	NA
AT3G52240	NA
AT3G22380	TIC
AT3G50630	ICK2
AT3G51400	NA
AT5G24150	SQE5
AT2G39000	NA
AT4G30790	NA
AT1G07230	NPC1
AT4G25620	NA
AT1G56010	anac021
AT1G67840	CSK
AT1G22630	NA
AT1G70000	NA
AT3G04350	NA
AT2G46550	NA
AT2G37050	NA

AT1G56220	NA
AT2G45080	cycp3;1
AT1G66840	PMI2
AT4G27470	ATRMA3
AT5G26230	MAKR1
AT1G45130	AtBGAL5
AT3G13040	NA
AT1G02720	AtGATL5
AT2G34150	ATRANGAP2
AT3G55610	P5CS2
AT3G07310	NA
AT4G37440	NA
AT3G19850	NA
AT2G17640	ATSERAT3;1
AT2G35680	NA
AT5G54080	AtHGO
AT4G38060	CCI2
AT4G39090	RD19
AT1G25560	AtTEM1
AT1G04280	NA
AT5G14390	NA
AT5G44410	NA
AT1G55020	ATLOX1
AT1G29400	AML5
AT2G45850	AHL9
AT1G30320	NA
AT5G58520	NA
AT3G09920	PIP5K9
AT5G64430	NA
AT2G26690	AtNPF6.2
AT3G20640	NA
AT3G25840	NA
AT1G17200	NA
AT4G18020	APRR2
AT3G16940	NA
AT2G40200	NA
AT2G18890	NA
AT5G25900	ATKO1
AT2G18750	NA
AT4G13100	NA
AT1G54710	ATATG18H
AT5G27280	NA
AT5G02250	ATMTRNASEII
AT1G60590	NA
AT5G01810	ATPK10
AT2G46060	NA

AT4G04435	NA
AT2G01570	RGA
AT1G68570	AtNPF3.1
AT1G75820	ATCLV1
AT3G03470	CYP89A9
AT3G02910	NA
AT4G03510	ATRMA1
AT1G10600	AMSH2
AT1G12280	SUMM2
AT3G47800	NA
AT1G61795	NA
AT2G23840	NA
AT5G08520	NA
AT5G40670	NA
AT1G60140	ATTPS10
AT2G27830	NA
AT4G05150	NA
AT4G28270	ATRMA2
AT4G12310	CYP706A5
AT1G67480	NA
AT4G38520	APD6
AT3G16180	NRT1.12
AT1G25440	BBX15
AT2G18960	AHA1
AT3G62770	AtATG18a
AT2G47240	CER8
AT1G60540	NA
AT5G27730	NA
AT5G45800	MEE62
AT3G17510	CIPK1
AT4G03415	PP2C52
AT5G37020	ARF8
AT3G05120	ATGID1A
AT5G48850	ATSDI1
AT5G05690	CBB3
AT1G31650	ATROPGEF14
AT1G30330	ARF6
AT3G44310	ATNIT1
AT3G10740	ARAF
AT1G54510	ATNEK1
AT5G27350	SFP1
AT3G15070	NA
AT1G01430	TBL25
AT3G56140	NA
AT1G72010	NA
AT5G43850	ARD4

AT4G11320	AtCP2
AT4G39770	TPPH
AT1G70160	NA
AT1G76590	NA
AT5G01720	NA
AT2G18915	ADO2
AT1G25550	NA
AT5G14880	KUP8
AT2G36895	NA
AT5G03960	IQD12
AT5G24165	NA
AT1G70300	KUP6
AT2G03550	NA
AT4G40060	ATHB-16
AT4G19160	NA
AT5G55530	NA
AT4G32980	ATH1
AT3G16520	UGT88A1
AT3G04760	NA
AT1G07280	NA
AT1G78890	NA
AT1G73980	NA
AT5G65970	ATMLO10
AT1G56460	NA
AT1G77920	TGA7
AT2G36350	NA
AT4G37250	NA
AT1G60940	SNRK2-10
AT3G28130	UMAMIT44
AT1G03090	MCCA
AT1G66330	NA
AT4G27710	CYP709B3
AT5G37790	NA
AT2G31800	NA
AT1G69360	NA
AT3G16460	JAL34
AT5G01520	AIRP2
AT2G32970	NA
AT4G13530	NA
AT5G01820	ATCIPK14
AT1G77870	MUB5
AT2G41560	ACA4
AT5G63710	NA
AT2G03310	NA
AT5G47560	ATSDAT
AT1G73920	NA

AT5G25610	ATRD22
AT1G55000	NA
AT3G45900	NA
AT3G45300	ATIVD
AT3G29390	RIK
AT4G28610	AtPHR1
AT2G37450	UMAMIT13
AT3G55070	NA
AT2G04690	NA
AT4G19170	CCD4
AT1G13260	EDF4
AT5G59430	ATTRP1
AT3G56590	NA
AT2G31560	NA
AT5G20030	NA
AT1G32530	NA
AT3G18930	NA
AT2G36800	DOGT1
AT1G49230	AtATL78
AT2G36792	NA
AT5G35670	iqd33
AT4G23890	CRR31
AT1G13080	CYP71B2
AT3G44880	ACD1
AT3G29035	ANAC059
AT2G24240	NA
AT5G62910	NA
AT1G44770	NA
AT3G09770	AIRP3
AT4G37330	CYP81D4
AT1G60800	AtNIK3
AT1G11350	CBRLK1
AT1G60490	ATVPS34
AT1G74840	NA
AT5G42680	NA
AT2G30100	NA
AT1G47128	RD21
AT5G11460	NA
AT2G17730	NIP2
AT2G18560	NA
AT1G78680	ATGGH2
AT4G02050	STP7
AT1G69080	NA
AT1G01770	NA
AT5G41110	NA
AT5G67385	NA

AT2G33060	AtRLP27
AT5G61270	PIF7
AT1G32540	LOL1
AT4G24050	NA
AT2G17890	CPK16
AT5G56860	GATA21
AT5G58440	SNX2a
AT3G55130	ABCG19
AT5G18460	NA
AT3G60850	NA
AT5G67420	ASL39
AT4G13830	DJC26
AT4G04610	APR
AT5G13770	NA
AT5G13730	SIG4
AT5G50450	NA
AT4G33150	LKR
AT3G30180	BR6OX2
AT5G65210	TGA1
AT3G06170	NA
AT1G73950	NA
AT1G74900	OTP43
AT1G19000	NA
AT5G38510	NA
AT5G19970	NA
AT1G71240	NA
AT3G07425	NA
AT5G46270	NA
AT5G27150	AT-NHX1
AT1G77280	NA
AT3G47160	NA
AT5G24930	ATCOL4
AT5G24120	ATSIG5
AT5G24155	NA
AT1G77480	NA
AT4G35750	NA
AT2G35170	NA
AT4G36380	ROT3
AT3G26300	CYP71B34
AT3G21670	AtNPF6.4
AT1G09010	NA
AT4G20070	AAH
AT4G12440	APT4
AT4G02075	PIT1
AT4G33666	NA
AT2G14080	NA

AT5G12350	NA
AT3G21760	HYR1
AT1G77760	GNR1
AT1G07200	SMXL6
AT1G16680	NA
AT1G78090	ATTPPB
AT1G12240	ATBETAFRUCT4
AT1G53510	ATMPK18
AT5G24520	ATTTG1
AT1G22770	FB
AT4G02480	NA
AT3G09162	NA
AT5G07670	NA
AT2G26980	CIPK3
AT1G28310	NA
AT2G42490	NA
AT1G18270	NA
AT5G59830	NA
AT3G54990	SMZ
AT4G35640	ATSERAT3;2
AT3G59300	NA
AT5G10860	CBSX3
AT3G45290	ATMLO3
AT5G15400	MUSE3
AT1G35290	ALT1
AT3G19030	NA
AT3G05400	NA
AT5G61420	AtMYB28
AT5G57630	CIPK21
AT1G03380	ATATG18G
AT1G37130	ATNR2
AT2G46690	SAUR32
AT4G23700	ATCHX17
AT4G32820	NA
AT1G19660	AtBBD2
AT1G78000	SEL1
AT3G56200	NA
AT5G13550	SULTR4;1
AT5G10030	OBF4
AT2G48110	MED33B
AT1G72500	NA
AT1G50840	POLGAMMA2
AT5G63190	NA
AT4G37925	NDH-M
AT3G61960	NA
AT3G63000	NPL41

AT3G52060	AtGnTL
AT4G37300	MEE59
AT1G08980	AMI1
AT5G58787	NA
AT5G07290	AML4
AT2G32540	ATCSLB04
AT1G27320	AHK3
AT2G35800	SAMTL
AT2G33835	FES1
AT1G59580	ATMPK2
AT5G56850	NA
AT1G16320	NA
AT1G07990	NA
AT2G25930	ELF3
AT2G39400	NA
AT5G10960	NA
AT5G64550	NA
AT2G22200	NA
AT4G02710	NET1C
AT3G28270	NA
AT3G13750	BGAL1
AT3G57190	PrfB3
AT2G39250	SNZ
AT3G20120	CYP705A21
AT4G20820	NA
AT5G15230	GASA4
AT4G00355	ATI2
AT5G42140	NA
AT4G01020	NA
AT5G04360	ATLDA
AT2G45620	URT1
AT4G28260	NA
AT3G22104	NA
AT4G17940	NA
AT1G25375	NA
AT1G21590	NA
AT2G22660	NA
AT1G77660	NA
AT2G30070	ATKT1
AT2G22890	NA
AT2G46890	NA
AT2G02080	AtIDD4
AT5G54980	NA
AT1G14890	NA
AT5G04290	KTF1
AT4G37225	NA

		AT5G16540	ZFN3
		AT1G26150	AtPERK10
		AT5G16410	NA
		AT2G01890	ATPAP8
		AT1G16710	HAC12
		AT2G29970	SMXL7
		AT5G48180	AtNSP5
		AT4G19860	NA
		AT5G16820	ATHSF3
		AT1G76890	AT-GT2
		AT2G32530	ATCSLB03
		AT5G04810	NA
		AT1G22360	AtUGT85A2
180'	257	AT2G13665	NA
		AT5G37600	ATGLN1;1
		AT1G44760	NA
		AT3G11280	NA
		AT3G59270	NA
		AT3G50740	UGT72E1
		AT5G41700	ATUBC8
		AT1G13740	AFP2
		AT1G62810	CuAO1
		AT5G53550	ATYSL3
		AT2G38310	PYL4
		AT4G12450	NA
		AT5G36220	CYP81D1
		AT3G16910	AAE7
		AT5G14090	AtLAZY1
		AT3G16190	NA
		AT4G06746	DEAR5
		AT1G70310	SPDS2
		AT2G38800	NA
		AT5G48000	CYP708
		AT1G43020	NA
		AT5G26280	NA
		AT5G54960	PDC2
		AT2G43750	ACS1
		AT3G26710	CCB1
		AT2G28670	ESB1
		AT3G23430	ATPHO1
		AT2G40100	LHCB4.3
		AT2G29720	CTF2B
		AT2G40113	NA
		AT1G53700	PK3AT
		AT3G61630	CRF6
		AT1G59870	ABCG36

AT2G05520	ATGRP-3
AT4G23670	NA
AT1G22400	ATUGT85A1
AT1G50420	SCL-3
AT1G64710	NA
AT1G52270	NA
AT4G16563	NA
AT1G77885	NA
AT3G14020	NF-YA6
AT2G36460	FBA6
AT3G16530	NA
AT4G00040	NA
AT1G80050	APT2
AT4G24350	NA
AT5G67290	NA
AT1G16650	NA
AT5G05440	PYL5
AT2G26650	AKT1
AT1G74880	NDH-O
AT5G03780	TRFL10
AT5G11670	ATNADP-ME2
AT4G22690	CYP706A1
AT1G78850	NA
AT5G43910	NA
AT1G75430	BLH11
AT3G26330	CYP71B37
AT2G31230	ATERF15
AT1G72300	PSY1R
AT3G48100	ARR5
AT5G65530	NA
AT4G21910	NA
AT2G24260	LRL1
AT3G13404	NA
AT4G21870	NA
AT2G24100	ASG1
AT1G27980	ATDPL1
AT2G17820	AHK1
AT5G05110	NA
AT4G23570	SGT1A
AT3G48990	AAE3
AT5G10180	AST68
AT5G07830	AtGUS2
AT4G14410	bHLH104
AT5G42180	PER64
AT5G54940	NA
AT2G26355	NA

AT4G38160	pde191
AT3G05410	NA
AT5G39030	NA
AT3G45310	NA
AT4G13580	NA
AT5G61412	NA
AT4G27300	NA
AT5G19260	FAF3
AT1G58602	NA
AT2G01290	RPI2
AT2G29180	NA
AT3G61440	ARATH;BSAS3;1
AT2G45660	AGL20
AT2G41700	ABCA1
AT5G44580	NA
AT3G60300	NA
AT4G26950	NA
AT2G45510	CYP704A2
AT5G37850	ATSOS4
AT2G40330	PYL6
AT1G11175	NA
AT5G61520	NA
AT5G28020	ATCYSD2
AT5G23920	NA
AT2G31110	TBL40
AT3G15353	ATMT3
AT3G17670	NA
AT3G16470	JAL35
AT1G73330	ATDR4
AT1G78580	ATTPS1
AT2G41720	EMB2654
AT4G39070	BBX20
AT4G21190	emb1417
AT5G43290	ATWRKY49
AT4G28250	ATEXPB3
AT2G01830	AHK4
AT2G35490	NA
AT3G04210	NA
AT1G50480	THFS
AT1G09430	ACLA-3
AT4G39780	NA
AT4G15330	CYP705A1
AT1G15125	NA
AT1G74890	ARR15
AT5G22460	NA
AT5G05860	UGT76C2

AT3G61430	ATPIP1
AT5G14730	NA
AT4G16250	PHYD
AT5G20740	NA
AT1G35560	AtTCP23
AT2G29340	NA
AT2G34470	PSKF109
AT3G01260	NA
AT1G77230	NA
AT1G10770	NA
AT1G13400	JGL
AT3G47250	NA
AT2G34490	CYP710A2
AT3G48740	AtSWEET11
AT1G08180	NA
AT1G13100	CYP71B29
AT2G46680	ATHB-7
AT4G21410	CRK29
AT5G11320	AtYUC4
AT2G29740	UGT71C2
AT5G25810	tny
AT3G49940	LBD38
AT2G36100	CASP1
AT1G19050	ARR7
AT5G11930	NA
AT3G62040	NA
AT2G32300	UCC1
AT1G77380	AAP3
AT3G16770	ATEBP
AT2G38010	NA
AT1G05570	ATGSL06
AT2G39310	JAL22
AT5G47990	CYP705A5
AT2G30870	ATGSTF10
AT3G48000	ALDH2
AT3G26210	CYP71B23
AT2G37200	NA
AT5G38610	NA
AT4G17870	PYR1
AT1G70560	CKRC1
AT3G62150	ABCB21
AT3G27190	UKL2
AT2G27310	NA
AT1G62200	AtNPF8.5
AT4G02850	NA
AT4G25940	NA

AT2G37130	NA
AT4G15700	NA
AT5G35732	NA
AT1G68220	NA
AT3G01210	NA
AT2G01590	CRR3
AT1G51070	bHLH115
AT3G46880	NA
AT5G61610	NA
AT3G25870	NA
AT3G45700	NA
AT5G48010	AtTHAS1
AT3G55230	NA
AT2G31160	LSH3
AT3G15356	NA
AT1G78830	NA
AT1G02860	BAH1
AT5G19250	NA
AT2G47910	CRR6
AT3G04520	THA2
AT5G04230	ATPAL3
AT5G66490	NA
AT1G60989	SCRL7
AT5G18140	DJC69
AT4G24660	ATHB22
AT2G33480	ANAC041
AT5G46780	NA
AT1G44970	NA
AT1G71880	ATSUC1
AT3G24463	NA
AT5G65510	AIL7
AT1G68238	NA
AT5G27380	AtGSH2
AT3G23790	AAE16
AT1G27030	NA
AT4G30250	NA
AT3G53180	NodGS
AT1G13110	CYP71B7
AT1G10470	ARR4
AT3G23550	NA
AT4G36670	AtPLT6
AT1G67810	SUFE2
AT5G55790	NA
AT4G14930	NA
AT5G67110	ALC
AT5G36160	NA

AT5G06570	NA
AT1G28570	NA
AT4G21850	ATMSRB9
AT1G45201	ATTLL1
AT2G38170	ATCAX1
AT2G26975	COPT6
AT3G05770	NA
AT3G26320	CYP71B36
AT1G53430	NA
AT5G61290	NA
AT2G28190	CSD2
AT5G02710	NA
AT5G59790	NA
AT2G34690	ACD11
AT5G20990	B73
AT5G62920	ARR6
AT5G52830	ATWRKY27
AT1G27020	NA
AT5G59090	ATSBT4.12
AT1G69520	NA
AT5G21482	ATCKX5
AT5G10280	ATMYB64
AT1G72200	NA
AT5G40390	RS5
AT3G45210	NA
AT3G58710	ATWRKY69
AT1G69760	NA
AT1G48320	DHNAT1
AT1G64680	NA
AT1G06160	ORA59
AT4G11290	NA
AT1G32450	AtNPF7.3
AT1G21100	IGMT1
AT1G31710	NA
AT3G22460	OASA2
AT3G63110	ATIPT3
AT5G46250	AtLARP6a
AT4G19810	ChiC
AT1G71740	NA
AT5G57930	APO2

References

© 2020 Parfums Houbigant Paris (2020) *Jean-François Houbigant*, *https://www.houbigant-parfum.com*. Available at: https://www.houbigant-parfum.com/.

Abenavoli, M. R. *et al.* (2001) 'Influence of coumarin on the net nitrate uptake in durum wheat', *New Phytologist*, 150(3), pp. 619–627. doi: 10.1046/j.1469-8137.2001.00119.x.

Abenavoli, M. R. *et al.* (2003) 'Coumarin inhibits the growth of carrot (Daucus carota L. cv. Saint Valery) cells in suspension culture', *Journal of Plant Physiology*, 160(3), pp. 227–237. doi: 10.1078/0176-1617-00867.

Abenavoli, M. R. *et al.* (2004) 'Coumarin differentially affects the morphology of different root types of maize seedlings', *Journal of Chemical Ecology*, 30(9), pp. 1871–1883. doi: 10.1023/B:JOEC.0000042407.28560.bb.

Abenavoli, M. R. *et al.* (2006) 'The inhibitory effects of coumarin on the germination of durum wheat (Triticum turgidum ssp. durum, CV. Simeto) seeds', *Journal of Chemical Ecology*, 32(2), pp. 489–506. doi: 10.1007/s10886-005-9011-x.

Abenavoli, M. R. *et al.* (2008) 'Effects of different allelochemicals on root morphology of Arabidopsis thaliana', *Allelopathy Journal*, 22(1), pp. 245–250.

Achard, P. *et al.* (2003) 'Ethylene Regulates Arabidopsis Development via the Modulation of DELLA Protein Growth Repressor Function', *The Plant Cell*, 15(12), pp. 2816–2825. doi: 10.1105/tpc.015685.

Achard, P. *et al.* (2007) 'The plant stress hormone ethylene controls floral transition via DELLA-dependent regulation of floral meristem-identity genes', *Proceedings of the National Academy of Sciences*, 104(15), pp. 6484–6489. doi: 10.1073/pnas.0610717104.

Achard, P. *et al.* (2009) 'Gibberellin Signaling Controls Cell Proliferation Rate in Arabidopsis', *Current Biology*. Elsevier Ltd, 19(14), pp. 1188–1193. doi: 10.1016/j.cub.2009.05.059.

Van Acker, R. *et al.* (2013) 'Lignin biosynthesis perturbations affect secondary cell wall composition and saccharification yield in Arabidopsis thaliana.', *Biotechnology for biofuels*, 6(1), p. 46. doi: 10.1186/1754-6834-6-46.

Adamowski, M. and Friml, J. (2015) 'PIN-Dependent Auxin Transport: Action, Regulation, and Evolution', *The Plant Cell Online*, 27(1), pp. 20–32. doi: 10.1105/tpc.114.134874.

Adfa, M. *et al.* (2010) 'Antitermite activities of coumarin derivatives and scopoletin from Protium javanicum Burm. f', *Journal of Chemical Ecology*, 36(7), pp. 720–726. doi: 10.1007/s10886-010-9807-1.

Afek, U. *et al.* (1999) 'Umbelliferone, a phytoalexin associated with resistance of immature Marsh grapefruit to Penicillium digitatum', *Phytochemistry*, 50(7), pp. 1129–1132. doi: 10.1016/S0031-9422(98)00671-2.

Agati, G. *et al.* (2012) 'Flavonoids as antioxidants in plants: Location and functional significance', *Plant Science*. Elsevier Ireland Ltd, 196, pp. 67–76. doi: 10.1016/j.plantsci.2012.07.014.

Al-Barwani, F. M. and Eltayeb, E. A. (2004) 'Antifungal compounds from induced Conium maculatum L.plants', *Biochemical Systematics and Ecology*, 32(12), pp. 1097–1108. doi: 10.1016/j.bse.2004.02.011.

Al-Wakeel, S. *et al.* (2013) 'Coumarin and salicylic acid activate resistance to *Macrophomina phaseolina* in *Helianthus annuus*', *Acta Agronomica Hungarica*, 61(1), pp. 23–35. doi: 10.1556/AAgr.61.2013.1.3.

Alabadí, D. *et al.* (2004) 'Gibberellins Repress Photomorphogenesis in Darkness', *Plant Physiology*, 134(3), pp. 1050–1057. doi: 10.1104/pp.103.035451.

Alabadí, D. *et al.* (2008) 'Gibberellins modulate light signaling pathways to prevent Arabidopsis seedling de-etiolation in darkness.', *The Plant journal : for cell and molecular biology*, 53(2), pp. 324–35. doi: 10.1111/j.1365-313X.2007.03346.x.

Alexieva, V. *et al.* (1995) 'Plant growth regulating activity of some phosphorus derivatives of coumarin', *Bulg.*

J. Plant Physiol, 21(July 2014), pp. 45–51.

Ali-Rachedi, S. *et al.* (2004) 'Changes in endogenous abscisic acid levels during dormancy release and maintenance of mature seeds: studies with the Cape Verde Islands ecotype, the dormant model of Arabidopsis thaliana', *Planta*, 219(3), pp. 479–488. doi: 10.1007/s00425-004-1251-4.

Aliotta, G. *et al.* (1993) 'Inhibition of radish germination and root growth by coumarin and phenylpropanoids', *Journal of Chemical Ecology*, 19(2), pp. 175–183. doi: 10.1007/BF00993687.

Aliotta, G., Fuggi, A. and Strumia, S. (1992) 'Coat-imposed dormancy by coumarin in radish seeds: the influence of light', *Giornale botanico italiano*, 126(5), pp. 631–637. doi: 10.1080/11263509209440368.

Alonso, J. M. *et al.* (2003) 'Genome-wide insertional mutagenesis of Arabidopsis thaliana.', *Science (New York, N.Y.)*, 301(5633), pp. 653–7. doi: 10.1126/science.1086391.

Amrhein, N. and Gödeke, K. H. (1977) 'α-aminooxy-β-phenylpropionic acid - a potent inhibitor of L-phenylalanine ammonia-lyase in vitro and in vivo', *Plant Science Letters*, 8(4), pp. 313–317. doi: 10.1016/0304-4211(77)90148-1.

Andersson, D. *et al.* (2009) 'Myrosinases from root and leaves of Arabidopsis thaliana have different catalytic properties', *Phytochemistry*. Elsevier Ltd, 70(11–12), pp. 1345–1354. doi: 10.1016/j.phytochem.2009.07.036.

Andreae, S. R. and Andreae, W. A. (1949) 'The metabolism of scopoletin by healthy and virus infected potato tubers.', *Canadian Journal of Research*, 27(2), pp. 15–22.

Andreae, W. A. (1952) 'Effect of scopoletin on indoleacetic acid metabolism', *Nature*, 170(4315), p. 83.

Andreae, W. A. and Andreae, S. R. (1953) 'STUDIES ON INDOLEACETIC ACID METABOLISM: I. THE EFFECT OF METHYL UMBELLIFERONE, MALEIC HYDRAZIDE, AND 2,4-D ON INDOLEACETIC ACID OXIDATION', *Canadian Journal of Botany*, 31(4), pp. 426–437. doi: 10.1139/b53-034.

Andriankaja, M. *et al.* (2012) 'Exit from Proliferation during Leaf Development in Arabidopsis thaliana: A Not-So-Gradual Process', *Developmental Cell*, 22(1), pp. 64–78. doi: 10.1016/j.devcel.2011.11.011.

Araniti, F. *et al.* (2015) 'Phytotoxic Potential and Biological Activity of Three Synthetic Coumarin Derivatives as New Natural-Like Herbicides', *Molecules*, 20(10), pp. 17883–17902. doi: 10.3390/molecules201017883.

Araniti, F. *et al.* (2017) 'Highlighting the effects of coumarin on adult plants of Arabidopsis thaliana (L.) Heynh. by an integrated -omic approach', *Journal of Plant Physiology*. Elsevier GmbH., 213, pp. 30–41. doi: 10.1016/j.jplph.2017.02.013.

Argueso, C. T., Raines, T. and Kieber, J. J. (2010) 'Cytokinin signaling and transcriptional networks', *Current Opinion in Plant Biology*, 13(5), pp. 533–539. doi: 10.1016/j.pbi.2010.08.006.

Ariizumi, T., Lawrence, P. K. and Steber, C. M. (2011) 'The Role of Two F-Box Proteins, SLEEPY1 and SNEEZY, in Arabidopsis Gibberellin Signaling', *Plant Physiology*, 155(2), pp. 765–775. doi: 10.1104/pp.110.166272.

Arnison, M. R. *et al.* (2004) 'Linear phase imaging using differential interference contrast microscopy', *Journal of Microscopy*, 214(1), pp. 7–12. doi: 10.1111/j.0022-2720.2004.01293.x.

Arvidsson, S. *et al.* (2008) 'QuantPrime - a flexible tool for reliable high-throughput primer design for quantitative PCR', *BMC Bioinformatics*, 9(1), p. 465. doi: 10.1186/1471-2105-9-465.

Asami, T. and Yoshida, S. (1999) 'Brassinosteroid biosynthesis inhibitors', *Trends in Plant Science*, 4(9), pp. 348–353. doi: 10.1016/S1360-1385(99)01456-9.

Audus, L. J. (1948) 'Studies on the pH-relationship of root growth and its inhibition by 2:4-Dicholorphenoxyacetic acid and Coumarin'. doi: 10.1111/j.1469-8137.1949.tb05112.x.

Audus, L. J. (1950) 'STUDIES ON THE PHYTOSTATIC ACTION OF 2:4-DICHLOROPHENOXYACETIC ACID AND COUMARIN THE REVERSIBILITY OF ROOT-GROWTH INHIBITIONS', *The New Phytologist*, 47(2), pp. 196–219.

Audus, L. J. and Quastel, J. H. (1947) 'Coumarin as a selective phytocidal agent', *Nature*, 160, pp. 330–331.

Avers, C. J. and Goodwin, R. H. (1956) 'Studies on Roots. IV. Effects of Coumarin and Scopoletin on the Standard Root Growth Pattern of Phleum pratense', *American Journal of Botany*, 43(8), p. 612. doi: 10.2307/2438877.

Azpiroz, R. *et al.* (1998) 'An Arabidopsis Brassinosteroid-Dependent Mutant Is Blocked in Cell Elongation', *The Plant Cell*, 10(2), pp. 219–230. doi: 10.1105/tpc.10.2.219.

Ba, R. *et al.* (2017) 'Maize Fungal Growth Control with Scopoletin of Cassava Roots Produced in Benin', *International Journal of Microbiology*, 2017, pp. 1–11. doi: 10.1155/2017/5671942.

Bagni, N. and Fracassini, D. S. (1971) 'The effect of coumarin derivatives on organogenesis and callus growth of Cichorium Intybus roots and Helianthus tuberosus tubers in vitro', *Experientia*, 27(10), pp. 1239–1241. doi: 10.1007/BF02286952.

Bai, M.-Y., Fan, M., *et al.* (2012) 'A Triple Helix-Loop-Helix/Basic Helix-Loop-Helix Cascade Controls Cell Elongation Downstream of Multiple Hormonal and Environmental Signaling Pathways in Arabidopsis', *The Plant Cell*, 24(12), pp. 4917–4929. doi: 10.1105/tpc.112.105163.

Bai, M.-Y., Shang, J.-X., *et al.* (2012) 'Brassinosteroid, gibberellin and phytochrome impinge on a common transcription module in Arabidopsis', *Nature Cell Biology*. Nature Publishing Group, 14(8), pp. 810–817. doi: 10.1038/ncb2546.

Bai, X. *et al.* (2012) 'Inhibitory Effect and Antifunal Mechanism of Umbelliferone on Plant Pathogenic Fungi', in *Advances in Intelligent and Soft Computing*, pp. 693–702. doi: 10.1007/978-3-642-27537-1_83.

Bao, F. *et al.* (2004) 'Brassinosteroids Interact with Auxin to Promote Lateral Root Development in Arabidopsis', *Plant Physiology*, 134(4), pp. 1624–1631. doi: 10.1104/pp.103.036897.

Barbez, E. *et al.* (2012) 'A novel putative auxin carrier family regulates intracellular auxin homeostasis in plants', *Nature*, 485(7396), pp. 119–122. doi: 10.1038/nature11001.

Barbez, E. *et al.* (2017) 'Auxin steers root cell expansion via apoplastic pH regulation in *Arabidopsis thaliana*', *Proceedings of the National Academy of Sciences*, p. 201613499. doi: 10.1073/pnas.1613499114.

Barbosa, I. C. R., Hammes, U. Z. and Schwechheimer, C. (2018) 'Activation and Polarity Control of PIN-FORMED Auxin Transporters by Phosphorylation', *Trends in Plant Science*, 23(6), pp. 523–538. doi: 10.1016/j.tplants.2018.03.009.

Barros, J. *et al.* (2019) '4-Coumarate 3-hydroxylase in the lignin biosynthesis pathway is a cytosolic ascorbate peroxidase', *Nature Communications*. Springer US, 10(1), pp. 1–11. doi: 10.1038/s41467-019-10082-7.

Barth, C. and Jander, G. (2006) 'Arabidopsis myrosinases TGG1 and TGG2 have redundant function in glucosinolate breakdown and insect defense', *Plant Journal*, 46(4), pp. 549–562. doi: 10.1111/j.1365-313X.2006.02716.x.

Baskin, J. M. and Baskin, C. C. (2004) 'A classification system for seed dormancy', *Seed Science Research*, 14(1), pp. 1–16. doi: 10.1079/SSR2003150.

Basler, E. and Mcbride, R. (1977) 'Interaction of coumarin, gibberellic acid and abscisic acid in the translocation of auxin in bean seedlings.', *Plant and Cell Physiology*, 18, pp. 939–947. doi: 10.1093/oxfordjournals.pcp.a075532.

Basu, M. *et al.* (2016) 'Effect of scopoletin on monoamine oxidases and brain amines', *Neurochemistry*

International, 93, pp. 113–117. doi: 10.1016/j.neuint.2016.01.001.

Basu, R. N. (1972) 'Effect of Non-auxin Chemicals on Translocation of Auxins in Cuttings of Phaseolus vulgaris (L.)', *Journal of Experimental Botany*, 23(2), pp. 357–365. doi: 10.1093/jxb/23.2.357.

Bates, D. *et al.* (2015) 'Fitting Linear Mixed-Effects Models Using lme4', *Journal of Statistical Software*, 67(1). doi: 10.18637/jss.v067.i01.

Baxter, I. *et al.* (2005) 'Genomic Comparison of P-Type ATPase Ion Pumps in Arabidopsis and Rice1 Genomic Comparison of P-Type ATPase Ion Pumps in Arabidopsis and Rice.', *Plant Physiology*, 138(3), pp. 1807–1807. doi: 10.1104/pp.104.900164.

Bayoumi, Soad A.L. *et al.* (2008) 'Biosynthesis of scopoletin and scopolin in cassava roots during post-harvest physiological deterioration: The E-Z-isomerisation stage', *Phytochemistry*, 69(17), pp. 2928–2936. doi: 10.1016/j.phytochem.2008.09.023.

Bayoumi, Soad A. L. *et al.* (2008) 'Investigation of Biosynthetic Pathways to Hydroxycoumarins During Post-Harvest Physiological Deterioration in Cassava Roots by Using Stable Isotope Labelling', *ChemBioChem*, 9(18), pp. 3013–3022. doi: 10.1002/cbic.200800515.

Van Bel, M. *et al.* (2018) 'PLAZA 4.0: an integrative resource for functional, evolutionary and comparative plant genomics', *Nucleic Acids Research*, 46(D1), pp. D1190–D1196. doi: 10.1093/nar/gkx1002.

Bellincampi, D., Cervone, F. and Lionetti, V. (2014) 'Plant cell wall dynamics and wall-related susceptibility in plant-pathogen interactions', *Frontiers in Plant Science*, 5(MAY), pp. 1–8. doi: 10.3389/fpls.2014.00228.

Benková, E. *et al.* (2003) 'Local, Efflux-Dependent Auxin Gradients as a Common Module for Plant Organ Formation', *Cell*, 115(5), pp. 591–602. doi: 10.1016/S0092-8674(03)00924-3.

Bennett, T. *et al.* (2016) 'Strigolactone regulates shoot development through a core signalling pathway', *Biology Open*, 5(12), pp. 1806–1820. doi: 10.1242/bio.021402.

Bennett, T. and Scheres, B. (2010) 'Root development—two meristems for the price of one?', in *Current topics in developmental biology*. Elsevier, pp. 67–102.

Bentley, J. A. (1958) 'The Naturally-Occurring Auxins and Inhibitors', *Annual Review of Plant Physiology*, 9(1), pp. 47–80. doi: 10.1146/annurev.pp.09.060158.000403.

Bernhard, R. A. (1959) 'Some Studies of Coumarin and Coumarin Analogues as Germination Inhibitors of Radish Seeds', *Botanical Gazette*, 121(1), pp. 17–21. doi: 10.1086/336035.

Berrie, A. M. M. *et al.* (1968) 'Studies on lettuce seed germination-I. Coumarin induced dormancy', *Phytochemistry*, 7(4), pp. 567–573. doi: 10.1016/S0031-9422(00)88228-X.

Bewley, J. D. (1997) 'Seed Germination and Dormancy.', *The Plant Cell*, 9(7), pp. 1055–1066. doi: 10.1105/tpc.9.7.1055.

Beyer, S. F. *et al.* (2019) 'The Arabidopsis non-host defence-associated coumarin scopoletin protects soybean from Asian soybean rust', *The Plant Journal*, 99(3), pp. 397–413. doi: 10.1111/tpj.14426.

Bhatia, N. *et al.* (2016) 'Auxin acts through MONOPTEROS to regulate plant cell polarity and pattern phyllotaxis', *Current Biology*. Elsevier, 26(23), pp. 3202–3208.

Bhosale, R., Maere, S. and De Veylder, L. (2019) 'Endoreplication as a potential driver of cell wall modifications', *Current Opinion in Plant Biology*. Elsevier Ltd, 51, pp. 58–65. doi: 10.1016/j.pbi.2019.04.003.

Biala, W. and Jasiński, M. (2018) 'The Phenylpropanoid Case – It Is Transport That Matters', *Frontiers in Plant Science*, 9(November), pp. 1–8. doi: 10.3389/fpls.2018.01610.

Bianco, M. Del and Kepinski, S. (2011) 'Context, Specificity, and Self-Organization in Auxin Respons', *Cold Spring Harbor Perspectives*, pp. 1–20.

Blaim, K. (1960) 'The Effect of Coumarin on Uptake of Water by Seeds', *Journal of experimental botany*, 11(33), pp. 377–380.

Blakeslee, J. J. *et al.* (2007) 'Interactions among PIN-FORMED and P-Glycoprotein Auxin Transporters in Arabidopsis', *The Plant Cell*, 19(1), pp. 131–147. doi: 10.1105/tpc.106.040782.

Blakeslee, J. J., Spatola Rossi, T. and Kriechbaumer, V. (2019) 'Auxin biosynthesis: spatial regulation and adaptation to stress', *Journal of Experimental Botany*, (June). doi: 10.1093/jxb/erz283.

Blas, C. (1868) 'Sur une nouvelle glucoside, la murrayine.', *Bull. Soc. Roy. Sci. Lettres, Beaux Arts. II.*, 26, pp. 303–318.

Bleecker, A. B. *et al.* (1998) 'The ethylene–receptor family from Arabidopsis : structure and function', *Philosophical Transactions of the Royal Society of London. Series B: Biological Sciences*. Edited by N. –H. Chua et al., 353(1374), pp. 1405–1412. doi: 10.1098/rstb.1998.0295.

Bleibtreu, H. (1846) 'Untersuchungen über Cumarin', *Justus Liebigs Annalen der Chemie*. Wiley Online Library, 59(2), pp. 177–198.

Blilou, I. *et al.* (2005) 'The PIN auxin efflux facilitator network controls growth and patterning in Arabidopsis roots', *Nature*, 433(7021), pp. 39–44. doi: 10.1038/nature03184.

den Boer, B. G. and Murray, J. A. (2000) 'Control of plant growth and development through manipulation of cell-cycle genes', *Current Opinion in Biotechnology*, 11(2), pp. 138–145. doi: 10.1016/S0958-1669(00)00072-0.

Boer, D. R. *et al.* (2014) 'Structural Basis for DNA Binding Specificity by the Auxin-Dependent ARF Transcription Factors', *Cell*, 156(3), pp. 577–589. doi: 10.1016/j.cell.2013.12.027.

Boerjan, W. *et al.* (1995) 'superroot, a Recessive Mutation in Arabidopsis, Confers Auxin Overproduction', *the Plant Cell Online*, 7(9), pp. 1405–1419. doi: 10.1105/tpc.7.9.1405.

Boerjan, W., Ralph, J. and Baucher, M. (2003) 'LIGNIN BIOSYNTHESIS', *Annual Review of Plant Biology*, 54(1), pp. 519–546. doi: 10.1146/annurev.arplant.54.031902.134938.

Boron, A. K. and Vissenberg, K. (2014) 'The Arabidopsis thaliana hypocotyl, a model to identify and study control mechanisms of cellular expansion', *Plant Cell Reports*, 33(5), pp. 697–706. doi: 10.1007/s00299-014-1591-x.

Borthwick, H. A. *et al.* (1952) 'A Reversible Photoreaction Controlling Seed Germination', *Proceedings of the National Academy of Sciences*, 38(8), pp. 662–666. doi: 10.1073/pnas.38.8.662.

Bou-Torrent, J. *et al.* (2008) 'PAR1 and PAR2 integrate shade and hormone transcriptional networks', *Plant Signaling and Behavior*, 3(7), pp. 453–454. doi: 10.4161/psb.3.7.5599.

Boullay, P. F. and Boutron-Charlard, A. F. (1825) 'Chimique de la Fève de Tonka', *J Pharm*, 11, pp. 480–487.

Bourgaud, F. *et al.* (2006) 'Biosynthesis of coumarins in plants: a major pathway still to be unravelled for cytochrome P450 enzymes', *Phytochemistry Reviews*, 5(2–3), pp. 293–308. doi: 10.1007/s11101-006-9040-2.

Braun, N. *et al.* (2012) 'The Pea TCP Transcription Factor PsBRC1 Acts Downstream of Strigolactones to Control Shoot Branching', *Plant Physiology*, 158(1), pp. 225–238. doi: 10.1104/pp.111.182725.

Braybrook, S. A. and Peaucelle, A. (2013) 'Mechano-Chemical Aspects of Organ Formation in Arabidopsis thaliana: The Relationship between Auxin and Pectin', *PLoS ONE*. Edited by M. Grebe. Public Library of Science, 8(3), p. e57813. doi: 10.1371/journal.pone.0057813.

Brown, D. E. *et al.* (2001) 'Flavonoids act as negative regulators of auxin transport in vivo in arabidopsis.', *Plant physiology*, 126(2), pp. 524–535. doi: 10.1104/pp.126.2.524.

Brown, S. A. (1962) 'Biosynthesis of the coumarins. III. The Role of Glycosides in the Formation of Coumarin by Hierochloe odorata', *Canadian journal of biochemistry and physiology*, 40(6801), pp. 607–18.

Brown, S. A., Towers, G. H. N. and Wright, D. (1960) 'BIOSYNTHESIS OF THE COUMARINS. TRACER STUDIES ON COUMARIN FORMATION IN HIEROCHLOË ODORATA AND MELILOTUS OFFICINALIS', *Canadian Journal of Biochemistry and Physiology*. NRC Research Press Ottawa, Canada, 38(1), pp. 143–156. doi: 10.1139/y60-016.

Brunoud, G. *et al.* (2012) 'A novel sensor to map auxin response and distribution at high spatio-temporal resolution', *Nature*, 482(7383), pp. 103–106. doi: 10.1038/nature10791.

Burgess, J. and Linstead, P. J. (1977) 'Coumarin inhibition of microfibril formation at the surface of cultured protoplasts', *Planta*, 133(3), pp. 267–273. doi: 10.1007/BF00380688.

Burström, H. (1954) 'Studies on Growth and Metabolism of Roots. XI. The Influence of Auxin and Coumarin Derivatives on the Cell Wall', *Physiologia Plantarum*, 7(3), pp. 548–559. doi: 10.1111/j.1399-3054.1954.tb07600.x.

Burton, R. A., Gidley, M. J. and Fincher, G. B. (2010) 'Heterogeneity in the chemistry, structure and function of plant cell walls', *Nature Chemical Biology*, 6(10), pp. 724–732. doi: 10.1038/nchembio.439.

Burtt, B. L. (1997) 'APIACEAE (UMBELLIFERAE)', *Bothalia*, 27(1), pp. 51–52. doi: 10.4102/abc.v27i1.657.

Cabello-Hurtado, F. *et al.* (1998) 'Coumarins in helianthus tuberosus: characterization, induced accumulation and biosynthesis', *Phytochemistry*, 49(4), pp. 1029–1036.

Cai, T. *et al.* (2016) 'The Efficacy of Umbelliferone, Arbutin, and N-Acetylcysteine to Prevent Microbial Colonization and Biofilm Development on Urinary Catheter Surface: Results from a Preliminary Study', *Journal of Pathogens*, 2016, pp. 1–6. doi: 10.1155/2016/1590952.

Cameron, F. K. (1910) 'Introduction to the study of the soil solution', 2(51), pp. 79–116.

Campbell, P. and Braam, J. (1999) 'In vitro activities of four xyloglucan endotransglycosylases from Arabidopsis', *The Plant Journal*, 18(4), pp. 371–382. doi: 10.1046/j.1365-313X.1999.00459.x.

de Candolle, A. P. (1832) *Physiologie végétale, ou exposition des forces et des fonctions vitales des végétaux: pour servir de suite à l'organograpie végétale, et d'introduction à la botanique géographique et agricole.* Vol. 3. Béchet.

Cao, D. *et al.* (2005) 'Loss of function of four DELLA genes leads to light- and gibberellin-independent seed germination in Arabidopsis', *Planta*, 223(1), pp. 105–113. doi: 10.1007/s00425-005-0057-3.

Cao, J. *et al.* (2011) 'Whole-genome sequencing of multiple Arabidopsis thaliana populations', *Nature Genetics*, 43(10), pp. 956–965. doi: 10.1038/ng.911.

Carpinella, M. C., Ferrayoli, C. G. and Palacios, S. M. (2005) 'Antifungal Synergistic Effect of Scopoletin, a Hydroxycoumarin Isolated from Melia azedarach L. Fruits', *Journal of Agricultural and Food Chemistry*, 53(8), pp. 2922–2927. doi: 10.1021/jf0482461.

Cecchetti, V. *et al.* (2013) 'Auxin controls Arabidopsis anther dehiscence by regulating endothecium lignification and jasmonic acid biosynthesis', *The Plant Journal*, 74(3), pp. 411–422. doi: 10.1111/tpj.12130.

Chabannes, M. *et al.* (2003) 'In situ analysis of lignins in transgenic tobacco reveals a differential impact of individual transformations on the spatial patterns of lignin deposition at the cellular and subcellular levels', *The Plant Journal*, 28(3), pp. 271–282. doi: 10.1046/j.1365-313x.2001.01159.x.

Chadchawan, S. *et al.* (1993) 'Arabidopsis cDNA sequence encoding myrosinase.', *Plant physiology*. American Society of Plant Biologists, 103(2), p. 671.

Chae, K. *et al.* (2012) 'Arabidopsis SMALL AUXIN UP RNA63 promotes hypocotyl and stamen filament elongation', *Plant Journal*, 71(4), pp. 684–697. doi: 10.1111/j.1365-313X.2012.05024.x.

Chaiwanon, J. and Wang, Z.-Y. (2015) 'Spatiotemporal Brassinosteroid Signaling and Antagonism with Auxin Pattern Stem Cell Dynamics in Arabidopsis Roots', *Current Biology*. Elsevier Ltd, 25(8), pp. 1031–1042. doi: 10.1016/j.cub.2015.02.046.

Chakraborty, M., Karun, A. and Mitra, A. (2009) 'Accumulation of phenylpropanoid derivatives in chitosan-induced cell suspension culture of Cocos nucifera', *Journal of Plant Physiology*. Urban & Fischer, 166(1), pp. 63–71. doi: 10.1016/J.JPLPH.2008.02.004.

Chandler, J. W. (2009) 'Local auxin production: a small contribution to a big field', *BioEssays*, 31(1), pp. 60–70. doi: 10.1002/bies.080146.

Chapman, E. J. *et al.* (2012) 'Hypocotyl transcriptome reveals auxin regulation of growth-promoting genes through GA-dependent and -independent pathways', *PLoS ONE*, 7(5). doi: 10.1371/journal.pone.0036210.

Chapman, E. J. and Estelle, M. (2009) 'Mechanism of Auxin-Regulated Gene Expression in Plants', *Annual Review of Genetics*, 43(1), pp. 265–285. doi: 10.1146/annurev-genet-102108-134148.

Chen, B.-X. *et al.* (2019) 'Coumarin-Induced Delay of Rice Seed Germination Is Mediated by Suppression of Abscisic Acid Catabolism and Reactive Oxygen Species Production', *Frontiers in Plant Science*, 10(June). doi: 10.3389/fpls.2019.00828.

Chen, R. *et al.* (1998) 'The Arabidopsis thaliana AGRAVITROPIC 1 gene encodes a component of the polar-auxin-transport efflux carrier', *Proceedings of the National Academy of Sciences*, 95(25), pp. 15112–15117. doi: 10.1073/pnas.95.25.15112.

Cheng, J. and Sun, W. (2001) 'Study on variety resistance of tobacco developing period to brown spot and the intergrated management techniques.', *Acta Phytopathologica Sinica*, 28, pp. 44–48.

Cheng, Y., Dai, X. and Zhao, Y. (2006) 'Auxin biosynthesis by the YUCCA flavin monooxygenases controls the formation of floral organs and vascular tissues in Arabidopsis', *Genes and Development*, 20(13), pp. 1790–1799. doi: 10.1101/gad.1415106.

Cho, H.-T. and Cosgrove, D. J. (2002) 'Regulation of Root Hair Initiation and Expansin Gene Expression in Arabidopsis', *The Plant Cell*, 14(12), pp. 3237–3253. doi: 10.1105/tpc.006437.

Cho, H. T. and Kende, H. (1997) 'Expression of expansin genes is correlated with growth in deepwater rice.', *The Plant Cell*, 9(9), pp. 1661–1671. doi: 10.1105/tpc.9.9.1661.

Choe, S. *et al.* (1998) 'The DWF4 gene of Arabidopsis encodes a cytochrome P450 that mediates multiple 22α-hydroxylation steps in brassinosteroid biosynthesis', *Plant Cell*, 10(2), pp. 231–243. doi: 10.1105/tpc.10.2.231.

Choi, H. and Oh, E. (2016) 'PIF4 Integrates Multiple Environmental and Hormonal Signals for Plant Growth Regulation in Arabidopsis', *Molecules and Cells*, 39(8), pp. 587–593. doi: 10.14348/molcells.2016.0126.

Chory, J., Nagpal, P. and Peto, C. A. C. (1991) 'Phenotypic and Genetic Analysis of det2, a New Mutant That Affects Light-Regulated Seedling Development in Arabidopsis.', *The Plant cell*, 3(5), pp. 445–459. doi: 10.1105/tpc.3.5.445.

Christie, J. M. *et al.* (2011) 'phot1 inhibition of ABCB19 primes lateral auxin fluxes in the shoot apex required for phototropism.', *PLoS biology*, 9(6), p. e1001076. doi: 10.1371/journal.pbio.1001076.

Christie, J. M. and Murphy, A. S. (2013) 'Shoot phototropism in higher plants: New light through old concepts', *American Journal of Botany*, 100(1), pp. 35–46. doi: 10.3732/ajb.1200340.

Christoffoleti, P. J. *et al.* (2015) 'Auxinic herbicides, mechanisms of action, and weed resistance: A look into recent plant science advances', *Scientia Agricola*, 72(4), pp. 356–362. doi: 10.1590/0103-9016-2014-0360.

Chung, Y. *et al.* (2011) 'Auxin stimulates DWARF4 expression and brassinosteroid biosynthesis in Arabidopsis', *The Plant Journal*, 66(4), pp. 564–578. doi: 10.1111/j.1365-313X.2011.04513.x.

Churchman, M. L. *et al.* (2006) 'SIAMESE, a Plant-Specific Cell Cycle Regulator, Controls Endoreplication Onset in Arabidopsis thaliana', *the Plant Cell Online*, 18(11), pp. 3145–3157. doi: 10.1105/tpc.106.044834.

Churngchow, N. and Rattarasarn, M. (2001) 'Biosynthesis of scopoletin in Hevea brasiliensis leaves inoculated with Phytophthora palmivora', *Journal of Plant Physiology*, 158(7), pp. 875–882. doi: 10.1078/0176-1617-00230.

Cifuentes-Esquivel, N. *et al.* (2013) 'The bHLH proteins BEE and BIM positively modulate the shade avoidance syndrome in Arabidopsis seedlings', *Plant Journal*, 75(6), pp. 989–1002. doi: 10.1111/tpj.12264.

Ciolfi, A. *et al.* (2013) 'Dynamics of the shade-avoidance response in Arabidopsis', *Plant Physiology*, 163(1), pp. 331–353. doi: 10.1104/pp.113.221549.

Claeys, H., De Bodt, S. and Inzé, D. (2013) 'Gibberellins and DELLAs: central nodes in growth regulatory networks.', *Trends in plant science*, pp. 1–9. doi: 10.1016/j.tplants.2013.10.001.

Clemens, S. and Weber, M. (2016) 'The essential role of coumarin secretion for Fe acquisition from alkaline soil', *Plant Signaling and Behavior*. Taylor & Francis, 11(2), pp. 1–6. doi: 10.1080/15592324.2015.1114197.

Clouse, S. D. (1996) 'Molecular genetic studies confirm the role of brassinosteroids in plant growth and development', *Plant J*, 10(1), pp. 1–8. doi: 10.1046/j.1365-313X.1996.10010001.x.

Clouse, S. D. (2011) 'Brassinosteroids', *The Arabidopsis Book*, 9(8), p. e0151. doi: 10.1199/tab.0151.

Clouse, S. D. (2015) 'A History of Brassinosteroid Research from 1970 through 2005: Thirty-Five Years of Phytochemistry, Physiology, Genes, and Mutants', *Journal of Plant Growth Regulation*. Springer US, 34(4), pp. 828–844. doi: 10.1007/s00344-015-9540-7.

Clouse, S. D., Langford, M. and McMorris, T. C. (1996) 'A Brassinosteroid-Insensitive Mutant in Arabidopsis thaliana Exhibits Multiple Defects in Growth and Development', *Plant Physiology*, 111(3), pp. 671–678. doi: 10.1104/pp.111.3.671.

Clouse, S. D. and Sasse, J. M. (1998) 'BRASSINOSTEROIDS: Essential Regulators of Plant Growth and Development', *Annual Review of Plant Physiology and Plant Molecular Biology*, 49(1), pp. 427–451. doi: 10.1146/annurev.arplant.49.1.427.

Cluis, C. P., Mouchel, C. F. and Hardtke, C. S. (2004) 'The Arabidopsis transcription factor HY5 integrates light and hormone signaling pathways', *Plant Journal*, 38(2), pp. 332–347. doi: 10.1111/j.1365-313X.2004.02052.x.

Cohen, A. J. (1979) 'Critical review of the toxicology of coumarin with special reference to interspecies differences in metabolism and hepatotoxic response and their significance to man', *Food and Cosmetics Toxicology*, 17(3), pp. 277–289. doi: 10.1016/0015-6264(79)90289-X.

Collett, C. E., Harberd, N. P. and Leyser, O. (2000) 'Hormonal interactions in the control of Arabidopsis hypocotyl elongation.', *Plant Physiology*, 124(2), pp. 553–562. doi: 10.1104/pp.124.2.553.

Collier, P. L. (1971) 'Studies related to natural procucts: Biosynthesis of Coumarins', in.

Colon-Carmona, A. *et al.* (1999) 'Spatio-temporal analysis of mitotic activity with a labile cyclin-GUS fusion

protein', *Science*, 20(4), pp. 503–208.

Cooke, T. J. *et al.* (2002) 'Evolutionary patterns in auxin action', *Plant Molecular Biology*, 49(3), pp. 319–338. doi: 10.1023/A:1015242627321.

Corbineau, F. *et al.* (2014) 'Ethylene, a key factor in the regulation of seed dormancy', *Frontiers in Plant Science*, 5(OCT), pp. 1–13. doi: 10.3389/fpls.2014.00539.

Cornman, I. (1947) 'The responses of onion and lily mitosis to coumarin and parasorbic acid.', *The Journal of experimental biology*, 23(3–4), pp. 292–297.

Correll, M. J. and Kiss, J. Z. (2005) 'The Roles of Phytochromes in Elongation and Gravitropism of Roots', *Plant and Cell Physiology*, 46(2), pp. 317–323. doi: 10.1093/pcp/pci038.

Cosgrove, D. *et al.* (2002) 'The Growing World of Expansins', *Plant Cell Physiology*, 43(12), pp. 1436–1444.

Cosgrove, D. J. (2000) 'Loosening of plant cell walls by expansins', *Nature*, 407(6802), pp. 321–326. doi: 10.1038/35030000.

Cosgrove, D. J. (2005) 'Growth of the plant cell wall', *Nature Reviews Molecular Cell Biology*, 6(11), pp. 850–861. doi: 10.1038/nrm1746.

Cosgrove, D. J. (2014) 'Plant Cell Growth and Elongation', in *eLS*. Chichester, UK: John Wiley & Sons, Ltd. doi: 10.1002/9780470015902.a0001688.pub2.

Costet, L., Fritig, B. and Kauffmann, S. (2002) 'Scopoletin expression in elicitor-treated and tobacco mosaic virus-infected tobacco plants', *Physiologia Plantarum*, 115(2), pp. 228–235. doi: 10.1034/j.1399-3054.2002.1150208.x.

Cottee, P. K., Bernays, E. A. and Mordue, A. J. (1988) 'Comparisons of deterrency and toxicity of selected secondary plant compounds to an oligophagous and a polyphagous acridid', *Entomologia Experimentalis et Applicata*, 46(3), pp. 241–247. doi: 10.1111/j.1570-7458.1988.tb01118.x.

Cowling, R. J. and Harberd, N. P. (1999) 'Gibberellins control Arabidopsis hypocotyl growth via regulation of cellular elongation', *Journal of Experimental Botany*, 50(337), pp. 1351–1357. doi: 10.1093/jxb/50.337.1351.

Cutler, H. G. *et al.* (2003) 'Allelopathy: Chemistry and mode of action of allelochemicals', *Planta Medica*. CRC Press, 22(3), pp. 217–239.

Czechowski, T. *et al.* (2005) 'Genome-Wide Identification and Testing of Superior Reference Genes for Transcript Normalization in Arabidopsis', *Plant Physiology*, 139(1), pp. 5–17. doi: 10.1104/pp.105.063743.

D'Amato, F. and D'Amato-Avanzi, M. G. (1954) 'The Chromosome-Breaking Effect of Coumarin Derivatives in the Allium Test', *Caryologia*, 6(2–3), pp. 134–150. doi: 10.1080/00087114.1954.10797467.

Dai, X. *et al.* (2013) 'The biochemical mechanism of auxin biosynthesis by an arabidopsis YUCCA flavin-containing monooxygenase', *Journal of Biological Chemistry*, 288(3), pp. 1448–1457. doi: 10.1074/jbc.M112.424077.

Dare, A. P. *et al.* (2017) 'Silencing a phloretin-specific glycosyltransferase perturbs both general phenylpropanoid biosynthesis and plant development Running Title: Silencing a phloretin-specific glycosyltransferase', pp. 1–14. doi: 10.1111/tpj.13559.

Darmawan, A. *et al.* (2012) 'Scopoletin, a coumarin derivative compound isolated from Macaranga gigantifolia Merr', *Journal of Applied Pharmaceutical Science*, 2(12), pp. 175–177. doi: 10.7324/JAPS.2012.21231.

Darwin, Charles and Darwin, F. (1881) *The power of movement in plants.*, *D. Appleton*.

Darwin, C. and Darwin, F. (1881) *The power of movements in plants.*, *Darwins Gesammelte Werke Bd. 13 (Schweizer-bartsche Verlagsbuchhandlung, Stuttgart)*.

Daviere, J.-M. and Achard, P. (2013) 'Gibberellin signaling in plants', *Development*, 140(6), pp. 1147–1151. doi: 10.1242/dev.087650.

Davière, J.-M., de Lucas, M. and Prat, S. (2008) 'Transcriptional factor interaction: a central step in DELLA function', *Current Opinion in Genetics & Development*, 18(4), pp. 295–303. doi: 10.1016/j.gde.2008.05.004.

Davière, J. M. and Achard, P. (2016) 'A Pivotal Role of DELLAs in Regulating Multiple Hormone Signals', *Molecular Plant*, 9(1), pp. 10–20. doi: 10.1016/j.molp.2015.09.011.

Dayan, F. E. and Duke, S. O. (2006) 'Clues in the search for new herbicides', *Allelopathy: A Physiological Process with Ecological Implications*, pp. 63–83. doi: 10.1007/1-4020-4280-9_3.

Delarue, M. *et al.* (1998) 'Sur2 mutations of Arabidopsis thaliana define a new locus involved in the control of auxin homeostasis', *Plant Journal*, 14(5), pp. 603–611. doi: 10.1046/j.1365-313X.1998.00163.x.

Deng, Y. and Lu, S. (2017) 'Biosynthesis and Regulation of Phenylpropanoids in Plants', *Critical Reviews in Plant Sciences*. Taylor & Francis, 36(4), pp. 257–290. doi: 10.1080/07352689.2017.1402852.

Depuydt, S. *et al.* (2016) 'How plant hormones and their interactions affect cell growth', *Molecular Cell Biology of Plants*.

Depuydt, S. and Hardtke, C. S. (2011) 'Hormone signalling crosstalk in plant growth regulation', *Current Biology*. Elsevier Ltd, 21(9), pp. R365–R373. doi: 10.1016/j.cub.2011.03.013.

Derbyshire, P. *et al.* (2007) 'Cell elongation in Arabidopsis hypocotyls involves dynamic changes in cell wall thickness', *Journal of Experimental Botany*, 58(8), pp. 2079–2089. doi: 10.1093/jxb/erm074.

Derbyshire, P., McCann, M. C. and Roberts, K. (2007) 'Restricted cell elongation in Arabidopsis hypocotyls is associated with a reduced average pectin esterification level', *BMC Plant Biology*, 7(1), p. 31. doi: 10.1186/1471-2229-7-31.

Derksen, H., Rampitsch, C. and Daayf, F. (2013) 'Signaling cross-talk in plant disease resistance', *Plant Science*, 207, pp. 79–87. doi: 10.1016/j.plantsci.2013.03.004.

Deropp, R. S. (1956) 'Kinetin and Auxin Activity.', *Plant physiology*, 31(3), pp. 253–4. doi: 10.1104/pp.31.3.253.

Dharmasiri, N. *et al.* (2005) 'Plant development is regulated by a family of auxin receptor F box proteins', *Developmental Cell*, 9(1), pp. 109–119. doi: 10.1016/j.devcel.2005.05.014.

Dharmasiri, N., Dharmasiri, S. and Estelle, M. (2005) 'The F-box protein TIR1 is an auxin receptor', *Nature*, 435(7041), pp. 441–445. doi: 10.1038/nature03543.

Dhawan, R. S. and Nanda, K. K. (1982) 'Stimulation of Root Formation on Impatiens balsamina L. cuttings by coumarin and the associated biochemical changes', *Biologia Plantarum*, 24(3), pp. 177–182. doi: 10.1007/BF02883658.

Dieterman, L. J. *et al.* (1964) 'Identification and quantitative determination of scopolin and scopoletin in tobacco plants treated with 2,4-dichlorophenoxyacetic acid', *Analytical Biochemistry*, 9(2), pp. 139–145. doi: 10.1016/0003-2697(64)90095-8.

Dill, A., Jung, H.-S. and Sun, T. -p. (2001) 'The DELLA motif is essential for gibberellin-induced degradation of RGA', *Proceedings of the National Academy of Sciences*, 98(24), pp. 14162–14167. doi: 10.1073/pnas.251534098.

Ding, Z. *et al.* (2008) 'Anti-Inflammatory Effects of Scopoletin and Underlying Mechanisms', *Pharmaceutical*

Biology, 46(12), pp. 854–860. doi: 10.1080/13880200802367155.

Ding, Z. *et al.* (2011) 'Light-mediated polarization of the PIN3 auxin transporter for the phototropic response in Arabidopsis', *Nature Cell Biology*, 13(4), pp. 447–452. doi: 10.1038/ncb2208.

Dixon, R. A., Liu, C. and Jun, J. H. (2013) 'Metabolic engineering of anthocyanins and condensed tannins in plants', *Current Opinion in Biotechnology*. Elsevier Ltd, 24(2), pp. 329–335. doi: 10.1016/j.copbio.2012.07.004.

Dixon, R. A. and Pasinetti, G. M. (2010) 'Flavonoids and Isoflavonoids: From Plant Biology to Agriculture and Neuroscience', *Plant Physiology*, 154(2), pp. 453–457. doi: 10.1104/pp.110.161430.

Djordjevic, M. A. *et al.* (1987) 'Clovers secrete specific phenolic compounds which either stimulate or repress nod gene expression in Rhizobium trifolii', *The EMBO Journal*, 6(5), pp. 1173–1179. doi: 10.1002/j.1460-2075.1987.tb02351.x.

Dobson, A. J. and Barnett, A. G. (2008) *An introduction to generalized linear models*. hapman and Hall/CRC.

Dolan, L. *et al.* (1993) 'Cellular organisation of the Arabidopsis thaliana root.', *Development (Cambridge, England)*, 119(1), pp. 71–84. Available at: http://www.ncbi.nlm.nih.gov/pubmed/8275865.

Dombrecht, B. *et al.* (2007) 'MYC2 Differentially Modulates Diverse Jasmonate-Dependent Functions in Arabidopsis', *The Plant Cell*, 19(7), pp. 2225–2245. doi: 10.1105/tpc.106.048017.

Downes, B. P. and Crowell, D. N. (1998) 'Cytokinin regulates the expression of a soybean β-expansin gene by a post-transcriptional mechanism', *Plant Molecular Biology*, 37(3), pp. 437–444. doi: 10.1023/A:1005920732211.

Drechsel, G., Raab, S. and Hoth, S. (2010) 'Arabidopsis zinc-finger protein 2 is a negative regulator of ABA signaling during seed germination', *Journal of Plant Physiology*, 167(16), pp. 1418–1421. doi: 10.1016/j.jplph.2010.05.010.

Du, J. *et al.* (2017) 'Identification and characterization of multiple intermediate alleles of the key genes regulating brassinosteroid biosynthesis pathways', *Frontiers in Plant Science*, 7(January), pp. 1–9. doi: 10.3389/fpls.2016.01893.

Dubois, M., Van den Broeck, L. and Inzé, D. (2018) 'The Pivotal Role of Ethylene in Plant Growth', *Trends in plant science*, (1642), pp. 1–13.

Duvel, J. (1905) 'Vitality of buried seeds.', *Bureau of Plant Industries, USDA Bulletin*, (83).

Ehlers, D. *et al.* (1995) 'HPLC analysis of tonka bean extracts', *Zeitschrift fur Lebensmittel-Untersuchung und -Forschung*, 201(3), pp. 278–282. doi: 10.1007/BF01193004.

Einhellig, F. A. *et al.* (1970) 'Effects of Scopoletin on Growth, CO2 Exchange Rates, and Concentration of Scopoletin, Scopolin, and Chlorogenic Acids in Tobacco, Sunflower, and Pigweed', *Bulletin of the Torrey Botanical Club*, 97(1), p. 22. doi: 10.2307/2483987.

Einhellig, F. A. (1996) 'Interactions Involving Allelopathy in Cropping Systems', *Agronomy Journal*, 88(6), p. 886. doi: 10.2134/agronj1996.00021962003600060007x.

Einhellig, F. A. and Kuan, L.-Y. (1971) 'Effects of Scopoletin and Chlorogenic Acid on Stomatal Aperture in Tobacco and Sunflower', *Bulletin of the Torrey Botanical Club*, 98(3), p. 155. doi: 10.2307/2484031.

Eng, R. C. and Sampathkumar, A. (2018) 'Getting into shape: the mechanics behind plant morphogenesis', *Current Opinion in Plant Biology*, 46, pp. 25–31. doi: 10.1016/j.pbi.2018.07.002.

Epstein, K. (2019) 'The Doomsday Vault's home is already altered by climate change . A report says it could get worse .', *the Washington Post*, 27 March. Available at: https://www.washingtonpost.com/climate-

environment/2019/03/27/doomsday-vaults-home-is-already-altered-by-climate-change-report-says-it-could-get-worse/.

Evans, M., Ishikawa, H. and Estelle, M. (1994) 'Responses of Arabidopsis roots to auxin studied with high temporal resolution: Comparison of wild type and auxin-response mutants', *Planta*, 194(2). doi: 10.1007/BF00196390.

Evans, M. L. and Cleland, R. E. (1985) 'The action of auxin on plant cell elongation', *Critical Reviews in Plant Sciences*, 2(4), pp. 317–365. doi: 10.1080/07352688509382200.

Evenari, M. (1965) 'Light and seed dormancy', in *Differenzierung und Entwicklung / Differentiation and Development*. Berlin, Heidelberg: Springer Berlin Heidelberg, pp. 2451–2494. doi: 10.1007/978-3-642-50088-6_61.

Farquharson, K. L. (2014) 'SAUR19 Links Auxin and Plasma Membrane H+-ATPases in Cell Expansion', *The Plant Cell*, 26(5), pp. 1835–1835. doi: 10.1105/tpc.114.127886.

Farshori, N. N. *et al.* (2011) '7-Hydroxy-coumarin derivatives: synthesis, characterization and preliminary antimicrobial activities', *Medicinal Chemistry Research*, 20(5), pp. 535–541. doi: 10.1007/s00044-010-9347-9.

Feldmann, K. A. *et al.* (1989) 'A Dwarf Mutant of Arabidopsis Generated by T-DNA Insertion Mutagenesis', *Science*, 243(4896), pp. 1351–1354. doi: 10.1126/science.243.4896.1351.

Fellenberg, C. and Vogt, T. (2015) 'Evolutionarily conserved phenylpropanoid pattern on angiosperm pollen', *Trends in Plant Science*. Elsevier Ltd, 20(4), pp. 212–218. doi: 10.1016/j.tplants.2015.01.011.

Fendrych, M., Leung, J. and Friml, J. (2016) 'Tir1/AFB-Aux/IAA auxin perception mediates rapid cell wall acidification and growth of Arabidopsis hypocotyls', *eLife*, 5(September2016), pp. 1–18. doi: 10.7554/eLife.19048.

Feng, S. *et al.* (2008) 'Coordinated regulation of Arabidopsis thaliana development by light and gibberellins', *Nature*, 451(7177), pp. 475–479. doi: 10.1038/nature06448.

Ferreira, F. J. and Kieber, J. J. (2005) 'Cytokinin signaling', *Current Opinion in Plant Biology*, 8(5), pp. 518–525. doi: 10.1016/j.pbi.2005.07.013.

Fleming, A. J. (1997) 'Induction of Leaf Primordia by the Cell Wall Protein Expansin', *Science*, 276(5317), pp. 1415–1418. doi: 10.1126/science.276.5317.1415.

Fortunato, A. E. *et al.* (2016) 'Diatom phytochromes reveal the existence of far-red-light-based sensing in the ocean', *Plant Cell*, 28(3), pp. 616–628. doi: 10.1105/tpc.15.00928.

Fourcroy, P. *et al.* (2014) 'Involvement of the ABCG37 transporter in secretion of scopoletin and derivatives by Arabidopsis roots in response to iron deficiency', *New Phytologist*, 201(1), pp. 155–167. doi: 10.1111/nph.12471.

Fourcroy, P. *et al.* (2016) 'Facilitated Fe Nutrition by Phenolic Compounds Excreted by the Arabidopsis ABCG37/PDR9 Transporter Requires the IRT1/FRO2 High-Affinity Root Fe2+ Transport System', *Molecular Plant*, 9(3), pp. 485–488. doi: 10.1016/j.molp.2015.09.010.

Franklin, K. A. *et al.* (2011) 'PHYTOCHROME-INTERACTING FACTOR 4 (PIF4) regulates auxin biosynthesis at high temperature', *Proceedings of the National Academy of Sciences*, 108(50), pp. 20231–20235. doi: 10.1073/pnas.1110682108.

Franklin, K. A. and Quail, P. H. (2010) 'Phytochrome functions in Arabidopsis development', *Journal of Experimental Botany*, 61(1), pp. 11–24. doi: 10.1093/jxb/erp304.

Frey, A. *et al.* (2012) 'Epoxycarotenoid cleavage by NCED5 fine-tunes ABA accumulation and affects seed

dormancy and drought tolerance with other NCED family members', *Plant Journal*, 70(3), pp. 501–512. doi: 10.1111/j.1365-313X.2011.04887.x.

Fridman, Y. and Savaldi-Goldstein, S. (2013) 'Brassinosteroids in growth control: How, when and where', *Plant Science*. Elsevier Ireland Ltd, 209, pp. 24–31. doi: 10.1016/j.plantsci.2013.04.002.

Friedrichsen, D. M. *et al.* (2002) 'Three redundant brassinosteroid early response genes encode putative bHLH transcription factors required for normal growth.', *Genetics*, 162(3), pp. 1445–56. Available at: http://www.ncbi.nlm.nih.gov/pubmed/12454087.

Friml, J. *et al.* (2002) 'Lateral relocation of auxin efflux regulator PIN3 mediates tropism in Arabidopsis', *Nature*, 415(6873), pp. 806–809. doi: 10.1038/415806a.

Friml, J. *et al.* (2003a) 'Efflux-dependent auxin gradients establish the apical-basal axis of Arabidopsis', *Nature*, 426(6963), pp. 147–153. doi: 10.1038/nature02085.

Friml, J. *et al.* (2003b) 'Efflux-dependent auxin gradients establish the apical–basal axis of Arabidopsis', *Nature*, 426(6963), pp. 147–153. doi: 10.1038/nature02085.

Friml, J. and Palme, K. (2002) 'Polar auxin transport - old questions and new concepts?', *Plant molecular biology*, 49, pp. 273–284.

Fritig, B., Hirth, L. and Ourisson, G. (1970) 'Biosynthesis of the coumarins: Scopoletin formation in tobacco tissue cultures', *Phytochemistry*, 9(9), pp. 1963–1975. doi: 10.1016/S0031-9422(00)85348-0.

Fu, X. and Harberd, N. P. (2003) 'Auxin promotes Arabidopsis root growth by modulating gibberellin response', *Nature*, 421(6924), pp. 740–743. doi: 10.1038/nature01387.

Fuentes, S. *et al.* (2012) 'Fruit growth in Arabidopsis occurs via DELLA-dependent and DELLA-independent gibberellin responses', *Plant Cell*, 24(10), pp. 3982–3996. doi: 10.1105/tpc.112.103192.

Fujiyama, K. *et al.* (2019) 'Structural insights into a key step of brassinosteroid biosynthesis and its inhibition', *Nature Plants*, 5(6), pp. 589–594. doi: 10.1038/s41477-019-0436-6.

Fukaki, H. *et al.* (2002) 'Lateral root formation is blocked by a gain-of-function mutation in the SOLITARY-ROOT/IAA14 gene of Arabidopsis.', *The Plant Journal*, 29(2), pp. 153–68. doi: 10.1046/j.0960-7412.2001.01201.x.

Fukuda, H. (2015) *Plant cell wall patterning and cell shape*. Wiley Online Library.

Gagne, J. M. *et al.* (2004) 'Arabidopsis EIN3-binding F-box 1 and 2 form ubiquitin-protein ligases that repress ethylene action and promote growth by directing EIN3 degradation', *Proceedings of the National Academy of Sciences*, 101(17), pp. 6803–6808. doi: 10.1073/pnas.0401698101.

Galbraith, D. W., Harkins, K. R. and Knapp, S. (1991) 'Systemic Endopolyploidy in Arabidopsis thaliana', *Plant Physiology*, 96(3), pp. 985–989. doi: 10.1104/pp.96.3.985.

Gallego-Bartolome, J. *et al.* (2012) 'Molecular mechanism for the interaction between gibberellin and brassinosteroid signaling pathways in Arabidopsis', *Proceedings of the National Academy of Sciences*, 109(33), pp. 13446–13451. doi: 10.1073/pnas.1119992109.

Gallego-Bartolomé, J. *et al.* (2011) 'Hierarchy of hormone action controlling apical hook development in Arabidopsis.', *The Plant journal : for cell and molecular biology*, 67(4), pp. 622–34. doi: 10.1111/j.1365-313X.2011.04621.x.

Gallei, M., Luschnig, C. and Friml, J. (2020) 'Auxin signalling in growth: Schrödinger's cat out of the bag', *Current Opinion in Plant Biology*, 53, pp. 43–49. doi: 10.1016/j.pbi.2019.10.003.

Galweiler, L. *et al.* (1998) 'Regulation of Polar Auxin Transport by AtPIN1 in Arabidopsis Vascular Tissue',

Science, 282(5397), pp. 2226–2230. doi: 10.1126/science.282.5397.2226.

Gangappa, S. N. and Botto, J. F. (2016) 'The Multifaceted Roles of HY5 in Plant Growth and Development', *Molecular Plant*. Elsevier Ltd, 9(10), pp. 1353–1365. doi: 10.1016/j.molp.2016.07.002.

Garcia, D. *et al.* (1995) 'Accumulation of scopoletin in Hevea brasiliensis infected by Microcyclus ulei (P. Henn.) V. ARX and evaluation of its fungitoxicity for three leaf pathogens of rubber tree', *Physiological and Molecular Plant Pathology*, 47(4), pp. 213–223. doi: 10.1006/pmpp.1995.1053.

Ge, W. and Steber, C. M. (2018) 'Positive and negative regulation of seed germination by the Arabidopsis GA hormone receptors, GID1a , b , and c', *Plant Direct*, 2(9), pp. 1–11. doi: 10.1002/pld3.83.

Geisler, M. and Murphy, A. S. (2006) 'The ABC of auxin transport: The role of p-glycoproteins in plant development', *FEBS Letters*, 580(4), pp. 1094–1102. doi: 10.1016/j.febslet.2005.11.054.

van Gelderen, K., Kang, C. and Pierik, R. (2018) 'Light Signaling, Root Development, and Plasticity', *Plant Physiology*, 176(2), pp. 1049–1060. doi: 10.1104/pp.17.01079.

Gendreau, E. *et al.* (1997) 'Cellular basis of hypocotyl growth in Arabidopsis thaliana.', *Plant physiology*, 114(1), pp. 295–305. doi: 114/1/295 [pii].

Gendreau, E. *et al.* (1999) 'Gibberellin and ethylene control endoreduplication levels in the Arabidopsis thaliana hypocotyl', *Planta*, 209(4), pp. 513–516. doi: 10.1007/s004250050755.

Gerhardt, C. F. (1846) *Grundriss der organischen Chemie: 2*. Schmidt & Grucker.

Ghosh, P., Sil, P. and Thakur, S. (1987) 'Spray reagent for the detection of coumarins and flavonoids on thin-layer plates', *Journal of Chromatography A*, 403(C), pp. 285–287. doi: 10.1016/S0021-9673(00)96364-7.

Giesemann, A., Biehl, B. and Lieberei, R. (1986) 'Identification of Scopoletin as a Phytoalexin of the Rubber Tree Hevea brasiliensis', *Journal of Phytopathology*, 117(4), pp. 373–376. doi: 10.1111/j.1439-0434.1986.tb04377.x.

Givel, M. (2003) 'A comparison of US and Norwegian regulation of coumarin in tobacco products', *Tobacco Control*, 12(4), pp. 401–405. doi: 10.1136/tc.12.4.401.

Glazebrook, J. (2005) 'Contrasting Mechanisms of Defense Against Biotrophic and Necrotrophic Pathogens', *Annual Review of Phytopathology*, 43(1), pp. 205–227. doi: 10.1146/annurev.phyto.43.040204.135923.

Gnonlonfin, G. J. B., Sanni, A. and Brimer, L. (2012) 'Review Scopoletin - A Coumarin Phytoalexin with Medicinal Properties', *Critical Reviews in Plant Sciences*, 31(1), pp. 47–56. doi: 10.1080/07352689.2011.616039.

Goh, T., Kasahara, H., *et al.* (2012) 'Multiple AUX/IAA–ARF modules regulate lateral root formation: the role of Arabidopsis SHY2/IAA3-mediated auxin signalling', *Philosophical Transactions of the Royal Society B: Biological Sciences*, 367(1595), pp. 1461–1468. doi: 10.1098/rstb.2011.0232.

Goh, T., Joi, S., *et al.* (2012) 'The establishment of asymmetry in Arabidopsis lateral root founder cells is regulated by LBD16/ASL18 and related LBD/ASL proteins', *Development*, 139(5), pp. 883–893. doi: 10.1242/dev.071928.

Gomez-Roldan, V. *et al.* (2008) 'Strigolactone inhibition of shoot branching.', *Nature*, 455(7210), pp. 189–94. doi: 10.1038/nature07271.

Gonzalez-Garcia, M.-P. *et al.* (2011) 'Brassinosteroids control meristem size by promoting cell cycle progression in Arabidopsis roots', *Development*, 138(5), pp. 849–859. doi: 10.1242/dev.057331.

Gonzalez, N. *et al.* (2010) 'Increased Leaf Size: Different Means to an End', *Plant Physiology*, 153(3), pp. 1261–1279. doi: 10.1104/pp.110.156018.

Goodwin, R. H. and Kavanagh, F. (1949) 'The Isolation of Scopoletin, a Blue-Fluorescing Compound from Oat Roots', *Bulletin of the Torrey Botanical Club*, 76(4), p. 255. doi: 10.2307/2482319.

Goodwin, R. H. and Pollock, B. M. (1954) 'Studies on Roots. I. Properties and Distribution of Fluorescent Constituents in Avena Roots', *American Journal of Botany*, 41(6), p. 516. doi: 10.2307/2438863.

Goodwin, R. H. and Taves, C. (1950) 'The Effect of Coumarin Derivatives on the Growth of Avena Roots', *American Journal of Botany*, 37(3), p. 224. doi: 10.2307/2437906.

Goplen, B. P., Greenshields, J. E. R. and Baenziger, H. (1957) 'The inheritance of coumarin in sweet clover', *Canadian Journal of Botany*, 35, pp. 583–594.

Goren, R. and Tomer, E. (1971) 'Effects of Seselin and Coumarin on Growth, Indoleacetic Acid Oxidase, and Peroxidase, with Special Reference to Cucumber (Cucumis sativa L.) Radicles', *Plant Physiology*, 47(2), pp. 312–316. doi: 10.1104/pp.47.2.312.

Gorz, H. J. and Haskins, F. A. (1969) 'Absence of Dominance of the Cu Gene in Influencing o-Hydroxycinnamic Acid Content in Melilotus alba', *Crop Science*, 9, pp. 2–5.

Gorz, H. J., Haskins, F. A. and Manglitz, G. R. (1972) 'Effect of Coumarin and Related Compounds on Blister Beetle Feeding in Sweetclover', *Journal of Economic Entomology*, 65(6), pp. 1632–1635. doi: 10.1093/jee/65.6.1632.

Goy, P. A. *et al.* (1993) 'Accumulation of scopoletin is associated with the high disease resistance of the hybrid Nicotiana glutinosa x Nicotiana debneyi', *Planta*, 191(2), pp. 200–206. doi: 10.1007/BF00199750.

Graña, E. *et al.* (2017) 'Auxin-like effects of the natural coumarin scopoletin on Arabidopsis cell structure and morphology', *Journal of Plant Physiology*. Elsevier, 218(July), pp. 45–55. doi: 10.1016/j.jplph.2017.07.007.

Greenham, K. and McClung, C. R. (2015) 'Integrating circadian dynamics with physiological processes in plants.', *Nature reviews. Genetics*. Nature Publishing Group, 16(10), pp. 598–610. doi: 10.1038/nrg3976.

Grones, P. *et al.* (2018) 'PID/WAG-mediated phosphorylation of the Arabidopsis PIN3 auxin transporter mediates polarity switches during gravitropism', *Scientific Reports*, 8(1), pp. 1–11. doi: 10.1038/s41598-018-28188-1.

Groot, S. P. C. and Karssen, C. M. (1987) 'Gibberellins regulate seed germination in tomato by endosperm weakening: a study with gibberellin-deficient mutants', *Planta*, 171(4), pp. 525–531. doi: 10.1007/BF00392302.

Grosser, J. W. and Chandler, J. L. (1986) 'In vitro multiplication of Swingle citrumelo rootstock with coumarin', *HortScience*. American Society for Horticultural Science, 21(3), pp. 518–520.

Grossmann, K. (2009) 'Auxin herbicides: current status of mechanism and mode of action', *Pest Management Science*, 66(2), pp. 113–120. doi: 10.1002/ps.1860.

Grove, M. D. *et al.* (1979) 'Brassinolide, a plant growth-promoting steroid isolated from Brassica napus pollen', *Nature*, 281(5728), pp. 216–217. doi: 10.1038/281216a0.

Gudesblat, G. E. *et al.* (2012) 'SPEECHLESS integrates brassinosteroid and stomata signalling pathways', *Nature Cell Biology*. Nature Publishing Group, 14(5), pp. 548–554. doi: 10.1038/ncb2471.

Gudesblat, G. E. and Russinova, E. (2011) 'Plants grow on brassinosteroids', *Current Opinion in Plant Biology*. Elsevier Ltd, 14(5), pp. 530–537. doi: 10.1016/j.pbi.2011.05.004.

Guibourt, N. J.-B. G. (1820) 'Histoire abrégée des drogues simples'. Paris: L. Colas : Méquignon-Marvis : L'auteur, p. 2 v. Available at: file://catalog.hathitrust.org/Record/009344795.

Guo, H. *et al.* (2015) 'Potential allelochemicals in root zone soils of Stellera chamaejasme L. and variations at

different geographical growing sites', *Plant Growth Regulation*. Springer Netherlands, 77(3), pp. 335–342. doi: 10.1007/s10725-015-0068-4.

Guo, H. and Ecker, J. R. (2003) 'Plant Responses to Ethylene Gas Are Mediated by SCFEBF1/EBF2-Dependent Proteolysis of EIN3 Transcription Factor', *Cell*, 115(6), pp. 667–677. doi: 10.1016/S0092-8674(03)00969-3.

Gupta, A., Singh, M. and Laxmi, A. (2015) 'Interaction between Glucose and Brassinosteroid during the Regulation of Lateral Root Development in Arabidopsis', *Plant Physiology*, 168(1), pp. 307–320. doi: 10.1104/pp.114.256313.

Gutiérrez-Barranquero, J. A. *et al.* (2015) 'Deciphering the role of coumarin as a novel quorum sensing inhibitor suppressing virulence phenotypes in bacterial pathogens', *Appl Microbiol Biotechnol*, 99(3303). Available at: https://doi.org/10.1007/s00253-015-6436-1.

Guzmán, P. and Ecker, J. R. (1990) 'Exploiting the triple response of Arabidopsis to identify ethylene-related mutants.', *The Plant Cell*, 2(6), pp. 513–523. doi: 10.1105/tpc.2.6.513.

Hagen, G. and Guilfoyle, T. (2002) 'Auxin-responsive gene expression: Genes, promoters and regulatory factors', *Plant Molecular Biology*, 49(3–4), pp. 373–385. doi: 10.1023/A:1015207114117.

Hager, A. (2003) 'Role of the plasma membrane H+-ATPase in auxin-induced elongation growth: Historical and new aspects', *Journal of Plant Research*, 116(6), pp. 483–505. doi: 10.1007/s10265-003-0110-x.

Hamerski, D., Schmitt, D. and Matern, U. (1990) 'Induction of two prenyltransferases for the accumulation of coumarin phytoalexins in elicitor-treated Ammi majus cell suspension cultures', *Phytochemistry*, 29(4), pp. 1131–1135. doi: 10.1016/0031-9422(90)85417-E.

Hamiaux, C. *et al.* (2012) 'DAD2 is an α/β hydrolase likely to be involved in the perception of the plant branching hormone, strigolactone.', *Current biology : CB*. Elsevier Ltd, 22(21), pp. 2032–6. doi: 10.1016/j.cub.2012.08.007.

Hanson, J. B. and Trewavas, A. J. (1982) 'Regulation of Plant Cell Growth : the Changing Perspective', *New Phytologist*, 90, pp. 1–18.

Hao, Y. *et al.* (2012) 'Interactions between HLH and bHLH factors modulate light-regulated plant development', *Molecular Plant*. © The Authors. All rights reserved., 5(3), pp. 688–697. doi: 10.1093/mp/sss011.

Hara, M., Umetsu, N. and Miyamoto, C. (1973) 'Inhibition of the biosynthesis of plant cell wall materials, especially cellulose biosynthesis, by coumarin', *Plant and Cell Physiology*, 28, pp. 11–28. doi: 10.1093/oxfordjournals.pcp.a074832.

Harada, H., Ohyama, K. and Cheruel, J. (1972) 'Effects of coumarin and other factors on the modification of form and growth of isolated mesophyll cells', *Zeitschrift für Pflanzenphysiologie*. Gustav Fischer Verlag Stuttgart, 66(4), pp. 307–324. doi: 10.1016/S0044-328X(72)80144-2.

Harada, H., Rossini, L. and Cheruel, J. (1971) 'Effect of coumarin on the growth of isolated mesophyll cells of Calystegia sepium L.', *Zeitschrift fur Pflanzenphysiologie.*

Harborne, J. B. (1999) 'Classes and functions of secondary products from plants.', in *In Walton NJ, Brown DE (eds), Chemicals form plants*. Imperial College Press, London, pp. 1–25. doi: 10.1111/j.1749-6632.1960.tb40950.x.

Hartwig, T. *et al.* (2012) 'Propiconazole is a specific and accessible brassinosteroid (BR) biosynthesis inhibitor for arabidopsis and maize', *PLoS ONE*, 7(5), pp. 1–11. doi: 10.1371/journal.pone.0036625.

Haruta, M. *et al.* (2010) 'Molecular Characterization of Mutant Arabidopsis Plants with Reduced Plasma Membrane Proton Pump Activity', *Journal of Biological Chemistry*, 285(23), pp. 17918–17929. doi:

10.1074/jbc.M110.101733.

Haruta, M. and Sussman, M. R. (2012) 'The Effect of a Genetically Reduced Plasma Membrane Protonmotive Force on Vegetative Growth of Arabidopsis', *Plant Physiology*, 158(3), pp. 1158–1171. doi: 10.1104/pp.111.189167.

Haskins, F. A. and Gorz, H. J. (1965) 'Absence of Dominance of the B Gene in Influencing β-Glucosidase Activity in Melilotus alba', *Agronomy and Horticulture*, 216, pp. 733–738.

Haskins, F. a and Gorz, H. J. (1970) 'Rapid Detection of o-Hydroxycinnamic Acid and Beta-Glucosidase in Melilotus alba', *Crop Science*, 10(5), p. 479. doi: 10.2135/cropsci1970.0011183X001000050006x.

Hategan, L. *et al.* (2014) 'Differential expression of the brassinosteroid receptor-encoding BRI1 gene in Arabidopsis', *Planta*, 239(5), pp. 989–1001. doi: 10.1007/s00425-014-2031-4.

Hayward, A. *et al.* (2009) 'Interactions between Auxin and Strigolactone in Shoot Branching Control', *Plant Physiology*, 151(1), pp. 400–412. doi: 10.1104/pp.109.137646.

He, J.-X. *et al.* (2005) 'BZR1 is a transcriptional repressor with dual roles in brassinosteroid homeostasis and growth responses.', *Science (New York, N.Y.)*, 307(5715), pp. 1634–8. doi: 10.1126/science.1107580.

He, Y. and Gan, S. (2004) 'A novel zinc-finger protein with a proline-rich domain mediates ABA-regulated seed dormancy in Arabidopsis', *Plant Molecular Biology*, 54(1), pp. 1–9. doi: 10.1023/B:PLAN.0000028730.10834.e3.

Hentrich, M. *et al.* (2013) 'The jasmonic acid signaling pathway is linked to auxin homeostasis through the modulation of YUCCA8 and YUCCA9 gene expression', *The Plant Journal*, 74(4), pp. 626–637. doi: 10.1111/tpj.12152.

Heo, J.-O. *et al.* (2011) 'Funneling of gibberellin signaling by the GRAS transcription regulator SCARECROW-LIKE 3 in the Arabidopsis root', *Proceedings of the National Academy of Sciences*, 108(5), pp. 2166–2171. doi: 10.1073/pnas.1012215108.

Hepler, P. K., Rounds, C. M. and Winship, L. J. (2013) 'Control of Cell Wall Extensibility during Pollen Tube Growth', *Molecular Plant*, 6(4), pp. 998–1017. doi: 10.1093/mp/sst103.

Heugebaert, T. (2015) *Perkin reaction towards coumarin formation.*, *Scent and Molecules*. Available at: https://scentandmolecules.wordpress.com/tag/vanilla/.

Heyn, A. N. J. (1931) 'Der Mechanismus der Zellstreckung', *Rec. Trav. Bot. Neerl.*, 28, pp. 113–244.

Heyn, A. N. J. (1940) 'The physiology of cell elongation.', *The Bot. Rev.*, 6(10), pp. 515–574.

Higgins, A. (2018) 'On its 10th anniversary, dispelling myths around the Arctic Circle's famed "doomsday" seed vault', *the Washington Post*. Available at: http://www.journals.cambridge.org/abstract_S0960258511000407.

Hijazin, T. *et al.* (2019) 'Uptake and modification of umbelliferone by various seedlings', *Phytochemistry*. Elsevier, 157(November 2018), pp. 194–199. doi: 10.1016/j.phytochem.2018.10.032.

Hillis, W. E. and Swain, T. (1959) 'Phenolic constituents ofPrunus domestica. III.—Identification of the major constituents in the tissues of victoria plum', *Journal of the Science of Food and Agriculture*, 10(10), pp. 533–537. doi: 10.1002/jsfa.2740101006.

Hino, F., Okazaki, M. and Miura, Y. (1982) 'Effect of 2,4-Dichlorophenoxyacetic Acid on Glucosylation of Scopoletin to Scopolin in Tobacco Tissue Culture', *Plant Physiology*, 69(4), pp. 810–813. doi: 10.1104/pp.69.4.810.

Hisanaga, T., Kawade, K. and Tsukaya, H. (2015) 'Compensation: A key to clarifying the organ-level regulation

of lateral organ size in plants', *Journal of Experimental Botany*, 66(4), pp. 1055–1063. doi: 10.1093/jxb/erv028.

Hogetsu, T., Shiboaka, H. and Shimokoriyama, M. (1974) 'Involvement of cellulose synthesis in actions of gibberellin and kinetin on cell expansion. Gibberellin-coumarin and kinetin-coumarin interactions on stem elongation', *Plant and Cell Physiology*, 272(15), pp. 265–272. doi: 10.1093/oxfordjournals.pcp.a075002.

Hohmann, U. *et al.* (2018) 'Mechanistic basis for the activation of plant membrane receptor kinases by SERK-family coreceptors', *Proceedings of the National Academy of Sciences of the United States of America*, 115(13), pp. 3488–3493. doi: 10.1073/pnas.1714972115.

Hohmann, U., Lau, K. and Hothorn, M. (2017) 'The Structural Basis of Ligand Perception and Signal Activation by Receptor Kinases', *Annual Review of Plant Biology*, 68(1), pp. 109–137. doi: 10.1146/annurev-arplant-042916-040957.

Holdsworth, M. J., Bentsink, L. and Soppe, W. J. J. (2008) 'Molecular networks regulating Arabidopsis seed maturation, after- ripening, dormancy and germination', *New Phytologist*, 179(1), pp. 33–54. doi: 10.1111/j.1469-8137.2008.02437.x.

Hollander, M. and Wolfe, D. A. (1973) *Nonparametric Statistical Methods*. second. New: Jonh Wiley & Sons.

Hooker, T., Millar, A. and Kunst, L. (2002) 'Significance of the expression of the CER6 condensing enzyme for cuticular wax production in Arabidopsis.', *Plant Physiology*, (129), pp. 1568–1580.

Hossain, D. *et al.* (2008) 'Suppressive effects of coumarins on pumpkin seedling growth and glutathione S - transferase activity', *Journal of Crop Science and Biotechnology*, 2008(3), pp. 187–192.

Houbigant Business, I. (2019) *The House of Houbigant - Parfumeurs depuis 1775*. Available at: https://www.houbigant-parfum.com/us_en/the-house-of-houbigant.html.

Hoult, J. R. S. and Payá, M. (1996) 'Pharmacological and biochemical actions of simple coumarins: Natural products with therapeutic potential', *General Pharmacology: The Vascular System*, 27(4), pp. 713–722. doi: 10.1016/0306-3623(95)02112-4.

https://www.thespicery.com (2020) *Picture Tonka Beans*. Available at: .

Hu, Y., Vandenbussche, F. and Van Der Straeten, D. (2017) 'Regulation of seedling growth by ethylene and the ethylene–auxin crosstalk', *Planta*. Springer Berlin Heidelberg, 245(3), pp. 467–489. doi: 10.1007/s00425-017-2651-6.

Hu, Y., Xie, Q. and Chua, N.-H. (2003) 'The Arabidopsis Auxin-Inducible Gene ARGOS Controls Lateral Organ Size', *The Plant Cell*, 15(9), pp. 1951–1961. doi: 10.1105/tpc.013557.

Hu, Z. *et al.* (2010) 'Strigolactones Negatively Regulate Mesocotyl Elongation in Rice during Germination and Growth in Darkness', *Plant and Cell Physiology*, 51(7), pp. 1136–1142. doi: 10.1093/pcp/pcq075.

Hu, Z. *et al.* (2014) 'Strigolactone and cytokinin act antagonistically in regulating rice mesocotyl elongation in darkness', *Plant and Cell Physiology*, 55(1), pp. 30–41. doi: 10.1093/pcp/pct150.

Hua, J. *et al.* (1995) 'Ethylene insensitivity conferred by Arabidopsis ERS gene', *Science*, 269(5231), pp. 1712–1714. doi: 10.1126/science.7569898.

Hua, J. and Meyerowitz, E. M. (1998) 'Ethylene Responses Are Negatively Regulated by a Receptor Gene Family in Arabidopsis thaliana', *Cell*, 94(2), pp. 261–271. doi: 10.1016/S0092-8674(00)81425-7.

Huq, E. and Quail, P. H. (2002) 'PIF4, a phytochrome-interacting bHLH factor, functions as a negative regulator of phytochrome B signaling in Arabidopsis.', *The EMBO journal*, 21(10), pp. 2441–50. doi: 10.1093/emboj/21.10.2441.

Hurban, P. *et al.* (2003) 'The auxin-induced transcriptome for etiolated Arabidopsis seedlings using a structure/function approach', *Functional & Integrative Genomics*, 3(4), pp. 135–143. doi: 10.1007/s10142-003-0093-7.

Hwang, I. and Sheen, J. (2001) 'Two-component circuitry in Arabidopsis cytokinin signal transduction', *Nature*, 413(6854), pp. 383–389. doi: 10.1038/35096500.

Hyun, Y. and Lee, I. (2006) 'KIDARI, Encoding a Non-DNA Binding bHLH Protein, Represses Light Signal Transduction in Arabidopsis thaliana', *Plant Molecular Biology*, 61(1–2), pp. 283–296. doi: 10.1007/s11103-006-0010-2.

Ikeda, M. *et al.* (2012) 'A Triantagonistic Basic Helix-Loop-Helix System Regulates Cell Elongation in Arabidopsis', *The Plant Cell*, 24(11), pp. 4483–4497. doi: 10.1105/tpc.112.105023.

Ikeda, M., Mitsuda, N. and Ohme-Takagi, M. (2013) 'ATBS1 INTERACTING FACTORs negatively regulate Arabidopsis cell elongation in the triantagonistic bHLH system', *Plant Signaling & Behavior*, 8(3), p. e23448. doi: 10.4161/psb.23448.

Imbert, M. P. and Wilson, L. A. (1970) 'Stimulatory and inhibitory effects of Scopoletin on IAA oxidase preparations from sweet potato', *Phytochemistry*. Pergamon, 9(8), pp. 1787–1794. doi: 10.1016/S0031-9422(00)85592-2.

Inoue, K., Nishihama, R. and Kohchi, T. (2017) 'Evolutionary origin of phytochrome responses and signaling in land plants', *Plant Cell and Environment*, 1, pp. 2502–2508. doi: 10.1111/pce.12908.

Inoue, T. *et al.* (2001) 'Identification of CRE1 as a cytokinin receptor from Arabidopsis', *Nature*, 409(6823), pp. 1060–1063. doi: 10.1038/35059117.

Dello Ioio, R. *et al.* (2007) 'Cytokinins Determine Arabidopsis Root-Meristem Size by Controlling Cell Differentiation', *Current Biology*, 17(8), pp. 678–682. doi: 10.1016/j.cub.2007.02.047.

Dello Ioio, R. *et al.* (2008) 'A Genetic Framework for the Control of Cell Division and Differentiation in the Root Meristem', *Science*, 322(5906), pp. 1380–1384. doi: 10.1126/science.1164147.

Itoh, T. (1976a) 'Microfibrillar orientation of radially enlarged cells of coumarin-and colchicine-treated pine seedlings', *Plant and cell physiology*. Japanese Society of Plant Physiologists, 17(2), pp. 385–398.

Itoh, T. (1976b) 'Microscopic and submicroscopic observation of the effects of coumarin and colchicine during elongation of pine seedlings', *Plant and Cell Physiology*, 17(2), pp. 367–384. doi: 10.1093/oxfordjournals.pcp.a075289.

Jacobs, M. and Rubery, P. H. (1988) 'Naturally Occurring Auxin Transport Regulators', *Science*, 241(4863), pp. 346–349. doi: 10.1126/science.241.4863.346.

Jaillais, Y. *et al.* (2011) 'Tyrosine phosphorylation controls brassinosteroid receptor activation by triggering membrane release of its kinase inhibitor', *Genes & Development*, 25(3), pp. 232–237. doi: 10.1101/gad.2001911.

Jain, N., Ascough, G. D. and Van Staden, J. (2008) 'A smoke-derived butenolide alleviates HgCl2 and ZnCl2 inhibition of water uptake during germination and subsequent growth of tomato – Possible involvement of aquaporins', *Journal of Plant Physiology*, 165(13), pp. 1422–1427. doi: 10.1016/j.jplph.2008.04.017.

Jankay, P. and Muller, W. H. (1976) 'THE RELATIONSHIPS AMONG UMBELLIFERONE, GROWTH, AND PEROXIDASE LEVELS IN CUCUMBER ROOTS', *American Journal of Botany*, 63(1), pp. 126–132. doi:

10.1002/j.1537-2197.1976.tb11792.x.

Jansson, E. and Svensson, S.-B. (1980) 'Coumarin effects on Glycine max hypocotyl explants.', *Physiologia Plantarum*, 48(1961), pp. 486–490.

Jensen, P. J., Hangarter, R. P. and Estelle, M. (1998) 'Auxin transport is required for hypocotyl elongation in light-grown but not dark-grown Arabidopsis', *Plant Physiology*, 116(2), pp. 455–462. doi: 10.1104/pp.116.2.455.

Jia, K.-P. *et al.* (2014) 'Strigolactone-regulated hypocotyl elongation is dependent on cryptochrome and phytochrome signaling pathways in Arabidopsis.', *Molecular plant*. Â© The Authors. All rights reserved., 7(3), pp. 528–40. doi: 10.1093/mp/sst093.

Jinpei Zhou *et al.* (2012) 'Synthesis and Antitumor Activity of Scopoletin Derivatives', *Letters in Drug Design & Discovery*, 9(4), pp. 397–401. doi: 10.2174/157018012799859972.

Jones, A. M. (1998) 'Auxin-Dependent Cell Expansion Mediated by Overexpressed Auxin-Binding Protein 1 ';, *Science*, 282(5391), pp. 1114–1117. doi: 10.1126/science.282.5391.1114.

Jones, L., Ennos, A. R. and Turner, S. R. (2001) 'Cloning and characterization of irregular xylem4 (irx4): A severely lignin-deficient mutant of Arabidopsis', *Plant Journal*, 26(2), pp. 205–216. doi: 10.1046/j.1365-313X.2001.01021.x.

Jurd, L., King, A. D. and Mihara, K. (1971) 'Antimicrobial properties of umbelliferone derivatives', *Phytochemistry*, 10(12), pp. 2965–2970. doi: 10.1016/S0031-9422(00)97333-3.

Kai, K. *et al.* (2006) 'Accumulation of coumarins in Arabidopsis thaliana', *Phytochemistry*, 67(4), pp. 379–386. doi: 10.1016/j.phytochem.2005.11.006.

Kai, K. *et al.* (2008) 'Scopoletin is biosynthesized via ortho-hydroxylation of feruloyl CoA by a 2-oxoglutarate-dependent dioxygenase in Arabidopsis thaliana', *The Plant Journal*, 55(6), pp. 989–999. doi: 10.1111/j.1365-313X.2008.03568.x.

Kallio, P. and Piiroinen, P. (1959) 'Effect of Gibberellin on the Termination of Dormancy in Some Seeds', *Nature*, 183(4678), pp. 1830–1831. doi: 10.1038/1831830a0.

Kant, S. and Rothstein, S. (2009) 'Auxin-responsive SAUR39 gene modulates auxin level in rice', *Plant Signaling & Behavior*, 4(12), pp. 1174–1175. doi: 10.4161/psb.4.12.10043.

Kapulnik, Y., Delaux, P.-M., *et al.* (2011) 'Strigolactones affect lateral root formation and root-hair elongation in Arabidopsis.', *Planta*, 233(1), pp. 209–16. doi: 10.1007/s00425-010-1310-y.

Kapulnik, Y., Resnick, N., *et al.* (2011) 'Strigolactones interact with ethylene and auxin in regulating root-hair elongation in Arabidopsis', *Journal of Experimental Botany*, 62(8), pp. 2915–2924. doi: 10.1093/jxb/erq464.

Kato, M. and Shimizu, S. (1985) 'Chlorophyll Metabolism in Higher Plants VI. Involvement of Peroxidase in Chlorophyll Degradation', *Plant and Cell Physiology*, 1301, pp. 1291–1301. doi: 10.1093/oxfordjournals.pcp.a077029.

Kauschmann, A. *et al.* (1996) 'Genetic evidence for an essential role of brassinosteroids in plant development', *The Plant Journal*, 9(5), pp. 701–713. doi: 10.1046/j.1365-313X.1996.9050701.x.

Keightley, A. M. *et al.* (1996) 'Coumarin and its 4- and 7- Substituted Derivatives as Retardants of Mitoses in Allium Root Promeristem', *International Journal of Pharmacognosy*, 34(2), pp. 105–113. doi: 10.1076/phbi.34.2.105.13192.

Kemmerling, B. *et al.* (2007) 'The BRI1-Associated Kinase 1, BAK1, Has a Brassinolide-Independent Role in Plant Cell-Death Control', *Current Biology*, 17(13), pp. 1116–1122. doi: 10.1016/j.cub.2007.05.046.

Ketring, D. L. and Morgan, P. W. (1972) 'Physiology of Oil Seeds', *Plant Physiology*, 50(3), pp. 382–387. doi: 10.1104/pp.50.3.382.

Khan, A. A. (1969) 'Cytokinin-Inhibitor Antagonism in the Hormonal Control of alpha-Amylase Synthesis and Growth in Barley Seed', *Physiologia Plantarum*, 22(1), pp. 94–103. doi: 10.1111/j.1399-3054.1969.tb07845.x.

Khanna, R. *et al.* (2004) 'A novel molecular recognition motif necessary for targeting photoactivated phytochrome signaling to specific basic helix-loop-helix transcription factors', *Plant Cell*, 16(11), pp. 3033–3044. doi: 10.1105/tpc.104.025643.

Kieber, J. J. *et al.* (1993) 'CTR1, a negative regulator of the ethylene response pathway in arabidopsis, encodes a member of the Raf family of protein kinases', *Cell*, 72(3), pp. 427–441. doi: 10.1016/0092-8674(93)90119-B.

Kierzkowski, D. *et al.* (2013) 'Interaction between Meristem tissue layers controls phyllotaxis', *Developmental Cell*. Elsevier Inc., 26(6), pp. 616–628. doi: 10.1016/j.devcel.2013.08.017.

Kim, T.-W. *et al.* (2009) 'Brassinosteroid signal transduction from cell-surface receptor kinases to nuclear transcription factors', *Nature Cell Biology*, 11(10), pp. 1254–1260. doi: 10.1038/ncb1970.

Kim, Y. H. *et al.* (2000) 'Scopoletin production induced resistance tobacco against TMV', *Plant Pathology Journal*, pp. 264–268.

Klebs, G. (1896) *Die bedingungen der fortpflanzung bei einigen algen und pilzen*. G. Fischer.

Kleinhofs, A., Haskins, F. A. and Gorz, H. J. (1966) 'Relationship of Phenylalanine Ammonia-lyase Activity to o-Hydroxycinnamic Acid Content in Melilotus alba', *Plant physiology*, 41, pp. 1276–1279.

Kleinhofs, A., Haskins, F. A. and Gorz, H. J. (1967) 'Trans-o-Hydroxycinnamic Acid Glucosylation in Cell-Free Extracts of Melilotus Alba*', *Phytochemistry*, 6, pp. 1313–1318.

Knobloch, K.-H. and Hahlbrock, K. (1977) '4-Coumarate:CoA ligase from cell suspension cultures of Petroselinum hortense Hoffm: Partial purification, substrate specificity, and further properties', *Archives of Biochemistry and Biophysics*. Academic Press, 184(1), pp. 237–248. doi: 10.1016/0003-9861(77)90347-2.

Knox, J. P. (1992) 'Cell adhesion, cell separation and plant morphogenesis', *The Plant Journal*, 2(2), pp. 137–141. doi: 10.1111/j.1365-313X.1992.00137.x.

Knox, J. P. (2008) 'Revealing the structural and functional diversity of plant cell walls', *Current Opinion in Plant Biology*, 11(3), pp. 308–313. doi: 10.1016/j.pbi.2008.03.001.

Knypl, J. S. (1960) 'Effect of Coumarin on the Growth of Rhodotorula rosea Cultures', *Nature*, (4717), pp. 933–934. Available at: http://link.springer.com/10.1007/BF02855967.

Knypl, J. S. (1961) 'Coumarin Vapours as the Stimulator of Oxygen Uptake by Sunflower Hypocotyls', *Nature*.

Knypl, J. S. (1963) 'A Fungistatic Action of Coumarin', *Nature*, (4897), p. 947.

Knypl, J. S. (1964a) 'Characteristic features of the coumarin induced growth', *Planta*, 61(4), pp. 352–360.

Knypl, J. S. (1964b) 'Coumarin-Induced Respiration of Sunflower', *Physiologia Plantarum*, 17, pp. 771–779.

Knypl, J. S. (1964c) 'IAA-and coumarin-dependent reversion of the CCC-induced retardation of growth.', *Current Science*, 33(17), pp. 518–519.

Knypl, J. S. (1964d) 'The coumarin-induced stimulation of germination and growth', *Die Naturwissenschaften*, 51(5), pp. 117–118. doi: 10.1007/BF00629625.

Knypl, J. S. (1966a) 'Action of (2-chloroethyl) trimethylammonium chloride, 2,4-dichlorobenzyl-tributylphophonium chloride, adn N-dimenthyl-amino-succinamic acid on IAA and coumarin induced growht

of sunflower hypocotyl sections', *Acta Societatis Botanicorum Poloniae*, 35(4), pp. 612–625.

Knypl, J. S. (1966b) 'Specific inhibitors of RNA and protein synthesis as suppressors of the IAA- and coumarin-induced growth responses', *Acta Societatis Botanicorum Poloniae*, 35(3).

Knypl, J. S. (1967a) 'Coumarin, Phosfon D and CCC - the Inhibitors of Chlorophyll and Protein Degradation in Senescing Leaf Tissue of Kale', *Flora oder Allgemeine botanische Zeitung. Abt. A, Physiologie und Biochemie*. Elsevier Masson SAS, 158(2), pp. 230–240. doi: 10.1016/s0367-1836(17)30310-5.

Knypl, J. S. (1967b) 'GROWTH RETARDANTS IN RELATION TO THE GERMINATION OF SEEDS: I. A PARADOXICAL CONCENTRATION EFFECT OF N,N -DIMETHYLAMINO-SUCCINAMIC ACID ON THE GERMINATION OF KALE SEEDS AFFECTED WITH COUMARIN', *Canadian Journal of Botany*, 45(6), pp. 903–913. doi: 10.1139/b67-092.

Knypl, J. S. (1967c) 'Growth retardants in relation to the germination of seeds', *Acta Societatis Botanicorum Poloniae*, 36(2), pp. 235–250.

Knypl, J. S. (1968) 'Coumarin- and indole-3-acetic acid-induced growth and respiration in sunflower as affected by 2-chloroethyl trimetylammonium chloride, actinomycin C1, puromycin and diazouracil', *Acta Societatis Botanicorum Poloniae*, 37(1), pp. 51–60.

Knypl, J. S. (1969) 'The Control of RNA, Protein and Chlorophyll Synthesis in Senescing Leaf Tissue of Kale by Coumarin and Growth Retardants', *Flora oder Allgemeine botanische Zeitung. Abt. A, Physiologie und Biochemie*. Elsevier Masson SAS, 160(3), pp. 217–233. doi: 10.1016/S0367-1836(17)30186-6.

Kobayashi, Y. *et al.* (2016) 'Joint genetic and network analyses identify loci associated with root growth under NaCl stress in Arabidopsis thaliana', *Plant, Cell & Environment*, 39(4), pp. 918–934. doi: 10.1111/pce.12691.

Kohlen, W. *et al.* (2012) 'The tomato CAROTENOID CLEAVAGE DIOXYGENASE 8 (S l CCD 8) regulates rhizosphere signaling, plant architecture and affects reproductive development through strigolactone biosynthesis', *New Phytologist*, 196(2), pp. 535–547. doi: 10.1111/j.1469-8137.2012.04265.x.

Kohmuenzer, S. (1965) 'Botanical and chemical studies of the collective species Gallium mollugo with reference to karyotypes growing in Poland. VI. Effects of extracts and some other chemical components of Galium molugo on the germination of seeds and growth of selected plant.', *Dissert. Pharm. Pharma*, 17, pp. 369–379.

Konishi, M. and Yanagisawa, S. (2008) 'Two different mechanisms control ethylene sensitivity in Arabidopsis via the regulation of EBF2 expression', *Plant Signaling & Behavior*, 3(9), pp. 749–751. doi: 10.4161/psb.3.9.6640.

Koorneef, M. *et al.* (1985) 'A gibberellin insensitive mutant of Arabidopsis thaliana', *Physiologia Plantarum*, 65(1), pp. 33–39. doi: 10.1111/j.1399-3054.1985.tb02355.x.

Koornneef, M., Bentsink, L. and Hilhorst, H. (2002) 'Seed dormancy and germination', 5(July), pp. 33–36. doi: 10.1093/jxb/erq063.

Koornneef, M. and Meinke, D. (2010) 'The development of Arabidopsis as a model plant', *Plant Journal*, 61(6), pp. 909–921. doi: 10.1111/j.1365-313X.2009.04086.x.

Koornneef, M., Rolff, E. and Spruit, C. J. P. (1980) 'Genetic control of light-inhibited hypocotyl elongation in Arabidopsis thaliana (L.) heynh.', *Zeitschrift für Pflanzenphysiologie*. Gustav Fischer Verlag Stuttgart, 100(2), pp. 147–160. doi: 10.1016/S0044-328X(80)80208.

Koornneef, M. and van der Veen, J. H. (1980) 'Induction and analysis of gibberellin sensitive mutants in Arabidopsis thaliana (L.) heynh.', *Theoretical and Applied Genetics*, 58(6), pp. 257–263. doi: 10.1007/BF00265176.

Koornneeff, M., Dellaert, L. W. M. and van der Veen, J. H. (1982) 'EMS- and relation-induced mutation frequencies at individual loci in Arabidopsis thaliana (L.) Heynh', *Mutation Research - Fundamental and Molecular Mechanisms of Mutagenesis*, 93(1), pp. 109–123. doi: 10.1016/0027-5107(82)90129-4.

Kopiersperre (2015) *Scopoletin*, *Wikipedia*. Available at: https://en.wikipedia.org/wiki/Scopoletin#/media/File:Scopoletin.svg.

Koren, D. *et al.* (2013) 'Strigolactone signaling in the endodermis is sufficient to restore root responses and involves SHORT HYPOCOTYL 2 (SHY2) activity.', *The New phytologist*, 198(3), pp. 866–74. doi: 10.1111/nph.12189.

Korte, A. and Ashley, F. (2013) 'The advantages and limitations of trait analysis with GWAS : a review Self-fertilisation makes Arabidopsis particularly well suited to GWAS', *Plant methods*, 9(1), p. 29.

Kosmann, C. P. (1844) 'Présence de la Coumarine dans l'Aspérule Odorante (Asperula odorata)', *J. Pharm*, 3(5), pp. 393–396.

Kosuge, T. and Conn, E. E. (1961) 'The metabolism of aromatic compounds in higher plants. III. The beta-glucosides of o-coumaric, coumarinic, and melilotic acids.', *The Journal of biological chemistry*, 236(1), pp. 1617–21. Available at: http://www.ncbi.nlm.nih.gov/pubmed/13753452.

Kováčik, J. *et al.* (2009) 'Salicylic acid-induced changes to growth and phenolic metabolism in Matricaria chamomilla plants', *Plant Cell Reports*, 28(1), pp. 135–143. doi: 10.1007/s00299-008-0627-5.

Kramer, E. M. and Bennett, M. J. (2006) 'Auxin transport: a field in flux', *Trends in Plant Science*, 11(8), pp. 382–386. doi: 10.1016/j.tplants.2006.06.002.

Křeček, P. *et al.* (2009) 'The PIN-FORMED (PIN) protein family of auxin transporters', *Genome Biology*, 10(12), p. 249. doi: 10.1186/gb-2009-10-12-249.

Kresge, N., Simoni, R. D. and Hill, R. L. (2005) 'Hemorrhagic Sweet Clover Disease, Dicumarol, and Warfarin: the Work of Karl Paul Link Disease, Dicumarol, and Warfarin: the Work of Karl Paul Link', *Journal of Biological Chemistry*, 280(17), pp. e5–e7. doi: 10.1074/jbc.X400013200.

Kretzschmar, T. *et al.* (2012) 'A petunia ABC protein controls strigolactone-dependent symbiotic signalling and branching.', *Nature*. Nature Publishing Group, 483(7389), pp. 341–4. doi: 10.1038/nature10873.

Kuhn, B. M. *et al.* (2011) 'Flavonols Accumulate Asymmetrically and Affect Auxin Transport in Arabidopsis', *Plant Physiology*, 156(2), pp. 585–595. doi: 10.1104/pp.111.175976.

Kuhn, B. M. *et al.* (2017) 'Flavonol-induced changes in PIN2 polarity and auxin transport in the Arabidopsis thaliana rol1-2 mutant require phosphatase activity', *Scientific Reports*, 7(January), pp. 1–13. doi: 10.1038/srep41906.

Kuhn, R. *et al.* (1943) 'über die chemische Natur der Blastokoline und ihre Einwirkung auf keimende Samen, Pollenkörner, Hefen, Bakterien, Epithelgewebe und Fibroblasten.', *Naturwissenschaften*, 31(39), pp. 468–468.

Kulich, I. and Žárský, V. (2014) 'Autophagy-related direct membrane import from ER/Cytoplasm into the vacuole or apoplast: A hidden gateway also for secondary metabolites and phytohormones?', *International Journal of Molecular Sciences*, 15(5), pp. 7462–7474. doi: 10.3390/ijms15057462.

Kumpf, R. P. *et al.* (2013) 'Floral organ abscission peptide IDA and its HAE/HSL2 receptors control cell separation during lateral root emergence', *Proceedings of the National Academy of Sciences*, 110(13), pp. 5235–5240. doi: 10.1073/pnas.1210835110.

Kupidlowska, E., Dobrzynska, K., *et al.* (1994) 'Effect of coumarin and xanthotoxin on mitochondrial structure, oxygen uptake, and succinate dehydrogenase activity in onion root cells.', *Journal of chemical*

ecology, 20(10), pp. 2471–80. doi: 10.1007/BF02036184.

Kupidlowska, E., Kowalec, M., *et al.* (1994) 'The Effect of Coumarins on Root Elongation and Ultrastructure of Meristematic Cell Protoplast', *Annals of Botany*, 73(5), pp. 525–530. doi: 10.1006/anbo.1994.1065.

Kurepa, J. *et al.* (2018) 'Modulation of auxin and cytokinin responses by early steps of the phenylpropanoid pathway', *BMC Plant Biology*. BMC Plant Biology, 18(1), p. 278. doi: 10.1186/s12870-018-1477-0.

Kushwah, S., Jones, A. M. and Laxmi, A. (2011) 'Cytokinin Interplay with Ethylene, Auxin, and Glucose Signaling Controls Arabidopsis Seedling Root Directional Growth', *Plant Physiology*, 156(4), pp. 1851–1866. doi: 10.1104/pp.111.175794.

Kutschera, U. (1994) 'The current status of the acid-growth hypothesis', *New Phytologist*, 126(4), pp. 549–569. doi: 10.1111/j.1469-8137.1994.tb02951.x.

Kutschera, U. and Niklas, K. J. (2013) 'Cell division and turgor-driven stem elongation in juvenile plants: A synthesis', *Plant Science*. Elsevier Ireland Ltd, 207, pp. 45–56. doi: 10.1016/j.plantsci.2013.02.004.

Lachowiec, J. *et al.* (2015) 'A Genome-Wide Association Analysis Reveals Epistatic Cancellation of Additive Genetic Variance for Root Length in Arabidopsis thaliana', *PLOS Genetics*. Edited by D. J. Kliebenstein, 11(9), p. e1005541. doi: 10.1371/journal.pgen.1005541.

Lacy, A. and O'Kennedy, R. (2004) 'Studies on coumarins and coumarin-related compounds to determine their therapeutic role in the treatment of cancer.', *Current pharmaceutical design*, 10(30), pp. 3797–3811. doi: 10.2174/1381612043382693.

Laibach, F. (1943) 'Arabidopsis thaliana (L.) Heynh. als Objekt für genetische und entwicklungsphysiologische Untersuchungen', *Bot. Archiv*, 44, pp. 439–455.

Lake, B. G. (1999) 'Coumarin metabolism, toxicity and carcinogenicity: relevance for human risk assessment.', *Food and chemical toxicology : an international journal published for the British Industrial Biological Research Association*, 37, pp. 423–453. doi: 10.1016/S0278-6915(99)00010-1.

Lakehal, A. and Bellini, C. (2019) 'Control of adventitious root formation: insights into synergistic and antagonistic hormonal interactions', *Physiologia Plantarum*, 165(1), pp. 90–100. doi: 10.1111/ppl.12823.

Lampugnani, E. R. *et al.* (2018) 'Building a plant cell wall at a glance', *Journal of Cell Science*, 131(2), p. jcs207373. doi: 10.1242/jcs.207373.

Lan, P. *et al.* (2011) 'ITRAQ protein profile analysis of arabidopsis roots reveals new aspects critical for iron homeostasis', *Plant Physiology*, 155(2), pp. 821–834. doi: 10.1104/pp.110.169508.

Laskowski, M. *et al.* (2006) 'Expression Profiling of Auxin-treated Arabidopsis Roots: Toward a Molecular Analysis of Lateral Root Emergence', *Plant and Cell Physiology*, 47(6), pp. 788–792. doi: 10.1093/pcp/pcj043.

Lau, O. S. and Deng, X. W. (2010) 'Plant hormone signaling lightens up: integrators of light and hormones', *Current Opinion in Plant Biology*. Elsevier Ltd, 13(5), pp. 571–577. doi: 10.1016/j.pbi.2010.07.001.

Lauressergues, D. *et al.* (2015) 'Strigolactones contribute to shoot elongation and to the formation of leaf margin serrations in Medicago truncatula R108', *Journal of Experimental Botany*, 66(5), pp. 1237–1244. doi: 10.1093/jxb/eru471.

Lavenus, J. *et al.* (2013) 'Lateral root development in Arabidopsis: fifty shades of auxin.', *Trends in plant science*, 18(8), pp. 450–8. doi: 10.1016/j.tplants.2013.04.006.

Leal, L. K. A. . *et al.* (2000) 'Antinociceptive, anti-inflammatory and bronchodilator activities of Brazilian medicinal plants containing coumarin: a comparative study', *Journal of Ethnopharmacology*, 70(2), pp. 151–159. doi: 10.1016/S0378-8741(99)00165-8.

Lee, J.-H. J. H. *et al.* (2014) 'Coumarins reduce biofilm formation and the virulence of Escherichia coli O157:H7', *Phytomedicine*. Elsevier GmbH., 21(8–9), pp. 1037–1042. doi: 10.1016/j.phymed.2014.04.008.

Lee, S. *et al.* (2002) 'Gibberellin regulates Arabidopsis seed germination via RGL2, a GAI/RGA-like gene whose expression is up-regulated following imbibition', *Genes & Development*, 16(5), pp. 646–658. doi: 10.1101/gad.969002.

Lee, S. *et al.* (2006) 'Overexpression of PRE1 and its homologous genes activates gibberellin-dependent responses in Arabidopsis thaliana', *Plant and Cell Physiology*, 47(5), pp. 591–600. doi: 10.1093/pcp/pcj026.

Lee, Y. K. *et al.* (2006) 'LONGIFOLIA1 and LONGIFOLIA2, two homologous genes, regulate longitudinal cell elongation in Arabidopsis', *Development*, 133(21), pp. 4305–4314. doi: 10.1242/dev.02604.

Leivar, P. and Quail, P. H. (2011) 'PIFs: Pivotal components in a cellular signaling hub', *Trends in Plant Science*. Elsevier Ltd, 16(1), pp. 19–28. doi: 10.1016/j.tplants.2010.08.003.

Levari, R. (1953) 'The effect of 2, 4-D and coumarin on respiration of germinating wheat and lettuce seeds', *Palest. J. Bot.(Jer. Ser.)*, 6, pp. 47–59.

Lewis, D. R. *et al.* (2009) 'Auxin transport into cotyledons and cotyledon growth depend similarly on the ABCB19 Multidrug Resistance-like transporter', *Plant Journal*, 60(1), pp. 91–101. doi: 10.1111/j.1365-313X.2009.03941.x.

Leyser, H. M. O. *et al.* (1993) 'Arabidopsis auxin-resistance gene AXR1 encodes a protein related to ubiquitin-activating enzyme E1', *Nature*, 364(6433), pp. 161–164. doi: 10.1038/364161a0.

Leyser, H. M. O. *et al.* (1996) 'Mutations in the AXR3 gene of Arabidopsis result in altered auxin response including ectopic expression from the SAUR-AC1 promoter', *The Plant Journal*, 10(3), pp. 403–413. doi: 10.1046/j.1365-313x.1996.10030403.x.

Leyser, O. (2018) 'Auxin signaling', *Plant physiology*. Am Soc Plant Biol, 176(1), pp. 465–479.

Li, C. *et al.* (2015) 'Effect of Scopoletin on Apoptosis and Cell Cycle Arrest in Human Prostate Cancer Cells *In vitro*', *Tropical Journal of Pharmaceutical Research*, 14(4), p. 611. doi: 10.4314/tjpr.v14i4.8.

Li, C. *et al.* (2019) 'Comprehensive expression analysis of Arabidopsis GA2-oxidase genes and their functional insights', *Plant Science*. Elsevier, 285(February), pp. 1–13. doi: 10.1016/j.plantsci.2019.04.023.

Li, J. *et al.* (2002) 'BAK1, an Arabidopsis LRR receptor-like protein kinase, interacts with BRI1 and modulates brassinosteroid signaling', *Cell*, 110(2), pp. 213–222. doi: 10.1016/S0092-8674(02)00812-7.

Li, J. *et al.* (2005) 'Plant Science: Arabidopsis H+-PPase AVP1 regulates auxin-mediated organ development', *Science*, 310(5745), pp. 121–125. doi: 10.1126/science.1115711.

Li, J. and Chory, J. (1997) 'A Putative Leucine-Rich Repeat Receptor Kinase Involved in Brassinosteroid Signal Transduction', *Cell*, 90(5), pp. 929–938. doi: 10.1016/S0092-8674(00)80357-8.

Li, L. and Deng, X. W. (2005) 'It runs in the family: regulation of brassinosteroid signaling by the BZR1–BES1 class of transcription factors', *Trends in Plant Science*, 10(6), pp. 266–268. doi: 10.1016/j.tplants.2005.04.002.

Li, N. *et al.* (2019) 'Signaling Crosstalk between Salicylic Acid and Ethylene/Jasmonate in Plant Defense: Do We Understand What They Are Whispering?', *International Journal of Molecular Sciences*, 20(3), p. 671. doi: 10.3390/ijms20030671.

Li, X. *et al.* (2011) 'Effects of a Coumarin Derivative, 4-Methylumbelliferone, on Seed Germination and Seedling Establishment in Arabidopsis', *Journal of Chemical Ecology*, 37(8), pp. 880–890. doi: 10.1007/s10886-011-9987-3.

Li, X. and Gao, M.-J. J. (2011) ‘Modulation of root branching by a coumarin derivative’, *Plant Signaling & Behavior*, 6(11), pp. 1654–1655. doi: 10.4161/psb.6.11.17768.

Liang, X. *et al.* (2012) ‘Involvement of COP1 in ethylene- and light-regulated hypocotyl elongation’, *Planta*, 236(6), pp. 1791–1802. doi: 10.1007/s00425-012-1730-y.

Lincoln, C., Britton, J. H. and Estelle, M. (1990) ‘Growth and development of the axr1 mutants of Arabidopsis.’, *The Plant Cell*, 2(11), pp. 1071–1080. doi: 10.1105/tpc.2.11.1071.

Lindman, C. A. M. (1901) *Hierochloe odorata*, *Bilder ur Nordens Flora*. Available at: https://es.wikipedia.org/wiki/Archivo:475_Hierochloe_odorata.jpg.

Linkies, A. *et al.* (2009) ‘Ethylene Interacts with Abscisic Acid to Regulate Endosperm Rupture during Germination: A Comparative Approach Using Lepidium sativum and Arabidopsis thaliana’, *The Plant Cell*, 21(12), pp. 3803–3822. doi: 10.1105/tpc.109.070201.

Linkies, A. and Leubner-Metzger, G. (2012) ‘Beyond gibberellins and abscisic acid: how ethylene and jasmonates control seed germination’, *Plant Cell Reports*, 31(2), pp. 253–270. doi: 10.1007/s00299-011-1180-1.

Liscum, E. and Reed, J. W. (2002) ‘Genetics of Aux/IAA and ARF action in plant growth and development’, *Plant Molecular Biology*, 49(3), pp. 387–400. doi: 10.1023/A:1015255030047.

Liu, C.-W. and Murray, J. (2016) ‘The Role of Flavonoids in Nodulation Host-Range Specificity: An Update’, *Plants*, 5(3), p. 33. doi: 10.3390/plants5030033.

Liu, H. *et al.* (2018) ‘AUX1 acts upstream of PIN2 in regulating root gravitropism’, *Biochemical and Biophysical Research Communications*. Elsevier Ltd, 507(1–4), pp. 433–436. doi: 10.1016/j.bbrc.2018.11.056.

Liu, W. *et al.* (2012) ‘Synthesis and in vitro antitumor activity of novel scopoletin derivatives’, *Bioorganic & Medicinal Chemistry Letters*. Elsevier Ltd, 22(15), pp. 5008–5012. doi: 10.1016/j.bmcl.2012.06.014.

Liu, X. *et al.* (2013) ‘Auxin controls seed dormancy through stimulation of abscisic acid signaling by inducing ARF-mediated ABI3 activation in Arabidopsis’, *Proceedings of the National Academy of Sciences*, 110(38), pp. 15485–15490. doi: 10.1073/pnas.1304651110.

Liu, Y. *et al.* (2007) ‘The α- and β-expansin and xyloglucan endotransglucosylase/hydrolase gene families of wheat: Molecular cloning, gene expression, and EST data mining’, *Genomics*, 90(4), pp. 516–529. doi: 10.1016/j.ygeno.2007.06.012.

Liu, Y. *et al.* (2012) ‘CCS52A2/FZR1, a cell cycle regulator, is an essential factor for shoot apical meristem maintenance in Arabidopsis thaliana’, *BMC Plant Biology*, 12(1), p. 135. doi: 10.1186/1471-2229-12-135.

Livak, K. J. and Schmittgen, T. D. (2001) ‘Analysis of Relative Gene Expression Data Using Real-Time Quantitative PCR and the 2−ΔΔCT Method’, *Methods*, 25(4), pp. 402–408. doi: 10.1006/meth.2001.1262.

Loewus, F. A. (1977) *The Structure, biosynthesis, and degradation of wood*, *Recent Advances In Phytochemistry (USA)*. Plenum Press. Available at: http://www.ghbook.ir/index.php?name=ر ساذه و ف رهنگ های ذویِ ن&option=com_dbook&task=readonline&book_id=13650&page=73&chkhashk=ED9C9491B4&Itemid=218&lang=fa&tmpl=component.

Lorenzo, O. *et al.* (2004) ‘JASMONATE-INSENSITIVE1 Encodes a MYC Transcription Factor Essential to Discriminate between Different Jasmonate-Regulated Defense Responses in Arabidopsis Author (s): Oscar Lorenzo , Jose M . Chico , Jose J . Sánchez-Serrano and Roberto Solano Published’, *Plant Cell*, 16(July), pp. 1938–1950. doi: 10.1105/tpc.022319.with.

Lorrain, S. *et al.* (2008) ‘Phytochrome-mediated inhibition of shade avoidance involves degradation of

growth-promoting bHLH transcription factors', *Plant Journal*, 53(2), pp. 312–323. doi: 10.1111/j.1365-313X.2007.03341.x.

De Lucas, M. *et al.* (2008) 'A molecular framework for light and gibberellin control of cell elongation', *Nature*, 451(7177), pp. 480–484. doi: 10.1038/nature06520.

Luccioni, L. G. (2002) 'Brassinosteroid Mutants Uncover Fine Tuning of Phytochrome Signaling', *PLANT PHYSIOLOGY*, 128(1), pp. 173–181. doi: 10.1104/pp.128.1.173.

Lundberg, D. S. and Teixeira, P. J. P. L. (2018) 'Root-exuded coumarin shapes the root microbiome', *Proceedings of the National Academy of Sciences*, 115(22), pp. 5629–5631. doi: 10.1073/pnas.1805944115.

Luo, X. M. *et al.* (2010) 'Integration of Light- and Brassinosteroid-Signaling Pathways by a GATA Transcription Factor in Arabidopsis', *Developmental Cell*. Elsevier Inc., 19(6), pp. 872–883. doi: 10.1016/j.devcel.2010.10.023.

Lupini, A. *et al.* (2010) 'Short-term effects of coumarin along the maize primary root axis', *Plant Signaling & Behavior*, 5(11), pp. 1395–1400. doi: 10.4161/psb.5.11.13021.

Lupini, A. *et al.* (2013) 'Gravitropic response induced by coumarin: Evidences of ROS distribution involvement', *Plant Signaling & Behavior*, 8(2), p. e23156. doi: 10.4161/psb.23156.

Lupini, A. *et al.* (2014) 'Coumarin interacts with auxin polar transport to modify root system architecture in Arabidopsis thaliana', *Plant Growth Regulation*, 72, pp. 1–9. doi: 10.1007/s10725-014-9893-0.

Lupini, A. *et al.* (2018) 'Coumarin enhances nitrate uptake in maize roots through modulation of plasma membrane H+-ATPase activity', *Plant Biology*. Edited by G. Thiel, 20(2), pp. 390–398. doi: 10.1111/plb.12674.

Luschnig, C. *et al.* (1998) 'EIR1, a root-specific protein involved in auxin transport, is required for gravitropism in Arabidopsis thaliana', *Genes & Development*, 12(14), pp. 2175–2187. doi: 10.1101/gad.12.14.2175.

Lyczakowski, J. J. *et al.* (2019) 'Structural imaging of native cryo-preserved secondary cell walls reveals presence of macrofibrils composed of cellulose , lignin and'. doi: 10.1101/648360.

Lymperopoulos, P., Msanne, J. and Rabara, R. (2018) 'Phytochrome and Phytohormones: Working in Tandem for Plant Growth and Development', *Frontiers in Plant Science*, 9(July), pp. 1–14. doi: 10.3389/fpls.2018.01037.

Ma, X. *et al.* (2016) 'SERKing Coreceptors for Receptors', *Trends in Plant Science*. Elsevier Ltd, 21(12), pp. 1017–1033. doi: 10.1016/j.tplants.2016.08.014.

Macias, M. L. *et al.* (1999) 'Effect of selected coumarins on spinach chloroplast photosynthesis', *Journal of Agricultural and Food Chemistry*, 47(5), pp. 2137–2140. doi: 10.1021/jf981121+.

Maher, E. P. and Martindale, S. J. B. (1980) 'Mutants of Arabidopsis thaliana with altered responses to auxins and gravity', *Biochemical Genetics*, 18(11–12), pp. 1041–1053. doi: 10.1007/BF00484337.

Malamy, J. E. and Benfey, P. N. (1997) 'Organization and cell differentiation in lateral roots of Arabidopsis thaliana.', *Development (Cambridge, England)*, 124(1), pp. 33–44. Available at: http://www.ncbi.nlm.nih.gov/pubmed/9006065.

Di Mambro, R. *et al.* (2019) 'The Lateral Root Cap Acts as an Auxin Sink that Controls Meristem Size', *Current Biology*. Elsevier Ltd., 29(7), pp. 1199-1205.e4. doi: 10.1016/j.cub.2019.02.022.

Mansour, M. H., Dimetry, N. Z. and Rofaeel, I. S. (1982) 'The role of coumarin as secondary plant substance in the food specificity of the cow pea aphid Aphis craccivora Koch', *Zeitschrift für Angewandte Entomologie*, 93(1–5), pp. 151–157. doi: 10.1111/j.1439-0418.1982.tb03581.x.

Maple, J. and Møller, S. G. (2007) 'Mutagenesis in Arabidopsis', *Methods in Molecular Biology*, 362, pp. 197–206. doi: 10.1385/1-59745-257-2:197.

Marchant, A. and Bennett, M. J. (1998) 'The Arabidopsis AUX1 gene: a model system to study mRNA processing in plants.', *Plant molecular biology*, 36(3), pp. 463–71. doi: 10.1023/a:1005961303167.

Mashiguchi, K. *et al.* (2011) 'The main auxin biosynthesis pathway in Arabidopsis', *Proceedings of the National Academy of Sciences of the United States of America*, 108(45), pp. 18512–18517. doi: 10.1073/pnas.1108434108.

Matern, U. (1991) 'Coumarins and Other Phenylpropanoid Compounds in the Defense Response of Plant Cells', *Planta Medica*, 57(S 1), pp. S15–S20. doi: 10.1055/s-2006-960224.

Matern, U., Lüer, P. and Kreusch, D. (1999) 'Biosynthesis of coumarins.', *Phytochemicals in Human Health Protection, Nutrition, and Plant defense*, pp. 623–637.

Mathews, S., Lavin, M. and Sharrock, R. A. (1995) 'Evolution of the Phytochrome Gene Family and Its Utility for Phylogenetic Analyses of Angiosperms', *Annals of the Missoure Botanical Garden*, 82(2), pp. 296–321.

Mathews, S. and Sharrock, R. A. (1997) 'Phytochrome gene diversity', *Plant, Cell and Environment*, 20(6), pp. 666–671. doi: 10.1046/j.1365-3040.1997.d01-117.x.

Matos, M. J. *et al.* (2015) 'Coumarins — An Important Class of Phytochemicals', in *Phytochemicals - Isolation, Characterisation and Role in Human Health*. InTech, p. 64. doi: 10.5772/59982.

Matsumoto, S. *et al.* (2012) 'Molecular cloning and functional analysis of the ortho-hydroxylases of p-coumaroyl coenzyme A/feruloyl coenzyme A involved in formation of umbelliferone and scopoletin in sweet potato, Ipomoea batatas (L.) Lam.', *Phytochemistry*. Elsevier Ltd, 74, pp. 49–57. doi: 10.1016/j.phytochem.2011.11.009.

Matthys, C. *et al.* (2016) 'The Whats, the Wheres and the Hows of strigolactone action in the roots', *Planta*, 243(6), pp. 1327–1337. doi: 10.1007/s00425-016-2483-9.

Mayer, A. M. and Evenari, M. (1952) 'The Relation between the Structure of Coumarin and its Derivatives, and their Activity as Germination Inhibitors', *Journal of Experimental Botany*, 3(2), pp. 246–252. doi: 10.1093/jxb/3.2.246.

Mazimba, O. (2017) 'Umbelliferone: Sources, chemistry and bioactivities review', *Bulletin of Faculty of Pharmacy, Cairo University*. Faculty of Pharmacy, Cairo University, 55(2), pp. 223–232. doi: 10.1016/j.bfopcu.2017.05.001.

McCarthy, D. J., Chen, Y. and Smyth, G. K. (2012) 'Differential expression analysis of multifactor RNA-Seq experiments with respect to biological variation', *Nucleic Acids Research*, 40(10), pp. 4288–4297. doi: 10.1093/nar/gks042.

McCullagh, P. and Nelder, J. A. (1989) '"Generalized Linear Models, London: Chapman and Hall"', *McCullagh2Generalised Linear Models*.

McGinnis, K. M. *et al.* (2003) 'The Arabidopsis SLEEPY1 Gene Encodes a Putative F-Box Subunit of an SCF E3 Ubiquitin Ligase', *The Plant Cell*, 15(5), pp. 1120–1130. doi: 10.1105/tpc.010827.

McKeon, T. A., Fernández-Maculet, J. C. and Yang, S.-F. (1995) 'Biosynthesis and Metabolism of Ethylene', in *Plant Hormones*. Dordrecht: Springer Netherlands, pp. 118–139. doi: 10.1007/978-94-011-0473-9_6.

De Meester, B. *et al.* (2017) 'Vessel-Specific Reintroduction of CINNAMOYL-COA REDUCTASE1 (CCR1) in Dwarfed ccr1 Mutants Restores Vessel and Xylary Fiber Integrity and Increases Biomass', *Plant Physiology*, 176(1), pp. 611–633. doi: 10.1104/pp.17.01462.

Melaragno, J. E., Mehrotra, B. and Coleman, A. W. (1993) 'Relationship between Endopolyploidy and Cell Size in Epidermal Tissue of Arabidopsis', *The Plant Cell*, 5(11), pp. 1661–1668. doi: 10.2307/3869747.

Mendrinna, A. and Persson, S. (2015) 'Root hair growth: it's a one way street', *F1000Prime Reports*, 7(February), pp. 1–6. doi: 10.12703/P7-23.

Mengiste, T. (2012) 'Plant Immunity to Necrotrophs', *Annual Review of Phytopathology*, 50(1), pp. 267–294. doi: 10.1146/annurev-phyto-081211-172955.

Merchante, C., Alonso, J. M. and Stepanova, A. N. (2013) 'Ethylene signaling: simple ligand, complex regulation', *Current Opinion in Plant Biology*. Elsevier Ltd, 16(5), pp. 554–560. doi: 10.1016/j.pbi.2013.08.001.

Merlot, S. *et al.* (2007) 'Constitutive activation of a plasma membrane H+-ATPase prevents abscisic acid-mediated stomatal closure', *EMBO Journal*, 26(13), pp. 3216–3226. doi: 10.1038/sj.emboj.7601750.

Metraux, J.-P. and Lionetti, V. (2014) *Plant cell wall in pathogenesis, parasitism and symbiosis*. Edited by J.-P. Metraux and V. Lionetti. Frontiers SA Media (Frontiers Research Topics). doi: 10.3389/978-2-88919-442-1.

Minamikawa, T., Akazawa, T. and Uritani, I. (1962) 'Isolation of Esculetin from Sweet Potato Roots with Black Rot', *Nature*, 195(4842), pp. 726–726. doi: 10.1038/195726a0.

Minamikawa, T., Akazawa, T. and Uritani, I. (1963) 'Analytical Study of Umbelliferone and Scopoletin Synthesis in Sweet Potato Roots Infected by Ceratocystis fimbriata', *Plant Physiology*, 38(5), pp. 493–497. doi: 10.1104/pp.38.5.493.

Misra, G. and Patnaik, S. N. (1959) 'Effect of Coumarin on the Germination and Growth of Rice Seedlings', *Nature*, 183(4666), pp. 989–990. doi: 10.1038/183989b0.

Mockaitis, K. and Estelle, M. (2008) 'Auxin Receptors and Plant Development: A New Signaling Paradigm', *Annual Review of Cell and Developmental Biology*, 24(1), pp. 55–80. doi: 10.1146/annurev.cellbio.23.090506.123214.

Moewus, F. (1949) 'Die Wirkung von Wuchs-und Hemmstoffen auf die Kressewurzel', *Biol. Zbl*, 68, p. 58.

Mogana, R., Teng-Jin, K. and Wiart, C. (2013) 'Anti-Inflammatory, Anticholinesterase, and Antioxidant Potential of Scopoletin Isolated from Canarium patentinervium Miq. (Burseraceae Kunth)', *Evidence-Based Complementary and Alternative Medicine*, 2013, pp. 1–7. doi: 10.1155/2013/734824.

Moloney, M. M., Elliott, M. C. and Cleland, R. E. (1981) 'Acid growth effects in maize roots: Evidence for a link between auxin-economy and proton extrusion in the control of root growth', *Planta*, 152(4), pp. 285–291. doi: 10.1007/BF00388251.

Mora-García, S. *et al.* (2004) 'Nuclear protein phosphatases with Kelch-repeat domains modulate the response to brassinosteroids in Arabidopsis', *Genes and Development*, 18(4), pp. 448–460. doi: 10.1101/gad.1174204.

Moreland, D. E. and Novitzky, W. P. (1987) 'Effects of Phenolic Acids, Coumarins, and Flavonoids on Isolated Chloroplasts and Mitochondria', in, pp. 247–261. doi: 10.1021/bk-1987-0330.ch023.

Morgan, P. W. and Powell, R. D. (1970) 'Involvement of Ethylene in Responses of Etiolated Bean Hypocotyl Hook to Coumarin', *Plant Physiology*, 45(5), pp. 553–557. doi: 10.1104/pp.45.5.553.

Morikawa, O. *et al.* (2011) 'ISOLATION OF UMBELLIFERONE AS A PRINCIPAL ALLELOCHEMICAL FROM THE PERUVIAN MEDICINAL PLANT Diplostephium foliosissimum (Asteraceae)', *Revista de la Sociedad Química del Perú*, 77(4), pp. 285–291.

Moseyko, N. and Feldman, L. J. (2001) 'Expression of pH-sensitive green fluorescent protein in Arabidopsis

thaliana', *Plant, Cell and Environment*, 24(5), pp. 557–563. doi: 10.1046/j.1365-3040.2001.00703.x.

Motte, H., Vanneste, S. and Beeckman, T. (2019) 'Molecular and Environmental Regulation of Root Development', *Annual Review of Plant Biology*, 70(1), pp. 465–488. doi: 10.1146/annurev-arplant-050718-100423.

Moubayidin, L. *et al.* (2010) 'The Rate of Cell Differentiation Controls the Arabidopsis Root Meristem Growth Phase', *Current Biology*. Elsevier Ltd, 20(12), pp. 1138–1143. doi: 10.1016/j.cub.2010.05.035.

Moubayidin, L., Di Mambro, R. and Sabatini, S. (2009) 'Cytokinin–auxin crosstalk', *Trends in Plant Science*, 14(10), pp. 557–562. doi: 10.1016/j.tplants.2009.06.010.

Mouchel, C. F. (2004) 'Natural genetic variation in Arabidopsis identifies BREVIS RADIX, a novel regulator of cell proliferation and elongation in the root', *Genes & Development*, 18(6), pp. 700–714. doi: 10.1101/gad.1187704.

Mravec, J. *et al.* (2009) 'Subcellular homeostasis of phytohormone auxin is mediated by the ER-localized PIN5 transporter', *Nature*, 459(7250), pp. 1136–1140. doi: 10.1038/nature08066.

Müller, A. *et al.* (1998) 'AtPIN2 defines a locus of Arabidopsis for root gravitropism control', *The EMBO Journal*, 17(23), pp. 6903–6911. doi: 10.1093/emboj/17.23.6903.

Murashige, T. and Skoog, F. (1962) 'A Revised Medium for Rapid Growth and Bio Assays with Tobacco Tissue Cultures', *Physiologia Plantarum*, 15(3), pp. 473–497. doi: 10.1111/j.1399-3054.1962.tb08052.x.

Muro-Villanueva, F., Mao, X. and Chapple, C. (2019) 'Linking phenylpropanoid metabolism, lignin deposition, and plant growth inhibition', *Current Opinion in Biotechnology*. Elsevier Ltd, 56, pp. 202–208. doi: 10.1016/j.copbio.2018.12.008.

Murray, R. D. H. (1989) 'Coumarins', *Natural Product Reports*, 6(6), p. 591. doi: 10.1039/np9890600591.

Murray, R. D. H., Méndez, J. and Brown, S. A. (1982) 'The natura, coumarins: Occurrence, Chemistry and Biochemistry.', *John Wiley & Sons*.

Nadal, M. and Paszkowski, U. (2013) 'Polyphony in the rhizosphere: Presymbiotic communication in arbuscular mycorrhizal symbiosis', *Current Opinion in Plant Biology*. Elsevier Ltd, 16(4), pp. 473–479. doi: 10.1016/j.pbi.2013.06.005.

Nagashima, A., Uehara, Y. and Sakai, T. (2008) 'The ABC Subfamily B Auxin Transporter AtABCB19 is Involved in the Inhibitory Effects of N-1-Naphthyphthalamic Acid on the Phototropic and Gravitropic Responses of Arabidopsis Hypocotyls', *Plant and Cell Physiology*, 49(8), pp. 1250–1255. doi: 10.1093/pcp/pcn092.

Nagatani, A., Reed, J. W. and Chory, J. (1993) 'Isolation and Initial Characterization of Arabidopsis Mutants That Are Deficient in Phytochrome A', *Plant Physiology*, 102(1), pp. 269–277. doi: 10.1104/pp.102.1.269.

Nakamura, A. *et al.* (2003) 'Brassinolide Induces IAA5, IAA19, and DR5, a Synthetic Auxin Response', *Plant physiology*, 133(4), pp. 1843–1853. doi: 10.1104/pp.103.030031.It.

Nakamura, A. *et al.* (2006) 'Arabidopsis Aux/IAA genes are involved in brassinosteroid-mediated growth responses in a manner dependent on organ type', *The Plant Journal*, 45(2), pp. 193–205. doi: 10.1111/j.1365-313X.2005.02582.x.

Nakaya, M. *et al.* (2002) 'Brassinosteroids control the proliferation of leaf cells of Arabidopsis thaliana', *Plant and Cell Physiology*, 43(2), pp. 239–244. doi: 10.1093/pcp/pcf024.

Nam, K. H. and Li, J. (2002) 'BRI1/BAK1, a receptor kinase pair mediating brassinosteroid signaling.', *Cell*, 110(2), pp. 203–12. doi: 10.1016/s0092-8674(02)00814-0.

Nandi, S. K., Tamta, S. and Palni, L. M. S. (2002) 'Adventitious root formation in young shoots of <i>Cedrus

deodara<i>', *Biologia Plantarum*, 45(3), pp. 473–476. doi: https://doi.org/10.1023/A:1016298524177.

Naoumkina, M. A. *et al.* (2010) 'Genome-wide analysis of phenylpropanoid defence pathways', *Molecular Plant Pathology*, 11(6), pp. 829–846. doi: 10.1111/j.1364-3703.2010.00648.x.

Née, G., Xiang, Y. and Soppe, W. J. (2017) 'The release of dormancy, a wake-up call for seeds to germinate', *Current Opinion in Plant Biology*, 35, pp. 8–14. doi: 10.1016/j.pbi.2016.09.002.

Neff, M. M. *et al.* (1999) 'BAS1: A gene regulating brassinosteroid levels and light responsiveness in Arabidopsis', *Proceedings of the National Academy of Sciences*, 96(26), pp. 15316–15323. doi: 10.1073/pnas.96.26.15316.

Negi, S., Ivanchenko, M. G. and Muday, G. K. (2008) 'Ethylene regulates lateral root formation and auxin transport in Arabidopsis thaliana', *The Plant Journal*, 55(2), pp. 175–187. doi: 10.1111/j.1365-313X.2008.03495.x.

Nelissen, H. *et al.* (2013) 'Kinematic Analysis of Cell Division in Leaves of Mono- and Dicotyledonous Species: A Basis for Understanding Growth and Developing Re fi ned Molecular Sampling Strategies', *Methods in Molecular Biology*, 959, pp. 247–264. doi: 10.1007/978-1-62703-221-6.

Nelson, N. and Harvey, W. R. (1999) 'Vacuolar and plasma membrane proton-adenosinetriphosphatases', *Physiological Reviews*, 79(2), pp. 361–385. doi: 10.1152/physrev.1999.79.2.361.

Nemhauser, J. L., Hong, F. and Chory, J. (2006) 'Different Plant Hormones Regulate Similar Processes through Largely Nonoverlapping Transcriptional Responses', *Cell*, 126(3), pp. 467–475. doi: 10.1016/j.cell.2006.05.050.

Nemhauser, J. L., Mockler, T. C. and Chory, J. (2004) 'Interdependency of Brassinosteroid and Auxin Signaling in Arabidopsis', *PLoS Biology*. Edited by Jeffrey Dangl, 2(9), p. e258. doi: 10.1371/journal.pbio.0020258.

Neumann, J. (1959) 'An Auxin-like Action of Coumarin', *Science*, 4(June), pp. 1675–1676.

Neumann, J. (1960a) 'The Nature of the Growth-Promoting Action of Coumarin', *Physiologia Plantarum*, 13(2), pp. 328–341.

Neumann, J. (1960b) 'The Nature of the Growth-Promoting Action of Coumarin', *Physiologia Plantarum*, 13(2), pp. 328–341. doi: 10.1111/j.1399-3054.1960.tb08035.x.

Neumann, J. (1960c) 'The Uptake of Coumarin by Helicanthus Hypocotyl Segments', *Science*, 12(15), p. 538.

Nishimura, T. *et al.* (2014) 'Yucasin is a potent inhibitor of YUCCA, a key enzyme in auxin biosynthesis', *Plant Journal*, 77(3), pp. 352–366. doi: 10.1111/tpj.12399.

Noguchi, T. *et al.* (1999) 'Brassinosteroid-insensitive dwarf mutants of Arabidopsis accumulate brassinosteroids.', *Plant physiology*, 121(3), pp. 743–52. doi: 10.1104/pp.121.3.743.

Noh, B. *et al.* (2003) 'Enhanced gravi- and phototropism in plant mdr mutants mislocalizing the auxin efflux protein PIN1', *Nature*, 423(6943), pp. 999–1002. doi: 10.1038/nature01716.

Noh, B., Murphy, A. S. and Spalding, E. P. (2001) 'Multidrug resistance-like genes of Arabidopsis required for auxin transport and auxin-mediated development', *Plant Cell*, 13(11), pp. 2441–2454. doi: 10.1105/tpc.13.11.2441.

Nonogaki, H. (2014) 'Seed dormancy and germination - emerging mechanisms and new hypotheses', *Frontiers in Plant Science*, 5(MAY), pp. 1–14. doi: 10.3389/fpls.2014.00233.

Nonogaki, H., Bassel, G. W. and Bewley, J. D. (2010) 'Germination—Still a mystery', *Plant Science*, 179(6), pp. 574–581. doi: 10.1016/j.plantsci.2010.02.010.

Nordborg, M. and Weigel, D. (2008) 'Next-generation genetics in plants', *Nature*, 456(7223), pp. 720–723. doi: 10.1038/nature07629.

Normanly, J. (1997) 'Auxin metabolism', *Physiologia Plantarum*, 100(3), pp. 431–442. doi: 10.1034/j.1399-3054.1997.1000304.x.

Normanly, J., Slovin, J. P. and Cohen, J. D. (2010) 'Auxin Biosynthesis and Metabolism', in *Plant Hormones*. Dordrecht: Springer Netherlands, pp. 36–62. doi: 10.1007/978-1-4020-2686-7_3.

Nozue, K. *et al.* (2015) 'Shade Avoidance Components and Pathways in Adult Plants Revealed by Phenotypic Profiling', *PLoS Genetics*, 11(4), pp. 1–26. doi: 10.1371/journal.pgen.1004953.

Nutile, G. E. (1945) 'INDUCING DORMANCY IN LETTUCE SEED WITH COUMARIN.', *Plant physiology*, 20(3), pp. 433–42. doi: 10.1104/pp.20.3.433.

Oh, E. *et al.* (2014) 'Cell elongation is regulated through a central circuit of interacting transcription factors in the Arabidopsis hypocotyl', *eLife*, 3, pp. 1–19. doi: 10.7554/eLife.03031.

Oh, E., Zhu, J. Y. and Wang, Z. Y. (2012) 'Interaction between BZR1 and PIF4 integrates brassinosteroid and environmental responses', *Nature Cell Biology*. Nature Publishing Group, 14(8), pp. 802–809. doi: 10.1038/ncb2545.

Oh, M.-H. *et al.* (1998) 'Soybean BRU1 Encodes a Functional Xyloglucan Endotransglycosylase That is Highly Expressed in Inner Epicotyl Tissues during Brassinosteroid-Promoted Elongation', *Plant and Cell Physiology*, 39(1), pp. 124–130. doi: 10.1093/oxfordjournals.pcp.a029283.

Ojala, T. *et al.* (1999) 'A Bioassay Using Artemia salina for Detecting Phototoxicity of Plant Coumarins', *Planta Medica*, 65(8), pp. 715–718. doi: 10.1055/s-1999-14049.

Ojala, T. *et al.* (2000) 'Antimicrobial activity of some coumarin containing herbal plants growing in Finland', *Journal of Ethnopharmacology*, 73(1–2), pp. 299–305. doi: 10.1016/S0378-8741(00)00279-8.

Ojewole, J. A. O. and Adesina, S. K. (1983) 'Cardiovascular and neuromuscular actions of scopoletin from fruit of Tetrapleura tetrapetra', *Planta Medica*, 49(2), pp. 99–102.

Olson, M. M. and Roseland, C. R. (1991) 'Induction of the Coumarins Scopoletin and Ayapin in Sunflower by Insect–Feeding Stress and Effects of Coumarins on the Feeding of Sunflower Beetle (Coleoptera: Chrysomelidae)', *Environmental Entomology*, 20(4), pp. 1166–1172. doi: 10.1093/ee/20.4.1166.

Olszewski, N., Sun, T. and Gubler, F. (2002) 'Gibberellin signaling biosynthesis, catabolism, and response pathways', *Plant Cell*, 14(Figure 1), pp. S61–S81. doi: 10.1105/tpc.010476.GAs.

Omelyanchuk, N. A. *et al.* (2016) 'A detailed expression map of the PIN1 auxin transporter in Arabidopsis thaliana root', *BMC Plant Biology*. BMC Plant Biology, 16(S1), p. 5. doi: 10.1186/s12870-015-0685-0.

Ooi, M. K. J. (2012) 'Seed bank persistence and climate change', *Seed Science Research*, 22(S1), pp. S53–S60. doi: 10.1017/S0960258511000407.

Ortega-Martinez, O. *et al.* (2007) 'Ethylene Modulates Stem Cell Division in the Arabidopsis thaliana Root', *Science*, 317(5837), pp. 507–510. doi: 10.1126/science.1143409.

Van Overbeek, J. and Went, F. W. (1937) 'Mechanism and Quantitative Application of the Pea Test', *Botanical Gazette*, 99(1), pp. 22–41. doi: 10.1086/334688.

Oyama, T., Shimura, Y. and Okada, K. (1997) 'The Arabidopsis HY5gene encodes a bZIP protein that regulates stimulus-induced development of root and hypocotyl', *Genes &Development*, pp. 2983–2995. doi: 10.1101/gad.11.22.2983.

Pałubicki, W., Kokosza, A. and Burian, A. (2019) 'Formal description of plant morphogenesis', *Journal of*

Experimental Botany, 70(14), pp. 3601–3613. doi: 10.1093/jxb/erz210.

Pan, L. *et al.* (2015) 'Phytotoxicity of umbelliferone and its analogs: Structure-activity relationships and action mechanisms', *Plant Physiology and Biochemistry*. Elsevier Masson SAS, 97, pp. 272–277. doi: 10.1016/j.plaphy.2015.10.020.

Pan, L. *et al.* (2017) 'Microbial Pathogenesis Antifungal activity of umbelliferone derivatives : Synthesis and structure-activity relationships', *Microbial Pathogenesis*. Elsevier Ltd, 104, pp. 110–115. doi: https://doi.org/10.1016/j.micpath.2017.01.024.

Pan, R. *et al.* (2009) 'Anti-arthritic effect of scopoletin, a coumarin compound occurring in Erycibe obtusifolia Benth stems, is associated with decreased angiogenesis in synovium', *Fundamental & Clinical Pharmacology*, 24(4), pp. 477–490. doi: 10.1111/j.1472-8206.2009.00784.x.

Pandya-Kumar, N. *et al.* (2014) 'Strigolactone analog GR24 triggers changes in PIN2 polarity, vesicle trafficking and actin filament architecture', *New Phytologist*, 202(4), pp. 1184–1196. doi: 10.1111/nph.12744.

Parry, G. *et al.* (2001) 'Quick on the uptake: Characterization of a family of plant auxin influx carriers', *Journal of Plant Growth Regulation*, 20(3), pp. 217–225. doi: 10.1007/s003440010030.

Parry, G. *et al.* (2009) 'Complex regulation of the TIR1/AFB family of auxin receptors.', *Proceedings of the National Academy of Sciences of the United States of America*, 106(52), pp. 22540–5. doi: 10.1073/pnas.0911967106.

Pastírová, A., Repčák, M. and Eliašová, A. (2004) 'Salicylic acid induces changes of coumarin metabolites in Matricaria chamomilla L.', *Plant Science*, 167(4), pp. 819–824. doi: 10.1016/j.plantsci.2004.05.027.

Paxton, J. D. (1981) 'Phytoalexins — A Working Redefinition', *Journal of Phytopathology*, 101(2), pp. 106–109. doi: 10.1111/j.1439-0434.1981.tb03327.x.

Peer, W. A., Cheng, Y. and Murphy, A. S. (2013) 'Evidence of oxidative attenuation of auxin signalling', *Journal of Experimental Botany*, 64(9), pp. 2629–2639. doi: 10.1093/jxb/ert152.

Peer, W. A. and Murphy, A. S. (2007) 'Flavonoids and auxin transport: modulators or regulators?', *Trends in Plant Science*, 12(12), pp. 556–563. doi: 10.1016/j.tplants.2007.10.003.

Pellino, M. *et al.* (2011) 'Selection of reference genes for quantitative real-time PCR expression studies of microdissected reproductive tissues in apomictic and sexual Boechera', *BMC Research Notes*, 4(1), p. 303. doi: 10.1186/1756-0500-4-303.

Peng, J. *et al.* (1997) 'The Arabidopsis GAI gene defines a signaling pathway that negatively regulates gibberellin responses', *Genes and Development*, 11(23), pp. 3194–3205. doi: 10.1101/gad.11.23.3194.

Peng, J. *et al.* (1999) '"Green revolution" genes encode mutant gibberellin response modulators', *Nature*, 400(6741), pp. 256–261. doi: 10.1038/22307.

Péret, B. *et al.* (2009) 'Arabidopsis lateral root development: an emerging story', *Trends in Plant Science*, 14(7), pp. 399–408. doi: 10.1016/j.tplants.2009.05.002.

Péret, B. *et al.* (2012) 'AUX/LAX genes encode a family of auxin influx transporters that perform distinct functions during arabidopsis development', *Plant Cell*, 24(7), pp. 2874–2885. doi: 10.1105/tpc.112.097766.

Perez-Rodriguez, E. *et al.* (2001) 'Excretion of coumarins by the Mediterranean green alga Dasycladus vermicularis in response to environmental stress', *Marine Biology*, 139(4), pp. 633–639. doi: 10.1007/s002270100588.

Pergo, É. M. *et al.* (2008) 'Bidens pilosa L. exhibits high sensitivity to coumarin in comparison with three

other weed species', *Journal of Chemical Ecology*, 34(4), pp. 499–507. doi: 10.1007/s10886-008-9449-8.

Perilli, S., Di Mambro, R. and Sabatini, S. (2012) 'Growth and development of the root apical meristem', *Current Opinion in Plant Biology*. Elsevier Ltd, 15(1), pp. 17–23. doi: 10.1016/j.pbi.2011.10.006.

Perilli, S., Moubayidin, L. and Sabatini, S. (2010) 'The molecular basis of cytokinin function', *Current Opinion in Plant Biology*, 13(1), pp. 21–26. doi: 10.1016/j.pbi.2009.09.018.

Perkin, W. H. (1868) 'On the Artificial Production of Coumarin and Formation of its Homologues.', *J. Chem. Soc.* The Royal Society of Chemistry, 21(0), pp. 53–63. doi: 10.1039/JS8682100053.

Pernisová, M. *et al.* (2009) 'Cytokinins modulate auxin-induced organogenesis in plants via regulation of the auxin efflux', *Proceedings of the National Academy of Sciences of the United States of America*, 106(9), pp. 3609–3614. doi: 10.1073/pnas.0811539106.

Perrella, G. *et al.* (2018) 'ZINC-FINGER interactions mediate transcriptional regulation of hypocotyl growth in Arabidopsis', *Proceedings of the National Academy of Sciences*, 115(19), pp. E4503–E4511. doi: 10.1073/pnas.1718099115.

Peterson, J. K. *et al.* (2003) 'Biological Activities and Contents of Scopolin and Scopoletin in Sweetpotato Clones', *HortScience*, 38(6), pp. 1129–1133.

Petrášek, J. and Friml, J. (2009) 'Auxin transport routes in plant development', *Development*, 136(16), pp. 2675–2688. doi: 10.1242/dev.030353.

Pickett, F. B., Wilson, A. K. and Estelle, M. (1990) 'The aux 1 mutation of Arabidopsis confers both auxin and ethylene resistance', *Plant Physiology*, 94(3), pp. 1462–1466. doi: 10.1104/pp.94.3.1462.

Piskurewicz, U. *et al.* (2008) 'The Gibberellic Acid Signaling Repressor RGL2 Inhibits Arabidopsis Seed Germination by Stimulating Abscisic Acid Synthesis and ABI5 Activity', *The Plant Cell*, 20(10), pp. 2729–2745. doi: 10.1105/tpc.108.061515.

Pitts, R. J., Cernac, A. and Estelle, M. (1998) 'Auxin and ethylene promote root hair elongation inArabidopsis', *The Plant Journal*, 16(5), pp. 553–560. doi: 10.1046/j.1365-313x.1998.00321.x.

Plackett, A. R. G. *et al.* (2012) 'Analysis of the developmental roles of the arabidopsis gibberellin 20-oxidases demonstrates that GA20ox1, -2, and -3 are the dominant paralogs', *Plant Cell*, 24(3), pp. 941–960. doi: 10.1105/tpc.111.095109.

Podbielkowska, M. *et al.* (1994) 'Coumarins as antimitotics', *Pharmaceutical Biology*, 32(3), pp. 262–273. doi: 10.3109/13880209409083004.

Podbielkowska, M. *et al.* (1995) 'Effect of Coumarin and its Derivatives on Mitosis and Ultrastructure of Meristematic Cells', *International Journal of Pharmacognosy*, 33(1), pp. 7–15. doi: 10.3109/13880209509088140.

Podbielkowska, M. *et al.* (1996) 'Effect of Two Furanocoumarins and Three Other Coumarins on Ultrastructure, ATPases and Acid Phosphatases in Meristematic Cells of Allium Cepa Root Tips', *International Journal of Pharmacognosy*, 34(2), pp. 96–104.

Pollock, B. M., Goodwin, R. H. and Greene, S. (1954) 'Studis on roots. II . Effects of Coumarin, Scopoletin and Other Substances on Growth.', *American journal of botany*, 41(6), pp. 521–529.

del Pozo, J. C. and Manzano, C. (2014) 'Auxin and the ubiquitin pathway. Two players–one target: the cell cycle in action', *Journal of Experimental Botany*, 65(10), pp. 2617–2632. doi: 10.1093/jxb/ert363.

Putwain, P. D. and Gillham, D. A. (1990) 'The significance of the dormant viable seed bank in the restoration of heathlands', *Biological Conservation*, 52(1), pp. 1–16. doi: 10.1016/0006-3207(90)90010-M.

Qiao, H. *et al.* (2009) 'Interplay between ethylene, ETP1/ETP2 F-box proteins, and degradation of EIN2 triggers ethylene responses in Arabidopsis', *Genes & Development*, 23(4), pp. 512–521. doi: 10.1101/gad.1765709.

Quail, P. *et al.* (1995) 'Phytochromes: photosensory perception and signal transduction', *Science*, 268(5211), pp. 675–680. doi: 10.1126/science.7732376.

Quail, P. H. (2002) 'Phytochrome photosensory signalling networks', *Nature Reviews Molecular Cell Biology*, 3(2), pp. 85–93. doi: 10.1038/nrm728.

Rademacher, W. (1991) 'Inhibitors of Gibberellin Biosynthesis: Applications in Agriculture and Horticulture', in *Gibberellins*. New York, NY: Springer New York, pp. 296–310. doi: 10.1007/978-1-4612-3002-1_29.

Rajniak, J. *et al.* (2018) 'Biosynthesis of redox-active metabolites in response to iron deficiency in plants', *Nature Chemical Biology*, 14(5), pp. 442–450. doi: 10.1038/s41589-018-0019-2.

Rakusová, H. *et al.* (2011) 'Polarization of PIN3-dependent auxin transport for hypocotyl gravitropic response in Arabidopsis thaliana', *Plant Journal*, 67(5), pp. 817–826. doi: 10.1111/j.1365-313X.2011.04636.x.

Razavi, S. M. (2011) 'Plant coumarins as Allelopathic Agents', *International Journal of Biological Chemistry*, pp. 86–90. doi: 10.3923/ijbc.2011.86.90.

Reda, A. S. and EI-Banhawy, E. M. (1986) 'Effect of Coumarin and gallic acid, Allelochemics, on survival, development and reproduction of the twospotted spider mite, Tetranychus urticae (acari: Tetranychidae)', *International Journal of Acarology*, 12(3), pp. 159–162. doi: 10.1080/01647958608683458.

Reddy, R. K. and Sharma, R. (1998) 'Spatial distribution and temporal regulation of phytochromes A and B levels in maize seedlings', *Plant Physiology and Biochemistry*, 36(10), pp. 737–745. doi: 10.1016/S0981-9428(98)80024-7.

Reed, J. W. *et al.* (2018) 'Three Auxin Response Factors Promote Hypocotyl Elongation', *Plant Physiology*, 178(2), pp. 864–875. doi: 10.1104/pp.18.00718.

Reed, J. W., Elumalai, R. P. and Chory, J. (1998) 'Suppressors of an Arabidopsis thaliana phyB mutation identify genes that control light signaling and hypocotyl elongation.', *Genetics*, 148(3), pp. 1295–310. Available at: http://www.ncbi.nlm.nih.gov/pubmed/9539443.

Reen, F. J. *et al.* (2018) 'Coumarin: a novel player in microbial quorum sensing and biofilm formation inhibition', *Applied Microbiology and Biotechnology*. Applied Microbiology and Biotechnology, 102(5), pp. 2063–2073. doi: 10.1007/s00253-018-8787-x.

Reinhardt, D. *et al.* (2003) 'Regulation of phyllotaxis by polar auxin transport', *Nature*, 426(6964), pp. 255–260. doi: 10.1038/nature02081.

Ren, H. and Gray, W. M. (2015) 'SAUR Proteins as Effectors of Hormonal and Environmental Signals in Plant Growth', *Molecular Plant*. Elsevier Ltd, 8(8), pp. 1153–1164. doi: 10.1016/j.molp.2015.05.003.

Repčák, M., Imrich, J. and Franeková, M. (2001) 'Umbelliferone, a stress metabolite of Chamomilla recutita (L.) Rauschert', *Journal of Plant Physiology*, 158(8), pp. 1085–1087. doi: 10.1078/0176-1617-00284.

Reuveni, M. and Cohen, Y. (1978) 'Growth retardation and changes in phenolic compounds, with special reference to scopoletin, in mildewed and ethylene-treated tobacco plants', *Physiological Plant Pathology*, 12(2), pp. 179–189. doi: 10.1016/0048-4059(78)90060-7.

Rice, E. L. (1987) 'Allelopathy: An Overview', in, pp. 8–22. doi: 10.1021/bk-1987-0330.ch002.

Rieu, I. *et al.* (2007) 'The gibberellin biosynthetic genes AtGA20ox1 and AtGA20ox2 act, partially redundantly, to promote growth and development throughout the Arabidopsis life cycle', *The Plant Journal*,

53(3), pp. 488–504. doi: 10.1111/j.1365-313X.2007.03356.x.

Riou-Khamlichi, C. (1999) 'Cytokinin Activation of Arabidopsis Cell Division Through a D-Type Cyclin', *Science*, 283(5407), pp. 1541–1544. doi: 10.1126/science.283.5407.1541.

Rizza, A. *et al.* (2017) 'In vivo gibberellin gradients visualized in rapidly elongating tissues', *Nature Plants*. Springer US, 3(October). doi: 10.1038/s41477-017-0021-9.

Rizza, A. *et al.* (2019) 'Visualizing Cellular Gibberellin Levels Using the nlsGPS1 Förster Resonance Energy Transfer (FRET) Biosensor', *Journal of Visualized Experiments*, 2019(143), pp. 1–9. doi: 10.3791/58739.

Rizza, A. and Jones, A. M. (2019) 'The makings of a gradient: spatiotemporal distribution of gibberellins in plant development', *Current Opinion in Plant Biology*. Elsevier Ltd, 47, pp. 9–15. doi: 10.1016/j.pbi.2018.08.001.

Robinson, M. D., McCarthy, D. J. and Smyth, G. K. (2010) 'edgeR: a Bioconductor package for differential expression analysis of digital gene expression data.', *Bioinformatics (Oxford, England)*, 26(1), pp. 139–40. doi: 10.1093/bioinformatics/btp616.

Robles, L., Stepanova, A. and Alonso, J. (2013) 'Molecular Mechanisms of Ethylene–Auxin Interaction', *Molecular Plant*, 6(6), pp. 1734–1737. doi: 10.1093/mp/sst113.

Rodriguez-Celma, J. *et al.* (2013) 'Mutually Exclusive Alterations in Secondary Metabolism Are Critical for the Uptake of Insoluble Iron Compounds by Arabidopsis and Medicago truncatula', *Plant Physiology*, 162(3), pp. 1473–1485. doi: 10.1104/pp.113.220426.

Rodríguez-Serrano, M. *et al.* (2014) '2,4-Dichlorophenoxyacetic acid promotes S-nitrosylation and oxidation of actin affecting cytoskeleton and peroxisomal dynamics', *Journal of Experimental Botany*, 65(17), pp. 4783–4793. doi: 10.1093/jxb/eru237.

Roman, G. *et al.* (1995) 'Genetic analysis of ethylene signal transduction in Arabidopsis thaliana: five novel mutant loci integrated into a stress response pathway.', *Genetics*, 139(3), pp. 1393–409. doi: https://www.genetics.org/content/genetics/139/3/1393.full.pdf.

Romano, C. P. *et al.* (1995) 'Transgene-mediated auxin overproduction in Arabidopsis: hypocotyl elongation phenotype and interactions with the hy6-1 hypocotyl elongation and axr1 auxin-resistant mutants.', *Plant Molecular Biology*, 27(6), pp. 1071–1083. doi: 10.1007/BF00020881.

Ron, A. and Mayer, A. M. (1959) 'The effect of coumarin on growth and respiration of Chlorella', *Bull Res. Counc. Israel Sect. D (Biol. Abst. 35: 28-87)*.

van Rongen, M. *et al.* (2019) 'Connective auxin transport contributes to strigolactone-mediated shoot branching control independent of the transcription factor BRC1', *PLOS Genetics*. Edited by S. Hake, 15(3), p. e1008023. doi: 10.1371/journal.pgen.1008023.

Rosas, U. *et al.* (2013) 'Integration of responses within and across Arabidopsis natural accessions uncovers loci controlling root systems architecture', *Proceedings of the National Academy of Sciences*, 110(37), pp. 15133–15138. doi: 10.1073/pnas.1305883110.

Rose, J. K. C. *et al.* (2002) 'The XTH Family of Enzymes Involved in Xyloglucan Endotransglucosylation and Endohydrolysis: Current Perspectives and a New Unifying Nomenclature', *Plant and Cell Physiology*, 43(12), pp. 1421–1435. doi: 10.1093/pcp/pcf171.

Ross, J. J., Murfet, I. C. and Reid, J. B. (1997) 'Gibberellin mutants', *Physiologia Plantarum*, 100(3), pp. 550–560. doi: 10.1034/j.1399-3054.1997.1000317.x.

Roudier, F. *et al.* (2003) 'The Medicago Species A2-Type Cyclin Is Auxin Regulated and Involved in Meristem Formation But Dispensable for Endoreduplication-Associated Developmental Programs', *Plant Physiology*,

131(3), pp. 1091–1103. doi: 10.1104/pp.102.011122.

Rouse, D. (1998) 'Changes in Auxin Response from Mutations in an AUX/IAA Gene', *Science*, 279(5355), pp. 1371–1373. doi: 10.1126/science.279.5355.1371.

Rozhon, W. *et al.* (2019) 'Inhibitors of brassinosteroid biosynthesis and signal transduction', *Molecules*, 24(23). doi: 10.3390/molecules24234372.

Rudorf, W. and Schwarze, P. (1958) 'Beiträge zur Züchtung eines cumarinfreien Steinklees und Untersuchungen Über Cumarin und verwandte Verbindungen', *Z. Pflanzenzüchtung*, 39, pp. 245–274.

Ruyter-Spira, C. *et al.* (2011) 'Physiological effects of the synthetic strigolactone analog GR24 on root system architecture in Arabidopsis: another belowground role for strigolactones?', *Plant physiology*, 155(2), pp. 721–34. doi: 10.1104/pp.110.166645.

Růžička, K. *et al.* (2007) 'Ethylene Regulates Root Growth through Effects on Auxin Biosynthesis and Transport-Dependent Auxin Distribution', *The Plant Cell*, 19(7), pp. 2197–2212. doi: 10.1105/tpc.107.052126.

De Rybel, B. *et al.* (2009) 'Chemical Inhibition of a Subset of Arabidopsis thaliana GSK3-like Kinases Activates Brassinosteroid Signaling', *Chemistry and Biology*, 16(6), pp. 594–604. doi: 10.1016/j.chembiol.2009.04.008.

De Rybel, B. *et al.* (2010) 'A novel Aux/IAA28 signaling cascade activates GATA23-dependent specification of lateral root founder cell identity', *Current Biology*, 20(19), pp. 1697–1706. doi: 10.1016/j.cub.2010.09.007.

De Rybel, B. *et al.* (2014) 'Integration of growth and patterning during vascular tissue formation in Arabidopsis', *Science*, 345(6197), pp. 1255215–1255215. doi: 10.1126/science.1255215.

Rymen, B. *et al.* (2010) 'Kinematic Analysis of Cell Division and Expansion', in *Plant Developmental Biology*, pp. 203–227. doi: 10.1007/978-1-60761-765-5_14.

Sachs, J. (1882) 'Vorlesungen über Pflanzen-Physiologie.', *Wilhelm Engelmann, Leipzig, Germany*.

Saibo, N. J. M. *et al.* (2003) 'Growth and stomata development of Arabidopsis hypocotyls are controlled by gibberellins and modulated by ethylene and auxins', *Plant Journal*, 33(6), pp. 989–1000. doi: 10.1046/j.1365-313X.2003.01684.x.

de Saint Germain, A. *et al.* (2013) 'Novel insights into strigolactone distribution and signalling', *Current Opinion in Plant Biology*, 16(5), pp. 583–589. doi: 10.1016/j.pbi.2013.06.007.

Sakai, H. *et al.* (1998) 'ETR2 is an ETR1-like gene involved in ethylene signaling in Arabidopsis', *Proceedings of the National Academy of Sciences*, 95(10), pp. 5812–5817. doi: 10.1073/pnas.95.10.5812.

Sakai, T. *et al.* (2001) 'Arabidopsis nph1 and npl1: Blue light receptors that mediate both phototropism and chloroplast relocation', *Proceedings of the National Academy of Sciences*, 98(12), pp. 6969–6974. doi: 10.1073/pnas.101137598.

Saleh, A. M. and Abu El-Soud, W. (2015) 'Evidence for "gibberellin-like" activity of coumarin', *South African Journal of Botany*. South African Association of Botanists, 100, pp. 51–57. doi: 10.1016/j.sajb.2015.05.010.

Saleh, A. M. and Kebeish, R. (2018) 'Coumarin impairs redox homeostasis in wheat aleurone layers', *Journal of Plant Research*. Springer Japan, 131(1), pp. 157–163. doi: 10.1007/s10265-017-0968-7.

Saleh, A. M. and Madany, M. M. Y. (2015) 'Coumarin pretreatment alleviates salinity stress in wheat seedlings', *Plant Physiology and Biochemistry*. Elsevier Masson SAS, 88, pp. 27–35. doi: 10.1016/j.plaphy.2015.01.005.

Saleh, A. M., Madany, M. M. Y. and González, L. (2015) 'The Effect of Coumarin Application on Early Growth and Some Physiological Parameters in Faba Bean (Vicia faba L.)', *Journal of Plant Growth Regulation*, 34(2),

pp. 233–241. doi: 10.1007/s00344-014-9459-4.

Salehin, M. *et al.* (2019) 'Auxin-sensitive Aux/IAA proteins mediate drought tolerance in Arabidopsis by regulating glucosinolate levels', *Nature Communications*, 10(1), p. 4021. doi: 10.1038/s41467-019-12002-1.

Salehin, M., Bagchi, R. and Estelle, M. (2015) 'SCF TIR1/AFB -Based Auxin Perception: Mechanism and Role in Plant Growth and Development', *The Plant Cell*, 27(1), pp. 9–19. doi: 10.1105/tpc.114.133744.

Salisbury, F. J. *et al.* (2007) 'Phytochrome coordinates Arabidopsis shoot and root development', *The Plant Journal*, 50(3), pp. 429–438. doi: 10.1111/j.1365-313X.2007.03059.x.

Sampathkumar, A. *et al.* (2014) 'Physical Forces Regulate Plant Development and Morphogenesis', *Current Biology*. Elsevier Ltd, 24(10), pp. R475–R483. doi: 10.1016/j.cub.2014.03.014.

San Antonio, J. P. (1952) 'The Role of Coumarin in the Growth of Roots of Melilotus alba', *Botanical Gazette*, 114(1), pp. 79–95.

Sánchez-Rodríguez, C. *et al.* (2010) 'Phytohormones and the cell wall in Arabidopsis during seedling growth', *Trends in Plant Science*, 15(5), pp. 291–301. doi: 10.1016/j.tplants.2010.03.002.

Sang, D. *et al.* (2014) 'Strigolactones regulate rice tiller angle by attenuating shoot gravitropism through inhibiting auxin biosynthesis', *Proceedings of the National Academy of Sciences*, 111(30), pp. 11199–11204. doi: 10.1073/pnas.1411859111.

Santner, A. A. and Watson, J. C. (2006) 'The WAG1 and WAG2 protein kinases negatively regulate root waving in Arabidopsis', *Plant Journal*, 45(5), pp. 752–764. doi: 10.1111/j.1365-313X.2005.02641.x.

Santner, A. and Estelle, M. (2010) 'The ubiquitin-proteasome system regulates plant hormone signaling', *The Plant Journal*, 61(6), pp. 1029–1040. doi: 10.1111/j.1365-313X.2010.04112.x.

Sargent, J. A. and Skoog, F. (1960) 'Effects of Indoleacetic Acid and Kinetin on Scopoletin-Scopolin Levels in Relation to Growth of Tobacco Tissues in Vitro', *Plant Physiology*, 35(6), pp. 934–941. doi: 10.1104/pp.35.6.934.

Sarkanen, K. V. and Ludwig, C. H. (1971) *Lignins. Occurrence, formation, structure, and reactions*.

Sasse, J. *et al.* (2015) 'Asymmetric Localizations of the ABC Transporter PaPDR1 Trace Paths of Directional Strigolactone Transport', *Current Biology*, pp. 647–655. doi: 10.1016/j.cub.2015.01.015.

Satbhai, S. B. *et al.* (2017) 'Natural allelic variation of FRO2 modulates Arabidopsis root growth under iron deficiency', *Nature Communications*. Nature Publishing Group, 8(1), p. 15603. doi: 10.1038/ncomms15603.

Satoh, S., Takahara, M. and Matsuda, K. (1976) 'Inhibition of the synthesis of microbial cellulose by coumarin', *Plant and Cell Physiology*, 17(5), pp. 1077–1080. doi: 10.1093/oxfordjournals.pcp.a075355.

Sauer, M., Robert, S. and Kleine-Vehn, J. (2013) 'Auxin: simply complicated', *Journal of Experimental Botany*, 64(9), pp. 2565–2577. doi: 10.1093/jxb/ert139.

Sawa, S. *et al.* (2002) 'The HAT2 gene, a member of the HD-Zip gene family, isolated as an auxin inducible gene by DNA microarray screening, affects auxin response in Arabidopsis', *Plant Journal*, 32(6), pp. 1011–1022. doi: 10.1046/j.1365-313X.2002.01488.x.

Scacchi, E. *et al.* (2010) 'Spatio-temporal sequence of cross-regulatory events in root meristem growth', *Proceedings of the National Academy of Sciences*, 107(52), pp. 22734–22739. doi: 10.1073/pnas.1014716108.

Scaffidi, A. *et al.* (2014) 'Strigolactone Hormones and Their Stereoisomers Signal through Two Related Receptor Proteins to Induce Different Physiological Responses in Arabidopsis.', *Plant physiology*, 165(3), pp. 1221–1232. doi: 10.1104/pp.114.240036.

Scarpella, E. (2006) 'Control of leaf vascular patterning by polar auxin transport', *Genes & Development*, 20(8), pp. 1015–1027. doi: 10.1101/gad.1402406.

Schaeffer, G. W., Buta, J. G. and Sharpe, F. (1967) 'Scopoletin and Polyphenol-Induced Lag in Peroxidase Catalyzed Oxidation of Indole-3-acetic Acid', *Physiologia Plantarum*, 20(2), pp. 342–347. doi: 10.1111/j.1399-3054.1967.tb07172.x.

Schaeffer, G. W., Haskins, F. A. and Gorz, H. J. (1960) 'Genetic control of coumarin Biosynthesis and Beta-Glucosidase activity in Melilotys alba', *Journal of Chemical Information and Modeling*, 3(3), pp. 268–271. doi: 10.1017/CBO9781107415324.004.

Schmid, N. B. *et al.* (2014) 'Feruloyl-CoA 6'-Hydroxylase1-Dependent Coumarins Mediate Iron Acquisition from Alkaline Substrates in Arabidopsis', *PLANT PHYSIOLOGY*, 164(1), pp. 160–172. doi: 10.1104/pp.113.228544.

Schmidt, H. *et al.* (2014) 'Metabolome Analysis of Arabidopsis thaliana Roots Identifies a Key Metabolic Pathway for Iron Acquisition', *PLoS ONE*. Edited by G. Muday, 9(7), p. e102444. doi: 10.1371/journal.pone.0102444.

Schreiner, O. and Reed, H. S. (1907) 'The production of deleterious excretions by roots', *Bulletin of the Torrey Botanical Club*. JSTOR, 34(6), pp. 279–303.

Schreiner, O., Reed, H. S. and Skinner, J. J. (1907) 'Certain organic constituents of soils in relation to soil fertility'. Govt. Print. Off.

Seo, M. *et al.* (2006) 'Regulation of hormone metabolism in Arabidopsis seeds: phytochrome regulation of abscisic acid metabolism and abscisic acid regulation of gibberellin metabolism', *The Plant Journal*, 48(3), pp. 354–366. doi: 10.1111/j.1365-313X.2006.02881.x.

Seo, M. *et al.* (2009) 'Interaction of light and hormone signals in germinating seeds', *Plant Molecular Biology*, 69(4), pp. 463–472. doi: 10.1007/s11103-008-9429-y.

Sequeira, L. (1964) 'Inhibition of indoleacetic acid oxidase in tobacco plants infected by Pseudomonas solanacearum.', *Phytopathology*, 54(9), p. 1078.

Sergeeva, E., Liaimer, A. and Bergman, B. (2002) 'Evidence for production of the phytohormone indole-3-acetic acid by cyanobacteria', *Planta*, 215(2), pp. 229–238. doi: 10.1007/s00425-002-0749-x.

Shalaby, S. and Horwitz, B. A. (2015) 'Plant phenolic compounds and oxidative stress: integrated signals in fungal–plant interactions', *Current Genetics*. Springer Berlin Heidelberg, 61(3), pp. 347–357. doi: 10.1007/s00294-014-0458-6.

Shani, E. *et al.* (2013) 'Gibberellins accumulate in the elongating endodermal cells of Arabidopsis root', *Proceedings of the National Academy of Sciences*, 110(12), pp. 4834–4839. doi: 10.1073/pnas.1300436110.

Shani, E. *et al.* (2017) 'Plant Stress Tolerance Requires Auxin-Sensitive Aux/IAA Transcriptional Repressors', *Current Biology*. Elsevier Ltd., 27(3), pp. 437–444. doi: 10.1016/j.cub.2016.12.016.

Sharan, M. *et al.* (1998) 'Effects of methyl jasmonate and elicitor on the activation of phenylalanine ammonia-lyase and the accumulation of scopoletin and scopolin in tobacco cell cultures', *Plant Science*, 132(1), pp. 13–19. doi: 10.1016/S0168-9452(97)00260-4.

Sharrock, R. A. and Clack, T. (2002) 'Patterns of Expression and Normalized Levels of the Five Arabidopsis Phytochromes', *Plant Physiology*, 130(1), pp. 442–456. doi: 10.1104/pp.005389.

Sharrock, R. A. and Quail, P. H. (1989) 'Novel phytochrome sequences in Arabidopsis thaliana: structure, evolution, and differential expression of a plant regulatory photoreceptor family.', *Genes & development*, 3(11), pp. 1745–1757. doi: 10.1101/gad.3.11.1745.

Shaw, C.-Y. *et al.* (2003) 'Antioxidant properties of scopoletin isolated fromSinomonium acutum', *Phytotherapy Research*, 17(7), pp. 823–825. doi: 10.1002/ptr.1170.

Shettel, N. L. and Balke, N. E. (1983) 'Plant Growth Response to Several Allelopathic Chemicals', *Weed Science*, 31(3), pp. 293–298. doi: 10.1017/S0043174500069034.

Shi, J.-H. and Yang, Z.-B. (2011) 'Is ABP1 an Auxin Receptor Yet?', *Molecular Plant*, 4(4), pp. 635–640. doi: 10.1093/mp/ssr050.

Shimizu, B.-I. (2014) '2-Oxoglutarate-dependent dioxygenases in the biosynthesis of simple coumarins', *Frontiers in Plant Science*, 5(November), pp. 1–7. doi: 10.3389/fpls.2014.00549.

Shinohara, N., Taylor, C. and Leyser, O. (2013) 'Strigolactone can promote or inhibit shoot branching by triggering rapid depletion of the auxin efflux protein PIN1 from the plasma membrane.', *PLoS biology*, 11(1), p. e1001474. doi: 10.1371/journal.pbio.1001474.

Shinomura, T. (1997) 'Phytochrome regulation of seed germination', *Journal of Plant Research*, 110(1), pp. 151–161. doi: 10.1007/BF02506854.

Shukla, Y. . *et al.* (1999) 'Phytotoxic and antimicrobial constituents of Argyreia speciosa and Oenothera biennis', *Journal of Ethnopharmacology*, 67(2), pp. 241–245. doi: 10.1016/S0378-8741(99)00017-3.

Silva, F. L. *et al.* (2014) 'Chemical constituents of Cardiospermum corindum L. and their distribution in Sapindaceae', *Biochemical Systematics and Ecology*, 57, pp. 137–140. doi: 10.1016/j.bse.2014.07.021.

Silva, W. P. K. *et al.* (2002) 'Isolation of scopoletin from leaves of Hevea brasiliensis and the effect of scopoletin on pathogens of H . brasiliensis', *Mycopathologia*, 600(153), pp. 199–202. doi: https://doi.org/10.1023/A:1014910132595.

Silverstone, A. L. (2001) 'Repressing a Repressor: Gibberellin-Induced Rapid Reduction of the RGA Protein in Arabidopsis', *the Plant Cell Online*, 13(7), pp. 1555–1566. doi: 10.1105/tpc.13.7.1555.

Silverstone, A. L., Ciampaglio, C. N. and Sun, T. (1998) 'The Arabidopsis RGA Gene Encodes a Transcriptional Regulator Repressing the Gibberellin Signal Transduction Pathway', *The Plant Cell*, 10(2), pp. 155–169. doi: 10.1105/tpc.10.2.155.

Simon, C. *et al.* (2010) 'The differential spatial distribution of secondary metabolites in Arabidopsis leaves reacting hypersensitively to Pseudomonas syringae pv. tomato is dependent on the oxidative burst', *Journal of Experimental Botany*, 61(12), pp. 3355–3370. doi: 10.1093/jxb/erq157.

Singh, A. P. and Savaldi-Goldstein, S. (2015) 'Growth control: Brassinosteroid activity gets context', *Journal of Experimental Botany*, 66(4), pp. 1123–1132. doi: 10.1093/jxb/erv026.

Sirko, A. *et al.* (2015) 'The family of LSU-like proteins', *Frontiers in Plant Science*, 5(JAN), pp. 1–9. doi: 10.3389/fpls.2014.00774.

Sirois, J. C. and Miller, R. W. (1972) 'The Mechanism of the Scopoletin-induced Inhibition of the Peroxidase Catalyzed Degradation of Indole-3-acetate', *Plant Physiology*, 49(6), pp. 1012–1018. doi: 10.1104/pp.49.6.1012.

Siwinska, J. *et al.* (2014) 'Identification of QTLs affecting scopolin and scopoletin biosynthesis in Arabidopsis thaliana', *BMC Plant Biology*, 14(1), pp. 1–14. doi: 10.1186/s12870-014-0280-9.

Skoog, F. and Miller, C. O. (1957) 'Chemical regulation of growth and organ formation in plant tissues cultured in vitro.', *Symposia of the Society for Experimental Biology*, 11, pp. 118–30. Available at: http://www.ncbi.nlm.nih.gov/pubmed/13486467.

Skoog, F. and Montaldi, E. (1961) 'Auxin-Kinetin Interaction Regulating the Scopoletin and Scopolin Levels in

Tobacco Tissue Cultures', *Proceedings of the National Academy of Sciences*, 47(1), pp. 36–49. doi: 10.1073/pnas.47.1.36.

Slobodníková, L. *et al.* (2016) 'Antibiofilm Activity of Plant Polyphenols', *Molecules*, 21(12), p. 1717. doi: 10.3390/molecules21121717.

Smalle, J. *et al.* (1997) 'Ethylene can stimulate Arabidopsis hypocotyl elongation in the light.', *Proceedings of the National Academy of Sciences of the United States of America*, 94(6), pp. 2756–2761. doi: 10.1073/pnas.94.6.2756.

Smith, H. (2000) 'Phytochromes and light signal perception by plants - An emerging synthesis', *Nature*, 407(6804), pp. 585–591. doi: 10.1038/35036500.

Smith, R. A. *et al.* (2001) 'Induction of umbelliferone in sweet potato cell suspension culture using mercuric chloride', *Biotechnology Letters*, 23(17), pp. 1397–1400. doi: 10.1023/A:1011660722402.

Smith, W. K. (1938) 'Relation of bitterness to the toxic principle in sweetclover', *Journal of Agricultural Research*, 57(2), pp. 145–154.

Snook, M. E., Chortyk, O. T. and Csinos, A. S. (1991) 'Black Shank Disease Fungus Inhibition of Growth by Tobacco Root Constituents and Related Compounds', in *Acs Symposium Series*, pp. 388–398. doi: 10.1021/bk-1991-0449.ch027.

Somerville, C. (2004) 'Toward a Systems Approach to Understanding Plant Cell Walls', *Science*, 306(5705), pp. 2206–2211. doi: 10.1126/science.1102765.

Somerville, C. and Koornneef, M. (2002) 'A fortunate choice: The history of Arabidopsis as a model plant', *Nature Reviews Genetics*, 3(11), pp. 883–889. doi: 10.1038/nrg927.

Sondheimer, E., Tzou, D. S. and Galson, E. C. (1968) 'Abscisic Acid Levels and Seed Dormancy', *Plant Physiology*, 43(9), pp. 1443–1447. doi: 10.1104/pp.43.9.1443.

Sorin, C. *et al.* (2005) 'Auxin and Light Control of Adventitious Rooting in Arabidopsis Require ARGONAUTE1', *Plant Cell*, 17(May), pp. 1343–1359. doi: 10.1105/tpc.105.031625.1.

Sozzani, R. and Iyer-Pascuzzi, A. (2014) 'Postembryonic control of root meristem growth and development', *Current Opinion in Plant Biology*. Elsevier Ltd, 17(1), pp. 7–12. doi: 10.1016/j.pbi.2013.10.005.

Spartz, A. K. *et al.* (2012) 'The SAUR19 subfamily of SMALL AUXIN UP RNA genes promote cell expansion', *Plant Journal*, 70(6), pp. 978–990. doi: 10.1111/j.1365-313X.2012.04946.x.

Spartz, A. K. *et al.* (2014) 'SAUR Inhibition of PP2C-D Phosphatases Activates Plasma Membrane H + -ATPases to Promote Cell Expansion in Arabidopsis', *The Plant Cell*, 26(5), pp. 2129–2142. doi: 10.1105/tpc.114.126037.

Spartz, A. K. *et al.* (2017) 'Constitutive Expression of Arabidopsis SMALL AUXIN UP RNA19 (SAUR19) in Tomato Confers Auxin-Independent Hypocotyl Elongation', *Plant Physiology*, 173(2), pp. 1453–1462. doi: 10.1104/pp.16.01514.

Stahmann, M. A., Huebner, C. F. and Link, K. P. (1941) 'Studies on the hemorrhagic sweet clover disease. 5. Identification and synthesis of the hemorrhagic agent.', *Journal of Biological Chemistry*, 138, pp. 513–527.

Stallknecht, G. F. (1972) 'Coumarin-induced Tuber Formation on Excised Shoots of Solanum tuberosum L. Cultured in Vitro.', *Plant physiology*, 50(3), pp. 412–3. doi: 10.1104/pp.50.3.412.

Stanga, J. P. *et al.* (2013) 'SUPPRESSOR OF MORE AXILLARY GROWTH2 1 controls seed germination and seedling development in Arabidopsis.', *Plant physiology*, 163(1), pp. 318–30. doi: 10.1104/pp.113.221259.

Stark, R., Grzelak, M. and Hadfield, J. (2019) 'RNA sequencing: the teenage years', *Nature Reviews Genetics*.

Springer US, 20(11), pp. 631–656. doi: 10.1038/s41576-019-0150-2.

Steenackers, W. *et al.* (2017) 'cis-Cinnamic Acid Is a Novel, Natural Auxin Efflux Inhibitor That Promotes Lateral Root Formation.', *Plant physiology*, 173(1), pp. 552–565. doi: 10.1104/pp.16.00943.

Steenackers, W. J. *et al.* (2016) 'The allelochemical MDCA inhibits lignification and affects auxin homeostasis', *Plant Physiology*, 172(October), p. pp.01972.2015. doi: 10.1104/pp.15.01972.

Steffens, B. *et al.* (2001) 'The auxin signal for protoplast swelling is perceived by extracellular ABP1', *The Plant Journal*, 27(6), pp. 591–599. doi: 10.1046/j.1365-313X.2001.01103.x.

Steffens, B. and Rasmussen, A. (2016) 'The physiology of adventitious roots', *Plant Physiology*, 170(2), pp. 603–617. doi: 10.1104/pp.15.01360.

Stepanova, A. N. (2005) 'A Link between Ethylene and Auxin Uncovered by the Characterization of Two Root-Specific Ethylene-Insensitive Mutants in Arabidopsis', *the Plant Cell Online*, 17(8), pp. 2230–2242. doi: 10.1105/tpc.105.033365.

Stepanova, A. N. *et al.* (2007) 'Multilevel interactions between ethylene and auxin in Arabidopsis roots.', *The Plant cell*, 19(7), pp. 2169–85. doi: 10.1105/tpc.107.052068.

Stepanova, A. N. *et al.* (2011) 'The Arabidopsis YUCCA1 Flavin Monooxygenase Functions in the Indole-3-Pyruvic Acid Branch of Auxin Biosynthesis', *The Plant Cell*, 23(11), pp. 3961–3973. doi: 10.1105/tpc.111.088047.

Stepanova, A. N. and Alonso, J. M. (2016) 'Auxin catabolism unplugged: Role of IAA oxidation in auxin homeostasis', *Proceedings of the National Academy of Sciences of the United States of America*, 113(39), pp. 10742–10744. doi: 10.1073/pnas.1613506113.

Stevenson, T. M. and White, W. J. (1940) 'Investigations Concerning the Coumarin Content of Sweet Clover: I. The Breeding of a Low-Coumarin Line of Sweet Clover—Melilotus alba', *Scientific Agriculture*. NRC Research Press, 21(1), pp. 18–28.

Stewart, J. L. and Nemhauser, J. L. (2010) 'Do trees grow on money? Auxin as the currency of the cellular economy.', *Cold Spring Harbor perspectives in biology*, 2(2), pp. 1–13. doi: 10.1101/cshperspect.a001420.

Stirnberg, P., Furner, I. J. and Ottoline Leyser, H. M. (2007) 'MAX2 participates in an SCF complex which acts locally at the node to suppress shoot branching.', *The Plant journal : for cell and molecular biology*, 50(1), pp. 80–94. doi: 10.1111/j.1365-313X.2007.03032.x.

Stortenbeker, N. and Bemer, M. (2019) 'The SAUR gene family: The plant's toolbox for adaptation of growth and development', *Journal of Experimental Botany*, 70(1), pp. 17–27. doi: 10.1093/jxb/ery332.

Strader, L. C. *et al.* (2004) 'Recessive-interfering mutations in the gibberellin signaling gene SLEEPY1 are rescued by overexpression of its homologue, SNEEZY', *Proceedings of the National Academy of Sciences*, 101(34), pp. 12771–12776. doi: 10.1073/pnas.0404287101.

Street, I. H. *et al.* (2007) 'The AT-hook-containing proteins SOB3/AHL29 and ESC/AHL27 are negative modulators of hypocotyl growth in Arabidopsis', *The Plant Journal*, 54(1), pp. 1–14. doi: 10.1111/j.1365-313X.2007.03393.x.

Stringlis, I. A. *et al.* (2018) 'MYB72-dependent coumarin exudation shapes root microbiome assembly to promote plant health', *Proceedings of the National Academy of Sciences*, 115(22), pp. E5213–E5222. doi: 10.1073/pnas.1722335115.

Su, Y.-H., Liu, Y.-B. and Zhang, X.-S. (2011) 'Auxin–Cytokinin Interaction Regulates Meristem Development', *Molecular Plant*. The Authors 2011., 4(4), pp. 616–625. doi: 10.1093/mp/ssr007.

Sun, H. *et al.* (2014) 'Scopoletin is a phytoalexin against Alternaria alternata in wild tobacco dependent on jasmonate signalling', *Journal of Experimental Botany*, 65(15), pp. 4305–4315. doi: 10.1093/jxb/eru203.

Sun, H. *et al.* (2017) 'Ethylene signalling is essential for the resistance of Nicotiana attenuata against Alternaria alternata and phytoalexin scopoletin biosynthesis', *Plant Pathology*, 66(2), pp. 277–284. doi: 10.1111/ppa.12568.

Sun, T. P., Goodman, H. M. and Ausubel, F. M. (1992) 'Cloning the arabidopsis GA1 locus by genomic subtraction', *Plant Cell*, 4(2), pp. 119–128.

Sun, Y. *et al.* (2010) 'Integration of Brassinosteroid Signal Transduction with the Transcription Network for Plant Growth Regulation in Arabidopsis', *Developmental Cell*. Elsevier Inc., 19(5), pp. 765–777. doi: 10.1016/j.devcel.2010.10.010.

Sunita, K., Kumar, P. and Singh, D. K. (2014) 'Seasonal variation in toxicity of citral against Fasciola larva', *Asian Pacific Journal of Tropical Biomedicine*, 4(May), pp. S584–S588. doi: 10.12980/APJTB.4.2014C1102.

Supek, F. *et al.* (2011) 'REVIGO Summarizes and Visualizes Long Lists of Gene Ontology Terms', *PLoS ONE*. Edited by C. Gibas, 6(7), p. e21800. doi: 10.1371/journal.pone.0021800.

Suzuki, H. *et al.* (2009) 'Differential expression and affinities of Arabidopsis gibberellin receptors can explain variation in phenotypes of multiple knock-out mutants', *The Plant Journal*, 60(1), pp. 48–55. doi: 10.1111/j.1365-313X.2009.03936.x.

Svensson, S.-B. (1971) 'The effect of coumarin on root growth and root histology', *Physiologia Plantarum*, 24(3), pp. 446–470.

Svensson, S.-B. (1972a) 'A Comparative Study of the Changes in Root Growth, Induced by Coumarin, Auxin, Ethylen, Kinetin and Gibberellic Acid', *Physiol Plant*, (26), pp. 115–135.

Svensson, S.-B. (1972b) 'The Effect of Coumarin on Growth, Production of Dry Matter, Protein and Nucleic Acids in Roots of Maize and Wheat and the Interaction of Coumarin with Metaholic Inhibitors', *Physiol Plant*, 27, pp. 13–24.

Swarup, K. *et al.* (2008) 'The auxin influx carrier LAX3 promotes lateral root emergence', *Nature Cell Biology*, 10(8), pp. 946–954. doi: 10.1038/ncb1754.

Swarup, R. (2001) 'Localization of the auxin permease AUX1 suggests two functionally distinct hormone transport pathways operate in the Arabidopsis root apex', *Genes & Development*, 15(20), pp. 2648–2653. doi: 10.1101/gad.210501.

Swarup, R. *et al.* (2004) 'Structure-Function Analysis of the Presumptive Arabidopsis Auxin Permease AUX1', *The Plant Cell*, 16(11), pp. 3069–3083. doi: 10.1105/tpc.104.024737.

Swarup, R. *et al.* (2005) 'Root gravitropism requires lateral root cap and epidermal cells for transport and response to a mobile auxin signal', *Nature Cell Biology*, 7(11), pp. 1057–1065. doi: 10.1038/ncb1316.

Swarup, R. *et al.* (2007) 'Ethylene Upregulates Auxin Biosynthesis in Arabidopsis Seedlings to Enhance Inhibition of Root Cell Elongation', *The Plant Cell*, 19(7), pp. 2186–2196. doi: 10.1105/tpc.107.052100.

Swarup, R. and Bhosale, R. (2019) 'Developmental Roles of AUX1/LAX Auxin Influx Carriers in Plants', *Frontiers in Plant Science*, 10(October), pp. 1–14. doi: 10.3389/fpls.2019.01306.

Symons, G. M. *et al.* (2008) 'The hormonal regulation of de-etiolation', *Planta*, 227(5), pp. 1115–1125. doi: 10.1007/s00425-007-0685-x.

Szekeres, M. *et al.* (1996) 'Brassinosteroids rescue the deficiency of CYP90, a cytochrome P450, controlling cell elongation and de-etiolation in Arabidopsis', *Cell*, 85(2), pp. 171–182. doi: 10.1016/S0092-

8674(00)81094-6.

Taguchi, G. *et al.* (2000) 'Scopoletin uptake from culture medium and accumulation in the vacuoles after conversion to scopolin in 2,4-D-treated tobacco cells', *Plant Science*, 151(2), pp. 153–161. doi: 10.1016/S0168-9452(99)00212-5.

Taguchi, G. *et al.* (2001) 'Plant hormone regulation on scopoletin metabolism from culture medium into tobacco cells', *Plant Science*, 160(5), pp. 905–911. doi: 10.1016/S0168-9452(00)00464-7.

Takahashi, K., Hayashi, K. I. and Kinoshita, T. (2012) 'Auxin Activates the Plasma Membrane H + -ATPase by Phosphorylation during Hypocotyl Elongation in Arabidopsis', *Plant Physiology*, 159(2), pp. 632–641. doi: 10.1104/pp.112.196428.

Takahashi, T. *et al.* (1995) 'The DIMINUTO gene of Arabidopsis is involved in regulating cell elongation', *Genes and Development*, 9(1), pp. 97–107. doi: 10.1101/gad.9.1.97.

Takemura, T. *et al.* (2013) 'Discovery of coumarin as the predominant allelochemical in Guricidia sepium', *Journal of Tropical Forest Science*, 25(2), pp. 268–272.

Tal, B. and Robeson, D. J. (1986) 'The Metabolism of Sunflower Phytoalexins Ayapin and Scopoletin', *Plant Physiology*, 82(1), pp. 167–172. doi: 10.1104/pp.82.1.167.

Tam, V. *et al.* (2019) 'Benefits and limitations of genome-wide association studies', *Nature Reviews Genetics*. doi: 10.1038/s41576-019-0127-1.

Tan, A. M. and Low, F. C. (1975) 'Phytoalexin production by Hevea brasiliensis in response to infection by collectotrichum gloesporioides and its effect on other fungi.', *International Rubber Conference, Kuala Lumpur (Malaysia)*.

Tan, S. *et al.* (2020) 'Salicylic Acid Targets Protein Phosphatase 2A to Attenuate Growth in Plants', *Current Biology*. Elsevier, 30(3), pp. 381-395.e8. doi: 10.1016/j.cub.2019.11.058.

Tanaka, Y. *et al.* (1983) 'Biochemical changes in secondary metabolites in wounded and deteriorated cassava roots.', *Agricultural and Biological Chemistry*, 47(4), pp. 693–700. doi: 10.1271/bbb1961.47.693.

Tang, W. *et al.* (2008) 'Proteomics studies of brassinosteroid signal transduction using prefractionation and two-dimensional DIGE', *Molecular and Cellular Proteomics*, 7(4), pp. 728–738. doi: 10.1074/mcp.M700358-MCP200.

Tanimoto, M., Roberts, K. and Dolan, L. (1995) 'Ethylene is a positive regulator of root hair development in Arabidopsis thaliana', *The Plant Journal*, 8(6), pp. 943–948. doi: 10.1046/j.1365-313X.1995.8060943.x.

Tao, Y. *et al.* (2008) 'Rapid Synthesis of Auxin via a New Tryptophan-Dependent Pathway Is Required for Shade Avoidance in Plants', *Cell*, 133(1), pp. 164–176. doi: 10.1016/j.cell.2008.01.049.

Tartoura, K., da Rocha, A. and Youssef, S. (2004) 'Synergistic interaction between coumarin 1,2-benzopyrone and indole-3-butyric acid in stimulating adventitious root formation in Vigna radiata (L.) Wilczek cuttings: I. Endogenous free and conjugated IAA and basic isoperoxidases', *Plant Growth Regulation*, 42(3), pp. 253–262. doi: 10.1023/B:GROW.0000026507.90898.8a.

Terzaghi, W. B. and Cashmore, A. R. (1995) 'Light-Regulated Transcription', *Annual Review of Plant Physiology and Plant Molecular Biology*, 46(1), pp. 445–474. doi: 10.1146/annurev.pp.46.060195.002305.

The Arabidopsis Genome Initiative, X. (2000) 'Analysis of the genome sequence of the flowering plant Arabidopsis thaliana', *Nature*, 408(6814), pp. 796–815. doi: 10.1038/35048692.

Thieme, C. J. *et al.* (2015) 'Endogenous Arabidopsis messenger RNAs transported to distant tissues', *Nature Plants*, 1(4), p. 15025. doi: 10.1038/nplants.2015.25.

Thimann, K. V and Bonner, W. D. (1949) 'Inhibition of Plant Growth by Protoanemonin and Coumarin, and Its Prevention by Bal.', *Proceedings of the National Academy of Sciences of the United States of America*, 35(6), pp. 272–6. Available at: http://www.pubmedcentral.nih.gov/articlerender.fcgi?artid=1063020&tool=pmcentrez&rendertype=abstract.

Thomann, A. *et al.* (2009) 'Arabidopsis CULLIN3 Genes Regulate Primary Root Growth and Patterning by Ethylene-Dependent and -Independent Mechanisms', *PLoS Genetics*. Edited by P. S. Schnable, 5(1), p. e1000328. doi: 10.1371/journal.pgen.1000328.

Thomas, S. G., Phillips, A. L. and Hedden, P. (1999) 'Molecular cloning and functional expression of gibberellin 2- oxidases, multifunctional enzymes involved in gibberellin deactivation', *Proceedings of the National Academy of Sciences*, 96(8), pp. 4698–4703. doi: 10.1073/pnas.96.8.4698.

Thomé, O. W. (1885a) *Anthoxanthum odoratum*, *Flora von Deutschland, Österreich und der Schweiz*. Available at: https://commons.wikimedia.org/wiki/File:Illustration_Anthoxanthum_odoratum0.jpg.

Thomé, O. W. (1885b) *Melilotus officinalis*, *Flora von Deutschland, Österreich und der Schweiz*. Available at: https://fr.wikipedia.org/wiki/Mélilot_officinal#/media/Fichier:Illustration_Melilotus_officinalis1.jpg.

Tian, Q. and Reed, J. W. (1999) 'Control of auxin-regulated root development by the Arabidopsis thaliana SHY2/IAA3 gene.', *Development (Cambridge, England)*, 126(4), pp. 711–21. Available at: http://www.ncbi.nlm.nih.gov/pubmed/9895319.

Timmerman, M., Wassarman, P. M. and Pourquié, O. (2010) *Plant Development*, *Developmental Biology*.

Tissier, A. F. *et al.* (1999) 'Multiple Independent Defective Suppressor-mutator Transposon Insertions in Arabidopsis: A Tool for Functional Genomics', *The Plant Cell*, 11(10), pp. 1841–1852. doi: 10.1105/tpc.11.10.1841.

To, J. P. C. *et al.* (2004) 'Type-A Arabidopsis Response Regulators Are Partially Redundant Negative Regulators of Cytokinin Signaling', *The Plant Cell*, 16(3), pp. 658–671. doi: 10.1105/tpc.018978.

Tsai, H. H. and Schmidt, W. (2017) 'Mobilization of Iron by Plant-Borne Coumarins', *Trends in Plant Science*. Elsevier Ltd, 22(6), pp. 538–548. doi: 10.1016/j.tplants.2017.03.008.

Tsuchiya, Y. *et al.* (2010) 'A small-molecule screen identifies new functions for the plant hormone strigolactone.', *Nature chemical biology*, 6(10), pp. 741–749. doi: 10.1038/nchembio.435.

Tsukagoshi, H., Busch, W. and Benfey, P. N. (2010) 'Transcriptional regulation of ROS controls transition from proliferation to differentiation in the root', *Cell*. Elsevier Ltd, 143(4), pp. 606–616. doi: 10.1016/j.cell.2010.10.020.

Tsukaya, H. (2019) 'Re-examination of the role of endoreduplication on cell-size control in leaves', *Journal of Plant Research*, 132(5), pp. 571–580. doi: 10.1007/s10265-019-01125-7.

Turner, J. H. (1933) 'The Viability of Seeds', *Bulletin of Miscellaneous Information (Royal Gardens, Kew)*, 1933(6), p. 257. doi: 10.2307/4115450.

Ubeda-Tomás, S. *et al.* (2009) 'Gibberellin Signaling in the Endodermis Controls Arabidopsis Root Meristem Size', *Current Biology*, 19(14), pp. 1194–1199. doi: 10.1016/j.cub.2009.06.023.

Ubeda-Tomás, S., Beemster, G. T. S. and Bennett, M. J. (2012) 'Hormonal regulation of root growth: Integrating local activities into global behaviour', *Trends in Plant Science*, 17(6), pp. 326–331. doi: 10.1016/j.tplants.2012.02.002.

Uhrstrom, I. and Svensson, S.-B. (1979) 'The Effect of Coumarin on Young's Modulus in Sunflower Stems and Maize Roots and on Water Permeability in Potato Parenchyma', *Physiologia Plantarum*, 45(1), pp. 41–44.

doi: 10.1111/j.1399-3054.1979.tb01660.x.

Umehara, M. *et al.* (2008) 'Inhibition of shoot branching by new terpenoid plant hormones.', *Nature*, 455(7210), pp. 195–200. doi: 10.1038/nature07272.

Uritani, I. (1999) 'Biochemistry on postharvest metabolism and deterioration of some tropical tuberous crops.', *Botanical Bulletin of Academia Sinica*, 40, pp. 177–183.

Valle, T. *et al.* (1997) 'Antifungal activity of scopoletin and its differential accumulation in Ulmus pumila and Ulmus campestris cell suspension cultures infected with Ophiostoma ulmi spores', *Plant Science*, 125(1), pp. 97–101. doi: 10.1016/S0168-9452(97)00057-5.

Vandenbussche, F. *et al.* (2010) 'The auxin influx carriers AUX1 and LAX3 are involved in auxin-ethylene interactions during apical hook development in Arabidopsis thaliana seedlings', *Development*, 137(4), pp. 597–606. doi: 10.1242/dev.040790.

Vandenbussche, F., Verbelen, J. P. and Van Der Straeten, D. (2005) 'Of light and length: Regulation of hypocotyl growth in Arabidopsis', *BioEssays*, 27(3), pp. 275–284. doi: 10.1002/bies.20199.

Vanholme, B., El Houari, I. and Boerjan, W. (2019) 'Bioactivity: phenylpropanoids' best kept secret', *Current Opinion in Biotechnology*. Elsevier Ltd, 56, pp. 156–162. doi: 10.1016/j.copbio.2018.11.012.

Vanholme, R. *et al.* (2010) 'Lignin Biosynthesis and Structure', *Plant Physiology*, 153(3), pp. 895–905. doi: 10.1104/pp.110.155119.

Vanholme, R. *et al.* (2012) 'A systems biology view of responses to lignin biosynthesis perturbations in Arabidopsis.', *The Plant cell*, 24(9), pp. 3506–29. doi: 10.1105/tpc.112.102574.

Vanholme, R. *et al.* (2013) 'Caffeoyl Skikimate Esterase (CSE) Is an Enzyme in the Lignin Biosynthetic Pathway in Arabidopsis', *Science*, 341(September), pp. 1103–1106.

Vanholme, R. *et al.* (2019) 'COSY catalyses trans-cis isomerization and lactonization in the biosynthesis of coumarins.', *Nature plants*. Springer US. doi: 10.1038/s41477-019-0510-0.

Vanneste, S. and Friml, J. (2009) 'Auxin: A Trigger for Change in Plant Development', *Cell*, 136(6), pp. 1005–1016. doi: 10.1016/j.cell.2009.03.001.

Vanneste, S. and Friml, J. (2013) 'Calcium: The Missing Link in Auxin Action', *Plants*, 2(4), pp. 650–675. doi: 10.3390/plants2040650.

Vasconcellos, F. (2006) *Dicoumarol*, *Wikipedia*. Available at: https://en.wikipedia.org/wiki/File:Dicumarol.svg.

Vázquez, A. (1973) 'Effect of umbelliferone on rooting in bean cuttings', *Plant Science Letters*, 1(11), pp. 433–438. doi: 10.1016/0304-4211(73)90080-1.

Vázquez, A. (1974) 'Effect of umbelliferone, as rooting stimulator, on endogenous growth substances in bean cuttingsVliv umbeliferonu jako stimulátoru zakořeňování na endogenní růstové látky v řízcích fazole', *Biologia Plantarum*, 16(4), pp. 308–311. doi: 10.1007/bf02921243.

Velasquez, S. M. *et al.* (2016) 'Auxin and Cellular Elongation', *Plant Physiology*, 170(3), pp. 1206–1215. doi: 10.1104/pp.15.01863.

Velasquez, S. M. *et al.* (2019) 'Auxin-dependent xyloglucan remodelling defines differential tissue expansion in Arabidopsis thaliana', *BioRxiv*, pp. 1–25. doi: https://doi.org/10.1101/808964.

Veldstra, H. and Havinga, E. (1943) 'Untersuchungen Uber phflanzliche wuchsstoffe VII', 314(1931).

Verstraeten, I., Schotte, S. and Geelen, D. (2014) 'Hypocotyl adventitious root organogenesis differs from

lateral root development.', *Frontiers in plant science*, 5(September), p. 495. doi: 10.3389/fpls.2014.00495.

Vert, G. *et al.* (2005) 'Molecular Mechanisms of Steroid Hormone Signaling in Plants', *Annual Review of Cell and Developmental Biology*, 21(1), pp. 177–201. doi: 10.1146/annurev.cellbio.21.090704.151241.

Vialart, G. *et al.* (2012) 'A 2-oxoglutarate-dependent dioxygenase from Ruta graveolens L. exhibits p-coumaroyl CoA 2'-hydroxylase activity (C2'H): a missing step in the synthesis of umbelliferone in plants', *The Plant Journal*, 70(3), pp. 460–470. doi: 10.1111/j.1365-313X.2011.04879.x.

Vieten, A. *et al.* (2005) 'Functional redundancy of PIN proteins is accompanied by auxin-dependentcross-regulation of PIN expression', *Development*, 132(20), pp. 4521–4531. doi: 10.1242/dev.02027.

Vogel, A. (1820) 'Darstellung von Benzoesäure aus der Tonka-Bohne und aus den Meliloten - oder Steinklee - Blumen', *Annalen der Physik und der physikalischen Chemie*, 64(2), pp. 161–166. doi: 10.1002/andp.18200640205.

Voges, M. J. E. E. E. *et al.* (2019) 'Plant-derived coumarins shape the composition of an Arabidopsis synthetic root microbiome', *Proceedings of the National Academy of Sciences*, 116(25), pp. 12558–12565. doi: 10.1073/pnas.1820691116.

Vogt, T. (2010) 'Phenylpropanoid biosynthesis', *Molecular Plant*. The Author. All rights reserved., 3(1), pp. 2–20. doi: 10.1093/mp/ssp106.

Wang, C. *et al.* (2015) 'Insights into the origin and evolution of the plant hormone signaling machinery', *Plant Physiology*, 167(3), pp. 872–886. doi: 10.1104/pp.114.247403.

Wang, H. *et al.* (2009) 'Regulation of Arabidopsis Brassinosteroid Signaling by Atypical Basic Helix-Loop-Helix Proteins', *The Plant Cell*, 21(12), pp. 3781–3791. doi: 10.1105/tpc.109.072504.

Wang, J. P. *et al.* (2018) 'Improving wood properties for wood utilization through multi-omics integration in lignin biosynthesis', *Nature Communications*. Springer US, 9(1). doi: 10.1038/s41467-018-03863-z.

Wang, W., Bai, M. Y. and Wang, Z. Y. (2014) 'The brassinosteroid signaling network-a paradigm of signal integration', *Current Opinion in Plant Biology*. Elsevier Ltd, 21, pp. 147–153. doi: 10.1016/j.pbi.2014.07.012.

Wang, Yin *et al.* (2013) 'Plant cell wall lignification and monolignol metabolism', *Frontiers in Plant Science*, 4(July), pp. 1–14. doi: 10.3389/fpls.2013.00220.

Wang, Yuan *et al.* (2013) 'Strigolactone/MAX2-Induced Degradation of Brassinosteroid Transcriptional Effector BES1 Regulates Shoot Branching', *Developmental Cell*. Elsevier Inc., 27(6), pp. 681–688. doi: 10.1016/j.devcel.2013.11.010.

Wang, Z.-Y. *et al.* (2011) 'Brassinosteroid Signaling Network and Regulation of Photomorphogenesis', *Annual Review of Genetics*, 46(1), pp. 701–724. doi: 10.1146/annurev-genet-102209-163450.

Waters, M. T. *et al.* (2014) 'The karrikin response system of Arabidopsis', *Plant Journal*, 79(4), pp. 623–631. doi: 10.1111/tpj.12430.

Waywood, E. R., Oaks, A. and Maclachlan, G. A. (1956) 'The enzymatically catalyzed oxidation of indoleacetic acid.', *Canadian Journal of Botany*, 34, pp. 905–926.

Wehmer, C. (1911) 'Die pflanzenstoffe, botanisch-systematisch bearb: chemische bestandteile und zusammensetzung der einzelnen pflanzenarten, rohstoffe und produkte.', *Phanerogamen*, 1.

Wei, C. and Lintilhac, P. M. (2003) 'Loss of stability—a new model for stress relaxation in plant cell walls', *Journal of Theoretical Biology*, 224(3), pp. 305–312. doi: 10.1016/S0022-5193(03)00167-X.

Wei, C. and Lintilhac, P. M. (2007) 'Loss of Stability: A New Look at the Physics of Cell Wall Behavior during Plant Cell Growth', *Plant Physiology*, 145(3), pp. 763–772. doi: 10.1104/pp.107.101964.

Wei, Z. and Li, J. (2016) 'Brassinosteroids Regulate Root Growth, Development, and Symbiosis', *Molecular Plant*. Elsevier, 9(1), pp. 86–100. doi: 10.1016/j.molp.2015.12.003.

Wen, J., Lease, K. A. and Walker, J. C. (2004) 'DVL, a novel class of small polypeptides: overexpression alters Arabidopsis development', *The Plant Journal*, 37(5), pp. 668–677. doi: 10.1111/j.1365-313X.2003.01994.x.

Went, F. W. (1934) *On the pea test method for auxin, the plant growth hormone*.

Went, F. W. (1939) 'Further Analysis of the Pea Test for Auxin', *Bulletin of the Torrey Botanical Club*, 66(6), p. 391. doi: 10.2307/2481039.

Went, F. W. and Thimann, K. K. V (1937) 'Phytohormones', *New York: Macmillan Company*.

Whittaker, R. H. and Feeny, P. P. (1971) 'Allelochemics: Interactions between Species', *Science*, 171(3973), pp. 757–770.

Widhalm, J. R. and Dudareva, N. (2015) 'A familiar ring to it: Biosynthesis of plant benzoic acids', *Molecular Plant*. Elsevier Ltd, 8(1), pp. 83–97. doi: 10.1016/j.molp.2014.12.001.

Wikipedia (2008) *Chemical structure of coumarin*. Available at: https://nl.wikipedia.org/wiki/Coumarine#/media/Bestand:Cumarin2.svg.

Wilkinson, G. N. and Rogers, C. E. (1973) 'Symbolic Description of Factorial Models for Analysis of Variance', *Applied Statistics*, 22(3), p. 392. doi: 10.2307/2346786.

Willige, B. C. *et al.* (2011) 'Gibberellin regulates PIN-FORMED abundance and is required for auxin transport-dependent growth and development in Arabidopsis thaliana.', *The Plant cell*, 23(6), pp. 2184–95. doi: 10.1105/tpc.111.086355.

Winkler, B. C. (1967) *Quantitative Analysis of Coumarins by Thin Layer Chromatography, Related Chromatographic Studies, and the Partial Identification of a Scopoletin Glycoside Present in Tobacco Tissue Culture.* The University of Oklahoma.

de Wit, M., Lorrain, S. and Fankhauser, C. (2014) 'Auxin-mediated plant architectural changes in response to shade and high temperature', *Physiologia Plantarum*, 151(1), pp. 13–24. doi: 10.1111/ppl.12099.

Woeste, K. E., Ye, C. and Kieber, J. J. (1999) 'Two Arabidopsis Mutants That Overproduce Ethylene Are Affected in the Posttranscriptional Regulation of 1-Aminocyclopropane-1-Carboxylic Acid Synthase', *Plant Physiology*, 119(2), pp. 521–530. doi: 10.1104/pp.119.2.521.

Woldemariam, M. G. *et al.* (2013) 'NaMYC2 transcription factor regulates a subset of plant defense responses in Nicotiana attenuata', *BMC Plant Biology*, 13(1), p. 73. doi: 10.1186/1471-2229-13-73.

Wolf, S., Hématy, K. and Höfte, H. (2012) 'Growth Control and Cell Wall Signaling in Plants', *Annual Review of Plant Biology*, 63(1), pp. 381–407. doi: 10.1146/annurev-arplant-042811-105449.

Won, C. *et al.* (2011) 'Conversion of tryptophan to indole-3-acetic acid by tryptophan aminotransferases of Arabidopsis and YUCCAs in Arabidopsis', *Proceedings of the National Academy of Sciences of the United States of America*, 108(45), pp. 18518–18523. doi: 10.1073/pnas.1108436108.

Woodward, A. W. and Bartel, B. (2005) 'Auxin: Regulation, action, and interaction', *Annals of Botany*, 95(5), pp. 707–735. doi: 10.1093/aob/mci083.

Worsham, A. D.Klingman, G. C. and Moreland, D. E. (1962) 'Promotion of Germination of Striga asiatica Seed by Coumarin Derivatives and Effects on Seedling Development', *Nature*, 195, pp. 199–201.

Wu, C.-X. *et al.* (2015) 'Discovery and Weed Inhibition Effects of Coumarin as the Predominant Allelochemical of Yellow Sweetclover (Melilotus officinalis)', *International Journal of Agriculture and Biology*, 18(01), pp. 168–175. doi: 10.17957/IJAB/15.0082.

Wu, H. S. *et al.* (2008) 'Allelopathic impact of artificially applied coumarin on Fusarium oxysporum f.sp. niveum', *World Journal of Microbiology and Biotechnology*, 24(8), pp. 1297–1304. doi: 10.1007/s11274-007-9602-5.

Wu, J. *et al.* (2019) 'phyB Interacts with BES1 to Regulate Brassinosteroid Signaling in Arabidopsis', *Plant and Cell Physiology*, 60(2), pp. 353–366. doi: 10.1093/pcp/pcy212.

Wulff, H. *et al.* (1998) 'Alkoxypsoralens, Novel Nonpeptide Blockers of Shaker -Type K + Channels: Synthesis and Photoreactivity', *Journal of Medicinal Chemistry*, 41(23), pp. 4542–4549. doi: 10.1021/jm981032o.

Xia, Y. *et al.* (2007) 'Determination of scopoletin in rat plasma by high performance liquid chromatographic method with UV detection and its application to a pharmacokinetic study', *Journal of Chromatography B*, 857(2), pp. 332–336. doi: 10.1016/j.jchromb.2007.07.023.

Xie, X., Kagawa, T. and Takano, M. (2014) 'The phytochrome B/phytochrome C heterodimer is necessary for phytochrome C-mediated responses in rice seedlings.', *PloS one*, 9(5), p. e97264. doi: 10.1371/journal.pone.0097264.

Xuan, W. *et al.* (2015) 'Root Cap-Derived Auxin Pre-patterns the Longitudinal Axis of the Arabidopsis Root', *Current Biology*, 25(10), pp. 1381–1388. doi: 10.1016/j.cub.2015.03.046.

Xue, J. *et al.* (1995) 'The myrosinase gene family in Arabidopsis thaliana: gene organization, expression and evolution', *Plant molecular biology*. Springer, 27(5), pp. 911–922.

Yamaguchi, S. (2008) 'Gibberellin Metabolism and its Regulation', *Annual Review of Plant Biology*, 59(1), pp. 225–251. doi: 10.1146/annurev.arplant.59.032607.092804.

Yang, C. *et al.* (2015) 'Ethylene Signaling in Rice and Arabidopsis: Conserved and Diverged Aspects', *Molecular Plant*, 8(4), pp. 495–505. doi: 10.1016/j.molp.2015.01.003.

Yang, D.-L. *et al.* (2012) 'Plant hormone jasmonate prioritizes defense over growth by interfering with gibberellin signaling cascade', *Proceedings of the National Academy of Sciences*, 109(19), pp. E1192–E1200. doi: 10.1073/pnas.1201616109.

Yang, L. *et al.* (2017) 'Exposure to Umbelliferone reduces Ralstonia solanacearum biofilm formation, transcription of type III secretion system regulators and effectors and virulence on tobacco', *Frontiers in Microbiology*, 8(JUN), pp. 1–10. doi: 10.3389/fmicb.2017.01234.

Yang, L. *et al.* (2018) 'Response of Plant Secondary Metabolites to Environmental Factors', *Molecules*, 23(4), p. 762. doi: 10.3390/molecules23040762.

Yao, D.-D. *et al.* (2017) 'Effect of coumarin on Italian ryegrass seed germination and seedling growth', *Acta Prataculturae Sinica*, 2, p. 15.

Yaoya, S. *et al.* (2004) 'Umbelliferone Released from Hairy Root Cultures of Pharbitis nil Treated with Copper Sulfate and Its Subsequent Glucosylation', *Bioscience, Biotechnology, and Biochemistry*, 68(9), pp. 1837–1841. doi: 10.1271/bbb.68.1837.

Yikrazuul (2010) *Umbelliferon*, *Wikipedia*. Available at: https://nl.wikipedia.org/wiki/Umbelliferon#/media/Bestand:Umbelliferone.svg.

Yin, R. *et al.* (2014) 'Kaempferol 3-O-rhamnoside-7-O-rhamnoside is an endogenous flavonol inhibitor of polar auxin transport in Arabidopsis shoots', *New Phytologist*, 201(2), pp. 466–475. doi: 10.1111/nph.12558.

Yin, Y. *et al.* (2002) 'BES1 Accumulates in the Nucleus in Response to Brassinosteroids to Regulate Gene Expression and Promote Stem Elongation', *Cell*, 109(2), pp. 181–191. doi: 10.1016/S0092-8674(02)00721-3.

Yin, Y. *et al.* (2005) 'A New Class of Transcription Factors Mediates Brassinosteroid-Regulated Gene

Expression in Arabidopsis', *Cell*, 120(2), pp. 249–259. doi: 10.1016/j.cell.2004.11.044.

Yoshimitsu, Y. *et al.* (2011) 'Transcription of DWARF4 plays a crucial role in auxin-regulated root elongation in addition to brassinosteroid homeostasis in arabidopsis thaliana', *PLoS ONE*, 6(8). doi: 10.1371/journal.pone.0023851.

Youn, J.-H. *et al.* (2016) 'ARF7 increases the endogenous contents of castasterone through suppression of BAS1 expression in Arabidopsis thaliana', *Phytochemistry*, 122, pp. 34–44. doi: 10.1016/j.phytochem.2015.11.006.

Yuksel, B. and Aksoy, O. (2017) 'Cytological Effects of Coumarin on the Mitosis of Lens culinaris Medik', *Fresenius Environmental Bulletin*, 26(11), pp. 6400–6407.

Zádníková, P. *et al.* (2010) 'Role of PIN-mediated auxin efflux in apical hook development of Arabidopsis thaliana.', *Development (Cambridge, England)*, 137(4), pp. 607–17. doi: 10.1242/dev.041277.

Zentella, R. *et al.* (2007) 'Global Analysis of DELLA Direct Targets in Early Gibberellin Signaling in Arabidopsis', *The Plant Cell*, 19(10), pp. 3037–3057. doi: 10.1105/tpc.107.054999.

Zhang, D.-W. *et al.* (2015) 'Induction of plant virus defense response by brassinosteroids and brassinosteroid signaling in Arabidopsis thaliana', *Planta*, 241(4), pp. 875–885. doi: 10.1007/s00425-014-2218-8.

Zhang, J. *et al.* (2009) 'Flavones and flavonols play distinct critical roles during nodulation of Medicago truncatula by Sinorhizobium meliloti', *Plant Journal*, 57(1), pp. 171–183. doi: 10.1111/j.1365-313X.2008.03676.x.

Zhang, J. *et al.* (2016) 'DAO1 catalyzes temporal and tissue-specific oxidative inactivation of auxin in Arabidopsis thaliana', *Proceedings of the National Academy of Sciences of the United States of America*, 113(39), pp. 11010–11015. doi: 10.1073/pnas.1604769113.

Zhang, L.-Y. *et al.* (2009) 'Antagonistic HLH/bHLH Transcription Factors Mediate Brassinosteroid Regulation of Cell Elongation and Plant Development in Rice and Arabidopsis', *The Plant Cell*, 21(12), pp. 3767–3780. doi: 10.1105/tpc.109.070441.

Zhang, M. *et al.* (1998) 'The relationship between maturity or senescence of tobacco leaves and brown spot.', *Acta Phytopathologica Sinica*, 28, pp. 49–54.

Zhang, S. *et al.* (2017) 'Quorum sensing-disrupting coumarin suppressing virulence phenotypes in Vibrio splendidus', *Applied Microbiology and Biotechnology*. Applied Microbiology and Biotechnology, 101(8), pp. 3371–3378. doi: 10.1007/s00253-016-8009-3.

Zhang, Z.-L. *et al.* (2011) 'SCARECROW-LIKE 3 promotes gibberellin signaling by antagonizing master growth repressor DELLA in Arabidopsis', *Proceedings of the National Academy of Sciences*, 108(5), pp. 2160–2165. doi: 10.1073/pnas.1012232108.

Zhao, B. *et al.* (2018) 'Core cis -element variation confers subgenome-biased expression of a transcription factor that functions in cotton fiber elongation', *New Phytologist*, 218(3), pp. 1061–1075. doi: 10.1111/nph.15063.

Zhao, J. *et al.* (2013) 'Arabidopsis thaliana AHL family modulates hypocotyl growth redundantly by interacting with each other via the PPC/DUF296 domain', *Proceedings of the National Academy of Sciences*, 110(48), pp. E4688–E4697. doi: 10.1073/pnas.1219277110.

Zhao, M. *et al.* (2012) 'Expansins are involved in cell growth mediated by abscisic acid and indole-3-acetic acid under drought stress in wheat', *Plant Cell Reports*, 31(4), pp. 671–685. doi: 10.1007/s00299-011-1185-9.

Zhao, Y., Christensen, S K, *et al.* (2001) 'A role for flavin monooxygenase-like enzymes in auxin biosynthesis.', *Science (New York, N.Y.)*, 291(5502), pp. 306–9. doi: 10.1126/science.291.5502.306.

Zhao, Y., Christensen, Sioux K., *et al.* (2001) 'A Role for Flavin Monooxygenase – Like Enzymes in Auxin Biosynthesis', *Science*, 291(January), pp. 306–310. doi: 10.1126/science.291.5502.306.

Zhao, Y. (2010) 'Auxin biosynthesis and its role in plant development', *Annu Rev Plant Biol*, 61, pp. 49–64. doi: 10.1146/annurev-arplant-042809-112308.Auxin.

Zhao, Y. (2012) 'Auxin biosynthesis: A simple two-step pathway converts tryptophan to indole-3-Acetic acid in plants', *Molecular Plant*. Â© The Author. All rights reserved., 5(2), pp. 334–338. doi: 10.1093/mp/ssr104.

Zheng, K. *et al.* (2017) 'Involvement of PACLOBUTRAZOL RESISTANCE6/KIDARI, an Atypical bHLH Transcription Factor, in Auxin Responses in Arabidopsis', *Frontiers in Plant Science*, 8(October), pp. 1–13. doi: 10.3389/fpls.2017.01813.

Zheng, X. *et al.* (2011) 'AUXIN UP-REGULATED F-BOX PROTEIN1 regulates the cross talk between auxin transport and cytokinin signaling during plant root growth', *Plant Physiology*, 156(4), pp. 1878–1893. doi: 10.1104/pp.111.179812.

Zheng, Z. *et al.* (2016) 'Local auxin metabolism regulates environment-induced hypocotyl elongation', *Nature Plants*, 2(April), p. 16025. doi: 10.1038/nplants.2016.25.

Zhong, S. *et al.* (2012) 'A molecular framework of light-controlled phytohormone action in arabidopsis', *Current Biology*, 22(16), pp. 1530–1535. doi: 10.1016/j.cub.2012.06.039.

Zhong, S. and Chang, C. (2018) 'Ethylene Signalling: The CTR1 Protein Kinase', in *Annual Plant Reviews online*. Chichester, UK: John Wiley & Sons, Ltd, pp. 147–168. doi: 10.1002/9781119312994.apr0478.

Zhou, L. *et al.* (2008) 'Simultaneous analysis of coumarins and secoiridoids in Cortex Fraxini by high-performance liquid chromatography–diode array detection–electrospray ionization tandem mass spectrometry', *Journal of Pharmaceutical and Biomedical Analysis*, 47(1), pp. 39–46. doi: 10.1016/j.jpba.2007.12.009.

Zhou, Y. *et al.* (2018) 'HAIRY MERISTEM with WUSCHEL confines CLAVATA3 expression to the outer apical meristem layers', *Science*, 361(6401), pp. 502–506. doi: 10.1126/science.aar8638.HAIRY.

Ziegler, J. *et al.* (2015) 'Non-targeted profiling of semi-polar metabolites in Arabidopsis root exudates uncovers a role for coumarin secretion and lignification during the local response to phosphate limitation', *Journal of Experimental Botany*, 67(5), pp. 1421–1432. doi: 10.1093/jxb/erv539.

Zobel, A. M. and Brown, S. A. (1989) 'Localization of daphnetin and umbelliferone in different tissues of Daphne mezereum shoots', *Canadian Journal of Botany*, 67(5), pp. 1456–1459. doi: 10.1139/b89-194.

Zobel, A. M. and Brown, S. A. (1995) 'Coumarins in the interactions between the plant and its environment', *Allelopathy J*, 2(1), pp. 9–20.

Zobel, R. W. (2016) 'Arabidopsis: An Adequate Model for Dicot Root Systems?', *Frontiers in Plant Science*, 7(FEB2016), pp. 5–7. doi: 10.3389/fpls.2016.00058.

Zou, J. *et al.* (2006) 'The rice HIGH-TILLERING DWARF1 encoding an ortholog of Arabidopsis MAX3 is required for negative regulation of the outgrowth of axillary buds', *Plant Journal*, 48(5), pp. 687–696. doi: 10.1111/j.1365-313X.2006.02916.x.

Curriculum vitae

Personal

Personal data

- Stan Van Praet
- Born the 18th of November 1992
- Married
- Leegtestraat 26A, 8020 Ruddervoorde, Belgium
- stan.vanpraet@gmail.com
- +32484619090
- https://www.linkedin.com/pub/stan-van-praet/a5/155/553

Professional goals

I am a life science professional, finishing my PhD at the VIB-UGent Center for Plant Systems Biology. Two-thirds of my PhD I have spent on the Ghent University Global Campus in South Korea, establishing a new research facility. Managing projects, enrolling protocols, establishing sustainable structures and implementing creative strategic solutions is what strongly interest me. Therefore, I want to pursue a career in the life science sector as project leader.

Work experience

2015 – present	Doctoral researcher	VIB-UGent Center for Plant Systems Biology (PSB)
	Fundamental molecular research in plants. - Establishing a plant science lab at the Ghent University Global Campus (GUGC) in South Korea - Head of the greenhouse facilities at GUGC, maintaining and managing the facilities as well as crop protection - Collaborating with the University of Cambridge: application of the in house developed tool of the Sainsbury Laboratory in my project - Knowledge transfer of the PSB to GUGC - Organizer of the first GUGC Research Symposium (team of 3)	
2008 – 2015	Several summer- and weekend-jobs	
	- *BVBA Verhegge Marc, Zedelghem, Belgium:* constructing pavements and sewage system - *BVBA Demeulenaere, Ruddervoorde:* constructing floors and bathrooms - *Joxx, Brugge*: Installing bouncy castles - *BVBA Den Baes, Ruddervoorde:* helping in car garage - *Piefferoen, Ruddervoorde and Wingene*: chicken hatchery and farm - *KBC Ruddervoorde*: Goalkeeper trainer (volunteer work)	

Education

2019 forthcoming	Doctor of physiology (Ph.D.) in Biotechnology and biochemistry	Ghent University
2015	Master of Science in Biology *Summa cum laude*	Ghent University
2013	Bachelor of Science in Biology *Magna cum laude*	Ghent University
2010	Science and Sports (Wetenschappen-Sport)	Vrij Handels- en Sportinstituut, Bruges

Interpersonal skills

Coaching and teaching	- Coaching and training master students and researchers of different backgrounds and cultures - Teaching different practical sessions and lectures to 1st, 2nd and 3rd year bachelor students bio-engineering - Head of the practical of plant biology (histology) for 2nd-year bachelor students bio-engineering (5 years)	2015 – 2019

Leadership	- Co-Founding the Lab of Plant Growth Analysis at GUGC
	- Leading the meetings with the constructors (COGAS) of the growth facilities at GUGC and direction the communication to the lab
	- Assisting Academic Staff (AAP) representative of GUGC, representing their interest to the management of GUGC and the board of directors of Ghent University
	- Student representative at Ghent university
	  o Study programme committee of Biology
	  o Council of the Faculty of Science
	  o The student council of the Faculty of Science (StuW), of which 2 years as vice-chairman
	- Students representative in mid and high school
		2015 – 2019
		2016 – 2019
		2015 – 2018
		2010 – 2015
		2004 - 2010

Entrepreneurial	- Founder and manager of the Faculty football team of the Incheon Global Campus (FC the Songdo Socks) - Organizer of the first Research symposium at the Ghent University Global Campus - Co-founder of StuW - Project responsible of StuW - Co-founder of the 'cursuscruisen' programme in Biology at UGent	2015 – 2019 2018 2010 – 2014 2011 – 2014 2011 – 2013
Communication	- Presenting our research to specialist in the field, at our campus in South Korea, at conferences as well as in Cambridge - Presenting our research in laymen terms to non-specialist in the field, as well as to several stakeholders in South Korea (board of directors, deans, ministry of education of Korea etc.)	2015 – present

Scientific expertise

- Molecular Genetic tools (e.g. RT-qPCR and RNAseq)
- Microscopy (microtome sectioning, light, fluorescence and confocal)
- Priva (software of growth facilities)
- Statistics (R)
- GIMP
- Inkscape
- Microsoft office
- General laboratory practices

Language skills

	Understanding		Producing	
	Listening	Reading	Speaking	Writing
Dutch	Native			
English	Excellent	Excellent	Fluent	Very good
French	Limited	Basic	Poor	Poor

Additional information:

Personality

- Responsible
- Driven
- Respectful
- Social
- Meticulous
- Optimistic

Grants:

- Awarded Dehousse scholarship for doctoral research (4-year grant)
- Awarded the Francine Ronsse price for my master dissertation
- Awarded the Scientist of the year graduate in High School

Additional Degrees:

- Driver license – B 2011
- Official Hunting License 2013
- Diploma of official Bee-Keeper (Erkenningsnummer: 16327) 2014

Additional courses followed:

- Technology Transfer Course 2019
- GIMP and Inkscape initiation 2019
- Assistant Lecture training 2018
- Galaxy 2017 and 2018
- Electronic Lab Book 2017
- Effective oral presentation of Jean-Luc Dumount 2016

Hobbies and passions:

At the age of 5, I started as a goalkeeper, and ever since my life has been full of sports. Currently, I'm playing futsal, rugby and every now and then I'm out for a good run. Besides sports, I am passionate about nature, experiencing wild-life, I do some amateur photography and love to hunt and travel. My experience in falconry and dog training taught me a lot about patience and persistence. My interest in brewing and distilling processes resulted in brewing my own beer and wine. I also have a special interest in economics and management in order to try to understand how society functions. I love reading (non-fiction) books and the Flemish newspaper 'De Tijd'.

References

- Professor Dr Nico Callewaert (Ghent University), VIB Science director of the VIB-UGent Center for Medical Biotechnology
    - nico.callewaert@ugent.vib.be
    - +32 9 331 36 30/ 264 93 03
- Professor Dr Dirk Inzé (Ghent University), VIB Science director of the VIB-UGent Center for Plant Systems Biology
    - dirk.inze@ugent.vib.be
    - +32 9 331 38 00 / 06
- Professor Dr Geert De Jaeger (Ghent University), VIB Group Leader
    - geert.dejaeger@ugent.vib.be
    - +32 9 331 38 70
- Professor Dr Ir Stephen Depuydt (Ghent University Global Campus), director of the Lab of Plant Growth Analysis, PhD supervisor
    - stephen.depuydt@ghent.ac.kr
    - +32472 35 37 40
- Professor Dr Ir Bartel Vanholme (Ghent University), VIB Project Leader, PhD co-supervisor
    - bartel.vanholme@ugent.vib.be
    - +32 9 331 38 40

Upon request, additional references can be obtained.

Scientific

In addition to my personal CV, written in order the find a new opportunity in my future, underneath I will give some broader information on my scientific CV, in order to fulfil all requirements to obtain my PhD. Hereby I only focus on the trainings and skills obtained during my PhD, not the ones in my free-time, or previous career.

Trainings

- **Technology Transfer Course** **2019**
  - 1 full week course
  - Organised and lectured by the VIB innovations and business team
- **GIMP and Inkscape initiation** **2019**
  - 1 full day
  - Organised by the VIB
- **Career guidance training** **2019**
  - Job orientation, constructing CV and motivation letterIn total 2 full days
  - Organised by Lucia Smith
- **Leadership Skills in Science** **2018**
  - 2 hours
  - Plant Biology Conference, Montreal
- **Assistant Lecturer training** **2018**
  - 1 full week
  - 'Doctoraatsassistenten training of the UGent'
- **Galaxy** **2017, 2018**
  - 2 times 1 full day
  - Organised by the UGent in 2017, and by the VIB in 2018
- **Electronic Lab Book** **2017**
  - 1 full day
  - Organised by the VIB
- **Effective oral presentation** **2016**
  - 5 full days, spread over 3 weeks
  - Given by Jean-Luc Dumount

Symposia and conferences

- **2018: Plant Biology Conference, Montreal, Québec**
  - Title: "Coumarin-induced cell elongation depends on the interplay between auxin signalling, auxin transport and gibberellic acid biosynthesis."
  - Abstract ID: 481704
  - Authors: Stan Van Praet[1,2,3], Jonas De Saeger[1,2,3], Bartel Vanholme[1,2], Dirk Inzé[1,2,], Stephen Depuydt[1,2,3]
  - Poster presentation, presented by Stan Van Praet.
  - 14th until the 18th of July 2018
- **2018: Ghent University Global Campus Research Symposium, 119 Songdomunwha-Ro, Incheon**
  - Title: "Coumarin-induced cell elongation depends on the interplay between auxin signalling, auxin transport and gibberellic acid biosynthesis."
  - Authors: Stan Van Praet[1,2,3], Jonas De Saeger[1,2,3], Bartel Vanholme[1,2], Dirk Inzé[1,2,], Stephen Depuydt[1,2,3]
  - Poster presentation, presented by Stan Van Praet
  - 2018.08.24
- **2016: Annual meeting of the Korean Society of Phycology, Jeju Island, Korea.**
  - An algae-based natural compound screen to improve plant growth
  - Authors: Stan Van Praet, Jonas De Saeger, Jihae Park, Taejun Han and Stephen Depuydt.
  - 28-30/09/2016
  - Presentation by Stephen Depuydt
- **2016: 27th International Conference on Arabidopsis Research (ICAR), Gyeong Ju, Korea.I**
  - An algae-based natural compound screen to improve plant growth
  - Authors: Stan Van Praet, Jonas De Saeger, Jihae Park, Taejun Han and Depuydt Stephen
  - Poster presentation, presented by Stephen Depuydt
  - June 29 - July 3, 2016

Collaborations and experiences abroad

2015-2019	4 year collaboration, in which 7-8 months a year were spent in South Korea, the rest in Belgium	Ghent University Global Campus, South Korea UGent-VIB centre for Plant Systems Biology
2018	3 weeks research stay in order to complete training on in vivo imaging of FRET biosensors for the phytohormone gibberellin.	Sainsbury Laboratory, Cambridge University
2018	Collaboration with Elke Barbez, to use her HPTS tool. She performed the experiments for us.	Kleine-Vehn Lab

Publications

A1

- **Toward the molecular understanding of the action mechanism of *Ascophyllum nodosum* extracts on plants**
- Jonas De Saeger & Stan Van Praet1 & Danny Vereecke & Jihae Par & Silke Jacques & Taejun Han & Stephen Depuydt
  - *Jonas De Saeger, Stan Van Praet and Danny Vereecke contributed equally to this work.*
- Journal of Applied Phycology
- https://doi.org/10.1007/s10811-019-01903-9

B2

- **How Plant Hormones and Their Interactions Affect Cell Growth**
- Stephen Depuydt, Stan Van Praet, Hilde Nelissen, Bartel Vanholme and Danny Vereecke
- Book: Molecular Cell Biology of the Growth and Differentiation of Plant Cells
- Edited by Ray J. Rose
- CRC Press 2016
- Pages 174–195
- Print ISBN: 978-1-4987-2602-3
- eBook ISBN: 978-1-4987-2603-0
- DOI: 10.1201/b20316-14

Involvement in training young scientist, students and technicians

Guiding students

2018	**Tutor master thesis:** Unravelling the role of the Phenylpropanoid pathway during coumarin-induced hypocotyl elongation in *Arabidopsis thaliana*	Mathias Thijs
2018-2019	**Technical expertise:** Guiding post-docs and PhD students in the lab.	Jelena Acimovic, Debbie Botterman and Lena Vlaminck
2017-2018	**Guiding internship:** Unravelling the mode-of-action of coumarin during coumarin-induced hypocotyl elongation in *Arabidopsis thaliana* via a GWAS-analysis	Kiseong Lee
2017-2018	**Technical expertise:** Role of SA in plant defence against *Rhodococcus fascians*	Lien Lietaer
2016-2017	**Technical expertise:** Towards fast and reliable screening methods for biostimulants to improve plant growth.	Fanny Baudoin

Teaching

2018	Plant physiology: 'Brassinosteroid signalling'	3rd Bachelor Bio-Engineering Ghent University Global Campus
2015-2019	Head of the practical of Plant Biology 6 practicals/semester, 5 semesters	2nd Bachelor Bio- Engineering Ghent University Global Campus
2017	Plant Physiology Preparations and guiding lecturers in preparations of *Arabidopsis* seedlings	Ghent University Global Campus
2016	Molecular Biology 1 practical	2nd Bachelor Bio- Engineering Ghent University Global Campus
2015	Lecturer of the practical of General Biology 10 practicals/semester, 1 semester	Ghent University Global Campus

Involvement in organizational task in the laboratory/department/faculty/university

2015-2019	**PhD-Student representative:** - Member of the Faculty Board - Member of the Intercampus Board - Monthly meetings with the management	Ghent University Global Campus
2016-2019	**Head of the greenhouse facilities:** - Installing and fine-tuning of the growth conditions via the Priva software - Maintenance of the Cogas growth facilities - Pest control of Rice and Arabidopsis - Technical support for all growth facilities - Leading all meetings with Cogas.	Ghent University Global Campus
2018	**Organizer of the first Research symposium at the Ghent University Global Campus**	Ghent University Global Campus
2017-2018	**PhD-Student representative:** - Member of the Study Programme Committee	Ghent University Global Campus

Acknowledgements

This part brought back a memory from when I was in high-school. They had the tradition, in our last year, to thank all the teachers for their tremendous effort in teaching us. I was, probably, the first to oppose that idea and I still remember the facial expression of my 'religion-teacher' (the organizer) when I said I only wanted to thank some teachers but not all. Today, I still believe in this spirit. What does it mean to thank someone in this section here or anywhere else, because tradition predicts? This would mean the thanks are just part of the job and, in fact, meaningless. I did not want to thank some teachers at the time because they were just doing their job, and some even weren't. I, however, wanted to thank especially the numerous teachers that went that extra mile to push us forward, to make us really understand their course and to guide us in our young and rebellious life. For example, my biology teacher that learned me all about genetics and shared my passion for birds. When I was late from school, it was because of him, thank you Johan Buckens for encouraging my biology heart and my interest in genetics, it brought me all the way to Korea to perform a PhD in Plant Genetics.

Therefore, here, I want to thank my two supervisors Bartel and Stephen, not only for 'just doing your job' but for going that extra mile for me. Thank you, Bartel, for the numerous coffees together, either face to face or via the well-known online channels. Your pretty face was never any of my interest, but your warm heart, your listening-ear and your broad understanding of the issues I was facing, were of enormous importance to me. Thank you for your advice, both scientifically as well as my mentor. Special thanks as well for all your wet lab work. It ranged from taking care of my plants and harvesting the seeds every semester again when I was in Korea, to even sowing and harvesting a complete EMS screening experiment. Seldom have I met a superior that is so down to earth and likes to still pull up his sleeves and do the job. I loved it!

Stephen, thank you for your trust in me, your eagerness to bring me to Korea and your unconditional support during this PhD. It has been a hell of an adventure with unmeasurable impact on my self-development, o man, what did I love it! It has been a track with ups and downs and I am very grateful for it. Special thanks for your writing advice and the multiple re-writing of everything. My name is Stan Of Talking, and not 'of writing', let's say that has been clear. Without your help, I would never have been able to finish it. Thank you for that.

Here, I also especially want to thank my parents. Mom, Dad, if it wasn't from you, I was working in construction. And although I dreamed and hoped many times during the writing of this 'pain-in-the-***-book' that I was working in construction, tiling or bricklaying, I'm o so grateful. Still a few steps to take to obtain my PhD, but hopefully soon, your son Stan that hated school so much, will not only have obtained a master but soon a PhD as well. This is all because of you, I simply never would have finished high school in the science track and would have started working as carpenter or mason. Many people do not understand how tough I made it for you in my young age and how smart and gentle you could confess me of the importance of education and a good degree if you have the talents for it. Thank you for all!

Darling, that first year in Korea, without you at my side was terrible. It is very simple, I was not complete. I remember how much I suffered, at the beginning of our relationship, to adjust to living with two. There was simply no time in my schedule for that. But the chemistry of love is inscrutable and I'm very grateful for that. Thank you for giving me my personal space, for understanding me better than I do myself and for accepting me who I'm. With you at my side, home or in Korea, it all is so much better than alone. Since September, I have

been writing day and night and almost every weekend, making me ‘grumpy grumbler’ (read: ‘brompie brompot’). The impact this had on us and especially on you cannot be underestimated. Only a magnificent strong lady like you can bear all of this without ever complaining. In a few sentences, I will finish this manuscript and from then onwards I’m all yours again honey. I’m looking forward to our marriage soon and building at our future together. Darling, I love you very much!

Of course, last but not least, I want to thank all the people that have guided me during my PhD and our Korea adventure. Thank you, Dirk, for your support all the way from the start to now. Thank you Lieve, Geert and Steffen for the moments together in Korea. It was always nice to see some Flemisch smiles trying the Korean food and beer together. Thank you, Nico, for all the fun moments together and for your advice in my career. Logically, I want to thank all my friends in Korea as well as home, but hey I definitely thanked you already numerous times in real life, see you soon, hopefully, accompanied by an Orval, Sint-Bernardus or Triple Karmeliet. Take care!